A Dendroclimatological Investigation of *Phyllocladus aspleniifolius* (Labill.) Hook. f.

by

Kathryn J. Allen, B.Ec., Grad. Dip. Env. St. (Hons.)

Submitted in fulfilment
of the requirements
for the degree of
Doctor of Philosophy

School of Geography and Environmental Studies
University of Tasmania
Hobart
Australia

August 1998

March 1993
Keating is voted top man. ***Truth****'s page 3 girl has enormous breasts, too much make-up and an ugly beach ball. Di is visiting the anti-royalists in Devonshire Row. Some jerk the other side of the bar is demanding the penultimate Guiness and shoves the greasy paper with his 'anytime you need a man, love' number on it across the bar towards the fuzzy barmaid. He smiles his 'I'll be your poet laureate anytime' smile because he knows the barmaid is into poetry. He forgets he isn't. His billowing gut is too full of Guiness to realise that the barmaid is flying above all the old coots on the wrong side of the bar, waiting for the crash after two weeks of hash and heavy alcohol abuse. She's been diving, sliding and spinning, cramming all of London's cheap sugar, grease and Guiness men into the crisp packet barges floating in Camden Loch.*

January 1994
Wondering whose body it is attached to these foreign arms, who it is thinking with this head when the big guys from the States roll in on the last big breaker of 1993. Taking a ride with this new head and new body to forget about London. To the big hill in the west, under the Cap. Watching the sun spill blood then drown just off the coast of home, allowing the Huon fronds to catch hair to play it into nature's cautious breeze. The silence of orange stratocumulus end each day's journey back into this self, and, just as dusk stalks the lake, blows the phylloclade across the pathway of my breath.

March 1995
A tic trying to burrow into the indeterminate fat layer of the thigh, leech between the toes – that's what you're here for, and the reunion with the easterly weather squatting on these eastern mountains. At Ralph's hotel at the top, one thousand years of solitude speaks in confused syllables, laughs in disjointed sentences, secretes messages in the intervals of speech. The Japanese tourists testing out Ralph's echo hall wear plastic K-Mart weather protection and can smell our wet thermals. They know we're here to work because we're swearing in Australian about the broken corer. We tell them we're doing the Phylloclade rap, trying to turn on the weather tap. They nod and mutter urban Japanese things to one another, will forget about trees until the next time they buy a genuine wooden souvenir of a Tasmanian apple 1000 years older than they are. They all sit on the left hand side of their bus as it clings to the steep incline, and listen to their Mr. Nice-Guy guide verbalising the politics of Australian science, as they edge back down the road towards the tentative safety of Ringarooma, then the surer safety of Launceston. We watch the clouds play games with history and laugh because they were somehow convinced we were doing science up here.

October 1996
Some geek on the dendroforum is talking dendromusic – literal translation of tree-ring widths and densities to symphonic masterpieces recited by Bristlecone Pine, Brahms lullabies from the Sequoias. Beethoven will be performed by Huon Pine, live tonight at the ABC Odeon, Liverpool St; the Pencil Pine roll'n'roll thunder band will be on, baby, thrashin' it sick down the Town Hall. Too many scientists practice piano and play jazz. I am hoping the trees will give them Leonard Cohen live and play everything in D minor. That octave fail to be octaves, instead becoming irregular, alternating, refusing to obey the statistician's periodicities. I am wondering if hoarse Celerytop musettes would whisper as the storm clouds swept in, or if Ralph's trees write Irish jigs, or famous bush ballads; if the chant of tree corroboree might be heard until the year white settlers floated in on filthy magic carpets. I am wondering if I rode the carpet to shore, or if I am a tree running the Tasmanian earth with science as an excuse.

Declaration

This is to certify that this thesis contains no material which has been accepted for a degree or diploma, not any material which has been previously published or written by another person except where due reference has been made.

Kathryn J. Allen

Authority of access

This thesis may be made available for loan and limited copying in accordance with the Copyright Act of 1968.

Kathryn J. Allen

Abstract

A network of fifteen *Phyllocladus asplenifolius* (Celerytop Pine) chronologies for Tasmania, Australia, is developed. These sites effectively form north-south and east-west transects across the state, ranging in elevation from sea level to 850m above sea level. Crossdating is established between sites spread across the state, indicating the existence of a common broadscale control mechanism. The growth response to a number of climatic variables, including maximum and minimum temperature, precipitation, zonal and meridional indices, and the Southern Oscillation Index is investigated. The most prominent features of the response functions produced for these variables are a consistency across sites in their response, especially so for northern sites, and a significant and negative correlation with prior growing season temperatures.

High frequency variability in the quasibiennial range dominates the spectra of ring width series and is investigated in an attempt to determine whether it contains statistically significant climate information. Strong evidence for the influence of a climatic factor is not apparent, although the influence of the Zonal Index may be significant.

Maximum temperature, the variable most consistently and most strongly correlated with ring widths, is used as the basis for climatic reconstruction on time scales greater than 2 years. Attempts to reconstruct climate by the more traditional technique of principal components regression were unsatisfactory, with insufficient variance due to climate being explained. Structural time series analysis is adapted for dendroclimatic reconstruction and some improvements in models result.

The structural time series reconstructions show some differences between different regions of the state over the twentieth century which apparently did not exist in the previous century. While these reconstructions approximately trace the trend of increasing temperatures indicated by high altitude *Lagarostrobos franklinii* (Huon Pine) and instrumental records over the past century, there remain some significant differences in reconstructions from the two species. Different optimal temperatures for photosynthesis associated with elevational differences of sites are consistent with these differences.

In large part, the limitations revealed through an examination of climate response of this species, and through the development of models for climatic reconstruction, relate to physiological questions concerning the species and point to a need for more detailed investigation of physiological aspects of species used for dendroclimatic work. Such investigations would allow a fuller utilisation of the potential offered by these species, and networks of them, as well as opening the way to a better understanding of resultant climatic reconstructions.

Acknowledgments

In expressing gratitude to those people below, I hope, probably in vain, that I have not omitted anyone. Firstly, much thanks and many drinks to those who have supervised me: Roger Francey, Manuel Nunez and Kelvin Michael. Without their continuous support and guidance I would have a: become clinically depressed and, b: very probably embarked upon a journey to ∞ on some dimly lit plane orthogonal to this one. It is impossible to sufficiently convey to Ed Cook the gratitude I feel for providing ingredients for thought, persistent encouragement, the long term loan of essential equipment without which this project would never have come into being, frustrated email conferences about the basics of dendrochronology and statistics, generally putting up with me, and finally and most importantly, for the whiskey. To those who made my stay at Lamont-Doherty pleasant, possible and educational, thankyou. Invaluable 'dendro talk' sessions (dry or wet) with Mike Peterson, Trevor Bird, Mike Barbetti, Guus van der Geer and David Pepper were sources of additional inspiration. And to the on-site 'dendro-head', Brendan Buckley, a huge thankyou for all the support and discussions over three of the past four years, providing me with the *Lagarostrobos* chronologies and the daily raising of sagging spirits at 3pm. Thankyou to those who took the time to help put me on the right path (?) as far as plant physiology/ecology is concerned: Mike Battaglia, Steve Harris, Tim Brodribb, Phil Barker, Jamie Kirkpatrick, and Susie Hester. For those who provided me with meteorological information/data, don't look too closely at what I've done (or not done) with it - Doug Shepherd, Mike Pook (Bureau of Meteorology), Ian Searle, Christina Neball and David Wilson (HEC). And just when I thought I could safely forget all about that Economics degree I recklessly completed whilst still in tender youth, David McDonald re-reminded me of the absolute and irreverent existence of econometrics. Without his guidance and support, a very large part of one chapter of this thesis would still be trying to find the formula for the big bang.

To all those who aided me with field work, I am forever indebted - without your help I would still be out there. Without a car. Most probably swinging from tree to tree. Thanks for various scrub bashing forays, the many squashed meals with lots of beans, lentils, rotting vegetables and alcoholic fruit, and the general entertainment provided by your injuries: Jol Desmarchelier (Mr IgorPro, who will never venture into the scrub with me again) and Di Sward, Janet Smith, Trevor Innes, my father, brother Paul, Nigel Locket, David Young, David Harries, José Valiente, Winfried Hoerr, Johnathan Marsden-Smedley, Mike Power, Steve Harris, and Kelvin Michael. In addition, thankyou to those who allowed me access to sites, or provided invaluable and time-saving information about sites: Forestry Tasmania in Hobart, St Helens, Scottsdale, Fingal and Deloraine; ANM New Norfolk; North Forests, Burnie; Parks and Wildlife, Hobart.

Peter Cornish happily (and rather foolishly) allowed me access to the Geology workshop; Malcom Hughes, at the TRL, Tucson, Arizona allowed access to Tasmanian samples collected by V. LaMarche, and Rex Adams provided general assistance during my Tucson sojourn. For the (in)voluntary, painful and time consuming perusal of various dismembered limbs of the draft I thank the mathematically pedantic and exacting Ken Peters (whom I shall never satisfy), Mona Loofs, Albert Goede, Trevor Bird, Harry 'Buck' Valentine, Tim Brodribb, Steve Harris and David Allen.

For the marathon of endurance of those in the department, especially my fellow Libran room mates, the long suffering Janet Smith and Roger Dawson, and departmental technical staff, a huge thankyou. Thanks to those who nursed me through bad moods and bad times, as well as the manic good times: Ange and Blun Bresnehan, Terence Liow, Maryanne Tamvakis, John and Barbara Norris, Paavo Jumppanen, Michael and Phillipa Power, Trevor Innes, Adam Friend and Dan Sinclair. Thankyou for all the hugs, chocolates, bushwalks through vegetation and weather (both of which were horizontal), candlelit rock climbs, imitation of Emperor Penguins in the Southern Ocean, and many other tame distractions. Finally, it is impossible to sufficiently express thanks for the support my extended family has given me through the past few years.

Table of Contents

List of Figures

List of Tables

Glossary

AIC	Akaike Information Criterion
AR	Autoregressive
AR(n)	Autoregressive, order n
ARM_M	Arm River
ARMA	Autoregressive moving average
ARSTAN	Program for data standardisation and statistical analysis
ASL	Average segment length
BCH	Buckley's Chance *Lagarostrobos franklinii* chronology
BEN_E	Ben Ridge Road
BIOCLIM	Biogeographical database
BLT_E	Blue Tier
CE	Coefficient of efficiency statistic
$CLAY_S$	Clayton's Lagoon
COFECHA	Data quality control program
DALR	Dry Adiabatic Lapse Rate
DW	Durbin-Watson statistic
EPS	Expressed population signal
ESM_E	East Shelf Maria Island
FC_M	February Creek
$FISH_M$	Fisher River
HAR	Harman River *L. franklinii* chronology
HEC	Hydro-Electric Corporation
HIGH	High elevation *L. franklinii* (>700 m ASL)
KF	Kalman Filter
KOA_M	Kia-Ora Creek
LJH	Lake Johnson *L. franklinii* chronology
LOW	Low elevation *L. franklinii* (<700 m ASL)
LCR_S	Lower Cole Road

LMH	Lake Marilyn High *L. franklinii* chronology
LML	Lake Marilyn Low *L. franklinii* chronology
LVH	Lake Vera Huon *L. franklinii* chronology
MA	Moving average
MI	Meridional Index
ML	Maximum Likelihood
MS_x	Mean sensitivity
MSE	Mean Square Error
MSLP	Mean Sea Level Pressure
MTM	Multiple Taper Method
MTREAD	Mt. Read *Lagarostrobos franklinii* chronology
MUR_W	Mt. Murchison
N_{BS}	Bowman-Shenton test for normality
NID	Normally Independently Distributed
PC	Principal Component
PCA	Principal Component Analysis
PDSI	Palmer Drought Severity Index
$PILL_M$	Mt Pillinger
PM	Product Means test
QBO	Quasibiennial Oscillation
QBORW	Quasibiennial Oscillation in Ring Widths
r	Pearson's product moment correlation coefficient
$\overline{R}$	Average series intercorrelation
R^2	Coefficient of Determination
R_D^2	Coefficient of determination, based on differenced data
RCS_W	Race Course Spur
RE	Reduction of error statistic
RFR_E	Ralph's falls Road
ρ	Spearman rank correlation coefficient
SNR	Signal to Noise Ratio
SLP	Sea Level Pressure

SO	Southern Oscillation
SOI	Southern Oscillation Index
SPR_S	Scott's Peak Road
SRT	Stanley River *Lagarostrobos franklinii* chronology
SSF	State Space Form
SST	Sea Surface Temperature
STAMP™	Structural Time Series Analyser, Modeller and Predictor software package
STHPB	Subtropical High Pressure Belt
STS	Structural Time Series
TPI	Transpolar Index
WEY_W	Wey River
yBP	years Before Present
ZI	Zonal Index

Chapter 1: Introduction

1.1 Preface

Global climate change over the past century has been well documented by numerous sources (Nicholls and Lavery 1992, Nicholls and Kariko 1993, Angell 1994, Grosiman and Easterling 1994, Hulme and Zhao 1994, Jones 1994, Nicholson 1994, Vinnikov *et al.* 1994, Wilson and Hansen 1994 among others). In comparison with the Northern Hemisphere, the Southern Hemisphere has a relative dearth of climatological records. Prior to 1900, the situation is exacerbated by a lack of instrumental records.

Whether or not current climatic changes are principally due to natural variability or to anthropogenic effects is presently highly topical. In order to address such questions, an examination of past climate is desirable, requiring the use of proxy climate indicators to study fluctuations and change prior to the period of instrumental records. Each proxy climate indicator has a different geographic and temporal range, accuracy, and resolution (Bradley 1985). Large numbers of these proxy climate records have been gleaned from ice cores, pollen cores, marine sediment cores, ice cores, bore–holes, tree rings and speleotherms. Deep-sea sediment cores and pollen spectra from lakes and swamps may span long time intervals but generally have low time resolution (Heusser and Shackleton 1994, Thompson *et al.* 1995, MacPhail 1980, Colhoun *et al.* 1991). Other proxy climate indicators such as ice cores (Bender *et al.* 1994), varved lake sediments (Hajdas *et al.* 1995), laminated speleotherms (Roberts *et al.* 1998), corals (McCulloch *et al.* 1994) and tree ring sequences all have the potential of annual to sub-annual time resolution but usually cover shorter time spans. Tropical corals have the potential to offer a weekly resolution (McCulloch *et al.* 1994).

Southern Hemisphere palaeoclimate research has largely been concentrated on ice cores, tree rings, and pollen analysis. Much of the tree ring work did not begin until the early 1970s and has been concentrated on the higher latitude land masses of South America, New Zealand and Tasmania. In southern Africa the growing season is poorly defined, making the detection of annual rings a difficult task.

Previous investigations of *Lagarostrobos franklinii* in Tasmania (e.g. Cook *et al.* 1991, 1992, 1996a & b, Buckley 1997) have yielded a continuous proxy temperature record extending back prior to 2100 BC, and another as yet discontinuous tree-ring record back to about 10,000 yBP which has been used for radiocarbon calendar calibration (Barbetti *et al.* 1992). This long–lived species is, however, limited to fire protected areas in the west and southwest of Tasmania. Because there exists considerable variation between the climate of eastern and western Tasmania, this geographical constraint may be significant. By contrast, *Phyllocladus aspleniifolius* is shorter lived but widely distributed across the State and may provide complementary information to the *L. franklinii* record. Due to its broad geographical distribution, *P. aspleniifolius* tree ring records should also be useful in the delineation of east/west differences and circulation changes which result in radically different conditions between the east and west. Fritts *et al.* (1979), Meko *et al.* (1993) and Salinger *et al.* (1994) have previously used spatial networks of sample sites in investigations of large scale climatic phenomena. For the purposes of this study, climatic data are considered as either monthly or seasonal variables, and the period of interest extends back over the last 1000 years. The climatic variables of interest in this study are maximum and minimum temperature, precipitation, Zonal and Meridional Indices and the Southern Oscillation Index (SOI).

Its adaptability means that *Phyllocladus aspleniifolius* is found in a wide range of environments, and this provides a further opportunity to examine the influence of a number of environmental characteristics on ring width.

1.2 Literature review

1.2.1 Dendrochronology

Dendrochronological methods have been widely used in a number of disciplines including ecology, climatology, hydrology, geomorphology, the development of regional fire histories, and archaeology and establishing the radiocarbon timescale (Schulman 1945, Fritts *et al.* 1965, Fritts 1971, Stockton and Fritts 1973, Dean 1978, McPhail *et al.* 1983, Cook *et al.* 1987, Payette *et al.* 1985, Jacoby *et al.* 1988, Barbetti *et al.* 1992, Jacoby *et al.* 1992, Luckman 1993,

Nanson *et al.* 1995, Brown and Sieg 1996). The study of dendrochronology is based upon variations contained in the annual growth band found in trees. Variations in ring width, ring density (latewood, earlywood, average density), stable isotopes ($\delta^{18}O$, $\delta^{13}C$, $\delta^{13}C\backslash\delta^{12}C$, δD) and trace elements contained in rings are all variables which have been previously investigated (e.g. McKinnell and Shepherd 1971, Epstein and Yapp 1976, Pearman *et al.* 1976, Francey 1981, Francey and Farquhar 1982, Leavitt and Long 1982, Baes and McLaughlin 1984, White *et al.* 1985, D'Arrigo *et al.* 1992). However, not all trees have annual bands. Many species, unsuitable for dendrochronological studies, display multiple rings for any one year, the number being inconsistent from year to year (LaMarche 1982). In conifers such as those studied here, annual rings appear as sheaths of cells in concentric rings in a cross section of the stem (Figure 1.1). In temperate areas these annual rings are generally the result of an annual growth flush beginning in spring and ending in autumn. In the tropics, where seasonality is not as distinct as in more temperate regions, the application of traditional dendrochronological methods has been more challenging. Nevertheless, a burgeoning research effort has indicated that there is sufficient seasonality to allow the formation of annual rings in some species (e.g. Ogden 1981, Eckstein *et al.* 1981, Ash 1983, Jacoby 1989, Buckley *et al.* 1995, Hughes 1995, Tsou 1995, Pumijumnong *et al.* 1995).

The active vascular cambium can be defined as those portions of phloem and xylem where cells are enlarging, but still able to divide (Fritts 1976). Cambial activity is initiated by favourable climatic conditions. New cells become differentiated into phloem and xylem, and the tree's diameter increases mainly as a result of cell division (Wilson 1964). As the rate of cell division slows towards the end of the annual growth flush, the width of the active cambial zone declines to that of the dormant state. Auxins are important in the initiation of cambial activity which starts in the upper part of the tree and extends downwards. Cell division begins under the buds, and proceeds from the stem tip down to the base of the tree.

Early in the season, new cells are thin-walled and the newly formed wood light coloured and porous. This is known as the earlywood (Figure 1.1). In contrast, latewood is formed later in the season and contains cells which are

radially flattened and have thicker cell walls. It is both darker in colour and denser. Latewood first appears near the base of the tree and then 'moves up' (Brown 1970), the opposite direction to which early season growth is initiated in the tree. False rings (Figure 1.1) may be formed as a response to sudden changes — e.g. a cold spell in the middle of the growing season, followed by a return to normal conditions, storms, or mid-season drought (Kramer 1964).

Both internal and external factors limit tree growth. External factors include 'macro' climatic factors, soil minerals, herbivores, microsite factors such as shading, and soil moisture. Internal factors include available food, minerals, growth regulators, enzymes, and water. Interactions between the two groups of factors are complex and internal factors are regulated by the combination of the external factors which influence growth in the current season but also carry-over effects from previous seasons.

Various hormones are important in regulating growth (Brown 1970) (Table 1.1). Auxin influences apical dominance, trophic responses, vascular tissue

Hormone	Rate of cell division	Rate of cell expansion	Direction of cell expansion	Differentiation (gene expression)
Auxin	+	+	↕	+
Cytokinins	+	*	*	+
Ethylene	+/-	+/-	↔	+
Abscisic acid	-	-	*	+
Gibberellins	+	+	↕	+

Table 1.1. **Hormonal influences on basic cellular processes. + positive effect, - negative effect, * little or no effect, vertical arrow longitudinal expansion, horizontal arrow radial expansion. Adapted from Raven *et al.* (1992)**

differentiation, promotion of cambial activity, inhibition of fruit and leaf abscission, inhibition/promotion of flowering, and also the stimulation of fruit development. Cytokinins affect cell division, promotion of shoot formation, and the delay of leaf senescence. Ethylene affects fruit ripening, leaf and flower senescence, leaf and fruit abscission, while abscisic acid influences stomatal closure, the induction of photosynthate transport from leaves to developing seeds,

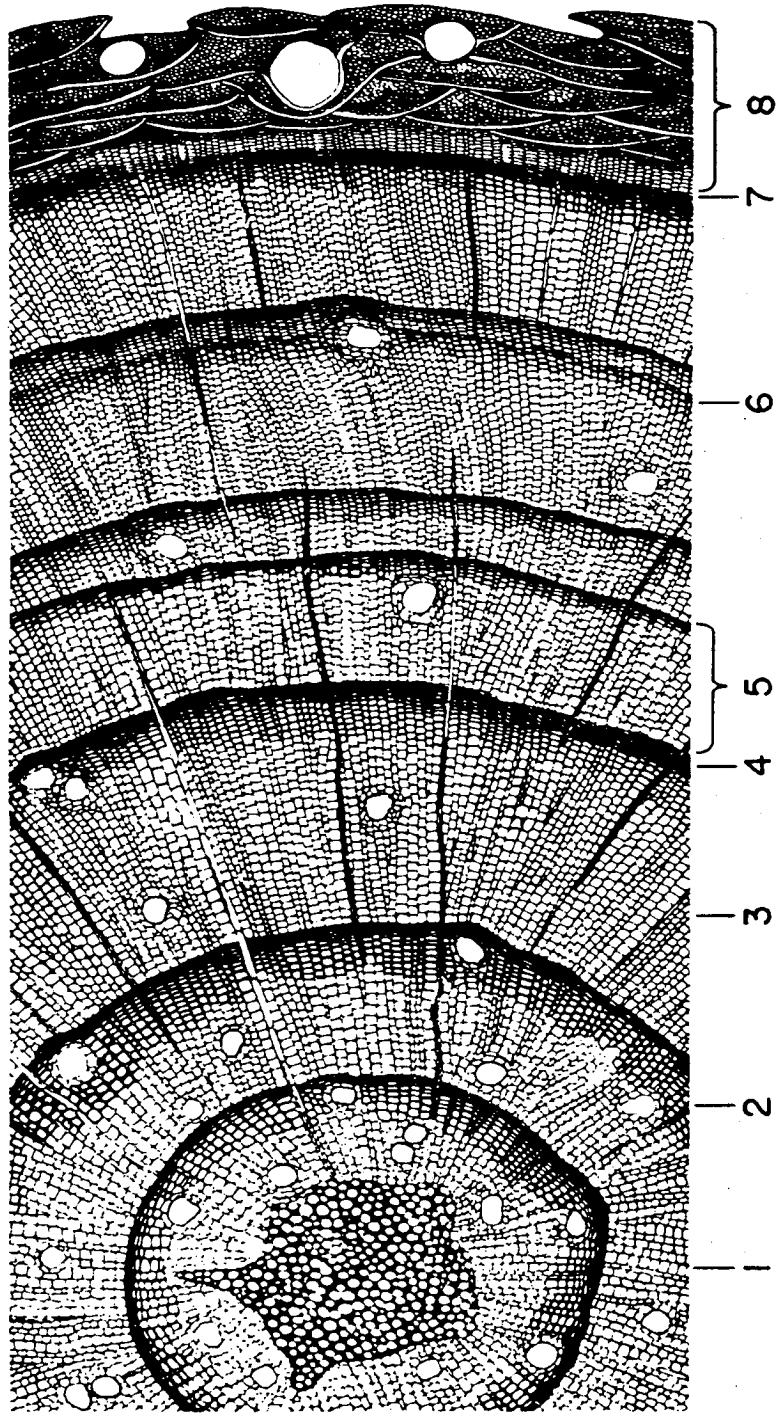

Figure 1.1: **Cross section of a typical conifer showing: 1. pith; 2. resin duct; 3. earlywood cells; 4. latewood cells; 5. annual ring; 6. false intra-annular ring; 7. cambium; 8. bark. Adapted from Ferguson (1970)**

induction of storage protein synthesis in seeds, and embryogenesis. Gibberellins play a role in hyper-elongation of shoots by stimulating cell division and cell elongation, and they also induce seed germination (Raven *et al.* 1992). Shashkin and Fritts (1995) have discussed the importance of growth promoters and inhibitors in determining cambial growth.

For different species in different situations, different external climatic factors will be important. Fritts (1958) found maximum summer temperature to have the highest correlation with radial growth for *Fagus grandifolia*, followed by soil moisture; Kozlowski and Peterson (1962) pointed out that temperature was most important in spring for *Pinus resinosa,* while in summer, when temperatures were less limiting, soil moisture became important; Parker (1976) described tree-ring parameters from sites in Canada as being temperature sensitive. In contrast, Zahner (1963) stressed the importance of late season moisture deficits on latewood formation and Kramer (1964) suggested that the width of the latewood zone would be greater if water stress was not severe. The actual density of the latewood has proven useful in crossdating and climatic reconstruction. McKinnell and Shepherd (1991), Kellomäki (1979), and D'Arrigo *et al.* (1992) have found temperature and density to be correlated, while Parker and Henoch (1971) and Cleaveland (1986) have commented on the correlation of latewood density with precipitation and runoff as well as with temperature. Different limiting factors are the likely cause of these different relationships.

It is well known that temperature has a number of important effects on plant growth. In general terms, each species will have an optimal temperature range. Outside this range a species will not be working at full efficiency. This relationship can be summarised by a temperature response curve (Figure 1.2). Temperature changes affect hormonal action which in turn stimulates seed germination, flower initiation, induction or breaking of dormancy as well as tissue growth (Salisbury and Ross 1992). Low temperatures can inhibit growth through a short growing season coupled with restraints on cell division processes.

The effects of moisture stress in plants of mesic environments have been extensively investigated, particularly in relation to crop yields. Even moderate water stress can produce a profound impact on growth. Cellular growth, photosynthesis, and the activity of enzymes are all affected by water stress

(Henckel 1964, Salisbury and Ross 1992). For some species it is likely that latewood formation, and cessation of growth, are initiated by a lack of moisture (Kramer 1964).

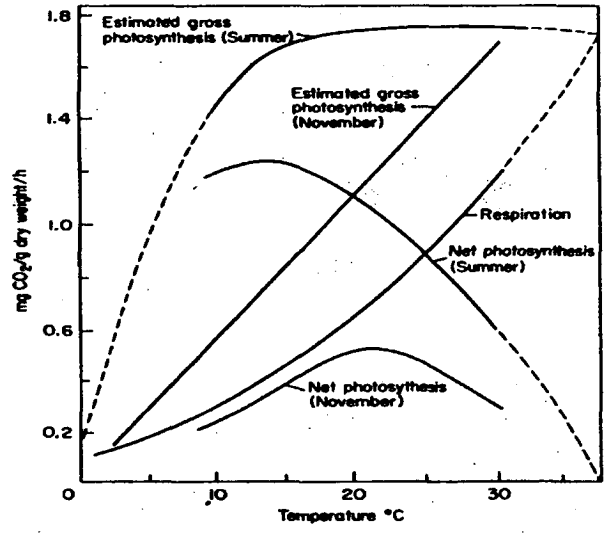

Figure 1.2: **The apparent relationship between temperature and estimated gross photosynthesis, net photosynthesis, and respiration in *Pinus longaeva* during summer and the month of November (Northern Hemisphere). Dashed lines represent extrapolated data, and respiration is assumed to occur at the same relative rates throughout the day and throughout the year. Source: Fritts (1976)**

Stand dynamics are a further group of external factors limiting growth. In an investigation of *Pinus resinosa*, Kozlowski and Peterson (1962) have found dominant and suppressed trees of the same species within a given stand to respond differently to environmental stimuli. Dominant trees grew fastest, and their growth started earlier and finished later than suppressed trees below canopy level, which grew more slowly and more erratically and also had a shorter growing season. In this context, the differences inferred by Zelawski *et al.* (1973) to exist in the photosynthesis of plants dependent on diffuse radiation and those of the same species relying on direct radiation, are important.

Tranquillini (1964) has found elevation to have a number of effects upon plant growth, the most immediately obvious involving the general inverse relationship between temperature and elevation. A high level temperature inversion may, however, result in increasing temperatures at higher elevations.

Buckley (1997) has identified the temperature inversion at approximately 700 m ASL, found to exist in the southwest of Tasmania by Kirkpatrick *et al.* (1996), as a potentially important factor in the differentiation of high and low-mid altitude responses in *Lagarostrobos franklinii* in the west of the State. Other important changes also occur with elevation: as altitude increases, the amount of global radiation received rises; in clear weather, diffuse radiation decreases with elevation, but in overcast conditions the opposite occurs. Additional examples of changes with altitude are decreasing absolute humidity but increasing relative humidity, increased precipitation, and optimal temperatures for photosynthesis being 2–4 ^{0}C lower than at lower elevations (Tranquillini 1964, Read and Busby 1990). In terms of ring widths, LaMarche (1974a) has identified differences between the low frequency components of chronologies at the lower and upper forest borders. In contrast, high frequency variations were in agreement.

Aspect, in combination with slope angle, is a further important consideration which can influence internal growth factors. A site with a northerly aspect in the Southern Hemisphere enjoys solar radiation for a much larger proportion of the day in contrast to one with a southerly aspect. A steeply sloping site with a northerly aspect would be more likely to experience moisture deficits than one on a more gentle south-facing slope.

The distribution of some plants is restricted to specific soil types. In Tasmania, for example, trees such as *Eucryphia lucida* are restricted to the poorest quality soils. Competitive pressure from other species precludes this species from more fertile sites. Other species, such as *Phyllocladus asplenifolius*, although mostly found on very poor soils, are occasionally present on more fertile substrates. This variety of soil types suitable for the species may have implications for factors affecting growth rates on different sites.

1.2.1.1 Basic principles of dendrochronology

Perhaps the best known principle of plant growth is the *principle of limiting factors* which simply states that a process proceeds only as fast as it is allowed by the most limiting factor. This limiting factor may change across the range of a single species. At high elevations, the limiting factor is most likely to

be temperature, while on steep slopes further down moisture may be limiting growth. At other sites, competitive pressures may be limiting growth. For a dendroclimatological study to be most useful for climate reconstruction purposes, growth should be climatically limited.

The *principle of sensitivity* derives from the principle of limiting factors. A sensitive tree-ring series shows a response to year-to-year changes in the variable of interest. A complacent series shows little change from year to year. Site selection is crucial in attaining a sensitive series (Figure 1.3). For an investigation into past temperature fluctuations, sampling is best conducted where

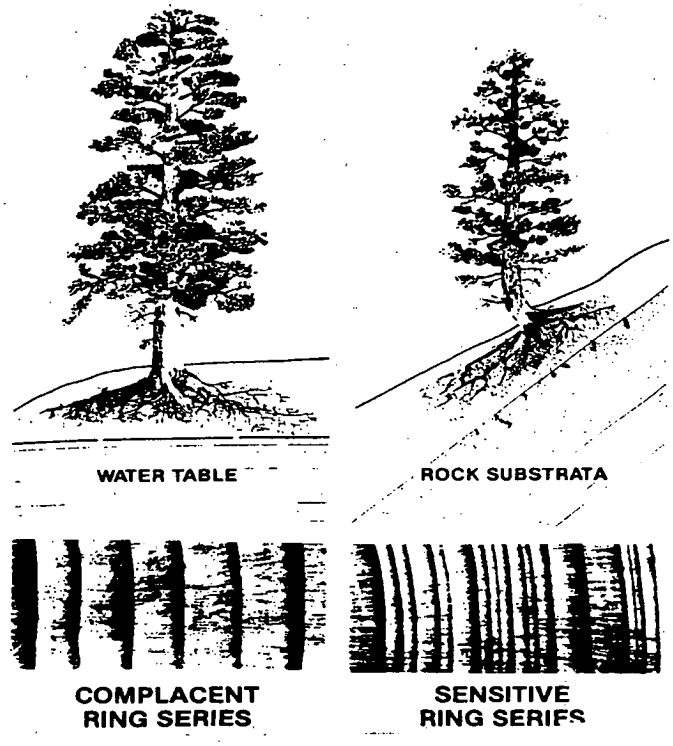

Figure 1.3: **Complacent and sensitive ring series for a moisture sensitive species. A. a site where water is in constant supply; B. a site where water supply is limited. Adapted from Swetnam *et al.* (1985)**

temperature is the most limiting factor to growth, such as sites close to the treeline, or at high latitudes. Investigations into precipitation histories have been most productive in more arid regions.

The key to building long dendrochronological records is the ability to *crossdate*. Crossdating refers to temporal matching of the sequences of narrow and wide rings of one sample with the sequence of another (Figure 1.4). All samples to be used in the development of a chronology from an individual site must crossdate with one another. To be in error by a single year destroys the integrity of a chronology, and any further investigation based on an incorrect

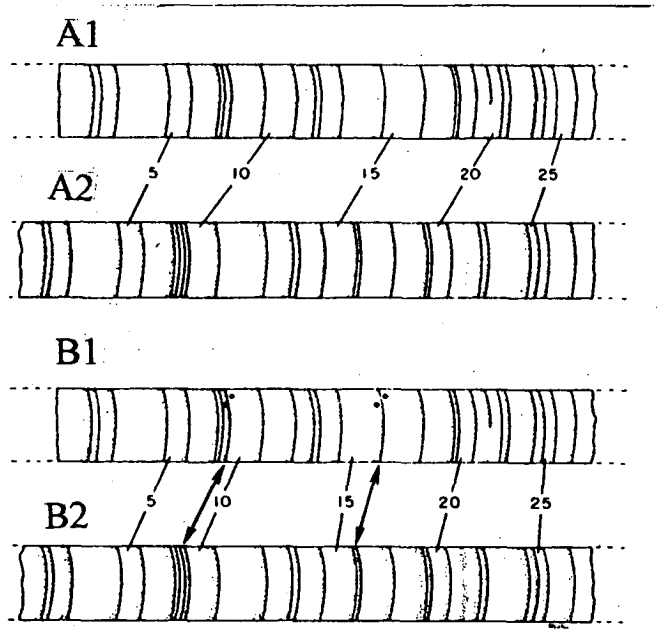

Figure 1.4: **Crossdating of ring sequences makes it possible to recognise where rings are locally absent or where false rings appear. Patterns of wide and narrow rings are compared amongst specimens. In the above diagram, every fifth ring is numbered. Rings in A match until ring 9. Ring 9 occurs as a narrow ring in A2. In B1 positions of inferred absence are marked by two dots, the false ring at ring 21 is recognised, and patterns in all ring widths are synchronously matched. Bold arrows indicate same year rings on B1 and B2. Source: Fritts (1976)**

chronology will be fundamentally flawed. Essentially, the premise of crossdating is that climatic influences are regional and will therefore affect different individuals in a similar manner (Fritts 1976). Crossdating of samples of a species from distant sites demonstrates a regional influence on cambial growth (Douglass 1920). Sites which do not crossdate are subject to more localised controls. Microsite influences cause differences between individuals at the same site and, if more limiting than regional climatic conditions, will prohibit crossdating.

A further important consideration is the principle of *replication.* If replication is inadequate, a large variability in ring width between samples is commonly observed, and can be described in terms of a low signal-to-noise ratio (SNR). The amount of required replication will depend on the site characteristics and the species itself. It must be adequate to counter two types of variability: within-tree variability and between-tree variability. Greatest variability within a tree is observed at its base and least variability is observed at its crown (Schweingruber 1990). To sample at crown level, however, places significant restrictions on series lengths which may be obtained. It is common to sample at breast height in order to get a minimum variability for the maximum period of years possible. Horizontal variability can be caused by wounding, ring wedging, microsite, and species characteristics. Variation between trees in the same stand will depend on site variability and the sensitivity of each individual to these characteristics. Replication must be sufficient to attain crossdating both within and between individuals.

1.2.2 Previous dendroclimatological work in the Tasmanian/New Zealand sector

Much of the previous dendroclimatological research in Tasmania was initiated in the early 1970s as part of a wider project by the Tree Ring Laboratory, Tucson, Arizona. During this project a total of 14 *Phyllocladus asplenifolius*, 4 *Athrotaxis cupressoides*, 2 *Athrotaxis selaginoides*, 2 *Nothofagus cunninghamii*, and 1 *Nothofagus gunnii* chronologies were developed (see LaMarche *et al.* 1979). Of these, the same 11 chronologies (four different species) were used jointly in both a temperature (LaMarche and Pittock 1982) and a streamflow reconstruction (Campbell 1980). A principal component analysis of the sites used by these authors showed that most variance was due to species differences.

The major single species reconstructions from the State so far have come from *Lagarostrobos franklinii* (e.g.Cook *et al.* 1992, Buckley 1997). The longest of these currently extends back continuously to 2100 BC. These reconstructions examine one species, and are thus free of any problems associated with using a number of different species in a single analysis. Such problems include differing response windows and differing responses to the same climate variables.

Buckley's (1997) investigation also isolates a large variation in the response of the species with altitude. This is an important point to note, as it demonstrates that the response of a species to a single climate variable is not uniform across its range.

The high altitude temperature reconstruction from Mt Read reveals particularly cool periods around 300 BC and 1890 AD, and particularly warm periods around 400 BC, 700 AD, and post 1960. The five warmest periods found by Buckley were 1476–1500, 1855–1879, 1965–1989, 1020–1044, 1873–1898; the five coolest periods were 1925–1949, 1345–1369, 1210–1237, 1890–1914. Cook *et al.* (1996a) have found evidence of oscillatory modes of 31, 56, 77 and 200 years in the Mt Read *L. franklinii* reconstruction.

Although of a shorter duration than Tasmanian *Lagarostrobos franklinii* reconstructions, New Zealand chronologies (Stewart Island) based on *Halocarpus biformis* (from 1460s) show increasing cambial growth since 1850, and low cambial growth in the early 1600s (D'Arrigo *et al.* 1995a & b, D'Arrigo *et al.* 1997). Salinger *et al.* (1994) have used five different New Zealand species to reconstruct temperature, Zonal and Meridional Indices, and concluded that the use of a number of species may elucidate more regional phenomena than the use of one species with a limited range.

In New Zealand, Palmer (1989) has found *Phyllocladus trichomanoides* to be sensitive to summer temperatures, although only 30% of the variation in ring widths could be explained by climatic variations. The summer temperature reconstruction was, however, highly correlated with Norton *et al.*'s (1989) temperature reconstruction from *Nothofagus menziesii* and *Nothofagus solandri*. *P. trichomanoides* and *P. glaucus* have been found to provide a conservative record of temperature and, unlike Norton *et al.*'s (1989) reconstruction, do not show the same depressed temperatures around the turn of the century followed by increasing temperatures. Salinger *et al.*'s (1994) reconstruction suggests depressed temperatures just prior to the turn of century, and the same post 1950s warming as D'Arrigo *et al.* (1995a & b) have found. Norton *et al.* did not find this warming but have found evidence of warming post 1970. It is possible that the

inability of the chronology to reflect warming from the 1950s is due to site locations (Norton *et al.* 1989).

Ogden (1982) has commented that differences between the New Zealand *Phyllocladus* spp. and *Nothofagus* spp. are akin to the differences between *Athrotaxis* spp. and *Phyllocladus* spp. chronologies from Tasmania. This observation has been based largely on statistics such as mean sensitivity and autocorrelation characteristics, and in view of this, *Lagarostrobos franklinii* with low mean sensitivity and high first order autocorrelation, is better compared to *Athrotaxis* species (with similar characteristics) than *Phyllocladus* species which have low first order autocorrelation and high mean sensitivity, apparent in the rings of the species as a quasibiennial oscillation in ring width.

1.3 Objectives

Although *Phyllocladus aspleniifolius* has been the subject of previous dendroclimatological work, it has been so in conjunction with other species, and no separation on the basis of species has been made (Campbell 1980, La LaMarche and Pittock 1982). Prior dendrochronological work (e.g. Ogden 1978a, Dunwiddie and LaMarche 1980, Campbell 1980, Bird *et al* 1990) has indicated that the species has high dendroclimatological potential due to its high sensitivity, broad distribution, reasonable longevity, and spatially consistent response to climate.

This study is centred on the climate response of *Phyllocladus aspleniifolius* to those variables mentioned earlier, namely, the air temperature records (both maximum and minimum), Zonal and Meridional Indices and the SOI. Previous work by LaMarche and Pittock (1982) has shown that tree-ring response to precipitation is site dependent and highly erratic, but precipitation has also been included in this study. The individual sites are extraordinarily varied in their community and floristic structure, geology and topography. Therefore, a cursory examination of the ring width variation along a number of 'gradients' is desirable.

The essential purpose of this study is to establish whether or not *Phyllocladus aspleniifolius* has an important role to play in the reconstruction of Tasmanian palaeoclimates. More specifically, the objectives are:

1. To examine the climate response of *P.aspleniifolius* and compare it with the response of New Zealand *Phyllocladus* species, and that of other Tasmanian species.

2. To examine whether or not the climate response of *Phyllocladus aspleniifolius* changes with altitude in a way comparable to *Lagarostrobos franklinii*.

3. To attempt climate reconstruction solely from this species, and identify and analyse any apparent regional differences in Tasmanian palaeoclimates

4. To compare any climatic reconstruction from this species with that of *Lagarostrobos franklinii* in addition to testing the crossdating between the two species.

5. To assess how important various site characteristics are for radial growth.

6. To investigate whether the quasibiennial oscillation apparent in the rings, and commented on by other workers, is a significant climatic signal.

1.4 Outline and structure of thesis

Chapter 2 presents a summary of the physical Tasmanian environment, followed by more specific site descriptions which serve to highlight environmental differences between the sites. Chapter 3 outlines the dendrochronological approach to the species, and presents chronology details and the results of intersite correlations, as well as making an initial comparison with *Lagarostrobos franklinii* chronologies. Relevant climatic data are presented and discussed in Chapter 4. In Chapter 5, the response of *Phyllocladus aspleniifolius* to climate is outlined. The origin of the quasibiennial oscillation in the rings, and its impact upon the climate signal seen in the rings is investigated in Chapter 6. Chapter 7 discusses the issues surrounding climatic reconstruction from this species, and

how these reconstructions compare with those of *L. franklinii*. Chapter 8 presents the conclusions by linking the findings of previous chapters.

Chapter 2 The Physical Environment and Physiology of *Phyllocladus aspleniifolius*

2.1 Introduction

This chapter describes each sampled site in the context of its locality, and presents a broader picture of the Tasmanian environment in which each locality fits. Ecological information about *Phyllocladus aspleniifolius*, as for other Tasmanian rainforest species, is relatively scarce. A summary of the available information about *P. aspleniifolius* is presented, and the rationale of the sampling strategy is discussed.

2.1.1 An overview of the Tasmanian environment

Tasmania is an island of approximately 64,000 square kilometres lying between 40^0 and 44^0 S, and 144^0 and 149^0 E, and situated in what are commonly known as the 'roaring forties' latitudes. Tasmania can be subdivided into two distinct regions by what is often known as 'Tyler's Line' (Sustainable Development Advisory Council 1996). The rugged west coast with complex topographical and geological detail, high rainfall and dense forests contrasts with the tabular mountains and structural basins of the east which support mostly sclerophyll forests and extensive grasslands. Along the east coast, sandy beaches and peninsulas form a series of bays. Contrasts between the two regions are largely due to a combination of geology, climate and geomorphic evolution (Jones 1977). At least four episodes of Quaternary glaciation have been identified (Colhoun and Fitzsimons 1990).

2.1.1.1 Climate

Tasmania is characterised by a temperate maritime climate (Langford 1965). The dominant influence on the climate of the State are the prevailing westerlies. The mountainous west gives way along the Western Tiers to the eastern part of the State which receives substantially less precipitation than the west, due to a rainshadow effect.

Gentilli (1972) described seven major climatic subregions (Figure 2.1) Bassian islands, Northeastern block, Northern slopes, Eastern ridge, Western slopes, Central Plateau, and the Southern block. The Bassian Islands have a maritime and mild climate; the Northern slopes have heavier rainfall and temperatures are more variable; the Northeastern block consists of the cooler and

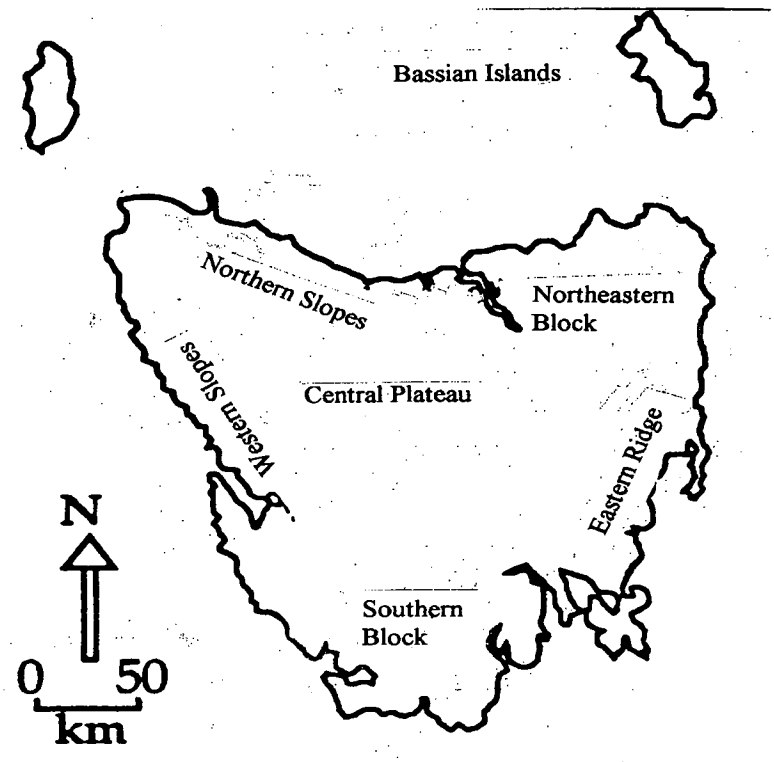

Figure 2.1: **Gentilli's climatic regions of Tasmania: the Bassian islands, the Northeastern Block, the Northern Slopes, Eastern ridge, Western slopes, Central Plateau, and the Southern block**

wetter northeastern highlands and the warmer and drier coastal region. On the Western slopes, winter is the wettest and coldest season while summers are mild; the Central Plateau is the coldest region in winter, and precipitation is particularly high along its western margin; the Eastern ridge experiences more precipitation in autumn and spring, and has a longer dry period than other regions; the Southern block has cooler summers than the Western slopes, but is warmer towards its eastern extent, and short term variability is highest in this region, due to topography (Gentilli 1972).

The movement of the Subtropical High Pressure Belt (STHPB) has a major controlling influence on the seasonal (and longer time scale) climate of the State. It moves southward in the summer months, and frontal systems generally pass to the south of the State. In the winter months, the STHPB migrates north and frontal systems move through the region at lower latitudes, bringing increased rainfall to the west in particular.

Precipitation across the State is extremely variable, ranging from an annual average of over 3600 mm per year at Lake Margaret, to less than 600 mm per year at Oatlands situated in the Midlands area (Figure 2.2). This variation can be ascribed largely to changes in elevation and topography. Heavy precipitation in the west coast region is a result of a combination of frontal and orographic effects. The extent of this precipitation over eastern areas is limited by strength of the airstream, synoptic system intensity and moisture availability (Shepherd 1995). On the west coast the majority of precipitation falls in the winter months, while near the east coast, it is much more evenly distributed, especially at lower elevations. An increase in precipitation is observed at the east coast due to orographic uplift of occasional easterly airflow— this is particularly evident in the Gray – St Marys region (Gentilli 1972). An extensive covering of snow, frost and ice is common in west, southwest and northeast highlands during the winter months. Heavy rainfall on the east coast is commonly associated with variable east coast cyclones (Troup and Clarke 1965) which can produce Statewide rain and overcast conditions for a number of consecutive days.

Temperatures are generally mild throughout the year, but can reach as high as 42 ^{0}C in late summer, and well below freezing in winter at high elevations. Warmer summers are generally experienced in the east, except the northeastern highlands which are subject to cooler summers, comparable to those of other alpine areas in the State (Figure 2.3a & b). Average maximum temperatures show a strong elevational gradient for January, but are less pronounced for July (Figures 2.3a & b). Minimum temperatures also show this pattern for both months, but again, the pattern is weaker in July.

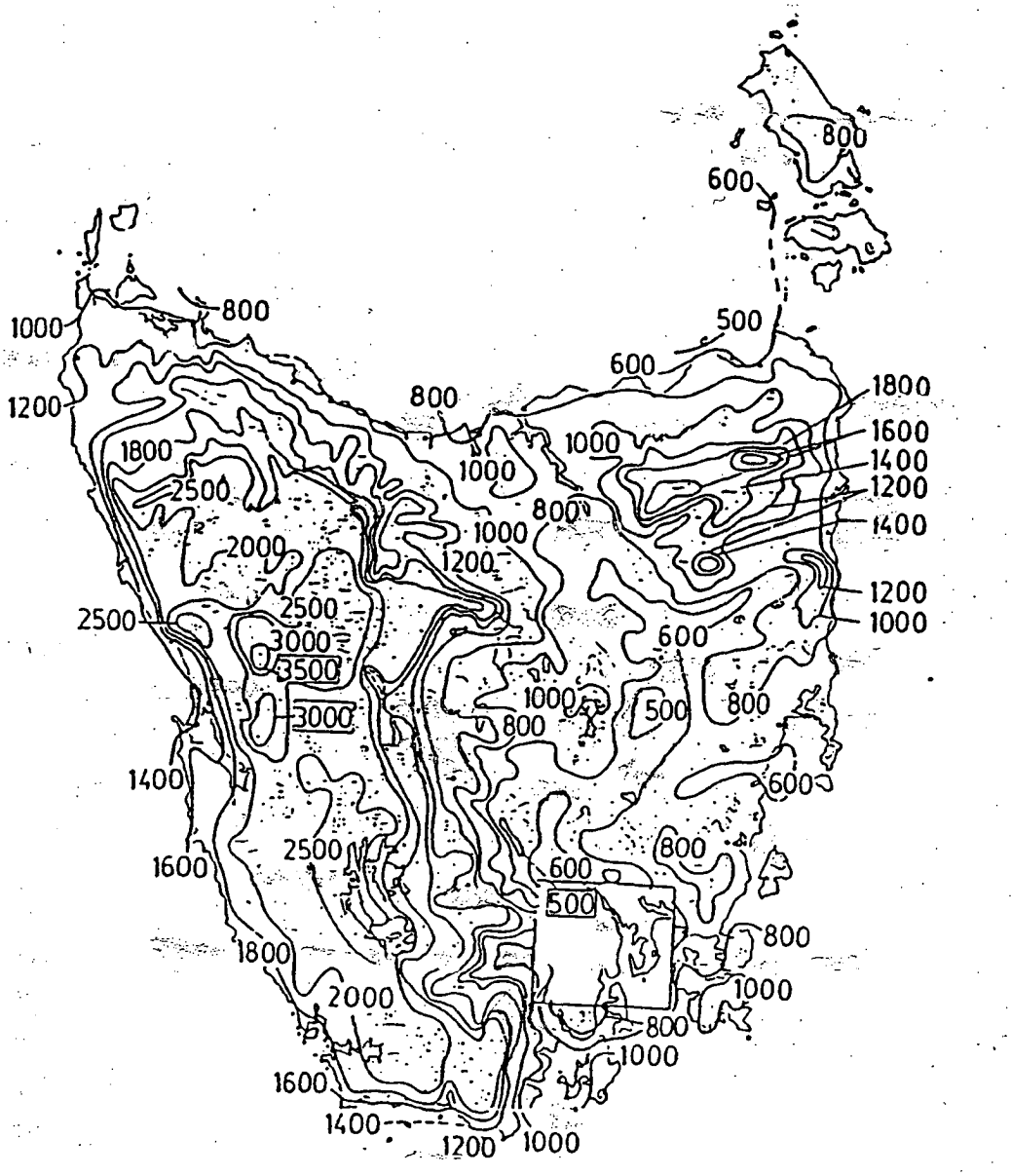

Figure 2.2: **Average annual precipitation (mm) across Tasmania. Source: Barker (1993)**

2.1.1.2 Vegetation

A wide diversity of habitat exists in the State (Jackson 1965). Two basic vegetation types are observed: one with a closer affinity to New Zealand and South America, the 'Gondwanan element' (Cullen 1991) which dominates the west coast region, and the other of eastern Tasmania which bears a closer affinity with the 'Australian element.' Approximately 1600 species of vascular plant

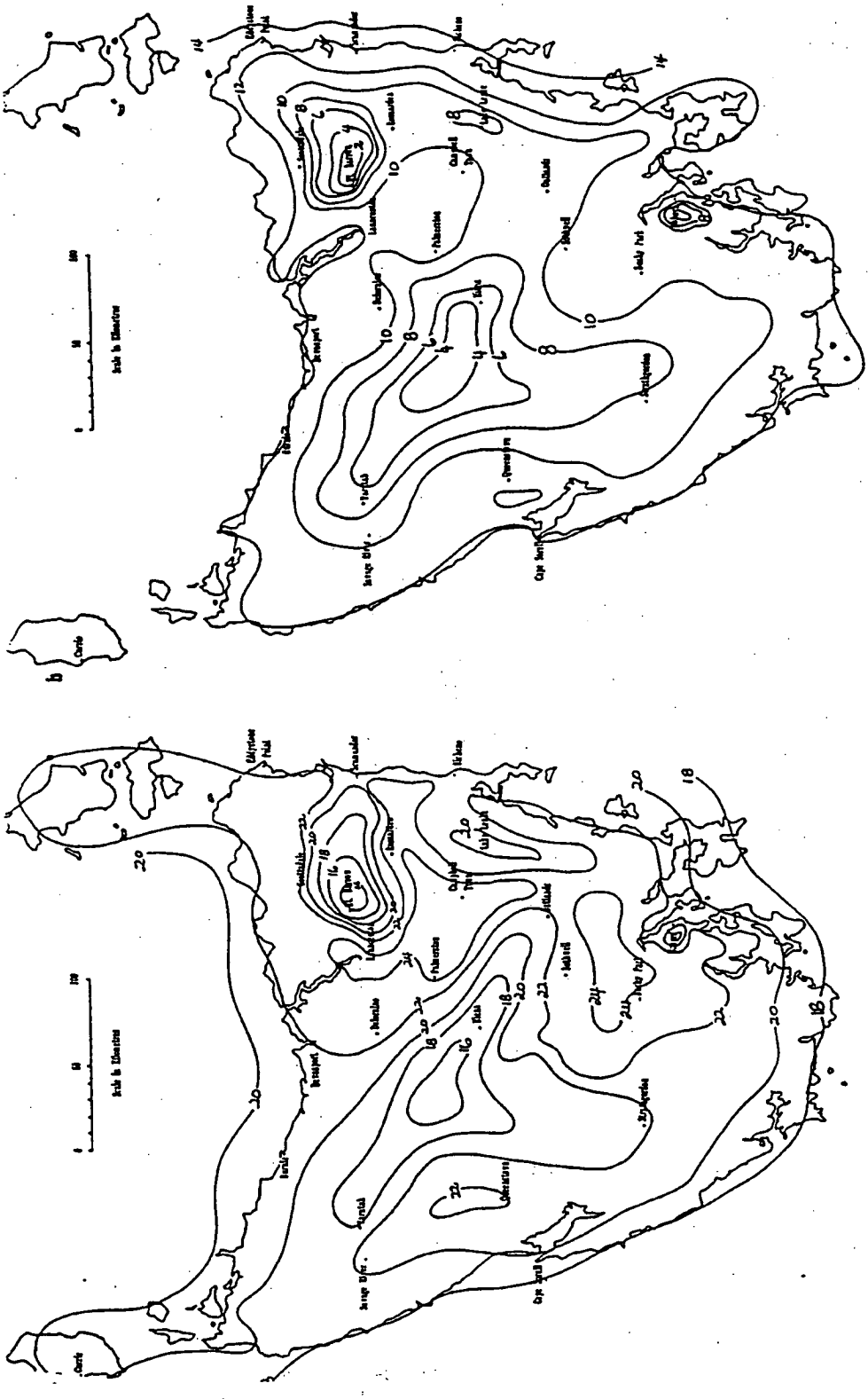

Figure 2.3a: **Average maximum and minimum January temperatures (°C). Source: Barker (1993)**

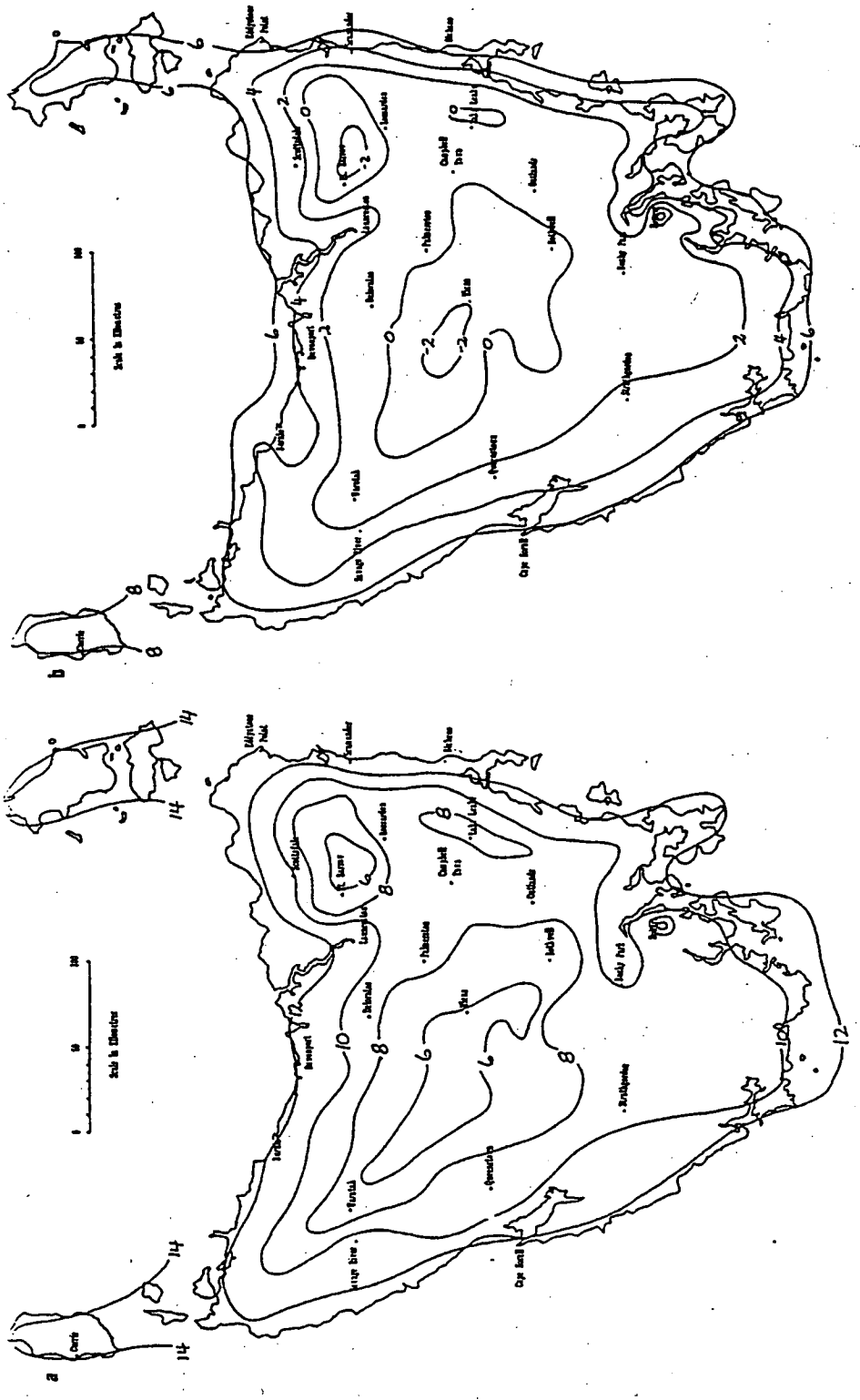

Figure 2.3b: Average maximum and minimum July temperatures (°C). Source: Barker (1993)

species are native to Tasmania, and 20% of these are endemic (Duncan 1991). The proportion of endemic species increases from north to south, and varies with geological substrate.

Kirkpatrick (1991) separated vegetation into seven zones. Cool temperate rainforest is representative of the 'Gondwanan element' of the vegetation. Wet forests are dominated by sclerophyllous species which mostly require fire for successful regeneration (Gilbert 1959, Wells 1991); dry schlerophyll forests represent the 'Australian element' of the vegetation, and exist in areas receiving less than 1000 mm precipitation per year (Williams 1991). Buttongrass moorlands are described as treeless vegetation dominated by graminoids with the frequent occurrence of woody shrub species (Balmer 1991). Grassy vegetation includes only those species in the Poacaea family (Kirkpatrick 1991); wetlands are defined as vegetated or temporarily unvegetated areas covered by water less than 4 m deep for several months of the year. (Harwood 1991). Coastal vegetation is adapted to salt spray and dessicating winds (Harris 1991).

The role of fire in the Tasmanian landscape is crucial in the determination of vegetation type and has been responsible, in combination with climatic change, for changing relative distributions of the Gondwanan and the more fire-tolerant Australian elements. Where fire has been absent for thousands of years, temperate rainforest flourishes (Cullen 1987) and may contain the fire-intolerant conifer species *Lagarostobos franklinii, Athrotaxis selaginoides,* and *Athrotaxis cupressoides*. A frequently fired landscape becomes dominated by heathy sedgelands (Kirkpatrick 1977). Fire-tolerant *Eucalyptus* species can also be found in fire-maintained habitat. Marginal rainforest patches on the east coast are assumed to be remnants from times when the climate was more suitable for its survival (Neyland and Brown 1993).

Fossil evidence suggests that the Gondwanan element of the vegetation has been present for at least 40 million years and has undergone very little evolutionary change. In addition, a much wider occurrence of this element in the past is suggested by the fossil evidence (MacPhail 1980, Hill 1990a).

2.1.1.3 Geology and soils

Tasmania's geology is complex. The oldest rocks are Precambrian, predominantly siliceous meta-sediments and form a north–south belt from the Forth River area in the north of the State to Port Davey in the south (Scanlon 1984). Jurassic dolerites dominate the central portion of the State, extending towards the east coast. In the northeast, Devonian granite batholiths intrude the mainly Palaeozoic Mathinna beds which are composed primarily of sandstone and coarse siltstone (Burrett and Martin 1989). These granite batholiths dominate the geological terrain of the northeast and are an important source of mineralisation in the northeast of the State (Groves *et al.* 1977). The northeastern area is topographically isolated by the Tamar tectonic basin. Along the northwest coast of the State, Tertiary basalts are widespread and locally extend into the eastern region.

The predominant groups of Tasmanian soils are the podzols and podzolics that have been developed on siliceous sediments, meta-sediments and felsic igneous rocks. They contrast with the more fertile black and brown earths of the Midlands and southeastern regions which have been developed on substrates of mafic igneous rocks such as dolerite and basalt and have a high degree of silt and clay. Most soils are acidic and strongly leached, and the organic matter content increases with increasing moisture availability and increasing altitude (Nicholls and Dimmock 1965). In the northwest of the State, and small parts of the northeast, rich red krasnozems, developed on basalt, are seen. Skeletal soils, typical of steep slopes, derived from siliceous parent material occur widely throughout the southwest of the State.

2.1.2 *Phyllocladus aspleniifolius*

Phyllocladus aspleniifolius (Labill.) Hook.f. (Podocarpaceae) is a dioecious gymnosperm with a wide ecological and geographical distribution in Tasmania. It is classified as a dominant of cool temperate rainforest in the State, along with *Nothofagus cunnninghamii, Eucryphia lucida, Atherosperma moschatum, Athrotaxis selaginoides, Athrotaxis cupressoides, Lagarostrobos*

franklinii and *Diselma archerii* (Jarman and Brown 1983). The presence of the genus *Phyllocladus* in southeastern Australia extends back at least as far as the Late Eocene, and evidence suggests that the genus was present throughout Tertiary times (Hill 1990a). The timing of the extinction of the genus in Victoria is uncertain (MacPhail 1981, Hill 1990a). Samples of *P. arberensis* dating back to Late Eocene times have been found in Tasmania (Hill 1990b). The only *Phyllocladus* species now remaining in Australia is the Tasmanian endemic *P. aspleniifolius* which has living relatives in New Zealand (*P. alpinus, P. trichomanoides, P. glaucus*) and Malesia (*P. hypophyllus*) (Whitmore 1981). The leaf structure of the species has not changed since Tertiary times (Hill 1990a).

From about 13,000 yBP to 9000 yBP, *Phyllocladus aspleniifolius* became increasingly dominant in the rainforest landscape of the west coast (Colhoun and Van De Geer 1986, Colhoun *et al.* 1991, Colhoun *et al.* 1992), pointing to opportunistic behaviour of species such as *Phyllocladus*. A rapid Early Holocene expansion of the moderately cold–sensitive and widely dispersed *Phyllocladus* saw an association with *Eucalyptus* spp. which lasted for 1500–2000 years (2–3 forest generations). By 9000 yBP the same niche had been captured by *Nothofagus cunninghamii*, resulting in competition and the formation of different associations, the structure and composition of which have been further modified by site quality (MacPhail 1981). The 'rise' of the species in the Mid–Late Holocene saw its association with *Dicksonia* and *Lagarostrobos* on fertile soils, and with *Eucryphia* and *Anodopetalum* on infertile soils. The Early Holocene sequence of *Eucalyptus – Eucalyptus / P.aspleniifolius – N. cunninghamii* reversed in the Late Holocene (MacPhail 1980) as climate in southeastern Tasmania since the Mid–Holocene became increasingly drought and frost prone.

Today, *Phyllocladus aspleniifolius* is not only extensively distributed on the west coast and in the central highlands but is also found in rainforest or wet forest pockets on the east coast (Figure 2.4). Neyland (1990) suggested that specific topographic occurrences on the Tasmanian east coast may be due to cloud being trapped in these valleys in summer which would increase the effective precipitation of these sites.

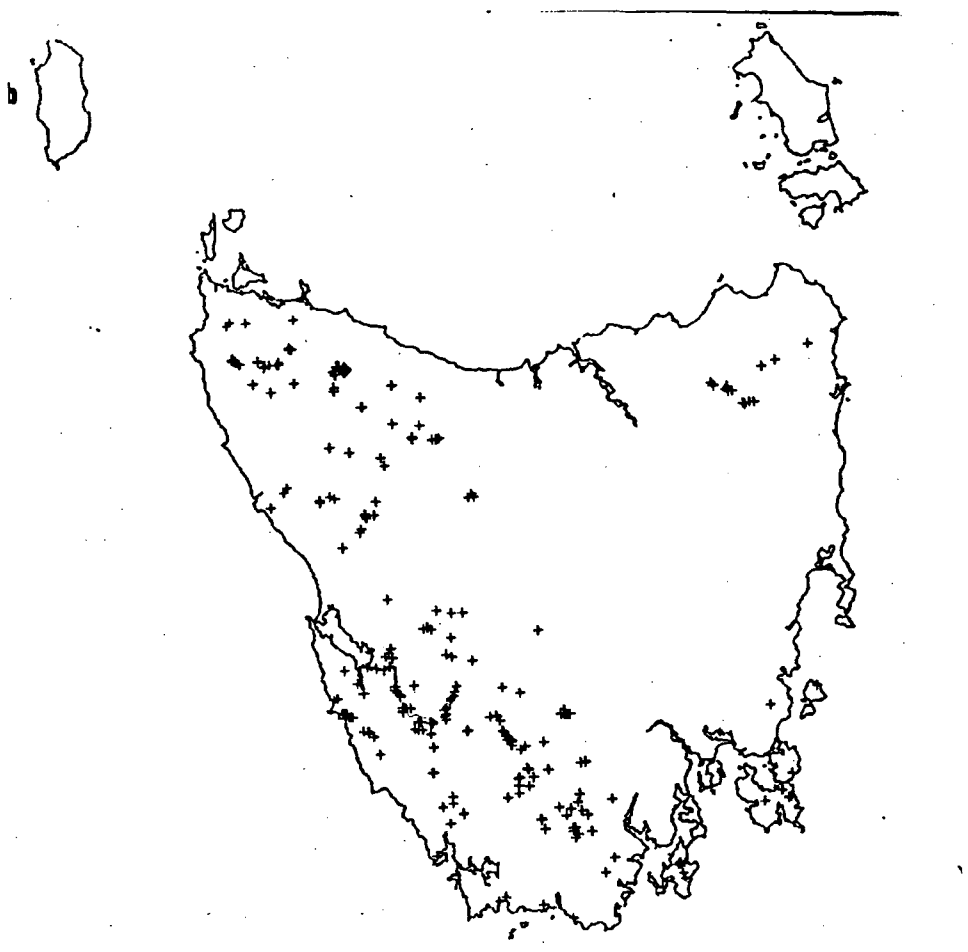

Figure 2.4: **Present day distribution of *Phyllocladus aspleniifolius*. Sites extracted from the TASFORHAB data base. Some known sites are not shown in the Figure — for example a site above 1000 m ASL exists at the northern end of Great Lake in the central highlands. Source: Barker (1993)**

Altitudinally, the range of *Phyllocladus aspleniifolius* extends from sea level to around 1050 m ASL, the optimal range being defined as 400–800 m ASL (Figure 2.5). Most individuals can be found at sites with an annual precipitation of about 900–2500 mm. Figure 2.6 shows the climatic envelope in which *P. aspleniifolius* is found. Barker (1993) found that precipitation was more important than temperature in explaining the distribution of the species.

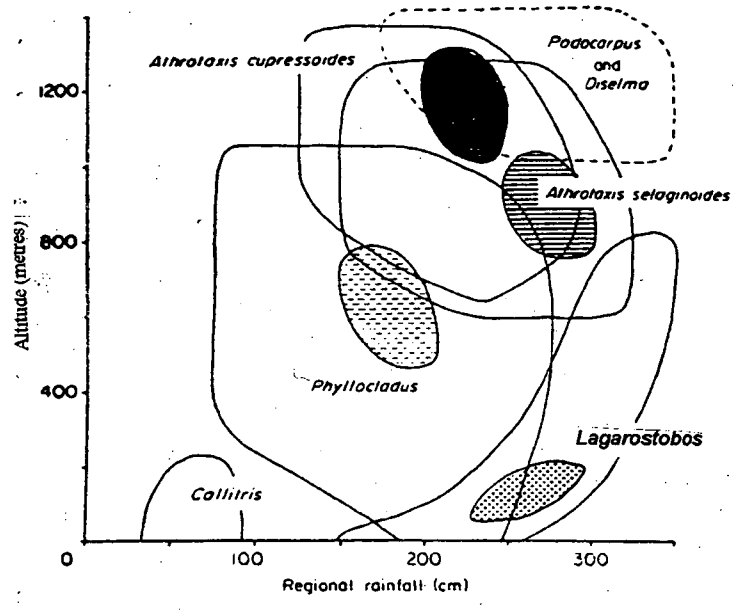

Figure 2.5: **Altitudinal distributions of some Tasmanian conifers in areas of different regional precipitation. The shaded area in each species distribution (except *Callitris*) represent those areas of the altitude/precipitation gradients in which the species, where present, usually forms a significant proportion of the forest biomass, i.e. the 'optimum' conditions for the species. The ranges of *Phyllocladus aspleniifolius* and *Lagarostrobos franklinii* overlap at low elevations and moderate to heavy precipitation. Note that areas where each species is noted to form a significant proportion of the forest canopy do not overlap. Adapted from Ogden (1978a)**

2.1.2.1 Habitat

It is probable that, although widely distributed, the occurrence of *Phyllocladus aspleniifolius* is restricted predominantly by climate. The species has been shown to be insensitive to soil fertility, nutrient level and pH (Barker 1993). This insensitivity partly explains its versatility. However, these factors are still important influences on its growth. On richer soils, such as those derived from basalt, nutrient uptake and metabolism are more efficient (Barker 1993), and growth more rapid.

Although found on both fertile and infertile soils, as well as in a range of community types, *Phyllocladus aspleniifolius* is more commonly found on infertile soils which support 'implicate' rainforest assemblages. Implicate rainforest forests are defined as being relatively species rich by Tasmanian standards, have low broken canopies and incomplete dominance (Cullen 1987).

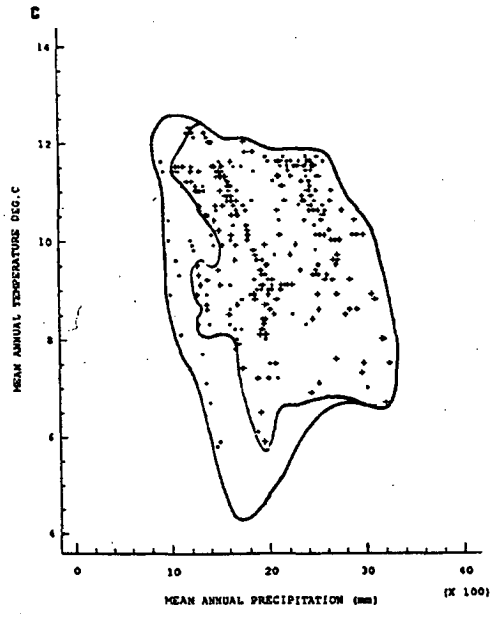

Figure 2.6: **The climatic envelope of *Nothofagus spp.* (outer) with the distribution of *P aspleniifolius* (inner) overlaid. Adapted from Barker (1993)**

'Callidendrous' forests, by contrast, conform to the popular idea of cool temperate rainforest (Jarman *et al.* 1984) and occupy more fertile sites, have closed canopies, open understories and are usually dominated by *Nothofagus cunninghamii*. 'Thamnic' rainforest is intermediate between callidendrous and implicate rainforest, and generally contains a well developed shrub layer in the understorey (Jarman *et al.* 1984). On less fertile and poorer quality implicate rainforest sites, *P. aspleniifolius* is observed in all strata (Barker 1993). It is likely that the low growth rate of *N. cunninghamii* on these sites is an important factor in the commonly observed domination of these sites by *P. aspleniifolius* and *Eucryphia lucida*. On these low nutrient sites, the growth rate of *P. aspleniifolius* exceeds that of other species, allowing it a significant advantage (Read 1995). On the more fertile callidendrous sites, the competitive pressure of the faster growing *N. cunninghamii* excludes, to a large degree, slower growing species such as *P. aspleniifolius* at low to mid–altitudes (Read 1995).

Further explanation of the success of *Phyllocladus aspleniifolius* on infertile sites may relate to the presence of root nodules with mycorrhizal associations that allow an increased uptake of phosphorous. This enables growth enhancement of *P. aspleniifolius* by up to seven times that of plants without the

mycorrhizal association (Barker 1993). Nelson (1964) found a ten-fold increase in photosynthate translocation in plants with mychorrhizal associations.

Phyllocladus aspleniifolius is also observed in wet mixed forest communities (Gilbert 1959, Kirkpatrick *et al.* 1988) that are likely to be fire–maintained disclimaxes (Barker and Kirkpatrick 1994). Where *P. aspleniifolius* is present at these sites, it is present only as mature individuals, and regeneration is not commonly observed, except in forest gaps. By contrast, regeneration in implicate rainforest is continuous (Barker 1993).

Where *Phyllocladus aspleniifolius* islands occur on hilltops, the site is often bereft of other rainforest species (Barker and Kirkpatrick 1994). Little Mount Michael, at Blue Tier in northeastern Tasmania, is a prominent example.

2.1.2.2 Ecophysiology

Phyllocladus aspleniifolius is light demanding, and the optimum growing environment for the species is probably under good light levels. Despite this, the species has been found intolerant to high light and high temperature environments (Read 1985, Barker 1993).

The adult photosynthetic organs of *Phyllocladus aspleniifolius* are not leaves, but flattened branch structures; in this characteristic it is unique amongst the podocarps. In addition, the 'leaf' morphology of the species shows a relatively high variability for a conifer (Brodribb 1996). Optimum temperature for photosynthesis of *P. aspleniifolius* has been found to be 15 ^{0}C in trees acclimated to 8 ^{0}C, 19 ^{0}C in trees acclimated to 20 ^{0}C, and 20 ^{0}C in trees acclimated to 30 ^{0}C (Read and Busby 1990). Little photosynthesis occurs at temperatures below approximately 8 ^{0}C. The infrequency of *P. aspleniifolius* specimens at higher altitudes (above 800 m ASL) is consistent with this observation (Read and Busby 1990). Bird *et al.* (1990) expected subcanopy trees to be more responsive to light fluctuations than trees in the canopy, and this expectation was confirmed by Read (1985) and Barker (1993) who both suggested that diffuse radiation may be more important for the growth of *P. aspleniifolius* than direct radiation. Photosynthesis is greater in forest gap trees than in canopy trees when photosynthetically active radiation (400–700 nm) is low; this being due to a reduction in the rate of stomatal

conductance in the canopy level trees (Read 1985, Barker 1993). Although this implies the importance of diffuse radiation, other environmental factors are important in photosynthesis (Barker 1993).

Foliage is not particularly frost resistant (Read and Hill 1988), and may be particularly vulnerable in years when bud-break is delayed and frost hardening does not occur until very late. The timing of leaf expansion of *Phyllocladus aspleniifolius* is generally later than that for other species, and the species also has a relatively long foliar development period (Barker 1993). Greatest frost hardening occurs at higher altitudes. Minimum and maximum frost hardening of foliage has been reported at -5.5 and -14.1 ^{0}C, respectively, for *P. aspleniifolius* at 980 m ASL, and -3.8 and -11.1 ^{0}C for specimens at 700 m ASL. Two New Zealand species of the genus, *P. trichomanoides* and *P. aplinus* display a similar frost resistance to low elevation members of the Tasmanian species (Sakai *et al.* 1981).

Foliage development, onset of female and male strobili, budswell and pollen release are all affected by altitude (Barker 1995). At higher altitudes, foliage development occurs over a longer time period. The slow development of foliage may also mean that the current year's foliage is photosynthetically inefficient until late summer the following year (Barker 1993). Abscission of leaves between 4 and 12 years old has been observed by Barker (1995). The oldest of these leaves occupied full sunlight positions in the canopy. Currently, there is little known about leaf efficiency of the species and the effect of aging on the leaf efficiency.

2.1.2.3 Establishment and regeneration

Establishment of young seedlings in forests depends on a number of factors. *Phyllocladus aspleniifolius* is sensitive to fire but is usually the first rainforest species to recolonise a site after fire (Kirkpatrick 1977). Establishment after fire is dependent on soil-stored seed and bird dispersal. This bird dispersal of seed, as well as the ecological amplitude of the species, may help explain its broad geographic range. Although disturbance is important to the establishment of *P. aspleniifolius* (personal observation), endogenous, non–catastrophic disturbances

are sufficient to maintain populations. Sexual reproduction is usual in the species, with only very rare instances of vegetative regeneration observed (Barker 1995).

Male and female primordia of *Phyllocladus aspleniifolius* form in the previous season (Tomlinson *et al.* 1989). This prior season development of primordia may represent an attempt to remain reproductively active for as long as possible, or may act to ensure the completion of the reproductive cycle in the short growth season (Mark 1970). Female cone development generally begins 1–2 weeks before pollen release over a 5–6 week period (Barker 1993). Little year-to-year phenological variation in development has been observed, and this in itself may be due to the short duration of the growing season in addition to the relatively long time required for foliar development (Barker 1993). A period of seed dormancy is required before germination occurs (Read 1985, Barker 1993), new seedlings reflecting seed germination from two seasons prior. The variation in seed production from year to year may result in a number of suitable habitats not being utilised in years of low seed production.

Gap and elevated microsites are preferred by *Phyllocladus aspleniifolius* seedlings for establishment. Gap environments, created by endogenous events such as tree fall, allow increased light availability at the forest floor, while elevated microsites may afford some protection against foraging. However, survivability at these sites is significantly less than for seedlings establishing on mossy logs, stump mounds and moss. The reasons for this may be related to competition from other regenerating species in gaps and, for those seedlings establishing on buttresses, the effect of reduced light availability (Barker and Kirkpatrick 1994). The seedling establishment of *P. trichomanoides* in New Zealand is known to be dependent on full daylight conditions (Bieleski 1959). For the spring germination, however, low light intensity was found to be sufficient.

Size class distributions (Barker and Kirkpatrick 1994) show that few very large individuals of *Phyllocladus aspleniifolius* exist despite high levels of recruitment to the early phases of growth, indicating a high natural attrition rate, of up to 90% (Barker 1993).

2.1.2.4 Climatic correlates for annual growth

Previous work examining the climatic response of *Phyllocladus aspleniifolius* is not unanimous in its opinion as to which climatic variables are the most important. The early study of Ogden (1977) suggested a positive response of *P. aspleniifolius* to early summer precipitation and a negative response to higher than average summer temperatures. Ogden (1982), although repeating the above information, recommended caution until more detailed work was undertaken. In a later study, however, Read and Busby (1990) also concluded growth was sensitive to summer precipitation and high temperatures. These conclusions were based on photosynthetic responses and information derived from the BIOCLIM database.

However, other investigations have shown that the correlation of ring widths with the prior season's conditions is dominant. Campbell (1980) found a negative response to the prior season's maximum temperature associated with a positive response to precipitation of the same season. Likewise, LaMarche and Pittock (1982) demonstrated a predominantly negative response to temperature of the prior season. Temperature was found to be the most important factor, and this is in accordance with the idea that temperature is more likely to be a limiting factor in a mesic forest environment than precipitation (LaMarche and Pittock 1982, Ogden 1982, Bird *et al.* 1990). A positive response to winter temperatures, and a negative response to dormant season precipitation, has been found by both these groups of workers (and also for New Zealand species of *Phyllocladus*). The response to precipitation was found to be inconsistent amongst sites (LaMarche and Pittock 1982), and is most probably a partial reflection of the complexity of the Tasmanian topography.

2.1.2.5 Biennial fruiting cycle and mast seedings

A further complication in working with *Phyllocladus aspleniifolius* is the visually and statistically apparent quasibiennial oscillation in ring widths. This oscillation is not, however, evident to the same degree in all specimens. To date, it has been accepted generally that this bienniality in the ring widths of this species, and other species in New Zealand, is predominantly a biological

expression of the species which does not reflect climatological information (Ogden 1982, Francey *et al.* 1984), although Dunwiddie (1982) briefly mused on the possibility that it contained a climatic signal.

One biologically based explanation relates to the observed oscillation in quantity of produced seed (Read 1989, Barker 1993, 1995). This oscillation may not be synchronous between sites (Barker 1995), indicating the likelihood of a predominantly biological cause.

Mast seeding for *Phyllocladus aspleniifolius* is known to have occurred in 1982 and 1989 (Barker 1995). In both cases, the current and previous summers were warm and dry, suggesting that a climatic stimulus is important for mast seeding events. By implication, this intimates the importance of climate in biennially oscillating seed production. It is plausible that geographic variability in climate is responsible for the oscillation not being synchronous between sites (Barker 1993).

2.2 Site selection

Sites are clustered into four regions: East, Mersey, West and Southwest. Figure 2.7 shows the location of selected tree ring sites.

At the time of initial project planning, the goal was a more rigorous approach to streamflow reconstruction than had previously been attempted for Tasmania. It was also the intention to examine the possible zonality of any climatically related changes. Therefore, both an east–west transect, and a north–south transect of catchments containing *Phyllocladus aspleniifolius* and with relatively long streamflow records, were constructed. The rivers were: the Hellyer in the west, the Mersey, the South Esk in the East, and the Florentine in the Southwest. Within each of these catchments a number of tree ring sites were selected, the number depending on the availability of sites. Three sites from each catchment were deemed as a minimum requirement for each region. Suitable sites in the headwaters of the rivers were limited, meaning that generally, only three sites in a catchment were sampled. The exception to this was the Mersey Valley where more sites, although of a younger age, were available.

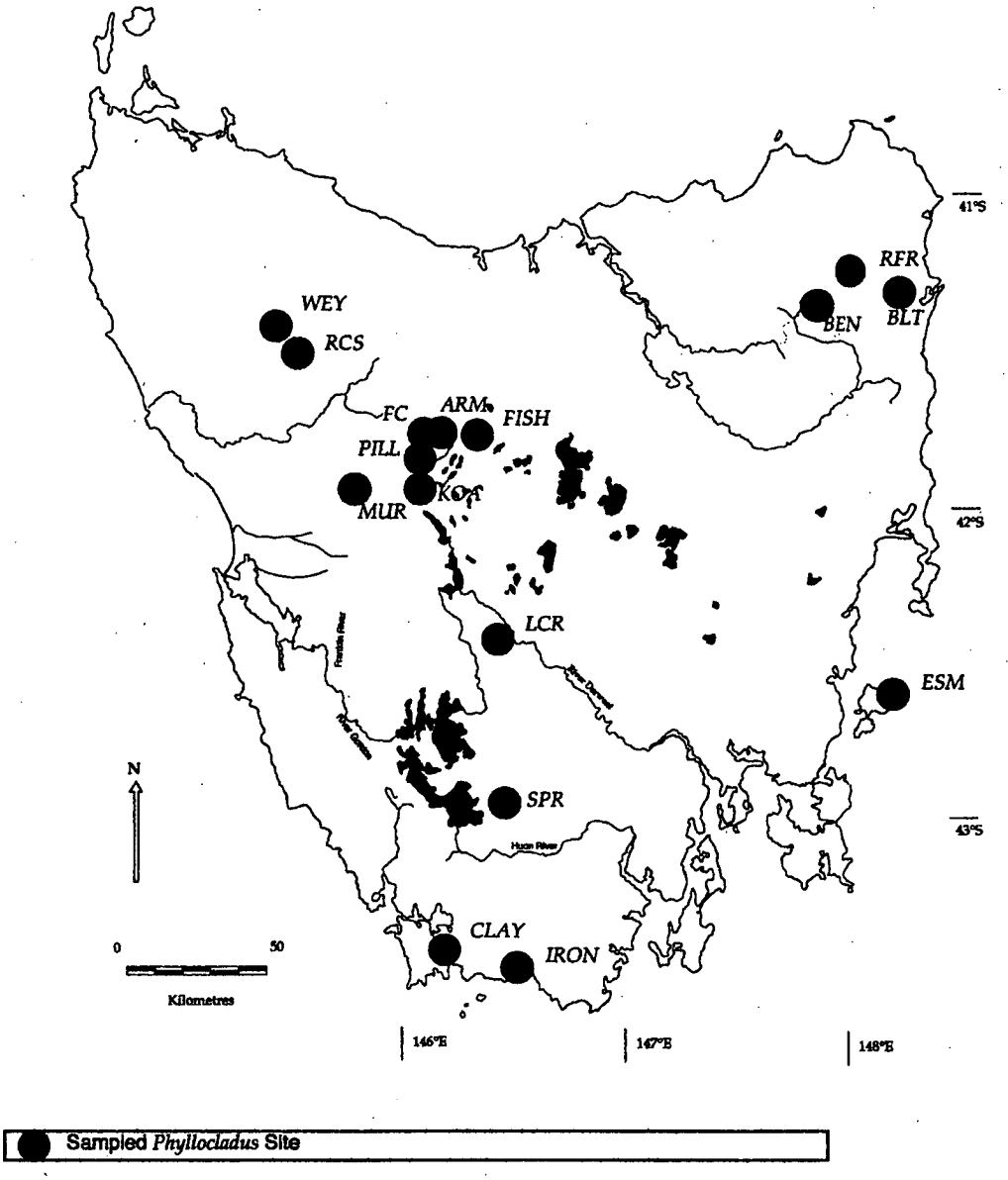

Figure 2.7: **Location of *Phyllocladus aspleniifolius* sampling sites**

Early response function analysis (Chapter 5) of sampled sites suggested a much more consistent, and generally stronger, response to maximum and minimum temperatures than to precipitation, and hence streamflow. Although several of the sites existed at relatively high altitudes (east coast), and apparently close to their upper elevational limits in an area (southwest), a number of additional sites were sampled outside the catchment areas to augment the existing data set. Two of these sites were in the temperature limited southwestern area of

the State, and another towards the upper limit of the species' distribution in a thamnic/implicate rainforest environment on the west coast. A fourth additional site on an island in close proximity to the east coast, sampled as part of an unrelated study, has also been included for comparison purposes.

The change of emphasis meant that some of the sites previously sampled would not be optimal for inclusion in a temperature reconstruction. These sites have been included however, in the discussion of response function analysis. They have not been used for attempted climate reconstructions.

Because *Phyllocladus aspleniifolius* is an extraordinarily versatile species for a rainforest dominant (Barker 1995), some examination of varied topographical, altitudinal, geological and floristic situations at tree–ring sampling sites is desirable. This wealth of information could yield important clues as to relationships between radial growth and site characteristics. To this end, data collected in the field included:

- slope
- aspect
- a brief topographical description
- main species present (nomenclature follows Buchanan (1995))
- rainforest type
- geology
- site drainage characteristics
- the direction from which each core was taken
- soil pH - one soil sample was taken from the A1 horizon at each site, and its pH was assessed by use of a Hannah^{TM} pH meter. A 5:1 mixture of distilled water and soil from the site was tested.
- a very subjective estimate of current 'light conditions' for the canopy of each specimen

2.3 Site descriptions

Each site name includes a one letter subscript suffix denoting the region in which it is located. These are: E for East, M for Mersey, W for West and S for Southwest.

2.3.1 The East

The northeastern highlands are the only area on the east coast containing sufficiently extensive stands of *P. aspleniifolius* to enable selection of a number of sites. Two sites were sampled in the Mt. Victoria area (RFR_E and BEN_E), with a third, just east of the catchment area (BLT_E) being added at a later date. The three northeastern sites lie to the north and east of the Ben Lomond massif ($41^0$15'–$41^0$30' S) and, as a group, are at the highest sampled elevation. All three sites are dominated by *Nothofagus cunninghamii* and have a W/NW or N/NW aspect (see Table 2.1). The fourth east site, on Maria Island, differs from these three sites in a number of important ways, and was not originally intended to be part of this study.

BLT_E

BLT_E is situated on the plateau of Blue Tier, close to Poimena, an abandoned tin mining settlement. Despite tin mining activities in the immediate area, the sampled 'subsites', close enough to one another to be called a single site, appear relatively undisturbed. One subsite was an exception, in that it has previously experienced a relatively high degree of disturbance. Blue Tier has been sampled previously by LaMarche *et al.* in the mid to late 1970s, and samples obtained in this study are used both to update and add to the chronology developed in the late 1970s (see LaMarche *et al.* 1979). All samples taken from the most disturbed area have been obtained by previous workers.

The crowns of most sampled trees are visible above the general canopy layer and others were at canopy level, indicating a greater reliance on direct rather than diffuse radiation (Figure 2.8). One subsite, with a number of younger trees, has crowns at or below the canopy layer, implying a greater reliance on diffuse radiation. A further subsite dominates the summit of Little Mount Michael. Numerous small drainage lines which eventually flow into the George River are evident in all three subsites.

The forest dominants are *Nothofagus cunninghamii, Phyllocladus aspleniifolius* and *Eucryphia lucida* with an understorey consisting of *Blechnum wattsii, Gahnia grandis,* and *Tasmannia lanceolata.* At the disturbed edge of the forest, invading species include *Leptospermum nitidum, Olearia algida* and

Juncus sp. The forest type grades from thamnic to callidendrous. In a number of cases, a broken canopy layer due to tree fall was apparent, allowing a greater amount of light into the stand. Devonian granite underlies the region (McClenaghan and Williams 1982).

RFR_E

Ralph's Falls Road (RFR_E) lies on the northern flank of Mt. Victoria, to the west of BLT_E. In the 1970s, a road partly built in the 1920s and '30s, was continued through the site to St Columba Falls and has only recently been completed. The construction has led to some significant disturbance close to the road where many felled trees were sampled. In addition, many living trees not far from the road may have been affected by the increased light availability (Figure 2.9). Interbedded sandstone, siltstone and mudstone, which are part of the Mathinna Beds (N. Allen, University of Tasmania, pers. comm.), underlie this site and drainage lines flow through to the steep north–facing cliffs giving rise to Cash's and Ralph's Falls.

Vegetatively, the site can be described as thamnic–callidendrous grading forest with a moderate stand density. It is dominated by a mixture of *Nothofagus cunninghammi Phyllocladus aspleniifolius* and *Atherosperma moschatum. Blechnum wattsii* is the dominant ground cover, with occurrences of *Gahnia grandis* and *Blechnum nudum.* At the disturbed edge of the forest, *Histiopteris incisa, Pittosporum bicolor, Tasmannia lanceolata, Olearia argophylla, Acacia melanoxylon, Oxylobium* sp., *Gaultheria hispida, Aristotelia penduncularis, Leptospermum scoparium* and *Juncus* sp. can be observed. Most *Phyllocladus* individuals have crowns at canopy level. The oldest samples obtained in this study came from this site, with a few specimens being over 1000 years old when felled as part of the road construction process.

BEN_E

BEN_E takes its name from Ben Ridge Road which runs along a broad ridge separating the Ringarooma and South Esk catchments. There are two subsites within approximately 2 km of one another. One is situated on the main road itself,

and backs onto a disused quarry (Figure 2.10). The second is to the north, on a spur road, recently built for forestry purposes. The first subsite shows a relatively high level of disturbance with some 'forest thinning' having occurred some 20–30 years ago, significantly altering the light conditions for the understorey. The first subsite is thamnic–callidendrous disturbed rainforest, and the second, callidendrous forest, disturbed at the road edge. Both subsites are dominated by large *Nothofagus*. Both sites are similar in species composition with any differences being due to the age of disturbance. The second subsite has only been disturbed comparatively recently, and has, as a result, fewer invading species. The site on Ben Ridge Road itself also supports some *Eucryphia lucida,* and *Atherosperma moschatum.* At the disturbed edge is a mosaic of *Acacia dealbata, Nothofagus cunninghammii, Dicksonia antarctica, Eucalyptus obliqua, Blechnum nudum, Blechnum wattsii, Pimelea* sp., *Gaultheria hispida, Eucryphia milligania, Oxylobium* sp., and *Montoca* sp. At the second subsite, the forest is dominated by *N. cunninghamii* with some mature *P. aspleniifolius* also present. No juvenile *Phyllocladus* are observed. Very little ground cover other than litter is apparent and this site is callidendrous. Where *Phyllocladus* occur, crowns are generally at canopy level. Both subsites are on wet, flat ground, with few drainage lines apparent. At both sites, light is available for most of the day, and trees are largely dependent on direct rather than diffuse radiation. As for BLT_E, granite underlies the site. Dieback of both *Nothofagus* and *Phyllocladus* is apparent at subsite one.

ESM_E

The 'East shelf Maria Island' site is a thamnic relict rainforest site on the steep east facing cliffs of Maria Island which lies off the east coast of the Tasmanian mainland. The site is south of the Bishop and Clarke summit. The growth form of individuals at this site on dolerite talus is unusually contorted with spreading branches. The stand is immediately adjacent to a young stand of *Callitris rhomboidea* (Figure 2.11) and represents a unique association of rainforest and climax dry forest (Olesen *et al.* in prep.). Other species present in the rainforest element are *Atherosperma moschatum* and *Anopterus glandulosus.*

Upslope is the dolerite peak of Mt Bishop and Clarke, and downslope are Permian siliceous sediments.

Site	*Altitude (m ASL)*	*Forest type*	*Soil pH*	*Slope (°)*	*Aspect*	*Rock type*	*Distur-bance*
BLT_E	720–750	thamnic	4.38	5–15	W/NW	Granite	Y
RFR_E	820–850	thamnic	4.42	5–10	W/NW	San/Silt	Y
BEN_E	750	tham/call	4.02/4.35	0–5	N/NW	Granite	Y
ESM_E	550–600	thamnic	6.73	10–40	E	Dolerite	N
ARM_M	600–700	mixed	4.62	5–10	S/SE	Sch/quar	Y
FC_M	750–800	mixed	5.10	0–10	SE	Sch/quar	Y
$FISH_M$	460–480	mixed	5.15	0–20	SE	Sch/quar	Y
KOA_M	650–750	tham/call	4.16	10–40	E/SE	Mu/sand	N
$PILL_M$	700–800	mixed	4.97	15–35	W/NW	Mu/silt	N
MUR_W	550–600	tham/impl	4.58	10–40	NE	Basalt	N
RCS_W	500–550	tham/impl	4.40	0–5	W/N	Basalt	Y
WEY_W	540	thamnic	6.17	5–15	W/NW	Basalt	Y
LCR_S	500	mixed	4.06	0–5	S/SE	Silt/shale	Y
SPR_S	550–600	imp/tham	4.22	5–10	S/SE	Dolomite	N
$CLAY_S$	20	mixed	-	5–10	S/SE	Sch/quar	N
$IRON_S$	620–640	implicate	-	10–30	SSE	Sch/quar	N

Table 2.1: **Site Characteristics. tham = thamnic rainforest, impl = implicate, call = callidendrous. Disturbance refers to obvious anthropogenic disturbance only: where this has been extensive, the site was considered as disturbed, where little human influence is apparent, the site is not considered disturbed. A large range in the slope of a site indicates a high variability across the site. San/Silt — sandstone/siltstone, Sch/quar — schists/quartzites, Mu/sand — mudstone/sandstone, Mu/silt — mudstone/siltstone, Silt/shale — siltstone/shales.**

2.3.2 Mersey Valley

The headwaters of the Mersey lie jointly in the Cradle Mt.–Lake St Clair and the Walls of Jerusalem National Parks in central Tasmania.

Mersey Valley sites are situated in the glaciated landscape of central Tasmania, where topography can change dramatically within short distances. As a result, these sites are very variable as a group. However, all but KOA_M have been anthropogenically disturbed by forestry and/or hydroelectric operations leading to the expectation that most sites in this area would be of relatively poor dendroclimatological potential. Human activities have meant that very few older

Figure 2.8: **Forest interior at BLT_E. near the summit of Little Mt. Michael. Two *Phyllocladus aspleniifolius* individuals can be seen in the background. the lower photograph looks northeast into the site and the crown of a *Phyllocladus aspleniifolius* individual emerges above the general canopy layer (centre)**

Figure 2.9: **The upper frame looks south along Ralph's Falls Road, showing the disturbed forest edge, mainly a mixture of *N. cunninghamii*, *B. nudum*. The crowns of some *P. aspleniifolius* are visible in the background. The lower frame shows the callidendrous forest interior to the west of the road**

Figure 2.10: **Ben Ridge Road, subsite 1 Upper picture shows the disturbed interior of site. Several stems of relatively young *Phyllocladus aspleniifolius* can be seen in the background, while ground cover shows clear evidence of disturbance, and light penetrates the forest to reach the forest floor. Lower frame shows the disused quarry immediately behind subsite 1 Around the edge of the site are numerous young sclerophyllous plants, sedges, and *Juncus* sp. An old disused road runs down the eastern side of the site (left side of photograph). Crown of a *Phyllocladus aspleniifolius* specimen is clear in the centre of the photograph**

Figure 2.11: **East Shelf ,Maria Island, looking to the south into the *Callitris* forest. Note the scree slope on which the forest is growing. The second photograph looks southwest at the site, showing the steep slope on which the forest sits**

trees exist and sites generally show high levels of disturbance. Only two sites of the five in this catchment are relatively free of such disturbances, and one of these has been subject to a number of fires in more recent times. However, sites have been sampled given that no alternative catchment close to this area exists. In addition, the one undisturbed site in the catchment (KOA_M), which has not been subject to fire in the past century, also has a number of characteristics desirable in streamflow reconstruction (see below). These sites of the Mersey are wet forest rather than rainforest assemblages. KOA_M, which has not been extensively disturbed, is the only rainforest site.

ARM_M

The Arm River site is on the western, southeast–facing bank of the Arm river which feeds into the Mersey. A number of small drainage lines, draining into the Arm river are present in *Eucalyptus delegatensis* and *E. obliqua* mixed forest. The rainforest portion of the vegetation is predominantly *Nothofagus cunninghamii* and *Phyllocladus aspleniifolius.* Further upslope, *Phyllocladus* is no longer present and *Nothofagus cunninghamii* is dominant and *Atherosperma moschatum* subdominant. The understorey is dominated by *Pomaderris apetala*, *Histiopteris incisa* and *Blechnum nudum*, with other sclerophyllous species also intermittently present (Figure 2.12).

Abundant evidence of disturbance over a long time period exists, and trees are relatively young. The crowns of the straight, tall and well spaced *Phyllocladus* generally form the canopy layer in combination with a *Eucalypt* species. As evidence of the youth of the site, many trees show signs of recent and/or continuing branch abscission below the crown.

FC_M

The site at February Creek is approximately 6 km south of ARM_M, and floristically similar, although stand density is considerably higher, indicative of the youth of many of the trees. To the west, the land rises to meet the Cradle Mt–Lake St Clair National Park. Forestry disruption is again clear in the area, along with evidence of fire. The site has a southeasterly aspect. Overtopping the

rainforest species are numerous *Eucalyptus delegatensis* and *E. obliqua*. The site itself grades from mixed forest to disturbed wet sclerophyll forest. No drainage lines exist in the immediate vicinity of cored trees, with the exception of one small part of the site situated on flatter swampy ground containing the oldest trees on the site. At the edge of the forest are *Telopea truncata* and *Epacridacea* sp., *Hakea lissospermum, Monotoca glaucus, Pittosporum bicolour* and *Leptospermum scoparium* (Figure 2.13).

FC_M, ARM_M and $FISH_M$ are all situated on Precambrian sediments, classified as schists/ quartzites (Macleod *et al.* 1961).

$FISH_M$

Situated near the confluence of Snake Creek and the Fisher River, the site is surrounded by steep slopes on all sides. Essentially, $FISH_M$ is a disturbed patch of *Nothofagus cunninghamii–Atherosperma moschatum* remnant rainforest. The general area is dominated by *Eucalyptus delegatensis/E. obliqua*, and wet schlerophyll species were reinvading at the disturbed edge. The stand contains individuals of mixed age, with some *Phyllocladus aspleniifolius* individuals being greater than 350 years old. *Acacia dealbata, Pomaderris apetala, Epacridacea* sp., *Monotoca submutica, Lomatia tasmanica, Hakea lissospermum,* and *Dianella tasmanica* are prominent at the disturbed edges. Although all trees sampled have crowns in the canopy layer, topography limits the duration of the solar day for this site (Figure 2.14).

$PILL_M$

The Mt Pillinger site lies along the western flank of the mountain and much of it is in an area subjected to fires over the last 200 years. The southern end of stand, characteristic of relatively young rainforest, contains the older individuals sampled at this site. The oldest trees sampled in the stand were approximately 130 years old. Although not initially sampled, the stand has been sampled on a later visit, mainly because its relatively high elevation strongly suggested the probability of a temperature response. Dominant *Eucalypts* rising above the rainforest species at the northern end of the stand are *Eucalyptus subcrenulata* and *E. delegatensis*. *Nothofagus cunninghamii* dominated the

pockets of 'purer'-rainforest. Stand density is very high amongst the youngest trees of the site but sampled trees occupy more open positions. The northern part of the stand shows evidence of recent fires. The position of the site on the steep northwestern part of the mountain limits the duration of solar radiation and the broken canopy layer means that both diffuse and direct solar radiation are important at this site. Figure 2.15 shows only the far southern end of the stand which is characteristic of the rainforest assemblage rather than the fire–disturbed vegetation evident at the northern end of the stand.

Geologically, the underlying rock of the site consists of Permian marine sediments belonging to the 'Fern Tree group' which itself consists of pebbly mudstones and siltsones with occasional conglomerates and poorly sorted sandstones (Macleod *et al.* 1961).

KOA$_M$

The Kia-Ora site is contiguous to the Mersey River with a view of Cathedral Mountain to the east and southeast. It extends up the western side of the valley and is dominated by *Nothofagus cunninghamii, Phyllocladus aspleniifolius* and *Athrotaxis selaginoides.* Its position in the steep sided north–south aligned Mersey valley means that bright sunlight is available only during the middle of the day. Crowns of the majority of trees are present at canopy level in the mostly callidendrous forest. At the northern edge of the site is wet forest, grading to thamnic rainforest, and then to callidendrous rainforest at the southern end of the site. At the more thamnic northern end of the site, the understorey contained mostly *Anodopetalum biglandulosum* and *Cenerrhenes nitida*, with occasional specimens of *Gahnia grandis* and *Richea pandanifolia* (Figure 2.16). The predominant ground cover immediately south of this zone, in the callidendrous forest, is leaf litter. Fire has been absent for some time, as evidenced by large individuals of fire-intolerant *Athrotaxis selaginoides.* No drainage lines are evident across the site. The closest sampled tree to the river is at least 10 m above it. Most trees are in excess of 15 m above, and 20 m west, of the river. Minimal disturbance is apparent at the site, although a rejuvenated walking track passes through the stand to join the popular Overland Track.

Figure 2.12: Arm River. The upper picture shows the open forest interior at ARM_M. Several of the trees in the picture were sampled. The second picture looks into the disturbed edge of the site from the west

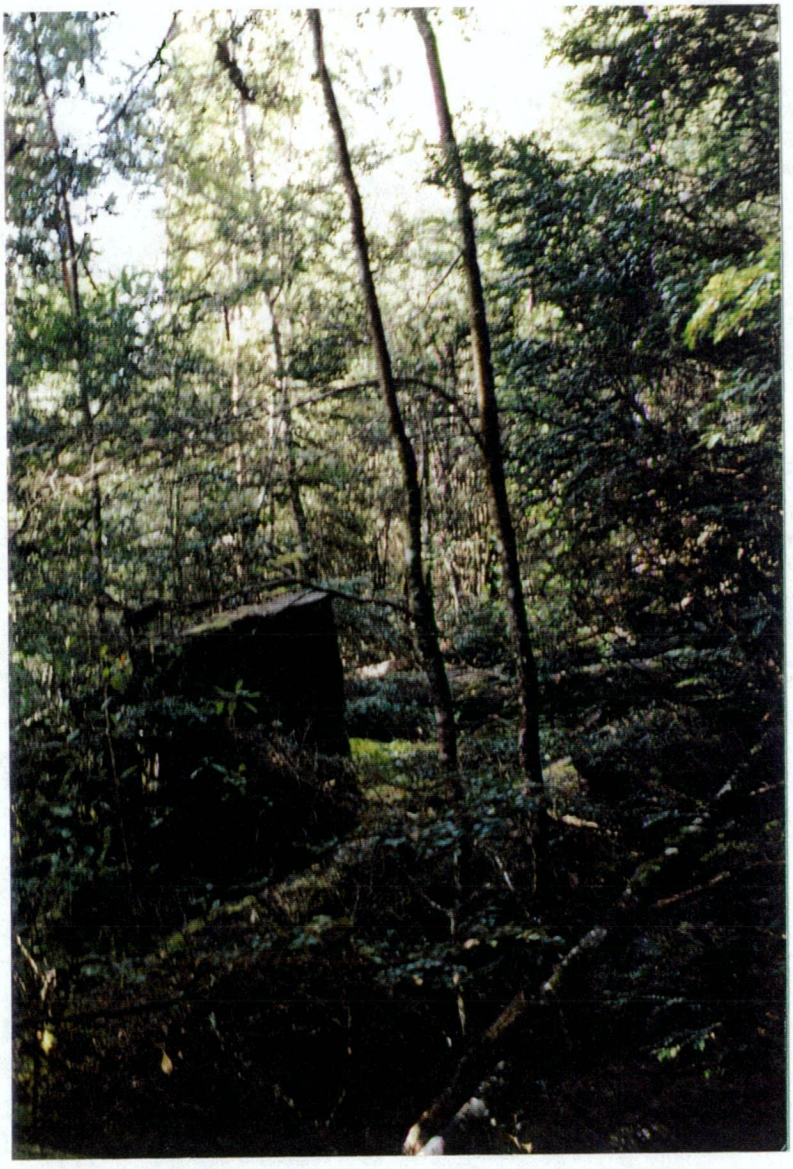

Figure 2.13: **February Creek. The interior of the site grades from a wet mixed forest association to a disturbed wet schlerophyll forest. *Phyllocladus* sampled at this site were relatively young, with only a few samples being greater than 200 years old**

Figure 2.15: **Fisher River. This site is close to the Fisher Power Station, in a narrow valley of relict rainforest. The upper frame shows the Fisher River, and the sampled site is just out of view towards the centre of the photograph. In the second photograph, the rainforest site can be seen**

Figure 2.16: **Mt Pillinger. The southern older, and undisturbed part of the Mt. Pillinger stand**

Figure 2.17: **Kia-Ora. The west bank of the Mersey River supports an open rainforest assemblage dominated by *P. aspleniifolius* and *A. biglandulosum*. In the foreground of the photograph is a multiple stemmed specimen of *A. biglandulosum*. To both sides of the photograph, *P. aspleniifolius* is visible**

Underlying the site are Permian sediments consisting of grey to dark grey and black mudstones with occasional grey sandstone, conglomerate, lenticles and fissile black shales, known as the 'Wallace Group' Macleod *et al.* (1961).

2.3.3 The West

Two of the three western sites are located relatively close to one another, and their local environments are similar. The third site, MUR_W, is considerably different in terms of both its location and environment. As was the case for the Mersey sites, the area has been subjected to extensive disturbance, particularly forestry operations. The two sites sampled in the headwaters of the river, south and east of Waratah, however, include specimens greater than 400 years old. The undisturbed site, MUR_W contains specimens of similar age.

RCS_W

Race Course Spur is situated in the North Forests concession area on the northwest coast, on steadily rising land which meets the rugged mountains of the west coast. To the north and west are the peaks of Mt Bischoff, Mt Pearse and St Valentines peak; to the east is the Cradle Mountain–Lake St Clair National Park. The area has been extensively logged for over 60 years and trees in the area are therefore likely to show some impact of logging in their ring widths. The RCS_W site is a small raised platform to the south and west of plantation *Eucalyptus nitens* (Figure 2.17). The small area of rainforest grades from implicate rainforest to a wet forest association before giving way to grassland/herbfield to the south, and is more than 500 years old. All sampled trees have crowns in the canopy layer of the forest and, because of the open nature of the area, receive a complete day of solar radiation. Direct radiation is therefore more important for these specimens than diffuse. The site is underlain by Cainozoic olivine-augite basalt (Spry 1962).

Nothofagus cunninghamii and *Phyllocladus aspleniifolius* dominate the site which also contains *Anodopetalum biglandulosum, Leptospremum scoparium,* and *Atherosperma moschatum.* Towards the edges of the site are the occasional *Eucalyptus obliqua, Banksia marginata, Telopea truncata* and *Leptospermum*

scoparium. The understorey is dominated by *Cennarhenes nitida* and *Gahnia grandis.*

WEY_W

The Wey River site is located at the confluence of the Wey and Hellyer rivers close to the Murchison highway. The axis of the valley runs from northwest to southeast. The construction of the Murchison highway to the west of the site is the nearest disturbance, as well as forestry operations (Figure 2.18). The site is disturbed thamnic rainforest dominated by *Nothofagus cunninghamii.* Other species present in the canopy layer include *Eucryphia lucida, Atherosperma moschatum* and *Nothofagus cunninghamii.* The shrubby understorey contains *Tasmannia lanceolata, Pimelea* sp., *Polystrichum proliferum* and *Blechnum nudum.* Disturbance has led to increased light availability within the stand which is underlain by Cainozoic olivine-augite basalt (Spry 1962).

MUR_W

A site on the eastern side of Mt Murchison, one of the additional sites sampled, has been chosen both for its proximity to the Mt Read *Lagarostrobos franklinii* site and its potentially higher elevation compared with the other west coast sites. However, although *Phyllocladus* are observed up to almost 700 m, individuals at higher elevations are only saplings. Most individuals grow at elevations between 550 and 650 m ASL, and all sampled specimens come from within this range.

In contrast with RCS_W and WEY_W, MUR_W is virtually undisturbed. Fire has been absent for a substantial time period, as evidenced by numerous large specimens of *Athrotaxis selaginoides.* To the south, along the eastern side of the mountain, the forest appears to be considerably younger than at the northern end: no *Athrotaxis selaginoides* have been observed, the stature of the forest is less and the trees younger. The forest grades from being implicate to thamnic. Most of the sampled site lies in more thamnic rainforest on relatively steep slopes on the northeast facing slope of the mountain (Figure 2.19). A number of drainage channels tending northeast are evident, and in periods of high rainfall can be expected to carry substantial flows. The profile of the mountain to the west results

Figure 2.17: **Racecourse Spur Upper frame shows the forest interior at the northern end of site. At far left of photograph, *Phyllocladus aspleniifolius* stems are visible. In the open foreground, dying *Anodopetalum biglandulosum* is observed.**
In the lower picture, the disturbed eastern edge of the rainforest platform is apparent. A few metres further east is young plantation *Eucalyptus nitida*. Several crowns of *P. aspleniifolius* are visible to the right of the photograph

Figure 2.18: **Wey River. Upper frame shows the disturbed edge of the forest, and the photograph is taken from Murchison Highway**
The lower picture shows the interior of stand. To the right of the photograph, is a sampled *Phyllocladus aspleniifolius* specimen on the steep banks of the Wey River

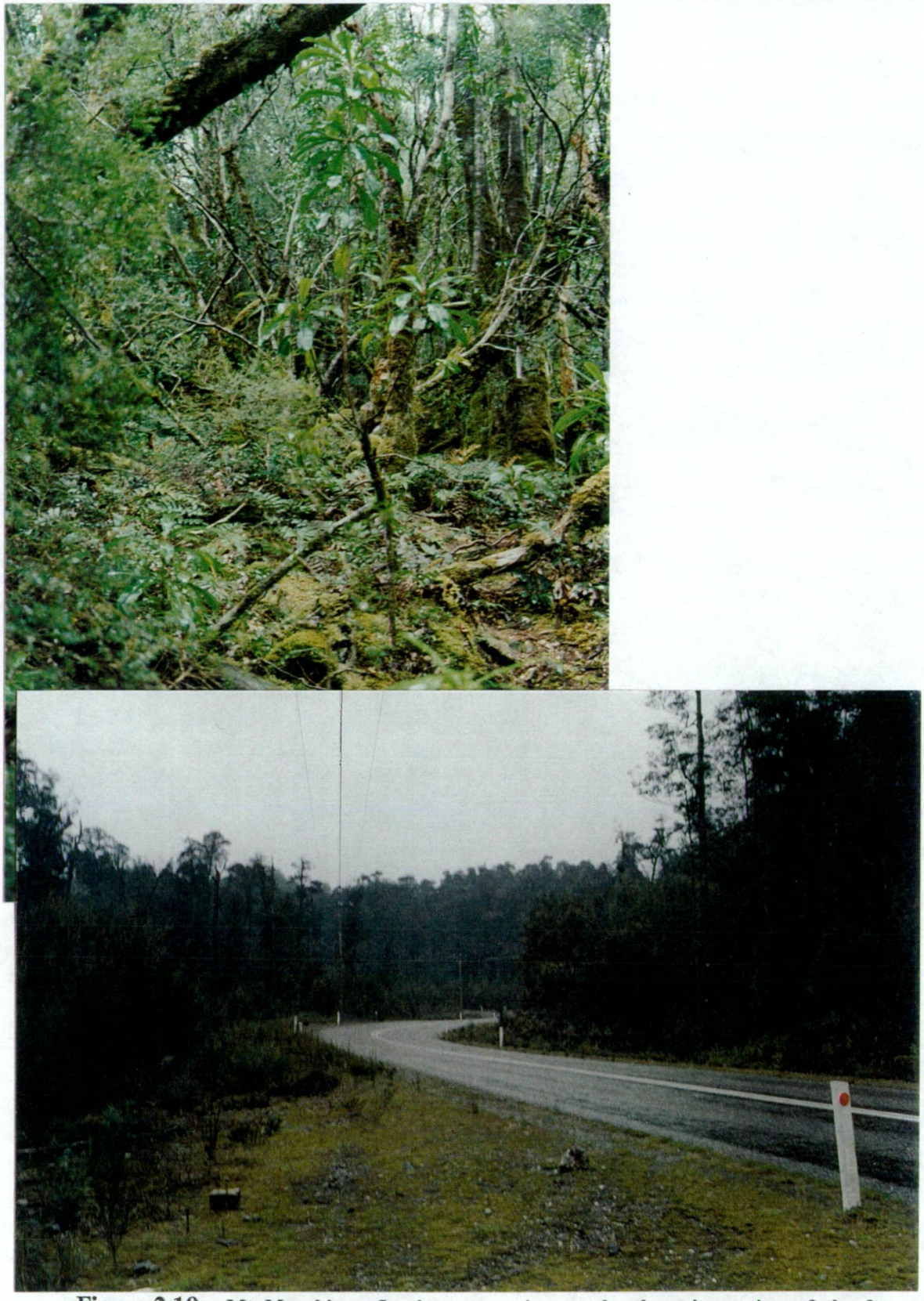

Figure 2.19: **Mt Murchison. In the upper picture, the thamnic portion of the forest interior is evident. The second photograph is taken from the Anthony road, and looks westwards towards the site. The site itself, however, is not visible due to low cloud cover, relatively common in this area.**

in bright sunlight being excluded in the late afternoon. Dominant canopy layer species at this site include *Phyllocladus aspleniifolius, Nothofagus cunninghamii* and *Athrotaxis selaginoides*. Above the '*Phyllocladus* zone' (above 650 m ASL), *Nothofagus cunninghamii* dominates the forest with *Atherosperma moschatum* occurring as subdominant. Other species in the forest are typical of thamnic/implicate rainforest assemblages, and include *Anodopetalum biglandulosum, Cenerrhenes nitida, Anopterus glandulosus, Blechnum nudum* and *Gahnia grandis.*

Cambrian volcanic deposits underlie the site (Banks 1962).

2.3.4 The Southwest

In addition to the northern transect of sites, a southern river has also been selected to form a north-south transect. Although many parts of the southwest have been relatively free of widespread anthropogenic effects, it has not been possible to find many catchments with sufficiently long streamflow records. The only river in the 'wilderness area' with a relatively long record is the Florentine, with a record extending continuously back to 1951. Two sites in the catchment were initially sampled, with a third site, $CLAY_S$, not in the catchment, being added at a later date.

LCR_S

The Lower Cole Road site lies immediately to the southwest of Wylds Crag. It is the most northern of the three widely dispersed southwest sites and is approximately halfway between $CLAY_S$, the southern most site, and MUR_S in the northwest. LCR_S is a good example of a mixed forest growing in a wet area, with an even-aged *Eucalyptus delegatensis* canopy layer over an assemblage of rainforest species dominated by *Phyllocladus aspleniifolius* and *Nothofagus cunninghamii* (Figure 2.20). Further upslope, the dominant rainforest species become *Atherosperma moschatum* and *N. cunninghamii*. The understorey consists predominantly of *Anodopetalum biglandulosum, Cenarrhenes nitida* and *Anopterus glandulosus*. Because tall *E. delegatensis* blocks a considerable proportion of incoming solar radiation, this site is largely dependent on diffuse radiation, except along its the southern edge. Recent forestry operations have

exposed the southernmost portion of the site to increased light intensity, and increased productivity in trees at the forest edge is a likely result of this. The site is underlain by siltstone and shale.

SPR_S

The Scott's Peak Road site is situated about 2–3 km south of the junction of Gordon Road and Scott's Peak Road. This site is an excellent example of implicate rainforest where the sampling regime (see Chapter 3) is impossible to follow (Figure 2.21). The canopy layer is uneven with crowns of all *Phyllocladus* sampled rising above most other vegetation. The implicate rainforest indicates poor soil quality. Dominant tree species are *Nothofagus cunninghamii* and *Phyllocladus aspleniifolius*. Dominant understorey species include *Anodopetalum biglandulosum, Cenarrhenes nitida, Prionotes cerinthoides, Anoptrous glandulosus, Gahnia grandis, Chococarpa gunnii, Richea pandanifolia* and *Orites diversifolia.* To the west, a gently sloping hill accommodates *Atherosperma moschatum*, replacing *Phyllocladus* as a forest dominant. To the south are the rugged peaks of Mt Anne and Mt Sarah Jane, to the west, Mt Wedge, and to the north, the Saw Back Range. Several drainage lines exist in the stand and drain into the upper reaches of the Florentine River. The site is underlain the site by middle Cambrian dolomite.

$CLAY_S$

Although $CLAY_S$ is located close to sea level, it was chosen for its extreme southerly position and the fact that a number of exposed stumps could be sampled for discs. It is unlikely to be precipitation limited.

Abundant evidence for old fires exists at Clayton's Lagoon, and Brown and Podger (1982) have discussed the floristics and fire regimes of the area. However, a proportion of the site appears to have been relatively unscathed by many of these fires over the past 400–500 hundred years and contains *Phyllocladus aspleniifolius*. The site is a mixture of two components: the older part being a rainforest assemblage, while the younger part is wet schlerophyll forest containing

Figure 2.20: **The disturbed southern edge of the Lower Cole road site. Large *Eucalyptus delegatensis* form the canopy layer, with the rainforest species below this. The second photograph shows a young *Phyllocladus aspleniifolius* seedling at the edge of the disturbed area**

Figure 2.21: **Implicate rainforest at Scott's Peak Road. Canopies of several *Phyllocladus aspleniifolius* specimens can be seen emerging above the general canopy layer. The dense rainforest at the site is apparent in the lower photograph. *Anodopetalum biglandulosum* stems dominate the picture**

Figure 2.22: **Interior of the wet forest at Clayton's Lagoon. At this part of the site, evidence for fire over the past 200 years is apparent. A sampled stump at the site is shown in the lower photograph, close to the 1933/34 fire boundary (J. Marsden-Smedley, University of Tasmania, pers. comm.)**

younger *P. aspleniifolius* individuals. In the rainforest, the dominant species are *Nothofagus cunninghamii* and *P. aspleniifolius.* The most abundant understorey species are *Anodopetalum biglandulosum*, *Anopterus glandulosus*, *Blechnum wattsii, Archeria* sp., *Gahnia grandis* and *Monotoca glaucus.* The wet schlerophyll forest contains *Eucalyptus nitida* as the dominant Eucalypt (Figure 2.22).

The site faces S/SE across the lagoon behind which rise hills enclosing the bay. Above the forest, the vegetation cover consists of button grass. Precambrian conglomerates in a sandstone–mudstone matrix underlie the site (Jones 1977).

IRON$_S$

Sampled trees on the south/south-southeast facing slopes of the Ironbound Range are close to the treeline at approximately 660 m ASL. These trees, like those of ESM$_E$, show a peculiar growth form. Unlike ESM$_E$, they are small, but similarly to ESM$_E$, the lateral extent of branches is much greater than for other sites. The immediate implication is that this reflects severe temperature limitation. The site is characterised by dense implicate forest, and includes stunted *Nothofagus cunninghamii*, *Eucryphia milliganii, Astelia alpina, Richea scoparia, Gahnia grandis, Orites diversifolia, Tasmannia lanceolata,, Leptospermum rupestre, Cenerrhenes nitida, Prionotes cerinthoides* and *Milligania* sp.. The general area has been disturbed only by a popular walking track. Track construction itself has resulted in some disturbance, but no other recent disturbance is evident. The broken canopy layer ensures a relatively high level of light penetration into the stand, but its southerly aspect limits the hours of sunshine it receives. The geology of the site is similar to CLAY$_S$.

2.4 Summary of site characteristics

Phyllocladus aspleniifolius is a member of the Gondwanan element of the vegetation and is a remarkably adaptable species with relatives in New Zealand and Malesia. It has a broad geographical and ecological range (Figures 2.2, 2.3, 2.4, 2.5), as evident from site descriptions. This wide distribution not only reflects broad limits of tolerance to climatic factors but is also aided by bird dispersal of

its seed. Perhaps one of the most intriguing aspects of the genus, in Tasmania as well as New Zealand, is a well defined, approximate biennial, oscillation in the ring widths, thus far attributed solely to biological causes. Previous work (Ogden 1978, 1982, Campbell 1980, Read and Busby 1990, Barker 1993) suggests that both temperature and moisture are important to the growth of *P. aspleniifolius*, and that the conditions of the previous season are especially important.

The environments of the west coast sites represent the most homogenous region, in terms of elevation and general forest environments. The RCS_W and WEY_W sites, however, are markedly different from MUR_W in terms of their slope, aspect and disturbance histories. In addition, they fall into the Northern Slopes (see Figure 2.1) classification of Gentilli (1972) while MUR_W is located on the Western slopes.

Although quite closely clustered, the Mersey valley sites differ greatly from one another. The most common factor between four of these sites is the high level of anthropogenic disturbance. All these sites fall into Gentilli's Northern Slopes region. The east coast sites, in the Northeastern block, also lie quite close to one another. The environments of BLT_E and RFR_E are more similar to one another than to BEN_E, although BEN_E and BLT_E are at similar altitudes. All three of these sites have experienced varying degrees of disturbance, RFR_E being the least disturbed of these three higher elevation sites. ESM_E is markedly different from these sites, and is likely to be more limited by precipitation due to its relatively low elevation and position on the steep eastern side of Maria Island. This site is one that is likely to have been maintained by sea fog and valley cloud (Neyland 1990).

The four sites of the Southwest are the most widely dispersed and this region also represents the most heterogeneous region in terms of site environments. These differences are apparent in elevation, forest type and floristics as well as geology. $CLAY_S$ and LCR_S both represent disturbed sites, the disturbance at LCR_S predominantly due to forestry operations while disturbance at $CLAY_S$ has been due to fires.

Chapter 3: Dendrochronology of *Phyllocladus aspleniifolius*

3.1 Introduction

The climatological usefulness of dendrochronological data is critically dependent on site selection and the confirmation of crossdating, as discussed in Chapter 2. However, in order to prepare data for dendroclimatic analysis, other signals present in ring widths but not related to the macroclimatic signal need to removed. Processes through which this can be done include what is known as standardisation of ring–width series and the computation of the mean ring–width chronology. After this, a chronology can be further assessed and analysed.

Chapter 3 outlines these processes, and describes the fifteen chronologies and their characteristics. Intersite comparisons are drawn, and some comparison with *Lagarostrobos franklinii* chronologies is made.

3.1.1 Standardisation

Standardisation aims to maximise the macroclimatic signal present in ring widths and to remove nonclimatic variance (including microclimatic information of no interest) from samples (Graybill 1982). This is achieved through the construction of stationary ring–width indices which are used in the computation of the mean ring–width chronology for a site. The process of standardisation is neither straightforward nor entirely objective.

A number of variables affect ring width. A simplified representation of sources of variance within a growth ring is:

$$G = C + A + D1 + D2 + E \qquad (3.1)$$

where G is total growth, C the macroclimate-related growth, A the age trend, $D1$ endogenous disturbance, $D2$ exogenous disturbance, and E is unexplained variation (Cook 1985). An endogenous disturbance is one originating from within the stand, an exogenous disturbance one that originates from without.

Tree fall, a common endogenous disturbance, alters both light and competition conditions for surrounding trees. Such endogenous disturbance resulting in increased light penetration, would be likely to result in increased cambial growth of light-preferring trees immediately adjacent to the site. This increased growth would persist for a number of years after the event, resulting in autocorrelation (see below). Other trees in the same stand, but distant from the disturbance, will not show this same trend. Importantly, endogenous disturbances are assumed to be transient and randomly distributed in time and space (Cook 1990). Exogenous disturbances on the other hand, generally affect an entire stand (Graybill 1982). Evidence of growth suppression in *Eucalyptus pauciflora* and *E. stellulata* due to insect attack (LaMarche 1978), and growth suppression in *Pinus echinata* possibly due to exposure to SO_2 and other combustibles (Baes and McLaughlin 1984), are examples of exogenous disturbances. Both exogenous and endogenous disturbance pulses will effect changes in ring-width series which are not attributable to climate.

Early workers in dendrochronology described the existence of an aging trend which is apparent in the ring widths (Douglass 1928, Hawley 1937, Bisset *et al.* 1951, Schulman 1951). This trend can generally be approximated as a negative exponential curve. If this aging trend is not accounted for, the subsequent mean ring–width chronology will reflect average raw growth — which will be partially a function of sample depth and changes in sample depth, and therefore not depict the influence of climate on average growth at a site. In addition, some trees will show more rapid growth than others, and this will lead to additional distortion of the mean chronology (Fritts 1971). Further distortion of the aging trend caused by competition and other endogenous disturbances will also affect the sequence of ring widths (Cook *et al.* 1990a).

Two broad classes of methodological alternatives for dealing with the aging trend are deterministic and stochastic respectively. Within each of these broad classes a number of alternatives exist. The choice of detrending technique will strongly affect the resultant chronology, with effects particularly evident in the lower frequencies.

The more elementary methods are deterministic, the most popular being the negative exponential curve and its various modifications (e.g. Fritts 1963,

Fritts *et al.* 1979, Graumlich and Brubaker 1986, D'Arrigo and Jacoby 1991, Scuderi 1993). Another group of deterministic detrending techniques apply polynomial functions to the time series (e.g. Fritts 1976, Graybill 1979, Till 1984). Stochastic detrending methods include the use of digital filtering (e.g. Guiot *et al.* 1982), exponential smoothing (Cook *et al.* 1990a), and differencing (e.g. Box and Jenkins 1970). These stochastic techniques recognise that the aging trend is modified by endogenous and exogenous events whereas deterministic methods do not.

The cubic smoothing spline, a digital filter where no weights are explicitly calculated, is a piecewise polynomial (Wold 1974) and is now used routinely by many investigators (e.g. Cook 1985, Stahle *et al.* 1988, Kelly *et al.* 1994). It is considered a superior approach to standardisation, as no assumptions are made with regard to the shape of the standardisation curve (Cook and Peters 1981). Other studies have made use of a double detrending method which first fits a negative exponential function to the time series, followed by the application of the stochastic smoothing spline to remove remaining variance considered to be nonclimatic in origin (e.g. Stahle *et al.* 1985). On rare occasions, no detrending method has been used (LaMarche 1974b).

It is not uncommon for deterministic detrending to grossly over- or under-estimate certain parts of a series. Although stochastic detrending is more flexible than deterministic detrending, it is also generally less objective.

A further issue to be considered in the standardisation process is what is known as the segment length curse (Cook *et al.* 1995). Essentially, this occurs when climatic change takes place over a longer time scale than individual trees typically live. Because standardisation techniques have been developed largely for comparatively young stands of trees, the situation where low-frequency changes in climate occur may become problematic in the standardisation of some series. Standardisation itself can remove a trend exceeding the life span of an individual.

The basic intention of standardisation is to obtain series which do not reflect non-macroclimatic information and which can be averaged to reflect average growth at a site. Index values are calculated so that each series can be adjusted for differential growth rates observed at a site. A stationary index series is produced by the division of the raw ring width by its expected value. This

expected value has been determined by the chosen detrending option. Division rather than subtraction is used because the local mean ring width is proportional to local variance (heteroscedasticity). The resultant series has a mean of 1.0 and a reasonably constant variance.

3.1.2 Computation of mean ring–width chronology

Once data has been appropriately detrended and each series converted to an index series, it is possible to 'amalgamate' all series from a site into an average series. The most elementary method of constructing a mean chronology would be to calculate the arithmetic mean across all detrended series at an individual site for each year. However, if outliers exist, the arithmetic mean is not the best estimator and may also be biased. A robust mean is both more efficient and less likely to be biased than the arithmetic mean when outliers are present. If outliers are not present then the cost associated with the use of the robust mean is reduced efficiency, and the arithmetic mean is more efficient. The robust mean is iteratively computed, and can be expressed as:

$$\overline{Y}_t^* = \sum_{j=1}^{m} w_t Y_t \qquad (3.2)$$

where $\overline{Y}_t^*$ is the biweight mean, Y_t represents tree ring indices for year t and sample j, m is the number of samples, and

$$w_t = \left\{1 - \left[\left(Y_t - \overline{Y}_t^*\right) / \left(cS_t^*\right)\right]^2\right\}^2 \qquad (3.3)$$

is a symmetric weight function when

$$\left[\left(Y_t - \overline{Y}_t^*\right) / \left(cS_t^*\right)\right]^2 < 1 \qquad (3.4)$$

otherwise 0.

S_t* is a robust measure of standard deviation of the frequency distribution.

$$S_t^* = median\{|Y_t - \overline{Y}|_t^2\} \quad (3.5)$$

and c is a constant which determines at what value an outlier is attributed a weight of 0. In the program used for analysis in this study, c is given a value of 9 (E. Cook, Lamont-Doherty Geological Earth Observatory, pers. comm.). The use of the more efficient estimator, where it is justified, will produce an averaged series with an homogeneous variance and an unbiased mean (Cook *et al.* 1990b).

3.1.3 Autoregressive modelling

Persistence in tree-ring series may occur not only due to endogenous and exogenous disturbance events, but also as a function of climatic events and species physiology. Persistence resulting from endogenous disturbance events, rather than climate or physiology, is unlikely to have been a site-wide occurrence. Physiological persistence related to climate may include bud formation, stem extension, or root development of the previous year (Fritts 1971, 1976) and is commonly observed in all or most individuals in a stand. Because persistence is unlikely to be identical from tree to tree within a stand (due to random endogenous disturbances), it is preferable that it be removed in order that an efficient estimator of the mean can be attained. This improvement may be achieved by autoregressive-moving average (ARMA) modelling. Cook (1985) outlined the mathematical development of ARMA models and the use of autoregressive (AR) modelling in detrending tree-ring series. An autoregressive series is one in which the current value, Y_t, is related to past values, $Y_{t-1}, Y_{t-2} \ldots Y_{t-k}$. A moving average (MA) specifies that the current value, Y_t, is related to past disturbances, $e_{t-1}, e_{t-2} \ldots e_{t-k}$. AR and moving average processes are equivalent to one another (Box and Jenkins 1970, Pankratz 1983, Cook 1985). An AR process where Y_t is dependent on Y_{t-1} only is an AR(1) process; an MA process in which Y_t is dependent only on e_{t-1} is denoted MA(1). An ARMA process is one where both of these processes operate, and if Y_t is dependent on Y_{t-1} and e_{t-1} only, the process is denoted as an ARMA(1,1) process. Mathematically, an $ARMA_{(p,q)}$ process can be represented as:

$$Y_t = \phi_p Y_{t-p} + \cdots + \phi_1 Y_{t-1} + e_t - \theta_1 e_{t-1} - \cdots - \theta_q e_{t-q} \qquad (3.6)$$

where Y_t is the index series at time t, e_t represents a serially random shock to the system at time t, ϕ are the AR coefficients and θ the MA coefficients. p denotes the order of the AR process, and q the order of the MA process. For the purposes of this study, only autoregressive processes have been considered, as these have been found to adequately apply to tree-ring series (Cook *et al.* 1990b). The order of autoregression present in a series can be determined by the Akaike Information Criterion (AIC) (Akaike 1974).

When modelling persistence for a group of time series (e.g. ring–width series), it is the *pooled* autoregression present which will theoretically be related to climate and species physiology (Cook *et al.* 1990b). In the dendrochronological context, pooled data are a combination of time series across all individuals at a site. A pooled model will reflect the common persistence structure of tree-ring series at the site, random effects attributable to microsite and physiology being averaged out (Cook 1985). Multivariate autoregressive modelling can be used to achieve the pooled model and has been shown to be robust in the face of out-of-phase fluctuations among series (Jones 1964, Cook *et al.* 1990b). The order of pooled autoregression present in a group of series can once again be estimated by the Akaike Information Criterion (AIC) (Akaike 1974).

The process of 'whitening' an original chronology with the intention of removing the effects of random endogenous disturbances involves the transformation of observations through the removal of the estimated autoregression (p). (ϕ restricted to be <1 for an AR(1) process). Prewhitening can be carried out as:

$$e_t = Y_t - \phi_1 Y_{t-1} - \cdots - \phi_p Y_{t-p} \qquad (3.7).$$

3.1.4 Summary statistics for chronologies

Several statistical measures have been developed for the specific purpose of assessing and interpreting tree ring chronologies. Those relevant to this study are briefly dealt with below.

Douglass initially described *mean sensitivity* as the '...mean percentage change from each measured yearly ring value to the next' (Douglass 1936 in Fritts 1976). It is now defined as:

$$MS_x = \left[1/(n-1)\right]\sum_{t=1}^{n-1} MS_{x,t} \qquad (3.8)$$

where

$$MS_{x,t} = \left|2(x_{t+1} - x_t)/(x_{t+1} + x_t)\right| \qquad (3.9)$$

x_t is ring width at year t, and n is the number of observations in the time series. The value of $MS_{x,t}$ ranges from zero to two. A zero value occurs if there is no difference between consecutive years, a value of two if a nonzero ring width lies next to a zero ring width. This statistic examines high frequency variability only. Strackee and Jansma (1992) pointed out that MS_x is a function of the standard deviation and first order autocorrelation, and that high values may be the result of a high standard deviation and a low first order autocorrelation, and vice versa.

The signal to noise ratio *(SNR)* is generally understood to be an indication of the signal contained in a number of data series. However, it is affected by both sample size and sample lengths, the relationship being a nonlinear one (Briffa and Jones 1990). A related statistic, less sensitive to sample size and sample lengths than the *SNR*, is the Expressed Population Signal (*EPS*). This is expressed as:

$$EPS = (N\bar{r})/\left[1 + (N-1)\bar{r}\right] \qquad (3.10)$$

where N refers to the number of series, and $\bar{r}$ to the average interseries correlation for the N series. *EPS* is an expression of how well the average of a finite number

of time series represents the population average (Wigley *et al.* 1984). There is no strict test for a threshold level of the statistic, but Wigley *et al.* (1984) discussed the necessity for a threshold value to be considerably higher than explained variance in a climatic reconstruction.

$\overline{R}$ is based on Pearson's product moment correlation, and is a measure of the average correlation for all series using the full overlaps of each pair of series, so the number of years used in computing each correlation may vary. The $\overline{R}$ result reported for each chronology is the average result for all series in the chronology.

Average segment length is merely an indication of the average length of individual data series in a chronology. If average segment length is short, resolvable frequency will be more limited than for a chronology with longer segment lengths. Average segment length has been calculated by summing the number of years in all samples containing a given year and dividing by the number of samples containing that year.

3.1.5 Analysis of chronologies

3.1.5.1 Principal Component Analysis

Principal component analysis (PCA) extracts both spatial and temporal information from a data set simultaneously (Lorenz 1956, Peters *et al.* 1981, Joliffe 1986). The covariance matrix of a set of independent variables is transformed to a matrix of principal components (PCs). PCs are linear combinations of variables weighted such that they are uncorrelated with one another (North *et al.* 1982). Each successive PC explains the maximum possible remaining variance, possesses both a spatial and a temporal pattern, and each is orthogonal to each of its predecessors. A linear combination of the variance contributed by each successive pattern will yield the original variables. This linear transformation of the data can be expressed as:

$$PCs = XL \qquad (3.11)$$

The original data (X) is multiplied by the new data, or loadings (L), to produce the *PCs*. Each PC generated by this process represents a 'global' mode of data behaviour. The use of principal components ensures that predictors are independent, or orthogonal, and each successive PC explains the maximum remaining variance in the data. Dimensionality of the problem (how many eigenvectors are considered 'important') may be reduced through the application of any one of a number of rules (see Craddock 1973, Guiot 1990).

When a PCA is performed on individuals at a single site, the percentage of variance contained in the first eigenvector is an indication of the common signal of individuals at that site. A full derivation and explanation of PCA is given in Jolliffe (1986).

While PCA has the advantages of orthogonality and the extraction of the maximum possible remaining variance in each successive PC, a major difficulty can be the physical interpretability of results. The first PC is often a 'compromise' component of the major 'clusters' in the data with the result that the loadings on all sites are moderated (Whetton 1986). Varimax rotation of components is commonly used to overcome this and other known problems associated with unrotated PC solutions (Richman 1986). It has the advantage of being able to identify group patterns in the data and is generally accepted as the most accurate of possible orthogonal rotations when applied to known data sets (Richman 1986). It aims to simplify the structure of the PCs.

3.1.5.2 Frequency domain analysis of chronologies

Spectral analysis techniques have long been used in examination of the frequency domain of time series. Spectral analysis is a technique used to describe the tendency for oscillations of given frequencies to occur in a data set (Bloomfield 1976), and its starting point is the calculation of the autocovariance function on which harmonic analysis is performed and estimates then smoothed.

The multiple taper method (MTM, Thomson 1982) of spectral analysis makes use of the eigenfunctions of the finite Fourier transform as data windows or 'tapers'. Tapering is a technique used to reduce bias, but in more traditional methods has the disadvantage of reducing sample size. Some of the more

popularly used tapers or 'windows' include the Blackman–Tukey, the Tukey–Hanning, and Hamming (Chatfield 1975). In MTM, where tapers which are orthogonal to one another are used, each successive eigenfunction (denoted as the K^{th} taper) is applied to the entire spectrum ($-\pi$, π) (Thomson 1982). The use of multiple orthogonal tapers is one way to overcome the increased variance which occurs at the expense of decreased sample size associated with other techniques (Percival and Walden 1993). Each of the K eigenfunctions, serve as the data tapers, and can be weighted such that all K eigenfunctions can be then be averaged to obtain the spectral estimates (see Percival and Walden 1993).

The use of eigenfunctions minimises leakage, produces consistent estimates and increases the number of degrees of freedom from two in other methods to two for each taper used (Percival and Walden 1993). The number of tapers used in any analysis may differ. Thomson (1982) has discussed the technique at some length.

The selection of the time-frequency bandwidth, W, will affect the resolution of the analysis:

$$W = j / (N\Delta t) \qquad j > 1 \quad (3.12)$$

where N is the number of observations, and Δt the time interval.

3.1.5.3 Cross-spectral analysis

Cross-spectral analysis is a linear statistical comparison of two time series in the frequency domain, examining relationships between two series over the entire range of frequencies. Comparison in the time domain involves the calculation of the cross covariance function. In cross-spectral analysis the equivalent is to calculate the coefficient of *coherency* between two series (Chatfield 1975). Coherency is an indicator of the relative proportion of coherent power in the total output power of a system at any particular frequency. If there is no noise in the system, the coherency will be one and, where there is no signal contained in the output, coherency will be zero. It depends only on the relative

magnitudes of coherent power spectral density and noise power spectral density (Jumppanen 1993). Squared coherency is that fraction of variance in one series that is linearly related to variance in the other series.

A further tool available in cross-spectral analysis is the phase spectrum. Phase angle denotes the 'off-set' of a periodicity in one data set with the same periodicity in the other data set being used in the analysis. The *phase spectrum* therefore depicts the phase relationship between the two series across the range of frequencies. For two series with a coherency at a given frequency that are in phase, the phase angle will be 0^{o}, while for two series with a coherency at a given frequency, but directly out of phase with one another, the phase angle will be 180^{o}. Negative phase relationships indicate that the input of the system (variable one) lags the output (variable two), while a positive phase relationship indicates output lagging input.

3.2 Methodology

3.2.1 Sampling

Frequent ring wedging (Figure 3.1) in *Phyllocladus aspleniifolius* resulted in a large number of locally absent rings, making crossdating difficult if not impossible for some core samples. Reasons for the occurrence of ring wedging were not clear, although it is possible that branch abscission was an important cause (Norton *et al.* 1987, Shigo 1985). Although it may be possible to observe relatively recent wedging in a living tree, it was not possible to observe past sites of wedging without destructive sampling. This source of relatively high variability, both around a single circuit and also between trees, meant that a greater number of samples were required in order to approximate a population signal than would have been the case if wedging were not a problem (LaMarche 1982).

Three to four cores were taken from each tree with an increment borer (30–75 cm) in an effort to accommodate the within-tree variability. For most sites, at least 20 trees were sampled. Wedging sites around the trunk and old injuries were avoided. Generally, two cores perpendicular to site slope were obtained, with the third and fourth cores taken from between these while

attempting to avoid likely compression wood (Low 1964, Westing 1965). However, for a number of trees at some sites, the immediate environment of the tree made this procedure impossible to follow and cores were obtained from wherever possible, for example, at sites MUR_W, RCS_W, SPR_S and $IRON_S$. In most cases cores were extracted from between 1.2 and 1.4 m above the ground. Cores were stored in plastic straws until dried and mounted. Procedures for both sample preparation and crossdating essentially followed Stokes and Smiley (1968).

Although the majority of samples were cores from living trees, a number of discs were obtained, particularly for the eastern sites. Many of those for BLT_E had previously been obtained by N. Allen and T. Bird in the late 1970s. Access to several additional samples cut by V. LaMarche at the same site, and stored at the Tree Ring Laboratory (TRL), Arizona, was also granted. Fresh discs were obtained from previously fallen trees for all of BLT_E, RFR_E and BEN_E. These discs were slowly air-dried for approximately 8 months to minimise checking and splitting of wood and then placed in a large oven over a period of three to four weeks at a temperature varying from 20–25 °C. Subjection to temperatures higher than this for extended periods of time resulted in checking and splitting of some samples.

All samples were sanded to 320 grit with the aid of a belt sander, after which an orbital sander was used to sand to 400 grit for all disc samples. Disc samples were then finished by hand sanding with 400–600 grit at which point the detailed ring structure was clearly visible. Core samples were sanded to 220 grit by a belt sander, followed by hand sanding with 400–600 grit sandpaper, as for disc samples.

3.2.2 Crossdating of individuals from a single site

Samples from an individual tree were first visually crossdated amongst themselves with the aid of a microscope by matching patterns of narrow and wide rings amongst cores. For discs, three radii from the phloem to the centre of the disc were marked and rings were checked between these radii. At times it was possible only to trace two or even one radius from the phloem to the centre of the disc. Same-tree cores were placed side by side and ring sequences checked across

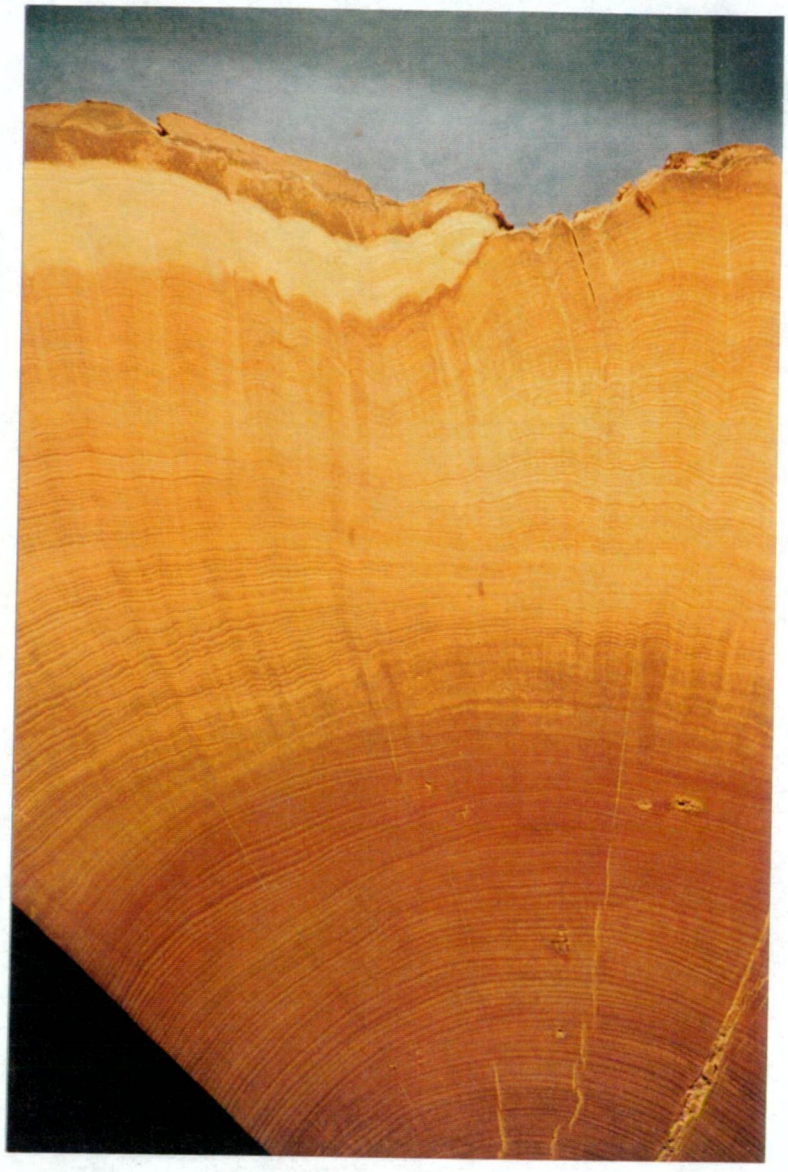

Figure 3.1: **Sample from BLT_E showing ring wedging. This sample could not be crossdated with other specimens from the same site and was discarded. In several cases, severe ring wedging meant that it was not possible to obtain three radii of measurements from an individual sample. At sites where only cores were taken, ring wedging was often the cause of samples being discarded as they did not even crossdate with other samples from the same tree**

the samples. 'Event years', or 'key years' were defined by Schweingruber *et al.* (1990) as visually conspicuous rings within a section of the sequence, in common between the majority of individuals at a site. Key year lists for each site were generated progressively (see Tables 3.1 and 3.2) and used for reference when crossdating. Frost rings were not a general feature of this species at the selected study sites and were therefore not used in crossdating. False rings were exceedingly rare, with only AD 1636 providing an example in three samples from the BLT_E site.

After visually crossdating the cores, a measuring stage with linear encoder attached to a digital display unit and a computer was used to measure ring width. After this, a data quality control program, COFECHA (Holmes 1994), was used to check dating of specimens. COFECHA identifies potential dating or measurement problems by comparing segments of one sample against those of another, or against a number of other samples. In several cases, dating of intra-site samples conflicted, but it was generally possible, by re-examination of the wood itself, field notes, the COFECHA output, and the overlaying of series plots on a light-table, to identify problematic series and subsequently rectify problems.

When locally absent rings were identified, the average ring width for other radii/cores from the same tree was substituted. The rationale behind this 'remedy' was the fact that many of the locally missing rings were due to ring wedging and therefore a zero value was not a good representation of growth for that year. In addition, a high number of zero values can distort data standardisation. Where there were no other samples from the same tree included in a chronology, a zero value was not altered. For the two sites ESM_E and $FISH_M$ this procedure resulted in a relatively high number of samples containing zero values. This occurred because often the only one sample from an individual could be dated successfully.

3.2.3 Chronology development

All the individual raw data series for several sites (BLT_E, RFR_E, KOA_M, RCS_W, SPR_S) were processed using a number of detrending schemes in order to determine which was the most appropriate. The options examined were: the negative exponential, double detrending where a negative exponential is first fitted to the data followed by a cubic smoothing spline and, finally, a cubic smoothing

spline. An examination of the plots of the raw data against each of these options, and resulting chronology statistics, suggested that a single detrending with a 128-year 50% cut-off cubic smoothing spline was most suitable. The use of a 128-year 50% cut-off smoothing spline meant that frequencies lower than this length were effectively removed. However, individual average sample lengths typically only varied between 130 and 260 years (see Table 3.3 below), and the implication of this was that it would not be possible to reliably identify periodicities of lengths considerably greater than 128 years, even without the limitation of the 128-year smoothing spline.

Figure 3.2 shows quite clearly the differences in growth patterns between trees at a single site. In its first 150 years of growth, BLT86B exhibits the classic negative exponential growth trend not seen in any of the other series shown. All series except BLT86B show increased growth in the last 30 or so years; each series appears to have its own periods of higher and lower growth not in concert with other series. At most sites, instances of myrtle wilt (Elliot *et al.* 1987, Packham 1991) were responsible for the occurrence of fallen and dying *Nothofagus cunninghamii* (personal observation). It is likely that such instances led to endogenous disturbance pulses in ring widths of nearby trees, therefore having caused some of the differences between individual series. The occurrence of such endogenous disturbances would illustrate the inappropriateness of deterministic detrending. Ring wedging, commonly observed in discs of *P. aspleniifolius*, and most probably associated with branch abscission (see Shigo 1985, Mattheck 1991), was also responsible for some of these differences.

All series, with the exception of FC_M, were modelled as AR(2) processes by program ARSTAN (originally developed by E.R. Cook) (Table 3.3). An examination of the wood itself shows this selection to be appropriate. For each site, a raw ring–width chronology (raw), a chronology which has been detrended and autoregressively modelled (residual), and a chronology which has had the pooled model of autocorrelation reincorporated into it (arstan) have been computed by programs ARSTAN and TURBO (TURBO developed by E.R. Cook).

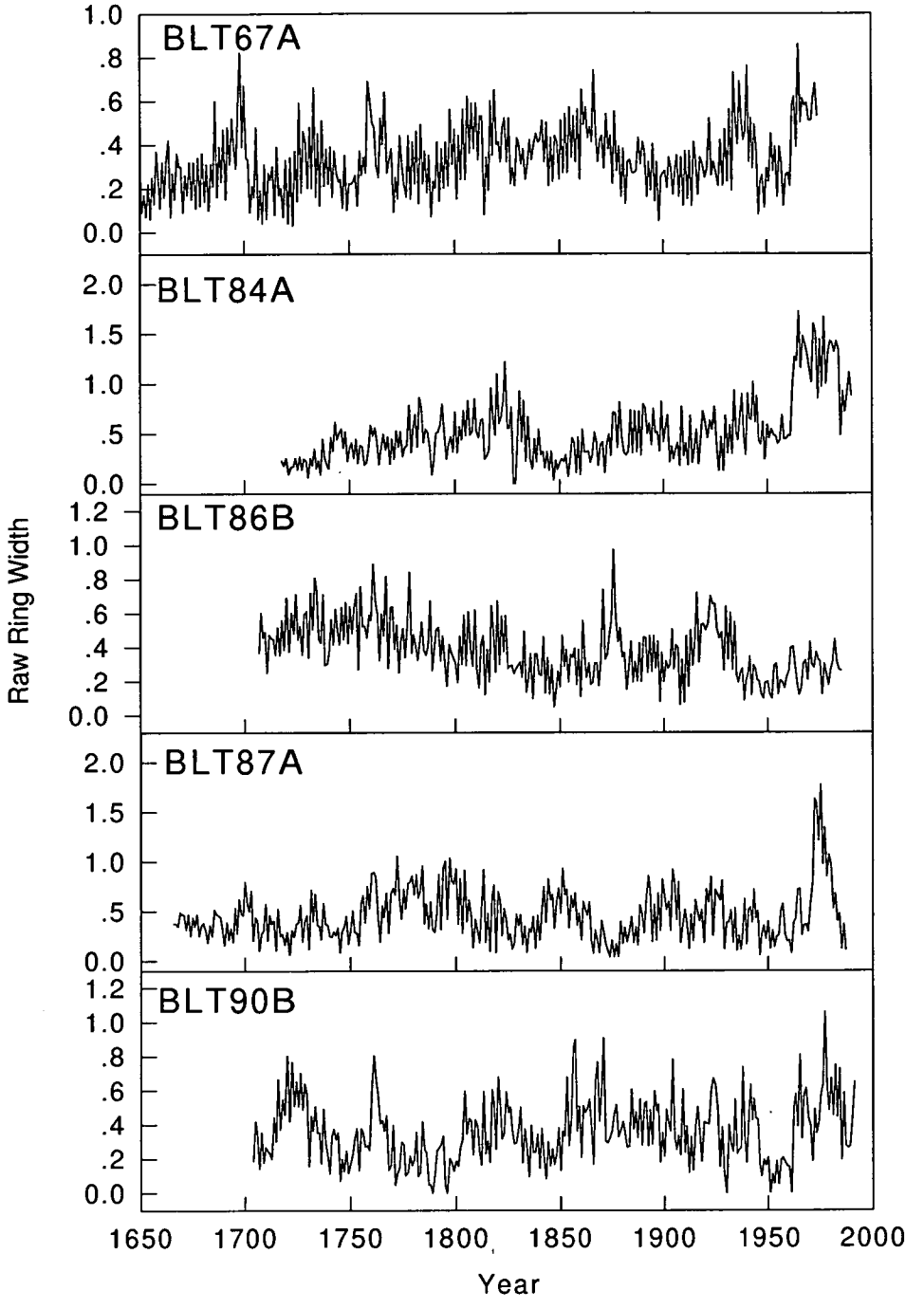

Figure 3.2: **Five samples from BLT_E showing different raw ring–width patterns. For many samples, a simple deterministic detrending of the series would result in dramatic over- or under-prediction for different time periods. Each sample shown here is shown over its entire measured length. The only sample which resembles the classic negative exponential growth trend is BLT86B**

In an attempt to minimise the problems that the 'segment length curse' introduces, short series of less than 100 years were discarded for most chronologies, excepting those of limited lengths that were created from living specimens only: $PILL_M$, $FISH_M$, FC_M and ARM_M.

3.2.4 Chronology analysis

3.2.4.1 Frequency domain analysis of chronologies

As an initial step, prior to estimation of the spectra, the autocorrelation coefficients of each chronology were calculated out to 20 lags in order to provide an initial indication of the autocorrelation structure of each series in relation to other series.

Following this analysis, a more detailed examination of the frequency domain characteristics of two series from each of East, West and Southwest regions was carried out. Sites in the Mersey, with the exception of KOA_M, were considered to be of too short a duration to yield information on relatively low frequency components present in ring–width data. In the East and West the longest series, RFR_E, BLT_E, MUR_W and RCS_W, were selected. In the Southwest, SPR_S and LCR_S were chosen. Sample depth for $CLAY_S$ was considerably poorer than either of these chronologies over most of its range. For the spectral analyses of the regional series, six data tapers were applied to the spectrum, each with a time-frequency bandwidth product of four. Thomson (1982) shows the form of the six tapers used. The use of six data tapers resulted in 12 degrees of freedom. Periods of analysis were 1300–1994 for BLT_E and RFR_E, 1590–1994 for MUR_W, and RCS_W, 1640–1994 for SPR_S and LCR_S.

3.2.4.2 Intersite comparisons

Intersite correlations

Correlations between all sites for the entire common length of both records were computed for residual chronologies (detrended and autoregressively modelled chronologies) in order to gain an impression of crossdating over the

entire period. However, a correlation obtained over the whole period may not reflect crossdating over smaller increments of time. To examine this, one chronology from each of the East (BLT_E), West (MUR_W) and Southwest (SPR_S) chronologies was chosen as a basis for comparison with all other chronologies over time. Each of these three analyses examined the correlation between successive 50-year periods in common between, for example, BLT_E and all other chronologies.

Principal Component Analysis

A PCA was conducted using the arstan chronologies (detrended, pooled model of autocorrelation reincorporated into the chronology) over the maximum length period containing the maximum number of sites, namely, 1750–1994.

The first two PCs of the unrotated PCA were significant (section 3.3.2.3), with eigenvalues greater than one (Craddock 1973). A Varimax rotation of these PCs was performed.

Cross-spectral analysis

Coherencies between the sites selected for spectral analysis were calculated using the MTM approach. In the first instance, coherency between sites in the same region was calculated, followed by coherency between sites from different regions. In this latter case, an average coherency between different regions was also calculated. For all analyses, six tapers, with a time-frequency bandwidth product of four were applied across the spectrum, resulting in 12 degrees of freedom. Time periods analysed were: 1300–1994 for the East, 1590–1994 for the West, and 1640–1994 for the Southwest. These time periods were those for which sample depths of each chronology in a region exceeded 10. Time periods of interregional analyses were limited by the shorter of the two regional chronologies used.

3.2.4.3 Comparison with *Lagarostrobos franklinii*

LaMarche (1974a) found that low frequency oscillations of high and low elevation sites (*Pinus longaeva*) were negatively correlated, while the high frequency oscillations were positively correlated. It is possible that such differences may also be evident in Tasmania, and that not all important differences between *Lagarostrobos franklinii* and *Phyllocladus aspleniifolius* will be directly species related. Buckley's (1997) discussion of the differences between HIGH and LOW *L. franklinii* sites is suggestive. The use of both a HIGH and a LOW *L. franklinii* site for comparison with *P. aspleniifolius* could therefore aid in the interpretation of apparent differences between the two species. Although this approach considers two variables (altitude and species differences) rather than just one, it must be recognised that differences in slope, aspect, soil type and other environmental variables have not been taken into account. It may be the case that one or several of these variables is the key to the differences reflected in ring–width series.

The simplest comparison between two series is to overlay them one on another. This approach was used as an initial comparison of the three regional *Phyllocladus aspleniifolius* chronologies and the MTREAD (Mt Read) and SRT (Stanley River) *Lagarostrobos franklinii* chronologies. MTREAD is at 950 m ASL, and SRT lies at 225 m ASL (Buckley 1997). The use of these two sites, at opposite extremes of Buckley's elevational gradient allows a preliminary sketch of the role of the two factors of elevation and species differences in the creation of disparities between the two sets of chronologies.

In addition to overlay plots, coherency spectra of the three regional *Phyllocladus aspleniifolius* chronologies and the HIGH and LOW *Lagarostrobos franklinii* were examined. Because coherency between *P. aspleniifolius* sites in the same region was high (Figure 3.25, and sections 3.3.3, 3.3.6 and 3.3.7 below), a regional chronology for each of these regions was constructed using those chronologies analysed in the cross-spectral analyses. These three regional chronologies were then used in the cross-spectral analyses with the higher elevation MTREAD and the lower elevation SRT *L. franklinii* chronologies. The time periods of the new regional chronologies were 1300–1994 East, 1590–1994

West, and 1580–1994 Southwest. Once again, only that portion of each chronology containing more than 10 samples was used.

For the calculation of all coherency spectra between the two species, six data tapers, each with a time-frequency bandwidth product of four were applied to the spectrum and the time periods analysed were restricted by the lengths of *P. aspleniifolius* chronologies. Because no confidence limits were provided for phase estimates, the point estimates of phase have not been utilised in this analysis. It is probable that such intervals would be quite wide (E. Cook, Lamont–Doherty Geological Earth Observatory, pers. comm.). This analysis is therefore based on the coherency spectra alone.

3.3 Results and discussion

3.3.1 Chronology description

Each chronology, along with sample depth and average segment length, is shown in Figures 3.3–3.17. In many cases it can be seen that standardisation has significantly altered the raw chronology and has removed what appeared to be low frequency variation.

3.3.1.1 Signature years

Although many key years differ between regions, some key years are common between regions. The frequency of signature rings more than 2σ below the mean is greater for the Southwest than for any other region and least for the East, indicating that the Southwest region is the most frequently stressed and the East the least frequently stressed of the four regions. Agreement between regions is greater in the case of narrow rings than for wide rings (Tables 3.1 and 3.2).
The large number of different key years indicates that differences between regions do exist.

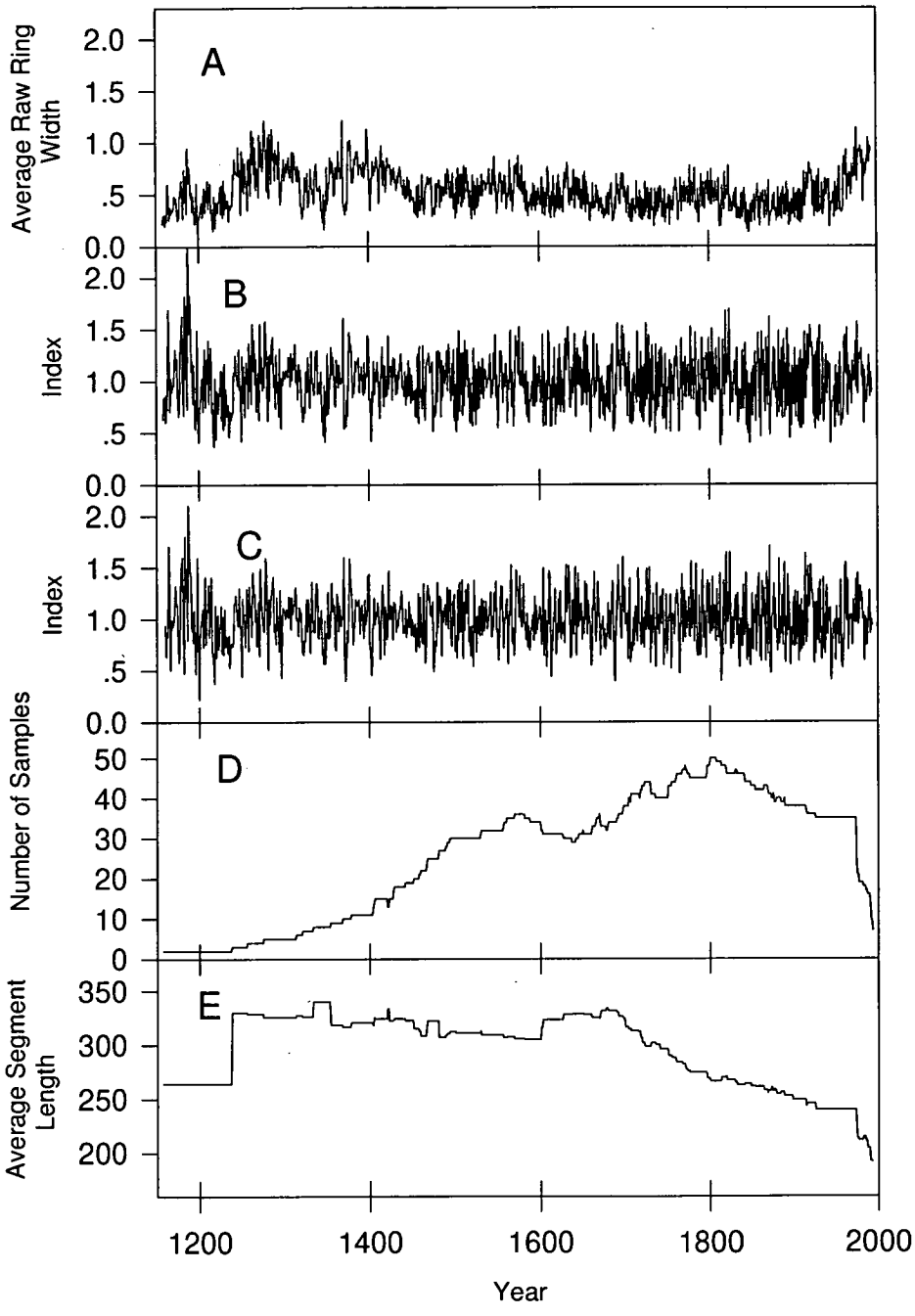

Figure 3.3: **Blue Tier (BLT_E) chronology: A. mean raw ring–width chronology; B. arstan chronology; C. residual chronology; D. sample depth; E. average segment length. Time span of chronology is 1156–1994. Standardisation has emphasised the late 1100s as a period of high growth while at the same time de-emphasising the increased growth in the latter decades of the twentieth century as seen in the RAW chronology. Average segment length and the number of samples included in the chronology are inversely related**

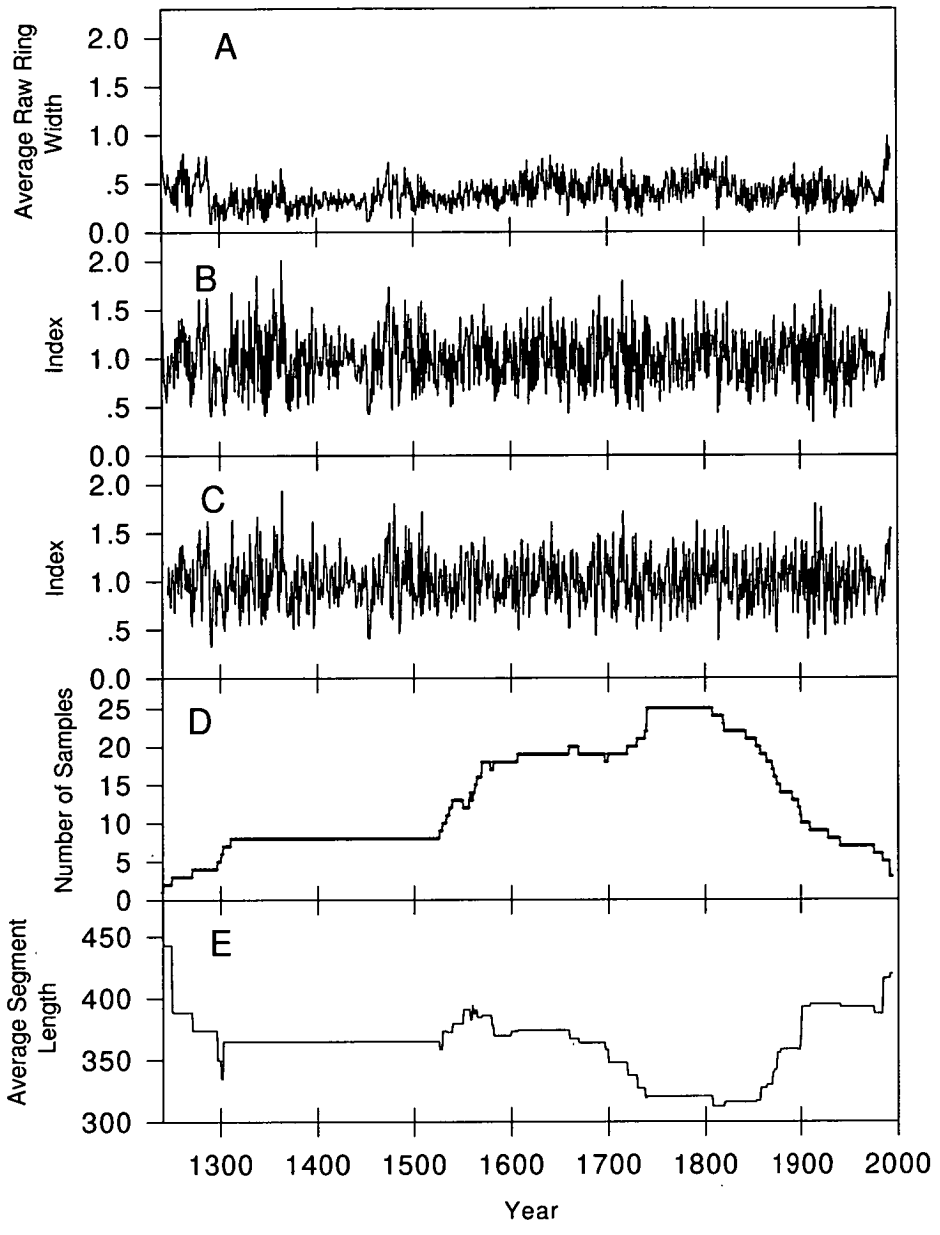

Figure 3.4: **Ralph's Falls Road (RFR_E) chronology: A. mean raw ring–width chronology; B. arstan chronology; C. residual chronology; D. sample depth; E. average segment length. For this chronology standardisation has removed what appeared to be low frequency variability on the order of 100–150 years. The effects of low sample depth in the earliest years have been de-emphasised by standardisation. The inverse relationship between sample depth and average segment length is particularly clear for the 1700–1900 time period. The fall in average segment length is due to the inability to crossdate over this period due to severe ring compression. Chronology time period is 1241–1994**

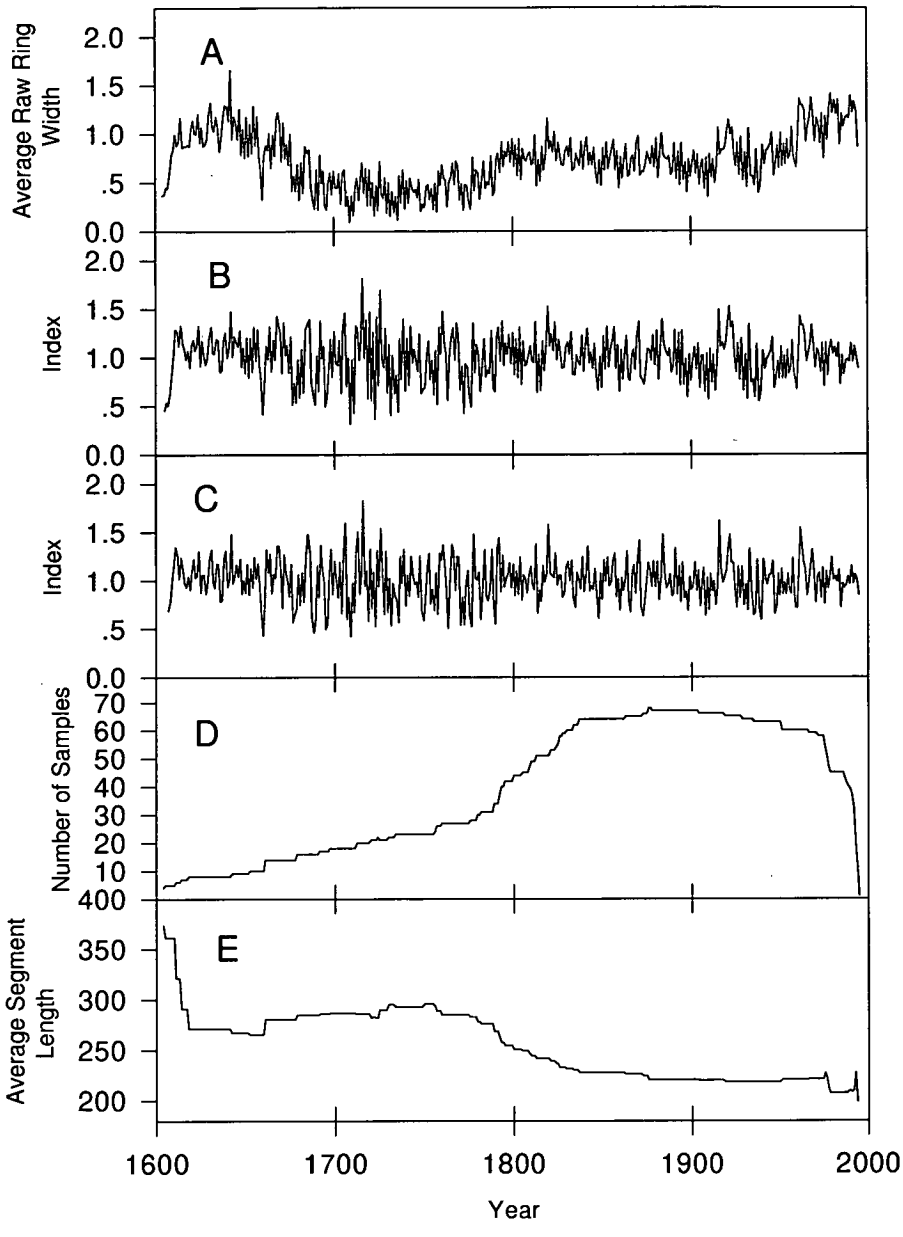

Figure 3.5: **Ben Ridge Road (BEN_E) chronology: A. mean raw ring–width chronology; B. arstan chronology; C. residual chronology; D. sample depth; E. average segment length. Standardisation has removed juvenile growth effects, and de-emphasised the variability, including the increased growth over the past 50 years evident in the RAW chronology. Once again there is an obvious inverse relationship between sample depth and average segment length. BEN_E spans the time period 1604–1994**

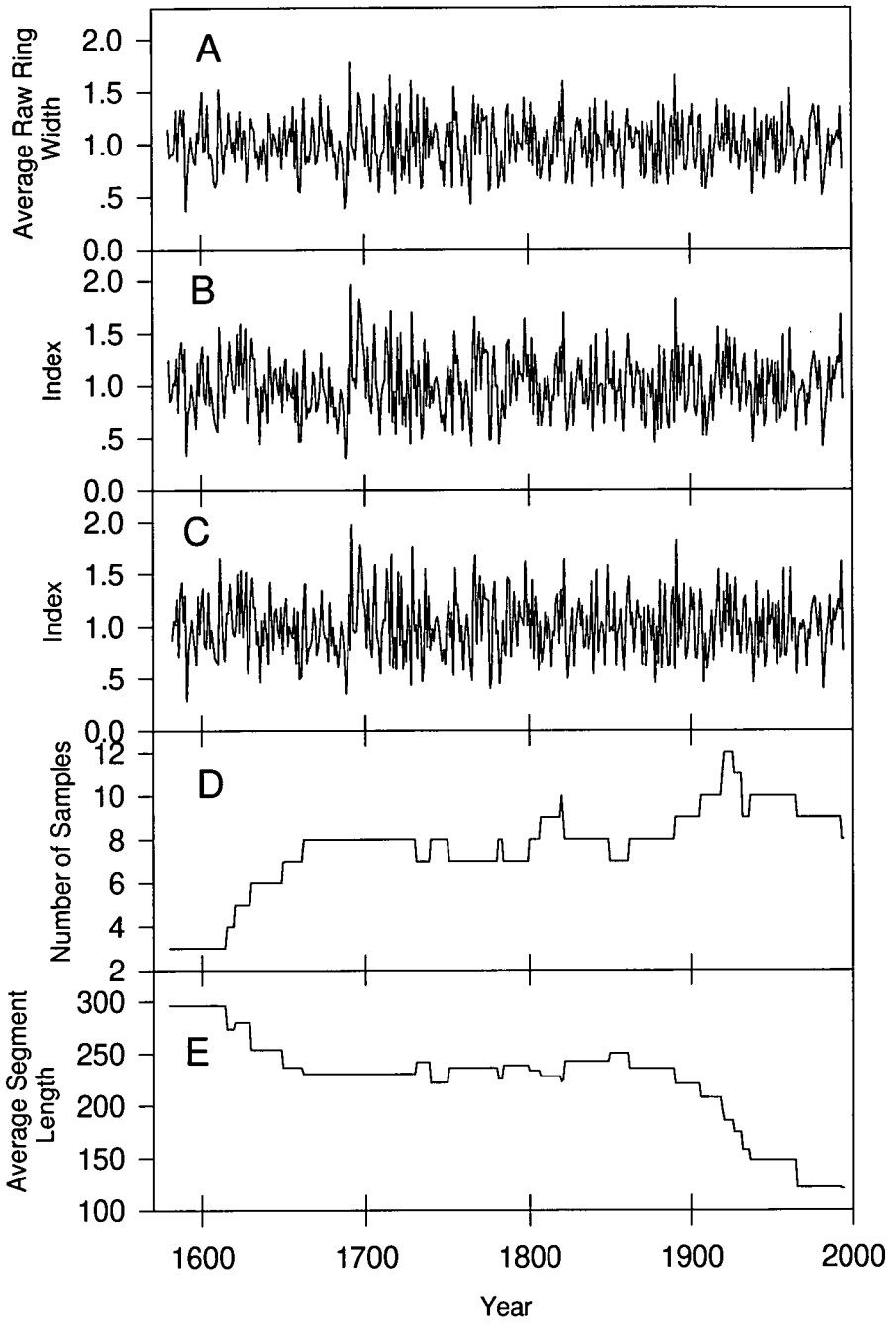

Figure 3.6: **East Shelf Maria Island (ESM_E) chronology: A. mean raw ring–width chronology; B. arstan chronology; C. residual chronology; D. sample depth; E. average segment length. Standardisation has not greatly altered the ESM_E chronology. Time span covered by the chronology is 1580–1994**

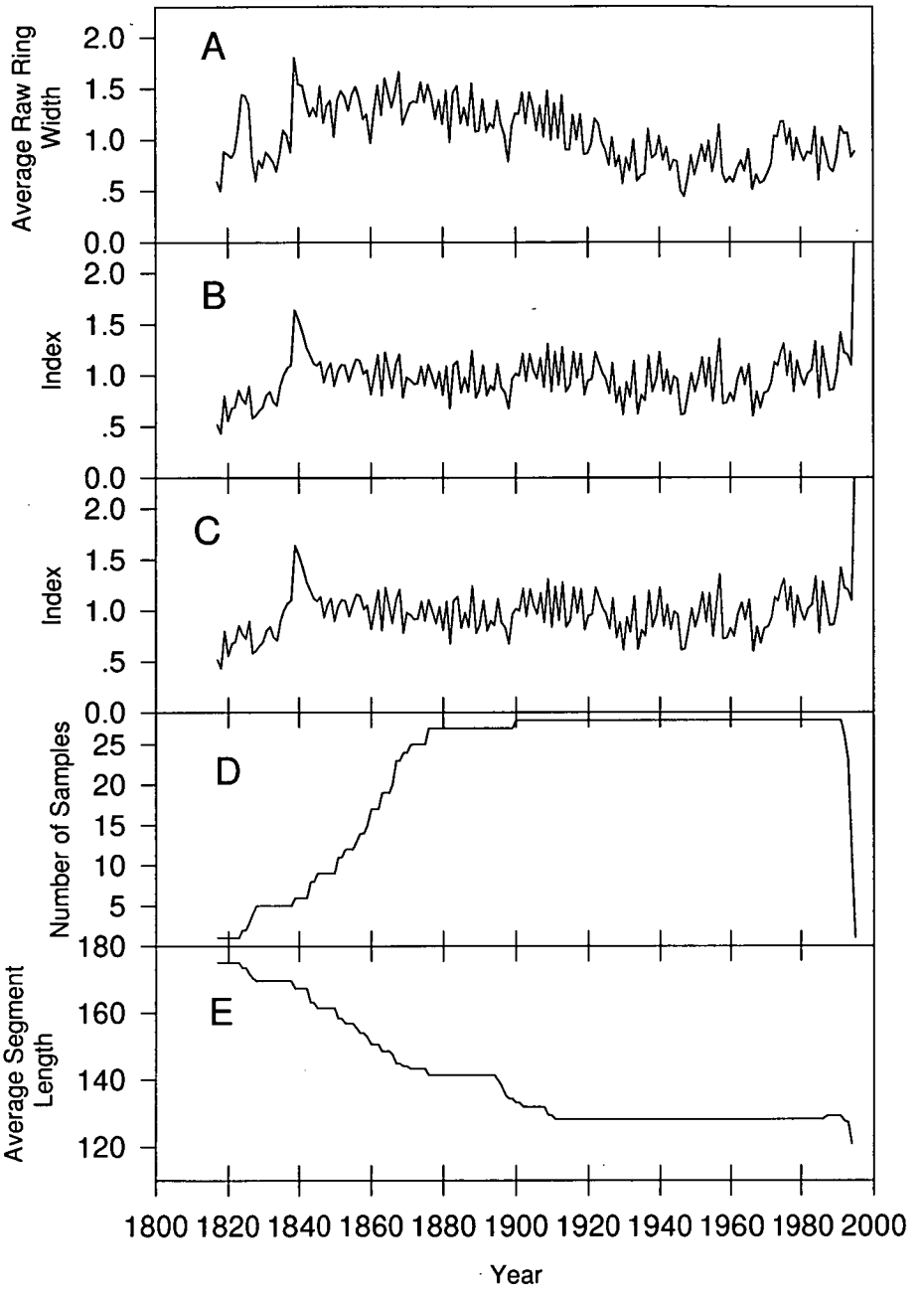

Figure 3.7: **Arm River (ARM_M) chronology: A. mean raw ring–width chronology; B. arstan chronology; C. residual chronology; D. sample depth; E. average segment length. Standardisation has removed variation in the early period which may well have been due to juvenile effects of individuals with staggered starting dates. ARM_M is a relatively young site which has been cleared in the past. Time span of the chronology is 1819–1994**

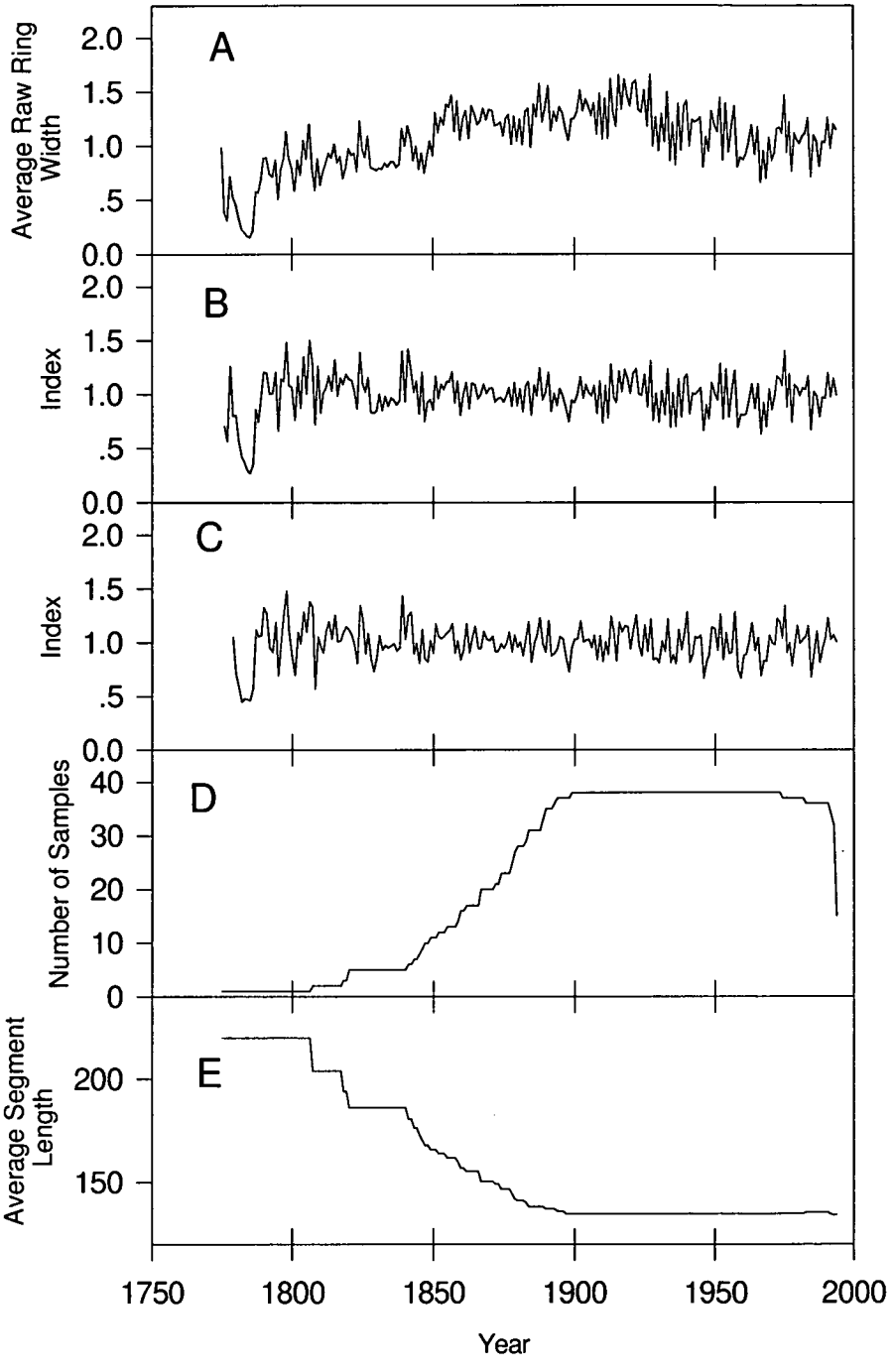

Figure 3.8: **February Creek (FC_M) chronology: A. mean raw ring–width chronology; B. arstan chronology; C. residual chronology; D. sample depth; E. average segment length. Standardisation has de-emphasised periods of both high and low growth. The chronology covers the period 1776–1994**

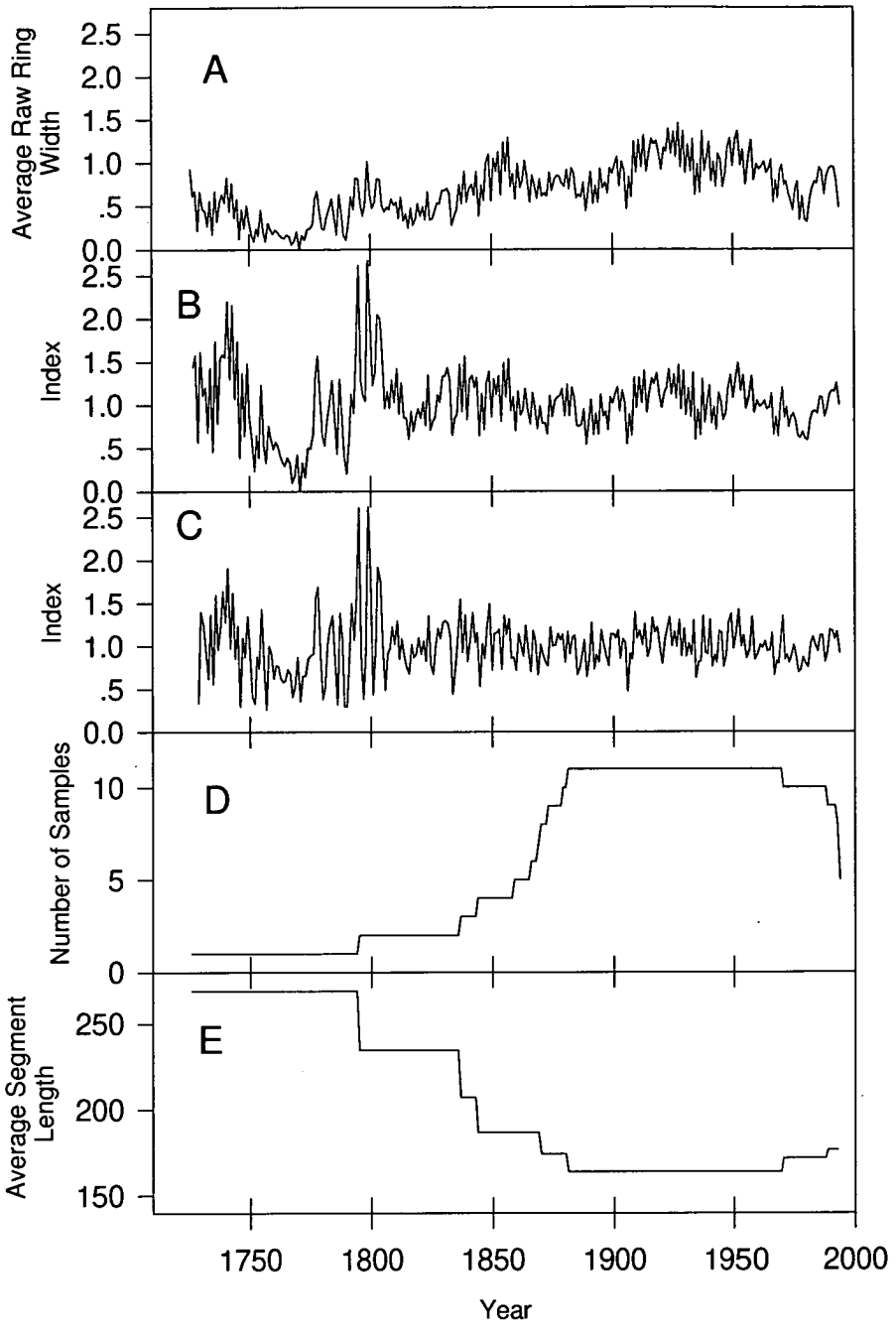

Figure 3.9: **Fisher River ($FISH_M$) chronology: A. mean raw ring–width chronology; B. arstan chronology; C. residual chronology; D. sample depth; E. average segment length. Standardisation has had the effect of emphasising features at the beginning of the chronology while de-emphasising later variation. The chronology covers the period 1726–1994**

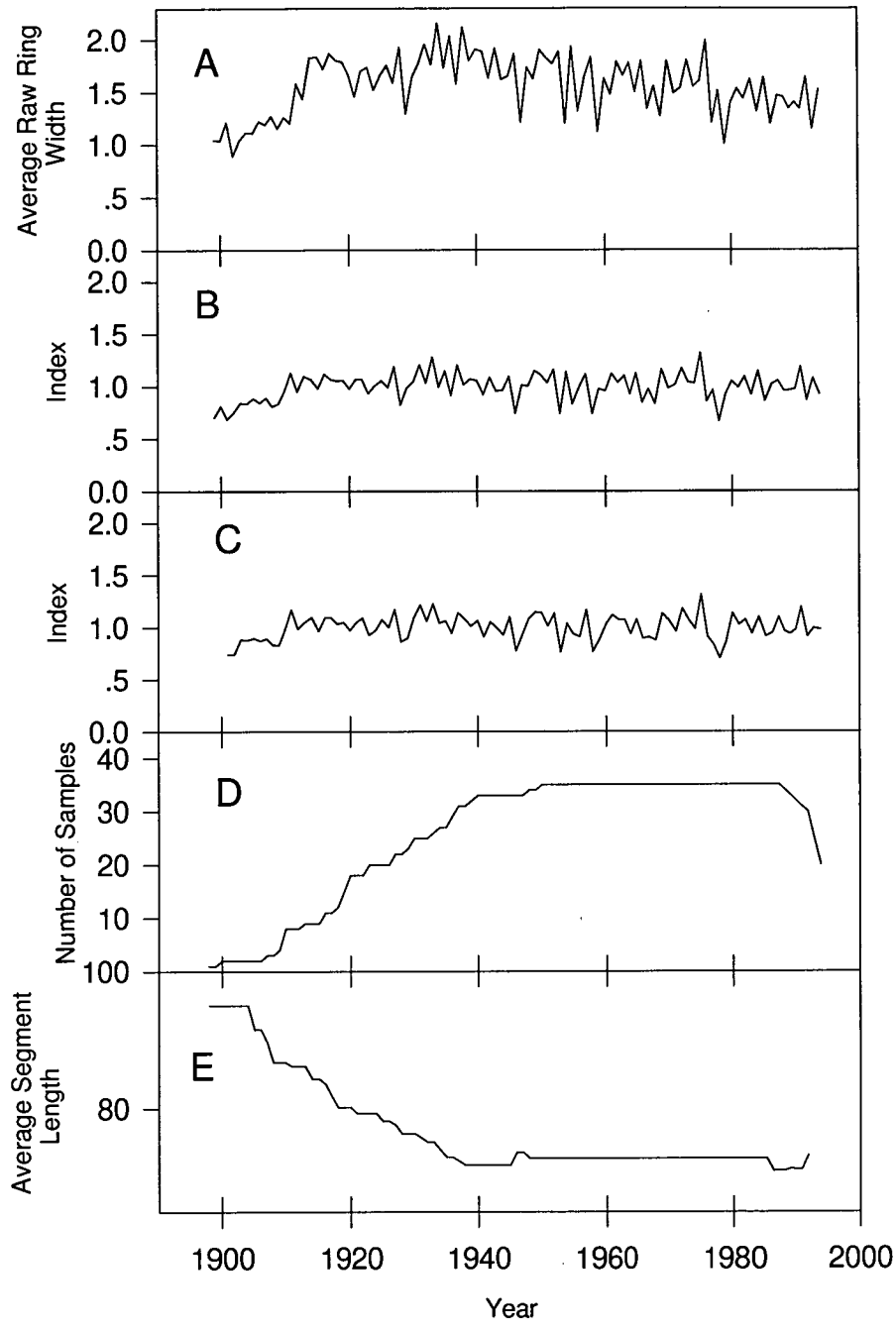

Figure 3.10: **Mt Pillinger ($PILL_M$) chronology: A. mean raw ring–width chronology; B. arstan chronology; C. residual chronology; D. sample depth; E. average segment length. The 'shape' of the Mt Pillinger chronology, the youngest of the 15 sites, has not been substantially altered by the standardisation process. However, the amplitude of the series has increased. Time span of the chronology is 1899–1994**

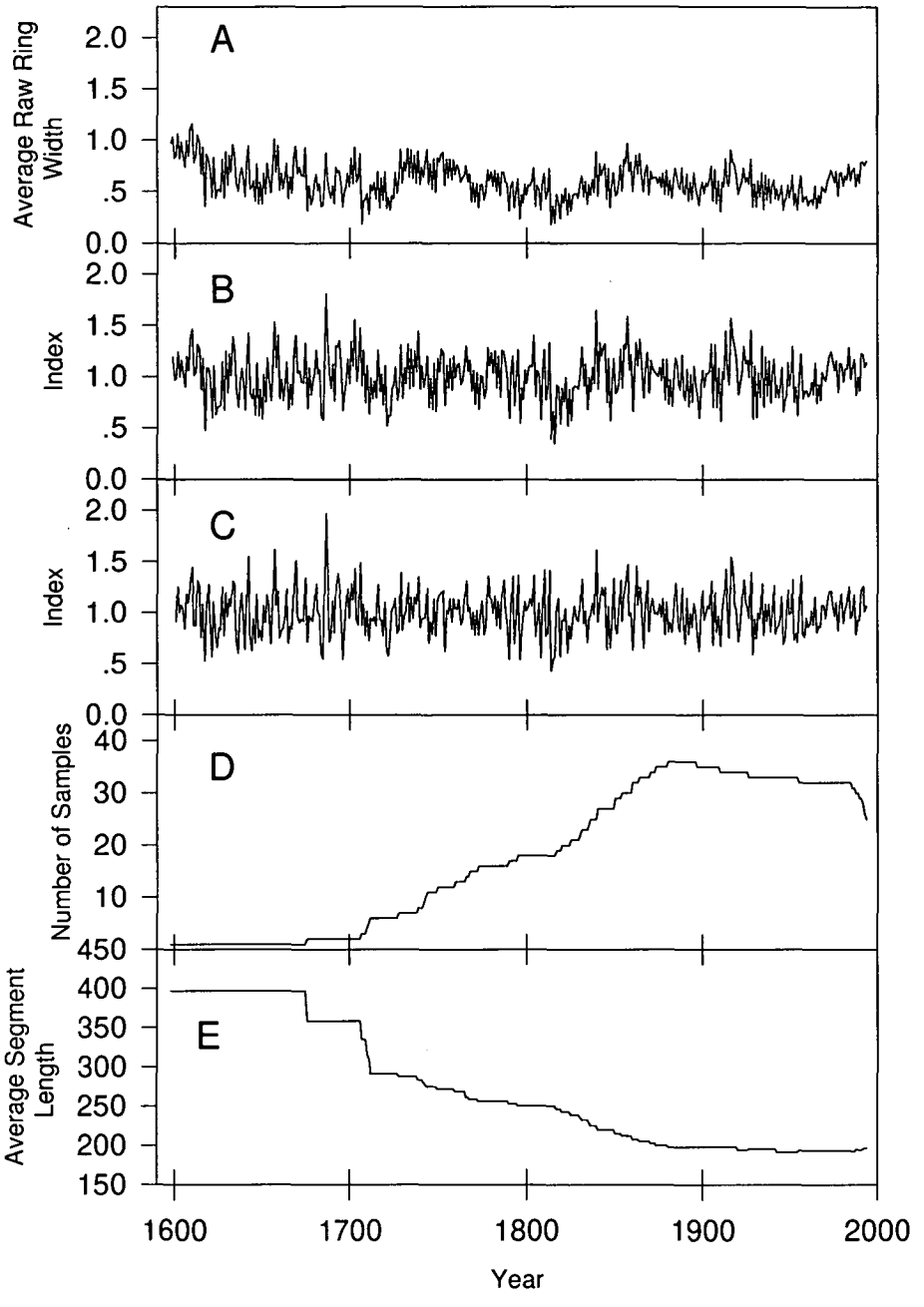

Figure 3.11: **Kia Ora (KOA_M) chronology: A. mean raw ring–width chronology; B. arstan chronology; C. residual chronology; D. sample depth; E. average segment length. Kia Ora is the longest of the Mersey chronologies, and standardisation has had the effect of removing some of the low frequency variation. Again, the inverse relationship between sample depth and average segment length is readily apparent. The chronology covers the period 1598–1994**

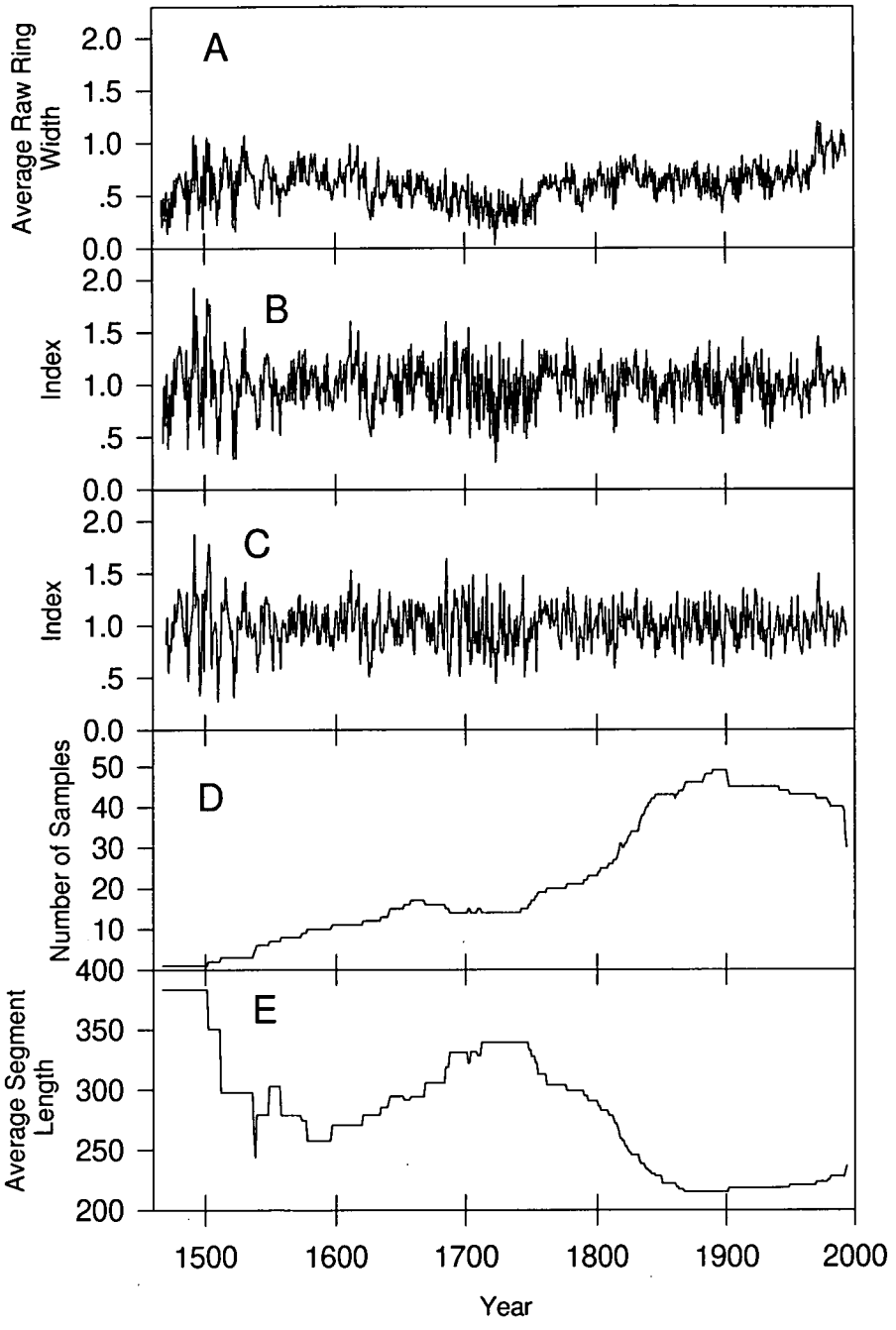

Figure 3.12: **Race Course Spur (RCS_W) chronology: A. mean raw ring–width chronology; B. arstan chronology; C. residual chronology; D. sample depth; E. average segment length. The standardisation of samples has resulted in the de-emphasis of the increased growth apparent in the RAW chronology and, while also de-emphasising low growth in the early 1700s has resulted in increased variation at about this time. Time period of the chronology is 1467–1994**

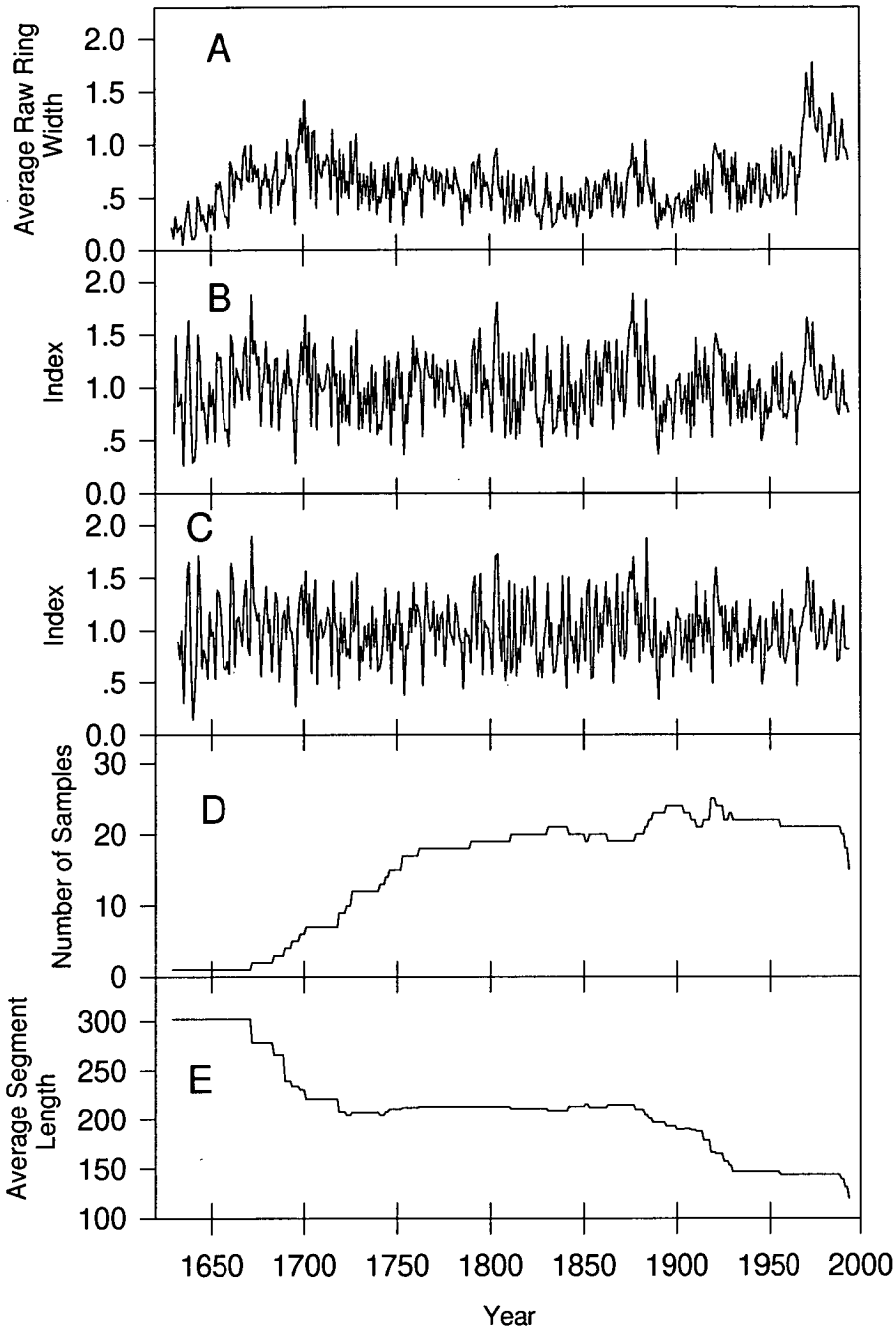

Figure 3.13: **Wey River (WEY_W) chronology: A. mean raw ring–width chronology; B. arstan chronology; C. residual chronology; D. sample depth; E. average segment length. Standardisation has had the effect of increasing the variability seen in the early years of the chronology and of de-emphasising the increased growth of the past 40 years seen in the RAW chronology. Time span of chronology is 1629–1994**

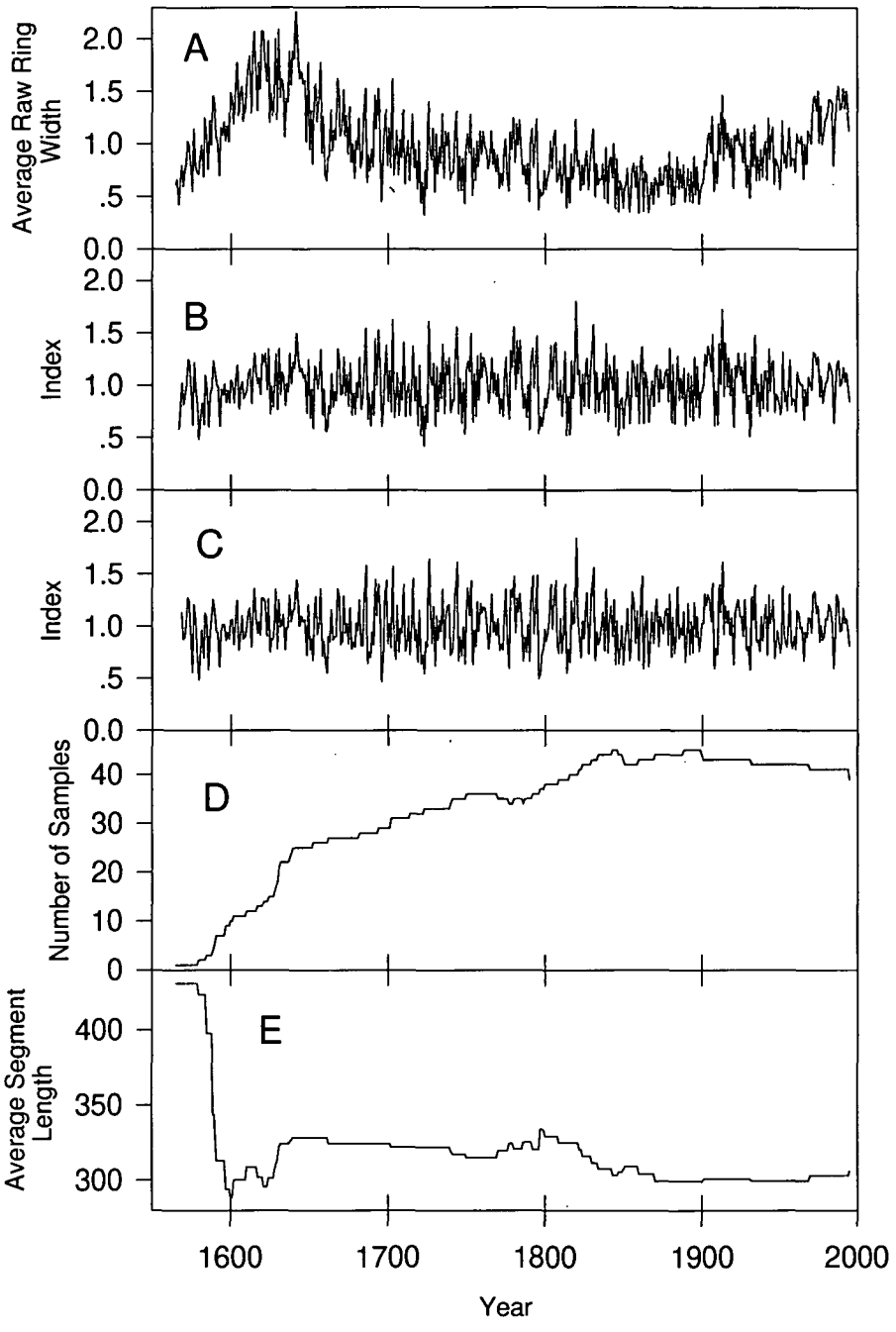

Figure 3.14: **Mt Murchison (MUR_W) chronology: A. mean raw ring-width chronology; B. arstan chronology; C. residual chronology; D. sample depth, E. average segment length. The Mt Murchison chronology has been dramatically affected by standardisation with early growth being de-emphasised as well as the later increased growth apparent in the RAW chronology. Chronology time span is 1565–1995**

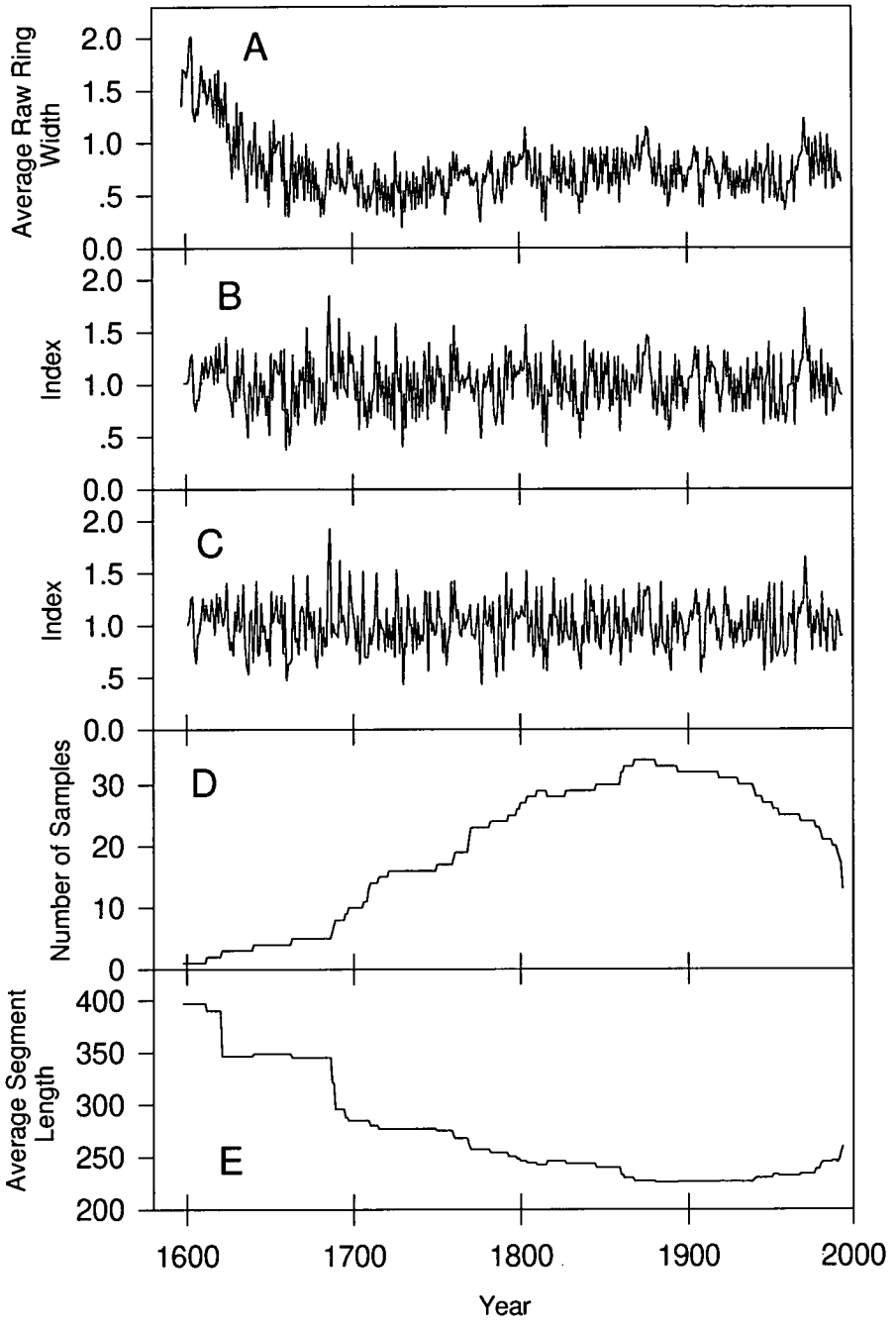

Figure 3.15: **Lower Cole Road (LCR_S) chronology: A. mean raw ring–width chronology; B. arstan chronology; C. residual chronology; D. sample depth; E. average segment length. The high growth in the early years of the chronology has been removed by standardisation. The chronology covers the period 1598–1994**

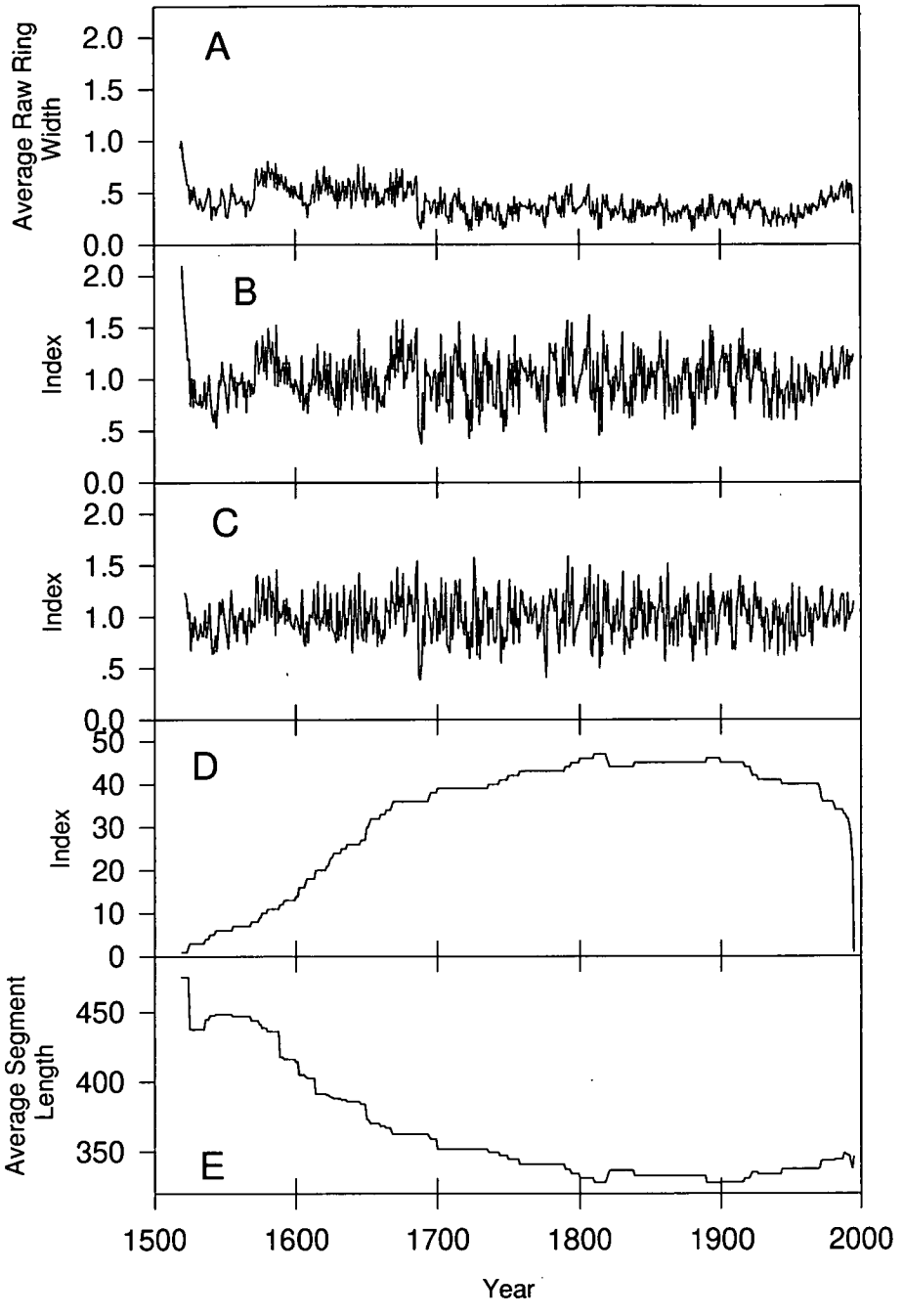

Figure 3.16: **Scott's Peak Road (SPR_S) chronology: A. mean raw ring–width chronology; B. arstan chronology; C. residual chronology; D. sample depth; E. average segment length. Standardisation has had the effect of downplaying low and high growth periods to some extent but the increased growth of the current century has not been removed. Time period of the chronology is 1519–1994**

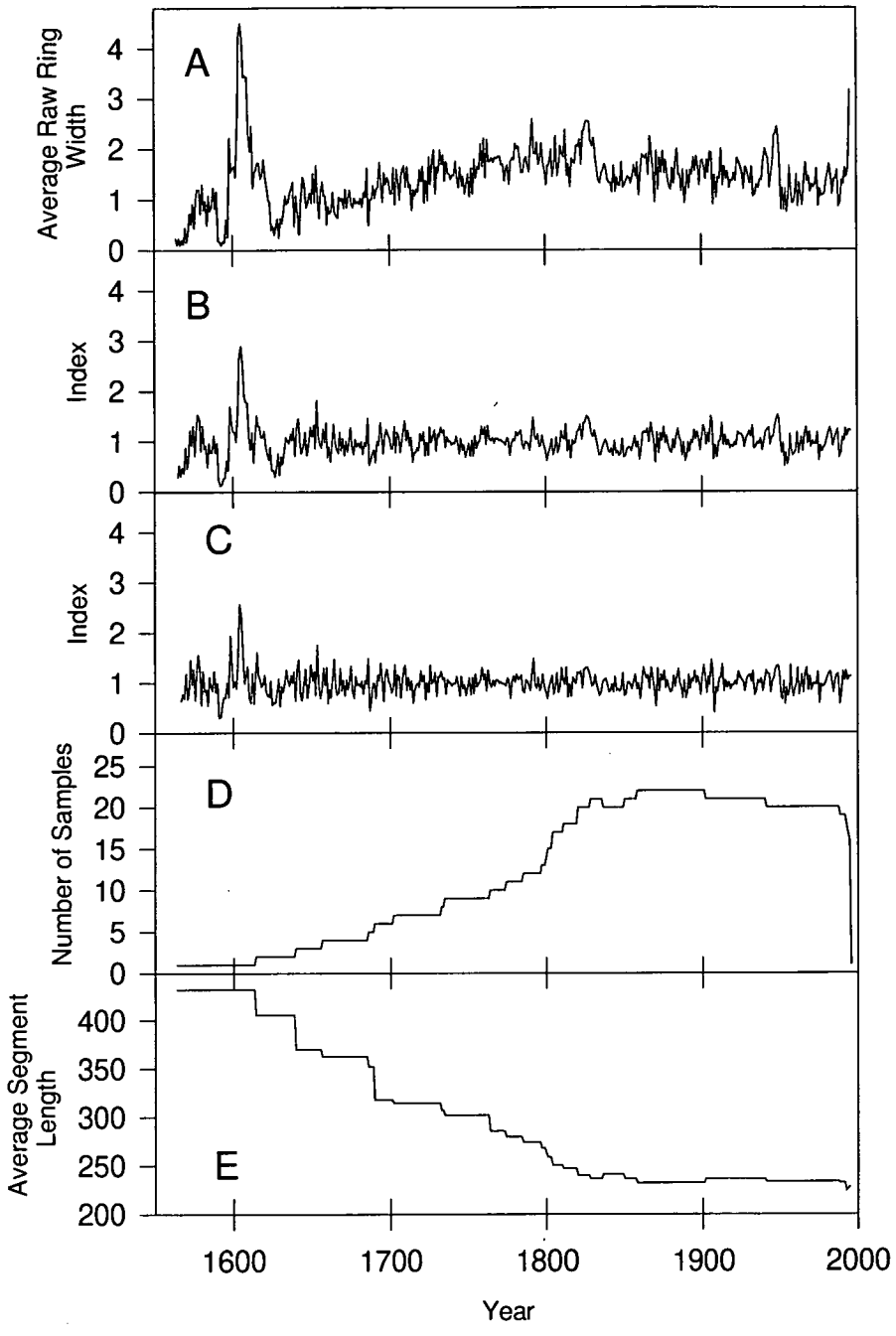

Figure 3.17: **Clayton's Lagoon ($CLAY_S$) chronology: A. mean raw ring–width chronology; B. arstan chronology; C. residual chronology; D. sample depth; E. average segment length. Standardisation has not removed the large spike in the early 1600s. This spike is likely to be the result of an aberration in a single specimen. The chronology covers the period 1564–1995**

East												
1271	1281	1290	1296	1297	1321	1324	1330	1336	**1347**	1349	1351	1353
1360	1361	1371	1372	1373	1375	1376	1381	1396	1413	1455	1457	1459
1466	1467	1476	1477	1478	1479	1485	1501	1503	1505	1510	1522	1558
1563	1570	1586	1588	1589	1593	1605	1608	1613	1619	1636	1637	1640
1643	1652	1660	1661	1681	1687	**1688**	1689	1699	1704	1709	1711	1721
1723	1732	1735	**1736**	1745	1749	1754	1758	1764	1771	1773	1776	1777
1782	1785	1789	1790	**1814**	1816	1828	1834	1835	1847	1848	1850	1860
1865	1866	1869	1873	1882	1892	1898	1908	1910	1912	1914	1926	1928
1930	1932	1935	1936	**1938**	1939	1946	1951	1958	1959	1960	1971	1985
Mersey												
1721	1722	1727	1745	1754	1771	1773	1776	1785	1790	**1793**	**1796**	1805
1811	**1814**	1815	1816	**1819**	1823	1825	1834	1845	1860	**1866**	1869	1892
1898	1906	1910	1928	1930	1934	1941	1946	1953	1955	1958	1959	1966
1978	1985	1988										
West												
1540	1541	1542	1552	1558	1586	1593	1608	1613	1619	**1627**	**1630**	1635
1650	1652	1660	**1661**	1677	1683	1687	**1696**	1704	1707	**1711**	1714	1719
1725	1730	1736	1740	1745	1747	1749	1754	1764	1771	1773	1777	1786
1796	1801	1808	1811	**1814**	1816	1828	1832	1845	**1847**	1850	1854	1860
1872	1880	1882	1889	1890	**1892**	**1898**	1908	1910	**1920**	1930	1934	**1946**
1985												
South												
1541	1542	1552	1565	1568	1571	1606	1608	1628	**1630**	**1632**	1640	1658
1663	1667	**1678**	**1687**	**1688**	1689	**1691**	1696	1711	**1721**	**1723**	**1725**	1728
1736	1745	1747	1749	1754	1758	1776	**1777**	1790	1796	1808	1809	1811
1816	1823	1835	**1836**	1838	1840	1854	1866	**1869**	1872	1880	1882	1889
1910	1920	1934	1936	**1946**	**1950**	1958	1966	**1976**	1989			

Table 3.1: **Regional signature rings. To generate this particular listing, all samples which crossdated within a region were used to develop a single chronology for that region. The dates shown are 1σ below the mean; dates in bold text are 2σ below the mean. Sample depth of chronologies is at least five for the time span considered. In most cases, this minimum sample depth is exceeded. Years in common between the three regions of longest duration, East, West and Southwest are 1608, 1661, 1687, 1711, 1723, 1745, 1754, 1777, 1790, 1814, 1816, 1866, 1908, 1910 and 1946. The years 1898 and 1908 are two very prominent pointer years in the *Lagarostrobos franklinii* chronologies. Only the West chronology shows the ring-width of 1898 to be more than 2σ below the mean**

East											
1241	1509	1604	1685	1716	1726	1729	1778	1784	1820	1824	1842
1871	1916										
Mersey											
1813	1839										
West											
1657	1686	1703	1716	1726	1744	1795	1820	1957			
South											
1555	1645	1686	1703	1726	1792	1831	1952	1957			

Table 3.2: **Wide marker rings for the four regions, generated in same manner as for Table 3.1. Ring widths for dates shown are 2σ above the mean. Sample depth of chronologies is at least five for the years considered. In most cases this minimum sample depth is exceeded. The year 1726 occurs as a wide ring for all regions except the Mersey**

3.3.1.2 Summary statistics

Summary statistics for regional and individual arstan chronologies are presented in Table 3.3. The longest chronologies are those of East sites, Blue Tier and Ralph's Falls Road. Longest average segment lengths are observed for RFR_E, SPR_S, MUR_W and BLT_E, and greatest maximum age occurs at these same sites and RCS_W. Figures 3.3–3.17 clearly show, as expected, there is a strong inverse relationship between average segment length and sample depth for shorter duration chronologies consisting solely of living samples. Longest records within these chronologies cover the whole period, with shorter records covering only the latter part of the period. In chronologies such as BLT_E, RFR_E and BEN_E (in which disc samples from dead trees are used) this inverse relationship is not as apparent. For RFR_E, a sudden decline in average segment length occurs in the eighteenth century. This is most probably due to severe compression of ring widths in many samples encountered in the 1710–1760 time period. As a result, this section (1710–1760) could not be dated, or crossdated, in these specimens and was therefore not used, meaning that segment lengths have been significantly shortened.

With regard to the segment length curse discussed above, the BLT_E chronology has many samples covering the earlier part of the chronology time span which end by about 1650–1700. In contrast, the majority of those samples covering the later period generally do not start until about 1650–1700, meaning that, in general, there is little overlap of samples containing the period 1650–1700. This in turn suggests that low frequency climatic change in the order of 400 or more years can not be reliably resolved from this chronology, regardless of the standardisation technique employed or individual sample lengths (referred to above). In the case of RFR_E, the inability to date a large proportion of samples covering the 1720–1850 period has resulted in a considerably reduced sample depth over this time period, which once again imposes a limit on the reliability of low frequency change or oscillations in this series. In this context some consideration should be given to the segment length curse when working in the frequency domain and considering low frequencies.

With reference to Table 2.1, those sites which experienced most rapid growth are generally located at lower altitudes and/or are disturbed mixed forest sites. Sites with higher median sample ages and with a greater maximum age of individual samples are, predictably, those sites with the longest chronologies (Table 3.3). Highest maximum age, or longest segment of a sample used in developing a chronology, occurs at the oldest site, RFR_E; lowest maximum age and shortest average segment length occurs at the youngest site, $PILL_M$. The greatest gap between maximum and median age occurs at RFR_E.

The presence of a canopy layer above the rainforest layer, and hence a greater dependence on diffuse radiation, does not appear to have made a large difference in growth rates at the LCR_S site compared to other sites (see Tables 2.1 and 3.3). The high altitude sites on the east coast, BLT_E and RFR_E experience the lowest growth rates with the exception of the implicate rainforest site SPR_S. The low rate of growth is possibly due to low soil fertility.

Table 3.3 reports average ring width for each site measured, the narrowest average ring-widths occurring at SPR_S and RFR_E. At $IRON_S$, for which no chronology could be developed, ring are generally narrower than at either RFR_E or

Chronology	*N*	*Period*	*ASL*	*Ring width*	*Max. age*	MS_x	*EPS*	$\overline{R}$	*%PC 1*	*AR*	*%AR*
BLT_E	83	1157–1994	258.70	0.523	462	0.51	0.939	0.47	52.55	2	11.80
RFR_E	25	1241–1994	358.60	0.426	617	0.32	0.910	0.43	40.30	2	16.40
BEN_E	49	1604–1994	210.90	0.828	374	0.38	0.932	0.55	47.47	2	14.30
ESM_E	19	1580–1994	166.70	0.902	386	0.34	0.677	0.47	60.76	2	2.40
$PILL_M$	35	1898–1994	70.60	1.623	95	0.15	0.924	0.47	44.11	2	17.40
ARM_M	37	1817–1994	128.20	1.139	172	0.21	0.876	0.44	35.45	2	19.20
$FISH_M$	11	1726–1994	146.40	0.908	269	0.34	0.677	0.42	42.38	2	18.40
FC_M	34	1775–1994	134.90	1.190	220	0.21	0.946	0.48	46.74	3	18.90
KOA_M	40	1598–1994	185.90	0.604	397	0.28	0.942	0.44	38.84	2	13.10
RCS_W	48	1467–1994	222.50	0.673	456	0.34	0.880	0.46	39.18	2	17.40
WEY_W	34	1629–1994	165.50	0.742	302	0.37	0.917	0.50	46.58	2	6.50
MUR_W	51	1565–1995	274.80	1.005	431	0.42	0.916	0.45	39.50	2	8.80
LCR_S	35	1598–1994	224.00	0.759	397	0.42	0.896	0.45	42.76	2	10.70
SPR_S	49	1519–1994	319.90	0.400	475	0.26	0.930	0.46	43.94	2	11.70
$CLAY_S$	23	1564–1995	228.30	1.759	432	0.32	0.837	0.35	35.21	2	12.70
$IRON_S$	17	NO CHRONOLOGY									

SPR_S. These trees are also subject to severe ring compression and as a consequence, dating is not possible. From ring counts, the minimum age of the site appears to be at least 300–400 years.

A large variation in sample size is evident and this largely reflects the number of rejected samples, as three cores have been taken from most trees, or three radii dated for most discs. Discarding samples less than 100 years in length has also limited the number of specimens in each chronology. At the $FISH_M$ site, only 11 trees have been cored, and a large proportion of cores have been rejected due to lack of crossdating. This chronology has not been used extensively in further analysis. At RFR_E, several instances of compression around the circumference of a single tree means that a sequence broken into several segments contains none of more than 100 years. In such instances all segments have been discarded, consequently reducing sample size. The use of longer segments, although at the expense of sample depth, has served as a first step in ameliorating the effects of the segment length curse discussed above.

A further striking feature of the chronologies is the occurrence of increased growth (prior to data standardisation) for all individual West chronologies (Figures 3.12A–3.14B) as well as for BLT_E (Figure 3.3A), BEN_E (Figure 3.5A), KOA_M (Figure 3.11A), LCR_S (Figure 3.15A), and SPR_S (Figure 3.16A) in the most recent decades. This has been removed by standardisation for most sites, the most notable exception being SPR_S. In all cases, the effects of low sample depth at the beginning of the chronologies have also been removed. A spike in the $CLAY_S$ chronology around 1600, not removed by standardisation, appears to be an aberration in the growth of a single specimen. Neither of the remaining Southwest chronologies depict the same feature.

AR(2) is the dominant mode of autoregression in the chronologies and its selection is supported by a visual examination of the wood (see Chapter 6). The percentage of variance due to autoregression varies considerably: from 2.49% for WEY_W to 19.2% at ARM_M. Associated with the selection of AR(2) are relatively high MS_x values (Campbell 1980). Coincidentally, highest mean sensitivity occurs for the oldest site, BLT_E, (0.51) and lowest for the youngest site, $PILL_M$ (0.15). Eis *et al.* (1965) have commented that young trees often produce relatively

wide rings in years in which older trees produce relatively narrow rings. This phenomenon should produce low MS_X values for young sites and higher MS_X values for older sites. This is not strictly the case for the *Phyllocladus aspleniifolius* sites, but the three youngest sites do have the lowest values of this statistic (Table 3.3). These three stands are also fairly even aged compared to other sites.

$\overline{R}$ varies from 0.35 at $CLAY_S$ to 0.55 at BEN_E, indicating poorest crossdating at $CLAY_S$, and best at BEN_E. The relatively high $\overline{R}$ for ESM is surprising in view of the difficulties of crossdating material at this site.

Highest *EPS* is attained for FC_M and lowest for ESM_E. Ten of the fifteen sites report an *EPS* greater than 0.9. Wigley *et al.* (1984) have pointed to a threshold of 0.85 as a very rough guide for indicating a minimum number of cores required before a sample can represent the population adequately. Those sites which fail to meet the 0.85 criterion are ESM_E, $FISH_M$ and $CLAY_S$. These three chronologies are noticeably the least well replicated and the number of samples contained in the optimal subsample, as selected by program ARSTAN, was low. The failure of these sites to meet the 0.85 threshold indicates that a larger number of samples is required so that the population the chronologies aim to reflect is adequately represented.

3.3.2 Analysis of chronologies

3.3.2.1 Frequency domain analysis

The correlograms (Figure 3.18) of chronologies show considerable differences in the autocorrelation structure across sites. BLT_E, RFR_E, BEN_E, KOA_M, RCS_W, MUR_W and LCR_S all show a strong tendency for oscillating positive and negative coefficients (ρ). For the East sites (excepting ESM_E), and for RCS_W and MUR_W, the coefficients are significantly different from lag-0 up to lag-3, and rapidly become statistically indistinguishable from zero beyond this point. In most cases the lag-2 effect is clearly seen, with ρ attaining its maximum value at this point (only ESM_E, and $CLAY_S$ fail to show this), supporting the selection of AR(2) as the dominant AR process (Table 3.3). $FISH_M$, ARM_M,

KOA_M, $PILL_M$, SPR_S and $CLAY_S$ all reveal a tendency for a decreasing value of the ρ coefficient as lag length increases. For these sites (excepting KOA_M) the effect of autocorrelation is not so quickly damped as for those sites exhibiting oscillating values of ρ. The most noticeable feature, by region, is the tendency for a decreasing value of ρ in Mersey and Southwest sites while the autocorrelative structure of the East sites displays a more oscillatory nature.

High frequency periodicity, close to the Nyquist frequency, dominates all spectra. Given the predominance of the AR(2) process in the chronologies (Table 3.3, Figure 3.18), this finding is not surprising. The results do not agree entirely with those of program ARSTAN which suggest an AR(3) process to be dominant for FC_M (Table 3.3). The correlograms also show lag-9 as dominant for ESM_E and lag-1 as the most important AR process for $CLAY_S$. The results of program ARSTAN do not suggest this to be the case. However, the high level of agreement between the techniques, and the high frequency periodicity in the spectra of Figure 3.19, confirm it as a feature of this species. Lower frequency periodicity is also indicated in all spectra, however. Both RFR_E and SPR_S indicate the existence of a periodicity of about 79 years and all sites, with the exception of RCS_W, show significant periodicity at about 10–11 years (Figure 3.19) which is not reflected in the correlograms of Figure 3.18.

The dominance of the spectra by high frequency components is highly unusual in species used in dendroclimatology (E. Cook, Lamont–Doherty Geological Earth Observatory, pers. comm.). The reason for this dominance by the approximate two-year oscillation is unclear. Suggestions that it may be related to leaf life time conflict with the observation that leaf life-time is in excess of 41 months (Read 1989), and also with Barker's (1993) observation of abscission of leaves between 4 and 12 years old. The reported quasibiennial seeding/fruiting of the species is a plausible explanation for the high frequency oscillation.

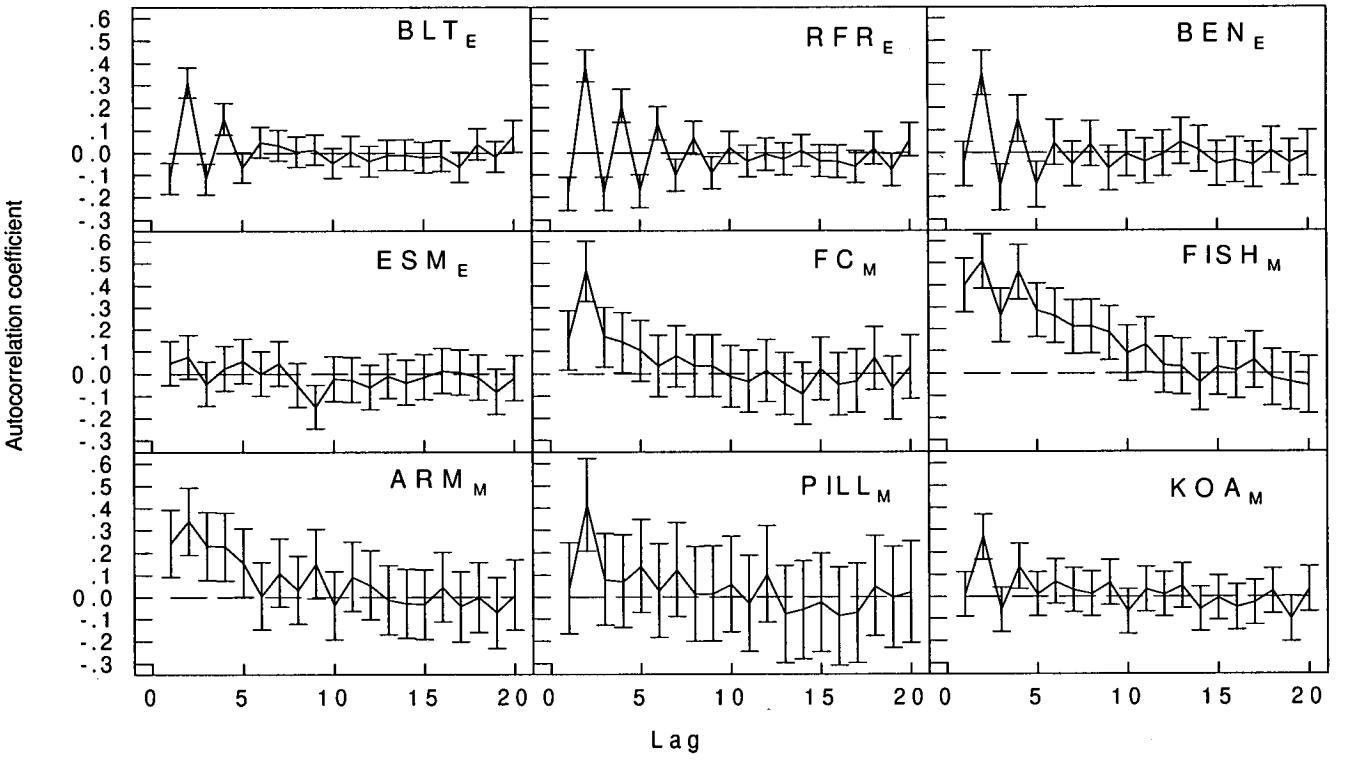

Figure 3.18: **Correlograms calculated out to 20 lags for each chronology using the entire length of each chronology. 95% confidence limits are shown**

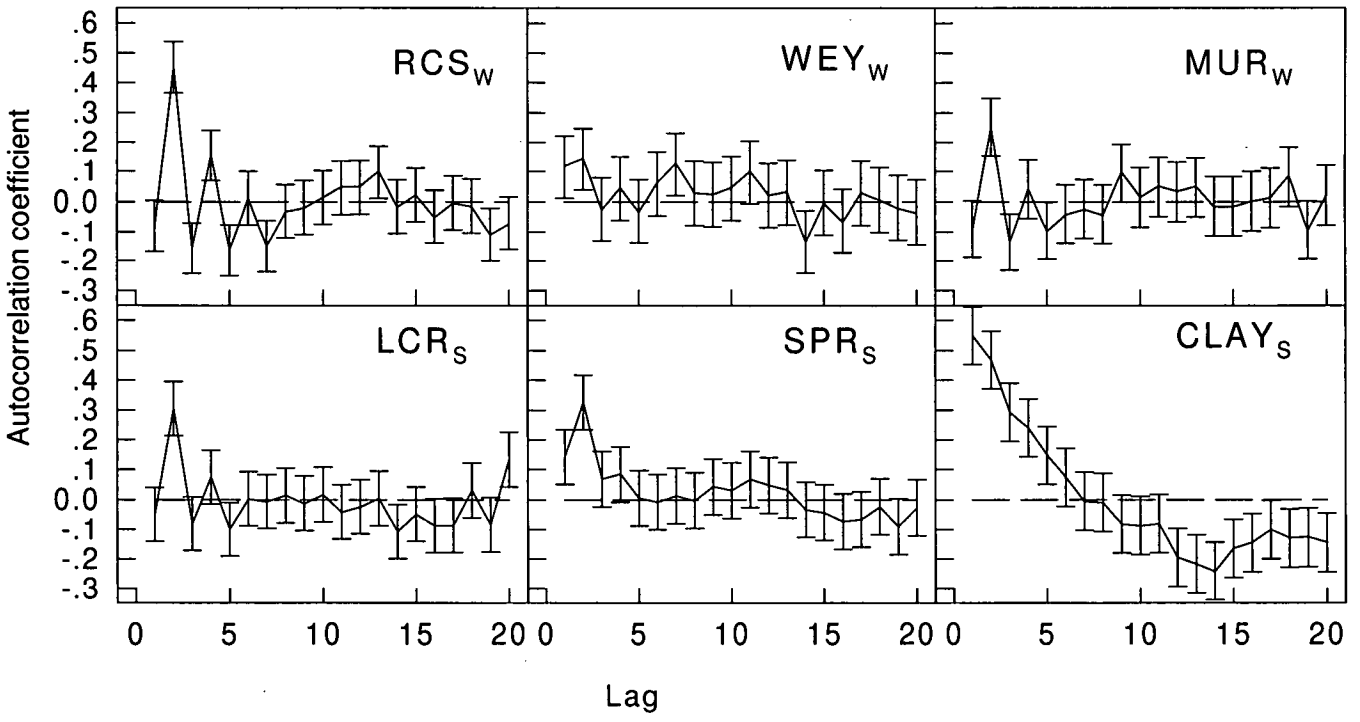

Figure 3.18 **continued: Correlograms calculated out to 20 lags for each chronology using the entire length of each chronology. 95% confidence limits are shown**

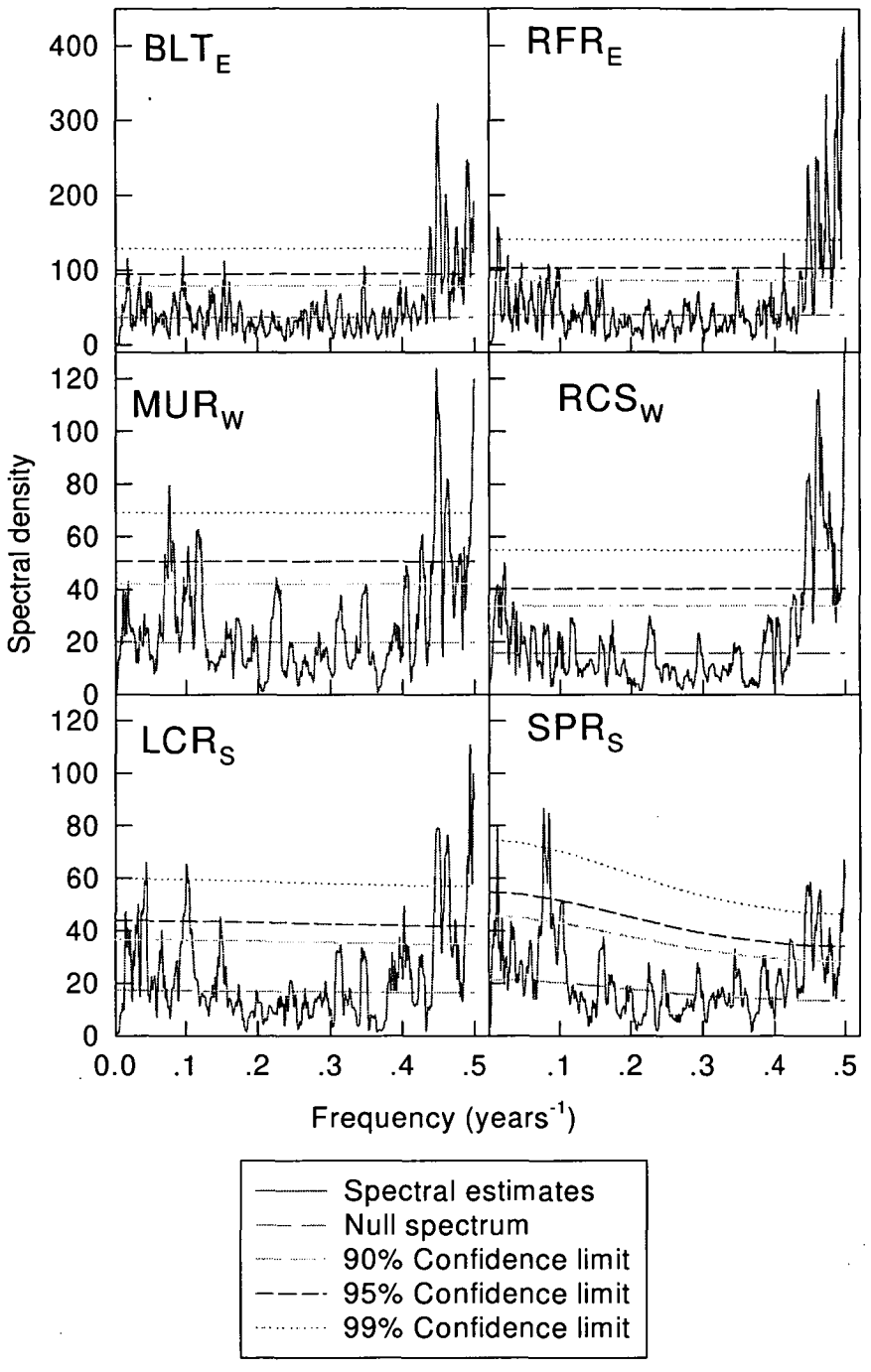

Figure 3.19: **MTM frequency spectra of selected chronologies. Periods corresponding to significant peaks at the 0.05 level occur at: BLT_E 60.2, 10.4, 6.6, 2.9, 2.3, 2.2, 2.1 and 2 years; RFR_E 78.7, 37.9, 11.9, 2.4, 2.2, 2.1 and 2 years; MUR_W 13.1, 12.2, 9.7, 2.3, 2.2 and 2 years; RCS_W 46.5, 2.2, 2.1 and 2 years; LCR_S 23.3, 9.9, 6.8, 2.5, 2.4, 2.2, 2.1 and 2 years; SPR_S 78.7, 12.8, 11.8, 2.4, 2.2, 2.1 and 2 years. Periods analysed are 1300–1994 for East sites, 1590–1994 for West sites and 1640–1994 for Southwest sites**

3.3.2.2 Intersite correlation and comparison

Highest inter-site correlations occur between West and Southwest sites with the exception of $CLAY_S$ (Table 3.4). BEN_E and BLT_E also show reasonably strong correlations with West and SPR_S and LCR_S sites (>0.5). Across most of the State significant correlations between sites are evident, thus verifying crossdating. Correlations between $CLAY_S$ and most other sites in the State are poor. ESM_E is also generally poorly correlated with other sites. In the case of ESM_E, individual site peculiarities are at least partially responsible for poor crossdating. The evidence of a number of fire boundaries on the edge of the $CLAY_S$ site suggests fire effects as one possible reason for the poor correlations between this site and others. Another possible explanation is that the far southwest of the Tasmania may be under different climatic controls from the rest of the State. Previous climatological work has suggested that such a difference does exist, but the lack of long climatic records for the area hamper efforts towards firmer conclusions. Due to the suggestiveness of past research, there is great interest in the further investigation of this issue (D. Shepherd, Bureau of Meteorology; R. Allan, CSIRO, pers. comm.). If all sites are significantly correlated with climatic variables, the lack of correlation between $CLAY_S$ and other sites adds weight to this suggestion. Mersey valley sites also suffer from poor crossdating with other sites, but this is likely to be due to their relative youth in addition to high levels of disturbance that are evident (Chapter 2).

In terms of temporal changes in crossdating, weakened crossdating exists between the Southwest and BLT_E over the 1901–1950 period (Figure 3.20). Although it appears that the pattern has become more north–south aligned rather than east–west aligned over the past two centuries, this may well merely be an artifact of an increased number of sites over time. Correlations of SPR_S with all other sites (Figure 3.22) do not show this north–south effect, although this site also demonstrates poor crossdating with the sites in the northeast over the past century. Correlations between East and West weaken in the 1900–1950 time period as seen in Figure 3.21, but Figure 3.20 does not support the view that this is a general characteristic of all sites in both regions.

3.3.2.3 Principal Component Analysis

The first unrotated PC merely expresses a whole State pattern where regions have not been differentiated. The second unrotated PC clearly separates the East sites from those in the rest of the State (Figure 3.23). The Varimax rotation serves to emphasise the difference between East sites and those in the rest of the State (Figure 3.24). The first rotated component reveals no clear pattern other than the isolation of the east coast sites. The second rotated component, however, shows a more obvious approximate northeast–southwest pattern in loadings; $CLAY_S$ possesses a considerably smaller loading than other sites and the northernmost western sites, RCS_W and WEY_W, show intermediate loadings. The loadings of the second component are also generally consistent with decreasing site elevations from the northeast to the far southwest.

Campbell (1980) has also performed a PCA, but used the ring widths of several different species in the one analysis. Her finding that the unrotated third eigenvector showed a distinction between the south and east of the State and the northwest is consistent with the results presented here.

Confounded possibilities prohibit finding a definitive explanation for the segregation of these two groups of sites. Not only are the East sites geographically remote from the other sites, they are also located at higher elevations. It is not implausible that reasons similar to those advanced by Buckley (1997) for differences between sites above and below a certain elevation are important here. Two other possible explanations are firstly, the spatial variability of climate, and secondly, biological differences between individuals in the East and those further west and south. Barker (1993) has found that physiological differences exist in the limits to growth of lowland (60m ASL) and highland provences (750m ASL) of *Phyllocladus aspleniifolius*. However, Barker has not indicated at what elevation plants are to be classed as 'highland' or as 'lowland'. It is therefore not clear which sites used in this study belong to which provenance, although it is clear that $CLAY_S$ falls into the lowland provenance, while BLT_E, RFR_E and BEN_E lie within the realm of Barker's highland provenance. Barker has commented that the differences may be either genetic or due to physiological plasticity of the species.

	BLT_E	RFR_E	BEN_E	ESM_E	ARM_M	$FISH_M$	FC_M	$PILL_M$	KOA_M	WEY_W	MUR_W	RCS_W	LCR_S	SPR_S	CLA_S
BLT_E	1.0	0.557	0.726	0.471	0.542	0.244	0.446	0.373	0.426	0.517	0.523	0.531	0.54	0.478	0.293
RFR_E		1.0	0.494	0.486	0.447	0.467	0.397	0.285	0.417	0.497	0.385	0.367	0.494	0.353	0.26
BEN_E			1.0	0.497	0.446	0.486	0.428	0.323	0.414	0.528	0.545	0.594	0.545	0.451	0.304
ESM_E				1.0	0.362	0.171	0.354	0.151^+	0.266	0.382	0.305	0.38	0.371	0.357	0.242
ARM_M					1.0	0.561	0.682	0.42	0.663	0.589	0.486	0.57	0.477	0.493	0.207
$FISH_M$						1.0	0.194	0.375	0.379	0.417	0.299	0.397	0.383	0.359	0.332
FC_M							1.0	0.585	0.397	0.408	0.325	0.461	0.368	0.294	0.143^+
$PILL_M$								1.0	0.435	0.473	0.365	0.44	0.377	0.223^+	0.093^+
KOA_M									1.0	0.514	0.581	0.62	0.527	0.513	0.28
WEY_W										1.0	0.575	0.636	0.559	0.557	0.339
MUR_W											1.0	0.723	0.591	0.673	0.385
RCS_W												1.0	0.604	0.623	0.367
LCR_S													1.0	0.628	0.421
SPR_S														1.0	0.353
CLA_S															1.0

Table 3.4: **Correlation matrix for residual chronologies. Correlations are Pearson's product moment correlation coefficient. Chronologies were correlated with one another over their entire common length. $^+$ indicates correlation was not significant at the 95% level.**

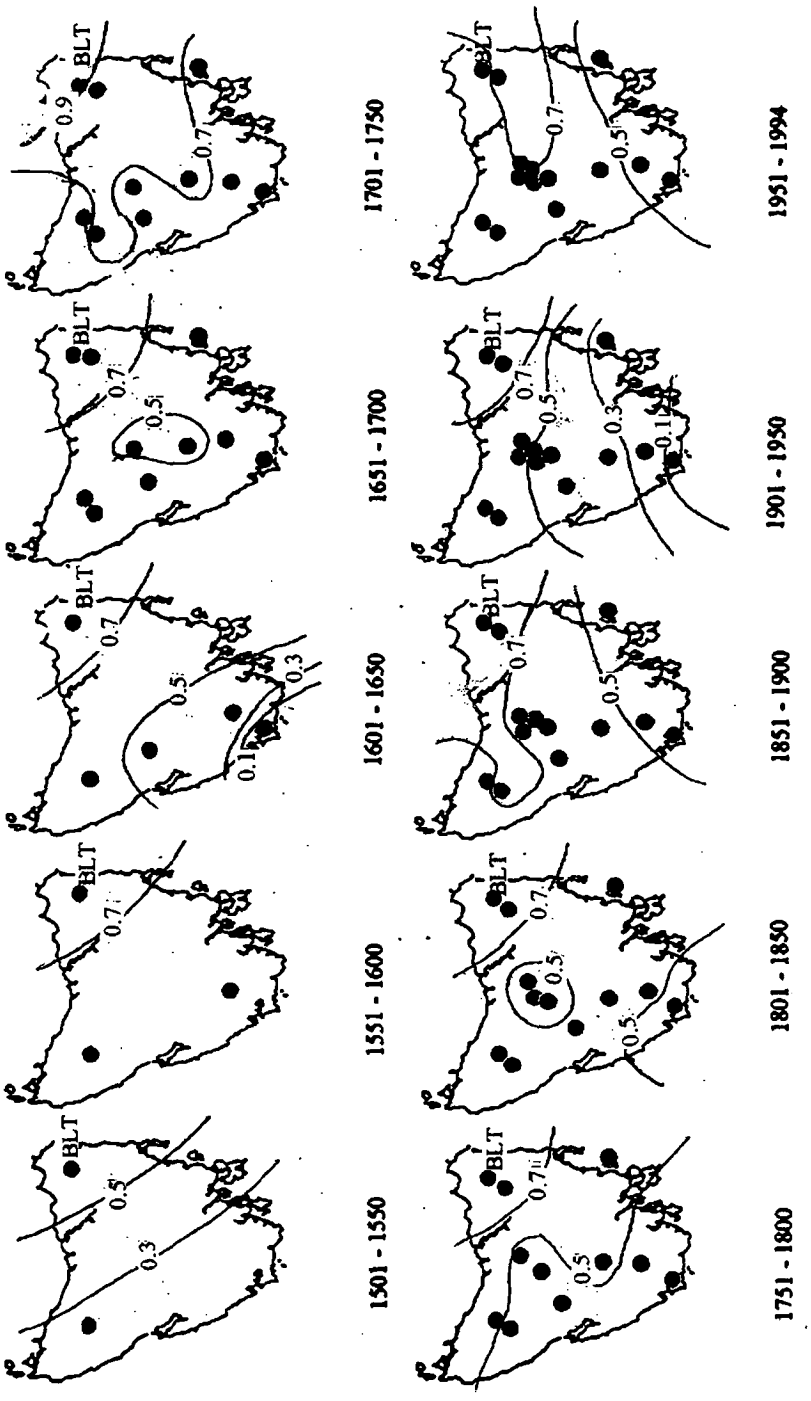

Figure 3.20: Correlation of BLT_E chronology with all other chronologies for consecutive 50 year periods, 1501–1994

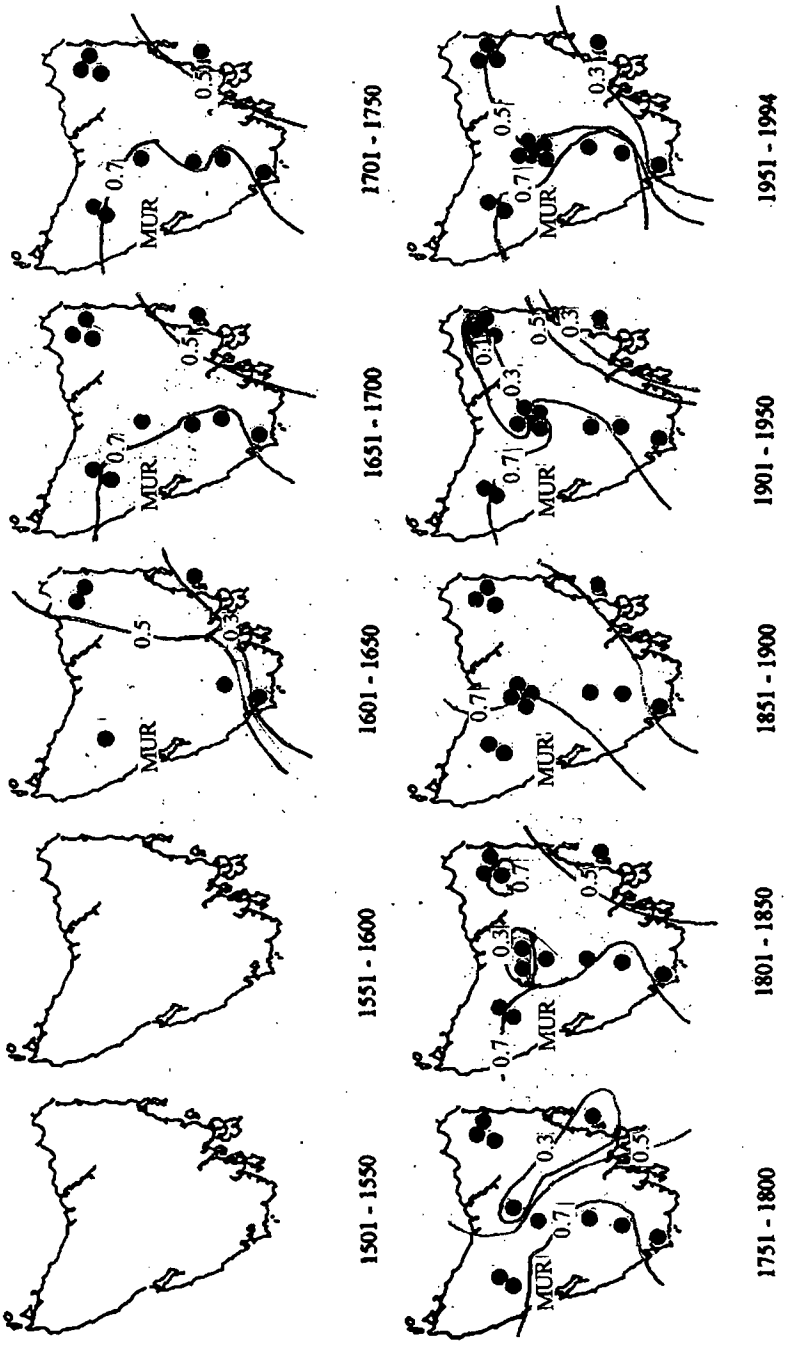

Figure 3.21: **Correlation of MUR_W chronology with all other chronologies for consecutive 50 year periods, 1601–1994**

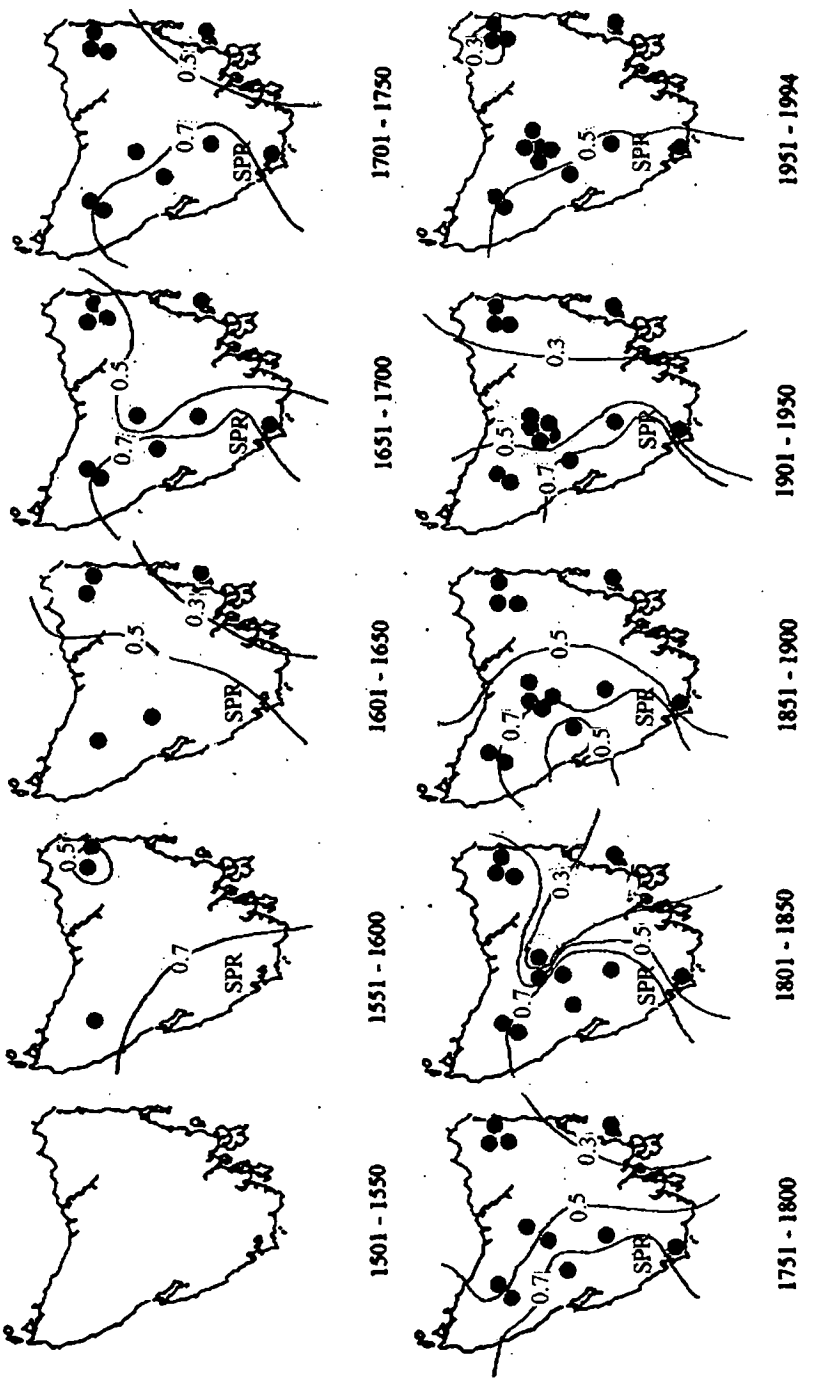

Figure 3.22: **Correlation of SPR_S chronology with all other chronologies for consecutive 50 year periods, 1551–1994**

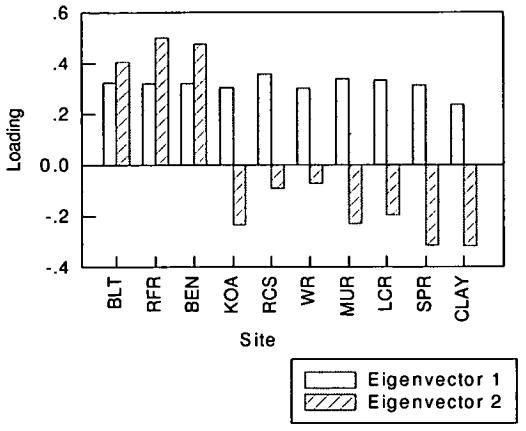

Figure 3.23: **Unrotated PC loadings on significant eigenvectors (those eigenvectors with eigenvalues greater than one). Loadings on all sites are positive and approximately the same for the first eigenvector, while the eastern sites have positive loadings and other sites negative loadings for the second eigenvector. Period of analysis is 1750–1994**

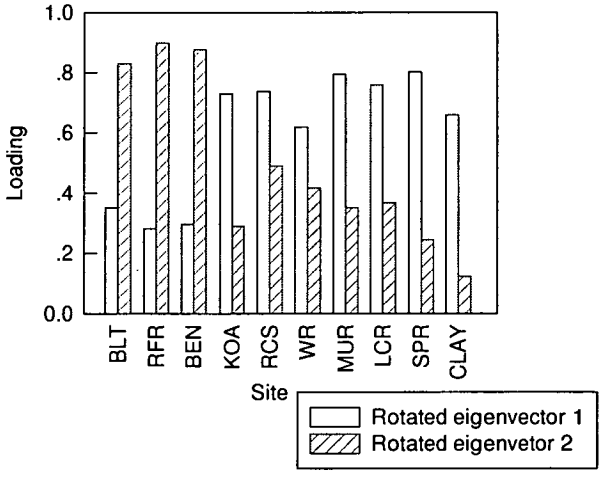

Figure 3.24: **Varimax loadings for sites covering the period 1750–1994. The Varimax rotation depicts the eastern sites as being distinctive for both the first and second eigenvectors**

3.3.2.4 Cross-spectral analyses of *Phyllocladus aspleniifolius* chronologies

Coherency between sites within the same region is significant over most frequencies at the 0.05 significance level (Figure 3.25). Coherency between regions is also demonstrably high, again being significant at the 0.05 level over most frequencies (Figures 3.26–3.28). This reinforces the successful crossdating of sites of the same region, as well as sites of different regions. Average coherency between sites of two regions represents a summary of the coherency between all sites in the two regions indicated in each plot (Figures 3.26–3.28). For all regions, coherency is greatest in the higher frequencies where greatest spectral power is indicated for autospectra. It is evident, looking at the average coherency for sites of two regions, that West and Southwest chronologies are more strongly coherent with one another than either are with the East sites. This is consistent with the results of the PCA.

3.3.2.5 Comparison with *Lagarostrobos franklinii*

Overlay plots of Phyllocladus aspleniifolius and Lagarostrobos franklinii

It is clear from Figures 3.29–3.31 that *Phyllocladus aspleniifolius* shows a much greater year to year variability than *Lagarostrobos franklinii*. This high frequency variation present in *P. aspleniifolius* is a much-noted feature of the species (Figure 3.18, 3.19, Campbell 1980, LaMarche and Pittock 1982, Bird *et al.* 1990), and is not shared by *L. franklinii*.

It is not uncommon for one species to show low/high growth while the other shows high/low, or close to average growth for the same year. A number of examples, with regard to the MTREAD chronology, are: around 1320, 1750–1880 (East, Figure 3.29), 1900–1920 (West and Southwest, Figures 3.30 and 3.31) and late 1670s–1690 (Southwest, Figure 3.31). Francey *et al.* (1984) commented on the nonsynchroneity of the formation of narrow rings in the two species. They did however, note some years for which narrow rings were formed in a number of different species, e.g. AD 1696/97 (shown as a narrow ring for West and Southwest in Table 3.1) and AD 1887/88.

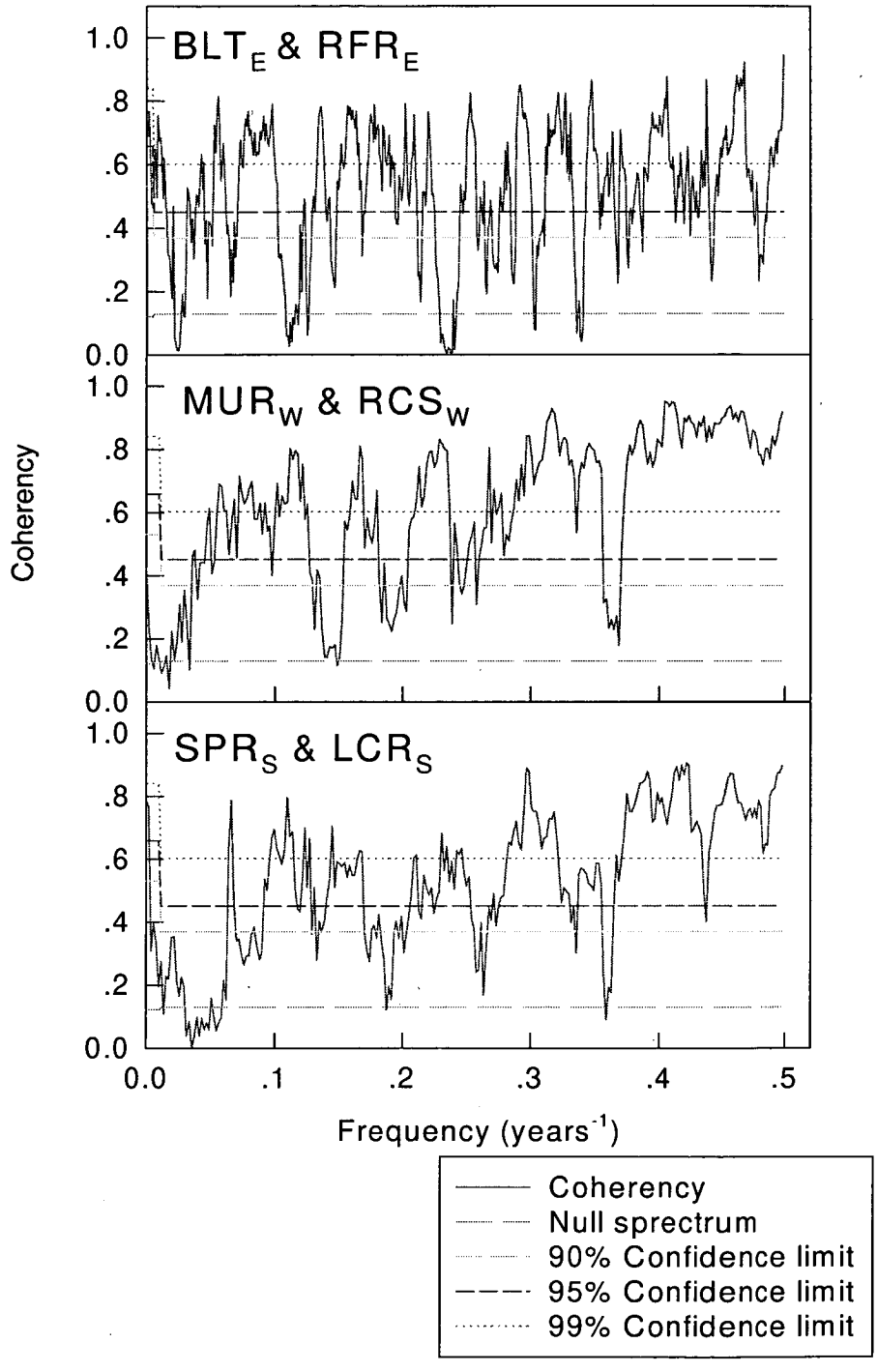

Figure 3.25: **Coherency between selected sites from the same region. Periods of analysis are: East sites, 1300–1994, West sites 1590–1994, Southwest sites 1640–1994. Coherency falls below the null spectrum (0.50 significance level) in the lower frequencies, but for the majority of frequencies is significant at the 0.05 level**

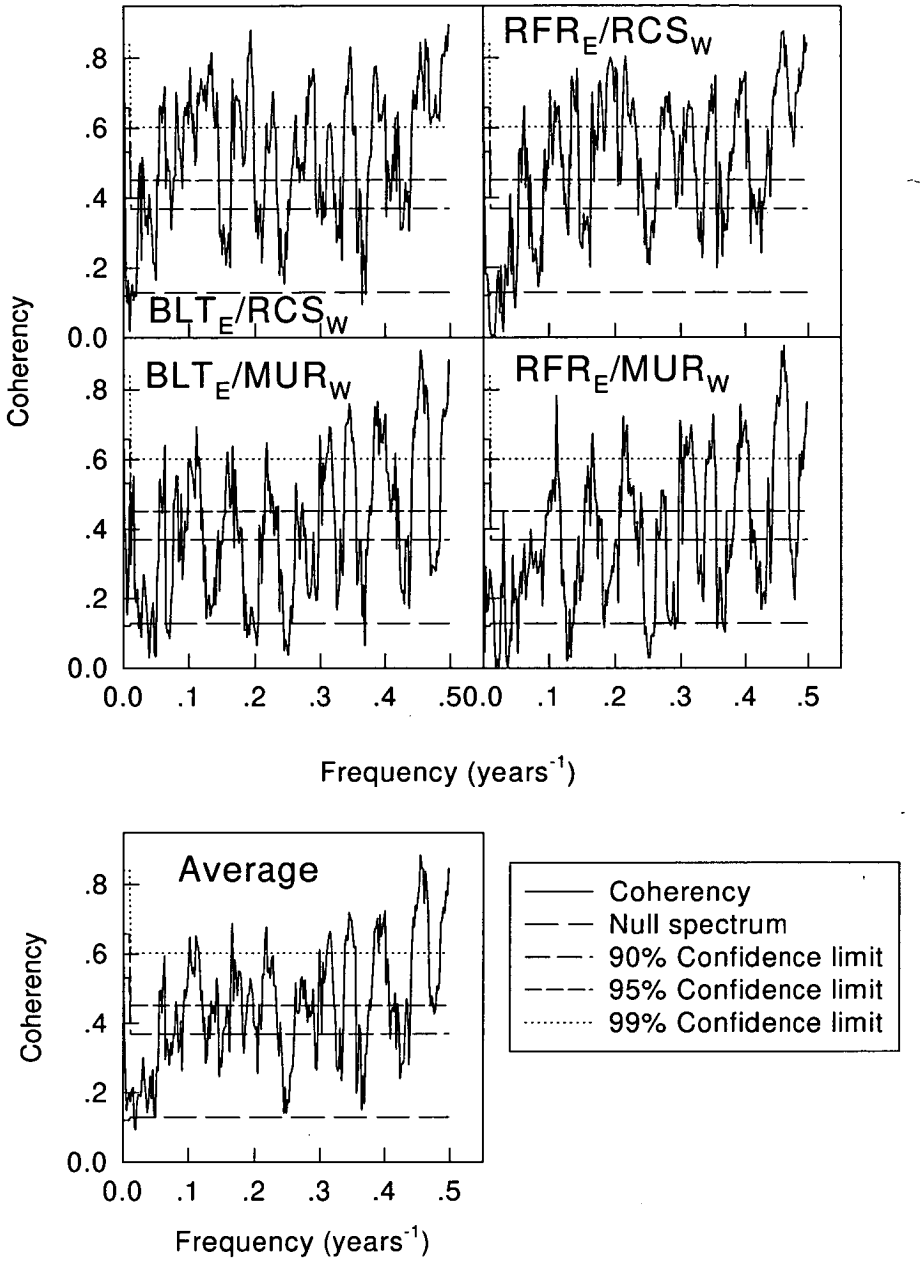

Figure 3.26: **Coherency of paired East and West chronologies, and average coherency between the sites of the East and West regions. Time period of analysis is 1590–1994. Coherency is apparent across most of the spectrum, but more so in the high frequencies.**

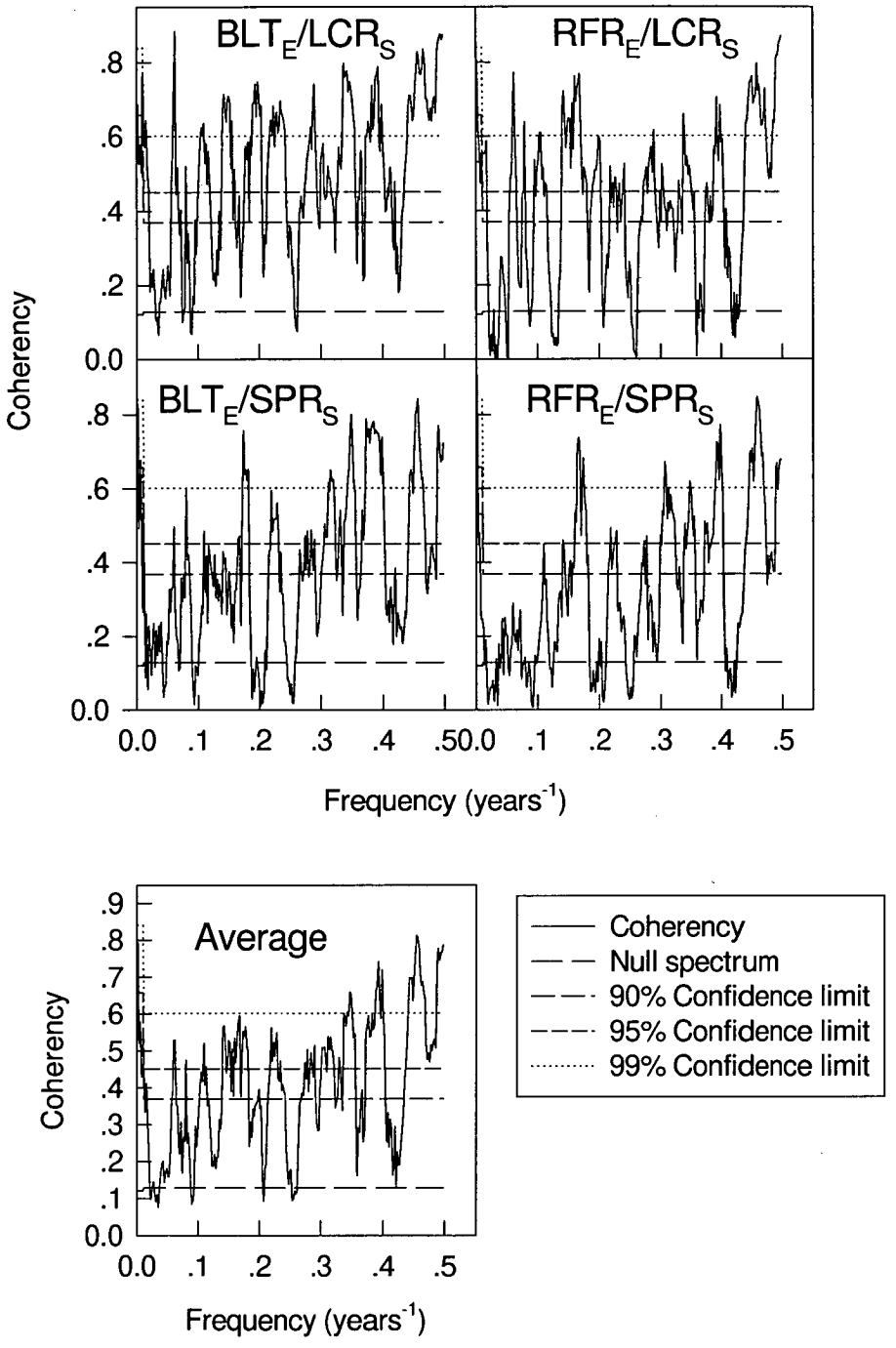

Figure 3.27: **Coherency of paired East and Southwest chronologies, and average coherency between the sites of the East and Southwest regions. Period of analysis is 1640–1994. Coherency is apparent across most of the spectrum, but between SPR$_S$ and East sites falls off considerably in the lower frequencies.**

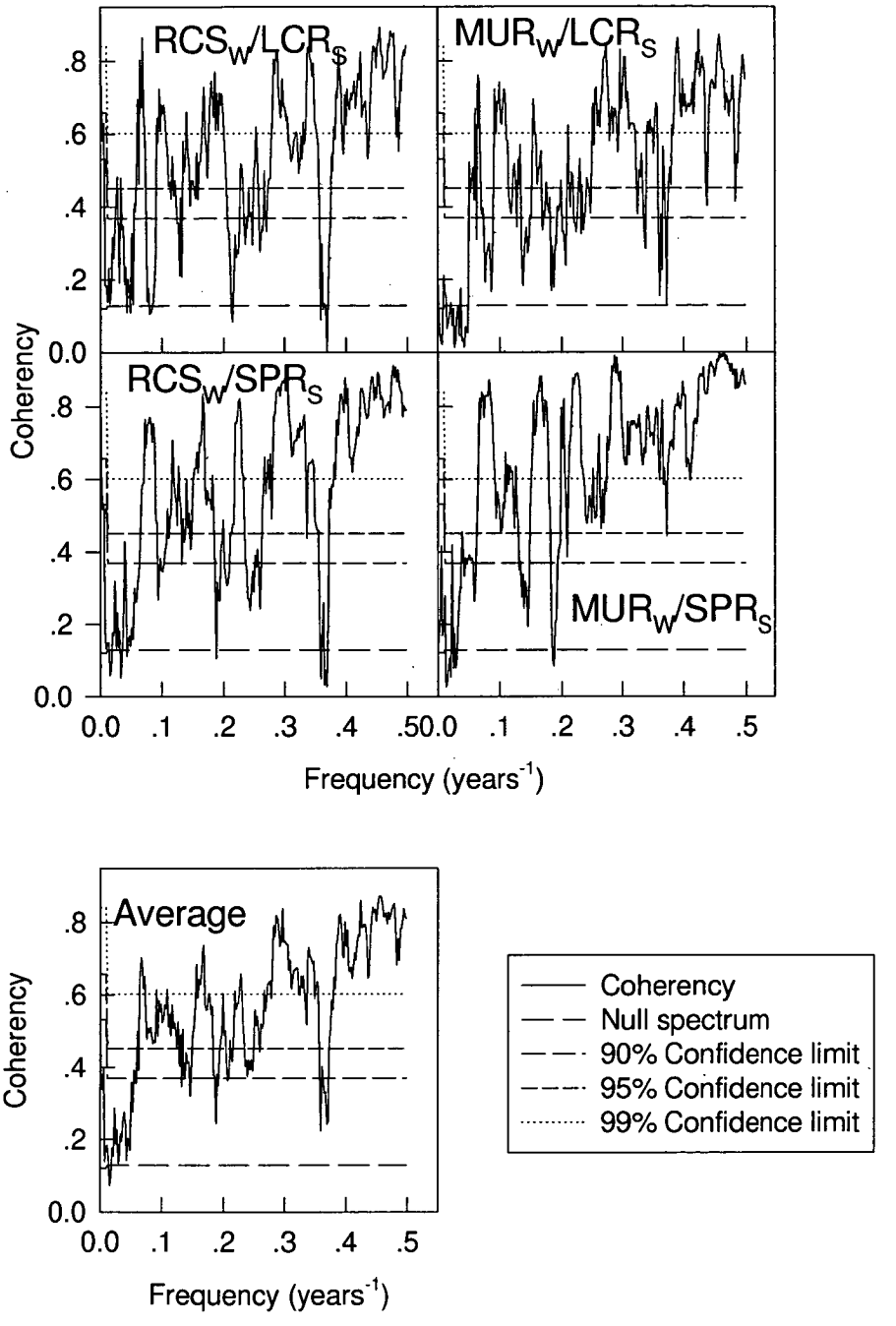

Figure 3.28: **Coherency of paired West and Southwest chronologies, and average coherency between site of the West and Southwest regions. Time period of analysis is 1640–1994. Coherency falls below the null spectrum (0.50 significance level) in the lower frequencies. Of the three regional comparisons, coherency is higher between West and Southwest sites.**

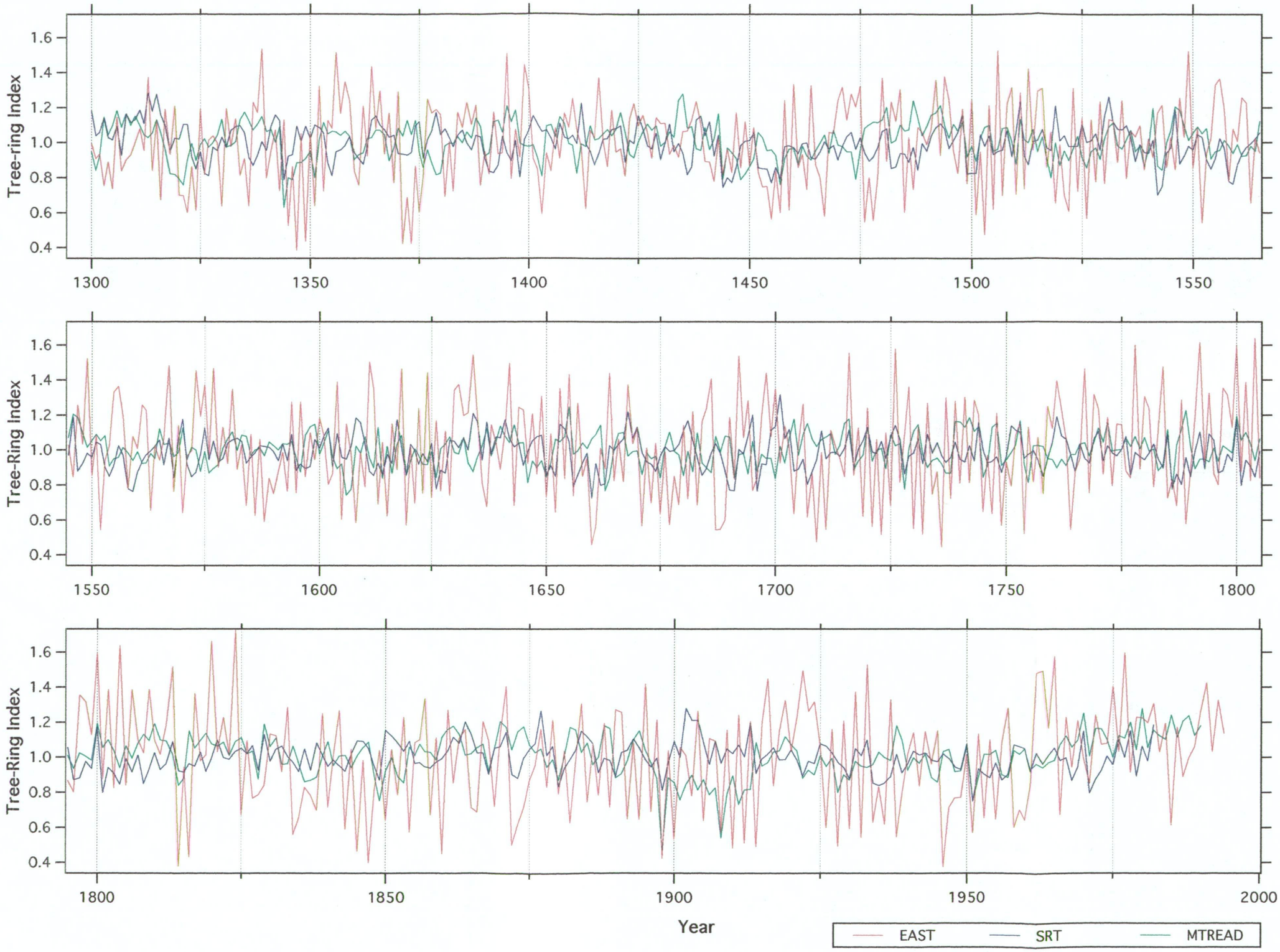

Figure 3.29: East *P. aspleniifolius* and MTREAD and SRT *L. franklinii* arstan chronologies over their common period, 1300-1990. Large and relatively sustained differences between the two series occur around 1320 and 1750-1880, and around 1960. Both species show an increase in growth since 1960, MTREAD showing increasing growth since about 1910. High frequency variability is considerably greater for *P. aspleniifolius* than for *L. franklinii*. Each frame is approximately 200 years.

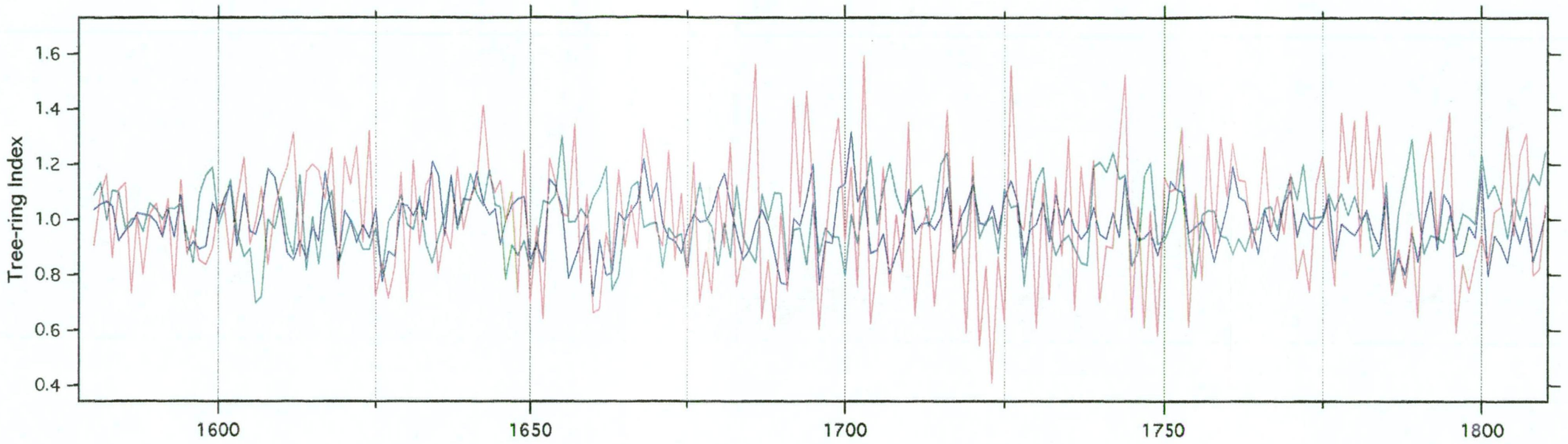

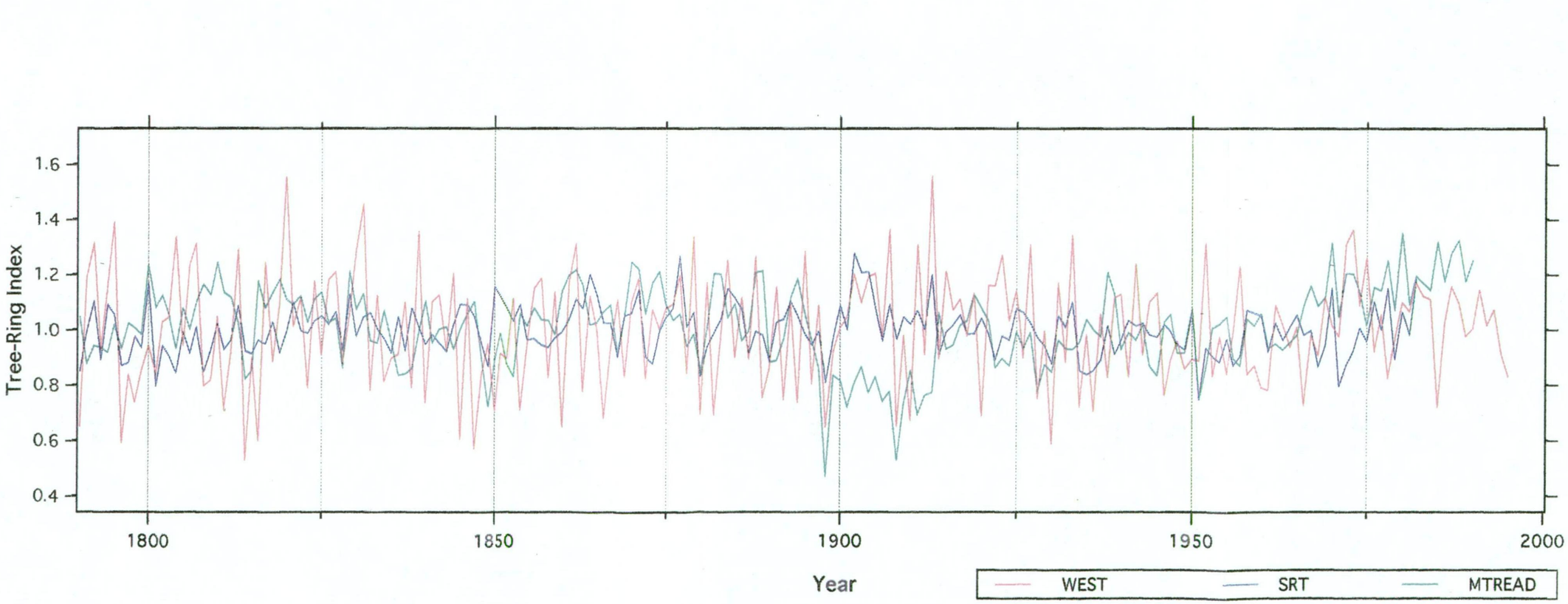

Figure 3.30: West *P. aspleniifolius* and MTREAD and SRT *L. franklinii* arstan chronologies over their common period, 1300-1990. Large and relatively sustained differences between the two series occur around 1320 and 1750-1880, and around 1960. Both species show an increase in growth since 1960, MTREAD showing increasing growth since about 1910. High frequency variability is considerably greater for *P. aspleniifolius* than for *L. franklinii*. Each frame is approximately 200 years.

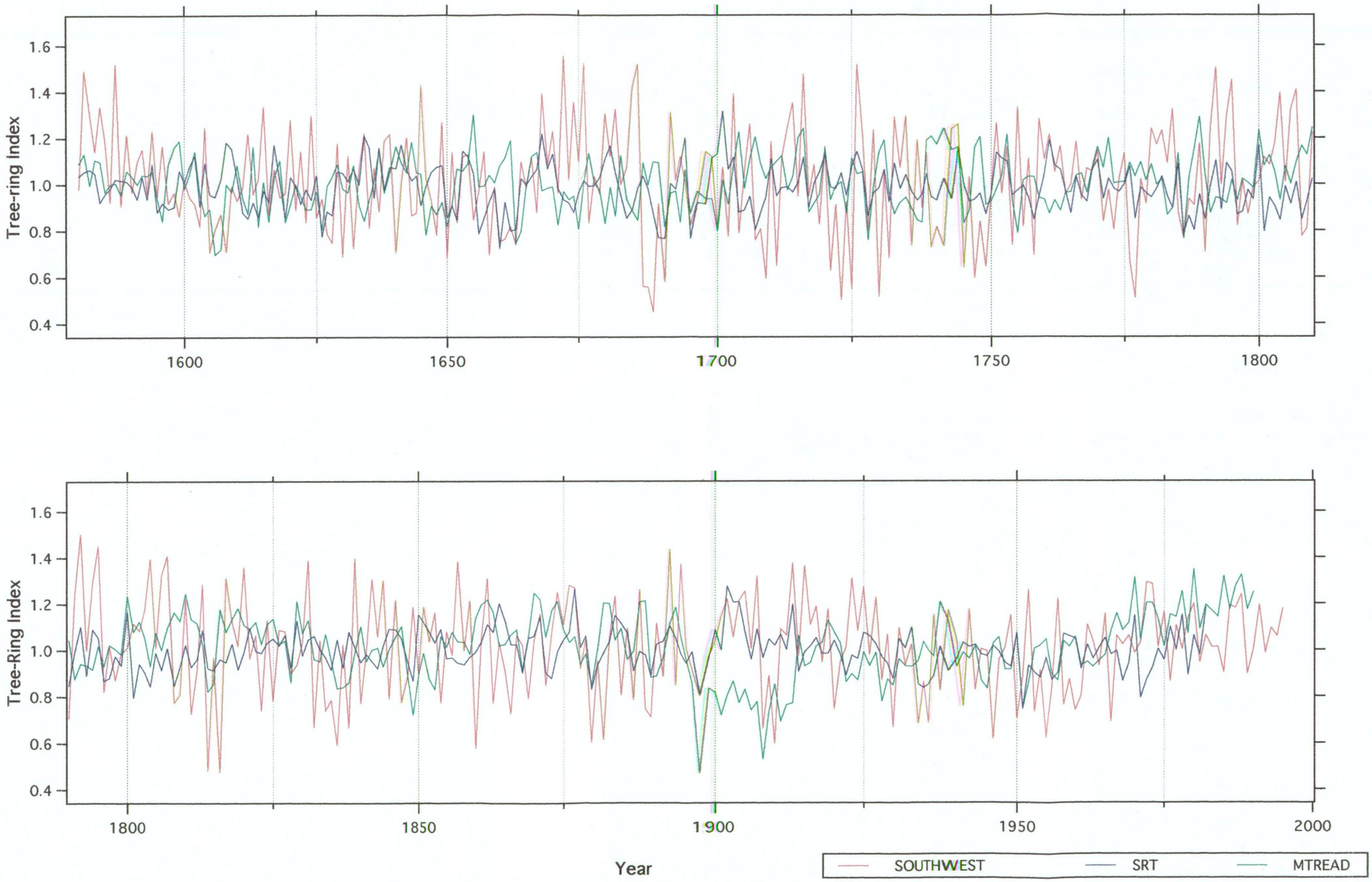

Figure 3.31: Southwest *P. aspleniifolius* and MTREAD and SRT *L. franklinii* arstan chronologies over their common period, 1580-1990. Large and relatively sustained differences between the two series occur around 1670-1690 and also just after the turn of the twentieth century. Both species show an increase in growth since 1960. High frequency variability of *P. aspleniifolius* is considerably greater than for *L. franklinii*. Each frame is approximately 200 years.

Both East and Southwest show a trend of increasing ring widths in the latter part of the twentieth century, in agreement with both *L. franklinii* chronologies. The West *P. aspleniifolius* chronology does not show this same general trend.

The prominent signature rings of 1898 and 1908, and the depressed growth around the turn of the twentieth century in general seen in the MTREAD chronology, is not evident in the SRT chronology, which indicates average to slightly above average growth for this time period (similar to West and Southwest *Phyllocladus aspleniifolius*). There are a number of other occasions where the index value of the SRT chronology is closer to that for *P. aspleniifolius*, for example, around 1700 East (Figure 3.29); 1606–1607, 1762–1765, 1787–1789 and 1807–1811 West (Figure 3.30); 1661–1662, 1760–1765 and 1807–1809 Southwest (Figure 3.31). There are also several cases where the MTREAD chronology traces the *P. aspleniifolius* chronologies more successfully than SRT, including the 1970s East (Figure 3.29), 1908–1910 West (Figure 3.30), and 1606–1607, 1908–1910 and the 1970s Southwest (Figure 3.31). At the turn of the twentieth century, the East ring–width series shows a strong high frequency variability not exhibited by either the West or Southwest. Neither MTREAD or SRT chronologies show a similar pattern.

Weaker crossdating between higher and lower elevation *Lagarostrobos franklinii* sites has been noted by Buckley (1997), and periods noted above where there are closer similarities between the lower elevation *L. franklinii* chronology and the *Phyllocladus aspleniifolius* chronologies also exist. This seems to indicate that higher and lower elevation sites are responding to different conditions (climatic and environmental), or are responding differently to the same conditions (LaMarche 1974a).

Cross-spectral analysis of Phyllocladus aspleniifolius and Lagarostrobos franklinii

Significant coherence (0.05 significance level) is observed between all three regional chronologies of this study and the MTREAD and SRT chronologies. In general, there is higher coherence across the spectrum between

East and MTREAD than between West or Southwest chronologies and MTREAD (Figure 3.32, Tables 3.5 and 3.6). This could be attributed in part to the greater length of the East chronology, but it is also possible that similar reasons to those causing differences between high and low elevation sites in LaMarche's (1974a) study are responsible. Significant coherence at frequencies lower than 50 years occur only between MTREAD and East. Two possible reasons for this are: firstly, that a greater time period has been analysed for this pair of chronologies and, secondly, that lower frequency oscillations are more apparent, and coherent, at higher elevation sites.

MTREAD and East	*SRT and East*	*MTREAD and West*	*SRT and West*	*MTREAD and Southwest*	*SRT and Southwest*
Frequency (years)	*Frequency (years)*	*Frequency (years)*	*Frequency (years)*	*Frequency (years)*	*Frequency (years)*
60.2	44.4	9.3	30.1	13.7	30.1
44.4	23.3	7.2	9.5	8.7	9.3
27.0	16.3	4.7	8.2	4.8	8.3
9.8	12.8	3.8	7.9	3.8	7.3
9.1	6.9	2.8	6.7	3.2	6.5
7.3	6.2	2.3	3.8	2.6	4.1
5.7	4.9	2.2	3.4	2.5	3.7
5.0	3.6	2.1	2.8	2.3	3.4
4.6	3.5		2.5	2.1	2.7
3.7	3.4		2.2		2.5
3.5	3.1				2.1
2.9	2.6				
2.7	2.5				
2.2	2.3				
2.1	2.2				

Table 3.5: **Significant (0.05 level) coherencies in years between MTREAD and *SRT L. franklinii* and regionalised *P. aspleniifolius* chronologies. Series lengths analysed are: MTREAD/East 1300–1990, MTREAD/West 1590–1990, MTREAD/Southwest 1580–1990, SRT/East 1300–1980, SRT/West 1590–1980, SRT/Southwest 1580–1980. Note the proportion of significant coherencies which occur in the high frequencies.**

For the West and Southwest, there is a noticeable increase in coherence with MTREAD at the higher-frequency end of the spectrum (Table 3.5, Figure 3.32). Significant high frequency coherence between West and Southwest and SRT, on the other hand, does not occur across as broad a range of frequencies in

this range as it does for MTREAD/West and MTREAD/Southwest. Lower frequency components, however, become more accentuated (significant), and a greater number of frequencies in the 5–15 years range are apparent (Table 3.5). In addition, a significant lower frequency coherence at approximately 30 years, not present when compared with MTREAD, is observed when West and Southwest chronologies are compared with SRT. Although significant low frequency coherence occurs between East and SRT, it has been de-emphasised (relative to coherence with MTREAD), as shown in Figure 3.32D. The coherence at 60.2 observed between MTREAD and East is not apparent between SRT and East.

No attempt has been made to assess the significance of the differences in the two sets of analyses, as this is beyond the scope of this study. However, it is interesting that West and Southwest show a greater similarity in the lower frequencies to SRT than to the higher elevation MTREAD. In addition, the coherence at lower frequencies is less significant for East/SRT than for East/MTREAD. The reasons for this are not clear, but as discussed above, could be due to a number of factors (LaMarche 1974a).

It is also possible that the differences observed are merely the result of using two different chronologies which contain different frequency domain information may have resulted in similar differences. However, results based on coherence between two further *L. franklinii* sites and *Phyllocladus aspleniifolius*, presented in Appendix 1, also show differences in coherency between higher and lower elevation sites.

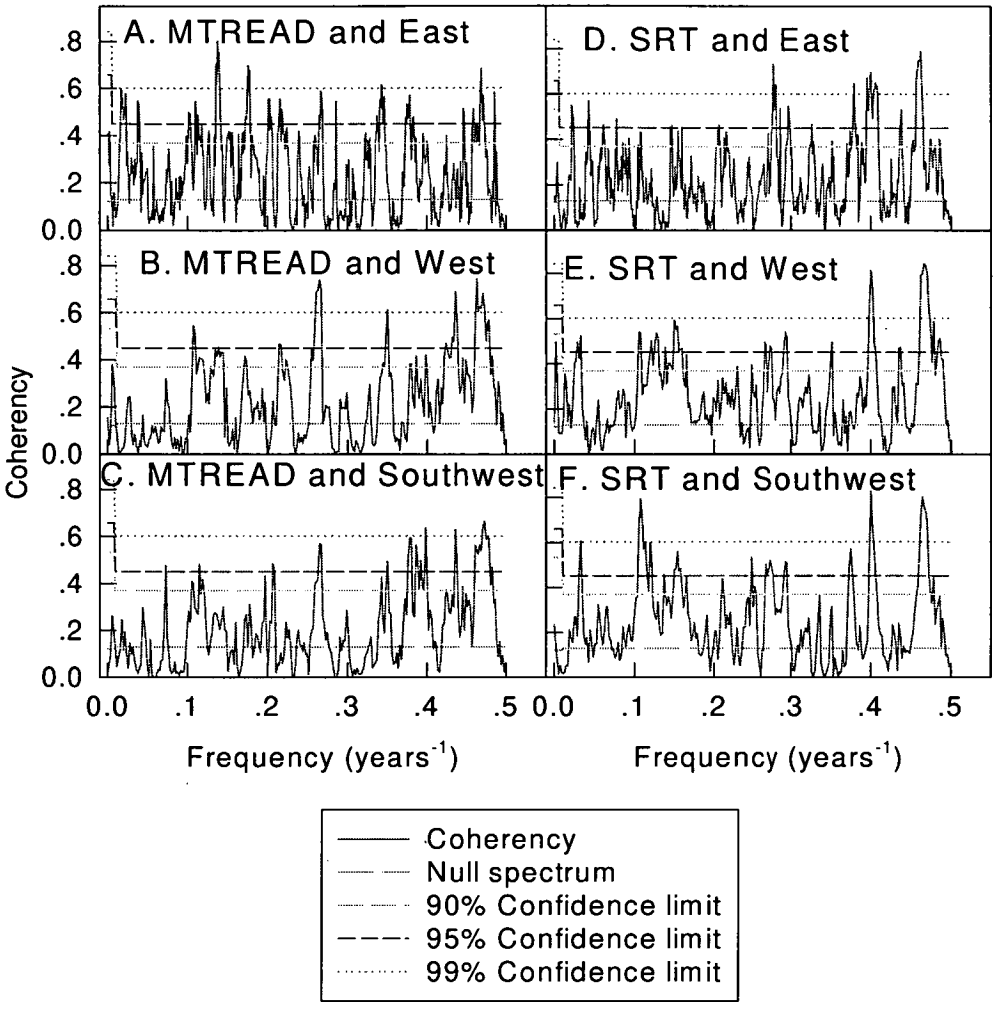

3.4 Summary

Tree ring data have been detrended using a 128-year 50% cut-off smoothing spline, effectively limiting frequency resolution to less than 128 years. However, greatest spectral power occurs in the high frequencies, with periodicities of 2–3 years. The time span of chronologies is very variable and general patterns in statistics, such as MS_X or $\overline{R}$, are not immediately discernible, although some generalities have been noted. These statistics, in part, reflect differences which can be attributed to a wide variety of site types and characteristics, but no firm

conclusions can be drawn regarding the influence of these site characteristics. This is consistent with Barker's (1993) finding that the species is insensitive to soil fertility and nutrient level. What is demonstrated however, is that a common signal between individuals on a single site does exist.

Evidence presented by correlation analysis, PCA and cross–spectral analysis all show crossdating between sites to be present. This intersite crossdating is evidence of a broadscale influence, such as climate, on cambial growth. There is a differentiation between East sites and West/Southwest sites, as shown by both the cross spectral analyses and the PCA. Weaker regional crossdating and regional correlations between sites around the turn of the century are a notable feature, and is further discussed in Chapter 7 in the context of climatic reconstruction.

The relationship between *Lagarostrobos franklinii* and *Phyllocladus aspleniifolius* is not clear. From a simple visual comparison of the time series of the two species, it is immediately obvious that the high frequency variation of *P. aspleniifolius* ring widths at least partially disguises any lower frequency commonality between the species. Coherency spectra indicate that coherence across the spectrum exists, but that it differs when comparing *P. aspleniifolius* sites with HIGH and LOW *L. franklinii* sites. This in turn suggests it is possible that an elevational grouping of plant response to climate may occur in some circumstances. Such an elevation dependent response in a single species is discussed by Buckley *et al.* (1997) for *L. franklinii* and this prospect is further discussed in Chapter 5 in the context of *P. aspleniifolius*.

It can be concluded from this that further work concentrated on elevational transects of a number of species would prove useful in a more rigorous study of the frequency domain properties of such sites as well as their differences in the time domain.

Chapter 4: Climatic Data

4.1 Introduction

Dendroclimatology has focused attention on both broad regional and quite localised phenomena. Localised studies have led to streamflow reconstructions (e.g. Stockton 1971, Campbell 1980), run-off histories (e.g. Schulman 1945), lake level reconstructions (e.g. Stockton and Fritts 1973, Brinkmann 1987), drought analysis based on the Palmer Drought Severity Index (PDSI) (e.g. Cook and Jacoby 1979, Meko *et al.* 1980, Stahle *et al.* 1985). Broad scale studies have been aimed at the reconstruction of variables such as the Southern Oscillation (SO) (e.g. Fritts *et al.* 1979, Gordon *et al.* 1985, Lough and Fritts 1985, Swetnam and Betancourt 1990), sea surface temperatures (SSTs) (e.g. D'Arrigo *et al.* 1993), and sea level pressure (SLP) (e.g. Fritts 1971, Fritts *et al.* 1979, Gordon *et al.* 1985). A number of studies have concentrated on temperature reconstruction in the Southern Hemisphere (e.g. Lara and Villalba 1993, Salinger *et al.* 1994, Cook *et al.* 1996). They extend relatively local temperature reconstructions to infer broader regional variations over long time periods. More recently, a dendroclimatic reconstruction of the transpolar index (TPI) has been particularly revealing (Villalba *et al.* 1997), linking the findings of a number of previous Southern Hemisphere tree ring studies.

Temperature and precipitation data are the most frequently reconstructed variables in dendroclimatic studies due largely to their ready availability. The Southern Oscillation, SST and SLP are broader scale phenomena which exert varying degrees of control over the temperature and precipitation of different regions of the globe.

The use of a number of sites in different regions of Tasmania immediately raises two issues: What differences, if any, can be ascribed to climatic variation on a regional scale, and what can be ascribed to microclimatic or microsite differences? This chapter describes the development and characteristics of the climatic data sets relevant to this study, namely: regional temperature and precipitation data sets, surface Meridional and Zonal indices, and the Southern Oscillation Index (SOI).

4.1.1 The Southern Oscillation Index

The Southern Oscillation Index (SOI) is a measure of pressure differences between Tahiti and Darwin, and has generated much recent discussion and research (e.g. Bjerknes 1969, Gill and Ramusson 1983, McBride and Nicholls 1983, Nicholls 1985, Lindesay and Vogel 1990, Graham and White 1993, Allan 1993, Allan *et al.* 1995, among others). The updated Ropelewski and Jones (1987) seasonalised SOI (1867–1996) is displayed in Figure 4.1 (data kindly provided by P. Jones, Climatic Research Centre, University of East Anglia). This index is similar to the Troup Index (McBride and Nicholls 1983) which is calculated on a monthly basis as

$$[(\text{Tahiti pressure-Darwin pressure}) \times 10] / \sigma$$

The seasonalised data does not reveal any long-term trend. In most recent years, however, values have been relatively low for all seasons. They were also lower around the turn of the century. The 1920–1960 period is one of generally higher than average values for autumn months. This is not discernible in the other seasonal series (Figure 4.1).

Trenberth (1976) has found evidence of a change in the SOI about 1954 which he related to weakening westerly flow. In agreement with this, McBride and Nicholls (1983) have noted an apparent westward shift in correlation between precipitation and the SOI over Australia between the two time periods 1933–53, and 1954–74. Furthermore, Allan *et al.* (1995), whose investigation is based on mean sea level pressure (MSLP), SST and surface winds and cloudiness, has noted that the 1920–41 period was one of weak teleconnections and ENSO events, and 1942–62 a transitional period. Conversely, the 1879–1900 and post 1963 periods show increased ENSO activity and more coherent teleconnections.

Although McBride and Nicholls (1983) have illustrated that the correlation between the SOI and Tasmanian weather is weak, it may well still be worth examining the data to see if correlation between ring widths in any region of the State and the SOI is significant.

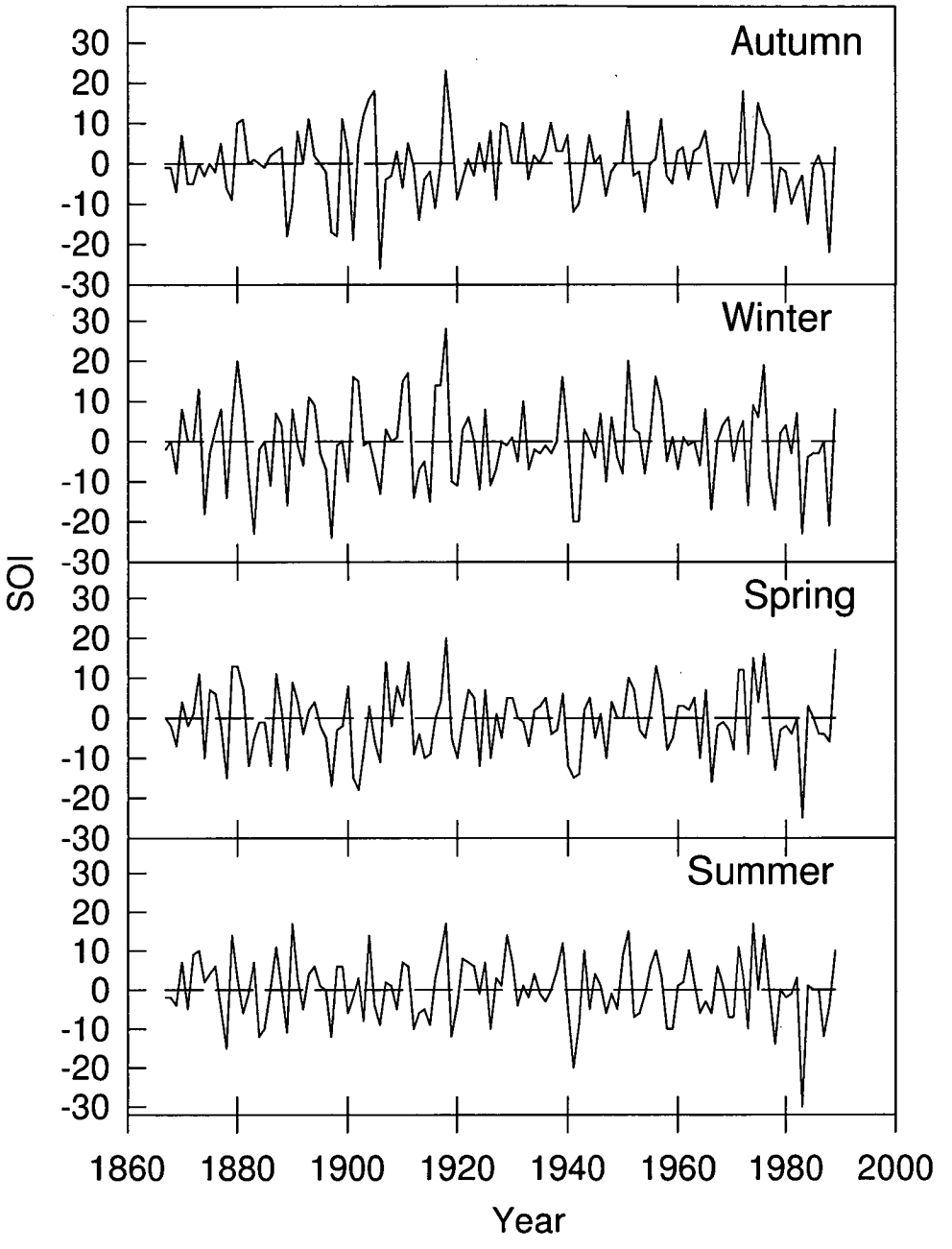

Figure 4.1: **Seasonalised SOI (pressure difference between Darwin and Tahiti). Seasonalisation has been based on the average value for each of the traditional seasons. Data source: Jones 1997 pers. comm. (updated from the data presented by Ropelewski and Jones 1987)**

Most variance in the SOI is contained in the 2–10 year band, and long-term periodicities of 40–50 and 90 years have been suggested by Anderson (1992). Enfield and Cid (1991) have commented on the nonstationary nature of ENSO episodes and provide evidence that the return intervals of strong and weak ENSO events are linked to solar activity. Nicholls (1992) has explained that the biennial oscillation embedded in the SOI is related to seasonal phase locking.

4.1.2 Zonal and Meridional indices

The Zonal Index (ZI) denotes the degree of east–west organisation of the circulation. A high value of the ZI implies strong midlatitude westerlies, while a low zonal index denotes weak westerly winds. The climate systems affecting the State's weather in high ZI years are significantly different from those dominant in low ZI years. Therefore, it is reasonable to assume that in some years or time periods, tree ring widths in the West or Southwest may not crossdate with those in the East. The Meridional Index (MI) is essentially the converse of the ZI, indicating the strength of north–south and south–north circulation. High values of the Meridional Index, and the accompanying low values of the ZI in the Tasmanian region, can be associated with blocking action in the Tasman Sea. Pittock (1973) has discussed correlations between meridional winds and ozone, and winds and temperatures in different levels in the troposphere and the stratosphere, indicating that the complementary Meridional and Zonal indices convey useful information on a number of parameters. Pook (1992) has found a negative relationship between the values of the ZI (as determined for the 500 hPa level) and ENSO events, and has confirmed that the Australian continent plays a critical role in this relationship.

Allen (1991) and Shepherd (1995) have both commented on the role of the zonal westerlies in producing rainfall across the State, and Harris *et al.* (1988) have pointed to the role of zonal winds in the determination of both inland and sea fisheries yields.

4.1.3 The Cook temperature series

An existing temperature series for Tasmania, the 'Cook temperature series' which amalgamates Launceston, Hobart and Low Head monthly average

temperatures, has not been employed although it has been used in previous investigations of *Lagarostrobos franklinii* (e.g. Cook *et al.* 1992). Two fundamental differences exist between the Cook series and the temperature indices constructed here (see below). The temperature indices for this study have been constructed for both average monthly maximum and minimum temperatures whilst the Cook series is an average of monthly maximum and minimum temperatures (mean monthly temperature). It is possible that significant information loss may occur through the use of an average of maximum and minimum temperatures. The derivation of separate maximum and minimum temperature series should allow isolation of any separate effects of these variables on tree growth.

Secondly, all *Lagarostrobos franklinii* sites used so far are situated in a relatively homogenous climatic zone, and it may therefore be assumed that they were subject to similar climatic conditions (excluding those related to vertical distribution) and that all sites can be adequately compared to a single series. However, to carry this assumption into a study of sites distributed throughout Tasmania may not be valid (Chapter 2).

4.2 Methodology

Six different climatic variables have been collected and analysed to test correlations with tree-ring widths (Chapter 5). These six variables are maximum and minimum temperatures, precipitation, a Zonal Index based on surface pressures, a Meridional Index again based on surface pressures, and the Southern Oscillation Index.

4.2.1 Temperature and precipitation data

For purposes of examining climate differentials, the State was divided into four regions based on clusters of *Phyllocladus asplenifolius* sites, these being East, Mersey, West and Southwest. The climate stations utilised are listed in Tables 4.1 and 4.2 and their location is shown in Figure 4.2. For both precipitation and temperature the problem was one of how to create an appropriate climate series against which to compare tree-ring data in the light of two issues. The first of these related to the extent to which a single station can be regarded as being representative of the regional climate. Blasing *et al.* (1981) found regional

precipitation data to be superior to single station data in isolated areas. On a related theme, Hughes (1978) found that precipitation data from a site 6 km distant from a tree-ring site in England resulted in 45% variance being attributed to climate and 28% to prior growth, as opposed to 34% to climate and 31% to prior growth when climate data collected 60 km away from the site was used. The second issue related to spatial differences. In Tasmania, the nature of the topography and differences in altitude can cause precipitation stations in close proximity to vary greatly in recorded rainfall over a given period (Bureau of Meteorology 1975). Most Tasmanian climate stations lie at relatively low altitudes, and form a denser network in more heavily populated regions, necessarily making them remote from *P. aspleniifolius* sites (Tables 4.1 and 4.2). Higher elevation climate stations in remote areas existed, but were often of short duration and/or suffered from large amounts of missing data. Figures 4.3a & b and 4.4a & b illustrate some of the problems associated with stations at different altitudes and in varied topographic settings. For the East region, higher elevation stations were 91086 (Ringarooma), 92004 (Upper Blessington), 92051 (Pyengana) and 92083 (Roses Tier) and had, on average, significantly higher winter precipitation than the lowland stations. While elevation remained an important distinguishing feature in precipitation received by west coast stations (e.g. 97006, Lake Margaret), two distinct groups were the 'northern stations' and the 'western stations', with the western stations receiving greater precipitation than the northern stations, as commented upon by Gentilli (1972). Monthly average temperatures were more coherent in terms of their yearly cycle, the two coastal stations being warmer than the inland stations for all months (Figure 4.4a & b). The above discussion illustrates that a simple average value for each month, especially in the case of precipitation data, is unlikely to be a reliable guide to abnormally wet/dry years across a region.

For this reason, data were regionalised using Meko's (1981) approach. The monthly data for each individual station were transformed into a series of standard normal deviates to create dimensionless indices that became functions of their own mean and standard deviation. These series were then averaged across a region for each month of each year to produce single series of monthly data (i.e.

12 series). Both orographic effects and potential bias resulting from the use of a single station, were reduced through the application of dimensionless indices.

East	*Place name*	*Period of record*	*Elevation (m ASL)*
91086	Ringarooma	1914–94	274
92004	Upper Blessington	1916–64	530
92012	Tower Hill	1914–94	234
92014	Germantown	1929–76	305
92020	Lewis Hill	1929–94	244
92033	St Helens	1914–94	5
92034	St Marys	1914–94	269
92051	Pyengana	1961–94	159
92083	Roses Tier	1957–94	840
Mersey			
91000	Deloraine	1914–90	235
91048	Latrobe	1914–94	30
91055	Lorinna	1916–63	280
91065	Mole Creek	1914–90	240
91119	Erriba	1958–94	590
West			
91011	Cape Grim	1914–94	21
91044	Irishtown	1914–94	55
91094	Stanley	1914–90	10
91109	Yolla	1914–91	335
97006	Lake Margaret	1914–94	680
97008	Queenstown	1914–94	183
97014	Waratah	1914–73, 89–94	615
Southwest			
94041	Maatsuyker Island	1914–94	147
95011	Maydena	1953–94	270
95012	Ouse	1917–94	190
95019	Uxbridge	1914–83	360
95026	Wayatinah	1958–90	20
95033	Ellendale	1914–68	226
97045	Arve Valley	1954–90	160
97053	Strathgordon	1968–94	320

Table 4.1: **Precipitation stations used in this study, elevation and period of record. Most of these stations have continuous records with few missing data. Lorinna (91052) has the most incomplete record of all the stations used. Very few stations with long data sets exist for the Southwest, and most of the stations shown are situated around the fringes of the area. Station elevation varies from sea level to 840 m ASL**

East	*Place name*	*Period of Record*	*Elevation (m ASL)*
91104	Launceston airport	1940–89	166
92033	St Helens	1914–75	5
92045	Eddystone Point	1914–94	13
Mersey			
91094	Stanley	1914–75	10
91119	Erriba	1962–93	590
97014	Waratah	1914–71	615
98001	King Island	1918–93	24
West coast			
91094	Stanley	1914–75	10
91119	Erriba	1962–93	590
97014	Waratah	1914–71	615
98001	King Island	1918–93	24
Southwest			
94041	Maatsuyker Island	1931–93	147
95003	Bushy Park	1936–93	60
97053	Strathgordon	1970–93	320

Table 4.2: **Temperature stations used in this study, their period of record and their elevation. No station in the Southwest, with ongoing data, commenced recording until the 1930s**

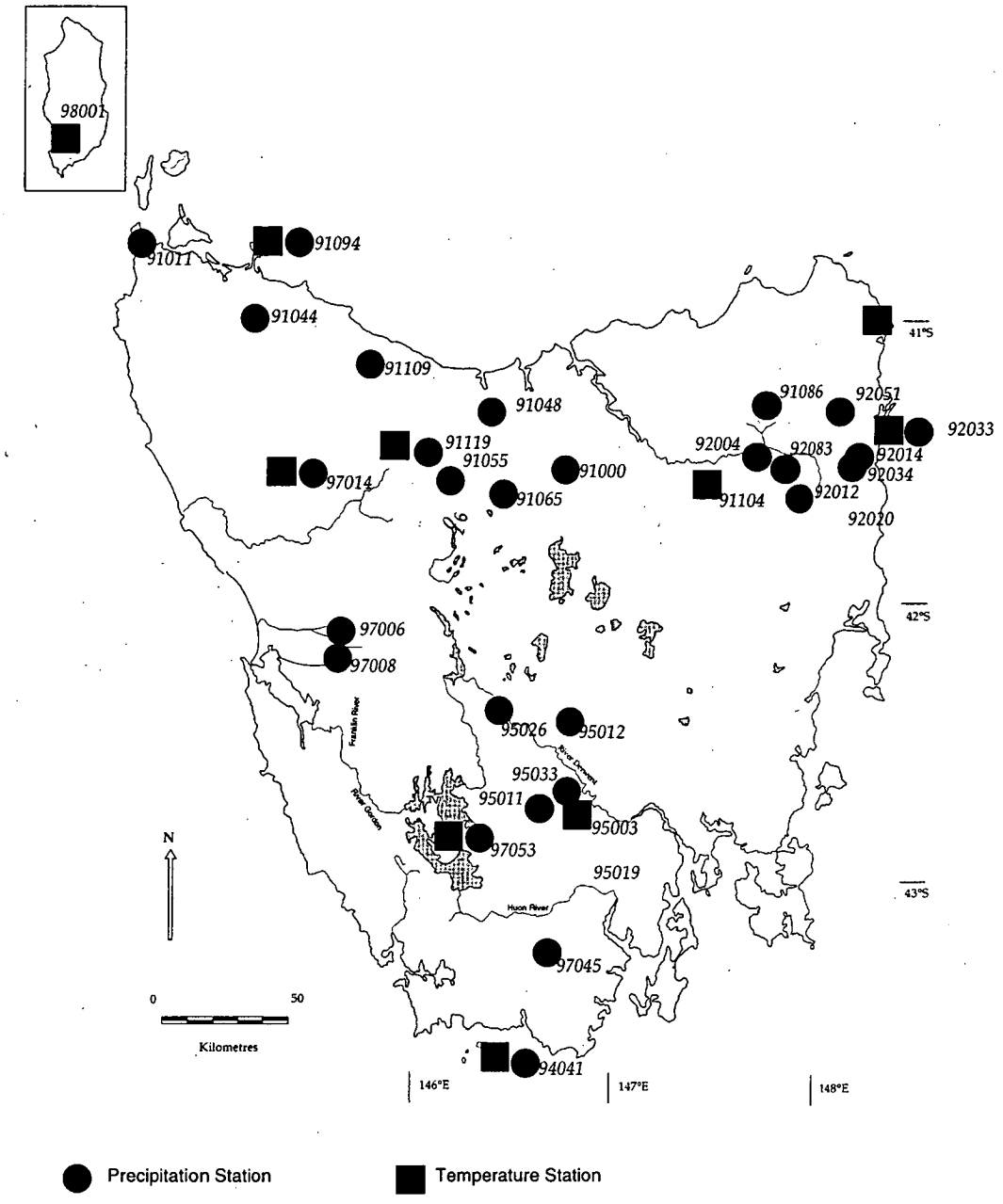

Figure 4.2: **Location of temperature and precipitation stations used in this study**

All temperature and precipitation stations used were selected initially on the length and completeness of their data, and proximity to tree-ring sites. Prior to the calculation of the indices, data were checked for normality by examination of scatterplots, and an appropriate transformation (described below) performed where necessary. Missing values were calculated through stepwise regression on

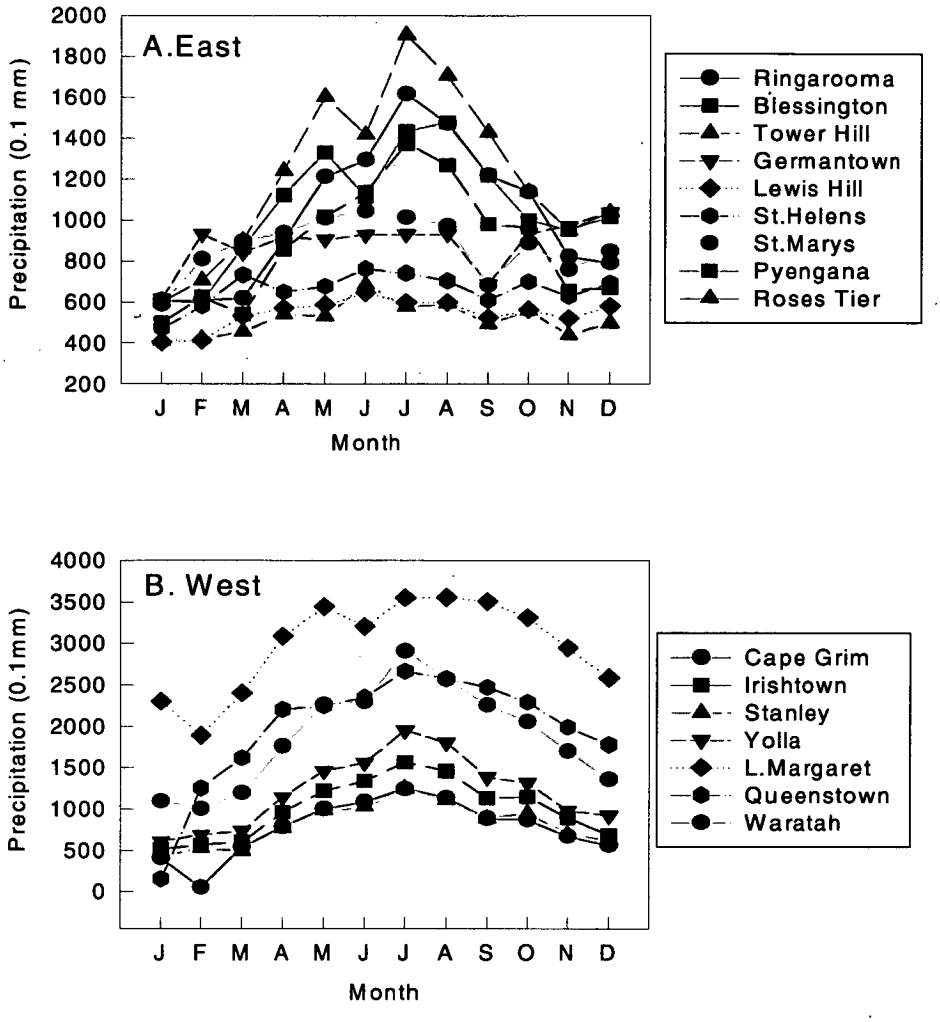

Figure 4.3: **A. Monthly precipitation averages for the East over period of record for each station. Periods of record used are: Ringarooma 1914–1994, Blessington 1916–1994, Tower Hill 1914–1994, Germantown 1929–1976, Lewis Hill 1929-1994, St. Helens 1914–1994, St. Marys 1914–1994, Pyengana 1961–1994, Roses Tier 1957–1994. See Table 4.1 for station numbers.**
B. Monthly precipitation averages for the West over period of record for each station. Cape Grim 1914–1994, Irishtown 1914–1994, Stanley 1914–1990, Yolla 1914–1991, Lake Margaret 1914–1994, Queenstown 1914–1994, Waratah 1914–1973 and 1989–1994. See Table 4.1 for station numbers

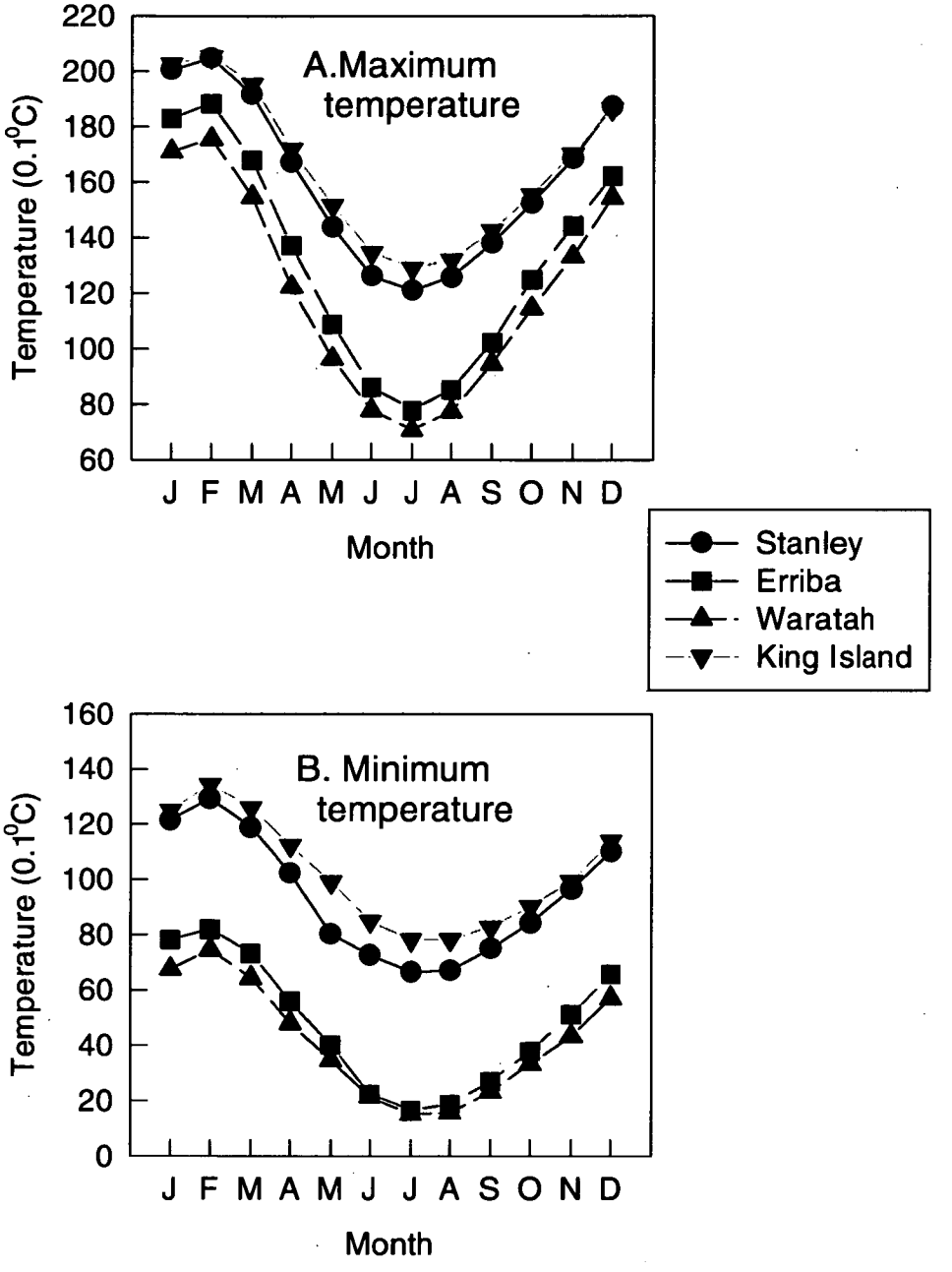

Figure 4.4: **A. Monthly averages of maximum temperatures for selected West stations over the period of record: Stanley 1914–1975, Erriba 1962–1993, Waratah 1914–1971, King Island 1918–1993. Minima and maxima are higher for all months in the coastal regions. See Table 4.2 for station numbers**
B. Monthly averages of minimum temperatures for selected West stations over the period of record. See Table 4.2 for station numbers

close proximity station data. The monthly data were then checked for homogeneity by the Mann–Kendall test (Holmes 1994) and double mass plots. Double mass plots examined a data set for changes in mean, while the Mann–Kendall test looked for a change in trend. All data prior to 1915 were eliminated as several stations failed to satisfy the homogeneity condition between 1910 and 1914. Regional indices were then calculated as described above.

4.2.1.1 Long-term temperature indices

Very few long-term temperature records exist in Tasmania (Table 4.2). This lack of data meant that West and Mersey data had to be pooled to form a single index series.

Examination of the distributions of station data indicated that, for most stations, neither skewness nor kurtosis were sufficiently serious to justify transformation of data. While data was not transformed, it must be noted that the distribution of data for 91104 was somewhat skewed. However, transformation of the data for the other stations resulted in skewed distributions. Therefore no data transformation was performed. Station 91104 was not rejected given the paucity of long term temperature data in the State. Standard normal deviates were then estimated, and averaged across all stations in a region, as outlined above.

4.2.1.2 Long-term precipitation indices

Out of the few reliable long-term stations in the State (Lavery *et al.* 1992), high quality sites used in the construction of precipitation indices included: 91011, 91109, 91044, 92012 and 97008 (Table 4.1, Figure 4.2). High elevation stations with records that did not extend back as far as 1915, but were almost complete, were also used in constructing indices as they would be more representative of actual conditions at tree-ring sites than lowland stations.

In no case were monthly precipitation station data normally distributed. A cube root transformation of data was used, following Stidd (1953) who found the cube root to be appropriate for transformation of rainfall data in both arid and

tropical regions and for time periods of a day to a year for individual stations. A log-normal transformation is often used in data normalisation but, at least in the case of Tasmanian precipitation data, it has been found to 'over-correct' for the skewness (D. Shepherd, Bureau of Meteorology, pers. comm.).

4.2.2 Zonal and Meridional indices

Measurements used in the construction of what is commonly known as the Zonal Index are taken at the 500 hPa level. Because measurements at this level extended back only as far as 1971, the Zonal Index for use in this study was constructed based on Mean Sea Level Pressure (MSLP) which has been recorded for some stations as far back as the 1890s. MSLP data for Hobart was subtracted from Melbourne MSLP (data supplied by the Bureau of Meteorology) to create a Zonal Index over the 1912–1996 period. Pook (1992) highlighted the problems associated with such an index based on a single longitude, but the calculated index was considered satisfactory in terms of a zonal pressure gradient across Tasmania for this study. Salinger *et al.* (1994) created a similar index using the pressure difference between Auckland and Christchurch and Cook *et al.* (1996) have examined pressure differences between paired eastern Australian stations. Creation of a Meridional Index across the State proved more problematical. Eastern Tasmanian stations began recording pressure information from 1939 (with the exception of Cape Bruny, which began in 1923), and many of these stations exhibited missing data. Although Cape Bruny had a relatively long record, Cape Sorell, which could have been used in conjunction with this station to create an index, had no data beyond 1971, and also had seven further years of missing data. The 'next best' set of stations — King Island and Low Head — although somewhat different in latitude, had full data sets, and were therefore selected to construct the Meridional Index.

4.2.3 Spectral analysis of climatic indices

Spectral analyses of monthly maximum and minimum temperature, precipitation, and Zonal and Meridional Indices were conducted over the entire time span available for each data set. For all series, the MTM spectral analysis technique was used, and six data tapers each with a time-frequency bandwidth

product of four were applied in all cases except for the MI. For the MI, three data tapers with time-frequency bandwidth products of two were used.

4.3 Results

4.3.1 Temperature and precipitation indices

Figures 4.5–4.8 illustrate the variation of Austral seasonal maximum and minimum temperatures and precipitation indices for the four regions over the 1915–1994 time frame. For the East and Mersey/West temperature data an upward trend in temperature is evident for most seasons since the 1940s. This is consistent with other independent findings (e.g. Cook *et al.* 1992, Jones and Briffa 1992, Jones 1994, Salinger *et al.* 1995). This trend is noticeably absent in the Southwest series. Torok and Nicholls (1996) and Plummer (1996) have stated that minimum temperatures have increased at a greater rate than maximum temperatures, and the index series are largely consistent with this. The lack of a recent upward trend in the southwest data conflicts with the five-year running mean for Maatsuyker Island (Adamson *et al.* 1988), but Shepherd (Bureau of Meteorology, pers. comm.) has found a considerably reduced year-to-year increase in temperature for southern Tasmanian stations compared with northern stations.

Precipitation indices suggest that there has been an increase in precipitation in the summer for the three northern regions (East, Mersey and West), as well as in autumn and winter for the Mersey and West. An increase in summer precipitation over southeastern Australia since about 1950 has previously been observed (Kraus 1954, Nicholls and Lavery 1992). Also, Srikanthan and Stewart (1991) commented on high winter rainfall in the latter part of the record, and a significant change in November rainfall over Tasmania. Nicholls and Kariko (1994) found that these increases have been largely due to an increase in the *number* of rainfall events while the *intensity* of these events has declined.

For all seasons, a consistently negative relationship between monthly precipitation and maximum temperature is observable (Table 4.3). For most months, this inverse relationship is significant at the 0.05 level, and may be

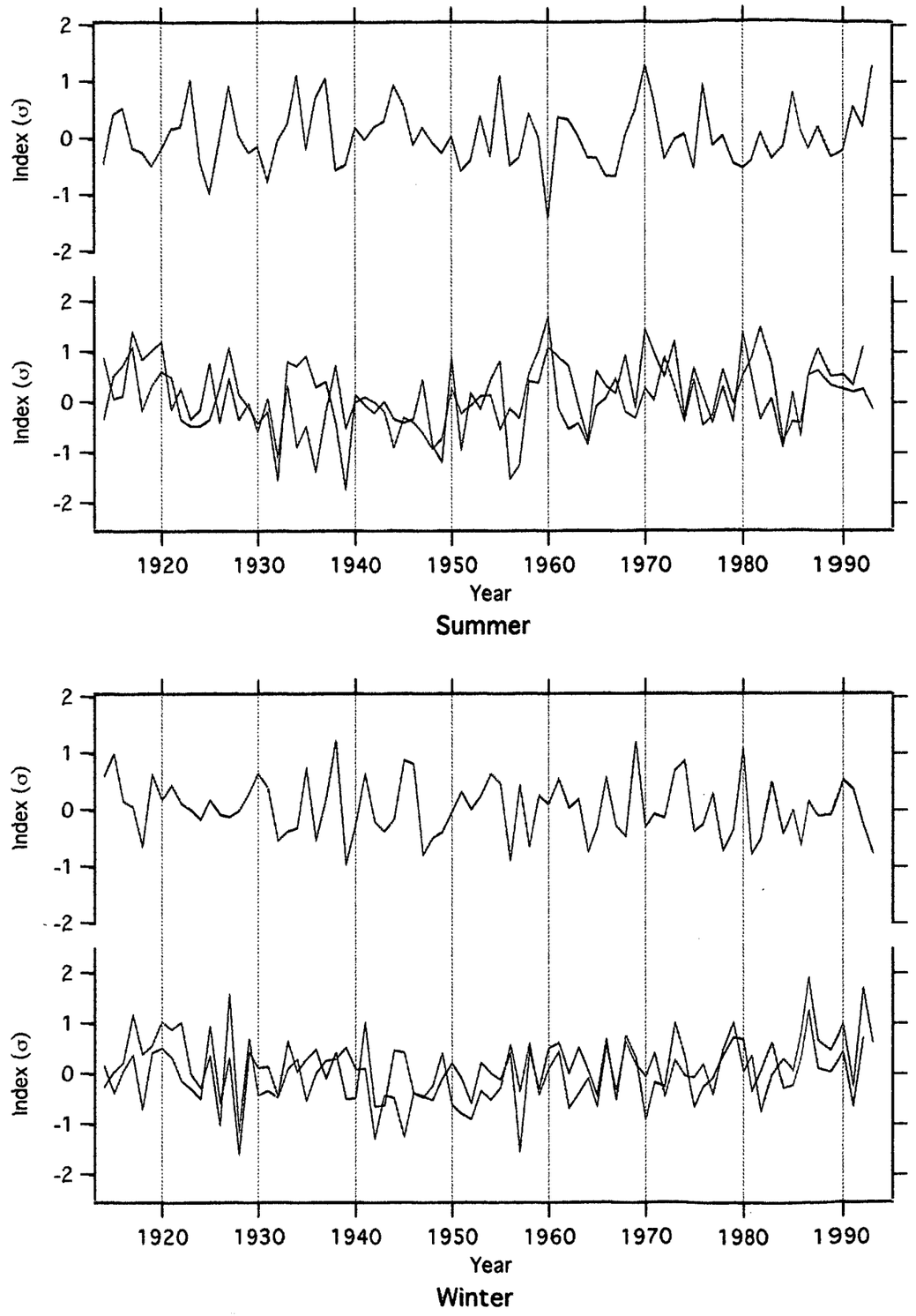

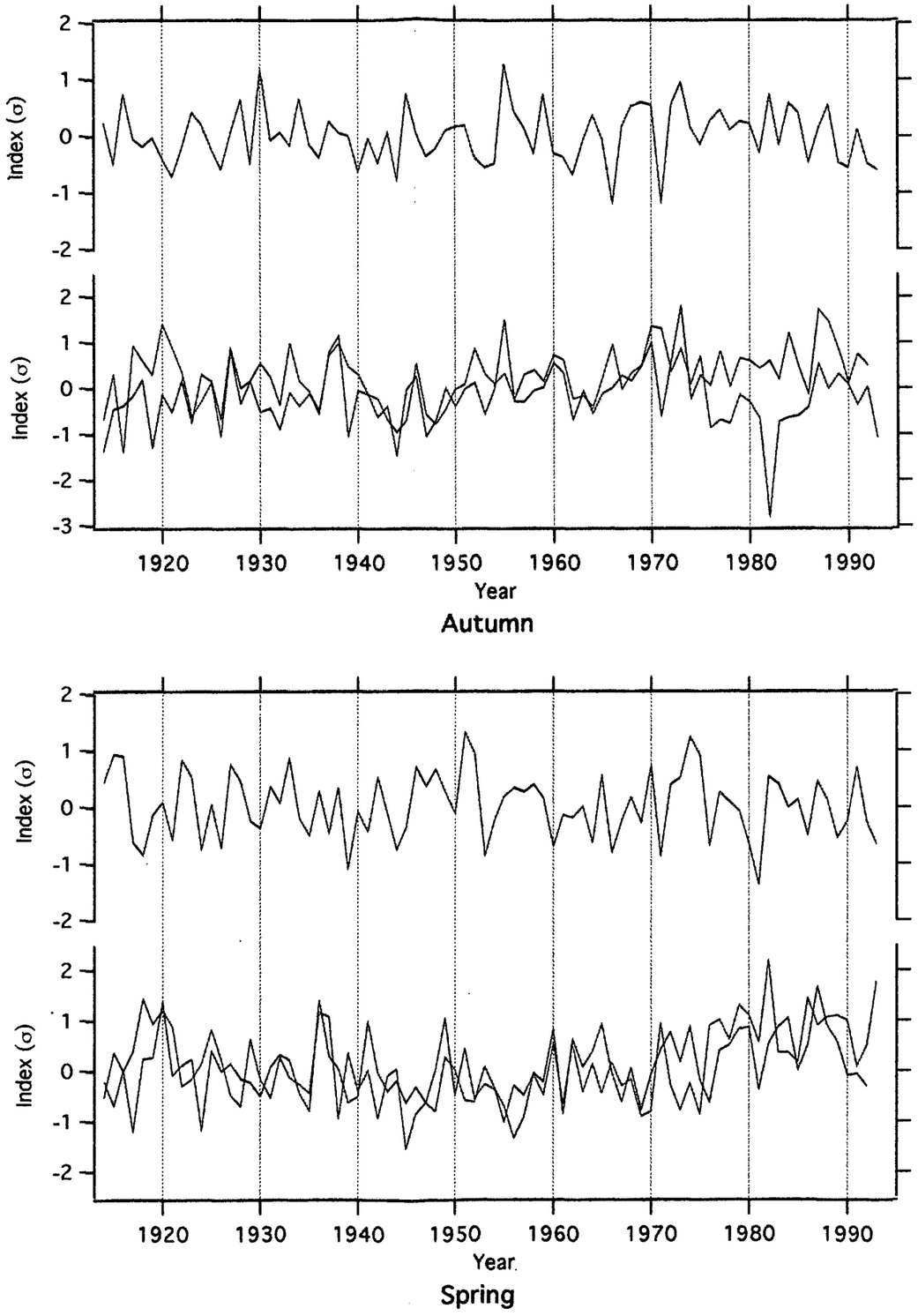

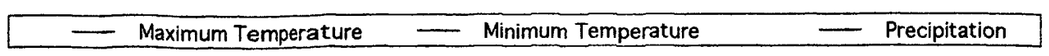

Figure 4.5: East coast seasonalised climate indices based on average standard normal deviates for a number of stations. Temperature data based on stations 91103, 92033 and 92045. Precipitation data based on 91086, 92004, 92012, 92014, 92020, 92033, 92034, 92051 and 92083. (see Tables 4.1 and 4.2)

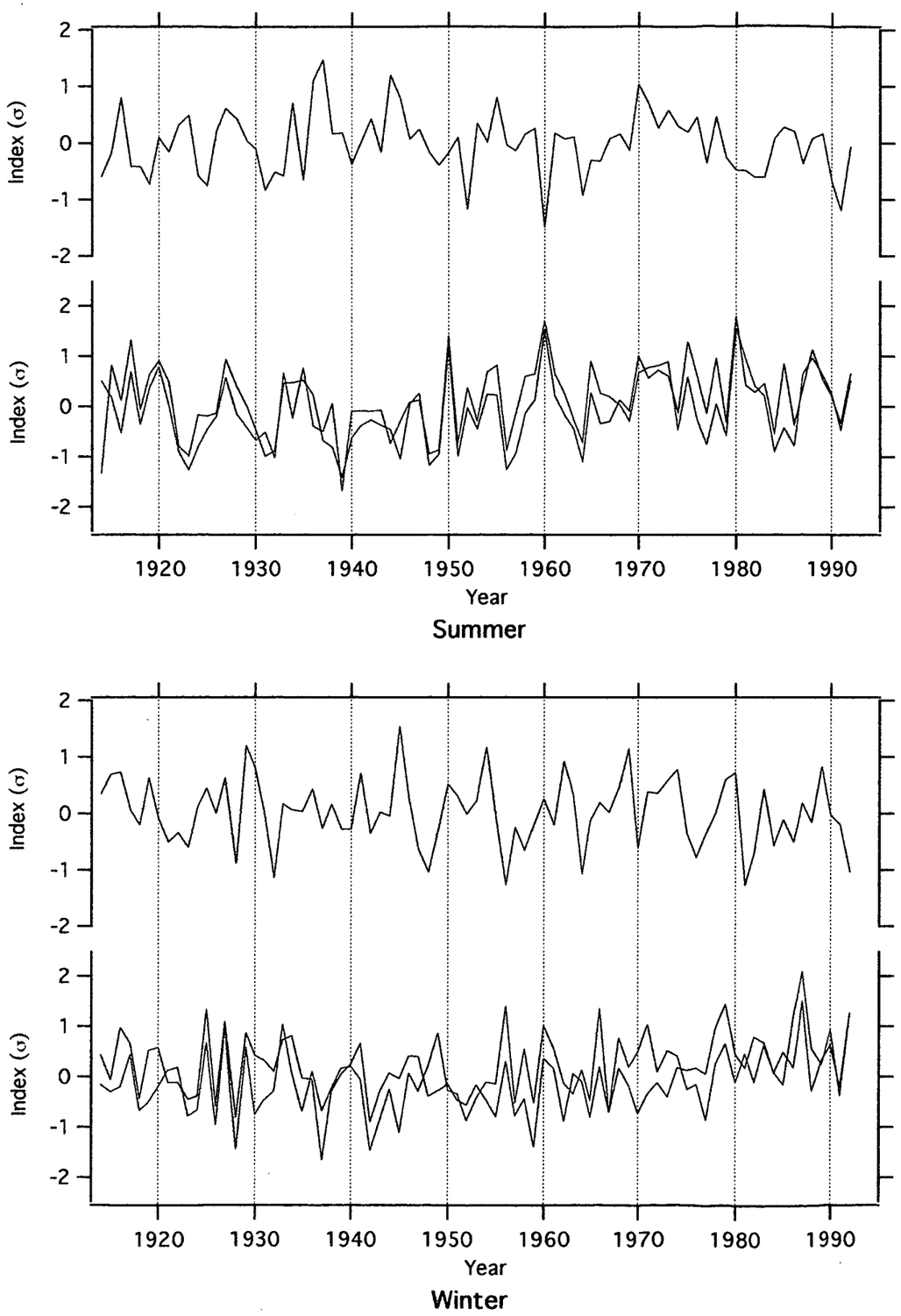

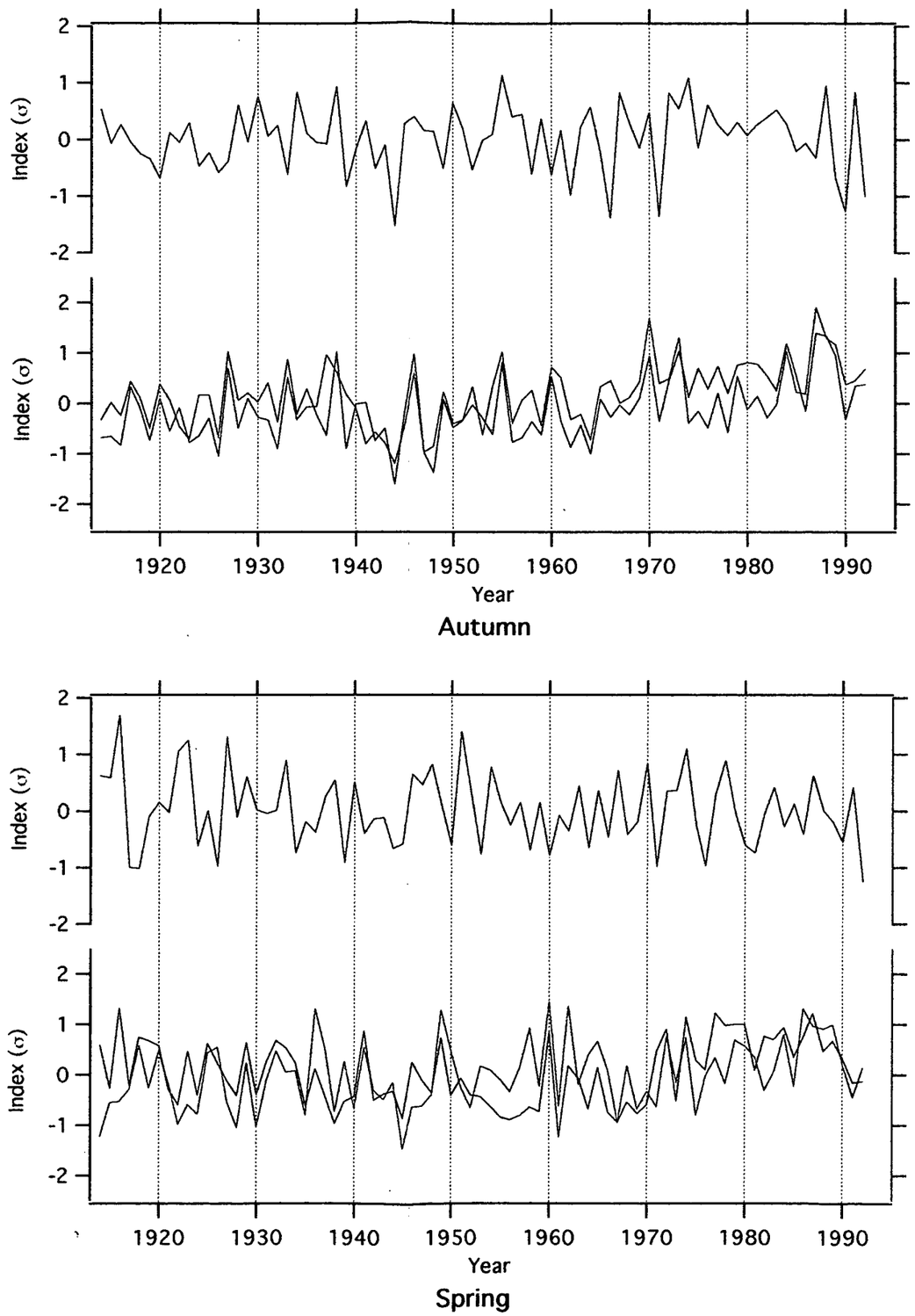

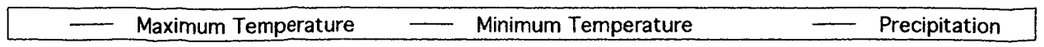

Figure 4.6: Mersey Valley seasonalised climate indices based on average standard normal deviates for a number of stations. Temperature data based on stations 91094, 91119, 97014 and 98001. Precipitation data based on 91000, 91048, 91055, 91065 and 91119. (see Tables 4.1 and 4.2)

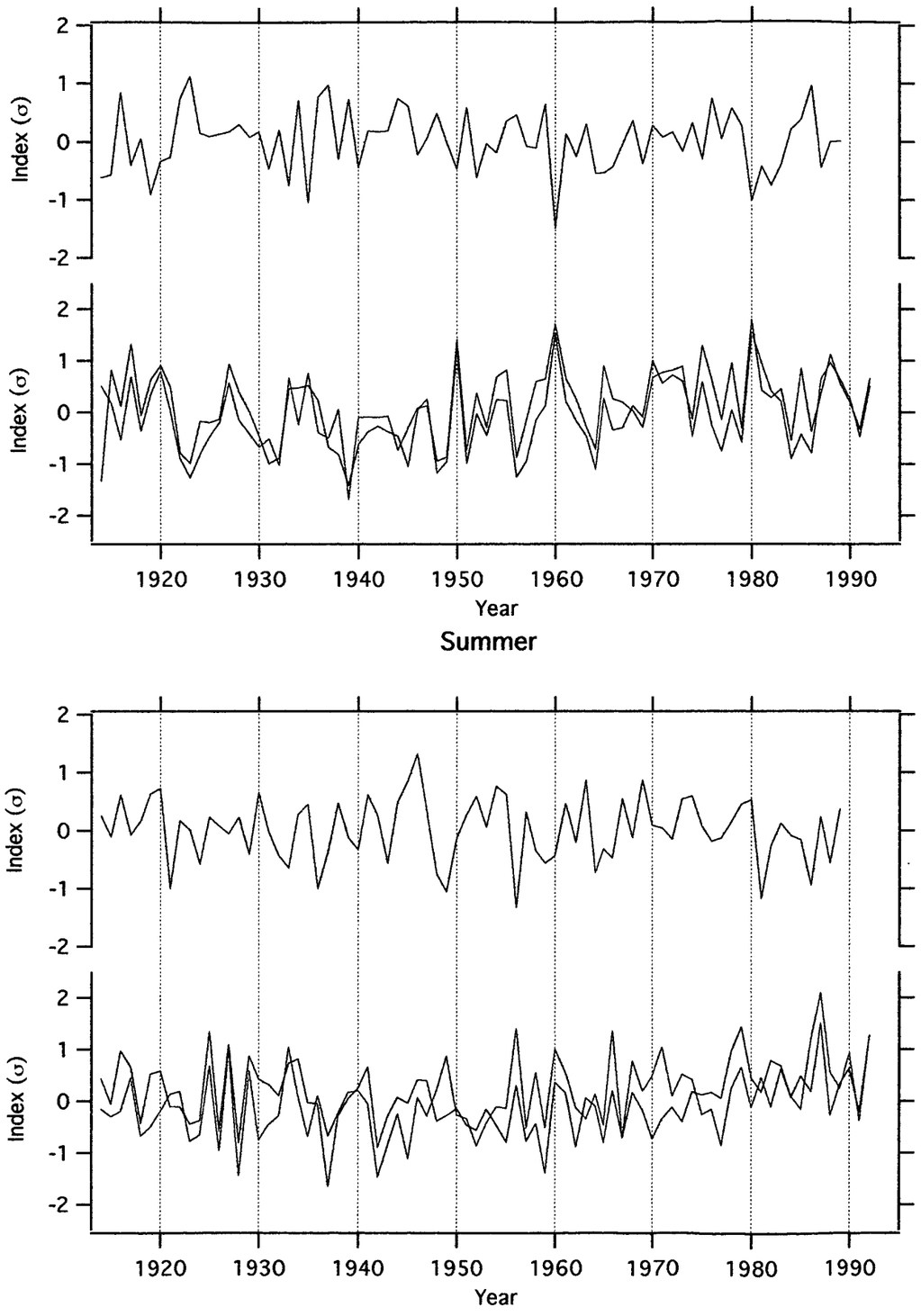

Figure 4.7: West coast seasonalised climate indices based on average standard normal deviates for a number of stations. Temperature data based on stations 91094, 91119, 97014 and 98001. Precipitation data based on 91011, 91044, 91094, 91109, 97006, 97008 and 97014. (see Tables 4.1 and 4.2)

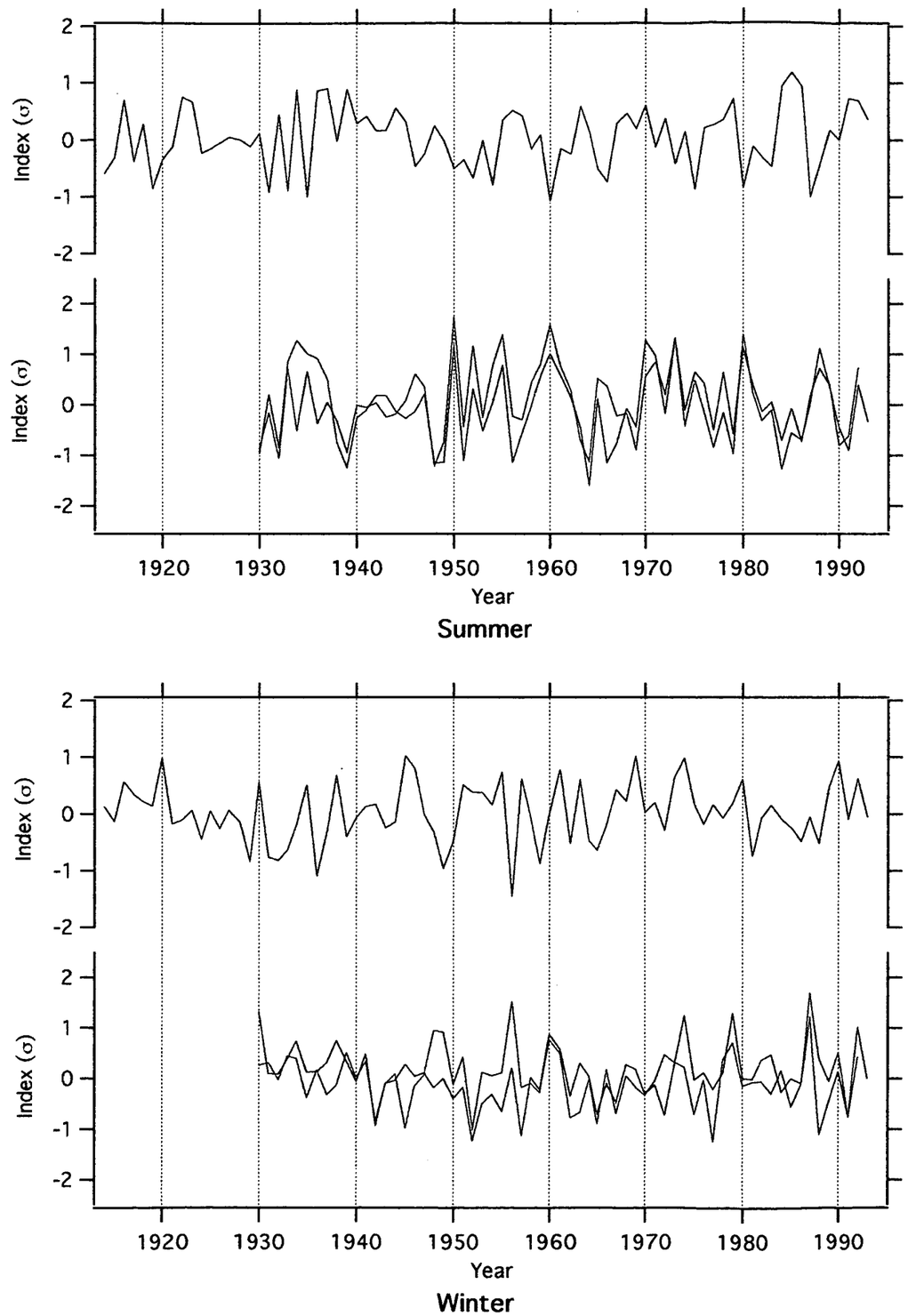

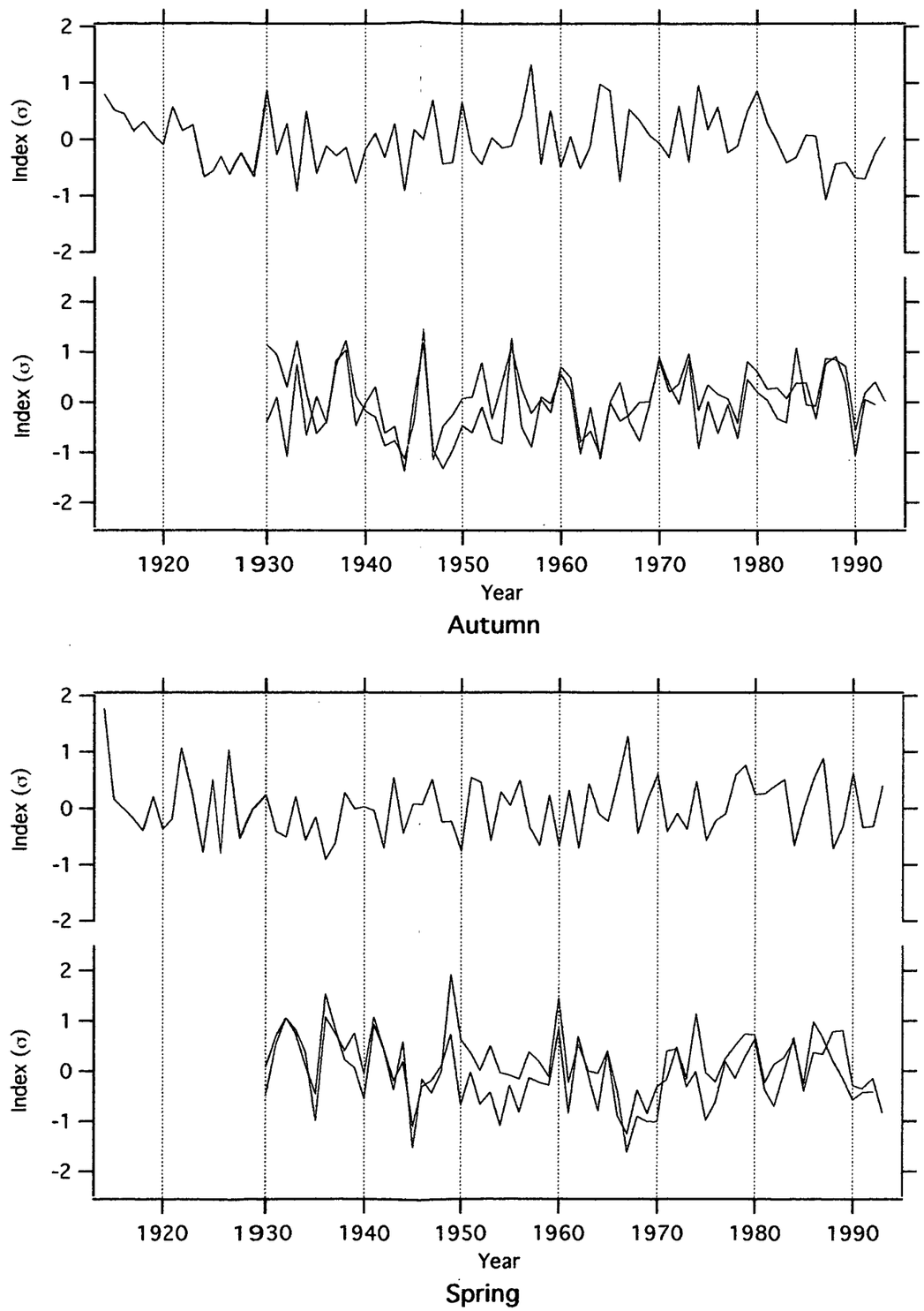

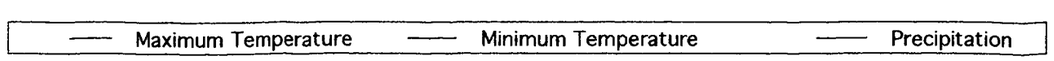

Figure 4.8: Southwest seasonalised climate indices based on average standard normal deviates for a number of stations. Temperature data based on stations 94041, 95003 and 97053. Precipitation data based on 94041, 95011, 95012, 95019, 95026, 95033, 97045 and 97053. (see Tables 4.1 and 4.2)

	East		*West*		*Southwest*	
	ρ	*Z*	*ρ*	*Z*	*ρ*	*Z*
January	-0.373	-3.21	-0.628	-4.66	-0.511	-4.05
February	-0.323	-2.78	-0.588	-4.36	-0.420	-3.33
March	-0.470	-4.04	-0.551	-4.09	-0.448	-3.56
April	-0.192	-1.65	-0.390	-0.29	-0.204	-1.62
May	-0.257	-2.21	-0.500	-3.27	-0.166	-1.31
June	-0.033	-0.29	-0.322	-2.39	0.173	1.38
July	-0.054	-0.46	-0.202	-1.50	-0.054	-0.43
August	-0.426	-3.68	-0.538	-3.99	-0.241	-3.31
September	-0.203	-1.74	-0.47	-3.49	-0.667	-1.94
October	-0.513	-4.42	-0.601	-4.46	-0.473	-3.76
November	-0.513	-4.41	-0.599	-4.46	-0.459	-3.88
December	-0.238	-2.05	-0.494	-3.67	-0.600	-4.77

Table 4.3: **Spearman Rank Correlation (ρ) of maximum temperature and precipitation indices for each region over the period of record: 1915–1994 East, 1915–1993 West, 1931–1994 Southwest. A |Z| >1.96 is significant at the 0.05 level. The inverse relationship between maximum temperature and precipitation becomes nonsignificant in June and July for the East, July for the West, and April–July and again in September for the Southwest**

attributed to higher cloud cover leading to greater rainfall and lower solar radiation. In addition, incident radiation on wet ground will be channelled into moisture evaporation rather than the heating of the ground and air above. Weakest relationships occur during late autumn and winter. This may be indicative of the occurrence of cold clear days at this time of year. Although this negative correlation is striking, the strength of it is unlikely to be time stable given the apparent increase in precipitation for some seasons of the year in conjunction with the undisputed general increase in temperature for the Southern Hemisphere. Salinger and Jones (1996) also commented on the inverse relationship between these two variables and a change in the relationship over time in an Australia-wide context.

4.3.1.1 Comparison with the Cook series

Although Buckley (University of Tasmania, pers. comm.) has found significant agreement between the Cook series and other coastal temperature series around Tasmania, correlation with the derived index series of this study (Table 4.4) suggest that it may be an inadequate representation of minimum and

	East mxt R^2	*West mxt R^2*	*Southwest mxt R^2*	*East mnt R^2*	*West mnt R^2*	*Southwest mnt R^2*
January	0.352	0.758	0.710	0.786	0.682	0.662
February	0.366	0.789	0.697	0.694	0.764	0.525
March	0.091	0.727	0.540	0.736	0.762	0.541
April	0.349	0.756	0.697	0.722	0.728	0.521
May	0.263	0.513	0.767	0.572	0.605	0.701
June	0.658	0.526	0.748	0.432	0.586	0.612
July	0.428	0.457	0.401	0.614	0.687	0.557
August	0.588	0.598	0.474	0.658	0.719	0.576
September	0.594	0.554	0.455	0.655	0.641	0.611
October	0.651	0.755	0.481	0.491	0.552	0.420
November	0.400	0.516	0.525	0.627	0.505	0.548
December	0.241	0.771	0.566	0.708	0.591	0.514

Table 4.4: **Correlation of Cook series and regional climate indices based on the coefficient of determination, R^2. mxt is maximum temperature, and mnt minimum temperature. Periods used: East 1915–1994, West 1915–1993, Southwest 1931–1994**

maximum temperatures for some months of the year for the East and Southwest. In particular, low R^2 values for the East, indicate poor predictive power. Monthly correlation of the Cook series with the maximum temperature index is weakest in the winter months for the West and Southwest, and in late summer/autumn for the East. For minimum temperature, the relationship with the Southwest data is weakest, particularly over the summer months. Weak relationships between both the East and Southwest series with the Cook series over the summer months are of particular concern for a regional dendroclimatic study concentrated on the months of the summer growing season.

Therefore, the use of one climate series, such as the Cook series, may in effect reduce spatially available information as well as leading to erroneous conclusions concerning the nature and strength of the relationship between *Phyllocladus asplenifolius* ring widths and climate in different areas of the State. Regional indices of maximum and minimum temperatures should more closely approximate the climatic conditions of sites than one Statewide climate series. In addition, the separation of maximum and minimum temperatures has the potential to reveal more detailed information concerning the response of the species to climate. For example, it is well known that varying maximum temperatures affect photosynthesis which in turn affects plant growth (Raven *et al.* 1992). In addition,

warm nights are known to be important in the reduction of plant biomass production (Pereira 1994). The use of a data set of averaged maximum and minimum temperatures will not enable the detection of effects such as these.

4.3.1.2 Spectral analysis of regional temperature and precipitation indices

The MTM spectra indicate a number of significant (at the 0.05 level) spectral peaks in monthly data sets (Figures 4.9–4.11). Significant periodicities coincident with the annual cycle occur in the East maximum temperature spectrum only. Temperature data for all three regions show significant periodicities at 1.6–1.95 years, in addition to a peak of approximately 6 years evident in West and Mersey, and Southwest maximum temperatures. East minimum temperatures shows a periodicity at 7–8 years. Precipitation data for Mersey, West and Southwest all have spectral peaks in the 2–2.15 year range, indicating the presence of a quasibiennial oscillation. No such peak occurs in the East precipitation spectrum, although Allen (1991) found evidence for a Statewide precipitation signal in the QBO band. Shepherd (1995) found evidence of the annual cycle in precipitation for the west and north of the State, but not for the east coast. The approximate 6 year periodicity evident in the West and Mersey data sets is consistent with evidence presented by Shepherd for a significant periodicity in precipitation of between 3.6 and 10 years. Spectral peaks at zero frequency, indicating a non-zero mean occurred in East and Mersey/West temperatures and Southwest maximum temperatures.

4.2.3 Zonal and Meridional indices

The seasonalised Zonal Index (Figure 4.12) shows, especially for spring, a slight decreasing trend. Conversely, the Meridional Index (Figure 4.13) shows an increasing gradient over the entire 1939–1996 period, particularly for spring and winter. This is in keeping with the observation of the southward movement of the STHPB and the associated weakening westerlies since 1930 (Deacon 1953, Lamb and Johnson 1961, Trenberth 1976, Cook *et al.* 1996).

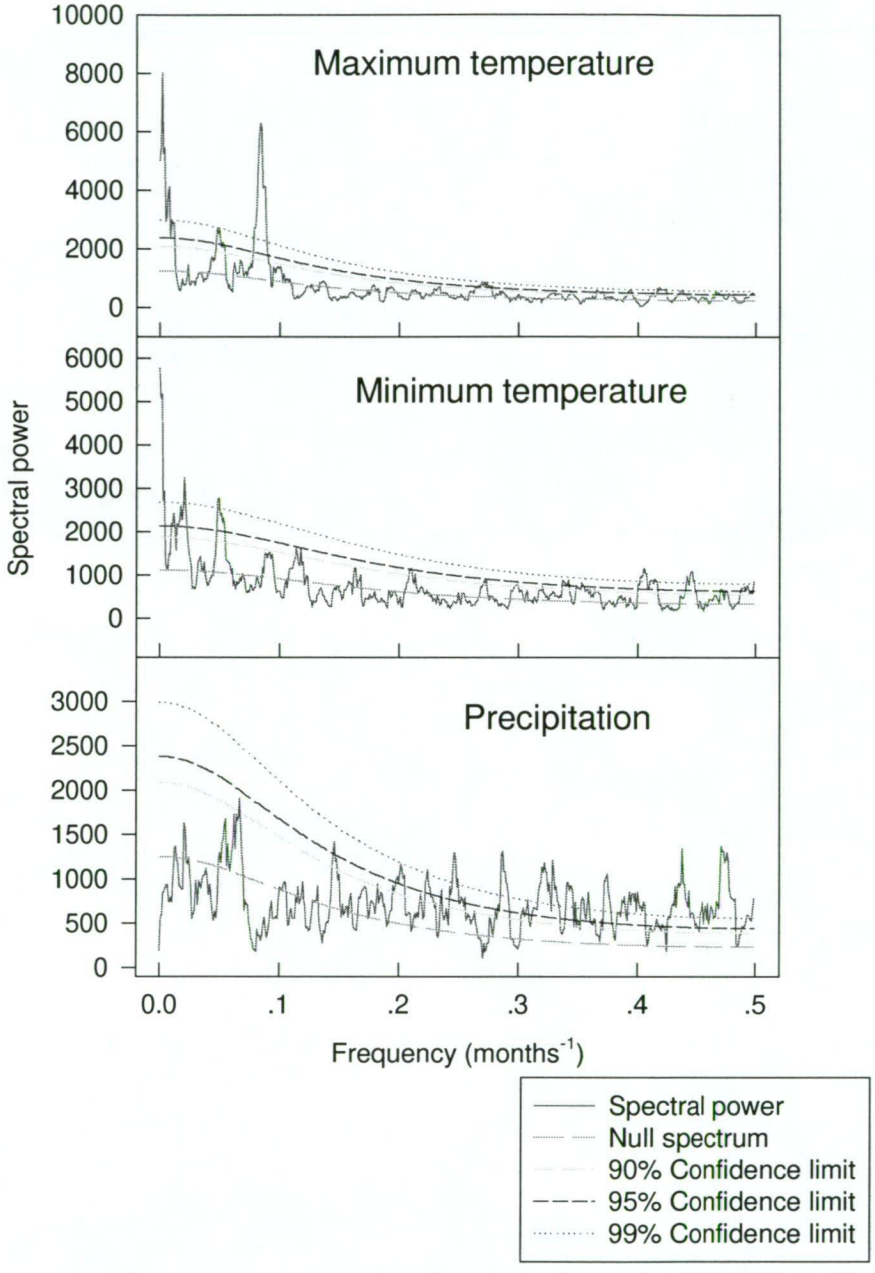

Figure 4.9: **Spectra of climate indices for East coast, monthly data. Significant spectral peaks (at 0.05) in maximum temperature occurred at 0 frequency, 1.6 and 1.04 years; for minimum temperature, 0 frequency, 8.5, 4.73 and 1.7, years; with no significant spectral peaks in precipitation data. Period of analysis is 1915–1994 for all data sets and six data tapers with time-frequency bandwidths of four have been applied**

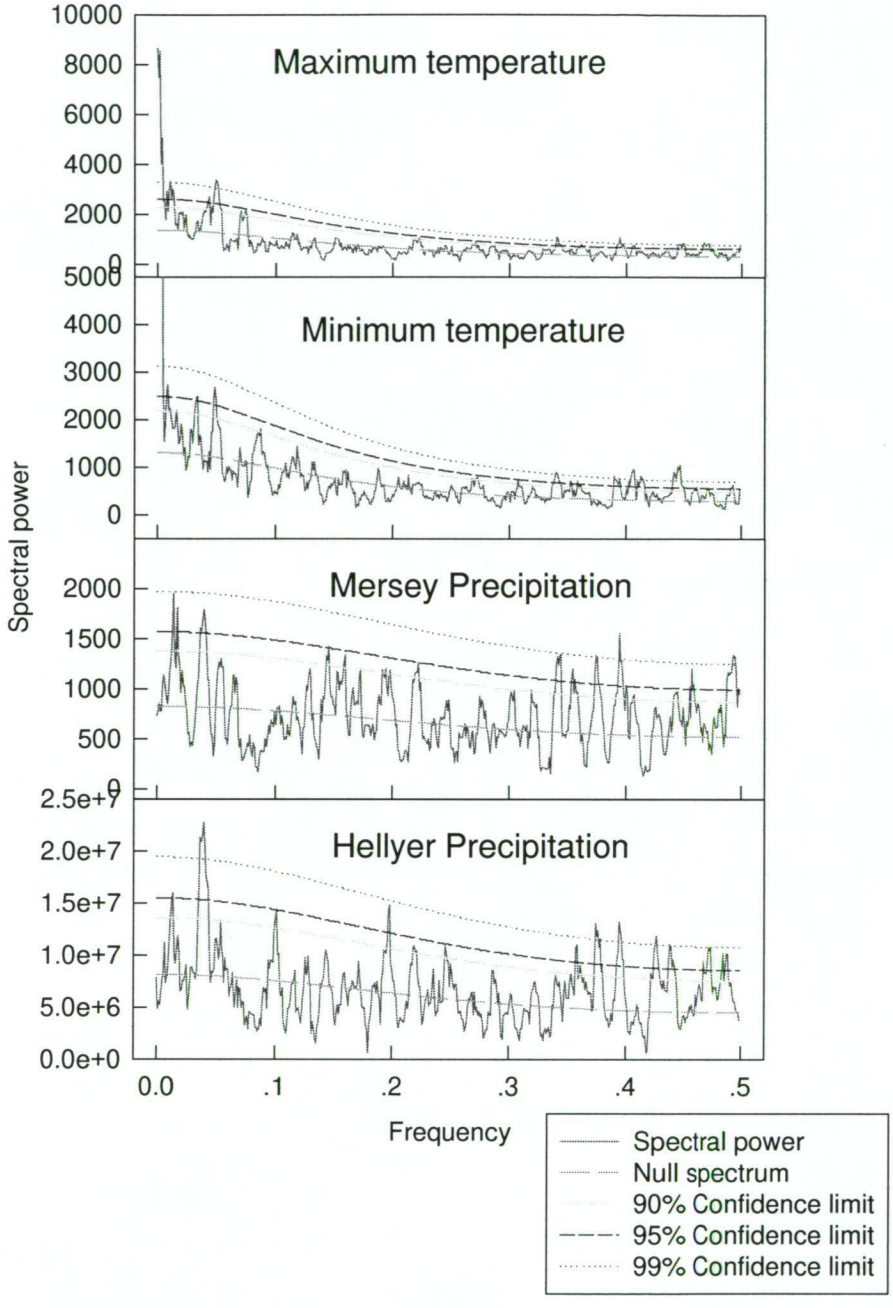

Figure 4.10: **Spectra of Mersey/West monthly climate indices. Significant spectral peaks for maximum temperature at occurred at frequencies lower than one year: a trend, 7.79, 1.94, 1.71 years; minimum temperature, trend, 1.73 years. Mersey precipitation 6.08, 5.02 and 2.13 years; Hellyer precipitation, 6.08 and 2.13 years. Period of analysis for temperature data is 1910–1993, for Mersey and Hellyer precipitation 1915–1992 and six data tapers with time-frequency bandwidths of four have been applied**

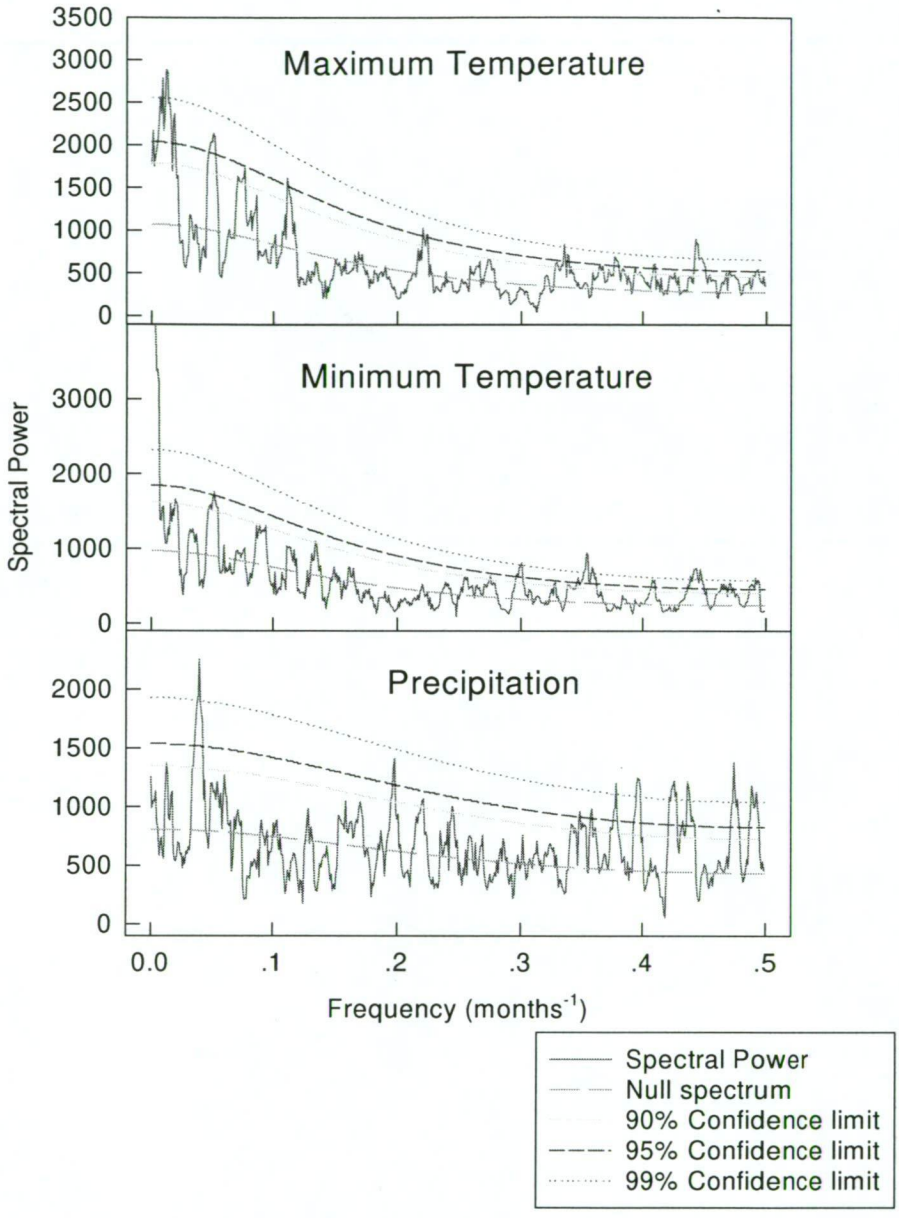

Figure 4.11: **Spectra of Southwest climate indices, monthly data. Significant spectral peaks (0.05 significance level) for periodicities greater than one year occurred at 10.4, 7.12, 4.48 and 1.6 years for maximum temperature; a trend and 1.6 years for minimum temperature; and 2.08 years for precipitation. Period of analysis is 1931–1994 for temperature and 1915–1994 for precipitation. Six data tapers with time-frequency bandwidths of four have been applied**

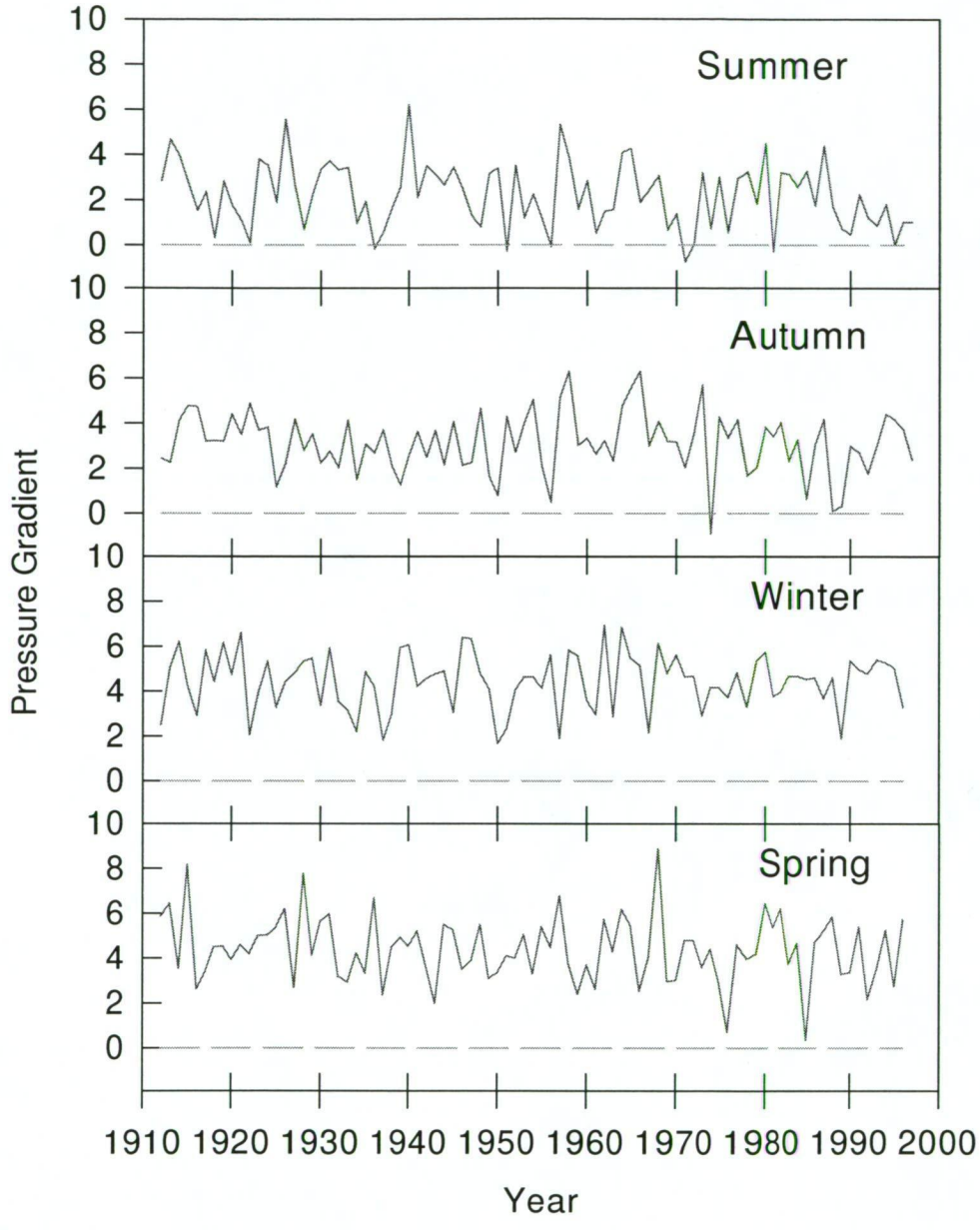

Figure 4.12: **Seasonalised Zonal Index: Melbourne minus Hobart MSLP. No trend was evident in the data set for any month. Negative values of the index occurred only in summer and autumn months, more commonly in the summer months. Data covers the 1912–1996 period**

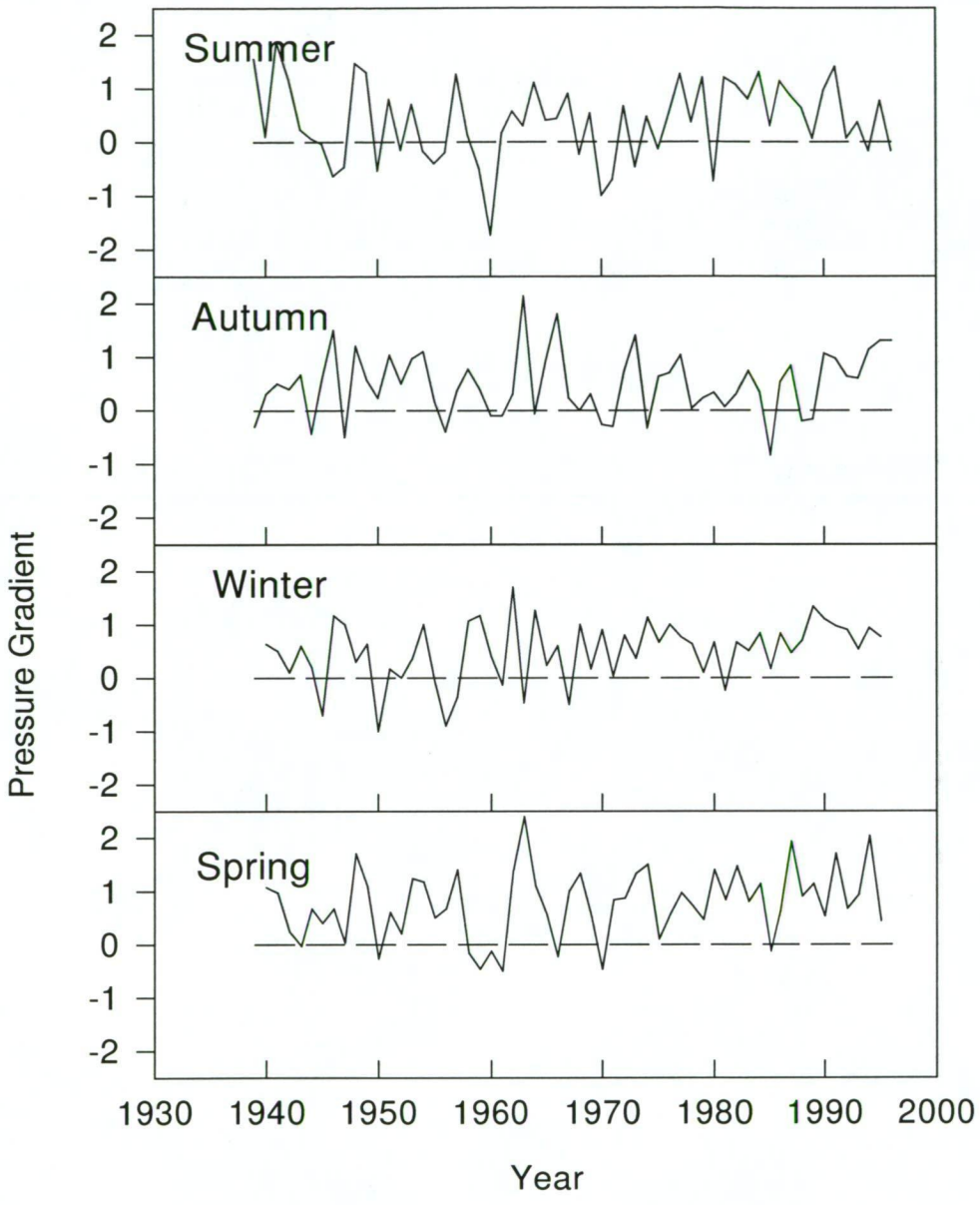

Figure 4.13: **Seasonalised Meridional Index, King Island minus Low Head. Decreased variability was evident for winter data after 1970 giving the impression of an upward trend, and a trend for spring data was also apparent over the 55-year period. Data spans the period 1939–1995**

4.2.3.1 Spectral analysis of the Zonal and Meridional indices

The strongest frequency peak in the Zonal Index represents the annual cycle (Figure 4.14). An additional significant peak at approximately 17 years is also apparent, with a plethora of significant peaks at less than one year evident. Although Makaroiannis *et al.* (1982) found spectral peaks at 13.9, 4.6, 3.5, 2.8 and 2.3 years, the results obtained in this study, are considerably different. Ropelewski *et al.*(1992) commented specifically on the biennial peak he observed in the zonal spectrum.

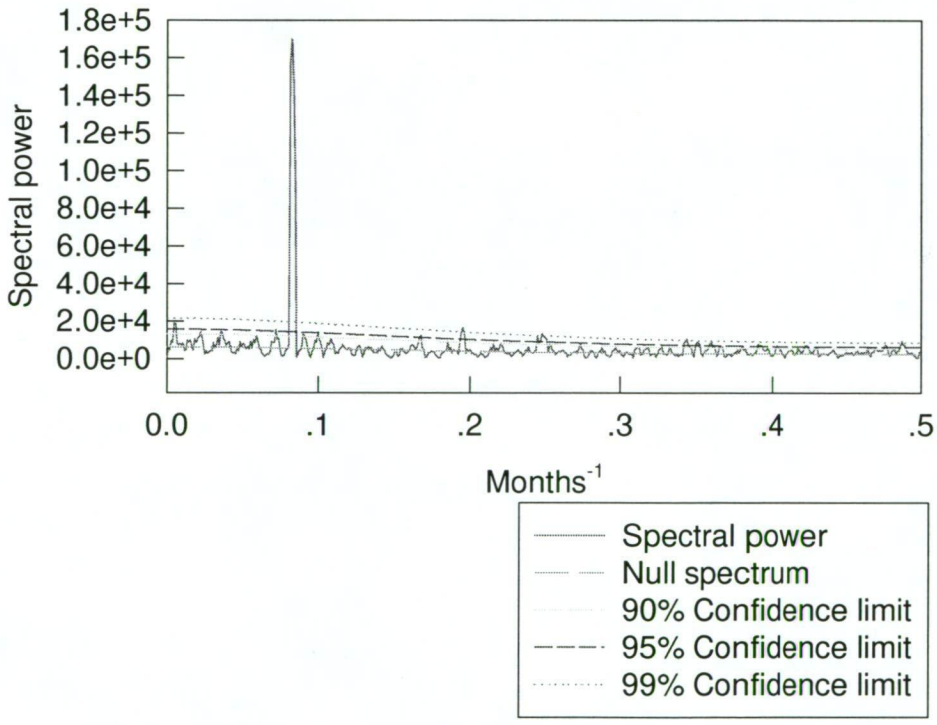

Figure 4.14: **MTM Spectra of monthly ZI. The only significant spectral peak of greater than one year occurs at a frequency of 0.0049 (17.01 years. The large spike represents the annual cycle, with a periodicity of 11.9 months. The Time period of analysis is 1912–1996 and six data tapers with time-frequency bandwidth products of four have been applied**

In the case of the MI, spectral analysis reveals a periodicity at approximately five years with a dominant peak at approximately 12 months. The obvious presence of the annual cycle in both the MI and ZI is encouraging.

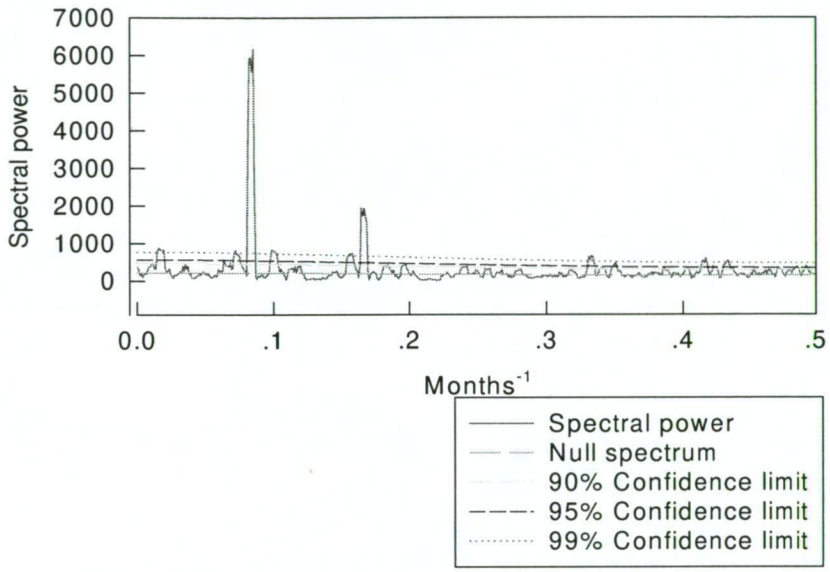

Figure 4.15: **MTM spectrum of monthly MI. The only significant peak of greater than one year occurs at 0.0156 (5.34 years). The large spike once again represents the annual cycle. Three data tapers with time-frequency bandwidth products of two have been applied. Period of analysis is 1940–1996**

4.4 Summary

Two temperature indices and one precipitation index have been derived for each of four regions within the State. While tree-ring widths will, in limiting circumstances, generally reflect more localised climatic information, it is possible that broader scale information may also be gleaned from trees. Therefore, the investigation of how ring widths of *Phyllocladus asplenifolius* relate not only to temperature and precipitation data but also to the SOI, ZI and MI, may reveal additional relationships that can potentially be used for climatic reconstruction

purposes. They can also be used to check the consistency of the tree's response to the more generally used temperature and precipitation variables. A number of previous studies have found significant correlations between such variables and ring-width indices.

Across the northern part of the State increasing temperatures over the current century are apparent, the most dramatic of these for the West. The trend of increasing temperatures does not appear to have occurred in the south of the State, and other evidence suggests that, although present, it is considerably less than for the north. Neither the ZI nor MI shows clear trends over time, although the winter MI is suggestive of an upward trend in winter. In most recent years the value of the SOI has been generally below average for autumn, winter and spring. Trends observed in the data sets developed here are in agreement with other climatic evidence for the Tasmanian sector.

Chapter 5: Climate Response of *Phyllocladus aspleniifolius*

5.1 Introduction

Strong association between climate variables and cambial growth is the foundation upon which climate reconstruction is built. The nature of the relationship between the tree and climate does not merely provide functional information for climate reconstruction, but has the potential to provide additional information concerning specific plant functions.

The general paucity of knowledge concerning the relationship of climate and cambial growth engenders a 'second best' approach of empirical modelling in order to attain some understanding of the processes involved. Certainly, in the case of Tasmanian conifers, the response function has been the most common method of determining which climate variable most limits cambial growth. Classic response function analysis involves a number of assumptions. The reproducibility of a postulated model is essential if climate reconstruction is the goal. Attempts to reproduce models of the climate response of *Phyllocladus aspleniifolius* for independent data sets have not been successful using the popular Principal Component Regression technique. This poor performance was therefore examined more closely in an attempt to ascertain what change in response, if any, had occurred and its implications for climate reconstruction from this species.

Because there exists a considerable literature on the nature of the climate response of *Lagarostrobos franklinii*, comparison of the responses of *L. franklinii* and *Phyllocladus aspleniifolius* may enable additional insight not possible by using a single species.

The basic thrust of this chapter is to address two issues: firstly, the nature of the response of *Phyllocladus aspleniifolius* to climate; and secondly, the temporal and spatial patterns of correlation. Particular emphasis is placed upon the dominant response mode as well as temporal variation. A brief outline of the calibration/verification process is provided at the outset, following which the two issues are addressed.

5.1.2 Calibration and Verification

Figure 5.1 is a simple diagrammatic representation of how climate affects ring widths. The climate of a given year will influence not only that year's growth, but also, through biological processes, the growth of subsequent years. This phenomenon is termed *physiological preconditioning* and some part of it is statistically expressed as autocorrelation (Figure 5.2). Autocorrelation is a violation of the important assumption of independent observations made by many models.

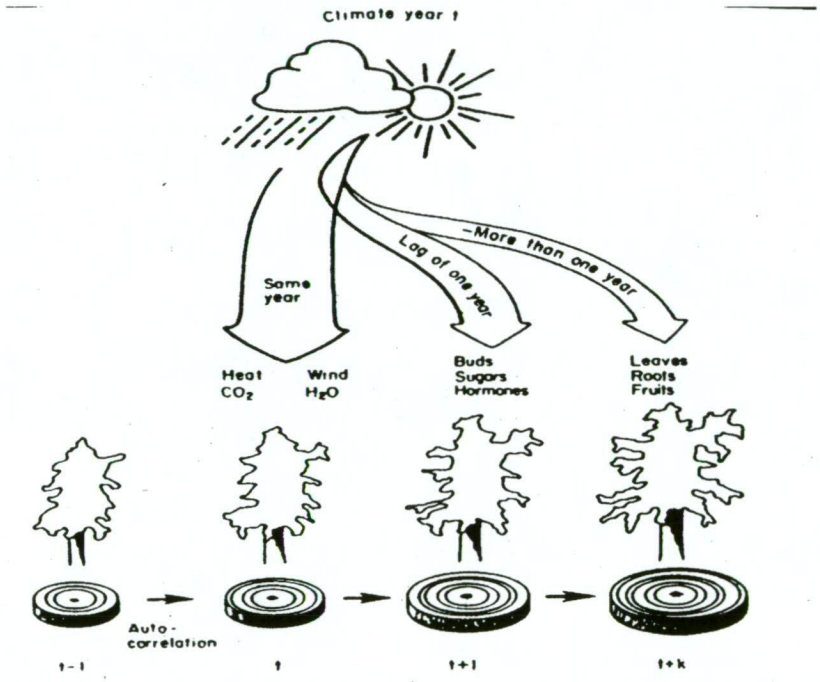

Figure 5.1: **Relationship between climate and ring width. Climate in any one year is modelled to have a large effect on ring width through heat, wind, carbon dioxide and water. However, it can also affect ring width of subsequent years through effects on sugars, hormones, buds, growth of leaves, roots, fruits and shoots. This effect upon growth in subsequent years results in the statistical process of autocorrelation. (Source: Fritts 1976, drawing by M. Huggins)**

For most dendrochronological studies the relationship between ring width and climate is assumed to be linear. When the data satisfy this assumption, a linear model may be applied. However, basic physiological processes do not generally show a linear response to externally applied conditions. In the most elementary terms, individual processes are generally characterised by a parabolic

response to external factors such as humidity, temperature, precipitation, available trace elements or minerals and so on. Above and below the optimal 'amount' of any one of these factors, growth becomes inhibited by this one factor. A simple

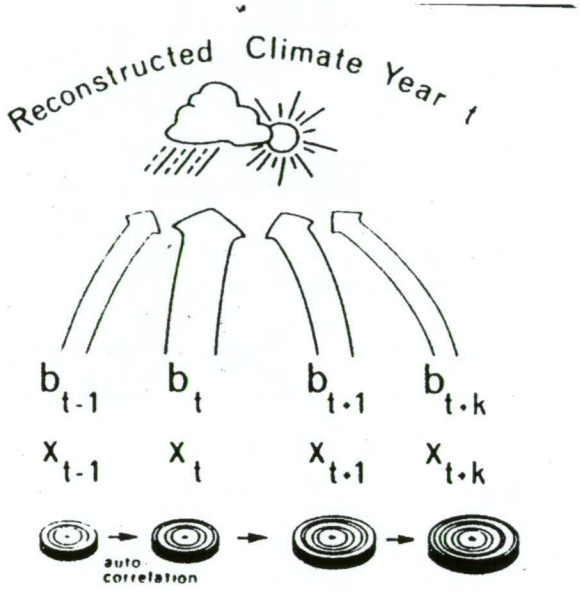

Figure 5.2: **Model for statistical calibration. Coefficients, b_t, are obtained and multiplied by corresponding ring-width indices and the products added to obtain an estimate of climate for a particular year. (Source: Fritts, 1976. Drawing by M Huggins)**

example is the existence of optimal and suboptimal temperatures for photosynthesis of Tasmanian rainforest species (Figure 5.3). A plausible hypothesis is that photosynthesis is limited by temperature and therefore that radial growth is temperature-limited. In such a case, fitting a linear relationship between growth and temperature for any of these species requires the qualifying assumption that only a single 'linear' portion of the mathematical representation of the process is relevant.

The statistical process of estimation of the relationship between climate and tree rings is known as *calibration*. *Verification* is the process whereby the calibrated model is tested against an independent data set. When climate is used as the independent variable and tree-ring width as the dependent variable, the relationship is known as the *response function*. Response functions are used to provide information on the nature of the response of the trees to climate variables.

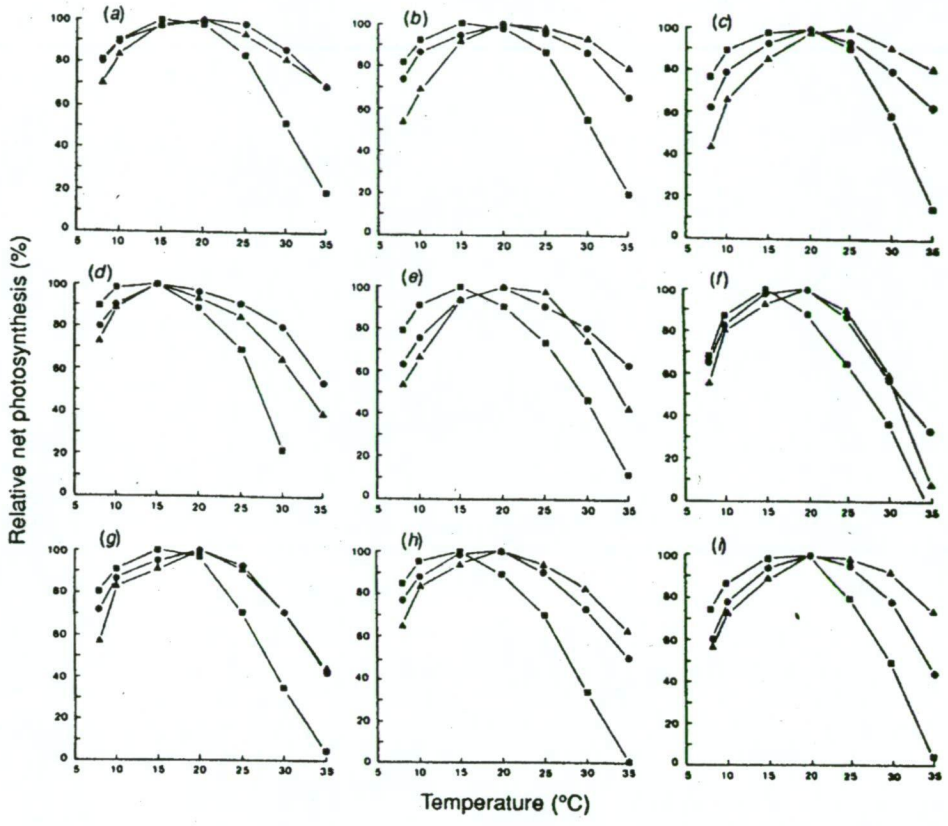

Figure 5.3: **The response of net photosynthesis to instantaneous temperature in foliage acclimated to 8 ^{0}C, 20 ^{0}C and 29 ^{0}C. Rates of photosynthesis are expressed as a percentage of the maximum rate of photosynthesis recorded at that acclimation temperature. Each point is the mean of five replicates. (a) *Nothofagus cunninghamii* (980m ASL), (b) *N. cunninghamii* (700m ASL), (c) *N. cunninghamii* (80m ASL), (d) *Athrotaxis selaginoides* (980m ASL), (e) *Nothofagus gunii* (980m ASL), (f) *Atherosperma moschatum* (700m ASL), (g) *Eucryphia lucida* (700m ASL), (h) *Phyllocladus aspleniifolius* (700m ASL), (I) *Lagarostrobos franklinii* (80m ASL). Source: Read and Busby (1990)**

If climate serves as the dependent variable and tree rings as the independent, then the relationship is known as the *transfer function*. Once a significant response of growth to certain climate variables has been found, this can be used to generate a transfer function where growth explains climatic variations, which can then be used to reconstruct climate. Hence, response and transfer functions are empirically established relationships between cambial growth and climate (Figures 5.1 and 5.2). While it makes sense to interpret response functions causally, the causal interpretation of transfer functions is nonsensical.

Although calibration may reveal the existence of a statistically significant relationship between climate variables and tree rings it does not necessarily follow that this is a direct causal relationship. The response of a plant to climate is complex, with one climate variable affecting a number of processes, which may compete, and one process is affected by several climatic variables. Nor does it follow that a response function is a measure of the relationship between ring widths and climate. Rather, it is a measure of the performance of a given model in the estimation of the relationship between ring widths and climate (Hughes *et al.* 1978). The calibration process involves a number of limiting assumptions:

1. The uniformitarian assumption which states that the response of a tree to climate is the same now as it has been in the past.
2. Conditions in the calibration period are analogous to past conditions.
3. The statistical relationship is justifiable in terms of the biological relationship — e.g. a linear model should model linear processes.
4. Observations of the dependent and independent variables are independent of one another. The problems of autocorrelation and multicollinearity violate the independence assumption.
5. Normality exists where required.

In response function analysis, the sign and magnitude of each element of a response function is an expression of the net effect of that variable on ring width (Fritts 1976), in the form defined by the model. High correlation of a climatic factor and ring width implies limitation of growth by that factor.

At first glance it might appear that multivariate regression is an appropriate medium through which to generate a good model. However, because multicollinearity of climate predictors may become problematic, the technique of multivariate regression after the extraction of principal components (PCs) is commonly used in the generation of both response and transfer functions. Interrelationships between 'independent' variables can lead to: difficulties in isolating the effects of separate variables; heightened sensitivity to deletion or addition of variables; inflated goodness-of-fit statistics; significant variables

appearing as insignificant. Using 'principal component regression' to generate a response function, PCs of climate data are used as independent variables in a multivariate regression relationship with tree-ring widths. Because PCs are, by definition, orthogonal to one another, the problem of multicollinearity is overcome. A number of other alternative approaches to response function analysis do exist, including the use of canonical correlation and regression analysis, and the separate use of high/low frequency components (e.g. Guiot *et al.* 1982, Cook *et al.* 1994).

A further violation of the independent observations assumption can be caused by autocorrelation, the existence of which in tree-ring series is well documented (Fritts 1971), and has been explained in Chapter 3. One common approach to dealing with autocorrelation in a time series is to remove it through autoregressive modelling. An alternative approach is to include prior growth as a predictor variable. Van Deusen (1991) points out that removal of autoregression from data prior to modelling is not strictly correct in a statistical sense, and that the appropriate place to be concerned with autocorrelation is in the residuals of the model.

There are several important ways in which a researcher may alter the final response function within the statistical framework of principal component regression. The first relates to potential independent variables. Fritts (1976) did not screen candidate independent variables, meaning that all variables were entered into the principal components analysis. Fritts and Wu (1986) have argued that minimisation of the number of predictors limited the descriptive ability of the response function. Cook *et al.* (1994), referring to transfer functions, stressed the likelihood of artificial predictability produced by this approach, and the importance, therefore, of parsimony. Their conclusions similarly apply to response functions. Screening of predictors was recommended such that only a subset of statistically significant independent variables was entered into the principal components analysis.

Secondly, the manner in which the number of PCs entering the multiple regression is selected also has important implications as a different number of PCs

will be selected by different techniques. Rules of dimension selection most pertinent to dendroclimatolology have been outlined by Guiot (1990).

Focusing specifically on response function analysis, Blasing *et al.* (1984) recognised a number of caveats:

1. Altering the number of variables to be transformed can change the shape of the response function in an unpredictable way.
2. The use of different criteria to select the number of eigenvectors entering into the regression can also change the shape of the response function. The addition of higher order eigenvectors explaining little variance may add meaningless information to the model, thereby degrading the quality of the response function.
3. Significant response function elements occur far more frequently than significant correlation function elements.

The outcome of these potential drawbacks has been the recommendation of the use of the correlation function, rather than the response function, as an initial step in the investigation of ring-width response to climate (Blasing *et al.* 1984). The correlation function is merely the set of correlation coefficients for the relationship between climate variables and growth over a given interval of time. Correlation functions have been used in this study.

Verification is integral to dendroclimatology and is intended to ensure that the calibrated model does not attain meaningful coefficients merely by chance. Verification of both response and transfer functions proceeds in the same manner. It is performed by testing the calibrated model (based on a *calibration* data set) on a portion of the data withheld from the calibration process (the *verification* data set). Due to the statistical optimisation procedures used in calibration procedure, it is unlikely that the calibrated model will perform as well on the verification data set as on the calibration data set (Cook *et al.* 1994). A calibrated model that performs well on an independent data set is considered to conform to the assumptions of the stated model and is hence both biologically and statistically

justifiable. If, on the other hand, the calibrated model can not be satisfactorily verified on the verification data set, questions concerning the true nature of the response to climate are raised. A popular approach to defining the calibration and verification periods is simply to split the climatic data set into halves, using one half for calibration and the other for verification. This commonly used split calibration–verification scheme can serve as an initial step in investigating the temporal stability of estimated models.

A number of statistical verification tests are commonly employed to test the goodness of fit of the calibrated model to the actual data in the independent period, and are described below. The same criteria for model selection are used for both the independent and dependent periods in order that genuine comparability can be achieved.

The *product means test* (PM) examines the number of times the sign of departures from the mean of the predicted and actual climate series agree or disagree (+ for agreement, - for disagreement), as well as the magnitudes of yearly changes. It uses the products of deviations from the respective means of the two series to look for differences in the two sample periods based on their signs. If the signs of these departures from their means are the same, the cross-product is positive. If the signs of the departures differ, it is negative. The difference between the absolute means of positive and negative products can be tested approximately by a standard *t* test for difference between the means of two samples. The null hypothesis is that the mean *positive* cross-product is significantly greater than the mean *negative* cross-product. Gordon and LeDuc (1981) commented that the PM test is likely to underestimate the value of the true relationship.

Pearson's R (r) or product moment correlation, is commonly applied in many statistical procedures and a description can be found in any basic statistics book (e.g. Mendenhall *et al.* 1989). It is a measure of the covariance of the two data sets which is insensitive to differences in mean and variance between the two (Fritts *et al.* 1990). As a parametric statistic, it will be sensitive to violation of the

normality assumption. Additionally, it detects only the linear correlation between the data sets.

Spearman's rank (ρ) correlation is a nonparametric test that measures association between two data sets by ranking the data of two data sets together and then testing the correlation of the assigned ranks. A description may be found in any basic statistics textbook which deals with nonparametric statistics.

The sensitivity of the *reduction of error* (*RE*) statistic reinforces its central position in verification (Fritts *et al.* 1990):

$$RE = 1 - \left[\sum_{i=1}^{n} (x_i - \hat{x}_i)^2 / \sum_{i=1}^{n} (x_i - \bar{x}_c)^2 \right] \qquad (5.1)$$

where x_i is the actual observation, $\hat{x}_i$ the estimated value, and $\bar{x}_c$, the mean of the observations over the calibration period. Basically, the *RE* looks at 1 minus the ratio of the total squared error of the regression estimates and the total squared error of the calibration data set, using the mean of the calibration period, $\bar{x}_c^2$, as the only estimate (Cook *et al.* 1994). The values of the statistic range from -∞ to +1. The significance of *RE* cannot be tested, but positive values indicate some skill of the model. Sample size may be important (Fritts *et al.* 1990). Due to its sensitivity, it is possible that a negative *RE* may be the result of only a few bad estimates.

The *coefficient of efficiency* (*CE*) is similar to *RE* and is expressed as:

$$CE = 1 - \left[\sum_{i=1}^{n} (x_i - \hat{x}_i)^2 / \sum_{i=1}^{n} (x_i - \bar{x}_v)^2 \right] \qquad (5.2)$$

where x_i again represents the actual observation, $\hat{x}_i$ the estimate of the observation, and $\bar{x}_v$ the mean of the verification data. The only difference is that *CE* uses the mean of the verification data, whereas *RE* uses the mean of the calibration data. If these means are the same, *CE* = *RE*. Otherwise *RE* is greater than *CE* by a factor related to the difference in the means (Cook *et al.* 1994). The

CE test is the most difficult of the above tests to pass. As for *RE*, no significance test is available, but a value greater than zero implies some skill in the model.

5.2 Methodology

The months for which the correlation function is calculated is commonly referred to as a 'climatic window'. Monthly data are commonly used for the calculation of this, with the data for each month being treated as a separate time series over *N* years. The correlation between the two series, one of climate data (e.g. maximum temperature for January), and one of ring-width index values, can then be calculated. This process is repeated for each month of the defined time interval. An example of a similar climatic window used for the calculation of the correlation function is: September of the prior year (year -1) through to May of the year following the current year (year +1), resulting in 21 months being used to calculate 21 monthly correlation coefficients over the 1885–1994 period (Buckley 1997).

Fritts and Wu (1986) argued that biological and statistical reasons justify the use of a climate window of more than 12 months and previous workers have found a pronounced response to the prior growing season for a number of Tasmanian species, including *Phyllocladus aspleniifolius* (e.g. Campbell 1980, LaMarche and Pittock 1982, Buckley 1997). On this basis, a 20–month window was selected for the calculation of correlation functions in this study. The window extended from September of the previous growing season through to April at the end of the current growing season.

Correlation functions were calculated for all sites with a view to examining both temporal and spatial stability. Following the estimation of correlation functions, PC regression models were calculated and reported for each site. The first of these models was based on maximum and minimum temperatures and precipitation data. Separate models have been calculated for each of the ZI, MI and SOI. Details of these models, for both the entire time period and for sub-periods, are discussed below.

After the calculation of correlation functions, response functions were calculated, calibrated and verified. For each site, the more traditional response

functions, based on both temperature and precipitation, were calculated first. Those monthly variables indicated as significant at the 0.05 level in the correlation analysis were entered into a PCA. PCs with eigenvalues greater than one (see Craddock 1973) were then used to generate the response models for each site. This approach followed Cook *et al.* (1994), who stressed the possibility of artificial predictability through the use of all possible independent variables in the estimation of PCs which would then be entered into a response function. The use of the principal component regression method provided information concerning the applicability of such models in the description of the relationship between climate variables and ring-width indices, but did not, strictly, describe the true relationship between the variables. The best order regression model was then selected by the AIC (see Chapter 3). The process of prewhitening data in order to remove autoregressive behaviour was outlined in Chapter 3, and the rationale behind this procedure is to ensure that later statistical tests are valid. Prewhitened residual chronologies for all sites were correlated against regional prewhitened monthly climate indices to produce correlation functions. Prewhitening of data, and the use of a 20-month window, resulted in the loss of several years of data: four years for the East, five years for the Mersey, three years for the West and two years for the Southwest.

Separate models were then estimated for each of the ZI, MI and SOI for all sites. Because the length of the $PILL_M$ chronology was less than the length of the available SOI time series, no response function for this site was calculated for this variable. In models based on the ZI, MI and SOI, monthly variables significant at the 0.1 level were allowed to enter the PCA analysis. The significance level was relaxed as these variables were not as specifically regional as the temperature and precipitation indices developed in Chapter 4. As for the above models, only those PCs with eigenvalues greater than one were entered into the regression analysis and the best order model selected by the AIC. Prewhitened data again resulted in the loss of several years of data. In the case of the SOI, ZI and MI, this was two years for all sites.

For all cases, it must be remembered that the use of these constant coefficient models highlights the unqualified assumption of constancy of the growth response to the climate variables over time.

5.2.1 Spatial Variability

In order to assess spatial variability of the climate–growth relationship, correlation functions for the entire period of available climate data, 1915–1994 East; 1915–1993 Mersey and West, 1932–1994 Southwest, were calculated in the manner described above. The time periods of response function models based on the SOI covered the period 1878–1994, those based on the MI covered the period 1942–1994, and those based on the ZI covered the period 1913–1993. Again, these were calculated as described above.

5.2.2 Temporal Variability

The first step in examining any temporal variability in the response to climate data was to explore the correlation functions for all sites based on two periods, an earlier and a later one. Response functions were then generated, based on these same periods.

For response functions based on temperature and precipitation data, two subperiods for each region were defined as follows: East 1920–1956 and 1957–1992; Mersey and West 1919–1954 and 1955–1990; and Southwest 1934–1962 and 1963–1992. For the ZI response functions the time periods used for all models were: 1913–1953 and 1954–1994; for the MI response functions these periods were 1942–1968 and 1969–1994; and for the SOI response functions time periods used were 1878–1936 and 1937–1994. In the first instance, the calculation of the response function was based on the earlier period (calibration), with verification tests performed on the later period. The order of these was then reversed, with the data of the later period being used as the calibration data set and the data of the earlier period as the verification data set.

The application of this split calibration–verification scheme, in conjunction with a visual examination of the correlation functions of the two periods, suggested the possibility of temporal instability (see Tables 5.1 and 5.2).

In view of this, an additional two tests, specifically designed to address such an issue, were employed. The first was the 'element matching test', (Gray *et al.*1981) and the second, based on the Kalman Filter (KF), searched for approximate step-function changes in the response.

These tests which are detailed below are largely based on the *individual* monthly independent variables. A possible change in response to the MI was not examined due to the shorter length of this series.

5.2.2.1 The element matching test

The 'element matching test' puts forward the null hypothesis that two response functions are statistically the same. In this study, the point of interest was whether two response functions from the same site, but based on different time periods, were statistically similar or not.

Each pair of traditional response functions for each site was generated using the early and late calibration data for the periods defined in section 5.2.2. One difference between the response functions derived above and those tested by the element matching test was the exclusion of precipitation from the calculation of the relevant response functions. This exclusion was done because there was no consistent and clear correlation of ring-width and precipitation data across time or space. Preservation of precipitation in the response function could have altered the response function in a way that masked a changing response to temperature. Previously, Palmer (1989) has found that the exclusion of precipitation data from stability tests of response functions allowed the derivation of temporally stable response functions for *Phyllocladus trichomanoides*.

For all cases, as explained above, prewhitening of the data led to a reduction in the number of years available for analysis. Where there were a number of consecutive significant or near significant correlations between ring widths and monthly climatic data, this was termed an interval of high correlation. Data for these months were averaged to produce one series of seasonalised regional temperature data for each of minimum and maximum temperatures. For the East, this was December–April of the prior season; for the Mersey,

January–April of the prior season; for the West, November–March of the prior season; and for the Southwest, November–January of the prior season. Both the seasonalised and monthly data were used in the generation of response functions for each site.

The SOI and ZI were also seasonalised over these same months, as well as for additional intervals in which correlation between ring widths and these indices was significant. For the East these additional periods of high correlation were November–January of the current year (SOI), July–August (ZI); for the Mersey, November–January of the current year (SOI), July–August (ZI); for the West, November–January of the current year (SOI), July–August (ZI); and for the Southwest, September–November of the current year (SOI). Separate response functions upon which to base the element matching test were estimated for each of these indices. The early and late time periods tested for the ZI were 1913–1953 and 1954–1994, and for the SOI were 1878–1936 and 1937–1994, respectively.

For the element matching test, 'standard response functions' were used: independent variables were not screened for significance but were all forced into the principal components analysis. Principal component amplitudes were back-transformed and expressed in terms of the original 40 independent variables (maximum and minimum temperature).

95% confidence intervals were then estimated for each element of the response functions based on both periods. Each pair of response functions for an individual site were then compared. Where confidence intervals overlapped for a given month, it was determined that there was an insignificant difference between the two point estimates (at the 0.05 level). Non-overlapping confidence intervals indicated statistically distinct responses for the two periods with regard to that particular month.

5.2.2.2 The Kalman Filter

The second test made use of the Kalman Filter (KF). Visser and Molenaar (1986) introduced the Kalman Filter into the field of dendrochronology in an

attempt to identify a response to pollution as distinct from a response to climate. The formulation of the KF may also be found in Visser and Molenaar (1986), and will be elaborated upon in the next chapter. The KF does not rely on the stationarity of time series data, nor, unlike regression analysis, are parameters assumed constant. It can therefore be used to detect approximate step function changes in the relationship between two time series (Gove and Houston 1996).

Two modes of response to climate variables are examined under this test. Firstly, a constant coefficient linear regression model was applied, which can be simply expressed as:

$$y_t = \alpha\beta_t + \varepsilon_t \qquad (5.3)$$

where y_t is the value of the tree-ring index series at year t, α contains the regression parameters, β_t contains the meteorological variables of interest for t = *1...N*, and the ε_t s are assumed to be normally distributed. Following this, a time-dependent model was calculated using the KF. In this second case, the α coefficient must be made stochastic and this is achieved by allowing the process to follow a random walk process. This model can be expressed as:

$$\begin{aligned} \alpha_t &= \alpha_{t-1} + \eta_t \\ y_t &= \alpha_t\beta_t + \varepsilon_t \end{aligned} \qquad (5.4a \text{ \& } b)$$

The value of the β_t coefficient has been made partially dependent on its prior value by the addition of equation 5.4b: this equation states that α_t will depend on the prior values of α. At each time step a new mean and variance of the estimate are calculated. This information is then used in the calculation of the next value of the coefficient. In essence, the Kalman Filter works by using previous information contained in prior observations to *update* the estimate. A fuller explanation of the Kalman Filter is given in Chapter 7, and Harvey (1989) thoroughly reviews its use in the context of Structural Time Series models.

After the parameters, α, have been estimated by the use of all prior information, they can be smoothed by using *all* available information, not just that contained in the prior values. A maximum likelihood (ML) function has been used to estimate these variances. The degree of change in the parameter will be dependent on this variance, as defined by the ML solution. If the parameters are constant, then time dependence is not indicated. If, on the other hand, the coefficients are not constant, time dependent behaviour has been identified. The two noise processes ε_t and η_t are assumed to be uncorrelated.

In the current study, the relationship between individual climate variables (maximum and minimum temperature) and ring-width indices was used to generate the α regression parameters. Those variables tested included maximum and minimum temperature, precipitation, the ZI and the SOI. The relationship between ring widths of each site chronology and each month of the 20-month climate window (as defined above) was tested for time-dependent behaviour. The time-dependent and non time-dependent models were compared through their AICs, and the model with the lowest AIC was chosen as the best one (Akaike 1974). As for Gray's test, both monthly and seasonalised data were used.

5.2.2.3 Climate data

Climate data of the individual regions were also examined by the division of the raw minimum and maximum temperature data into early and late periods, based on the calibration and verification periods. Not all stations used to construct indices (Chapter 4) could be used for this purpose, as data for some stations covered only one half of the record. Their use could therefore introduce a systematic bias into the results if the raw data, and not standardised indices, were used. The monthly data of the selected stations were then averaged across sites within a region for each month. Confidence intervals were calculated for each month of the two subsets of data. Climatic data were treated in this way in an attempt to provide an indication of how climate between the two periods had changed as opposed to how the climate *response* might have changed.

Stations used were:

Temperature:

East: 92033, 92045

Mersey/West: 91094, 97014, 98001

Southwest: 94041, 95003

Precipitation:

East: 91086,92004, 92012, 92014, 92020, 92033, 93034

West: 91011, 91044, 91094, 91109, 97006, 97008, 97014

Southwest: 94041, 95012, 95019

5.3 Results

5.3.1 Spatial Variability

5.3.1.1 Temperature and precipitation data

In all cases, KOA_M has been included in Figures of West data in order to aid readability of Figures of Mersey data. Generally, a significant negative correlation with prior season temperatures, and a positive correlation (not necessarily significant) with current late winter–spring temperatures, is discernible for all sites (Figures 5.4–5.7). Where the term 'growing season' has been used, it refers loosely to the warmer months of the October–April period. In a very general sense, the correlation with precipitation for the three northern regions alternates from positive to negative on a month-to-month basis. No clear patterns other than oscillations of this nature are apparent. Correlations for the Southwest do not show as strong an oscillatory tendency, although neither do they reveal a clearly defined pattern of correlation in the same sense that temperature data do.

Differences exist with respect to intervals of high correlation across sites. The correlation functions of Figures 5.4–5.7 are summarised in Table 5.1.

Maximum temperature

By June, all sites, with the exception of $CLAY_S$, have a positive correlation with maximum temperature. The prior season response however, is the most consistently significant feature of the correlation functions for all regions. Almost all sites show a negative response to temperature over the months December–March. Significant correlations in the current season's spring months for the East and Mersey are also apparent.

With regard to individual regions, the correlation of East sites with maximum temperature is in considerable agreement with the exception of ESM_E which shows a somewhat different pattern of response to maximum temperatures

	East	*Mersey*	*West*	*Southwest*
Maximum temperature	Dec–Apr(p,-)* Jun–Nov/Dec(c,+)*	Jan–Apr* (p,-) Jun-Oct (c,+)	Nov–Mar* (p,-)	Dec–Jan(p,-)* May–Sep (c,+)*
Minimum temperature	Mar–Apr(p,-)* Jun(c,+)	Jan–Apr* (p,-)	Feb–Apr(p,-)* Apr(c,+)	Feb–Mar (p,-) Jun(c,+)*
Precipitation	Jan(p,+)*	Jan(p,+)*	Jan(p,+)* Jul(c,-)*	Feb–Mar (p,+)* Sep(c,+)*

Table 5.1: **Summary of correlation functions in Figures 5.4–5.7. A 'p' in parentheses indicates prior season, and a 'c' current season. A + or a - indicates the sign of the correlation. For the Southwest, responses indicated are relevant only for LCR_S and SPR_S. A * indicates that the correlation is significant over part of the indicated period for more than one site at the 0.05 significance level.**

in the current season. Its correlation peaks in September and then falls to become significantly negative in January. Although Mersey valley sites all have a similar pattern in their correlation with prior season temperature data, there is a broad spread of correlation for the current growing season. The environments of these sites vary widely. $PILL_M$, the highest elevation site in the Mersey, can be expected to be the most temperature–limited site in that region. East and Mersey also show periods, greater than one month, of significant correlation between ring widths and maximum temperature in the current season which the West and Southwest do not. Rather, these two regions show significant correlation with individual months (Figures 5.4a–5.7a).

The majority of sites show a positive response to maximum temperature late in the growing season. Current season response to maximum temperature differs dramatically between the three Southwest sites. $CLAY_S$, close to sea level, has a positive and significant, or near significant, response to late winter–spring maximum temperature, while SPR_S and LCR_S have negative responses. This suggests that wetter, cooler conditions are preferred by trees at $CLAY_S$, while drier, warmer conditions are preferable for trees at SPR_S and LCR_S. The opposite is indicated for the prior season. The difference between $CLAY_S$ and the other two Southwest sites may be due to its considerably lower elevation and/or its proximity to the coast. SPR_S is positively correlated with winter maximum temperatures for longer than either LCR_S or $CLAY_S$. Even the Mersey Valley sites, noted in Chapter 2 for the diversity of their environments, do not show such a dramatic difference in their response to climate.

Minimum temperature

On the whole, response to minimum temperature is also coherent between sites within a region for the prior season. A significant negative correlation is evident in the prior season and its timing is slightly later than the significant negative correlation with maximum temperature (listed above). LCR_S and SPR_S show a significant negative correlation in December and $CLAY_S$ in March–April. In this light, it is interesting to note that Buckley (1997) has found that the statistically significant positive correlation of *Lagarostrobos franklinii* with mean temperature in the current growing season is largely driven by maximum temperature earlier in the growing season and by minimum temperature in April, at the end of the growing season. The reasons for Buckley's finding may well be similar to those for the negative prior season correlation in this study.

Precipitation

LaMarche and Pittock (1982) have noted that whereas the temperature response of Tasmanian conifers can be grouped by genus, the precipitation

Figure 5.4: Correlation of East residual chronologies with prewhitened climate indices. A: correlation with maximum temperatures, B: correlation with minimum temperatures, C: correlation with precipitation. 95% confidence limits are indicated and a zero line included. Time period of analysis was 1917–1993. Climatic window is September of the previous growing season to April at the end f the current growing season

Figure 5.5: Correlation of Mersey chronologies with climate indices. 95% confidence limits indicated. A: correlation with maximum temperatures, B: correlation with minimum temperatures, C: correlation with precipitation. 95% confidence limits are indicated and a zero line included. Time period of analysis was 1916–1993. Climatic window is September of the previous growing season to April at the end of the current growing season

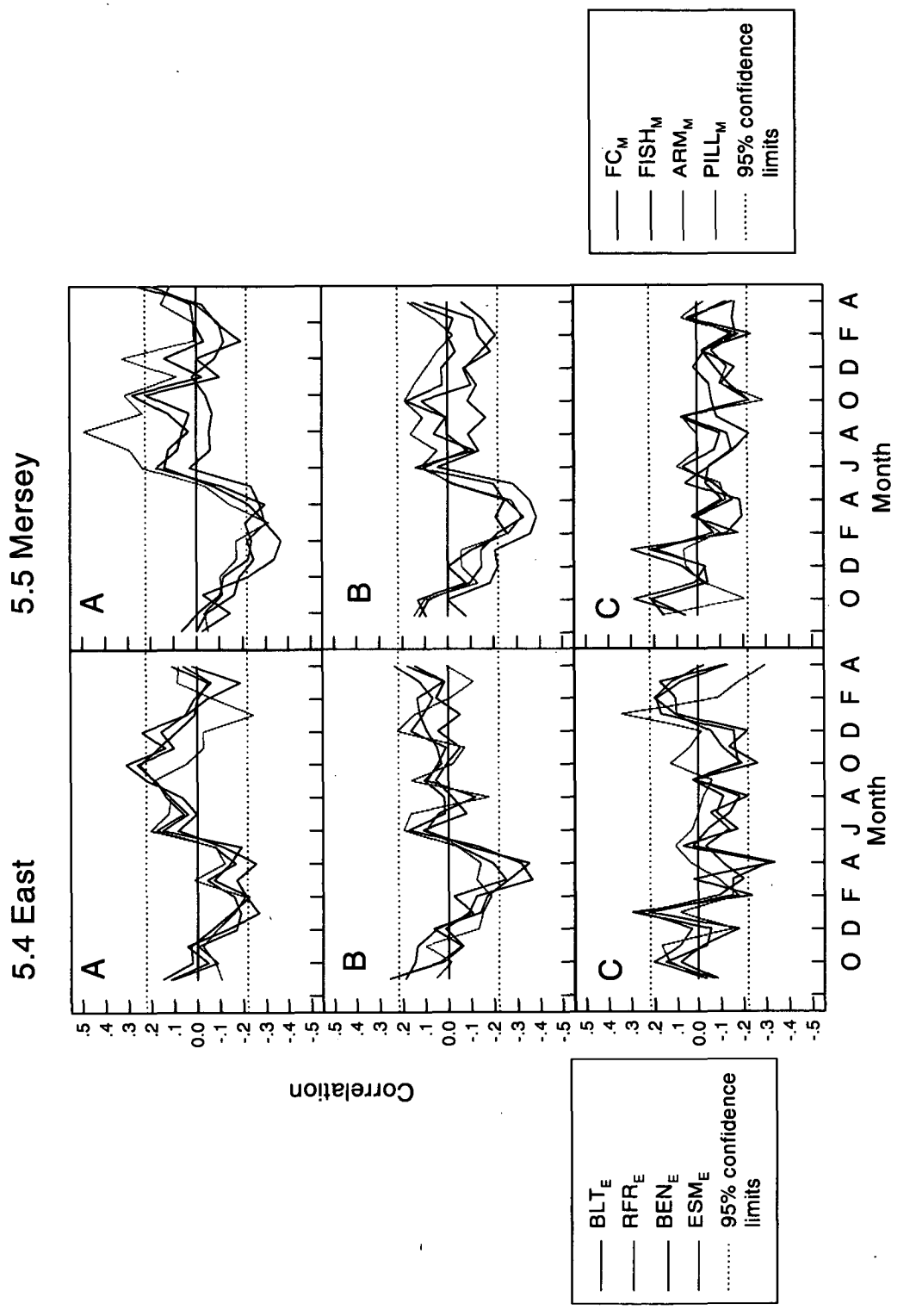
5.4 East
5.5 Mersey
A
B
C
Correlation
.5 .4 .3 .2 .1 0.0 -.1 -.2 -.3 -.4 -.5
O D F A J A O D F A O D F A J A O D F A
Month
BLT$_E$
RFR$_E$
BEN$_E$
ESM$_E$
95% confidence limits
FC$_M$
FISH$_M$
ARM$_M$
PILL$_M$
95% confidence limits

Figure 5.6: Correlation of West chronologies with climate indices. 95% confidence limits indicated. A: correlation with maximum temperatures, B: correlation with minimum temperatures, C: correlation with precipitation. 95% confidence limits are indicated and a zero line included. Time period of analysis was 1915–1992. Climatic window is September of the previous growing season to April at the end of the current growing season

Figure 5.7: Correlation of Southwest chronologies with climate indices. 95% confidence limits indicated. A: correlation with maximum temperatures, B: correlation with minimum temperatures, C: correlation with precipitation. 95% confidence limits are indicated and a zero line included. Time period of analysis was 1933–1993. Climatic window is September of the previous growing season to April at the end of the current growing season

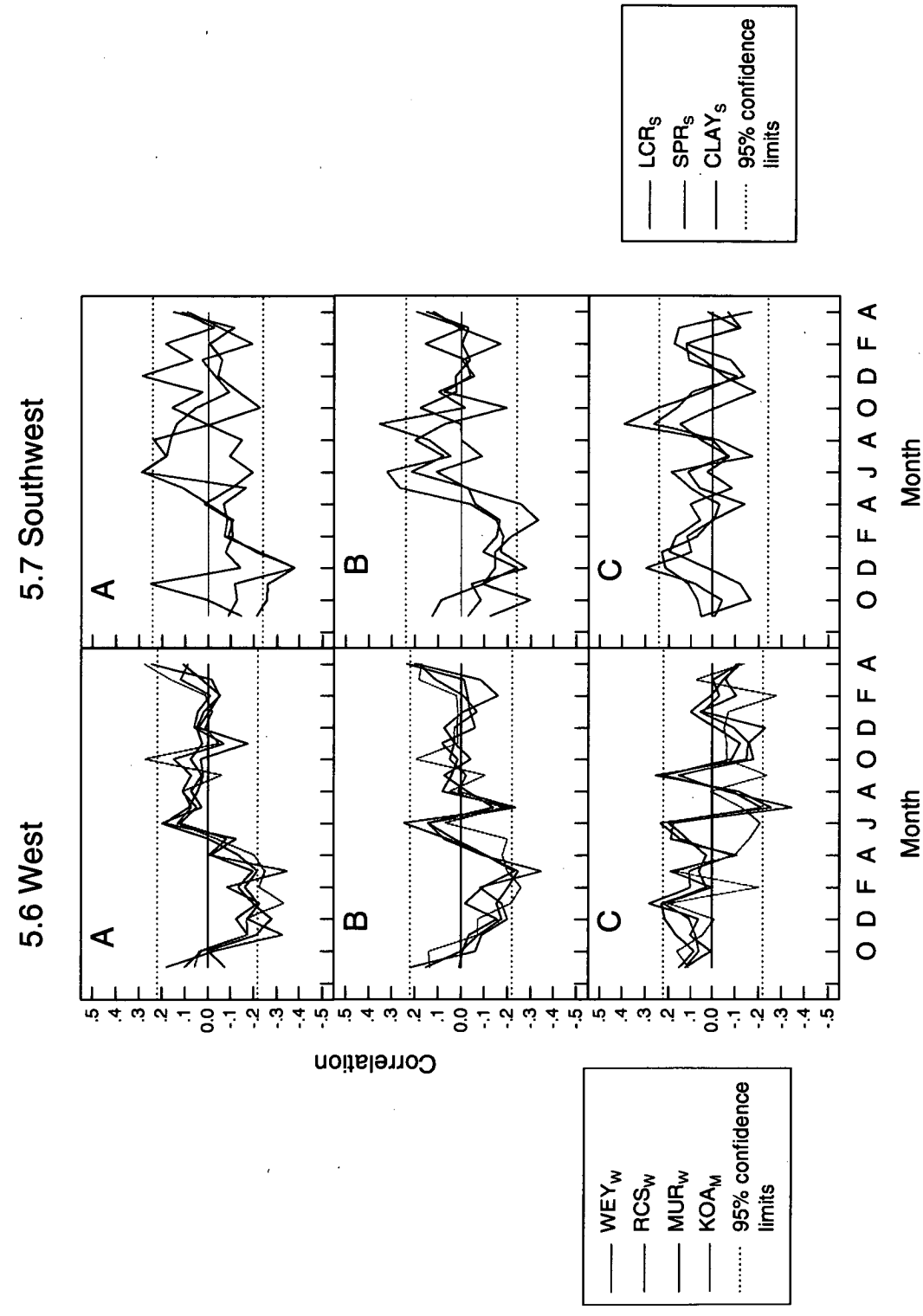
5.6 West
5.7 Southwest
A
B
C
Correlation
.5 .4 .3 .2 .1 0.0 -.1 -.2 -.3 -.4 -.5
O D F A J A O D F A
Month
WEY$_W$
RCS$_W$
MUR$_W$
KOA$_M$
95% confidence limits
LCR$_S$
SPR$_S$
CLAY$_S$
95% confidence limits

response can not. In this study, correlation with precipitation is not as clearly definedas that with temperature, but for the three northern regions there is a positive and significant correlation with prior January precipitation. For the Southwest, there is a positive correlation with December precipitation. For East sites, correlation with late current season precipitation approaches significance at the 0.05 level. Figures 5.4–5.7 show that there is a more positive response to precipitation in the prior season and a more negative correlation with it in the current season; this is most evident in the Mersey and West sites. Correlation of ring width and precipitation is particularly inconsistent for the East and Mersey regions.

5.3.1.2 Zonal and Meridional indices and the SOI

The consistency in patterns of correlation with the Meridional and Zonal Indices across the State is quite striking (Figures 5.8a & b – 5.11a & b). Correlation with the Zonal Index is positively significant/near significant for East, Mersey and West sites in November and March of the prior growing season, and significantly positively correlated for the winter months of July and August (Figures 5.8a – 5.11a). A positive correlation with the Zonal Index in the prior season is indicative of the importance to cambial growth of a stronger westerly air stream and increased rainfall over the State. Therefore, this finding is consistent with that above, namely, that a positive correlation of ring widths with precipitation and a negative correlation with temperature (see Chapter 4) of the prior season is important. The Southwest sites are significantly positively correlated with the Zonal Index in January of the prior growing season, with $CLAY_S$ being significant for February also, and LCR_S showing significance for the December–February period. For the Southwest a further period of significant and positive correlation can be seen for the months August–November, with correlations for $CLAY_S$ remaining significant for a longer period of time than the other Southwest sites. A similar, but less emphasised, feature is seen for West data, where the month of September (current season) shows significant correlation between ring-width indices and the ZI.

Correlations with the Meridional Index are also consistent in pattern across the State. Highest correlations are seen for the current growing season and are positive, the strongest correlations occurring for the East coast. The overlap of time periods for which there are positive correlations between ring-width and temperature and ring-width and the MI, suggests that a warm northerly airflow has a beneficial affect on ring-widths.

Significant correlations between ring width and the SOI (Figures 5.8c–5.11c), also show a general pattern of correlation across the State: more positive correlations in the prior growing season, and more negative correlations in the current summer. The majority of correlations for the 20–month window are negative, and this is consistent with more positive correlations with maximum temperature in the current growing season (Figures 5.4–5.7). For many sites, this negative correlation is significant in the current growing season, and this is especially the case for the generally cooler West and Southwest (Bureau of Meteorology 1993). The strongest negative relationships are again in the west and southwest of the State and Figures 5.8a–5.11a indicate that low values of the SOI are favourable to cambial growth in the West and Southwest. It is interesting to note that the same is much less obvious for the East. Only BLT_E becomes significantly negatively correlated with the SOI towards the end of the current growing season. Although no precipitation records of reasonable duration exist in the mountains close to the eastern sites, it is likely that BLT_E is drier than either of the remaining two eastern sites in the area (personal observation).

Although *significant* influence of the SOI on Tasmanian climate has not been detected by McBride and Nicholls (1983), effects of strong El Niño events on plant health have been observed on previous occasions (personal observation, T. Brodribb, University of Tasmania, J. Marsden-Smedley, University of Tasmania, M. Peterson, Forestry Tasmania pers. comm.), and there has been much discussion concerning the connection of mast seedings with El Niño events (e.g. Shapcott 1991, Barker 1993). In addition, Nicholls (1989) has examined the influence of SST on winter precipitation over Australia, finding the second of two main patterns of correlation is closely associated with the SOI. This pattern shows a negative relationship with Tasmanian precipitation that is opposite in sign to

Figure 5.8: Correlation of East chronologies with A. Zonal Index based on the period 1913–1994, B. Meridional Index based on the period 1939–1994, and C. the SOI based on the period 1878–1994. 95% confidence limits indicated. Climatic window is September of the previous growing season to April at the end of the current growing season

Figure 5.9: Correlation of Mersey chronologies with A. Zonal Index based on the period 1913–1994, B. Meridional Index based on the period 1939–1994, and C. the SOI based on the period 1878–1994. 95% confidence limits indicated. Climatic window is September of the previous growing season to April at the end of the current growing season

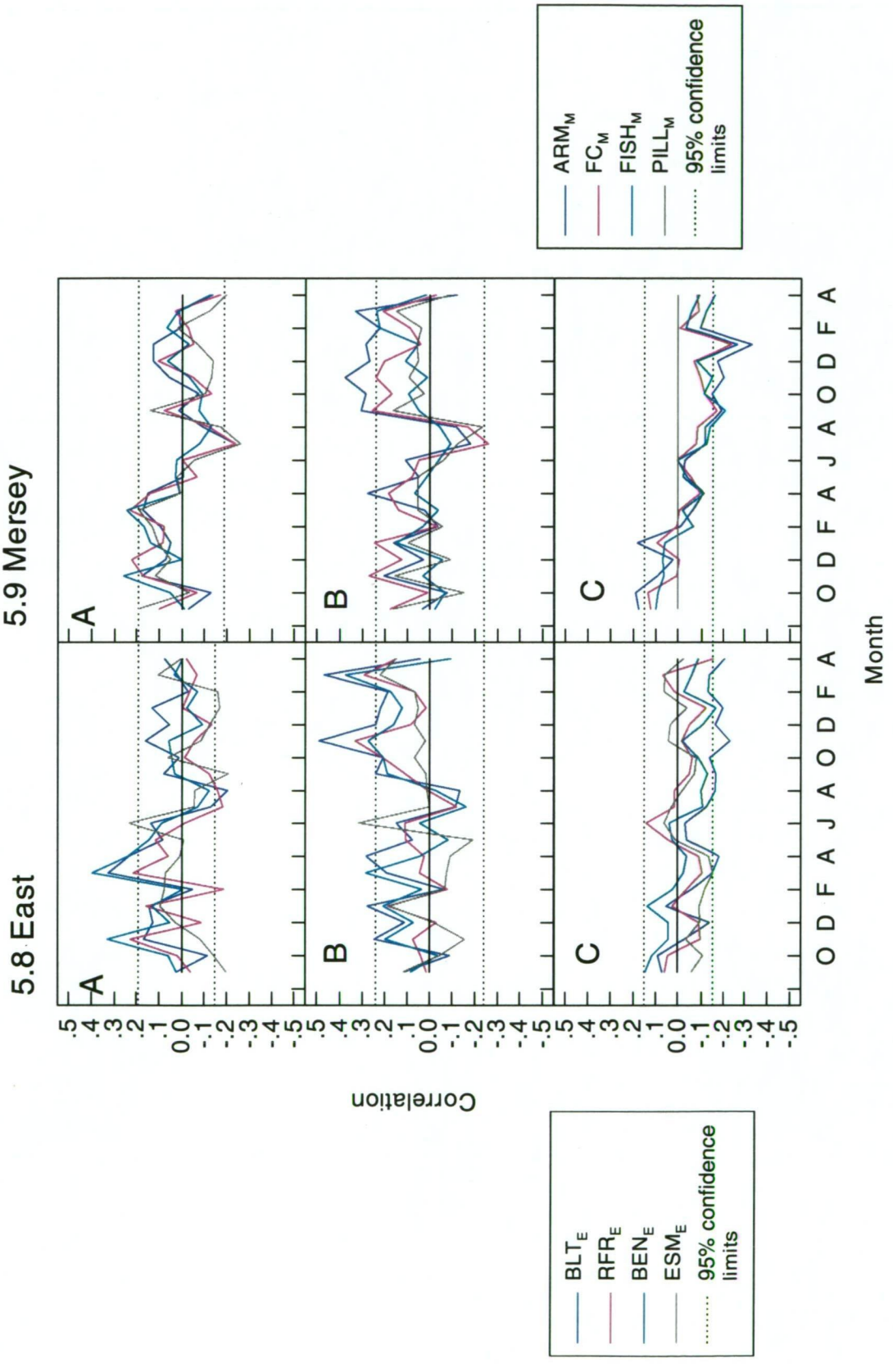
5.8 East
5.9 Mersey
A
B
C
Correlation
.5 .4 .3 .2 .1 0.0 -.1 -.2 -.3 -.4 -.5
O D F A J A O D F A
Month
BLT$_E$
RFR$_E$
BEN$_E$
ESM$_E$
95% confidence limits
ARM$_M$
FC$_M$
FISH$_M$
PILL$_M$
95% confidence limits

Figure 5.10: Correlation of West chronologies with A. Zonal Index based on the period 1913–1994, B. Meridional Index based on the period 1939–1994, and C. the SOI based on the period 1878–1994. 95% confidence limits indicated. Climatic window is September of the previous growing season to April at the end of the current growing season

Figure 5.11: Correlation of Southwest chronologies with A. Zonal Index based on the period 1913–1994, B. Meridional Index based on the period 1939–1994, and C. the SOI based on the period 1878–1994. 95% confidence limits indicated. Climatic window is September of the previous growing season to April at the end of the current growing season

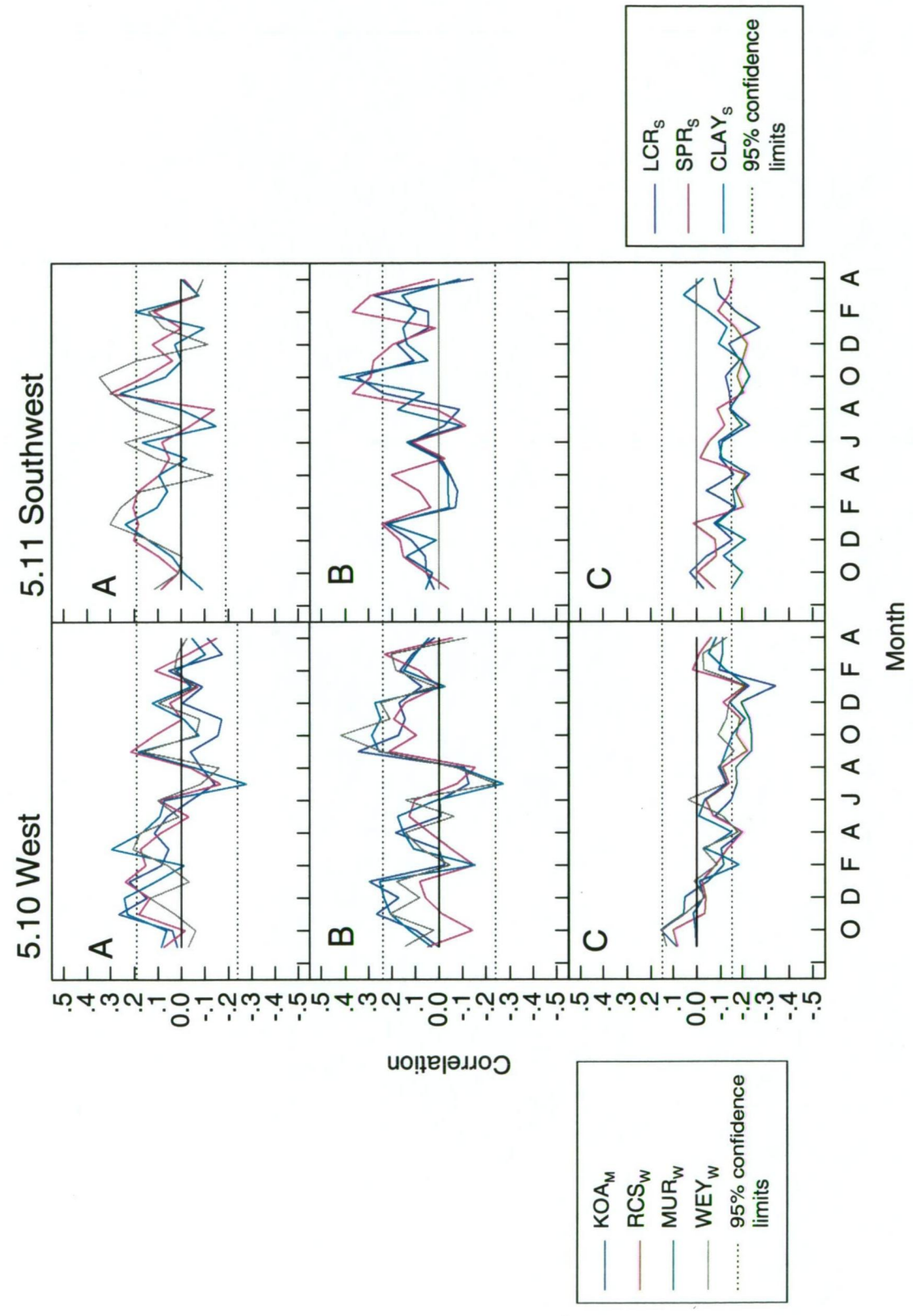
5.10 West
5.11 Southwest
A
B
C
Correlation
.5
.4
.3
.2
.1
0.0
-.1
-.2
-.3
-.4
-.5
O D F A J A O D F A
Month
KOA$_M$
RCS$_W$
MUR$_W$
WEY$_W$
95% confidence limits
LCR$_S$
SPR$_S$
CLAY$_S$
95% confidence limits

relationships over the rest of the country. The influence of the SOI on the *intensity* and *duration* of Tasmanian rainfall events (Nicholls and Kariko 1993) may be a partial source of its apparent importance to cambial growth.

5.3.2 Temporal Variability

5.3.2.1 Correlation Functions

Temperature and precipitation data

An inspection of Figures 5.12–5.15 reveals a distinct change in the timing of the peak 'high correlation interval' in the current season for all sites with the notable exception of the Southwest. For the three northern regions, the window of significant or near significant correlations has become narrower in the later period (Figures 5.12–5.15). In conjunction with this, there has been a 'shift' of highest correlations with maximum temperature in the current season from spring–summer to winter–spring. SPR_S displays a widened window of high correlations with maximum temperature over the winter months of the later period, while the timing of the correlation for the remaining Southwest sites remains similar, but visibly weaker, than for the early period.

The differences in early and late period correlation functions between ring widths and minimum temperatures are similar to the changes noted for correlations between ring widths and maximum temperature. The positive correlation with the late current season has become less important for both the East and Mersey, and there is a more consistent response in the winter months (Figures 5.12 and 5.13). This is not so clear for either the West or Southwest. In the West, correlation over the winter months has become positive in the later period after having been negative in the earlier period (significantly so in July). For the Southwest, correlations in the winter months mirror the change in correlation with maximum temperatures.

Changes in the relationship between precipitation and ring width are less easily describable in a general way, although less consistency between East sites is indicated (Figure 5.12). The same general picture of alternating oscillations from

month to month remains evident although some differences are apparent between the two periods.

In the prior season, negative relationships with temperature are generally less significant than in the later period and, in addition, fewer months are denoted as statistically significant. In the East the high correlation interval for maximum temperature has changed from December–April to February–April. A similar situation exists for minimum temperature (Figure 5.12). The same phenomenon has been observed for most sites across the State.

Zonal and Meridional Indices and the SOI

For East, Mersey and West sites, the consistency of correlations with the ZI is greater for the earlier than for the later period (Figure 5.16). The strongest positive correlation at these sites occurs in November of the previous growing season in the early period. In the later time period, this correlation has become nonsignificant, or significantly negative (West). A significant and positive correlation between ring-width indices and the March ZI, however, remains significant across both periods. The later period generally has a less easily summarised response, although the positive correlation of the spring months has become considerably more important, while the negative correlation of winter months less so. In the East, BLT_E and ESM_E change from being negatively correlated with the ZI in August to being positively correlated for the same month in the later period. A similar situation is seen for most sites in the Mersey region, with ARM_M and FC_M both strongly expressing the same feature. In the West, all sites show a significant correlation with the ZI in September of the later period which is absent in the earlier period; in the Southwest, LCR_S and SPR_S join $CLAY_S$ in becoming positively, and significantly, correlated with the ZI in the spring months. This does not appear consistent with changes in the correlation functions of temperature.

The negative response to the Zonal Index in the earlier period over the months of July to September suggests that cooler wetter conditions in this period were less favourable to growth, particularly for the East, Mersey and West (Figure 5.16). Why this is not the case for the generally cooler Southwest is not clear.

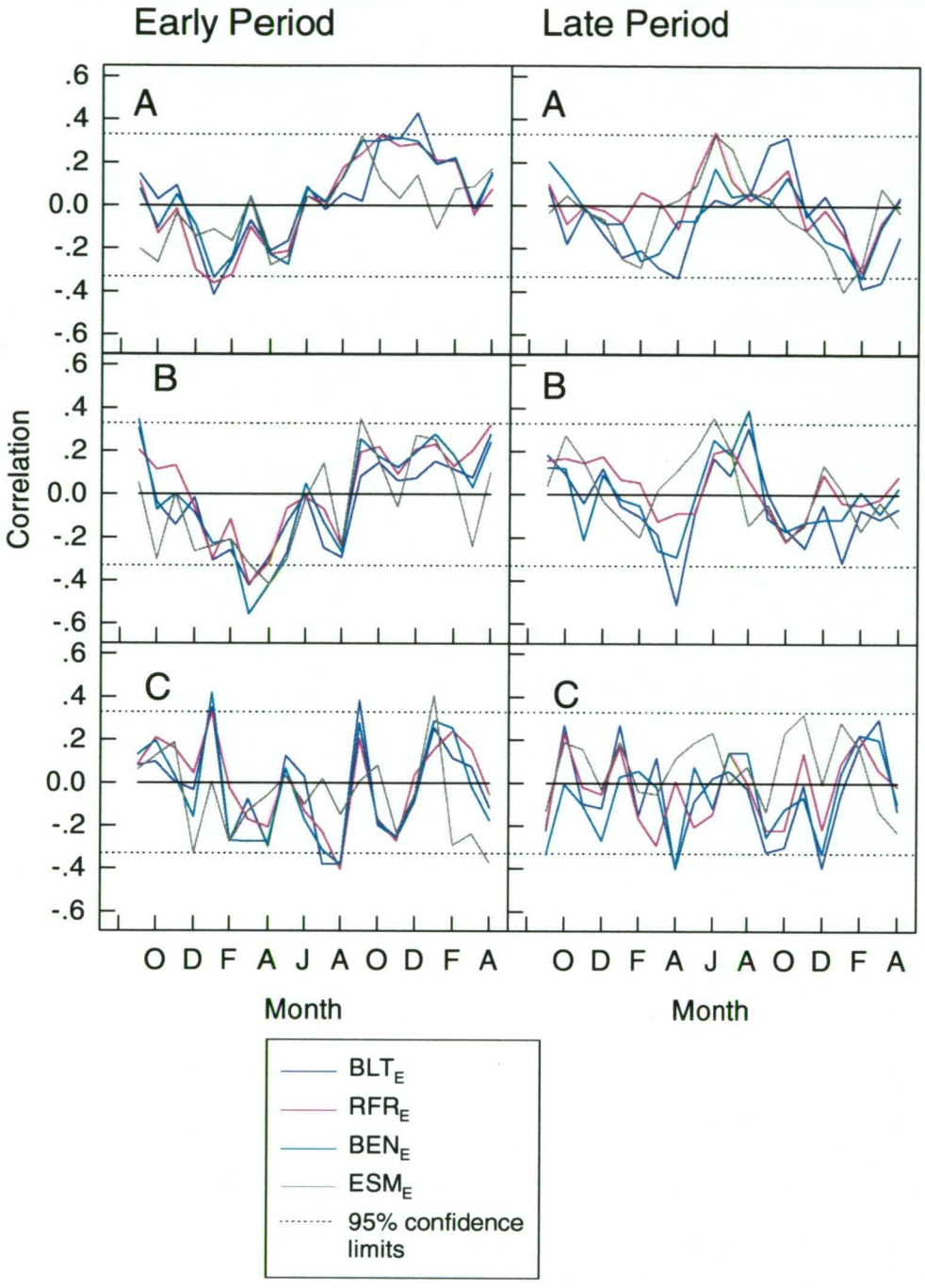

Figure 5.12: **Correlation of East chronologies and climate indices over two time periods. A. maximum temperature, B. minimum temperature, C. precipitation. Early period is 1920–1956, and late period. 1957–1992. Climatic window is September of the previous growing season to April at the end of the current growing season**

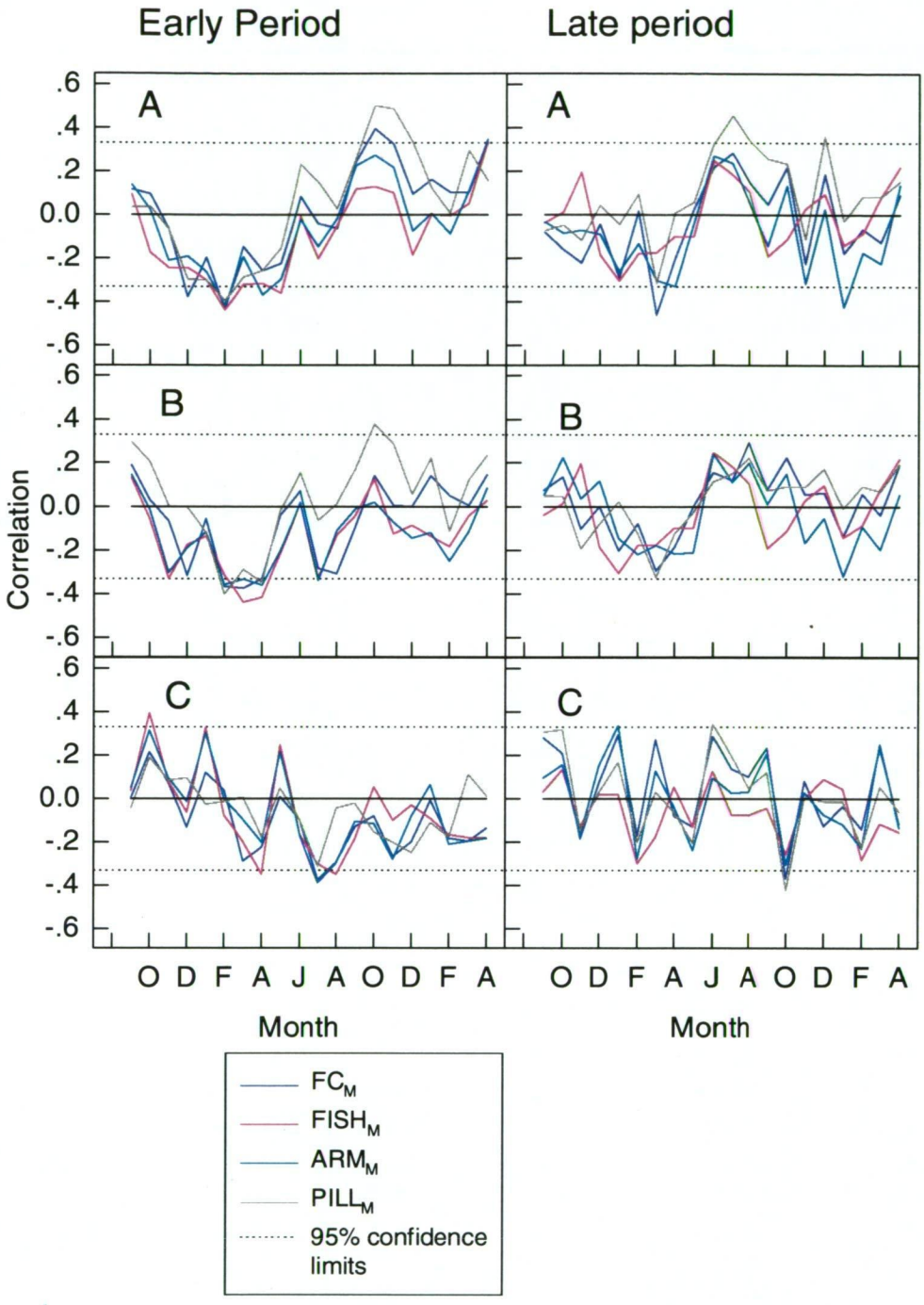

Figure 5.13: **Correlation of Mersey chronologies and climate indices over two time periods. A. maximum temperature, B. minimum temperature, C. precipitation. Early:1919–1954, late: 1955–1990. Climatic window is September of the previous growing season to April at the end of the current growing season**

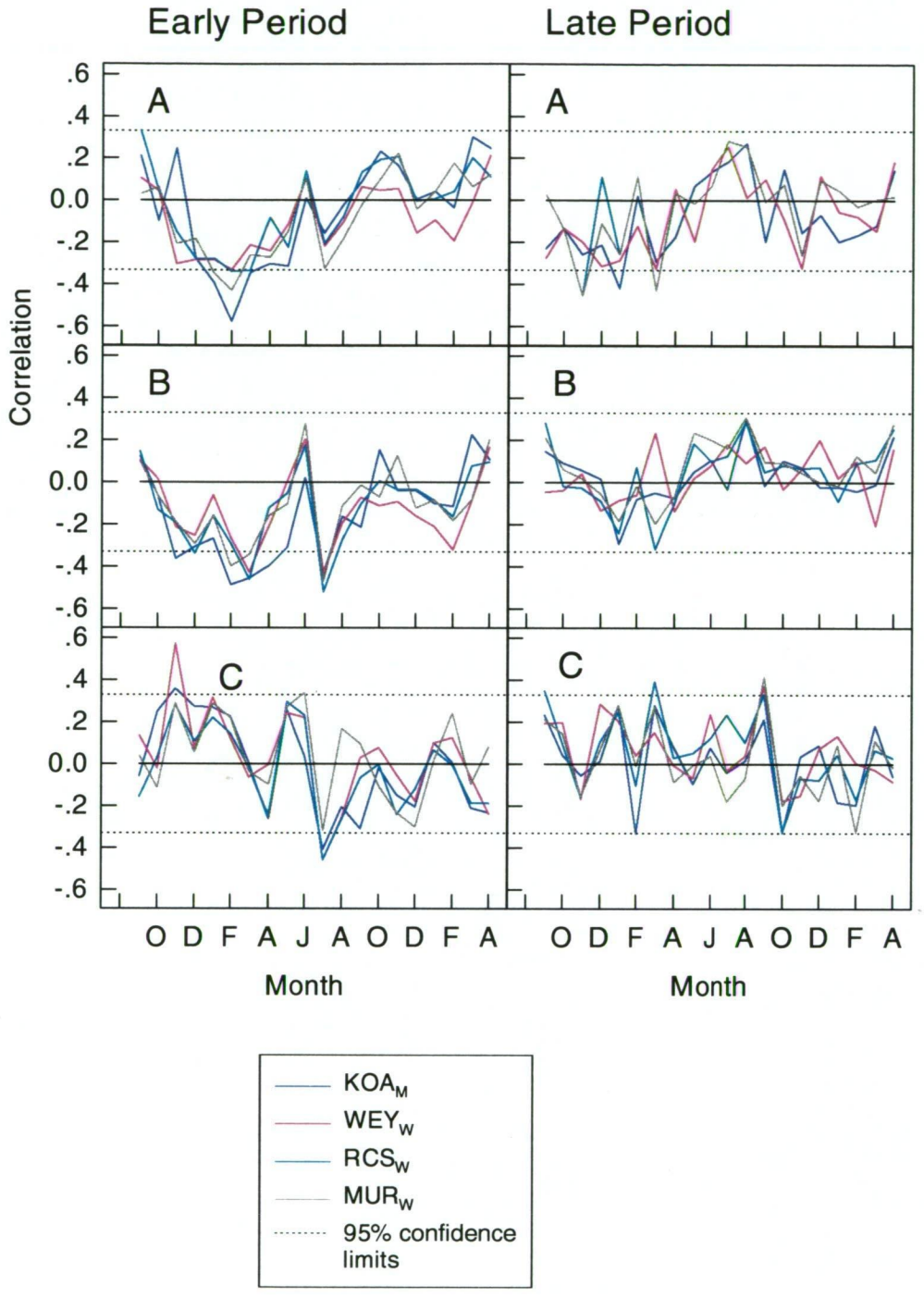

Figure 5.14: **Correlation of West chronologies and climate indices over two time periods. A. maximum temperature, B. minimum temperature, C. precipitation. Early:1919–1954, late: 1955–1990. Climatic window is September of the previous growing season to April at the end of the current growing season**

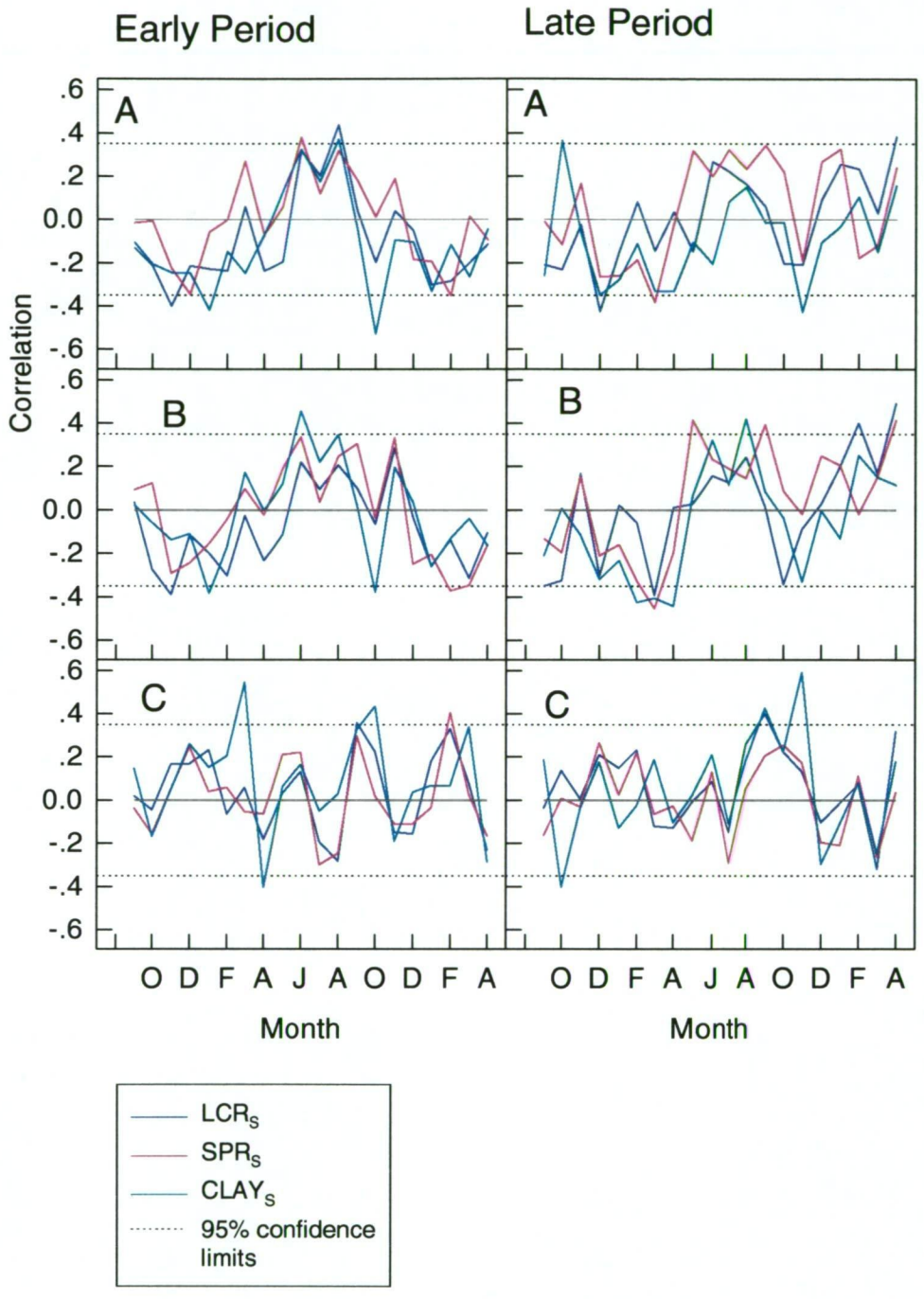

Figure 5.15: **Correlation of Southwest chronologies and climate indices over two time periods . A. maximum temperature, B. minimum temperature, C. precipitation. Early:1934–1962, late: 1963–1992. Climatic window is September of the previous growing season to April at the end of the current growing season**

The above interpretation is consistent, however, with a positive correlation with temperature and a negative correlation with precipitation at the same time of the year.

Current season correlations between ring widths of Mersey, West and Southwest sites and the MI have generally become less significant in the later period (Figure 5.17). As for other variables, the response to the MI across sites is more consistent in the earlier than the later time period. The most noticeable feature of correlations of chronologies and the MI in the early period is the strong late current season response, also apparent in the response over the whole period (Figures 5.8–5.11 and 5.17). For the East and Mersey, the prior autumn response has became relatively more important, while the late current season response is de-emphasised.

For both time periods, a consistent pattern of correlation between the SOI and ring-width indices is apparent for all regions (Figure 5.18). In the West and Southwest, correlations that are significantly negative in the current season of the earlier period become less significantly negative in the later period. In the East and Mersey, consistency between site response to this variable lessens in the later period compared to the earlier period, although the tendency for correlations to be more positive in the prior season and less positive in the current season remains. Whether or not any of these changes (including those discussed for temperature and precipitation) are significant cannot be assessed from these diagrams.

5.3.2.2 Response functions based on Principal Component Regression for the two periods

Temperature and Precipitation Data

An examination of the verification tests for calibrated response functions based on temperature and precipitation suggests that there are significant differences between the two periods. Table 5.2 presents a summary of variance explained by models based on temperature and precipitation in each sub-period,

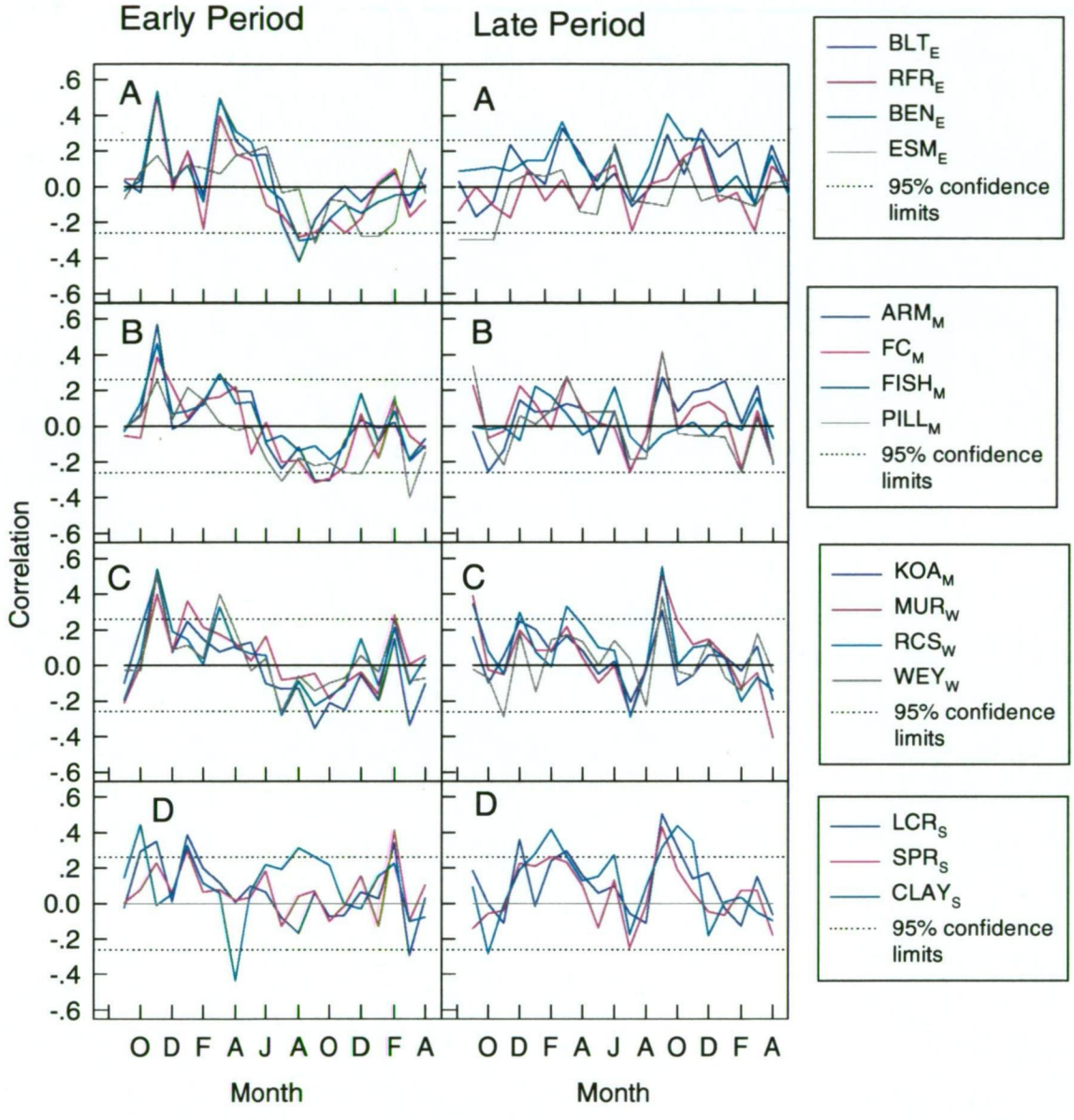

Figure 5.16: **Correlation of chronologies and the Zonal Index over two time periods. A. East, B. Mersey, C. West, D. Southwest. Time periods over which correlation functions have been calculated are: Early: 1913–1953, Late: 1954–1994. Climatic window is September of the previous growing season to April at the end of the current growing season**

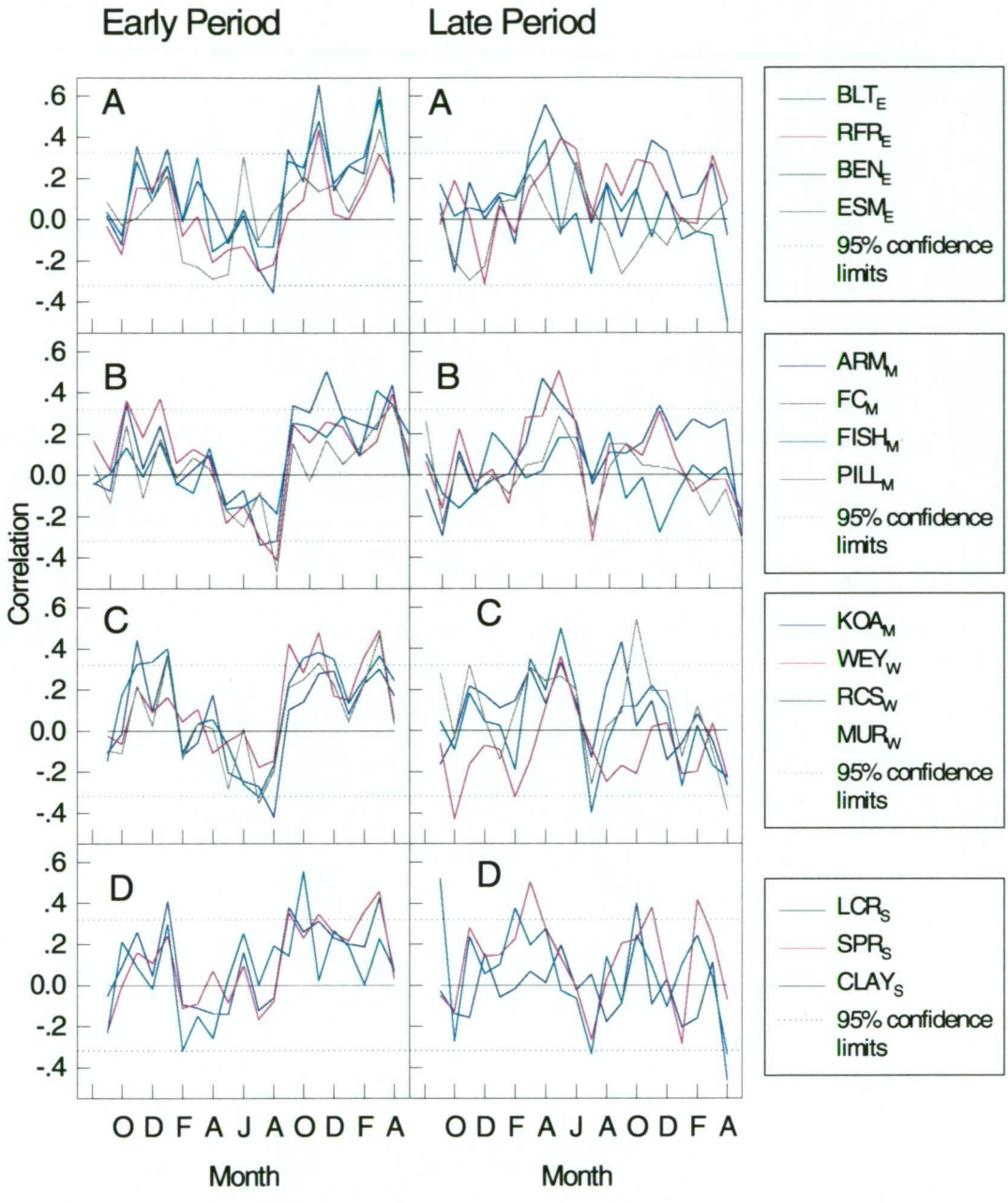

Figure 5.17: **Correlation of chronologies and the Meridional Index over two time periods. A. East, B. Mersey, C. West, D. Southwest. Time periods over which correlation functions have been calculated for all regions are: Early: 1942–1968, Late: 1969–1994. Climatic window is September of the previous growing season to April at the end of the current growing season**

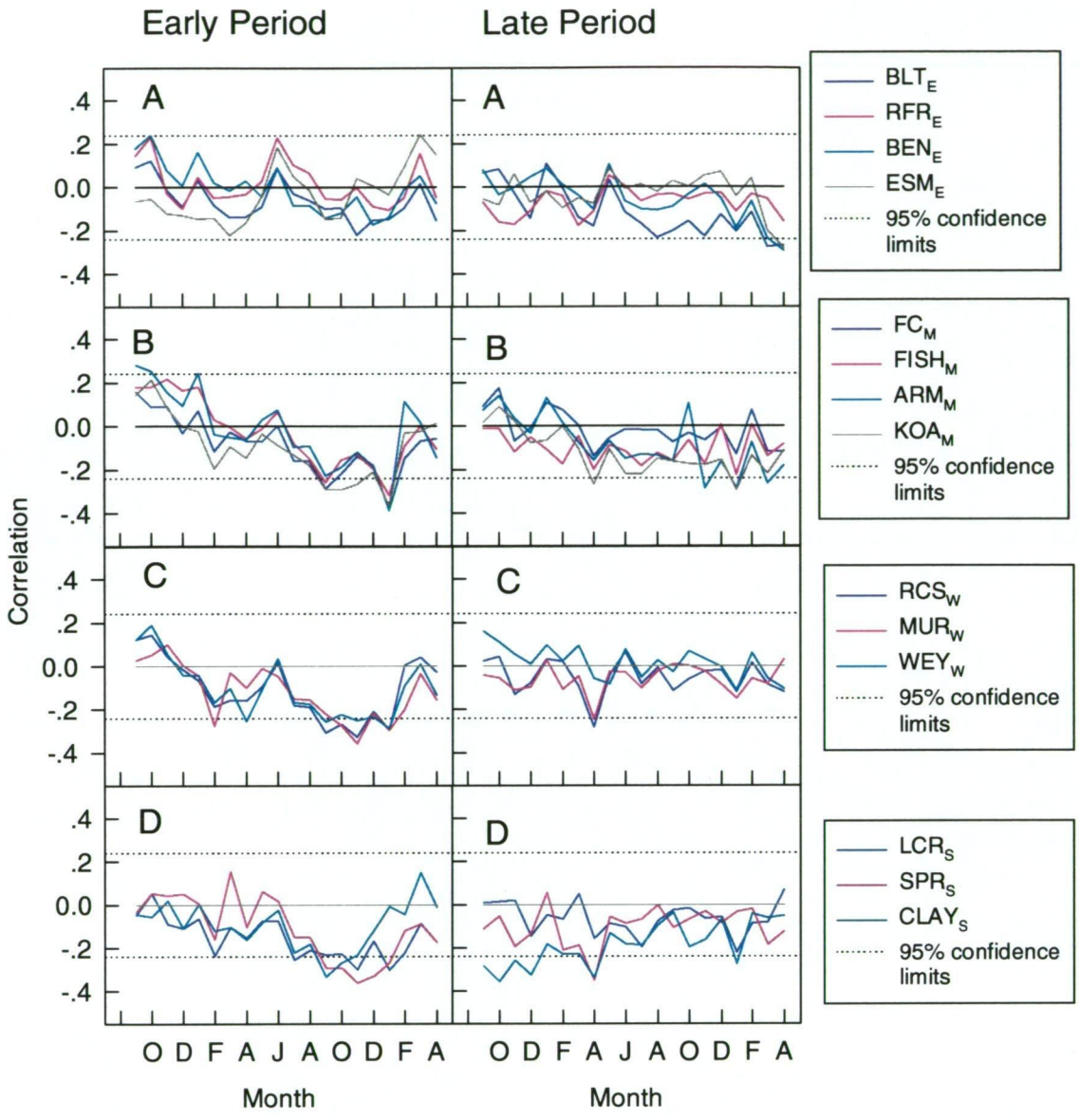

Figure 5.18: **Correlation of chronologies and the SOI over two time periods. A. East, B. Mersey, C. West, D. Southwest. Time periods over which correlation functions have been calculated are: Early: 1878–1937, Late: 1938–1996. Climatic window is September of the previous growing season to April at the end of the current growing season**

and also shows how many climate variables in the correlation functions are significant at the 0.05 level. For some sites, such as RFR_E, ESM_E and FC_M, there is a considerable change in the amount of variance in ring widths explained by climate. Table 5.1 reveals a somewhat disturbing tendency for considerably less variance to be explained by the climate in the second period for both the East and Mersey regions. The number of significant variables falls across most sites, $FISH_M$ being the most dramatic instance of this. On the other hand, SPR_S and LCR_S show a slight increase in explained variance in the second time period, while $CLAY_S$ shows only a slight decrease. In addition, there has been a concommitant increase in the number of significant variables for LCR_S and SPR_S.

Site	No. significant variables		% variance explained	
	early	late	early	late
BLT_E	7	6	45.69	40.78
RFR_E	6	2	41.44	11.72
BEN_E	6	5	52.26	45.12
ESM_E	7	3	45.49	18.49
FC_M	8	2	43.66	27.52
$FISH_M$	11	2	46.97	26.03
ARM_M	8	3	37.51	28.67
$PILL_M$	7	5	46.08	41.37
KOA_M	10	5	42.83	28.67
WEY_W	4	1	42.13	13.84
RCS_W	7	5	39.78	35.52
MUR_W	6	3	29.71	34.69
SPR_S	2	5	28.73	38.31
LCR_S	3	6	39.38	44.03
$CLAY_S$	9	9	46.54	40.94

Table 5.2: **Number of significant elements (0.05) in the correlation functions of maximum and minimum temperature and precipitation and explained variance of the model produced using these variables for early and late calibration periods. For each model, total number of variables is 60 (20 maximum temperature, 20 minimum temperature and 20 precipitation variables). Correlations for the East are based on the periods 1920–1956 and 1957–1992, for the Mersey, 1921–1956 and 1957–1992, for the West, 1919–1953 and 1954–1989, and for the Southwest, 1934–1963 and 1964–1993**

It is interesting to note that MUR_W, the southernmost of the West sites, like SPR_S and LCR_S, does not reveal a large change in explained variance across the two periods, although, unlike these sites, the number of significant variables has

decreased. However, Tables 5.3a & b belie any confidence that may have been entertained by Table 5.2 for these sites.

Tables 5.3a & b report results of the PC regression response functions based only on temperature and precipitation data. Results in Table 5.3a refer to models calibrated on the earlier time period while Table 5.3b reports results based on models calibrated against the data of the later period. In the early calibration period, no model for any site passes all verification tests. Most perform badly, failing not only *RE* and *CE* tests, but also displaying large decreases in explained variance (Tables 5.3a & b) when the model is tested on the verification data set. For 9 of 15 sites, the results of the *PM* test indicate that substantial differences exist between the calibration and verification periods. In a similar manner, both r and ρ show large falls in explained variation and differences between the two periods are suggested for all sites by *RE* and *CE*. Only $CLAY_S$ passes both the *RE* and *CE* tests in the early calibration period (Table 5.3a).

Differences between calibration and verification results are again observed when models are calibrated on the later data set. Models with largest falls in explained variance (r) are those for MUR_W, BEN_E, LCR_S, $CLAY_S$ and $PILL_M$. Although $CLAY_S$ appears to perform well in the early calibration period, and $FISH_M$ and ARM_M moderately well, only $FISH_M$, LCR_S and SPR_S pass the *RE* test in the later calibration period. The low sample depth of the $FISH_M$ chronology casts some doubt upon its quality (Table 3.3).

Zonal Index

Tables 5.4a & b, like Tables 5.3a & b, reveal little statistical consistency between the calibration and verification data sets for response functions based on both early and late calibration periods. As is the case for models based on temperature and precipitation data, models calibrated on one period generally fail to be successfully verified (Tables 5.6a & b). Of models calibrated on the ZI data of the early period, none pass the *RE* or *CE* tests (Table 5.4a). Once again, there are considerable differences in the amount of variation explained (r) in the calibration data and that explained in the verification data for both calibration periods.

In the later calibration period, 5 out of 15 models could not be formulated due to the absence of significant PCs (given the eigenvalue = 1 criterion) (Table 5.4b). Those models which could be formulated produced poor verification results with none passing the *RE* or *CE* tests.

The Meridional Index

Tables 5.5a & b once again demonstrate differences between the two periods similar to those noted for the above variables. The relatively short data set is likely to be a partial cause of such poor reproducibility of results.

The SOI

In contrast to temperature, precipitation, ZI and MI, several calibrated SOI models pass the *RE* and *CE* tests in both periods (Tables 5.6a & b). However, the variance explained is low and falls considerably from the calibration data set to the verification data set in all cases. As for the above cases, several models could not be formulated in the second period. This indicates that relationships between the SOI and ring widths are too insignificant to base models on.

5.3.2.3 Tests for Time-dependent behaviour

The element matching test —precipitation and temperature data

Gray *et al.*'s element matching test (Tables 5.7, 5.8) indicates a strong case for differences (at the 0.05 significance level) between the two periods. Very few elements for both time periods could be said to be drawn from the same population. Unfortunately, seasonalised data for individual sites fails on most occasions to produce response functions and, therefore, Gray's test could not be used to assess seasonalised data.

Table 5.3a

Site	*PM*	*r*	*ρ*	*RE*	*CE*
BLT_E	0.00 / 0.27	0.68 / 0.27	0.70 / 0.32	0.46 / -0.06	0.46 / -0.12
RFR_E	0.00 / 0.25	0.64 / 0.18	0.65 / 0.20	0.41 / -0.82	0.41 / -0.91
BEN_E	0.00 / 0.05	0.72 / 0.25	0.71 / 0.35	0.52 / -0.65	0.52 / -0.81
ESM_E	0.00 / 0.00	0.67 / 0.17	0.69 / 0.20	0.46 / -0.14	0.46 / -0.18
ARM_M	0.00 / 1.00	0.67 / 0.09	0.65 / 0.14	0.44 / -0.27	0.44 / -0.28
FC_M	0.00 / 0.14	0.69 / 0.23	0.65 / 0.29	0.47 / 0.09	0.47 / -0.15$^+$
$FISH_M$	0.00 / 0.25	0.68 / 0.22	0.67 / 0.28	0.46 / -0.09	0.46 / -0.13
$PILL_M$	0.00 / 0.03	0.61 / 0.29	0.62 / 0.32	0.38 / 0.00	0.38 / -0.04$^+$
KOA_M	0.00 / 0.44	0.65 / 0.27	0.61 / 0.18	0.43 / -0.40	0.43 / -0.85
WEY_W	0.04 / 1.00	0.65 / 0.06	0.66 / 0.03	0.42 / -0.22	0.42 / -0.36
RCS_W	0.00 / 1.00	0.63 / 0.19	0.64 / 0.12	0.39 / -0.12	0.39 / -0.15
MUR_W	0.01 / 1.00	0.54 / 0.01	0.53 / 0.03	0.30 /- 0.52	0.30 / -0.54
LCR_S	0.01 / 1.00	0.51 / 0.01	0.47 / -0.00	0.26 / -0.31	0.26 / -1.07
SPR_S	0.03 / 1.00	0.48 / -0.04	0.46 / -0.18	0.23 / -0.11	0.23 / -0.37
$CLAY_S$	0.00 / 0.01	0.68 / 0.46	0.70 / 0.51	0.47 / 0.12	0.46 / 0.12*

Table 5.3b

Site	*PM*	*r*	*ρ*	*RE*	*CE*
BLT_E	0.00 / 1.00	0.64 / 0.25	0.69 / 0.25	0.41 / -0.16	0.41 / -0.22
RFR_E	0.27 / 0.40	0.34 / 0.04	0.30 / 0.07	0.12 / -0.02	0.12 / -0.03
BEN_E	0.00 / 1.00	0.67 / -0.14	0.65 / -0.05	0.45 / -0.36	0.45 / -0.46
ESM_E	0.06 / 0.97	0.43 / 0.03	0.35 / 0.06	0.19 / -0.07	0.19 / -0.11
ARM_M	0.00 / 0.44	0.53 / 0.11	0.55 / 0.11	0.28 / -0.17	0.28 / -0.19
FC_M	0.00 / 0.02	0.51 / 0.32	0.52 / 0.26	0.26 / 0.14	0.26 / -0.01
$FISH_M$	0.00 / 1.00	0.64 / 0.14	0.62 / 0.13	0.41 / -0.62	0.41 / -0.69
$PILL_M$	0.00 / 0.31	0.50 / 0.37	0.47 / 0.36	0.25 / -0.22	0.25 / -0.29
KOA_M	0.01 / 0.04	0.54 / 0.41	0.51 / 0.32	0.29 / 0.01	0.29 / -0.26
WEY_W	0.01 / 1.00	0.37 / 0.02	0.48 / 0.05	0.14 / -0.15	0.14 / -0.39
RCS_W	0.05 / 0.08	0.60 / 0.27	0.65 / 0.19	0.36 / -0.16	0.36 / -0.19
MUR_W	0.00 / 1.00	0.59 / -0.33	0.64 / -0.27	0.35 / -0.42	0.35 / -0.44
LCR_S	0.00 / 0.40	0.54 / 0.30	0.46 / 0.28	0.56 / 0.05	0.56 / -0.24$^+$
SPR_S	0.00 / 0.13	0.75 / 0.11	0.83 / 0.03	0.56 / 0.07	0.56 / -0.42$^+$
$CLAY_S$	0.00 / 1.00	0.64 / 0.13	0.61 / 0.18	0.41 / -0.03	0.41 / -0.03

Tables 5.3a & b:Calibration and verification statistics for the model calibrated against temperature and precipitation data of a. the early, and b. the late calibration periods. The first number of each pair relates to the calibration period, the second to the verification period. *PM* is product means test (probability values), ρ the Spearman rank coefficient, *r* the Pearson product moment correlation, *RE* the Reduction of Error and *CE* the Coefficient of efficiency. In the calibration period, *RE* = *CE*. The East models are constructed over 1920–1956 and 1957–1992, Mersey over 1921–1956 and 1957–1992, West 1919–1953 and 1954–1989, Southwest 1934–1963 and 1964–1993. * indicates that both *RE* and *CE* tests have been passed, $^+$ indicates that the *RE* test has been passed

Table 5.4a

Site	*PM*	*r*	*ρ*	*RE*	*CE*
BLT_E	0.00 / 0.28	0.73 / 0.19	0.75 / 0.12	0.54 / -0.35	0.54 / -0.57
RFR_E	0.01 / 1.00	0.59 / -0.08	0.56 / -0.07	0.35 / -1.02	0.35 / -1.11
BEN_E	0.00 / 0.30	0.68 / 0.09	0.61 / 0.07	0.46 /- 0.52	0.46 / -0.56
ESM_E	0.01 / 0.00	0.39 / 0.14	0.44 / 0.14	0.15 / -0.02	0.15 / -0.03
ARM_M	0.00 / 1.00	0.59 / -0.22	0.57 / -0.19	0.35 / -0.49	0.35 / -0.52
FC_M	0.01 / 1.00	0.47 / -0.2	0.48 /-0.22	0.22 / -0.44	0.22 /- 0.48
$FISH_M$	0.01 / 0.26	0.47 /0.04	0.43 / 0.00	0.22 / -0.02	0.22 / -0.38
$PILL_M$	0.04 / 0.16	0.50 / 0.09	0.48 / 0.08	0.25 / -0.16	0.25 / -0.25
KOA_M	0.01 / 1.00	0.56 / -0.11	0.47 / -0.15	0.31 / -0.32	0.31 / -0.58
WEY_W	0.00 / 1.00	0.60 / -0.09	0.58 / -0.05	0.36 / -0.41	0.36 /-0.58
RCS_W	0.00 / 0.29	0.58 / 0.28	0.53 / 0.33	0.33 / -0.15	0.33 / -0.17
MUR_W	0.05 / 0.43	0.52 / -0.01	0.52 / -0.04	0.28 / -0.51	0.28 / -0.52
LCR_S	0.00 / 1.00	0.54 / -0.16	0.55 / -0.16	0.29 / -0.40	0.29 / -0.40
SPR_S	0.01 / 0.28	0.46 / 0.19	0.50 / 0.17	0.22 / -0.04	0.22 / -0.45
$CLAY_S$	0.00 / 1.00	0.65 / -0.17	0.62 / -0.18	0.42 / -0.59	0.42 / -0.60

Table 5.4b

Site	*PM*	*r*	*ρ*	*RE*	*CE*
BLT_E	0.04 / 0.38	0.44 / 0.25	0.51 / 0.25	0.20 / -0.12	0.20 / -0.35
RFR_E			NO MODEL		
BEN_E	0.00 / 0.27	0.53 / 0.00	0.47 / 0.04	0.28 / -0.14	0.28 / -0.14
ESM_E	0.00 / 0.47	0.43 / -0.12	0.37 / -0.10	0.18 / -0.23	0.18 / -0.23
ARM_M	0.00 / 0.29	0.42 / -0.10	0.48 / -0.13	0.17 / -0.12	0.17 / -0.15
FC_M			NO MODEL		
$FISH_M$			NO MODEL		
$PILL_M$	0.03 / 1.00	0.46 / -0.15	0.52 / -0.13	0.21 / -0.11	0.21 / -0.24
KOA_M			NO MODEL		
WEY_W			NO MODEL		
RCS_W	0.03 / 1.00	0.54 / 0.10	0.56 / 0.06	0.29 / -0.10	0.29 / -0.13
MUR_W	0.00 / 1.00	0.66 / -0.17	0.70 / -0.11	0.44 / -0.30	0.44 / -0.30
LCR_S	0.00 / 0.49	0.58 /0.04	0.61 / 0.12	0.34 / -0.21	0.34 / -0.23
SPR_S	0.03 / 0.26	0.47 / 0.10	0.44 / 0.14	0.22 / -0.25	0.22 / -0.95
$CLAY_S$	0.00 / 0.06	0.65 / 0.28	0.60 / 0.28	0.42 / -0.00	0.42 / -0.01

Tables 5.4a & b: Calibration and verification statistics for the model calibrated against ZI data of a. the early period, and b.the late period. The first number of each pair relates to the calibration period, the second to the verification period. *PM* is the product means test (probability values), *ρ* the Spearman rank coefficient, *r* the Pearson product moment correlation, *RE* the Reduction of error and *CE*, the Coefficient of efficiency. In the calibration period, *RE* = *CE* All models are constructed for the 1954–1994 period. * indicates that both *RE* and *CE* tests have been passed, + indicates that the *RE* test has been passed

Table 5.5a

SITE	*PM*	*r*	*ρ*	*RE*	*CE*
BLT_E	0.00 / 0.33	0.86 / 0.30	0.78 / 0.47	0.73 / -0.12	0.73 / -0.48
RFR_E	0.27 / 0.44	0.44 / 0.27	0.44 / 0.31	0.19 / -0.01	0.19 / -0.08
BEN_E	0.01 / 1.00	0.65 / -0.10	0.56 / -0.04	0.42 /- 0.94	0.42 / -0.94
ESM_E	0.16 / 0.16	0.44 / 0.013	0.40 / 0.09	0.19 / -0.12	0.19 / -0.29
ARM_M	0.00 / 0.07	0.59 / -0.22	0.70 / 0.42	0.35 / -0.49	0.35 / -0.52
FC_M	0.27 / 0.47	0.47 / -0.22	0.60 / -0.00	0.22 / -0.44	0.22 / -0.48
$FISH_M$	0.00 / 1.00	0.47 / 0.04	0.62 / 0.18	0.22 / -0.02	0.22 / -0.38
$PILL_M$	0.01 / 0.40	0.50 / 0.09	0.50 / -0.04	0.25 / -0.16	0.25 / -0.25
KOA_M	0.00 / 0.35	0.55 / 0.14	0.47 / 0.18	0.30 / -0.03	0.30 / -0.86
WEY_W	0.01 / 1.00	0.63 / -0.12	0.70 / 0.04	0.40 / -0.16	0.40 / -0.50
RCS_W	0.02 / 1.00	0.57 / 0.19	0.53 / 0.11	0.32 / 0.15	0.32 / -0.13
MUR_W	0.00 / 0.15	0.60/ 0.10	0.72 / 0.17	0.36 / -0.23	0.36 / -0.82
LCR_S	0.05 / 1.00	0.63/ -0.03	0.67 / 0.04	0.39 / -0.15	0.39 / -0.37
SPR_S	0.01 / 0.30	0.55 / 0.45	0.55 / 0.34	0.31 / -0.18	0.31 / -0.28
$CLAY_S$	0.01 / 0.30	0.55 / 0.24	0.53 / 0.29	0.31 / -0.17	0.31 / -0.17

Table 5.5b

SITE	*PM*	*r*	*ρ*	*RE*	*CE*
BLT_E	0.01 /0.31	0.67 / 0.44	0.68 / 0.34	0.45 / 0.12	0.45 / -0.06$^+$
RFR_E	0.00 / 1.00	0.47 / -0.20	0.50 /- 0.06	0.22 / -0.3	0.22 /- 0.43
BEN_E	0.04 / 1.00	0.55 / -0.21	0.52 / -0.41	0.30 / -0.25	0.30 / -0.26
ESM_E			NO MODEL		
ARM_M	0.02 / 0.27	0.49 / 0.33	0.49 / 0.30	0.24 / -0.01	0.24 / -0.267
FC_M	0.01 / 1.00	0.57 / 0.09	0.46 / -0.17	0.29 / -0.03	0.29 / -0.03
$FISH_M$			NO MODEL		
$PILL_M$			NO MODEL		
KOA_M	0.02 / 0.32	0.53 / -0.04	0.46 / -0.08	0.28 / -0.11	0.29 / -0.83
WEY_W	0.00 / 0.48	0.54 / 0.02	0.52 / 0.04	0.29 / -0.72	0.29 / -1.43
RCS_W	0.02 / 0.15	0.57 / 0.26	0.56 / 0.29	0.32 / -0.54	0.32 / -1.10
MUR_W	0.03 / 0.32	0.60 / 0.10	0.412 / 0.22	0.36 /-0.23	0.36 / -0.82
LCR_S	0.00 / 1.00	0.53 / 0.15	0.57 / 0.16	0.28 / -0.01	0.28 / -0.16
SPR_S	0.01 / 0.06	0.60 / 0.25	0.56 / 0.24	0.37 / -0.40	0.37 / -1.38
$CLAY_S$	0.01 / 1.00	0.65 / -0.25	0.61 / -0.16	0.42 / -0.54	0.42 / -0.55

Tables 5.5a &b: Calibration and verification statistics for the model calibrated against MI data of a. the early period, and b. the late period. The first number of each pair relates to the calibration period, the second to the verification period. *PM* is the product means test (probability values), *ρ* the Spearman rank coefficient, *r* the Pearson product moment correlation, *RE* the Reduction of error and *CE* the Coefficient of efficiency. In the calibration period, *RE* = *CE*. All regional models are calculated over the 1969–1994 period. * indicates that both *RE* and *CE* tests have been passed, $^+$ indicates that the *RE* test has been passed

Table 5.6a

Site	*PM*	*r*	*ρ*	*RE*	*CE*
BLT_E			NO MODEL		
RFR_E			NO MODEL		
BEN_E	0.01 / 1.00	0.29 / -0.14	0.31 / -0.13	0.09 / -0.15	0.09 / -0.16
ESM_E	0.11 / 1.00	0.32 / -0.12	0.35 / -0.18	0.10 / -0.12	0.10 / -0.12
ARM_M	0.01 / 0.07	0.45 / 0.26	0.41 / 0.23	0.20 / 0.06	0.20 / 0.06*
FC_M	0.34 / 0.44	0.34 / 0.09	0.35 / 0.12	0.12 / -0.03	0.12 / -0.04
$FISH_M$	0.01 / 0.16	0.36 / 0.17	0.36 / 0.16	0.13 / -0.01	0.13 / -0.03
$PILL_M$	NO MODEL — CHRONOLOGY TOO SHORT				
KOA_M	0.08 / 0.27	0.37 / 0.23	0.42 / 0.27	0.13 / 0.04	0.13 / 0.02*
WEY_W	0.01 / 1.00	0.33 / 0.14	0.32 / 0.10	0.11 / -0.08	0.11 / -0.11
RCS_W	0.01 / 0.26	0.35 / 0.08	0.37 / 0.20	0.13 / -0.12	0.13 / -0.13
MUR_W	0.00 / 0.04	0.41 / 0.09	0.41 / 0.09	0.17 / -0.20	0.17 / -0.24
LCR_S	0.00 / 1.00	0.33 / 0.12	0.36 / 0.08	0.11 / 0.02	0.11 / -0.09$^+$
SPR_S	0.27 / 1.00	0.39 / 0.08	0.42 / 0.18	0.15 / -0.01	0.15 / -0.11
$CLAY_S$	0.28 / 0.48	0.32 / 0.17	0.36 / 0.19	0.10 / 0.15	0.10 / 0.15*

Table 5.6b

Site	*PM*	*r*	*ρ*	*RE*	*CE*
BLT_E	0.13 / 1.00	0.34 / 0.16	0.44 / 0.17	0.11 / -0.01	0.11 / -0.10
RFR_E	0.02 / 1.00	0.33 / 0.05	0.34 / 0.10	0.10 / -0.08	0.10 / -0.10
BEN_E			NO MODEL		
ESM_E	0.05 / 1.00	0.28 / -0.15	0.27 / -0.12	0.08 / -0.20	0.08 / -0.20
ARM_M	0.01 / 0.30	0.34 / 0.21	0.34 / 0.18	0.11 / -0.02	0.11 / -0.02
FC_M			NO MODEL		
$FISH_M$			NO MODEL		
$PILL_M$	NO MODEL- CHRONOLOGY TOOSHORT				
KOA_M	0.15 / 0.11	0.33 / 0.21	0.35 / 0.26	0.11 / 0.04	0.11 / 0.03*
WEY_W			NO MODEL		
RCS_W	0.05 / 0.29	0.28 / 0.16	0.33 / 0.08	0.08 / -0.01	0.08 / -0.02
MUR_W			NO MODEL		
LCR_S			NO MODEL		
SPR_S	0.01 / 0.31	0.34 / 0.14	0.32 / 0.16	0.12 / -0.02	0.12 / -0.14
$CLAY_S$	0.00 / 0.31	0.43 / 0.15	0.43 / 0.15	0.19 / -0.13	0.19 / -0.13

Tables 5.6a & b: Calibration and verification statistics for the model calibrated against SOI data of the a. the early, and b. the late calibration periods. The first number of each pair relates to the calibration period, the second to the verification period. *PM* is the product means test (probability values), ρ the Spearman rank coefficient, *r* Pearson product moment correlation, *RE* the Reduction of error, *CE* the Coefficient of efficiency. In the calibration period, *RE* = *CE*. All models are constructed for the 1937–1994 period. A * indicates that both *RE and CE* tests have been passed, and $^+$ indicates the *RE* test has been passed

Site	*Proportion of nonoverlapping confidence intervals*	
	maximum temperature	*minimum temperature*
BLT_E	18/20	19/20
RFR_E	no model passed for second period	
BEN_E	no model passed for second period	
ESM_E	17/20	19/20
FC_M	19/20	18/20
$FISH_M$	no model passed for second period	
$PILL_M$	no model passed for second period	
ARM_M	17/20	17/20
KOA_M	18/20	19/20
WEY_W	no model passed for second period	
RCS_W	18/20	19/20
MUR_W	17/20	18/20
SPR_S	20/20	15/20
LCR_S	20/20	18/20
$CLAY_S$	18/20	18/20

Table 5.7: **Results of Gray's element matching test. Response functions are based on monthly maximum and minimum temperature data only. East models are based on the time periods 1920–1956 and 1957–1992; Mersey models on 1921–1956 and 1957–1992; West models on the periods 1919–1953 and 1954–1989; and Southwest on the periods 1934–1963 and 1964–1993**

Number of nonoverlapping confidence intervals (n)	*Probability*
15/20	3.66×10^{-16}
16/20	6.02×10^{-18}
17/20	7.45×10^{-20}
18/20	6.54×10^{-22}
19/20	3.65×10^{-24}
20/20	9.53×10^{-27}

Table 5.8: **Probabilities of *n* non overlapping confidence intervals in a response function. Probabilities based on the binomial distribution. Adapted from Gray *et al.* (1981)**

The Kalman Filter Test

The test based on KF for individual months (Table 5.9) reveals some evidence of approximate step function changes in the response to climate. Results for minimum and maximum temperatures, especially minimum temperature, for

the early autumn months of the prior growing season for northern sites suggest that the relationships between these variables and ring widths are time-dependent. Several precipitation variables are also denoted as being time-dependent, with some loose suggestion that a time-dependent relationship exists over the prior growing season. Palmer (1989) has commented on the temporally inconsistent

Site	*Maximum temperature*	*Minimum temperature*	*Precipitation*	*ZI*	*SOI*	
BLT_E	-	Mar-1, Apr-1		Mar-1		-
RFR_E	-	-		Mar-1		-
BEN_E	-	Mar-1, Apr-1	Jan-1	Mar-1		-
ESM_E	Jul	-	-	-		-
FC_M	-	-	-	-		-
$FISH_M$	-	-	Oct-1	-		-
$PILL_M$	-	-	Oct	-		-
ARM_M	-	-	-	-		-
KOA_M	Nov-1	Mar-1	Oct-1	-		-
WEY_W	-	-	Jul	-		-
RCS_W	Mar-1	Mar-1		Mar-1		-
MUR_W	-	Mar-1	-	-		-
SPR_S	Dec-1	-	-	-		Nov
LCR_S	-	-	-	Sep		-
$CLAY_S$		-	Mar-1	-		-

Table 5.9: **Results of time dependence tests based on Kalman Filter. Time-dependence between ring widths and each month of the 20 month window is tested for. Only those monthly variables for which a time-dependent relationship has been found are listed. For these models, the AIC of the model based on the KF is lower than for the constant coefficient model meaning that varying regression coefficients occur over time. A -1 suffix on a climatic variables indicates that the month of the prior year exhibits time-dependent behaviour. Models are based on the full period of available data: For temperature and precipitation: East models, 1915–1994; West models, 1915–1994; Southwest temperature 1931–1994, and Southwest precipitation 1915–1994. For the ZI, the time period used for model construction is 1912–1994; and for the SOI, 1876–1994 has been used**

response of *Phyllocladus trichomanoides* and *P. glaucus* to precipitation. In contrast to the above results, however, he has found that the inconsistency exists for the end of the current growing season. He also noted that the response appears dependent on the series time-periods tested.

Relationships between seasonalised data (temperature, precipitation, and the SOI) and ring widths did not suggest time-dependence. However, time-

dependent relationships between the ZI and ring-width indices are evident for $FISH_M$, KOA_M, RCS_W, MUR_W (prior to November–March), and SPR_S (November–January). The KF traces of the coefficients for these relationships are shown in Figure 5.19.

Three of the four sites show time-dependent behaviour in relation to maximum temperature, with maximum temperature becoming less important (Figure 5.20). The traces of those monthly parameters determined to be time-dependent, as suggested by the KF test, clearly show that the relationship between March (prior season) minimum temperatures and ring width has also become less defined over the period 1913–1994, the parameter values becoming less negative (Figure 5.21). The change over time is generally more pronounced than for minimum temperature coefficients. This appears to have been a continuous process over the time frame examined, but more rapid change, loosely approximating a step function in several cases, occurs after 1930. Essentially, the lower absolute values of the regression coefficients indicate that minimum temperature has become less limiting to cambial growth in the prior autumn.

Time-dependent responses to precipitation are less clear than those of temperature. However, four of the six sites where time-dependent behaviour has been detected show a weakening relationship with precipitation over time. Of these, the relationships for BEN_E, $FISH_M$ and KOA_M have become less positive over time, with WEY_W showing a less negative relationship for the month of July (Figure 5.22). With regard to the relationship between the ZI and ring-width indices, the positive relationship for the prior March early in the century has become weaker for sites showing a time-dependent relationship. LCR_S, with a suggestion of time-dependence for the September of the current growing season, does not follow the pattern shown for March.

Figure 5.23 shows time-dependent relationships for ZI and SOI. Three of the five sites indicating time-dependent relationship with monthly ZI data show coefficients that decrease in value over the whole time frame.

Broadly, there are definite suggestions of time-dependent relationships between ring-width index series and monthly climate variables. Gray's test indicates that there are significant differences between the two time periods for

Figure 5.19: KF traces for time-dependent seasonal relationships between seasonalised ZI and ring-width indices. A time-dependent relationship between the KOA_M, $FISH_M$, MUR_W, RCS_W and SPR_S chronologies and the ZI, zseasonalised over the November–March period of the prior growing season, is apparent. Data has been seasonalised by averaging the value of the ZI over theperiod from November to March. Time period of analysis is 1913–1994

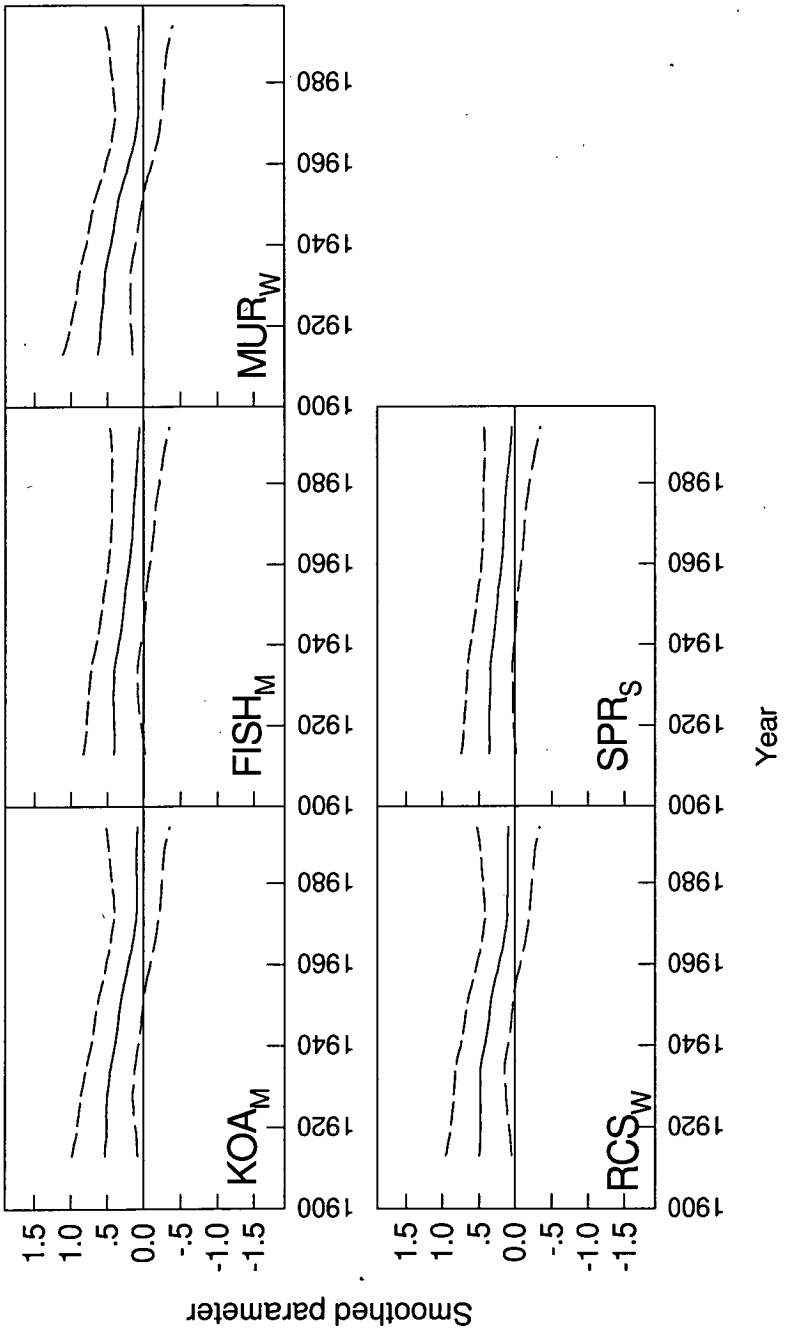
MUR_W
FISH_M
SPR_S
KOA_M
RCS_W
1900
1920
1940
1960
1980
1.5
1.0
.5
0.0
-.5
-1.0
-1.5
Year
Smoothed parameter

most months, while the KF test indicates that the nature of the change in relationship between autumn temperatures of the prior season and current growth, loosely approximates a step function. Why time-dependent relationships between seasonalised data and ring widths occur only in the case of the ZI is unclear.

5.3.2.4 Temperature and precipitation data

The monthly climate averages (Figure 5.24 and 5.25) show interesting differences between the two periods. There has been an increase in average maximum temperature for all months in the West, an increase in late winter to late summer in the East, while a decrease in average maximum temperatures for late winter to mid summer is implied for the Southwest. In the later period, average minimum temperature has increased in comparison with the early period for all seasons except autumn in the East; for summer and autumn in the West; and for summer, winter and spring in the Southwest. The increase evident in minimum temperature over autumn months in the East and West occurs for the same season as time-dependent relationships between minimum temperatures and ring widths are suggested to exist.

There has been little consistent change in precipitation for the East and West regions (Figure 5.25). Months showing significant increases in average precipitation over time are: April, May and September for the West; and April, May, August, November and December for the East. Months showing a significant decrease are: January, February and October in the West; and January–March, June and October in the East. Average Southwest precipitation reveals a much more striking pattern across the two time periods. Average recorded precipitation has increased significantly for the April-December period, with the exception of June and October.

Although the averages of the two periods differed for all the temperature variables, the superimposed 95% confidence intervals advise caution in making any inferences from the point estimates. There are no occasions where differences in the point estimates of the two time periods could be claimed to be significant.

Figure 5.20: KF traces for time-dependent relationships between maximum temperature and ring widths. Time-dependent behaviour is indicated for July (ESM_E), November of the prior season (KOA_M), March of the prior season (RCS_W), and December of the prior season (SPR_S). Time periods of analysis are: East, 1915–1994; 1915–1993;West,1915–1993; Southwest, 1933–1994

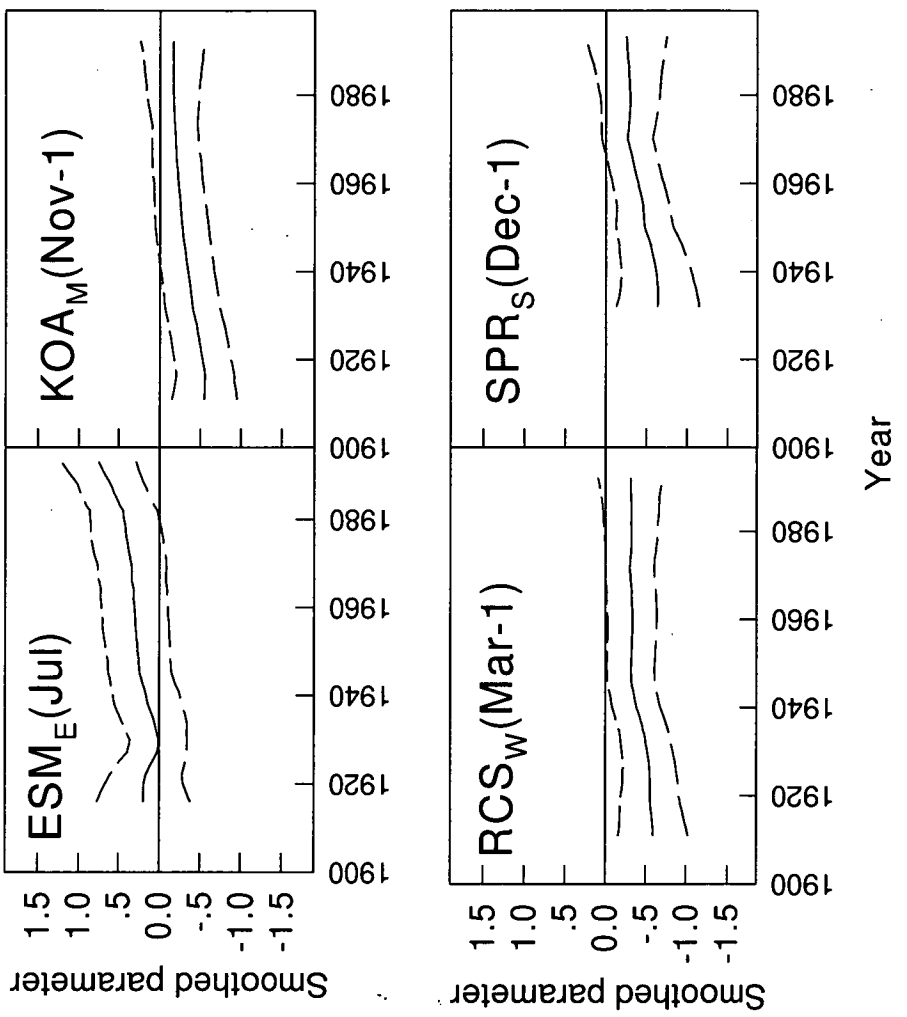
ESM$_E$(Jul)
KOA$_M$(Nov-1)
RCS$_W$(Mar-1)
SPR$_S$(Dec-1)
Smoothed parameter
1.5
1.0
.5
0.0
-.5
-1.0
-1.5
1900
1920
1940
1960
1980
Year

Figure 5.21: KF traces for time-dependent relationships between minimum temperature and ring widths. Time-dependent behaviour is indicated for March of the prior season (BLT_E and BEN_E), April of the prior season ($BLT_E(2)$, $BEN_E(2)$), March of the prior season (KOA_M, RCS_W, MUR_W). Time periods of analysis are: East, 1915–1994; Mersey, 1915–1993; West, 1915–1993; Southwest, 1933–1994

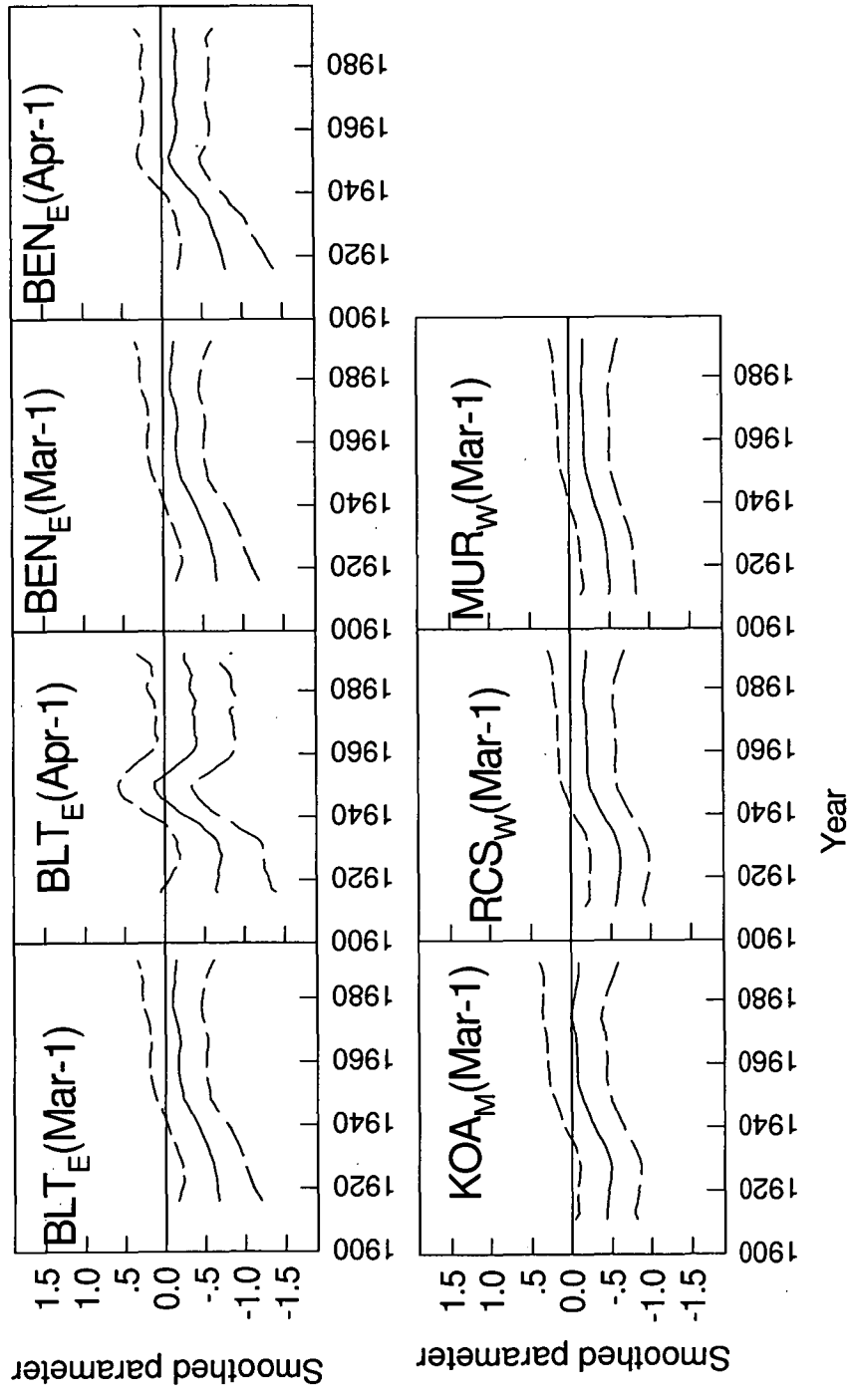
BLT$_E$(Mar-1)
BLT$_E$(Apr-1)
BEN$_E$(Mar-1)
BEN$_E$(Apr-1)
KOA$_M$(Mar-1)
RCS$_W$(Mar-1)
MUR$_W$(Mar-1)
1.5
1.0
.5
0.0
-.5
-1.0
-1.5
1900
1920
1940
1960
1980
Smoothed parameter
Year

Figure 5.22: KF traces for time-dependent relationships between precipitation and ring widths. Time-dependent behaviour is indicated for January of the prior season (BEN_E), October of the prior season ($FISH_M$ and KOA_M), October of the current season ($PILL_M$), and July (WEY_W) and March of the prior season ($CLAY_S$). Time periods of analysis are: East, 1915–1994; Mersey, 1915–1993; West, 1915–1993; Southwest, 1915–1994

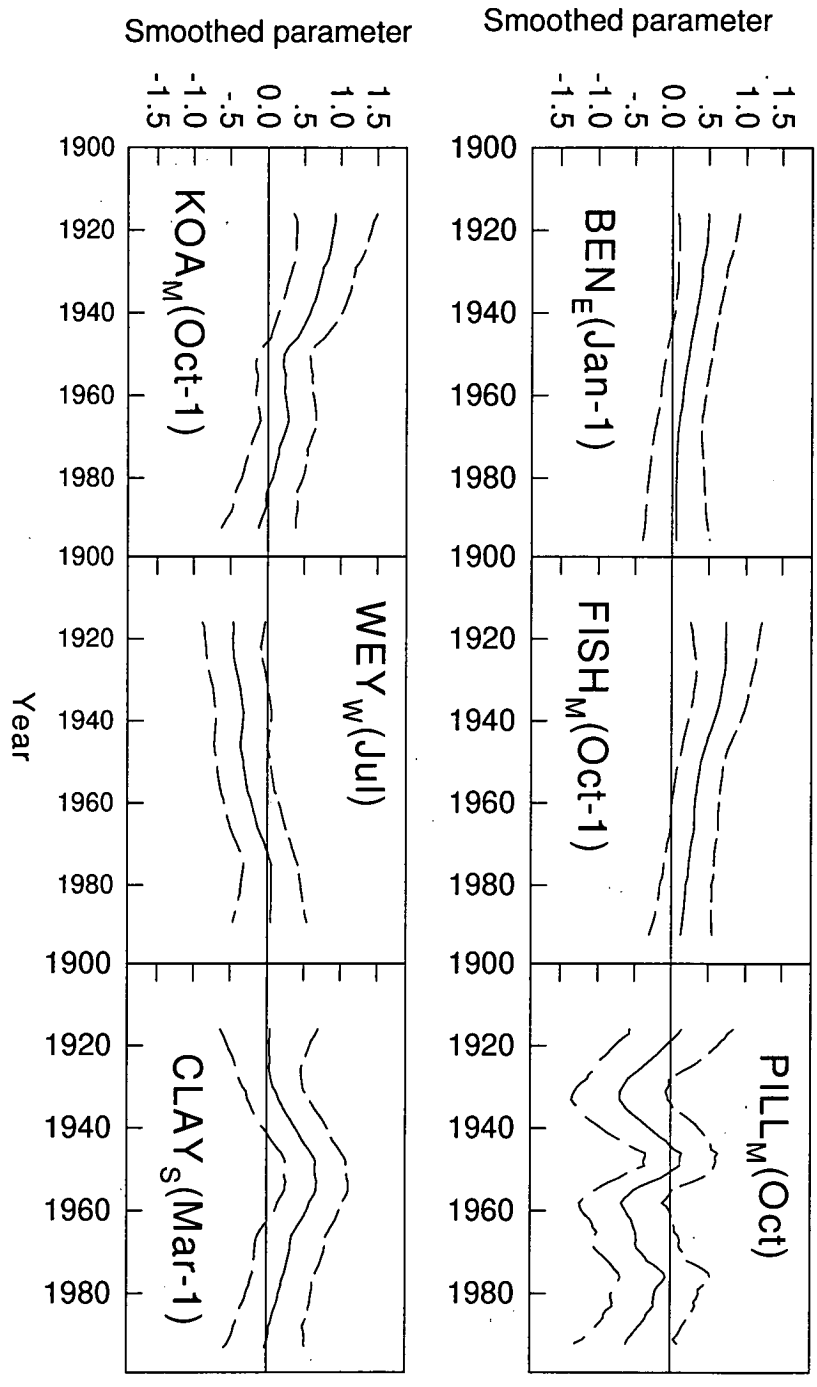
Smoothed parameter
Smoothed parameter
-1.5
-1.0
-.5
0.0
.5
1.0
1.5
1900
1920
1940
1960
1980
KOA$_M$(Oct-1)
WEY$_W$(Jul)
CLAY$_S$(Mar-1)
BEN$_E$(Jan-1)
FISH$_M$(Oct-1)
PILL$_M$(Oct)
Year

Figure 5.23: KF traces for time-dependent relationships between the ZI and ring widths, and between the SOI and ring widths. Time-dependent behaviour between the ZI and ring widths is indicated for March of the prior growing season for all sites shown except LCR_S which exhibits a time-dependent relationship for the September of the current growing season. Time period of analysis is 1913–1994. In the case of the SOI, time-dependent behaviour is indicated only for November of the current year (SPR_S), and the time period of analysis was 1878–1994

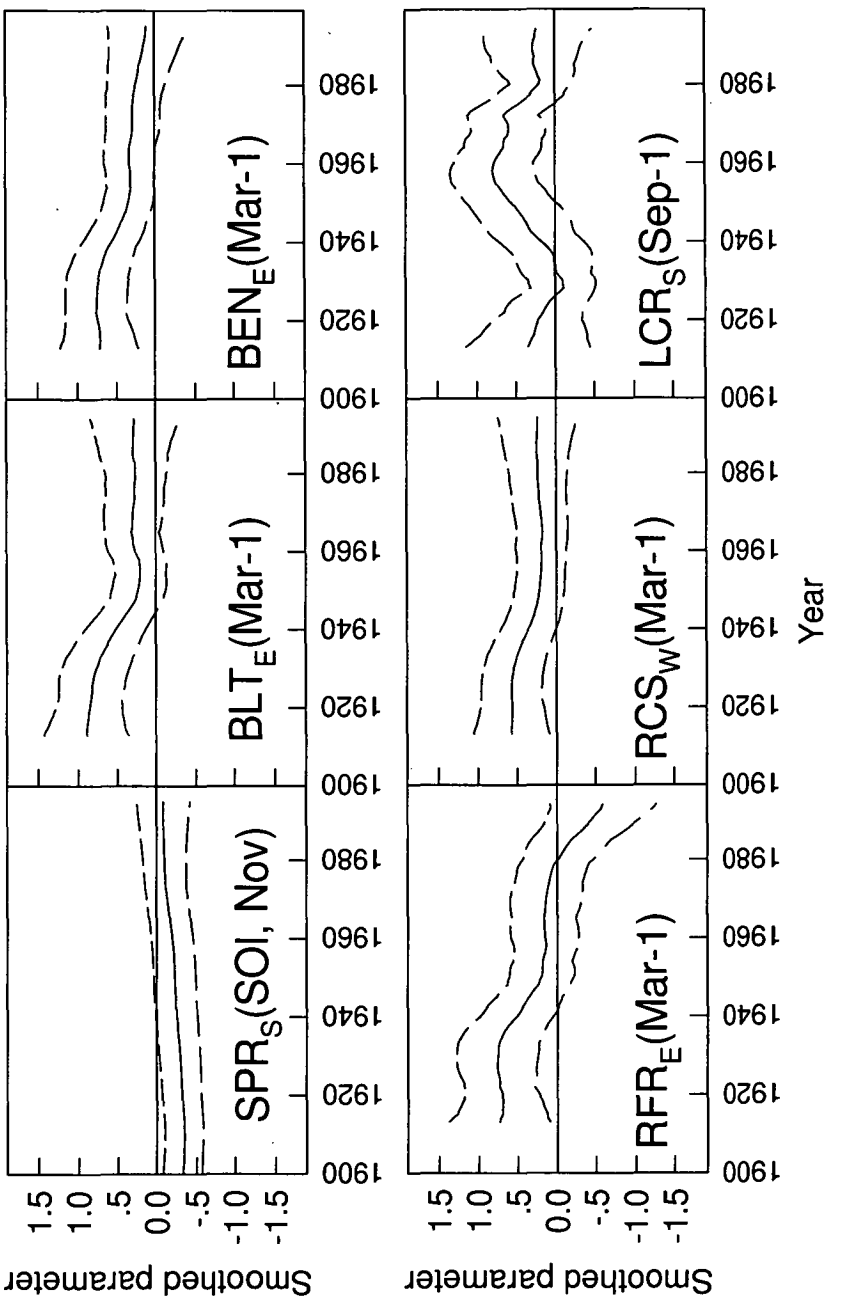
Smoothed parameter
1.5
1.0
.5
0.0
-.5
-1.0
-1.5
1900
1920
1940
1960
1980
SPR$_S$(SOI, Nov)
BLT$_E$(Mar-1)
BEN$_E$(Mar-1)
RFR$_E$(Mar-1)
RCS$_W$(Mar-1)
LCR$_S$(Sep-1)
Year

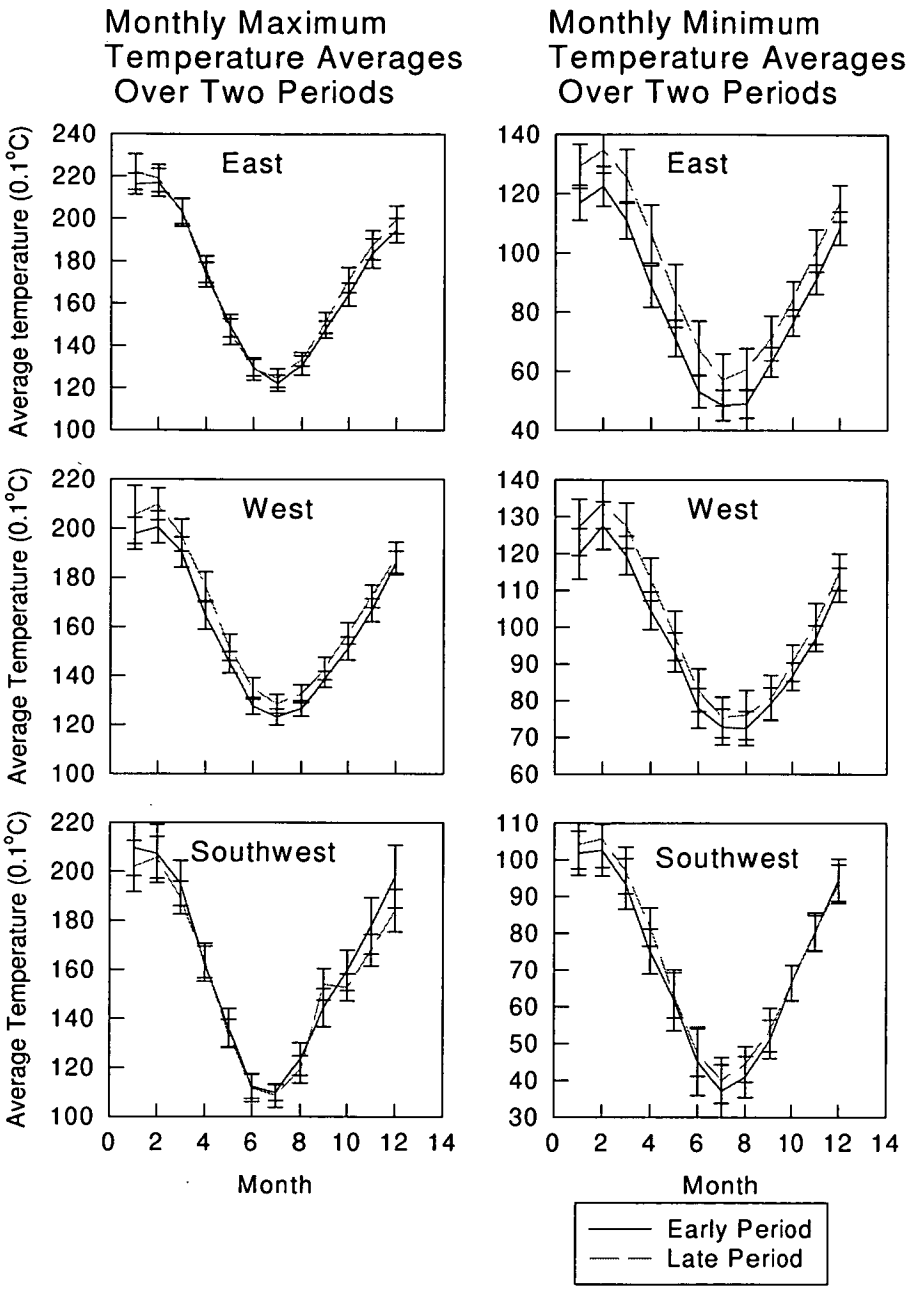

Figure 5.24: **Average monthly maximum (a) and minimum temperatures (b) for two time periods. Early period: East 1915–1954; West 1915–1953; Southwest 1932–1962. Late period: East 1955–1993; West 1954–1990; Southwest 1963–1992. Confidence intervals for point estimates are shown**

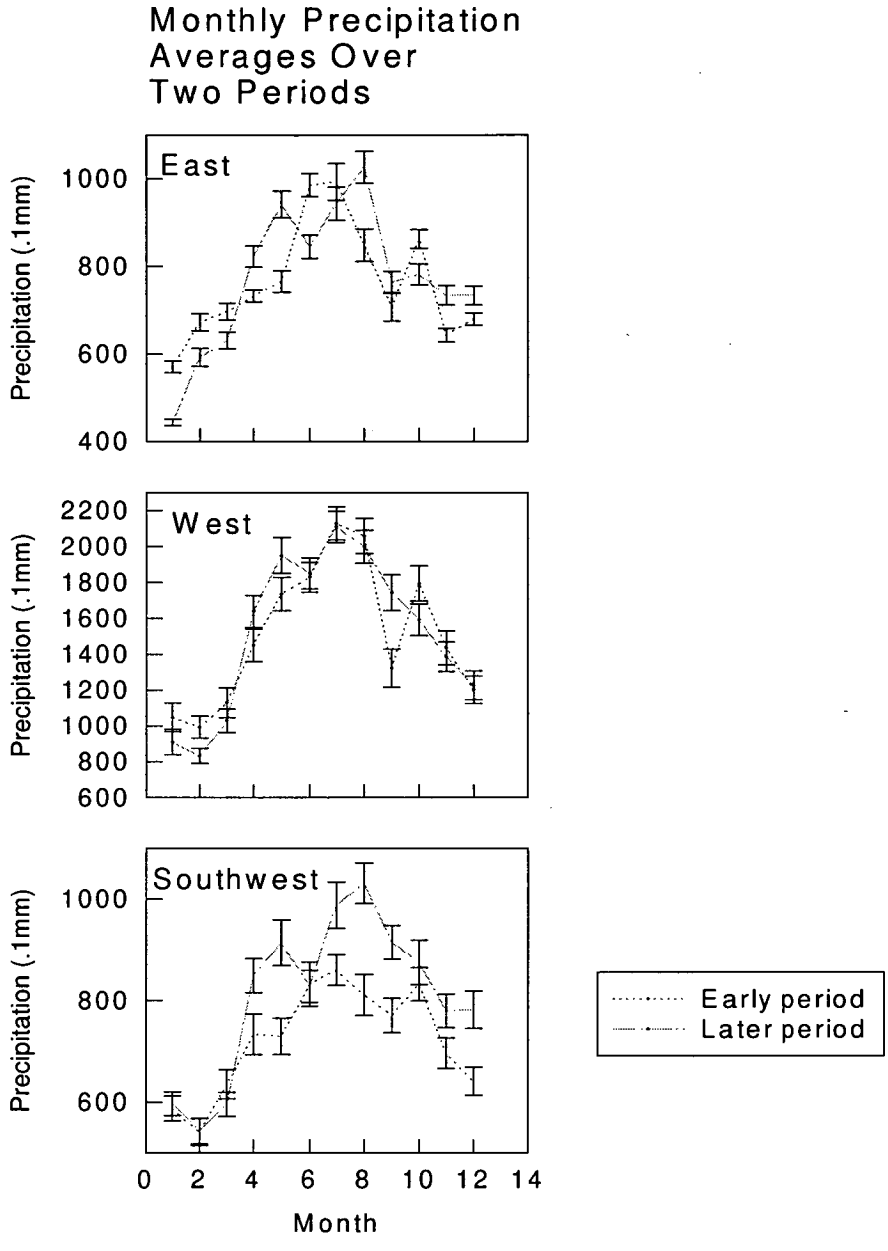

Figure 5.25: **Average monthly precipitation for two time periods. Early period: East 1915–1954; West 1915–1953; Southwest 1932–1962. Late period: East 1955–1993; West 1954–1990; Southwest 1963–1992. Confidence intervals for point estimates are shown**

However, increases in regional temperatures are supported by evidence from broader-scale phenomena (e.g. Jones 1994). For precipitation, however, a number of differences are shown to be statistically significant (Figure 5.25).

5.4 Discussion

5.4.1 The Dominant Response

The correlation functions (maximum temperature and precipitation) for the whole period (Figures 5.4–5.7) are broadly consistent with Campbell's (1980) *Phyllocladus aspleniifolius* response functions where a positive response to winter temperature was indicated over the period 1941–1970. Correlation with precipitation appears more complicated than that with temperature, and this is likely to predominantly reflect the varied topography of individual sites. Campbell's results also reveal a more complicated response to precipitation (as opposed to temperature) by *P. aspleniifolius*.

Consistency of precipitation response between sites within a single region differs across the four regions. The three western sites show the greatest similarity in their correlation with climatic data. As has been pointed out in Chapter 2, West sites are also more homogeneous in terms of their environmental variables than sites of other regions (Table 2.1), and it is indisputable that topography is an important control on precipitation received at a site. For the East, the closer proximity of the Ben Lomond massif to the BEN_E and RFR_E sites, compared to BLT_E, may have been responsible for those sites behaving quite differently from BLT_E in the current season with regard to precipitation. Conversely, topographical influences on local site precipitation in the West, may have been of less importance to the cambial growth of *Phyllocladus aspleniifolius* due to the considerably higher levels of precipitation in those regions. In conjunction with similar elevations and other microsite factors, this may partly explain the greater similarity of response to precipitation in the West region. Alternatively, it is not unreasonable to hypothesise that the climate of this area is more homogenous than that of other regions. Either of these reasons, or a combination of them, can account for a greater similarity of response to climatic variables. One further point

to note is that the use of a greater number of sites for the East and Mersey regions may have resulted in what appears to be greater variation in response to climate within these regions.

The ESM_E site, differentiated from other east coast sites by its position on the east-facing scree slopes of Maria Island, is especially likely to experience moisture stress earlier than other East sites during the warm season, and this is borne out by the inverse relationship between maximum temperature and precipitation of the current season from August to January (Figure 5.4). The late summer positive correlation between East ring width (Tasmanian mainland sites) and precipitation indicates that moisture stress occurring at the end of the season will result in a narrow ring. It is possible that this moisture stress is related to high temperatures which often occur at this time of year (Garfinkel and Brubaker 1980).

As discussed, there is an encouraging measure of consistency between the response of *Phyllocladus aspleniifolius* to the various climate indices. For example, a positive correlation with the Zonal Index in the prior season is consistent with wetter weather due to westerly flow and therefore cooler temperatures across the State. Similarly, a strong positive correlation with the Meridional Index in the early part of the current growing season is consistent with a northerly airflow producing warmer temperatures. The reason for the positive prior season response, at times verging on significance, is less clear in view of the responses to other climate variables.

The most coherent characteristic of the response functions is a strong negative correlation with prior growing season temperatures. It is this response which is discussed in detail below. This prior season response is a reported feature of other Tasmanian species: *Athrotaxis* sp. (not all sites sampled), *Nothofagus gunnii* (Campbell 1980) and low altitude *Lagarostrobos franklinii* (Buckley 1997). The prior season response is, at times, more important than the current season response to climate — e.g. west coast *Phyllocladus.* Many species have been noted to possess response functions which exhibit coefficients of opposite sign for current and previous growing season variables (e.g. temperature) (e.g. Fritts 1974, Scott 1972, Jacoby 1983, D'Arrigo *et al.* 1993, Kelly *et al.* 1994). At present, the reason for such a prior season response is unclear, although

current investigations of cambial growth will provide useful insights into the problem (e.g. Fritts and Shashkin 1995).

In the absence of detailed information of the nature that Fritts and Shashkin hope to provide, two sets of hypotheses concerning the reasons for the prior season temperature response will be entertained here. Neither set is truly testable based on the data currently available, but some additional data may be used to examine the second hypothesis more closely than it is possible to assess the first at this stage.

The first hypothesis is really a group of hypotheses which consider competition for available resources by various plant processes. Temperature is an important variable in the process of the photosynthetic conversion of energy to carbohydrates. It is well known that competition for carbohydrates between different parts of a plant exists, and that different processes occur at different times — e.g. root, shoot and fruit development (Raven *et al.* 1992). Processes which occur at the end of the one growing season compete with the storage of carbohydrates which can also be used for growth in the subsequent year. Kramer (1964) has put forward evidence indicating that early growth (earlywood) is largely supported by carbohydrates produced in the prior season. If late season processes deplete carbohydrate storage, then little remains at the beginning of the next growing season, and the plant is entirely reliant on instantaneously supplied resources for the production of carbohydrates (Periera 1994). For example, Buckley (1997) has argued that the significant and negative prior growing season response to temperature observed in lower elevation *Lagarostrobos franklinii* may be due to the depletion of stored carbohydrates and nutrients which are instead used in current growth. This process then serves to decouple growth and carbon assimilation rates, so that the storage of carbohydrates competes with current growth.

Two specific explanations under this 'umbrella' hypothesis, considered briefly here, are related to fruit and seed development and to leaf development, both of which occur late in the growing season. In *Phyllocladus aspleniifolius*, it is known that male and female primordia are laid down in the previous season. Male and female cones develop in November–December of the previous growing

season (Barker 1993). If the biennial oscillation observed in the ring widths is indeed related to oscillating seed production, then this could explain the lagged negative correlation with temperature, as carbohydrate is mobilised by reproductive growth at the expense of cambial growth in the following season (Kozlowski 1992).

Foliar development begins about November–December and lasts until approximately February–March, depending on elevation (Barker 1993). This relatively long foliar development period means that new foliage is unlikely to be photosynthetically efficient until the next season (Barker 1993). Large investment in new leaf initials is likely to deplete carbohydrate which may otherwise have been stored for woody growth early in the next season. There is evidence that carbohydrate accumulation occurs mainly in the later part of the season which is the same time as both foliage development and development of sexual primordia occur (Kozlowski 1973). Figures 5.4–5.7 clearly show that the timing of the negative correlation of temperature and cambial growth, at the end of the previous growing season, coincides with the timing of leaf and sexual primordia development.

Turning to the climate data, the two possibilities discussed above are tantamount to claiming that for years in which temperatures are high, carbohydrate is channelled into reproductive growth or foliar development, rather than into cambial growth. Conversely, in years when temperature is low and, therefore, the temperature resource for the production of carbohydrates is low, carbohydrates are stored and used for cambial growth in the following season, rather than reproductive growth or foliage development. From Figures 5 4–5.7, it is clear that if this is the case, the differential timing of negative correlations with maximum and minimum temperatures respectively may be important, reflecting different processes.

The literature, however, is not uniform in its view concerning competition between photosynthate storage and other growth processes. Kozlowski (1992) has suggested that, in gymnosperms, photosynthate produced after the end of the period of woody growth is used more in respiration than in accumulation of reserves, and that growth is influenced more by factors which affect carbohydrate

conversion to new tissues than by carbohydrate availability. Cannell and Dewar (1994) found that trees maintain moderate carbohydrate reserves at all times.

The second hypothesis relates to the climatic reduction of assimilation. The explicit assumption that photosynthesis is directly related to woody growth is generally considered reasonable (Bradford and Hsiao 1981, Schulz and Caldwell 1994). Plants become photo-inhibited by high light/temperature/water stress through the presence of an excess of absorbed light beyond that used in photosynthesis (Demmig-Adams and Adams 1992).

Many authors point to the crucial role of water stress in photo-inhibition, or in the reduction of assimilation (e.g. Zahner 1963, Bradford and Hsiao 1981, Kozlowski 1973, Kozlowski 1979, Kozlowski 1992, Cannell and Dewar 1994). The fact that relationships between cambial growth and precipitation are ill-defined in this study may merely reflect the fact that specific microsite information concerning moisture availability is required in order to assess the importance of precipitation to growth. Brodribb (University of Tasmania, pers. comm.) has also suggested that the monthly resolution of precipitation data may be too fine to enable a relationship between precipitation and cambial growth to be seen. Ong and Baker (1985) have pointed out that water deficit and heat stress are closely related, and Read (1985) and Barker (1993) have both noted the sensitivity of *Phyllocladus aspleniifolius* to high light and high temperature conditions. In Tasmania, high light conditions are generally associated with higher temperatures and reduced precipitation (Chapter 4). Therefore, while it is not optimal, nor strictly correct, to infer water stress from a negative relationship with temperature, it is not unreasonable to do so in the absence of more specific information.

Because woody growth is directly reliant on photosynthetic area (Bradford and Hsiao 1981), a suggested mechanism for temperature-reduced assimilation is related to leaf development, growth and abscission. Strongest evidence for a direct link between foliage and xylem growth is the familiar relationship between sapwood area and foliage biomass (Grier and Waring 1974, Kaufmann and Troendle 1981, Cannell and Dewar 1994). The chain of causality under the second hypothesis follows thus: a negative relationship with temperature in the prior season indicates that high temperatures/water stress inhibit growth of new

leaves as well as promoting leaf abscission. This means that there is less photosynthetic area in the *next* growing season, which in turn produces less woody growth. In cool summers, the opposite occurs. Annual variations in leaf abscission have been noted to reflect climatic variations, and the removal of less vigorous transpiring surfaces is an important drought resistance strategy in trees (Kozlowski 1973). The oldest leaves are shed first and water translocated to younger and more vigorous leaves. Ethylene is a powerful inducer of abscission and acts in association with cytokinins, abscisic acid and gibberellins. Late season defoliation will not have obvious inhibiting effects in the current year, but will affect cambial growth in the following year. In summary,

"*...Cambial growth which depends on a downward flow of carbohydrates and hormonal growth regulators from the leaves, varies greatly with leaf development, and...leaf development depends to a considerable extent on prior year weather.*" (Kozlowski 1979)

Read and Busby (1990) have indicated that the optimal temperature for photosynthesis in *Phyllocladus aspleniifolius* is 15 ^{0}C for trees acclimated to 8 ^{0}C (they examined responses in trees acclimated to 8 ^{0}C, 20 ^{0}C and 29 ^{0}C only). Temperatures are taken to be optimal for photosynthesis between 10 and 15 ^{0}C (Figure 5.26). The 8 ^{0}C acclimation temperature is used here as the field acclimation temperature of many of the sites being considered will more likely be closer to 8 ^{0}C than to 20 ^{0}C. To use 8 ^{0}C for all sites may not be strictly valid, but without more detailed microsite information it is not possible to discern which of the two acclimation temperatures is more suitable to use in the arguments developed below. In addition, although the absolute values of 10 and 15 ^{0}C are used in subsequent arguments, it is possible that these absolute values are not appropriate. The shape of the temperature/photosynthesis curves of various species, and the relative differences between them, are, however, considered to be reliable (T. Brodribb, University of Tasmania, pers. comm.).

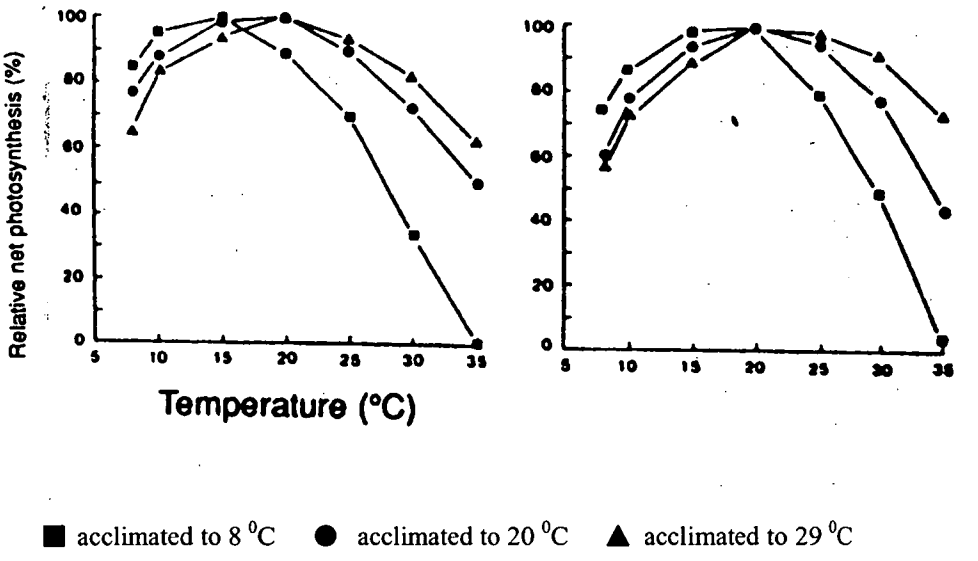

Figure 5.26: **The response of net photosynthesis to instantaneous temperatures in foliage acclimated to 8 °C, 20 °C, 29 °C. (a) *P. aspleniifolius* (700 m ASL), (b) *L. franklinii* (980 m ASL). Source: Read and Busby (1990)**

While regional index series can provide a general picture of the association between deviations from the regional mean and ring widths over time, the use of standard normal deviates prohibits their use for the examination of processes dependent on absolute temperatures. Figures 5.27–5.30 depict approximations of site temperatures. In each case, a nearby temperature station has been adjusted by the dry adiabatic lapse rate (DALR) to the approximate mean elevation maximum temperature of the sites in that region. When examining the change of maximum temperature with elevation, the DALR is the appropriate lapse rate to use for Tasmanian conditions (Nunez 1988). Using 15 °C and 10 °C, respectively, as the upper and lower thresholds for temperature-induced stress for photosynthesis, it is apparent that high temperatures over the summer period have the potential to limit woody growth of the following season (Figures 5.27–5.30) through the late season leaf abscission. The more common occurrence of temperatures above 15°C at lower elevations should result in these trees being more often high-temperature inhibited than those at higher elevations.

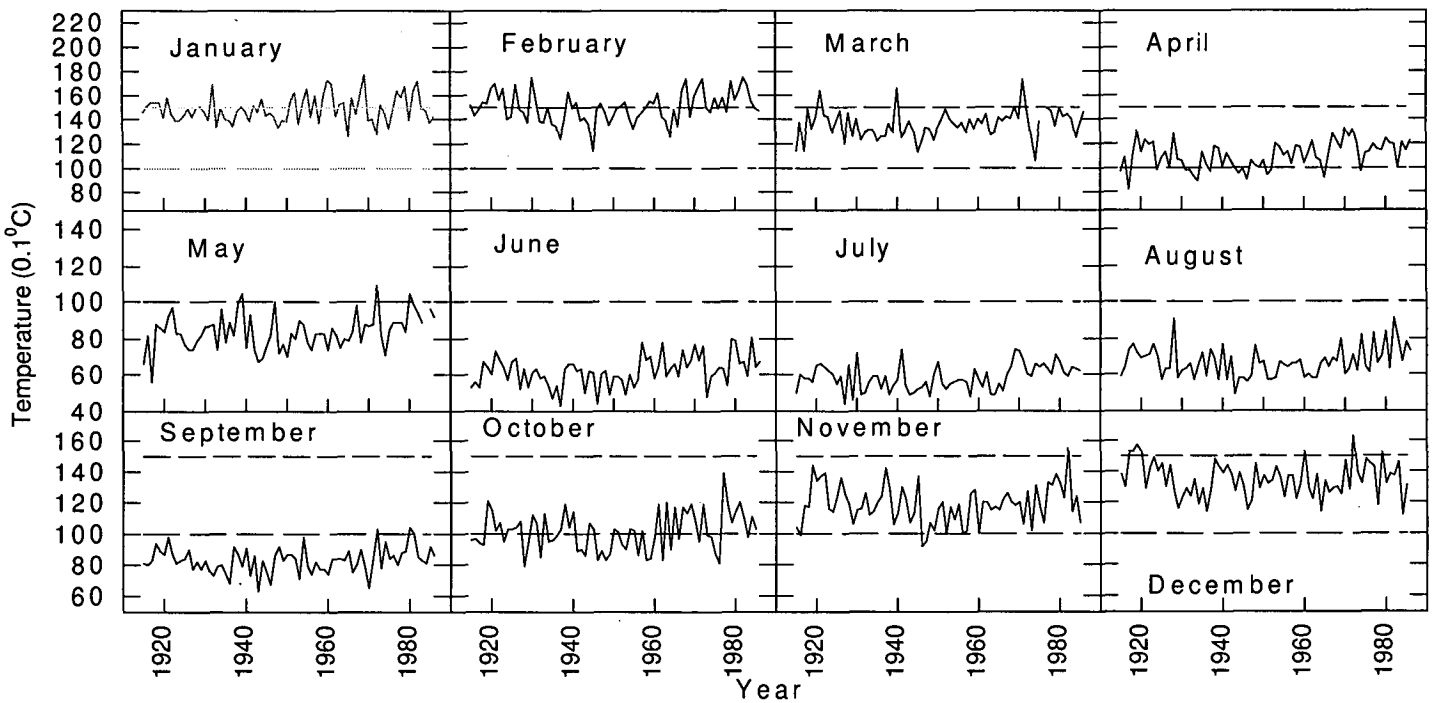

Figure 5.27: St Helens (92033) maximum temperature adjusted by the DALR to 750 m ASL. 10 ^{0}C–15 ^{0}C range is marked. Period of record is 1910–1994

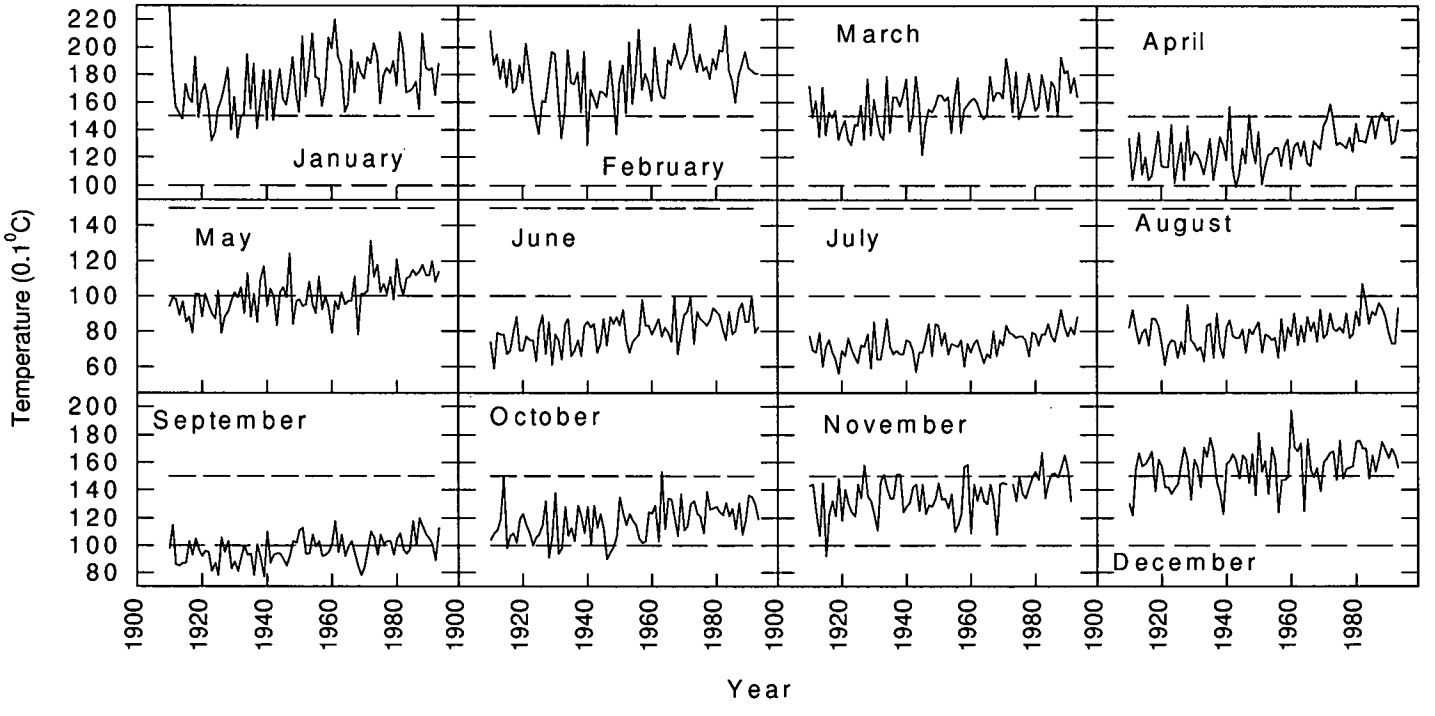

Figure 5.28: Waratah/Erriba (97014/91119) maximum temperature unadjusted. 10 ^{0}C–15 ^{0}C range is marked. Period of record is 1915–1994

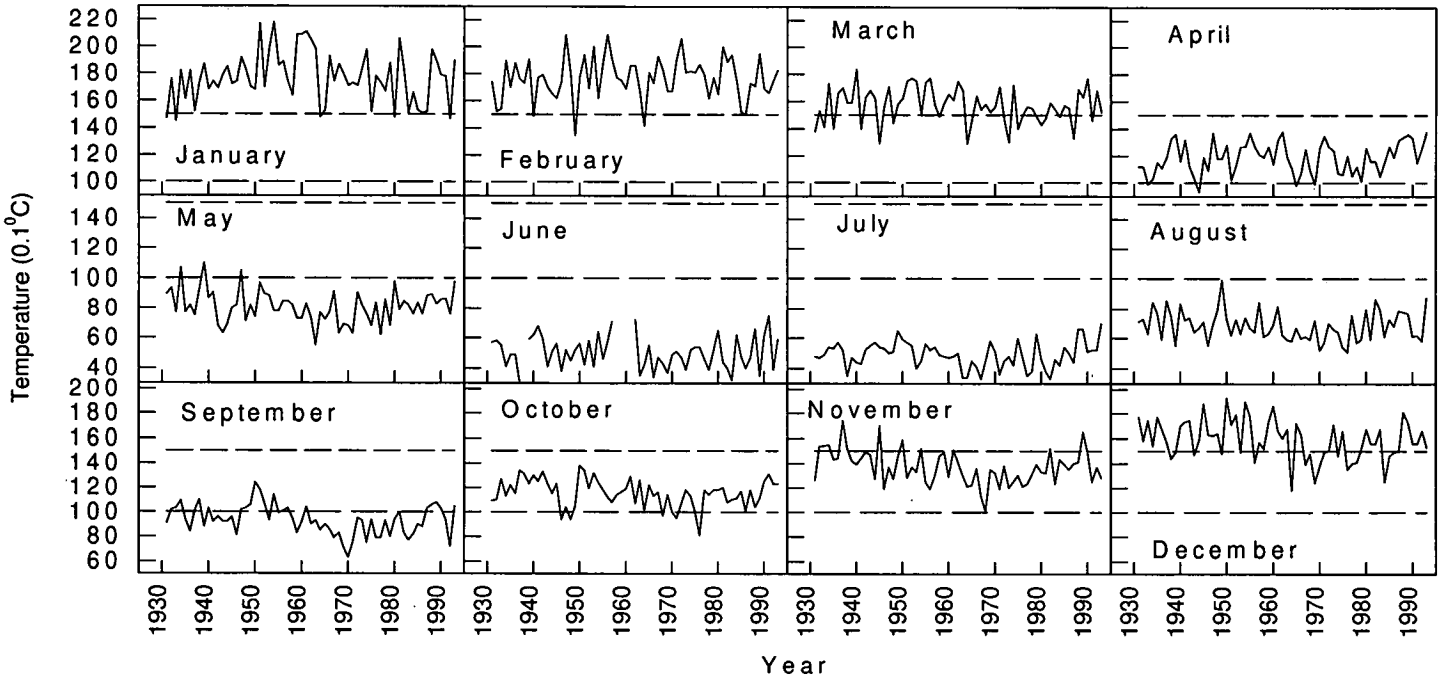

Figure 5.29: **Bushy Park (95003) maximum temperature adjusted by the DALR to 630 m ASL. 10 ^{0}C–15 ^{0}C range is marked. Period of record is 1933–1994**

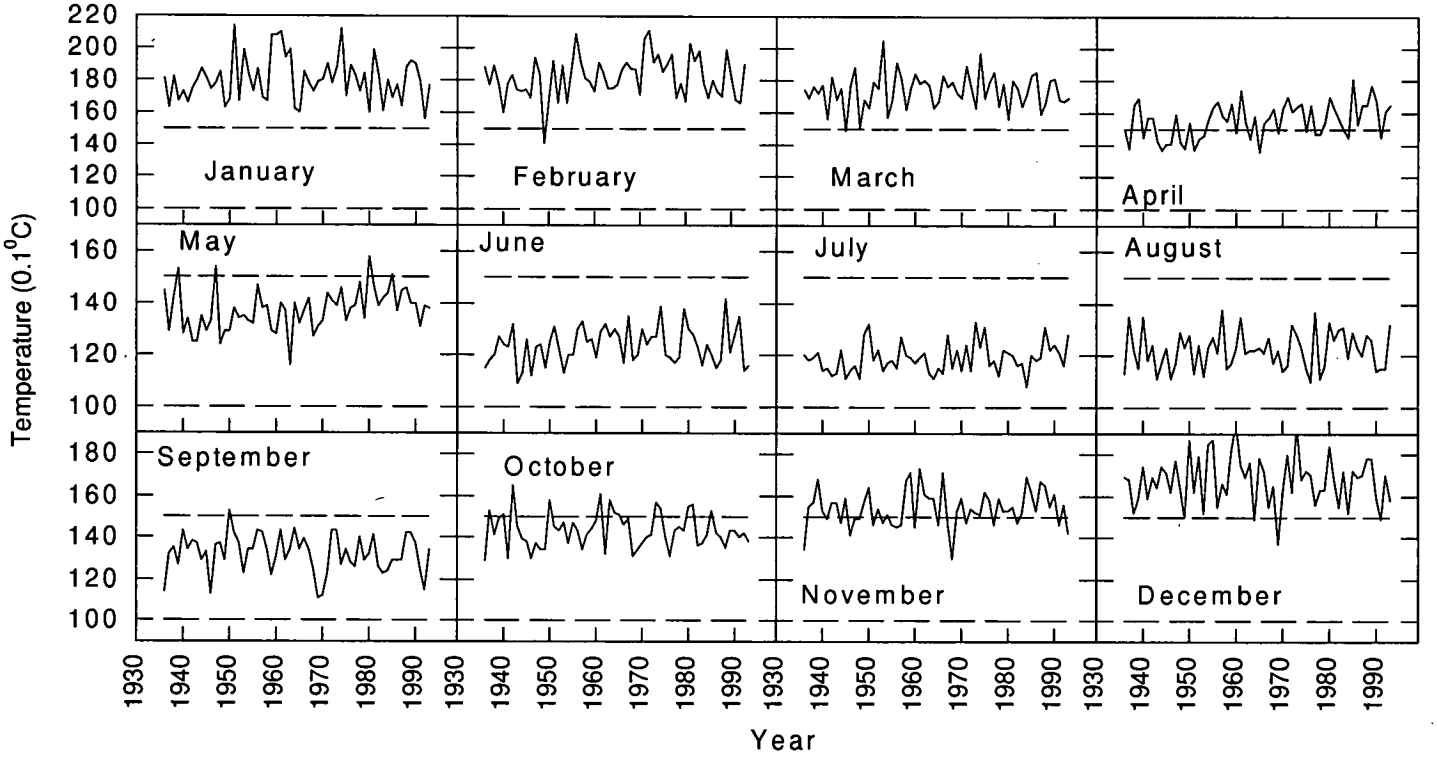

Figure 5.30: Maatsuyker (94041) maximum temperature adjusted by the DALR to 30 m ASL. 10 ^{0}C–15 ^{0}C range is marked. Period of record is 1934–1994

In contrast, any growth occurring in the months of June and July will be inhibited by low temperatures (Figures 5.27–5.30). It is known that the carbon balance of many temperate zone conifers is to some extent dependent on dormant season photosynthesis (Kramer and Kozlowski 1979, D'Arrigo and Jacoby 1993, Periera 1994). A winter response to temperature for these months is significant only for the Southwest and $PILL_M$, although approaching significance for other regions (Figures 5.4–5.7). The greater significance of the winter temperature response in the Southwest is therefore likely to be a reflection of generally lower mean, minimum and maximum temperatures for this region compared to the north and east of the State (Bureau of Meteorology 1993). $PILL_M$, at a relatively high elevation in the central region of the State, is similarly likely to experience lower temperatures than other sites in the north.

Table 5.10 divides the calendar year into three periods for the meteorological stations shown in Figures 5.27–5.30: that in which low temperatures are indicated to be limiting, that in which high temperatures are limiting, and that part of the year when temperatures fall roughly between 10 and 15 ^{0}C. Assuming an optimal temperature for photosynthesis at approximately 15 ^{0}C, the winter response (although not significant across all sites) of *Phyllocladus aspleniifolius* in the current year, as opposed to a response later in the warm season makes sense, particularly for the West and Southwest (Figures 5.4–5.7). Those sites at higher elevations (namely those in the East and $PILL_M$) show an extension of the interval of high correlation into the warmer months. The fact that temperatures at higher elevations remain below the high-temperature threshold into the later spring months may explain this feature.

If the photosynthesis hypothesis does describe what is occurring, these results serve to indicate that threshold effects may be important for *Phyllocladus aspleniifolius*. This has important implications for climate reconstruction.

The above argument can be extended to *Lagarostrobos franklinii*. The optimal temperature for photosynthesis of this species according to Read and Busby (1990) is 20 ^{0}C, associated with a range of 15–20 ^{0}C (assuming an acclimation of 8 ^{0}C) in which photosynthesis is less limited than by temperatures

Meteorological Station	*Low temperature inhibition*	*High temperature inhibition*	*No inhibition*
St. Helens	May–Sep	Jan, Feb	Mar, Apr, Nov, Dec
Waratah/Erriba	April–Aug/Sep	Dec–Mar	Oct, Nov, Apr
Bushy Park	Jun, Jul	Dec–Mar	Apr, May, Aug–Nov
Maatsuyker	-	Nov–Apr	May–Oct

Table 5.10: **Estimated site temperatures, using specific stations adjusted by DALR. Low temperature inhibition, temperature less than 10 ^{0}C; high temperature inhibition, temperature greater than 15 ^{0}C. St Helens data have been adjusted for 750 m ASL, the approximate elevation of both the BEN_E and BLT_E sites, Waratah/Erriba has not been adjusted - both stations are close to 600 m ASL, Bushy Park has been adjusted to 600 m ASL, and Maatsuyker Island adjusted to 20 m ASL**

outside this range. On the west coast, five of the seven *L. franklinii* sites occur at higher elevations than the three *Phyllocladus aspleniifolius* sites, and two at lower elevations. Figure 5.31 demonstrates, for this species, the more significant prior season response of Buckley's (1997) lower sites compared with the more significant current season response of higher sites. The sites at a higher elevation are unlikely to have assimilation rates reduced by high temperatures for long periods and therefore the prior season response, although present, is less likely to be statistically significant for these sites. Cambial growth for trees at these sites will be more limited by the availability of current photosynthate, and this is consistent with a dominantly positive response to current growing season temperatures (Kozlowski 1992). In contrast, it is likely that Buckley's two lower elevation sites, at 225 and 450 m ASL, would experience high temperature inhibition in warm summers and hence the greater negative significance of the prior growing season of these trees. Additionally, because *L. franklinii* has a higher optimal temperature for photosynthesis than *P. aspleniifolius*, it is logical that its growing season should begin later (November–April in Cook *et al.* 1991; January–April for high elevation sites in Buckley 1997) than that of *P. aspleniifolius.*

In an average summer on the West coast, maximum summer temperatures are approximately 16–18 ^{0}C at 600–650 m ASL (Bureau of Meteorology 1993). At these temperatures, *Lagarostrobos franklinii* sites are unlikely to be temperature-inhibited, while *Phyllocladus aspleniifolius* at the same elevation will

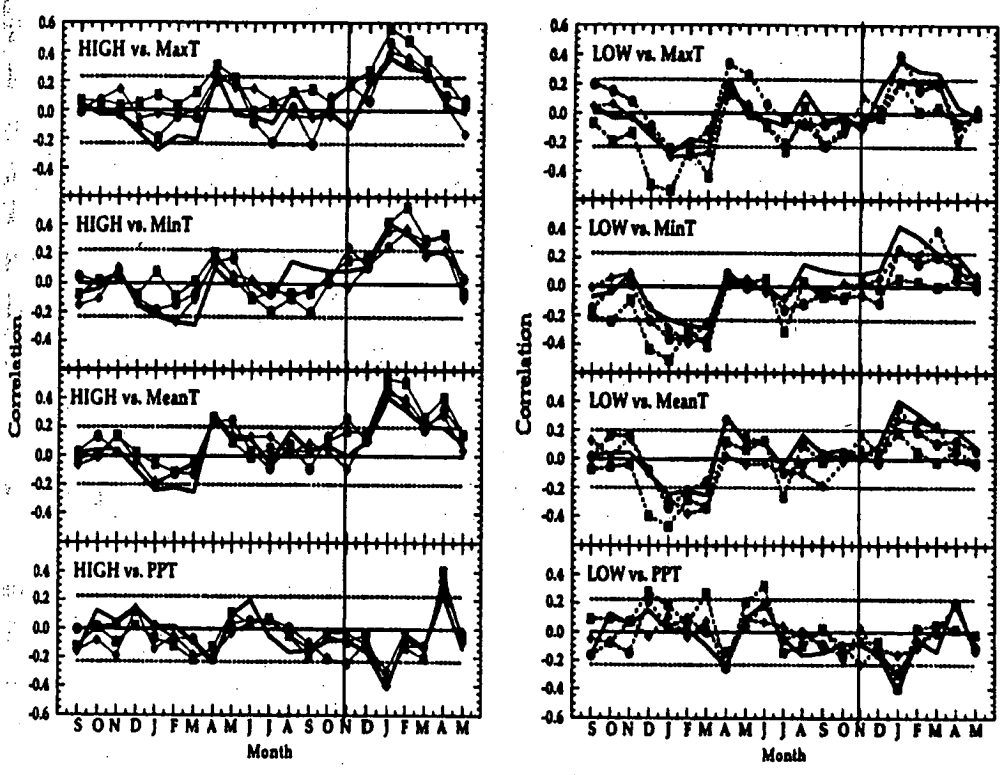

Figure 5.31: **Correlation of all seven *Lagarostrobos franklinii* chronologies with the Buckley temperature series (Buckley *et al.* 1997). MaxT is mean monthly maximum temperature, MinT mean monthly minimum temperature, MeanT mean monthly temperature (average of maximum and minimum temperature) and PPT, precipitation. A difference in the response of the high and low elevation sites is clear. Those sites above 700 m ASL (HIGH) have a distinct positive response to the current growing season whereas the lower sites (LOW) show a strong negative relationship with temperature of the prior growing season. HIGH sites are: LJH 950–1000 m ASL, BCH 800–900 m ASL, LML 700 m ASL, LMH 850 m ASL: and LOW sites are LML 700 m ASL, LVH 600 m ASL, HAR 450 m ASL, SRT 225 m ASL. LML, at 700 m ASL, has been included in both HIGH and LOW subgroups**

be. This may partly explain poor crossdating between the two species and, in particular, the sustained difference between the HIGH *L. franklinii* and the *P. aspleniifolius* stands at the turn of the twentieth century (Figure 3.26). It may also partially explain the difference at this time between the HIGH and LOW *L. franklinii* chronologies. According to the temperature/photosynthesis argument, the slightly above average growth of *P. aspleniifolius* and LOW *L. franklinii* at

this time can be explained by a greater available photosynthetic area. This is more likely to follow cooler than average summers at lower elevations. At the same time, the dramatically different record of the nearby, but higher elevation, *L. franklinii* is also consistent with cool summers that will be more restrictive to growth that is already limited by low temperatures (see Buckley 1997).

Although the hypothesis that the reduction of assimilation results in poor cambial growth in the following season would appear reasonable when examining the whole period for which instrumental records are available, other contenders for the explanation of the negative prior season response to temperature cannot be discounted. The umbrella hypothesis relating to competition by different parts of the tree for available resources remains an important hypothesis. The two hypotheses are not necessarily mutually exclusive as the photosynthesis argument outlined above makes the gross assumption that only maximum temperature is relevant, whereas the first hypothesis does not explicitly make this assumption.

5.4.2 Temporal Variation

Large differences between models calibrated on 'early' and 'late' period climatic data have previously been noted by a number of authors. Buckley (University of Tasmania, pers. comm.) has found differences between calibrated models for the early and late periods (1887–1939 and 1940–1990) based on mean monthly temperatures. These differences, however, are not significantly injurious to climate modelling, and temperature reconstructions have been performed successfully. In New Zealand, Palmer (1989) has been unable to successfully verify response functions, and has noted that while the response to temperature is similar over both time periods (1888–1931 and 1932–1974), precipitation response is not time stable. Norton *et al.* (1989) have also found large differences between sub-periods (1853–1915 and 1916–1979), along with Salinger *et al.* (1994) who have used the sub-periods 1863–1920 and 1921–1976 as early and late calibration periods, respectively. Both Norton *et al.* (1989) and Salinger *et al.* (1994) have found a higher proportion of variance explained by the calibrated

model based on the earlier period, and have detected considerable differences between the calibration and verification periods. Therefore, due to concerns of potential artificial predictability, only models calibrated on the later period have been used by Salinger *et al.* to reconstruct climate.

In the Northern Hemisphere, Briffa *et al.* (1998) have commented on increasing insensitivity over time of wood density, as well as ring width, to temperature changes occurring at high latitudes. As they pointed out, reconstructions based on these parameters for species or locations where such changes have occurred may well overestimate past temperatures unless this feature is accounted for.

With this in mind, it is therefore important to give some consideration to possible causes of changes in response functions found in this study. A number of possible explanations exist for the failure of *Phyllocladus aspleniifolius* response functions (based on either an early or a late calibration period). Each of these is considered in turn.

Outliers

Buckley (1997) has found that the omission of two outliers, the ring widths of the years 1899 and 1909, improved the resultant reconstructions. With regard to outliers in the maximum temperature data of this study, those values exceeding $\pm 2\ \sigma$ in the index series are 1987(+) for west coast winter maximum temperatures, 1983, 1985(-) east coast autumn temperatures, and 1983(+) spring maximum temperatures. None of these values exceed $\pm 3\sigma$ (Figures 4.4–4.6). In addition, two response models have been estimated for the whole period, based on maximum temperature. One of these is for BLT_E, and the other for MUR_W (Appendix 2). The model for MUR_W reveals no outliers, while for BLT_E an outlier is evident in the year 1983 (overprediction) only. Although the removal of these years can be expected to lead to better statistical results, it is unlikely that this procedure would lead to major changes in the models. This possibility can therefore be ruled out as the major cause of changes in the climate–growth relationship.

The no-analogue situation

Average monthly maximum temperatures for the late winter and spring months in the Southwest have fallen and then risen again (Figures 4.6 and 5.33). The fall in temperatures may explain the expanded response window for sites in this region, especially for SPR_S which is likely to be more closely linked to photosynthesis than other sites (Duncan *et al.* 1990). The simple grouping of data for the response function analysis into the two time periods, 1934–1962 and 1963–1992 (Southwest), may itself have promoted the result that cambial growth in the second time period was less low-temperature inhibited over the winter than in the first period. From Figure 5.29 it is apparent that winter temperatures decreased from the 1930s through to the early 1960s and then rose again to the 1990s. A similar argument can be mounted for other sites where temperatures fall throughout the early part of the record and then increase for the later period (these coinciding, in large part, with the periods used for calibration and verification). While this can be thought of as an example of the no-analogue situation, if the temperature response of the species were strictly linear, this situation would not arise. In addition, some preliminary results (not presented) again using multivariate linear regression after extraction of PCs, but with bootstrap estimation of variables (see Efron 1979, Guiot 1991), also failed to produce models which could be satisfactorily verified.

Climatic change and physiological processes

Examination of Figures 5.27–5.31 illustrates that in latter years temperature increases have occurred through the autumn, winter and spring months for these selected stations. Such increases may have had the effect of narrowing and 'shifting' the response window for northern sites. In contrast, late winter–spring–early summer temperatures in the Southwest appear to have decreased and, in view of this, the *broader* window of less significant correlations with maximum temperature is logical. However, the reason for reduced significance of these correlations is not clear. The fact that the coefficients of the independent variables (prior summer–autumn minimum temperatures, Figure 5.21) are non-constant is interesting in view of the fact that minimum

temperatures for the East and West in particular (Figure 5.24) have shown the largest increases for the summer–autumn months. The largest increases in maximum temperatures in the West also occur in the autumn months.

Although it must be stressed that increases in the regionally averaged maximum and minimum temperature indices are not statistically significant (Figure 5.24), the fact that broad-scale increases have occurred over the past century (Chapter 4) suggests that these more localised changes are in fact real, and can therefore be expected to influence plant growth in some way.

The greater consistency of correlations with temperature (except Mersey) for the earlier period implies a temperature regime more uniformly limiting to cambial growth across most of the State during that time. This is in agreement with data which show increasing temperatures in the second time period. It is also consistent with evidence of the KF traces. Figures 5.19–5.23 show that the negative relationship with temperature (maximum and minimum), and the positive relationship with the ZI for March of the prior growing season, has become less prominent over time for a number of sites.

A decrease in the consistency of temperature response between sites in the later period is suggestive of increasing relative importance of microsite factors. Given evidence provided by Torok and Nicholls (1996) and Plummer (1996), that minimum temperatures have risen at a greater rate than maximum temperatures, greater change in relationships between ring width and minimum temperatures (as opposed to maximum temperature) does seem reasonable. The reasons as to why the ESM_E shows a greater dependence on July maximum temperature are not apparent. The correlation between ring-widths and precipitation does not show a great deal of change in the site consistency over the two periods (Figures 5.12c–5.15c), but the KF traces suggest that the positive relationship has become less important over time, although the month for which change has occurred is not uniform across sites. This variable is not considered further.

Put in the context of the correlation functions (Figures 5.12–5.15) and the above evidence, the hypothesis that reduction in assimilation is the factor responsible for the negative relationship between maximum temperature of the prior season and cambial growth is not convincing. Plants which have been

previously inhibited by high temperatures/moisture stress at the end of the prior growing season can be expected to have become more limited over these months as temperatures have risen during the latter half of the twentieth century. The correlation functions of the two time periods do not suggest this, and neither do the calibration/verification statistics of Tables 5.3–5.6.

A consideration of the behaviour of *Lagarostrobos franklinii* does not make the matter any clearer. Although the photosynthesis hypothesis can be invoked to describe some of the differences between Buckley's HIGH and LOW sites, it does not explain other factors. For example, Buckley (University of Tasmania, pers. comm.) found fewer monthly variables to be significant in the response functions based on the second half of the twentieth century, indicating that conditions have become less limiting to growth over the latter part of the century. However, Buckley (1997) has also failed to find evidence of the dramatic post-1960 warming in trees at low elevation sites. This can be explained by the photosynthesis hypothesis: an increase in temperatures at these lower elevations is less likely to be evident as increased radial growth than at higher elevations as these lower elevation trees will have been operating closer to their optimal temperature conditions for photosynthesis (see Figure 5.26) prior to the observed temperature increases. Due to the parabolic nature of the relationship between temperature and photosynthesis, and hence woody growth, less gain in radial growth will be the result for a given increase in temperature at lower elevations. The only *Phyllocladus aspleniifolius* site which explicitly shows this feature, and retains it in the standardised version of the chronology, is SPR_S. The reason for this is unclear.

At the same time, evidence that higher elevation stands of *Lagarostrobos franklinii* exhibit increased growth since 1960, attributed to the observed post-1960s warming, while lower elevation stands do not, is also consistent with hypotheses relating to competition for resources. The phenomenon of increasing temperatures at high elevations where lower temperatures are more limiting to cambial growth can be expected to result in increased growth due to increased availability of carbohydrates, some of which may be allocated to cambial growth. At lower elevation where low temperatures are no longer the limiting factor to

growth, other factors consequently play more important roles in influencing the availability of carbohydrates than at higher elevation. Therefore, a statistical signal in ring widths, consistent with increasing temperatures, is less likely to be observed to the same degree in the time series of these low elevation sites than in the more temperature-limited higher elevation sites.

It is important to note, though, that those *L. franklinii* sites showing increased growth are responding more clearly to the current season, while those at lower elevation which do not show increased growth respond more significantly to the prior season (Figure 5.31). It is therefore possible that different mechanisms, other than those briefly discussed here, have produced the increased growth at Buckley's high elevation sites.

The preceding discussion is largely speculative and raises a number of issues that require further research, including a more detailed investigation of the species and its basic physiological characteristics, and more site-specific climate information such as cloud cover, solar radiation and moisture availability. The hypothesis put forward for the reduction of assimilation is a broad-brush concept only, and in the absence of detailed microsite information can not be tested. The umbrella hypothesis, relating to competition for carbohydrates between different parts and processes of the plant, appears to be more consistent with the evidence presented by the correlation functions based on the two separate time periods, but it also remains speculative.

Early climate reconstruction in Tasmania (e.g. Campbell 1980, LaMarche and Pittock 1982) has used multiple species networks where all species are combined in a single climatic reconstruction based on canonical regression analysis. Buckley (1997) has pointed out that different climate responses of different species render this approach somewhat questionable, and the discussions both here and by authors such as Read and Busby (1990) serve to highlight this point. The complication of a changing climate when precipitation has not necessarily fallen as temperatures have risen (Salinger and Jones 1996) increases uncertainties. This may in fact, be partially responsible for a substantial proportion of the 'noise' encountered in the response functions for *Phyllocladus aspleniifolius* based on early and late calibration periods. Climatic changes of this

nature will lead to different responses by different plant species depending on their physiological make-up, which is, by and large, genetically determined, although environmental influences may promote physiological plasticity.

The ability to utilise both high and low elevation sites of a single species in a study of climate may provide valuable complementary information to studies using only high elevation sites (e.g. LaMarche 1974a). Methods able to identify 'atypical' years where growth is high for one stand, but low for another (e.g. Dutilleul and Till 1989), may be particularly useful in this context. Beyond the use of a single species, it may, through an understanding of basic physiological processes, be possible to gain a more complete picture of the nature of changes in the environment by examining a number of species in parallel. In this manner, a multiple species network where responses are calculated for each individual species separately, but where these responses are then compared and further analysed after their computation, could prove exceedingly valuable to dendroclimatological investigations.

5.5 Summary and Conclusions

Despite wide differences in site conditions, reasonable coherence between sites in their response to temperature variables, the ZI, MI and SOI is apparent. The relationship of cambial growth with precipitation data is under considerable topographic control and, therefore, to use a regionally-constructed precipitation variable for climate construction would seem unsound. Correlation with the ZI, in particular, reinforces the integrity of the relationship with temperature indices. In order to satisfactorily assess the response of trees to moisture, highly localised information is probably necessary. The use of maximum and minimum temperatures as individual variables has shown that consistent differences do exist in their correlation with ring widths, and intimates that the correlation of each of these variables is important in cambial growth at different times. Further explanation of *how* these two variables might differentially affect plant processes obviously requires more detailed investigation in order to understand the mechanisms producing the statistical result.

The two hypotheses regarding the relatively strong prior season response to temperature (specifically maximum temperature) entertained here are by no means the only possible explanations. As numerous plant physiologists have pointed out, the lack of available moisture is the most likely direct link with photo-inhibition and reduction in assimilation, and the information collected in this study concerning moisture availability is not sufficiently accurate to explore this hypothesis more fully. Without additional detailed information concerning microclimatic conditions and physiological aspects of the species, it is not possible to affirm or reject either of the proposed hypotheses. A confirmation of the assimilation reduction hypothesis would acknowledge the importance of thresholds, and this in turn has the potential to enrich our understanding of the effects of climatic change on different species within various community complexes with differences in elevation, soil type, aspect, and topography. Work by Briffa *et al.* (1998) has alluded to the importance of thresholds, especially in a regime where climate is changing. The non-constant nature of the growth response to monthly temperature, as found by Briffa *et al.*, and in this study, presents a potentially serious obstacle to climate reconstruction. Although the only non-constant relationships between cambial growth and seasonalised data in this study occur between the ZI and ring widths, the fact that time-dependence exists in several monthly variables, in addition to seasonalised ZI, remains disturbing and requires further investigation.

It is also critical to note that the two above hypotheses have been raised on the premise of results produced by a statistical technique relying on a specific set of assumptions and, as stated, the assumption of constant regression coefficients is possibly inappropriate. Fundamentally then, it is not necessarily correct to claim that there is not a strong relationship between climate and the cambial growth of *Phyllocladus aspleniifolius* on the basis of these results. Rather, it is evident that the PC regression models of this chapter do not provide a good statistical explanation of cambial growth, as based on the climatic input. It may be the case that a more mathematically suitable model would show a clear relationship between input and output. Alternatively, it may be the case that the complexity of processes occurring between the time of 'information input' and 'ring-width

output' prohibit the finding of a relatively simple mathematical relationship of any form between the two. In terms of an easily 'extractable' growth response that can be used to generate a transfer function, it appears that *P. aspleniifolius* is an unsuitable climatic analogue. However, as Bryson (1985) reasons, the point at which something ceases to be a climatic analogue is really a statistical issue. With a greater understanding of plant processes and responses it may be possible to extend the envelope of climatic analogues in the dendrochronological arena to include a number of previously unsuitable species.

The implications of a non-constant temperature response are clear enough for climatic reconstruction. It automatically disqualifies the use of statistical and mathematical techniques which require constant coefficients. It also suggests that suppressed growth may be due to either high or low temperature inhibition. Without further independent evidence, it is not possible to discern which is the case. The only test used to examine seasonalised data, the KF test, has failed to show evidence of non-constancy in temperature data. On this basis, climatic reconstruction, based on seasonalised maximum temperature data, is tentatively considered in Chapter 7, whilst keeping in mind the non-constant response to temperature of individual months of the seasonalised period.

Chapter 6: The Quasibiennial Oscillation

6.1 Introduction

The presence of an approximate biennial oscillation in ring width in many specimens of *Phyllocladus aspleniifolius* is evident from a simple visual inspection (Figure 6.1). It is also apparent in the autospectra of *Phyllocladus aspleniifolius* chronologies in Chapter 3 which are dominated by frequencies in the 0.4–0.5 (2–2.5 year) range. Whether or not this oscillation is controlled primarily by biological factors, or whether it is a clear representation of a climatic variability, is an important issue to consider when attempting to reconstruct climate. It is important both in terms of the validity of removing it through autoregressive modelling as part of the 'biological noise', and also by enabling a better understanding of a climatic reconstruction such as that attempted in the next chapter.

Periodical phenomena have long been observed in plants. A commonly recognised periodicity is related to mast seedings where a large amount of fruit is set in a particular year, followed by a number of years with very little fruit set. The mast seeding phenomenon is well known in many species, including the Tasmanian endemics *Athrotaxis selaginoides, Athrotaxis cupressoides, Phyllocladus aspleniifolius* and *Lagarostrobos franklinii.* The period associated with mast seedings in these species is commonly 5–7 years (Shapcott 1991). Seeding cycles have been identified for some species by other workers including 3–5 years and 10–15 years (Monselise and Goldschmidt 1982, Kozlowski 1992, Woodward *et al.* 1994).

Many plant species, particularly those used in horticultural production, are known to exhibit approximate biennial seeding/fruiting cycles. They include numerous varieties of *Malus domestica* (apples), *Olea europaea* (olives), *Carya illinoensis* (pecan nuts), *Pistacia vera* (Middle East Pistachio nuts), some varieties of *Citrus sinensis* (oranges) and *Citrus limon* (lemons), *Persea americana* (avocado) and *Mangifera* (mango). A biennial fruiting cycle does not imply a strict adherence to a two-year cycle, and some 'on-years' will produce heavier crops than other 'on-years' (Monselise and Goldschmidt 1982). In the case of

Figure 6.1: **The biennial oscillation in ring widths; sample from BLT_E**

Phyllocladus aspleniifolius, a moderate seedfall year is frequently followed by a heavy seedfall year (Read 1989). The channelling of resources to reproductive organs at the expense of cambial growth in years of heavy fruit/seed set will impact upon other processes, and this impact will vary between different species (Kozlowski 1992). In an investigation based largely on 28 years of data for *Pseudotsuga menziesii,* Eis *et al.* (1965) found a distinct inverse relationship between cambial increment and cone production. They found this inverse relationship in the *current* growing season, suggesting that only current photosynthesis was relevant and that the storage of carbohydrates in anticipation of a heavy crop did not occur. However, it was suggested that a negative relationship between cambial increment of the current season and cone production of the *prior* season may exist if flower bud initiation occurs in the prior season (Eis *et al.* 1965). Elaborating upon this, Woodward *et al.* (1994) described the mechanism through which reproductive growth might occur at the cost of cambial growth in *Abies lasiocarpa.* Their argument was: because cones are strong carbohydrate and nitrogen sinks, and because buds differentiate in place of vegetative growth, cone production competes with cambial growth, and that the physical position of the cones is important. For *P. aspleniifolius* this argument implies that the negative relationship between prior season temperatures and cambial growth in *P. aspleniifolius* is in fact due to heavy reproductive commitment on an approximate 2-year cyclical basis. The authors did however, state the importance of both exogenous events such as climate and endogenous variables such as nutrient and hormone levels. These endogenous variables will be influenced by the history of growth and reproduction in response to climate.

Following on from this, Monselise and Goldschmidt (1982) have suggested that biennial fruit production requires an initial climatic trigger. To support their argument, Monselise and Goldschmidt (1982) cited evidence of co-ordination between fruit groves within a climatic district. In addition, Eis *et al.* (1965) reported the same result for many forest species, again implying climate to be an important factor. Woodward *et al.* (1994) found explicit relationships between climate and cone crops in *Abies lasiocarpa* and *Tsuga mertensiana*, the relationship being stronger in *A. lasiocarpa* indicating that species differences are important. However, Buszard and Schwabe (1995) have asserted that the fruiting

cycle itself is generally attributed to hormonal factors within the individual. This does not necessarily conflict with the findings by Eis *et al* (1965), Woodward *et al.* (1994) and Monselise and Goldschmidt (1982) because although the cycle might be controlled hormonally, climate will be important in regulating the levels of these hormones.

At the same time, several authors have previously pointed to the autonomy not only of individuals of a single species, but also of individual branches of a single tree (Harlet *et al.* 1942, Morettini 1950, Davis 1957 in Monselise and Goldschmidt 1982), seemingly in conflict with a climatic trigger hypothesis. But Eis *et al.* (1965) extended their above observation to suggest that either a complex regulator or a concentration of carbohydrates at some critical time in certain parts of the tree may be responsible for this autonomy. They then explained that the concentration of such a substance need not be uniform within an individual, nor at the same level within all individuals of a stand.

Jackson and Hamer (1980) on the other hand, found that warmer weather during the 1950s and 1960s in England led to yield increases of *Malus domestica* (Cox's Orange Pippin). Attempts to intervene and alter annual variability in yield did not succeed, and this have been be indicative of a strong climatic control on plant processes. It has also been found that some plants become biennial bearers under certain climatic conditions. Valencia oranges do not display biennial bearing behaviour in Spain, but in semi-arid Australia are known to be biennial producers (Monselise and Goldschmidt 1982).

The literature therefore appears to suggest that both macro- and microclimatic factors as well as hormonal controls are important in the determination of fruiting behaviour of the species concerned. Differences between species are also important.

Atmospheric quasibiennial oscillations (QBOs) have also been widely discussed in the climatological literature for several decades (e.g. Brier 1978, Trenberth 1975, 1980, 1981, Lau and Sheu 1988, van Loon and Labitzke 1988, Ropelewski *et al.* 1992, Jury *et al.* 1994, Goswami 1995, Kodera 1995), and represent one element in the myriad of cyclical climatic phenomena identified by many workers. These QBOs have been identified in sea surface temperatures, sea level pressure, temperature and precipitation, solar radiation and solar activity,

streamflow variability, variation of tropospheric ozone, zonal winds and snow patterns. Although interrelationships between different QBOs are believed to exist, evidence suggests a number of them to be unrelated (Trenberth 1980, Goswami 1995). Several workers have drawn links between QBOs, ENSO phenomena and the sunspot cycle, showing a QBO to be an integral part of ENSO phenomena (Nicholls 1992, Shepherd 1995), and the occurrence of El Niño events to be nonstationary over time with differing return times in periods of high and low solar activity (van Loon and Labitzke 1988, Enfield and Cid 1991, Ropelewski *et al.* 1992, Shiotani and Hasebe 1994, Goswami 1995). Low frequency variations in the strength and periodicity of El Niño events over time have been recorded (Quinn and Neal 1992, Anderson 1992, Enfield and Cid 1991), and similar variations have been found in atmospheric QBOs (Trenberth 1975, 1980, Lau and Sheu 1988). As outlined in Chapter 4, and also by several of the above authors, most of the variance associated with the SO lies in the 2–10 year band. Approximate two-year periodicities have been found in Tasmanian instrumental precipitation records (Allen 1991, Drosdowsky 1993, Shepherd 1995). Shepherd (1995) has found such an oscillation to exist in west coast data, and Allen (1991) has found evidence of a two-year spectral peak in precipitation across the State for all seasons. Approximate two- to three-year periodicities are seen in the spectra of temperature and precipitation for the West and Southwest indices in this study (Chapter 4). The significant negative correlation between temperature and precipitation over time (Chapter 4), implies that a QBO seen in precipitation data should also be reflected in temperature data. Periodicities of just under two years in temperature data are observed for all regions, and West and Southwest precipitation data show periodicities just over two years. Spectral analysis of the monthly ZI has not shown any significant periodicity in the QBO range.

The existence of atmospheric QBOs intensifies interest in the issue of whether or not approximate biennial oscillations in ring widths of dendrochronologically useful species are expressions of climatic oscillations. A handful of species used so far in dendrochronology exhibit such a bienniality in ring width. Norton *et al.* (1987) and Ahmed and Ogden (1985) have briefly discussed the tendency for alternating wide and narrow rings in the New Zealand

species *Agathis australis* and *Phyllocladus glaucus*. These oscillating ring-widths seemed to have been in synchrony between different sites (Ogden and West 1981), perhaps indicating a climatic stimulus.

As has been previously assumed for *Phyllocladus aspleniifolius,* this feature in the New Zealand species has been attributed either to two growth flushes per season (discounted by several studies — see Dunwiddie 1979, Ogden and West 1981, Palmer 1989 among others), or to a biennial flowering cycle. A more conservative opinion supports the hypothesis that a bienniality in ring widths is primarily caused by biennial fruiting of the species. Evidence discussed above suggests that while this may well be the case, the influence of climate is also important.

Many biological processes are dependent on climatic conditions. As far as *Phyllocladus aspleniifolius* is concerned, seedfall is initiated by changing moisture conditions coinciding with maximum leaf abscission (Barker 1993) and maximum leaf abscission occurs at times of leaf moisture stress at the end of summer (Kozlowski 1979). Furthermore, Nobori *et al.* (1995) have reported synchronous mast seeding of *Fagus crenata* for sites in northeast Japan. In these mast years, low ring widths have occurred either simultaneously with strong El Niño events, or the year prior to a strong El Niño event. Barker (1993.) intimated a similar coincidence of mast seedings and El Niño events in *P. aspleniifolius.*.

Conversely, Barker (1993) has also pointed to some evidence suggesting nonsynchronous heavy seedfall years for *Phyllocladus aspleniifolius* across the State. It is plausible that such nonsynchronous behaviour may be expressive of different climatic conditions across the State, although it is also possible that such nonsynchronous behaviour reflects a process under strong biological control. Good crossdating between different regions of the State for most periods (Chapter 3) implies that either seeding/fruiting does not impact sufficiently upon ring width variations to cause a problem (i.e. that the ring width oscillation is unconnected to seeding cycles); or, if the quasibiennial oscillation in ring widths (QBORW) is related to a seeding 'cycle', there is sufficient synchrony across the State to allow crossdating over most periods.

There are two basic questions of interest in connection with the issue of the QBORW. The first of these is whether or not the oscillation in ring width is

related directly to the biennial seed production noted by Read (1989). An oscillation related to seed production behaviour of the species is readily explainable by the tree diverting large amounts of resources away from wood production and into reproductive organs in a year of high seed production, thus producing a narrow ring (Eis *et al.* 1965, Cannell and Dewar 1994). The second question relates to whether or not (regardless of whether it is caused by alternate years of moderate and heavy seedfall) the ring width oscillation is representative of climatic conditions. These issues are not necessarily independent of one another.

Of the studies quoted above several examine the link between ring-width and fruiting, and several investigate the relationship between biennial oscillations in the amount of fruit set and climatic triggers. Eis *et al* (1965) and Woodward *et al.* (1994) both attempt to establish a link between climate and biennial oscillations in ring-width. Although mechanisms have been suggested by these authors for the chain of causality between climate, fruit set and ring width, they remain largely hypothetical at this stage.

The intention of this chapter is to ascertain through statistical analyses whether or not the clearly observable biennial oscillation in ring widths of this species is significantly associated with climate. It is not the intention of this chapter to examine whether or not the oscillation in ring width is directly related to oscillating seed production. Indeed, strictly statistical methods are unable to answer this question without physiological research.

6.2 Methodology

6.2.1 Cross spectral analysis

A climatically expressive QBORW in *Phyllocladus asplenifolius* should theoretically result in strong spectral coherencies between climatic data and ring width series at the 2–3 year periodicity in the frequency domain. The regional seasonalised climate indices (temperature and precipitation) constructed in Chapter 5, seasonalised SOI and the ZI were used in MTM cross spectral analyses with ring width. The SOI and ZI were both seasonalised over those months indicated as the growing season by maximum temperature data. In addition, the

SOI and ZI were seasonalised over consecutive months outside the growing season in which significant correlations were recorded between them and ring width indices (Figures 5.8–5.11). These data were seasonalised in the same manner as described in Chapter 5, namely by averaging across the relevant months. Table 6.1 reports those months for which data were seasonalised for each variable across the three regions.

	Maximum temperature	*Minimum temperature*	*Precipitation*	*SOI*	*ZI*
East	Dec–Apr	Dec–Apr	Jan–Mar	Dec–Apr	Dec–Apr
				Nov–Jan	Jul–Aug
West	Nov–Mar	Nov–Mar	Dec–Jan	Nov–Mar	Nov–Mar
				Sep–Jan	Jul–Aug
Southwest	Nov–Jan	Nov–Jan	Nov–Jan	Nov–Jan	Nov–Jan
				Sep–Nov	

Table 6.1: **Climatic variables used in cross spectral analyses. Temperatures have been seasonalised as in Chapter 5, and seasonalisation of the SOI and ZI also proceeded over these months by averaging. SOI and ZI were also averaged for additional months where significant correlation with ring width indices have been noted in Chapter 5**

Prior to calculation of MTM cross spectra between these seasonalised variables and ring width indices, individual MTM spectra, using three tapers with time- frequency bandwidth products of two for each of the seasonalised variables, were calculated and are shown in Figures 6.2–6.4. It is clear that seasonalised temperature data for all regions displayed significant spectral peaks (at the 0.05 level) in the QBO range. Only precipitation for the West and Southwest showed significant spectral peaks in this range. ZI, seasonalised over the growing season, also has spectral peaks in the QBO range. ZI data seasonalised over the winter months expressed a significant peak at the Nyquist frequency only (Figure 6.3). For the seasonalised SOI, few peaks fell into the commonly quoted QBO range (Figure 6.4), with only September–January showing a significant peak at 2.3 years. Therefore, any coherencies found in the QBO band between the SOI and ring width indices (based on the data sets described here) will be likely to be statistical artifacts.

Periods analysed in cross spectral analyses were 1914–1994 for East and West temperature and precipitation data and Southwest precipitation, 1931–1994 for Southwest temperature, 1912–1994 for the ZI and 1876–1994 for the SOI. The three regional arstan chronologies constructed in Chapter 3 were used in the analysis. Because the series were relatively short (both Southwest temperature series consisted of only 63 points) and because it was felt that the higher resolution in the high frequency range of the spectrum was less important than a greater number of degrees of freedom and reduced bias, six tapers, each with a time-frequency bandwidth product of four, were used for all cross spectral analyses in this chapter. The shortness of the series suggests that caution in interpreting the results is warranted for all cases, most especially for the Southwest.

6.2.2 Use of the Evolutive spectra

The term 'evolutive spectrum' refers to the spectrum of a series through time — i.e. as the series, and hence its spectrum, 'evolves'. As such it functions as a moving window. Beginning at the start of the series under consideration, a discrete time interval of a fixed length (N) is analysed in the frequency domain. The analysis is then conducted on the next time interval which is shifted forward T time units so that the time intervals analysed overlap one another by N-T. This continues until the end of the series is reached.

Table 3.3 reported that all chronologies, with the exception of FC, were dominated by an AR(2) process. While entire series lengths were dominated by this process, an assessment of variation in the process over time was not provided. If the QBORW is strongly related to climate, its power would be expected to wax and wane through time, as it is known that atmospheric QBOs exhibit some

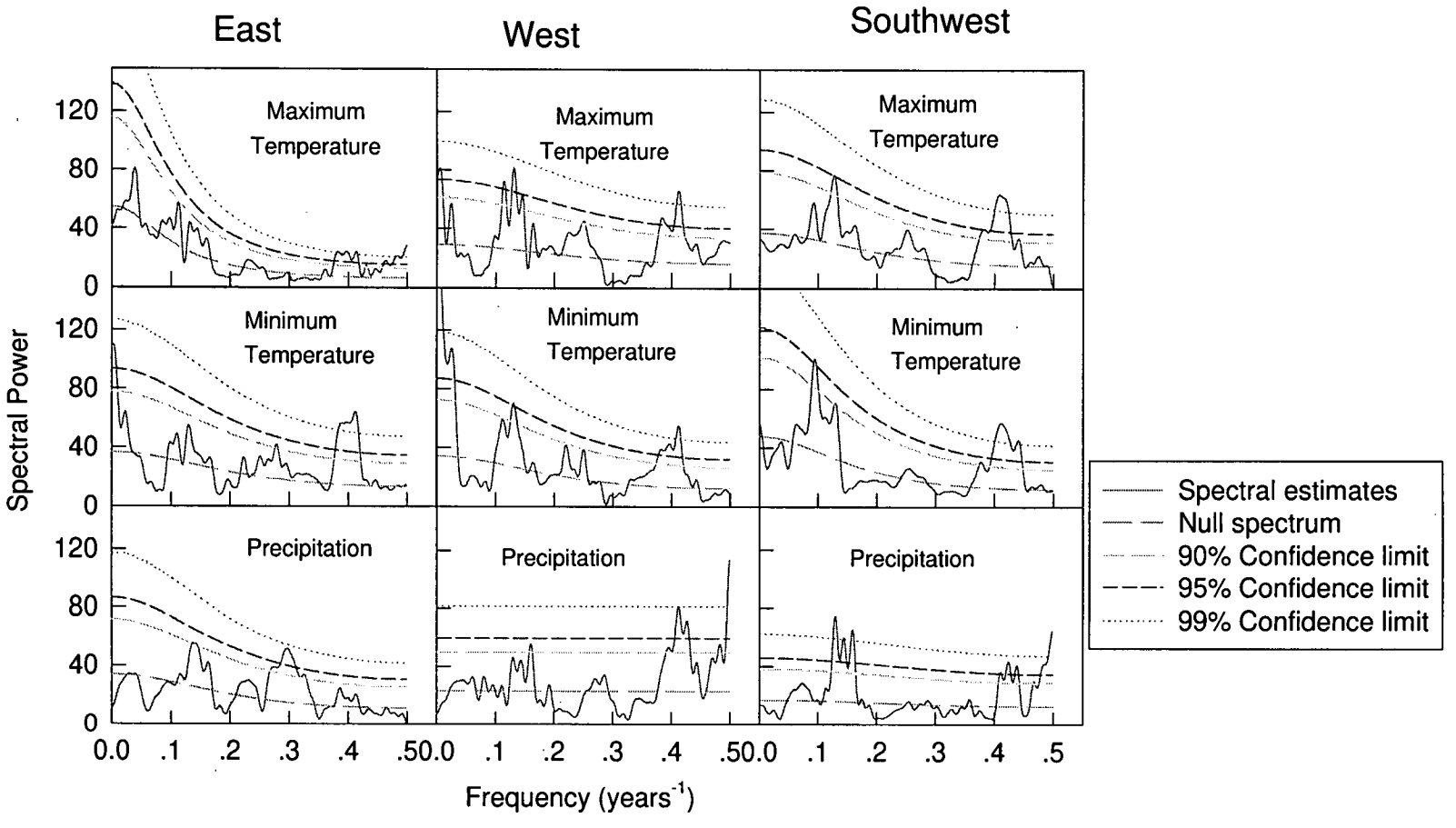
East
West
Southwest
Maximum Temperature
Minimum Temperature
Precipitation
Spectral Power
120
80
40
0
0.0
.1
.2
.3
.4
.5
Frequency (years-1)
Spectral estimates
Null spectrum
90% Confidence limit
95% Confidence limit
99% Confidence limit

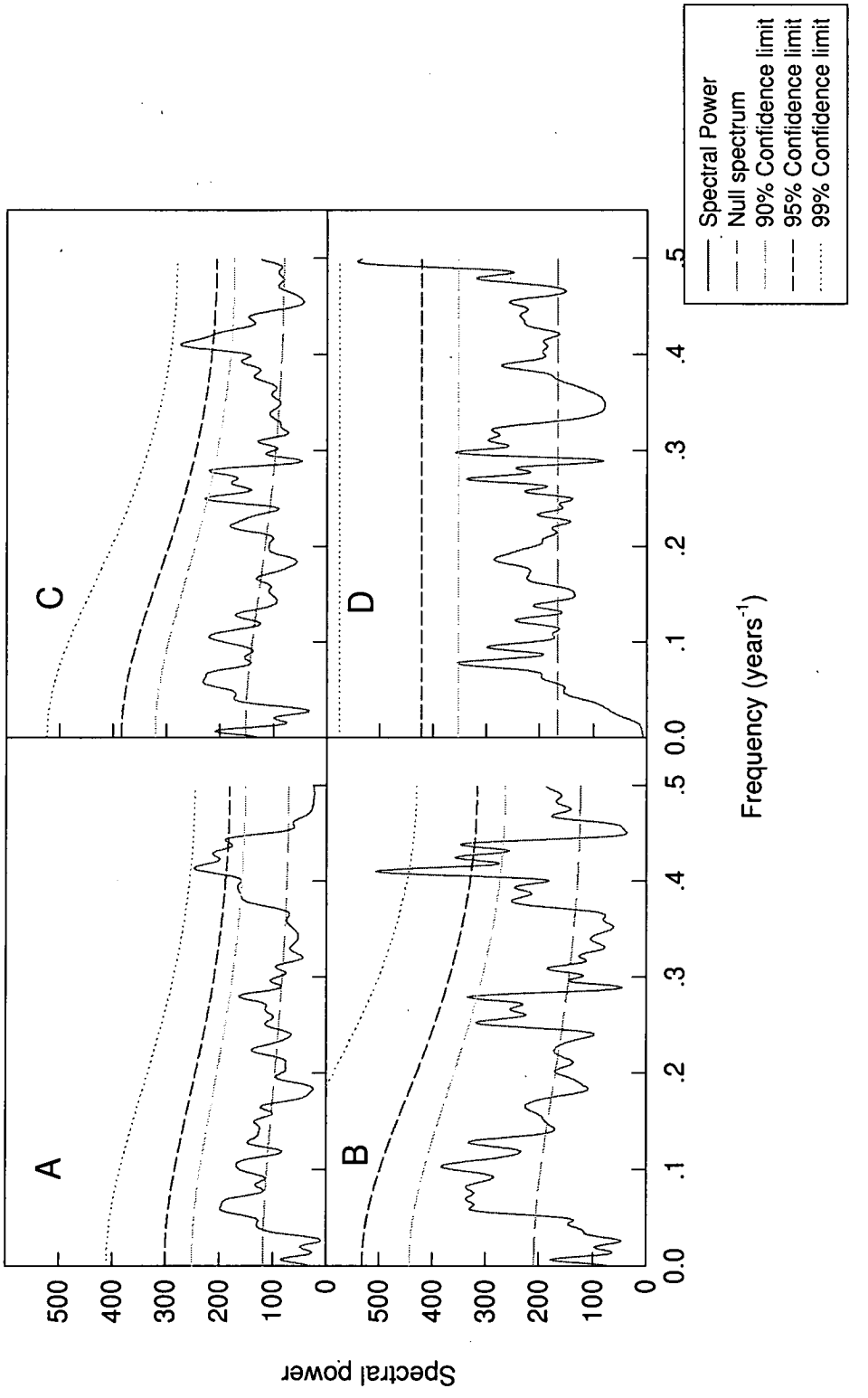
A
B
C
D
Spectral power
Frequency (years^{-1})
Spectral Power
Null spectrum
90% Confidence limit
95% Confidence limit
99% Confidence limit

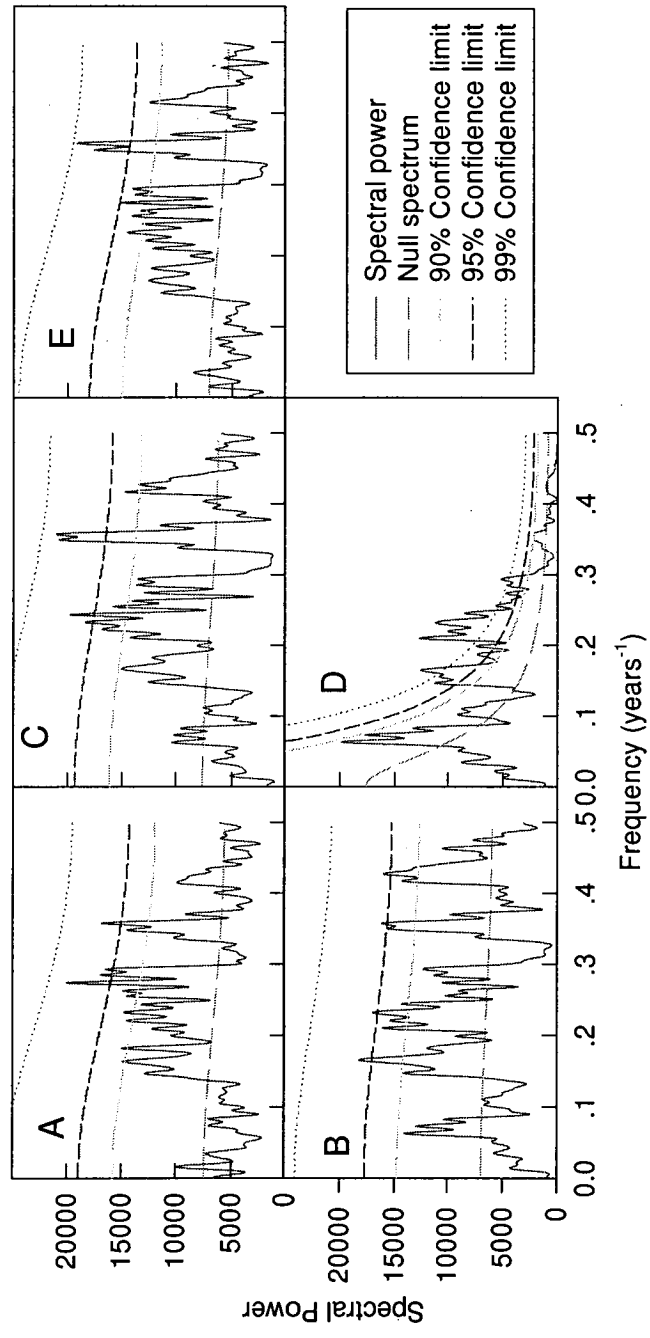
A
B
C
D
E
Spectral power
Null spectrum
90% Confidence limit
95% Confidence limit
99% Confidence limit
Spectral Power
Frequency (years^{-1})
0
5000
10000
15000
20000
0.0
.1
.2
.3
.4
.5

amplitude variation through time (e.g. Trenberth 1975, Lau and Sheu 1988, van Loon and Labitzke 1988, Ropelewski *et al.* 1992, Brádzil and Zolotokrylin 1995).

As for cross spectral analyses, the three regional chronologies developed in Chapter 3 were used. To track the high frequency components of the MTM spectra, 50 *(N)* year intervals overlapping the former by 10 *(T)* years were used. Six data tapers with time-frequency bandwidth products of four were applied to all series. Time periods analysed were 1300–1994 East, 1540–1994 West and 1550–1994 Southwest.

6.3 Results

6.3.1 Cross spectral analysis

Table 6.2 indicates those frequencies that provide significant coherencies between climate and ring width indices in the QBO band. A negative phase lag indicates that ring width lags climate, while a positive phase lag implies that climate lags ring width. The lack of confidence limits for phase estimates creates some problem with interpretation. The width of confidence intervals for the phase spectrum is linked to the strength of the coherence between variables. Confidence limits are likely to be wide rather than narrow given that most of the significant coherencies are not strong (E. Cook, Lamont-Doherty Geological Earth Observatory, pers. comm.). This means that no great weight can be placed upon the point estimates of phase shown in the Table 6.2. It must also be remembered that the shortness of the data sets cause some distortion. Therefore, although only negative phase lags make theoretical sense, coherencies with both positive and negative phase lags are provided below but no importance is attached to these reported phase lags.

The results obtained in Table 6.2 suggest that neither minimum temperature or precipitation are coherent with ring width in the QBO frequency range for all regions across the State. Maximum temperatures display a significant coherence with ring width in the QBO band for all regions. In each case, significant coherence occurs at 2.5–2.6 years, the coherence in excess of 0.6 for the East and West. Minimum temperatures are significantly coherent with ring width for East and West in the QBO band while precipitation is coherent in the

	Frequency (years $^{-1}$)	*Period (years)*	*Coherency*	*Phase (years)*
East				
Maximum temperature	0.3954	2.53	0.714	0.60
	0.4297	2.33	0.484	0.37
	0.4609	2.17	0.657	0.04
	0.4844	2.06	0.703	0.03
Minimum temperature	0.375	2.67	0.666	0.68
	0.3906	2.56	0.647	0.55
	0.4219	2.37	0.496	0.49
	0.4453	2.25	0.507	0.34
	0.4844	2.06	0.665	0.04
Precipitation	0.4375	2.29	0.492	0.94
SOI				
ZI	0.375	2.67	0.641	-0.74
	0.3906	2.56	0.673	-0.64
West				
Maximum temperature	0.3906	2.56	0.682	-0.07
Minimum temperature	0.4453	2.25	0.466	0.23
Precipitation				
SOI	0.4766	2.10	0.603	-0.30
	0.4766*	2.10	0.552	-0.05
ZI	0.3906	2.56		-0.42
	0.4062*	2.46	0.467	0.02
Southwest				
Maximum temperature	0.3906	2.56	0.477	0.44
	0.4375	2.29	0.595	0.37
Minimum temperature				
Precipitation	0.3516	2.84	0.456	
	0.4766	2.10	0.561	
SOI	0.3359	2.98	0.685	-0.21
	0.3359*	2.98	0.623	-0.21
ZI	0.4766	2.10	0.535	0.89
	0.3828*	2.61	0.491	-0.75
	0.3984*	2.51	0.493	-0.69

same spectral band for the East and Southwest. The SOI shows significant coherence with West and Southwest ring-widths at 2.1 and 2.98 years respectively, and periodicities of this order can be seen in the relevant seasonalised SOI data (Figure 6.4d & e). The coherence with the Southwest however, may be at a frequency too low to be considered consistent with other frequencies commonly referred to as being QBOs by other authors (cf. Holton and Lindzen 1972, Trenberth 1975, 1980, Lau and Sheu 1988, Jury *et al.* 1994).

Like maximum temperature, the ZI shows coherence in the QBO range for all regions. The periods at which coherency was found for the ZI were: 2.56 and 2.67 years (East), 2.56 years (West), and 2.61 and 2.51 years (Southwest). These periodicities are noticeably similar to those identified for coherence between ring widths and maximum temperature. The spectra of the seasonalised ZI (Figure 6.3) show peaks close to those frequencies at which ring widths and the ZI are reported to be significantly coherent. Significant periodicities apparent in tree ring index spectra (Chapter 3), range between 2 and 2.4 years. It is possible that some of the difference in the significant autospectral (ZI) and the coherence estimates may be attributable to differences in the resolution of the two analyses.

The point estimates of the negative phase lags for all these cases vary between 0.42 (approximately five months for the West) and 0.74 (approximately nine months for the East) years. In the case of maximum temperature, phase lags vary between -0.07 and 0.6 (approximately one and seven months respectively). It is important to note the *consistent* suggestion of coherence, for all regions, between ring widths and maximum temperature and the ZI at 2.5–2.7 years. These potentialities aside, the differences in the frequencies of significant coherence and those significant frequencies in autospectra of tree-ring chronologies may suggest that the QBORW phenomenon is not directly, or closely, associated with the atmospheric QBO expressed in the climatic data. This however, cannot, strictly, be determined here, and the importance of the different resolutions used for the two types of analyses is also unclear. In addition, the shorter time period available for the cross spectral analysis of the ZI and ring-widths may be a further cause for the above difference.

7.3.2 Evolutive Spectra

Figures 6.5–6.7 display the evolutive spectra for the three regional chronologies. Only those frequencies significant at the 0.05 level are shown. It is clear in all cases that significant frequencies in the QBORW range are present throughout the period covered by all chronologies. For West and Southwest chronologies, 'lower frequencies' in this range become less significant in the twentieth century, particularly so for the West. A further period from approximately 1740–1800 shows a similar phenomenon with insignificant power in the higher frequency end of the QBORW band in the Southwest. For these two chronologies, a noticeable expansion of significant frequencies in the QBORW bandwidth occurs from around 1800–1900, but then diminishes post-1940. In the East spectrum, frequencies in the QBORW range lose significance over the period 1400–1450. From about 1750 to the present day there is a broad response across the QBORW band in the East data contrasting with the West and especially the Southwest where those frequencies significant in the QBORW range become restricted to the 'higher frequencies'.

It is interesting to note the greater dominance by frequencies in the QBORW in the East over time as compared to the West and Southwest. The West spectrum shows considerably more 'lower frequency' significance particularly around 1670–1750 than either the Southwest or the East.

6.4 Discussion

The idea that inhibition of photosynthesis through water stress and high temperatures towards the end of the summer months is responsible for the negative relationship between the current year's growth and the prior year's temperature has been discussed in Chapter 5. Existence of the QBORW necessarily extends this hypothesis to imply that the QBORW itself is primarily a climatic expression of heat/water stress, regardless of whether or not the role of any seeding/fruiting 'cycle' is also important.

An alternative hypothesis briefly discussed in Chapter 5 suggested that the competition for resources by different plant processes is important in the determination of ring width. Therefore, a QBORW associated with alternate

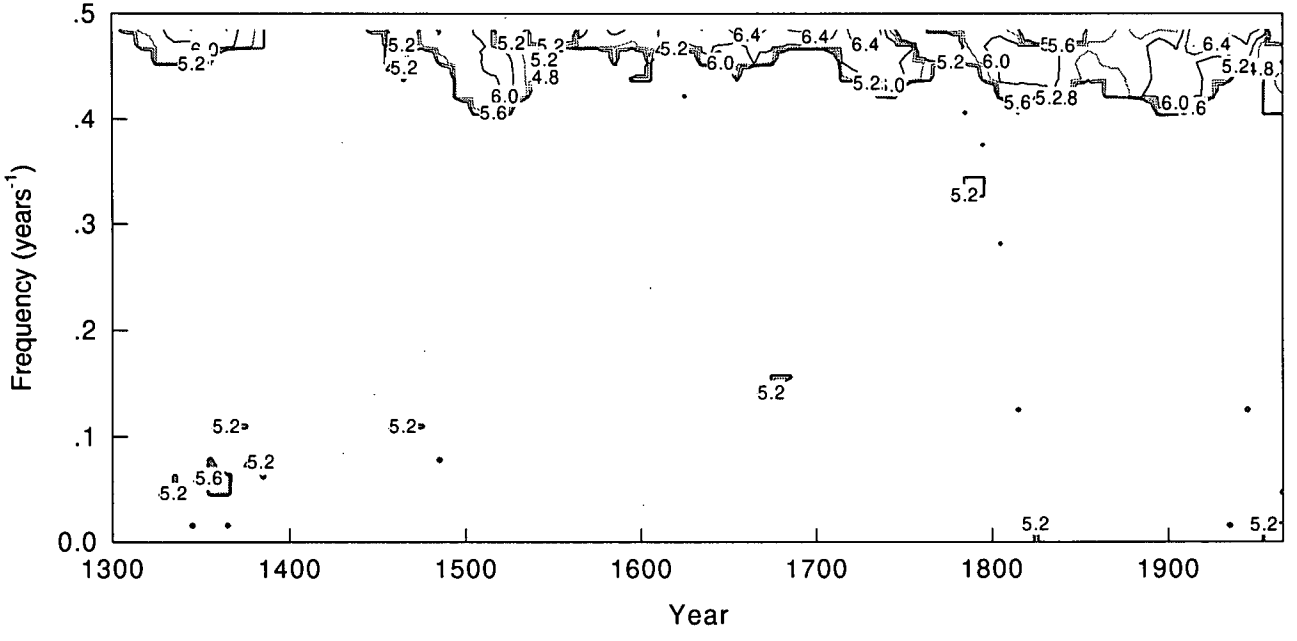

Figure 6.5: **Contour map of MTM evolutive spectrum for East regional chronology estimated with three data tapers with a time-frequency bandwidth product of four. Time span of analysis is 1300–1994. Only frequencies significant at 0.05 are shown. Contours indicate spectral power, and their range is 4.6 to 7.0. Contour interval is 0.4**

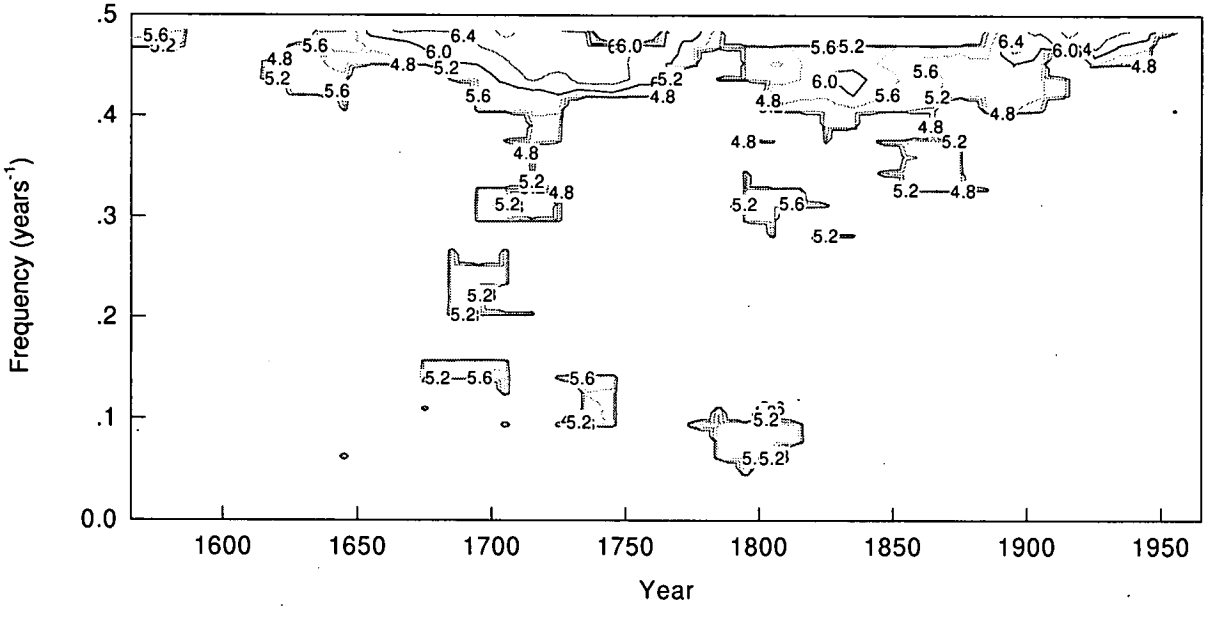

Figure 6.6: Contour map of MTM evolutive spectrum for West regional chronology estimated with three data tapers with a time-frequency bandwidth product of four. Time span of analysis is 1540–1994. Only frequencies significant at 0.05 are shown. Contours indicate spectral power, and their range is 4.6 to 7.0. Contour interval is 0.4

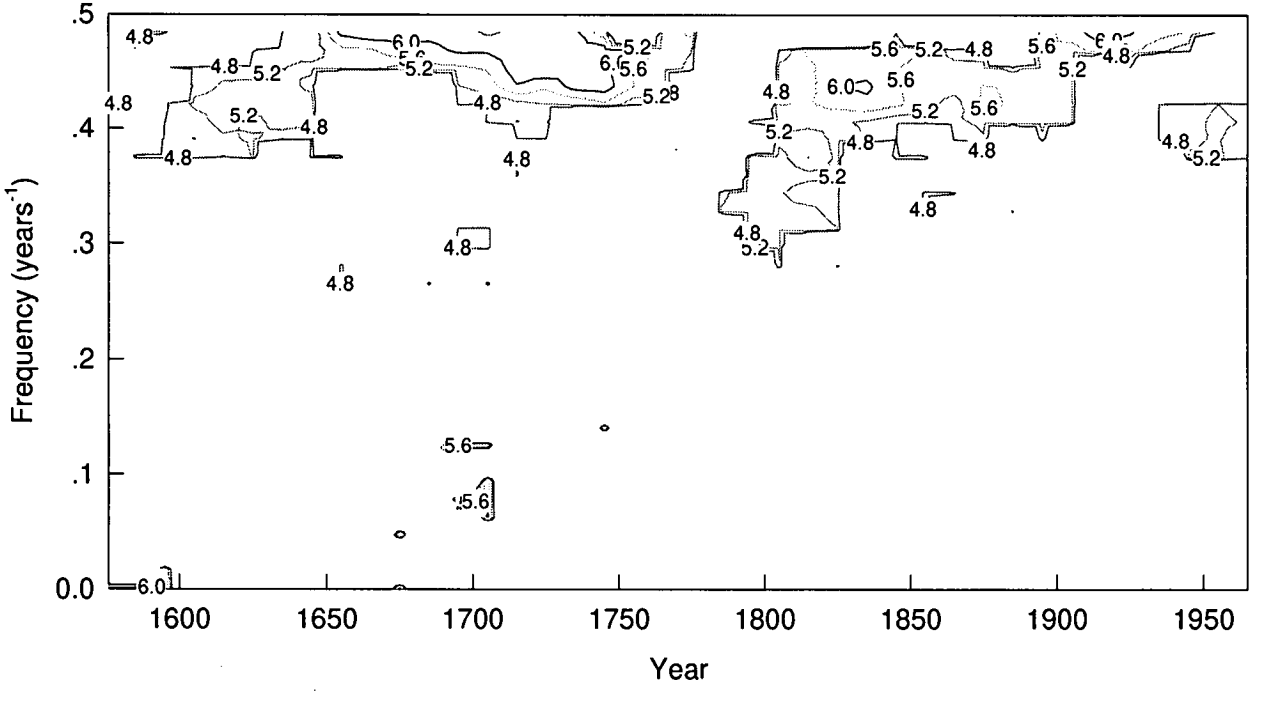

Figure 6.7: **Contour map of MTM evolutive spectrum for Southwest regional chronology estimated with three data tapers with a time-frequency bandwidth product of four. Time span of analysis is 1550–1994. Only frequencies significant at 0.05 are shown. Contours indicate spectral power, and their range is 4.6 to 7.0. Contour interval is 0.4**

moderate and heavy seedfall years implies that in years when a heavy seed crop is initiated (in the prior season), carbohydrate is mobilised by reproductive growth at the expense of future cambial growth.

A QBORW phenomenon produced in accordance with this alternative hypothesis (oscillating seed production) can be expected to be observed over the entire span of the tree's reproductive life. Eis *et al.* (1965) have suggested that the greater variation between the ring widths of individuals of older stands compared to younger stands is due to cone production. The reproductive life of tree species varies as does that of individual members of a single species. Factors such as whether the tree is a canopy level tree, whether it is shaded, and the age of the tree are important (Eis *et al.* 1965, Kozlowski 1992). Reproductive behaviour has been observed in *Phyllocladus aspleniifolius* as young as 12 years in a greenhouse situation and by approximately 30 years under more natural conditions (P. Barker, Forestry Tasmania, pers. comm.). As far as the chronologies here are concerned, these juvenile effects should not be present for two reasons: firstly, because the first years of each individual tree's growth are not included in samples taken at approximately breast height and, secondly, because where samples did contain very early years of growth which were measured, these years have been excluded through poor crossdating with other samples at the same site. Therefore, such effects will not be present in the regional chronologies. Although several time periods exist in which the QBORW is not significant at the 0.05 level (Figures 6.5–6.7), significant frequencies in the 2–3 year bandwidth are reasonably persistent through time. In this sense, the hypothesis that the QBORW is predominantly a biological expression cannot be rejected. This does not automatically suggest that the seeding/fruiting of the species is the only potential biological causal factor which would satisfy the hypothesis. Although the discussion in this chapter has targetted the role of oscillating seed production by *Phyllocladus aspleniifolius*, it is not possible to distinguish between different biological causes of the QBORW given currently available information. As Barker (1993) has pointed out, foliar development of the species also begins in the prior season, presumably consuming carbohydrates that would otherwise have been utilised in an alternative process. In order to distinguish between the relative and absolute importance of different biological processes on plant growth,

thorough physiological research would be required. The nonrejection of the hypothesis does not necessarily suggest that the QBORW is not representative of climatic conditions, as it is apparent from the writings of many researchers that climate has an important role to play in influencing these processes.

Similarly inconclusive evidence for the QBORW as a climatic expression is presented by cross spectral analyses. These suggest that the Zonal Index and/or maximum temperature may be related to the oscillatory signal observed in the ring widths, although the limited length of the climatic data sets invites caution in making such a conclusion. Of course, the implication that the QBORW is related to the zonal pressure gradient suggests in turn that temperature and precipitation anomalies are important in some capacity (e.g. Brázdil and Zolotokrylin 1995). This is despite the fact that evidence of this chapter fails to support this contention as far as minimum temperature and precipitation are concerned. For maximum temperature and the ZI, the common occurrence of coherence in the 2.5–2.6 year range is at least suggestive. The fact that maximum temperatures across the State will be more consistent than either minimum temperatures or precipitation, which will experience considerable topographic variation (Chapter 4), may be an important factor here, however. To further examine whether or not anomalies in the ZI are reflected in these three basic data sets, cross spectra of the seasonalised Zonal Index and seasonalised regional temperature and precipitation indices have been calculated (Figure 6.8).

The plots in Figure 6.8 show that there is significant coherence (at the 0.05 significance level) between both maximum and minimum temperatures and the Zonal Index across most frequencies for the West and Southwest in particular, generally discounting the idea that climate indices only represent strongly localised phenomena. Coherence between East minimum temperature and the Zonal Index is similarly high across most frequencies, but this is not the case for East maximum temperature. Despite this, all temperature series display significant coherence in the QBO band. Coherence between precipitation and the Zonal Index for seasonalised data is less consistent across the frequency range than is the case for temperature data. As expected, there is less significant coherence between the ZI and East precipitation than for West and Southwest

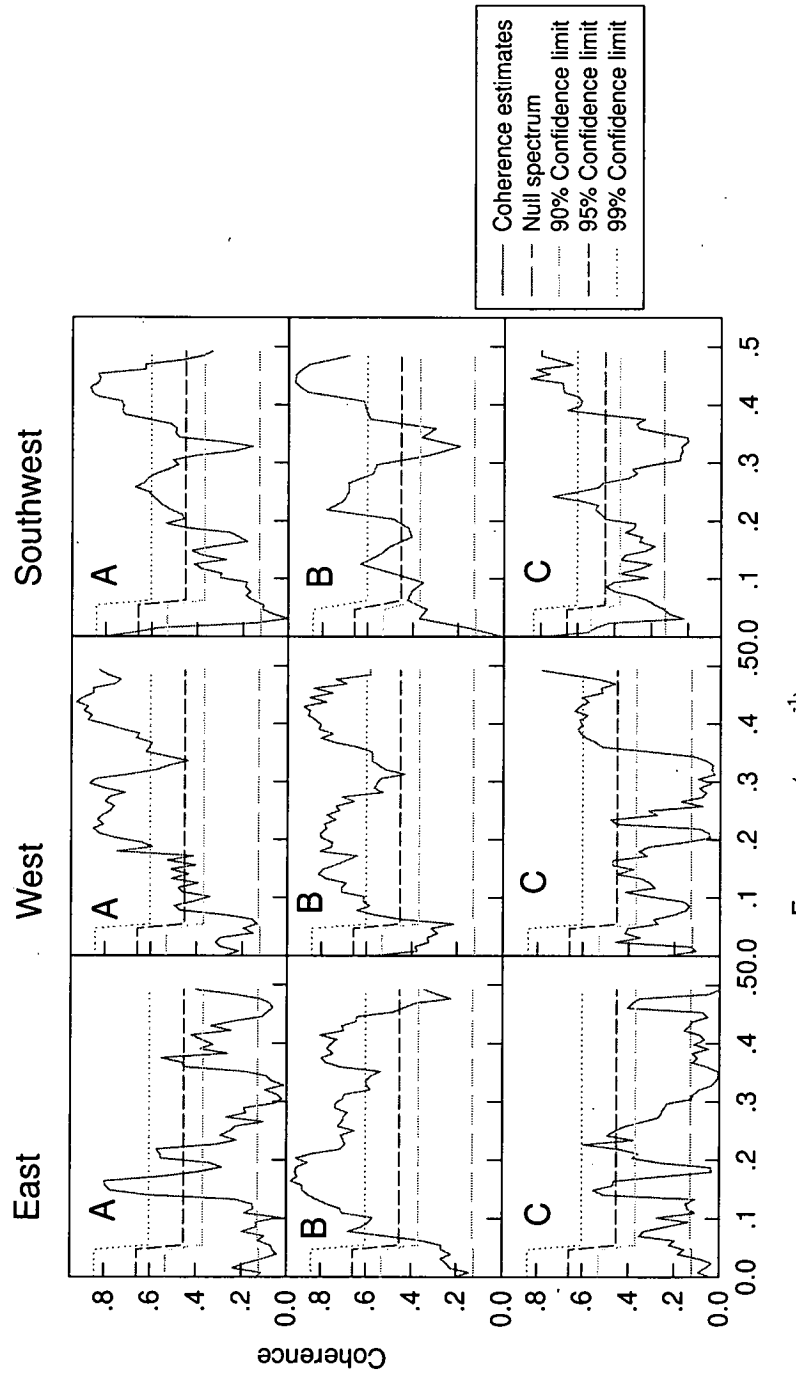
East
West
Southwest
A
B
C
Coherence
0.0
.2
.4
.6
.8
.1
.2
.3
.4
.50.0
.1
.2
.3
.4
.5
Frequency (years^{-1})
Coherence estimates
Null spectrum
90% Confidence limit
95% Confidence limit
99% Confidence limit

precipitation, most probably due to the East's greater dependence on precipitation generated by cyclonic depressions off the east coast as opposed to that brought by zonal winds. This lack of coherence appears to conflict with Shepherd (1995) who has found strong correlation between precipitation and the ZI for his eastern region, but weaker correlation for the western part of the State. However, he has made use of the Zonal Index constructed at the 500 hPa level which covered the period 1971–1989. In addition, data seasonalisation in his study proceeded on a different basis. For West and Southwest data, a broad band of significant coherence with precipitation is evident in the QBO range (Figure 6.8).

It is also interesting to note that ring width indices do not show a strong correlation with the ZI over a number of consecutive months (Chapter 5, Figures 5.8a–5.11a). It is possible that the whitening of both the chronologies and the climatic data by an AR(2) model (in Chapter 5) has removed the frequency at which correlation is present. It is also possible that the process of seasonalisation of the ZI has emphasised features which results in significant coherence between ring widths and the ZI becoming apparent.

The inference that surface pressure is causally linked to the QBORW requires further investigation for several reasons. It is possible that the QBORW is related in a complex manner to a number of climatic variables. It is also possible that an analysis based on finer resolution data in conjunction with physiological research may prove more enlightening. As pointed out above, the evidence that the ZI and maximum temperatures both demonstrate coherence at approximately the same frequency within the limited band of the QBO (Table 6.2) gives some weight to a claim of climatic forcing of the QBORW. At the same time, the weakest link in the chain of argument relates to the fact that periodicities of the order of 2.5–2.6 years have not been observed in the ring width indices themselves. However, it is plausible that differences in the time periods analysed have produced the above difference.

Although evolutive spectra do demonstrate fluctuations in significant spectral power of frequencies in the QBO band over time (Figure 6.4–6.6), there is no strong evidence presented by this technique to suggest that atmospheric QBOs have significant import for cambial growth in *Phyllocladus asplenifolius*.

However, Cook (Lamont-Doherty Geological Earth Observatory, pers. comm.) has found that greater amplitude fluctuation exists in the lower frequency (greater than 50 years) rather than the high frequency component of the spectrum of *Lagarostrobos franklinii* ring widths. It is possible that such amplitude fluctuation in lower frequency oscillations may be masking a clearer relationship between the QBORW and atmospheric QBOs. This then implies that the evolutive spectra may show little change in the significance of high frequency oscillations through time. This pattern is similar to what would be expected if the phenomenon were more closely related, in a statistical sense, to what have been denoted as 'biological processes' as opposed to 'climatic processes'. The determination of whether or not this is the case is beyond the scope of this chapter.

Strong evidence for the QBORW as a relatively clean climatic signal is, at best, tenuous. It must, however, be remembered that biological processes are generally dependent on external conditions such as climate (Zahner 1963, Henckel 1964, Eis *et al.* 1965, Kozlowski 1973, Haggar 1988, Demmig-Adams and Adams 1992, Kozlowski 1992, Fitchner *et al.* 1994, Larcher 1994, Lösch and Schulze 1994, Brodribb 1997 among many others).

6.5 Conclusions

In thinking of the tree as an agent whose growth is influenced by environmental factors, it is important to remember that climate is only one of many factors. The extent to which climatic information can be gleaned from the only 'output' variable considered here, ring widths, is a function of the way in which temperature, precipitation, humidity, solar radiation, soil moisture and so on, are processed and 'modified' within the 'black-box' of the tree to give a readily identifiable climatic signal in the output.

This chapter has attempted to ascertain whether statistical methods are able to discern a relatively straightforward relationship between the climatic variables considered (in some of which QBOs are well documented) and the output of the QBORW, apparent in many specimens. Results indicate that the relationship between input and output is far from simple, its nature eluding the statistical tools employed here. Rather than sophisticated statistical techniques whose objective is to establish a relationship between the inputs and outputs of a biological system, it

is clear that a greater understanding of the 'black-box' of species physiology is required in order to better understand how climate affects the output, and why, precisely, the QBORW exists. It is entirely possible that the physiological processes occurring within a tree result in climatic input becoming statistically insignificant in the output of ring widths. Simply denoting the process as biological, however, does not solve the problem, nor does it further understanding of plant processes as it fails to recognise that climate is an important factor in influencing or stimulating biological processes, as discussed by authors cited throughout this study. The 'statistical worth' of climatic information in the output, therefore, can not be properly understood without more detailed physiological investigation.

It is also important to recognise that only broadscale, or regionalised, climatic variables have been considered, and it is entirely plausible that the effect of microclimatic conditions on biological processes within an individual, and different parts of that individual, play a pivotal role in the relationship between climatic variables and ring widths. In other words, macroclimatic effects may be mediated by the microclimatic environment of the tree.

The fact that crossdating of sites across the State exists (Chapter 3) indicates the QBORW is synchronous between sites. This in itself is highly suggestive of a broadscale influence, but does not discount a predominantly biological 'source'. If the QBORW is a relatively unmodified expression of some climatic variable, the presence of the AR(2) process in the data requires careful consideration with respect to its representation, or nonrepresentation, in a dendroclimatic model. Of course, the same careful consideration is required if the QBORW contains very little climatic information. In essence, it is clear that a fuller understanding of plant physiology is required in order to illuminate the precise nature of linkages between processes such as moderate/heavy seeding years, foliar development, ring width oscillation, and the relative importance of various climatic stimuli for these processes. Such an understanding will enable the extraction of the maximum amount of climatic information contained within the ring widths of this species, and allow it to be used in a more meaningful manner in future work. At this juncture, the results obtained in this chapter do not

provide any clear indication of how the reconstruction presented in the next chapter is to be interpreted in the light of the QBORW.

Chapter 7: Climate Reconstruction

7.1 Introduction

The application of any biological model and its statistical formalisation imposes assumptions and restrictions on data and processes in order to produce a generalised description of the data generation process. The assumptions and restrictions of any one modelling method may or may not be appropriate for a given data set. A good model is commonly observed to have the following properties (Pankratz 1983, Harvey 1989, Koopman *et al.* 1995):

1. *Parsimony* — the model has few parameters. A simpler model is preferred to a more complicated one
2. *Good data coherence* — A good fit to the data is required. Residuals should be small and approximately random
3. *Consistency with prior knowledge*
4. *The inability to predict values which violate definitional constraints* (e.g. negative tree-ring growth)
5. *Structural stability* — the model should provide a good fit to the data outside the period used for calibration (i.e. verification)
6. *Is encompassing* — the model should encompass available information and be more general than any rival model

Although no conclusive evidence of a nonconstant response to seasonalised climate data could be shown in the Chapter 5, this does not preclude the possibility of a nonlinear response to seasonalised temperature. The QBORW, discussed in the previous chapter, represents a further complication in the reconstruction of climate from this species, especially in view of the fact that its origin is not known.

The more traditional method of PC regression, successfully used in Buckley's (1997) temperature reconstruction based on *Lagarostrobos franklinii*, was initially applied in this study, but poor results necessitated the search for a more encompassing technique which could improve model estimates. Structural

Time Series models are one class of models providing an alternative approach and, although they do not altogether solve the potential problems facing a climatic reconstruction based on *Phyllocladus asplenifolius*, they do improve model estimates. In the event of a nonconstant response to seasonalised climate data, for example, this technique would be no more valid than the PC regression technique. This is due to the fact that both techniques rely on a constant relationship between ring widths and independent (PC regression) or explanatory variables (Structural Time Series). Both techniques are inherently inhibited by the same problem: a lack of understanding of physiological processes and limits. In the context of this study the two most fundamental aspects affecting reliability or otherwise of climatic reconstructions are the presence of the QBO in ring widths and the suggestion of a nonconstant climate response. Despite these issues, climate reconstruction has been tentatively attempted in this chapter, and results compared to a *L. franklinii* maximum temperature reconstruction. This chapter describes the approach to climate reconstruction and compares the two techniques of PC regression and Structural Time Series. The limitations discussed in previous chapters need to be borne in mind when analysing these reconstructions, however.

7.1.1 Structural Time Series

Recently, interest in the use of econometric methods in the physical sciences has increased. The techniques of interest are not necessarily deterministic, nor as complex as models which rely on the current state of knowledge of the physical characteristics of a system. Instead, they represent an attempt to identify the major important behavioural modes contained within a data set, and place an emphasis on stochastic modelling (Shackley *et al.* 1998). A number of workers have applied such techniques to an examination of climatic data series (e.g. Tol and de Vos 1993, Tol 1994, Kaufman and Stern 1997, Stern and Kaufman 1997, Young 1997). Young (1997) emphasised the usefulness of first identifying model structure from information contained within the data set. Stern and Kaufman (1997) explicitly used a Structural Time Series approach in investigation of the dynamics of hemispheric temperature series.

Structural Time Series (STS) techniques have been widely used in econometric studies (e.g. Harvey and Todd 1983, Harvey and Durbin 1986, Crafts

et al. 1990, Mocan and Topyan 1993, McDonald and Hurn 1995). The ability to include frequency domain features, seasonality and autoregressive components, as well as a local rather than a global trend, represents an increased use of available information in a model, and can therefore be expected to improve model estimates. Although quite widely used in the social sciences, and economics in particular, the technique has not been extensively explored in the physical sciences, despite its suggested value (Watson and Engle 1983). STS models have previously been used in dendroclimatological studies to investigate the response, and changes over time in the response, of trees to climate (Gove and Houston 1996, Allen in press).

Components of an STS model are generally stochastic and evolve over time. Other methods which do not impose constancy of parameters have previously been used: Guiot *et al.* (1982) and Guiot (1985) separated data into high and low frequency parts, subsequently applying an assumption of linearity to the two separate series; Guiot *et al.* (1995) introduced an artificial neural network technique for the improvement of their response functions in the detection of tree response to atmospheric pollution; Van Deusen (1990) has used the Kalman Filter (KF), and statistical tests based on the prediction errors produced by it, in a model building approach to tree ring analysis. Figure 7.1 demonstrates the way in which gross assumptions of constancy may be restrictive.

STS models are models set up in terms of their components, which have a direct interpretation. For example, the decomposition of a given model may show the series to be modelled as the sum of a trend, seasonal component, irregular component and a cycle. Each of these has a direct interpretation. The following provides a useful generalised mathematical expression of the decomposition of a time series:

$$y = \mu + \gamma + \delta x + \psi + \varepsilon \qquad (7.1)$$

where y *is* the dependent variable (in this case, temperature)

μ = trend component

γ = seasonal component

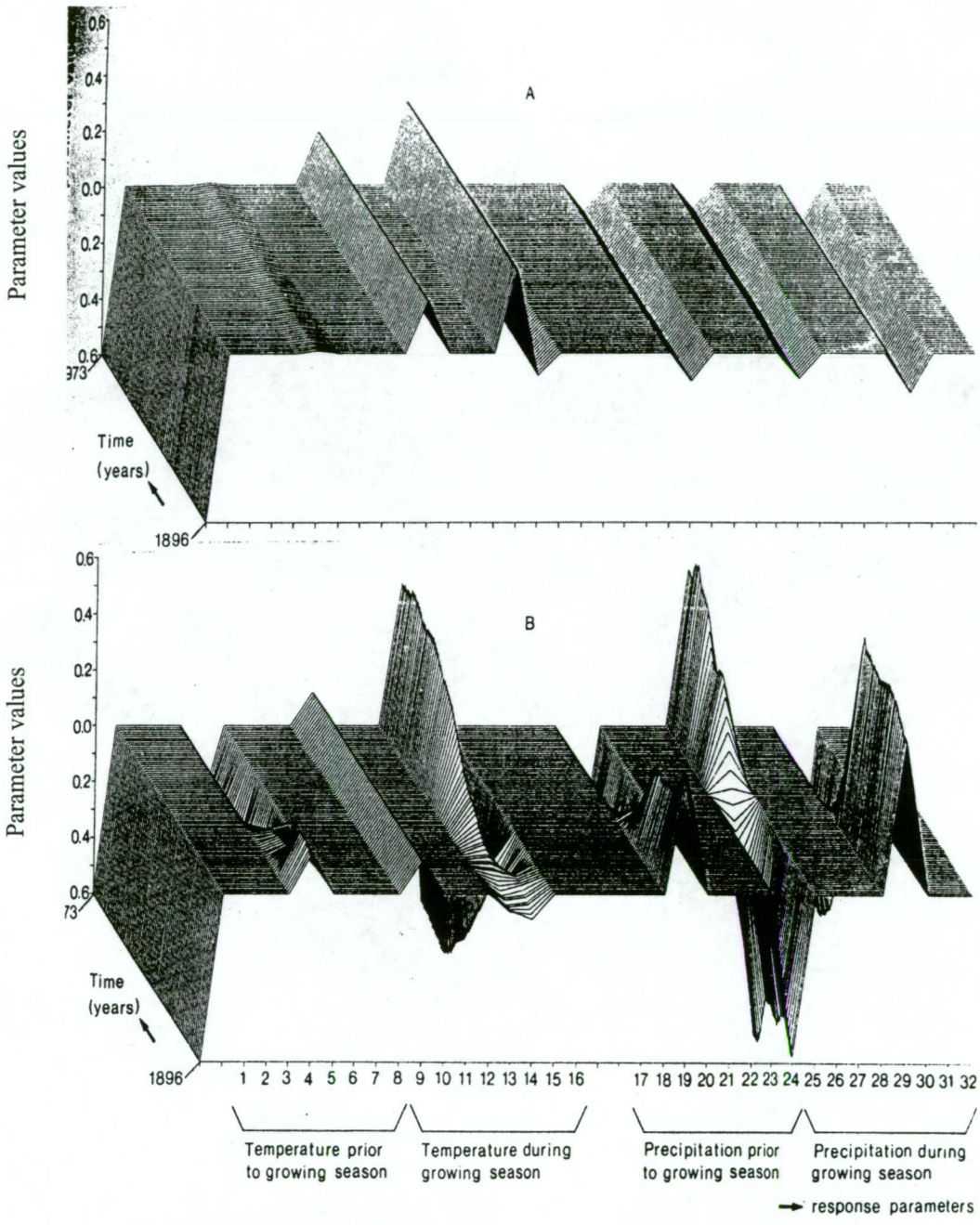

Figure 7.1: **Example of two response function estimates. Model A has been estimated by the ordinary least squares method generally applied in dendroclimatology. It gives average parameter values of a regression model. Model B has been estimated for the same data, but using the Kalman Filter. Source: Visser and Molenaar (1986)**

x = vector of explanatory variables

ψ = cyclical component

ε = irregular component

Trend can be defined as that part of a time series which when extrapolated gives the clearest picture of future long term movements in the series (Harvey 1989). It need not be constricted to be global, nor must it take a linear form. There are two parts to a trend: *Level* which refers to the value of the trend, and *slope* which may or may not be present. A locally linear trend can be expressed as:

$$\mu_t = \mu_{t-1} + \beta_{t-1} + \eta_t$$
$$\beta_t = \beta_{t-1} + \zeta_t \qquad (7.2)$$

where μ_t is a linear trend (level), η_t denotes a white noise process associated with the trend, β_t the slope of the trend, and ζ_t a white noise process associated with the slope of the trend. A white noise process can be defined as a set of serially unrelated random variables with constant mean and variance. The white noise processes, η_t and ζ_t, are mutually uncorrelated. If β_t = 0, then the process becomes a random walk.

Seasonal effects repeat themselves over a one-year time interval and are constrained to sum to zero over this period. They are generally included in a model as either trigonometric terms or as dummy variables. The following description treats the seasonal components as dummy variables. One way of allowing seasonal components to vary over time is to allow them to evolve as a random walk. This can be represented as:

$$\gamma_{jt} = \gamma_{j,t-1} + \omega_{jt} \qquad j = 1,...,s \text{ and } t = 1,...,T$$
$$E(\omega_j) = 0, VAR(\omega_j) = \sigma^2_{j\omega} \qquad (7.3)$$

where j denotes the j^{th} seasonal component and ω_j is white noise.

A *cyclical* phenomenon can be identified by an examination of the frequency domain. It repeats itself over time and can be defined in terms of its amplitude, frequency and phase. In STAMP™, the program used for STS analysis, the spectra are estimated as:

$$\hat{f}(\lambda_i) = 1/2\pi \sum_{j=-m}^{m} \omega_j p\left(\lambda_{i+j}\right) \qquad (7.4)$$

where m is window length, ω_j are the normalised weights constrained by $\omega_{-j} = \omega_j$ for $j = 0,.....m$. The method used by STAMP ™ applies a weighting procedure using Pascal's triangle (Koopman *et al.* 1995).

In the present case, *explanatory variables* are the PCs of ring widths, as will be explained below. x_t is the $k \times 1$ vector of explanatory variables, and δ contains the unknown parameters associated with them. It is important to note that, in this case, the term *explanatory variables* is not a term referring to all independent variables on the right hand side of equation (7.1). The explanatory variables enter the model in a manner similar to which independent variables enter a regression model.

The *irregular component* of the model, ε_t, captures nonsystematic movements, and is assumed to be normally and independently distributed with a mean of zero, and standard deviation σ, $\left(\text{NID}(0,\sigma)\right)$.

The application of any statistical model requires some prior information on the characteristics of the data, and this information can be obtained through data analysis. To apply candidate models blindly one model after another is akin to 'data mining', an '...uncritical examination of data sets for evidence of relationships without adequate prior consideration of potential behavioural hypotheses and without proper allowance for the process of selection of relationships when carrying out statistical tests' (p. 196 Harvey and Durbin 1986). It is relatively straightforward to interrogate both the spectrum and correlogram of the dependent data set. As in regression analysis, only relevant explanatory variables should be present in a model, and seasonal components should also be included only where appropriate. It should be noted that there is not necessarily a

unique solution to a problem when using the STS approach. Models are formulated on the basis of *a priori* information, goodness of fit and predictive power.

State Space Form (SSF) is a powerful tool opening the way for the handling of a wide range of time series models. Once in SSF, the Kalman Filter (discussed below) can be applied. The two basic components comprising SSF are known as the *measurement* and *transition* equations. The measurement equation is a statement of relations between the state variables (which may be unobservable) and the observations, while the transition equation serves as a description of the evolution of the characteristics of a physical process (Watson and Engle 1983). Following Harvey (1989), these are respectively:

$$y_t = Z_t \alpha_t + \varepsilon_t \qquad (7.5)$$

$$\alpha_t = T_t \alpha_{t-1} + R_t \eta_t \qquad (7.6)$$

$$\text{for } t = 1...N$$

Here, y_t, the dependent variable, represents temperature indices and can be expressed as a linear combination of the state and past errors (ε_t and η_t). α_t, the *state vector*, is an $m \times 1$ vector linking the observations with the measurement equation. In SSF, the state of the system contains all the information from the past and present history of the system which is necessary to describe present and future behaviour of the system. It will contain the generally stochastic components, for example, cycles, trend, and seasonality. Ideally, its length (m) should be minimised in order that the model remain as simple as possible. The aim is to set up the state vector such that it contains all relevant information for a model while at the same time being the minimum possible length.

Elements in the state and error matrices are called *hyperparameters*, may be unknown and govern the overall movement of the series. Z_t, T_t and R_t, are known as system matrices. Z_t is an $N \times m$ matrix, essentially containing the coefficients of the state vector for each time, t. These coefficients are generally nonstochastic, meaning that although they may change over time, they do so in a deterministic manner (Harvey 1989). This implies that the model is linear and,

that for any time period, y_t can be expressed as a linear combination of past and present ε_ts and η_ts and the initial state, α_0. T_t, an $m \times m$ matrix, contains information such as the sine and cosine terms of a trigonometrically defined cycle and the ARMA effects of stationary components; R_t is an $m \times g$ matrix, where g refers to the number of errors associated with the components of the system. In many cases there will be one error process for each component, meaning that g = m. In some cases, however, error process for one component may be the same as that for another, so that $g < m$. ε_t is an $N \times 1$ vector of serially uncorrelated disturbances: $\mathrm{E}(\varepsilon_t) = 0$, and $\mathrm{Var}(\varepsilon_t) = H_t$. η_t is also a $g \times 1$ vector of serially uncorrelated disturbances, i.e. $\mathrm{E}(\eta_t) = 0$, and $\mathrm{Var}(\eta_t) = Q_t$. Q_t and H_t are also system matrices.

Two further assumptions are required for the SSF formulation, and these are firstly, that:

$$E(\alpha_0) = a_0$$
$$VAR(\alpha_0) = P_0 \qquad (7.7)$$

and that the error terms, ε_t and η_t, are uncorrelated with each other and the initial state, implying independence of transition and measurement equations, i.e.:

$$E(\varepsilon_t \eta_s') = 0 \qquad \text{for all } s, t = 1,...,\mathrm{T}$$
$$E(\varepsilon_t \alpha_0') = 0$$
$$E(\eta_t \alpha_0') = 0 \qquad \text{for } t = 1,...,\mathrm{T} \qquad (7.8)$$

The estimation of structural time series parameters proceeds through the Kalman Filter, a recursive procedure through which the optimal estimator at a given time is attained. All available information, contained in previous observations, is used in estimation (Harvey 1989). This approach was first introduced to dendrochronology by Visser and Molenaar (1986) in an investigation of time dependent response of trees to climate.

The KF itself is composed of two equation sets known as the predicting and updating equations. Through the application of these equations, an updated estimate of y (equation (7.5)) is obtained. Their derivation is given in Harvey (1989) and their link, given the assumption of normality, with the state space formulation is made clear. The following is greatly elaborated upon in Harvey (1989). In the state space model, let a_{t-1} denote the optimal estimator of α_{t-1}. The covariance matrix of the estimation errors is:

$$P_{t-1} = E\left\{(\alpha_{t-1} - a_{t-1})(\alpha_{t-1} - a_{t-1})'\right\} \qquad (7.9)$$

Given a_{t-1} and P_{t-1}, the optimal estimator of the state at time t is defined as:

$$a_{t|t-1} = T_t a_{t-1} \qquad (7.10)$$

This is the mean of the conditional distribution of α_t, and is the optimal estimator of α_t in the sense that the MSE is minimised. $a_{t|t-1}$ is a vector of estimates associated with a particular realisation of observations. In essence, the new estimate of the state is dependent on the previous estimate. Equation (7.6) explains that the true state is dependent on the previous true state and an error term. The relation, therefore, of equation (7.6) to the estimator of (7.10) is obvious. The covariance matrix of estimation error is:

$$P_{t|t-1} = T_t P_{t-1} T_t' + R_t Q_{t-1} R_t' \quad t = 1,\ldots,N \qquad (7.11)$$

and is again dependent on the estimate of the covariance of the previous state. It is also dependent on the variances of the error terms, R_t and η_t in (7.6). Equations (7.10) and (7.11) are the *prediction equations* of the KF, applied at t-1, and the predicted values are then used in updating the estimates. The role of the *updating equations* is to calculate a new estimator of the state as new information (observation) arrives at time t. They are:

$$a_t = a_{t|t-1} + P_{t|t-1} Z_t' F_t^{-1} \left(y_t - Z_t a_{t|t-1} \right) \qquad (7.12)$$

$$P_t = P_{t|t-1} - P_{t|t-1} Z_t' F_t^{-1} Z_t P_{t|t-1} \qquad (7.13)$$

where $$F_t = Z_t P_{t|t-1} Z_t' + H_t \quad t = 1, \ldots, N \qquad (7.14)$$

Equation (7.12) is the mean of the multivariate normal distribution of α_t, conditional on the previous estimate, and (7.13) is a statement of its covariance matrix.

An underlying assumption is that both the disturbances and the initial state vector are normally distributed. The conditional distributions are also normal and therefore specified by their means and covariances as given above. If the disturbances and state vector are not normally distributed, then it is not assured that the KF will produce the conditional mean, although it will remain an optimal estimator in the class of all linear estimators. An exponential weighting function is used to place more weight on the most recent observations, and both the predictions and the estimator are continually updated as more observations become available. The amount of discounting of prior observations is dependent upon the relative values of the disturbances. The larger the disturbances, the greater the level of discounting of past observations.

The above section serves as a brief description of the 'mechanics' of STS. The estimation of the STS hyperparameters (cycles, trends, AR(p), seasonal terms) is based on the maximisation of a diffuse log likelihood function which is found by using the one-step-ahead predictions and their MSEs. Because the KF is unable to handle situations where the initial state is unknown, a variation of the KF, known as the *diffuse KF*, has been used for an initial stretch of data (de Jong and Chu-Chun-Lin 1994). The reader is referred to de Jong and Chu-Chun-Lin (1994) and Koopman *et al.* (1995) for a thorough discussion of this issue.

The software used in this study (STAMP^{TM}) uses an iterative quasi-Newton method for the optimisation of the likelihood function (Koopman *et al.* 1995). Newton methods search for a maximum or a minimum of a function, i.e. they search for the point at which the function has a zero gradient. STAMP^{TM} uses the Broyden–Fletcher–Golfarb–Shanno method of finding this point in

which a search direction is determined for the next step. A description of this method can be found in Press *et al.* (1992). The iterative process is concluded when three convergence criteria hold or if irregularities occur. A discussion of these criteria is given in Koopman *et al.* (1995) and comprehensive attention is given to the development of STS models in Harvey (1989), de Jonge and Chu-Chun-Lin (1994) and Koopman *et al.* (1995). This detail is well beyond the scope of this study and is not necessary in a basic comparison of results from the two techniques, PC regression and STS.

7.1.2 Model Testing

A number of tests are available for an STS model and fall into three basic categories: descriptive/diagnostic, goodness of fit statistics and predictive testing. Those measures relevant to this study are described briefly below.

7.1.2.1 Descriptive Statistics

Descriptive statistics provide an initial assessment of the characteristics of the residuals after the imposition of a model. It is desirable that for a given model the standard deviation of residuals from the mean be relatively small, they be normally distributed with a homogenous variance, and that any autocorrelation present prior to model formulation be successfully modelled and therefore not present in the residuals.

Normality

The Bowman–Shenton test (N_{BS}) is based on the third and fourth moments of the residuals and is defined as:

$$N_{BS}^{*} = (N/6)b_1 + (N/24)(b_2 - 3)^2 \qquad (7.15)$$

where b_1 denotes skewness and b_2 kurtosis. N is the number of observations. This can be tested against a χ_2^2 distribution. The null hypothesis is that the distribution of the residuals is normal.

Autocorrelation

The Durbin–Watson (DW) test is a well-known test for first order autocorrelation in a data set and is expressed as:

$$DW = \sum_{t=2}^{N}(e_t - e_{t-1})^2 / \sum_{t=1}^{N} e_t^2 \qquad (7.16)$$

where $0 < DW < 4$. A value close to zero implies positive autocorrelation and a value close to four corresponds to negative autocorrelation. A value of approximately two indicates no autocorrelation. The Box–Ljung portmanteau statistic (Ljung and Box 1978) is an extension of this test, examining data for the presence of autocorrelation up to lag p. The criterion on which the χ^2 test is based is:

$$\tilde{Q}(\hat{r}) = n(n+2)\sum_{k=1}^{m}(n-k)^{-1}\hat{r}_k^2 \qquad (7.17)$$

where n is the number of observations, k the value of the lag. The autocorrelation function for lag k, $\hat{r}_k$, can be defined as:

$$\hat{r}_k = \sum_{t=k+1}^{n}\hat{e}_t\hat{e}_{t-k} / \sum_{t=1}^{n}\hat{e}_t^2 \qquad (7.18)$$

The null hypothesis is that autocorrelation to lag p does not exist in the residuals.

Heteroscedasticity

A straight forward test for heteroscedasticity is based on an examination of the variance of two subsets of the residuals (Judge *et al.* 1988). The test statistic is:

$$H(h) = \sum_{t=N-h+1}^{N} v_t^2 / \sum_{t=d+1}^{d+1+h} v_t^2 \qquad (7.19)$$

where the numerator is the variance of the one data subset and the denominator the variance of the other. It can be tested against an $F_{(h,h)}$ distribution for significance, the null hypothesis being that model residuals are homogenous in variance.

7.1.2.2 Goodness of Model Fit Statistics

Coefficient of Determination (R^2)

For time series models a better measure of fit is R_D^2, where the first differences between the observations, rather than the observations themselves are used. This is expressed as:

$$R_D^2 = 1 - SSE / \sum_{t=2}^{T} (\Delta y_t - \Delta \bar{y}_t)^2 \qquad (7.20)$$

where $\Delta \bar{y}$ is the mean of the differences, and:

$$SSE = (T-d)\tilde{\sigma}^2 \qquad (7.21)$$

More details can be found in Harvey (1989).

Akaike Information Criterion (AIC)

Although R^2 and R_D^2 can be used to assess the fit of a given model to the data, a comparison of R^2 or R_D^2 across models is not strictly appropriate. The addition of explanatory variables can inflate the statistic without adding real value to a model. The *AIC* provides a well-established measure of fit that is commonly used to compare the fit of different models to a data set. It is, however, known to be inconsistent (Hurvich and Tsai 1989, Van Deusen 1990). The *AIC* corrected for this inconsistency is expressed as:

$$AIC_c = N * \log(MSE) + 2p + 2\{(p+1)(p+2)/(N-p-2)\} \qquad (7.22)$$

where N is the number of observations, p the number of model parameters and MSE the mean square error. The aim is to minimise the value of the *AIC*.

Component Tests

As well as testing the overall fit of a model, it is possible to examine the significance of individual components. The amplitude of a 'cycle' gives some insight into its relative importance. Deterministic stationary cycles can be tested against a χ^2 distribution for significance (see Harvey 1989). The numerical value of ρ, the coefficient of autocorrelation, can also be used as a gauge of the role played by autocorrelation in the residuals of the model. As in traditional regression analysis, the significance of the explanatory variables can be tested against a $t_{(n-1)}$ distribution for significance, as can trend present in the model.

7.1.2.3 Predictive Testing

In dendroclimatology, the calibration–verification procedure is considered fundamental. In principal component regression, a portion of the data is commonly withheld from the analysis and the calibrated model tested on this subset, as discussed in Chapter 5. The use of all previous information by the KF for updating the estimator renders the use of this split calibration–verification scheme inappropriate because information is lost, potentially resulting in large differences in estimates. In addition, when using frequency domain information (i.e. cycles) based on an analysis of an entire data set, the use of a split calibration–verification scheme is not strictly appropriate, especially if cyclical elements of relatively long period (compared to data set length) are included in the model. Predictive testing plays a similar role to the verification procedure of the PC regression models often used in dendroclimatology. It is, however, not equivalent to verification. Predictive testing can either be used to examine predictions at the end of sample or predictions of observations which have been withheld from analysis. Through predictive testing it is possible to assess the stability and usefulness of the postulated model.

The Chow test compares the one step ahead predictions with the actual values. For a model that is correctly specified, the *Chow* statistic is specified (within-sample testing) as:

$$Chow = \left[\left(N - l - d^*\right)/l\right] \sum_{t=N-l+1}^{N} w_t^2 \Big/ \sum_{t=d^*+1}^{N-1} w_t^2 \qquad (7.23)$$

and distributed as $F_{(l,N-l-d^*)}$, where w_t are recursive residuals for $t=d^* + 1...N$ where $d^* = d + k$, k is the number of explanatory variables in the model (Koopman *et al.* 1995), and N is the number of observations. l relates to the number of observations in the subperiod. These residuals are standardised residuals obtained with an augmented KF. Further discussion of this may be found in Harvey (1989) and Koopman *et al.* (1995). The null hypothesis is that the predictions and the actual data do not substantially differ.

For a misspecified model with a spuriously good fit, the *Chow* test will lead to a rejection of the null hypothesis that a suitable model has been specified. However, a low value of the statistic does not necessarily imply that the model is good; it may be the case that the fit of the model in the post-sample period is just as poor as in the sample period.

7.2 Methodology

Initially, the transfer functions for *Phyllocladus aspleniifolius* were based on PC regression models for which both an early and a late calibration period were tested. Whole period PC regression models were also calculated as a basis of comparison with STS models for which the whole period was used.

Maximum temperatures of the prior summer/autumn were used as the dependent variable in all *Phyllocladus aspleniifolius* models. Climatic data were seasonalised as discussed in Chapter 5; for the East, January to April of the prior year; for West, November to March of the prior year; and for the Southwest, September to January of the prior season. Independent (PC regression) or explanatory variables (STS) were the PCs of tree chronologies in each region. Each region was modelled separately. Sites used in the regional models were: East — BLT_E, RFR_E and BEN_E; West — KOA_M, RCS_W, WEY_W and MUR_W;

Southwest — LCR_S, SPR_S and $CLAY_S$. ESM_E (East) was excluded on the basis of its particularly poor quality after 1900. The shortness of record and the generally poor quality of the Mersey chronologies other than KOA_M also precluded their use in climatic reconstruction. The quite different response of $CLAY_S$, as opposed to SPR_S and LCR_S, to prior summer/autumn temperature, is likely to be a problematic element in the Southwest reconstruction.

7.2.1 PC Regression

Maximum temperature data were seasonalised, as described in Chapter 5, by averaging across the relevant months. Chapter 5 reported that strongest correlations with maximum temperature were recorded for the prior season, and it is therefore prior season reconstructions which will be attempted and analysed here. Both climatic and tree-ring data were prewhitened prior to modelling in order that subsequent statistical tests were valid. This resulted in the loss of two years of data (tree rings being modelled as AR(2) processes, climate as AR(1), as selected by the AIC_C). All candidate independent variables (residual chronologies in a region) significant at the 0.05 level were entered into the PCA. Only those PCs with an eigenvalue of one or greater were included as independent variables in the regression, with seasonalised maximum temperature (described above) as the dependent variable. Time spans of the early and late calibration periods were: East 1919–1955 and 1956–1994; West 1913–1953 and 1954–1993; Southwest 1933–1963 and 1964–1994. The entire period was used for the estimation of the STS models because the method is not suited to the use of separate calibration and verification periods due to the utilisation by the KF of all prior information in the updating of the estimator (see above). Therefore, PC regression models for the whole period were also estimated for comparison with STS models. The periods covered by these models were: East 1916–1993, West 1915–1993, Southwest 1933–1994.

In addition, a whole period model based on Buckley's (1997) HIGH *Lagarostrobos franklinii* sites was estimated for the purposes of comparison with an STS model for the same species. Because no temperature reconstruction was based on LOW *L. franklinii* sites due to their reported weaker link with climatic data (Buckley 1997), no attempt was made to use these sites. Current season

January–April maximum temperatures were seasonalised, again by averaging across this time period, and used as the dependent variable. This period was defined by Buckley (1997) as the 'high correlation interval' for the HIGH *L. franklinii* sites. The time span of the calibration period was 1913–1993.

All of these regression models are based on the assumption that ring width variation is essentially limited by maximum temperature (see Chapter 5). The maximum temperature of the prior season is being estimated from the ring width of the current season in the *Phyllocladus asplenifolius* models.

7.2.2 STS Reconstructions

Because STS models are designed to incorporate autoregression and include cyclical elements, chronologies which have not had autoregressive effects removed were used (Chapter 3). This contrasts with the use of the residual chronologies, which have had autoregressive effects removed, for the estimation of PC regression models. Some differences between the results of the two techniques can therefore be expected due to this difference.

Explanatory variables included in the model were once again the PCs of ring width for an individual region. Explanatory variables not significant ($p = 0.10$) in the STS models were eliminated. For all STS models, trend was modelled as a random walk.

The spectra of seasonalised maximum temperature for the East did not show significant spectral peaks greater than 2.3 years (Figure 7.2). The correlogram while not showing a classical AR(1) pattern, was suggestive of an AR(1) process. On the basis of this, an AR(1) term was included in the model. No cycles were incorporated, and explanatory variables, significant at the 0.10 level, were the first and third eigenvectors.

For West seasonalised maximum temperature data, four cyclical elements were indicated as being significant (Figure 7.2). The lowest frequency cycle, however, was of a frequency too low to be resolvable given the length of the data set. Other periodicities occurred at 7.6 years and 2.42 years, with lesser peaks at 8.7 and 3.3 years. The peak at 3.3 years was significant at the 0.10 level, but not at 0.05. Initially three cycles were included in the model, but one of these had an amplitude which approached zero, and goodness of fit statistics suggested that the

model was not the best available model. Therefore only two cycles were included in the model. The correlogram of West seasonalised maximum temperature did not show strong evidence of being an AR(1) process. The first and the third eigenvectors, significant at the 0.10 level were included in the model along with the two cycles.

For the Southwest, spectral peaks of greater than two years were evident at 7.8 and 2.44 years (Figure 7.2). Two cycles were included in the model on this basis. Only the first eigenvector was significant at the 0.10 level.

Periods covered by the STS models were: East 1915–1993, West 1911–1993, and Southwest 1933–1994. A further model was estimated for *Lagarostrobos franklinii*, covering the time period 1915–1993. The correlogram suggested the suggested the presence of an AR(1) process in the temperature data (January–April average). No significant (0.05) spectral peaks were identified in the seasonalised January–April temperature data, other than one at zero frequency (Figure 7.2). Therefore, no cyclical component was included. This model used the four PCs of ring width which were all significant at the 0.1 level as explanatory variables as well as including an AR(1) term.

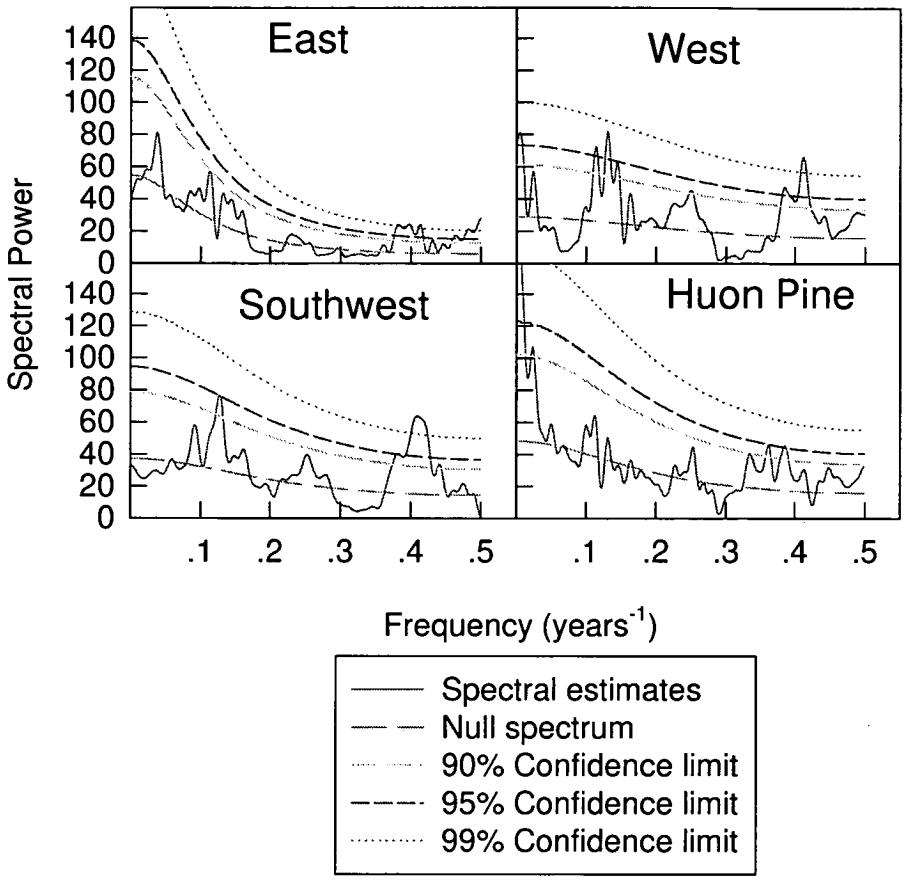

Figure 7.2: **Multiple Taper Method (MTM) spectra of seasonalised maximum temperature data. Periods analysed were: East 1915–1994, West 1915–1993, Southwest 1931–1994; Huon Pine 1914–1993. Three data tapers with time-frequency bandwidths of two were applied to all series. Significant spectral peaks (0.05) present were 0.3984 (2.51 years), 0.499 (2 years) in the East maximum temperature series; 0.0049 (204.08 years, and obviously nonsensical in this analysis) 0.1133 (8.83 years), 0.4121 (2.43 years) in the West; 0.4082 (2.5 years) for Southwest maximum temperatures. For the Huon Pine series no significant peaks were evident other than at zero frequency**

7.3 Results

7.3.1 PC regression results based on the split calibration/verification scheme

The forms of the PC regression models for the early and late calibration periods are:

East

$$mxt\_1 = 0.383PC1 + \varepsilon \quad \textit{(early)} \qquad mxt\_1 = -0.484PC1 + \varepsilon \quad \textit{(late)}$$
$$(0.000) \qquad\qquad (0.000) \qquad (7.24)$$

West

$$mxt\_1 = 0.516PC1 + \varepsilon \quad \textit{(early)} \qquad mxt\_1 = 0.486PC1 + \varepsilon \quad \textit{(late)}$$
$$(0.000) \qquad\qquad (0.000) \qquad (7.25)$$

Southwest

$$mxt\_1 = -0.416PC1 + \varepsilon \quad \textit{(early)}$$
$$(0.025) \qquad (7.26)$$

where *mxt_1* signifies maximum temperature of the prior summer/autumn months, and *PC1* refers to the first principle component. Numbers in parentheses refer to significance levels.

For all models, with the exception of the late calibration Southwest in which no PCs pass the eigenvalue = 1 test (see Craddock 1973), only the first eigenvector is retained, resulting in simple regression models. Although East and Southwest models (early period) pass the stringent *CE* test, explained variance is low, 14.7 and 17.3 % respectively (Table 7.1). The West model does not pass the *CE* test, although explained variance is 27%. In the later period, explained variance for the East increases to 24% while decreasing to 24% for the West. No model has been produced for the Southwest in the later period. It is noticeable that the West model fails to pass the *CE* test in both the early and late calibration periods. Additionally, it is interesting to observe that for the West, a greater amount of explained variance occurs in the earlier period, while for the East,

more variance is explained in the later period (Table 7.1). The small amounts of explained variance make it inadvisable to base a climatic reconstruction on any of these models.

A	*PM*	*R*	*ρ*	*RE*	*CE*
East	0.02 / 0.01	0.38 / 0.43	0.40 / 0.31	0.15 / 0.10	0.15 / 0.06
West	0.00 / 0.09	0.56 / 0.45	0.60 / 0.45	0.32 / 0.04	0.32 / -0.39
Southwest	1.00 / 0.10	0.42 / 0.36	0.36 / 0.32	0.17 / 0.19	0.17 / 0.07

B	*PM*	*R*	*ρ*	*RE*	*CE*
East	0.01 / 0.02	0.49 /0.38	0.50 / 0.39	0.24 / 0.07	0.24 / 0.05
West	0.06 / 0.02	0.49 / 0.57	0.49 / 0.59	0.24 / 0.08	0.24 / -0.42
Southwest	NO MODEL PASSED				

Table 7.1: **Calibration and verification statistics for regional transfer functions based on prior summer/autumn maximum temperatures. A. Early calibration period: East 1918–1955, West 1913–1953, Southwest 1933–1963. B. Late calibration period; East 1956–1994, West 1954–1993, Southwest 1964–1994. The first number in each pair represents the calibration period and the second represents the verification period. *R* is the coefficient of determination and ρ the Spearman rank correlation coefficient. Figures for the product means test, *PM*, are probability levels, and the null hypothesis that the differences between the actual and predicted values are not significant. *RE* is the reduction of error statistic and *CE* the coefficient of efficiency (described in Chapter 5). For the calibration period, *RE* = *CE*.**

7.3.2 Whole Period Reconstructions

7.3.2.1 PC Regression Models

Models for both species retain only the first eigenvector and are:

East

$$mxt\_1 = 0.372 PC1 + \varepsilon \qquad (7.27)$$

$$(0.000)$$

West

$$mxt\_1 = 0.353 PC1 + \varepsilon \qquad (7.28)$$

$$(0.000)$$

Southwest

$$mxt\_1 = -0.548PC1 + \varepsilon \qquad (7.29)$$
$$(0.000)$$

L. franklinii

$$mxt = -0.522PC1 + \varepsilon \qquad (7.30)$$
$$(0.000)$$

Estimated and actual temperatures for these models are shown in Figure 7.3. None of the three *Phyllocladus aspleniifolius* models provide a good visual fit, although they do appear to generally trace the series trend successfully. Due to the low explained variance of the *P. aspleniifolius* PC regression models, both for the whole period and for early and late calibration periods (see Table 7.7), the resultant reconstructions are neither compared nor explored further.

The *Lagarostrobos franklinii* PC regression model, although it does not explain a large proportion of the variance in maximum temperatures, is a better fit to the data than the *P. aspleniifolius* models (Figure 7.3), and this is confirmed by the results of Table 7.7 (see below).

7.3.2.2 STS Models

For each of the following models, the form of the model is reported followed by a tabulated report (Tables 7.2–7.5) of the estimated parameters of the model. The fitted structural time series models are:

Figure 7.3: Actual and estimated maximum temperatures (σ). Left hand column are the PC regression estimates and right hand column shows the STS estimates. Time frame is 1911–1994. For all STS models, with the exception of the East, estimation appears to be better in the earlier part of the time period. It is evident that PC regression models fail to capture much of the variability of the actual temperature indices for the three *P. aspleniifolius* models. However, in the case of *L. franklinii*, the PC regression model appears superior to the STS model, especially in latter years

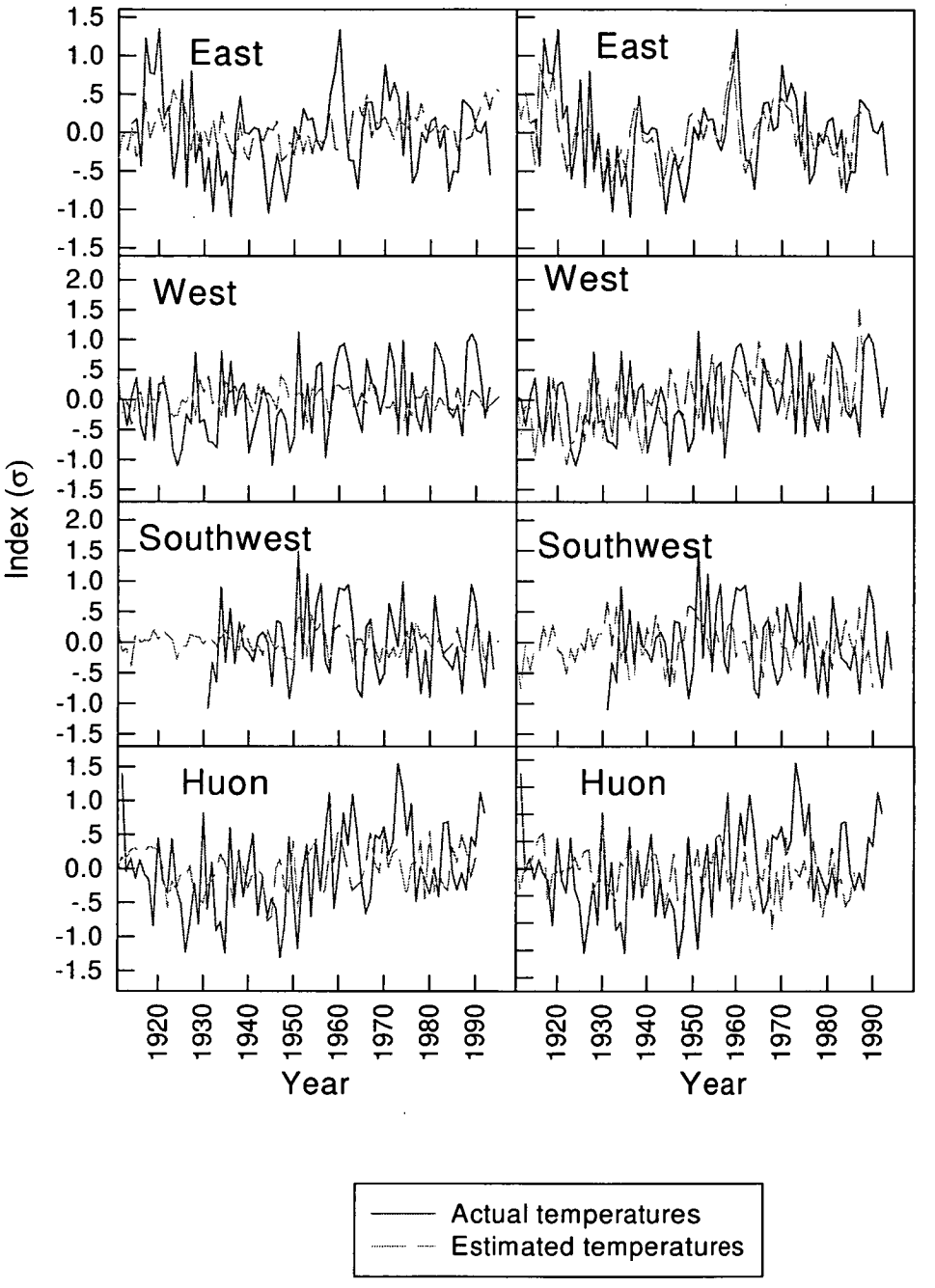
East
East
West
West
Southwest
Southwest
Huon
Huon
Index (σ)
Year
Year
1920
1930
1940
1950
1960
1970
1980
1990
Actual temperatures
Estimated temperatures

East

$$mxt\_1 = level + AR(1) - PC1 - PC3 + \varepsilon \qquad (7.31)$$

Parameter	*Estimate*	*Standard Error*	*t statistic*
level	0.023	0.152	0.147
AR(1)	0.759		
PC1	-0.123	0.030	-4.120
PC3	-0.189	0.102	-1.852

Table 7.2: **Estimated parameters of East STS model. Estimate of *level* is given for the final state, i.e. at time *T*. Estimate for AR(1) parameter refers to the value of the ρ coefficient. A *t* statistic greater than 1.64 indicates significance at the 0.1 level and one greater than 1.96 is significant at the 0.05 level**

West

$$mxt\_1 = level + \psi_1 + \psi_2 + PC1 + PC3 + \varepsilon \qquad (7.32)$$

Parameter	*Estimate*	*Standard error*	*t statistic*
level	0.167	0.176	0.948
ψ_1	0.097(A), 5.149(λ)	0.168	
ψ_2	0.122(A), 8.506(λ)	0.229	
PC1	-0.185	0.034	-5.393
PC2	-0.179	0.106	-1.682

Table 7.3: **Estimated parameters of West STS model. Estimate of *level* is given for the final state, i.e. at time *T*. For ψ_1 and ψ_2, the first value (A) refers to the amplitude of the cycle and the second value (λ) to the period in years of the cycle. A *t* value of 1.64 indicates significance at the 0.1 level, and one greater than 1.96 indicates significance at the 0.05 level**

Southwest

$$mxt\_1 = level + \psi_1 + \psi_2 + PC1 + \varepsilon \qquad (7.33)$$

Parameter	*Estimate*	*Standard error*	*t statistic*
level	-0.023	0.061	-0.384
ψ_1	0.124(A), 4.865(λ)	0.212	
ψ_2	0.155(A), 9.07(λ)	0.132	
PC1	-0.235	0.056	-4.218

Table 7.4: **Estimated parameters of Southwest STS model. Estimate of *level* is given for the final state, i.e. at time *T*. For ψ_1 and ψ_2, the first value (A) refers to the amplitude of the cycle, and the second value (λ) to the period in years of the cycle. A *t* value of 1.64 indicates significance at the 0.1 level, and one greater than 1.96 indicates significance at the 0.05 level**

L. franklinii

$$mxt = level + AR(1) + PC1 + PC2 + PC3 + PC4 + \varepsilon \qquad (7.34)$$

Parameter	*Estimate*	*Standard error*	*t statistic*
level	-0.048	0.192	-0.252
AR(1)	0.212		
PC1	0.080	0.046	1.752
PC2	-0.244	0.110	-2.216
PC3	-0.310	0.111	-2.778
PC4	-0.441	0.141	-3.140

Table 7.5: **Estimated parameters of *L. franklinii* STS model. Estimate of *level* is given for the final state, i.e. at time *t*. Estimate for AR(1) parameter refers to the value of the ρ coefficient. For ψ_1 and ψ_2, the first value (A) refers to the amplitude of the cycle and the second value (λ) to the period in years of the cycle. A *t* value of 1.64 indicates significance at the 0.1 level and one greater than 1.96 indicates significance at the 0.05 level**

In the STS models, the explanatory variables, which enter the model in the same manner as independent variables in a regression, are deterministic. That is they do not vary over time. Despite the fact that the level is not statistically significant it has been included in the models as its non-inclusion leads to erratic and highly misleading temperature retrodictions being produced by resultant models. This has been ascertained by an examination of longer period temperature series such as the Cook and Buckley temperature series.

Table 7.6 reports descriptive statistics for each of the above models. The DW test indicates that very little first order autocorrelation remains in the residuals, although the Q statistic implies that significant autocorrelation (lags greater than one year) remains in the West (at the 0.05 significance level). The distribution of the residuals for each of the models, (7.31)–(7.34), are indicated to be homogenous for East, West and *Lagarostrobos franklinii* models with the critical value of the F statistic being 1.44 (0.05 significance level). The critical value for the Southwest is $F = 1.61$, also indicating that heterogeneity of residuals is not significant in the Southwest either (0.05 significance level).

	Std Error	*BS*	*DW*	*Q*
East	0.444	0.615	2.051	12.590
West	0.487	1.190	2.021	14.290
Southwest	0.506	1.510	2.087	10.400
L. franklinii	0.544	0.963	1.941	7.403

Table 7.6: **STS Model diagnostics. The Bowman–Shenton (BS) test is a test of data normality. No value for any site is significant (0.05). DW is the Durbin–Watson statistic, centred around 2 for a series with no autocorrelation, and Q is the Box–Ljung Portmanteau statistic (Ljung and Box 1978) which tests for autocorrelation out to lag *p*. No significant autocorrelation remains in East, Southwest or for *L. franklinii* (0.05 significance level), although *Q* for the West is significant at the 0.05 level**

Cycle periodicities for the West are reported by the model as 5.1 and 8.5 years. For the Southwest the periodicities are 4.86 and 9.06 years. It is probable that the differences between these estimates and the MTM estimates of periodicities in the temperature data (8.83 and 2.43 years West; 2.5 years for Southwest), most particularly for the Southwest, are partially due to the technique of estimating the

spectra in STAMP™. The initial values of periodicities at the start of the iteration procedure are 5 and 8 years for both the West and Southwest.

Plots of STS estimated and actual temperatures are shown in Figure 7.3. There is a visually apparent improvement over the PC regression models shown in the same Figure. Goodness of fit statistics suggest very definite improvements for all three *Phyllocladus aspleniifolius* models through the use of STS, both in terms of explained variance and model AIC_Cs (Table 7.7). It must be remembered, however, that the formulation of R^2 and R_D^2 differs and that this difference may well explain a considerable amount of the difference between the values of these goodness of fit statistics. The AIC_C for the Southwest is the least satisfactory of the three STS models. This may be due to the same reason that a PC regression model cannot be formulated in the later calibration period. As far as *Lagarostrobos franklinii* models are concerned, results suggest that the performance of the STS model is inferior to that of PC regression which has a lower AIC_C than the STS model (Table 7.7). A larger amount of explained variance in the STS model (as reported by R_D^2) is likely to be caused by the inclusion of extra variables, inflating the statistic.

	East	*West*	*Southwest*	*Lagarostobos*
R^2(PCREG)	0.138	0.117	0.149	0.252
AIC_C(PCREG)	-7.130	-13.600	-5.810	-19.330
R_D^2 (STS)	0.307	0.349	0.286	0.307
AIC_C (STS)	-35.586	-30.550	-22.503	-6.027
CHOW (STS)	0.065	0.346	0.538	0.650

Table 7.7: **Goodness of fit statistics for PC Regression and STS models. The Chow statistic (χ^2) is a measure of similarity between actual and estimated values. The significance level is reported here and indicates a possible model misspecification for the East (0.1 significance). This may be related to the above suggestion that autocorrelation of greater than one lag remained significant in the data at the 0.1 significance level**

The improvement in explained variance for *Phyllocladus aspleniifolius* models justifies some tentative discussion of the STS temperature reconstructions. All three STS reconstructions show a great deal of similarity to one another over the nineteenth century, especially over the period 1830–1910, indicating a

similarity of conditions across the State (Figure 7.4). The periods 1815–1830 and 1915–1923, and the early 1980s, are instances of clear differences in the reconstructions. Temperatures for the West deviate positively from the long-term mean to a greater extent than for the East over 1815–1830, and for the East and Southwest in the early 1980s. Over the period 1915–1923, the east coast shows positive deviation from the mean, while the West, negative (on the whole). The year 1947 is indicated as being greater than 1σ below average for the Southwest while approaching the long-term mean temperature for East and West. There is a further anomaly between the Southwest and the more northern regions in the late 1960s/1970s. Again, these years are indicated to be cooler than average for the Southwest, but warmer than average for the West and East. In summary, warmer than average periods indicated by reconstructions are 1810–1830 (West), mid 1840s, mid 1880s – late 1890s (West), 1915–1923 (East), late 1950s, mid 1960s – early 1970s, early 1980s (West). The northern reconstructions both indicate increasing temperatures, especially over the 1930–1960 period, most obviously so in the West. Cooler than average periods occur for 1818–1824 (East), mid 1880s – mid 1890s (East), 1915–1945 (West), 1929–1945 (East) and early 1980s (East). Temperature index series for the twentieth century indicate warmer than average conditions for the East from 1915–1921, in the late 1950s, the late 1960s – early 1970s; for the West temperatures are approximately average between 1910–1920, and since the 1950s have generally been above the long-term mean (Figures 4.4–4.7 and 7.3). This lends some credence to the reconstructions. However, the differences of the reconstructions in the late 1960s through to the late 1970s do not appear to be faithfully reproduced records of temperature, especially in the Southwest.

Because the *Lagarostrobos franklinii* and *Phyllocladus aspleniifolius* reconstructions are based on different climatic windows, it is not valid to compare them statistically. A basic visual comparison, however, of the PC regression *L. franklinii* reconstruction and the STS *P. aspleniifolius* West reconstruction reveals some quite striking differences in the periods: 1810–1815, 1849, the late 1890s and 1908, when *L. franklinii* indicates colder than average temperatures and the

Figure 7.4: **Regional *Phyllocladus* maximum temperature reconstructions for East, West and Southwest. Over the nineteenth century the three regional time series move closely together in accordance with one another. In contrast, the three series show quite different movements over the twentieth century. Differences between East and West are readily discernible for the periods 1820–1830 and 1910–1930. Differences between East and Southwest are most evident in the twentieth century, particularly for the periods 1915–1920, the early 1930s, late 1960s–early 1970s. Differences between West and Southwest are most emphasised for the periods 1915–1920 and the early 1980s.**

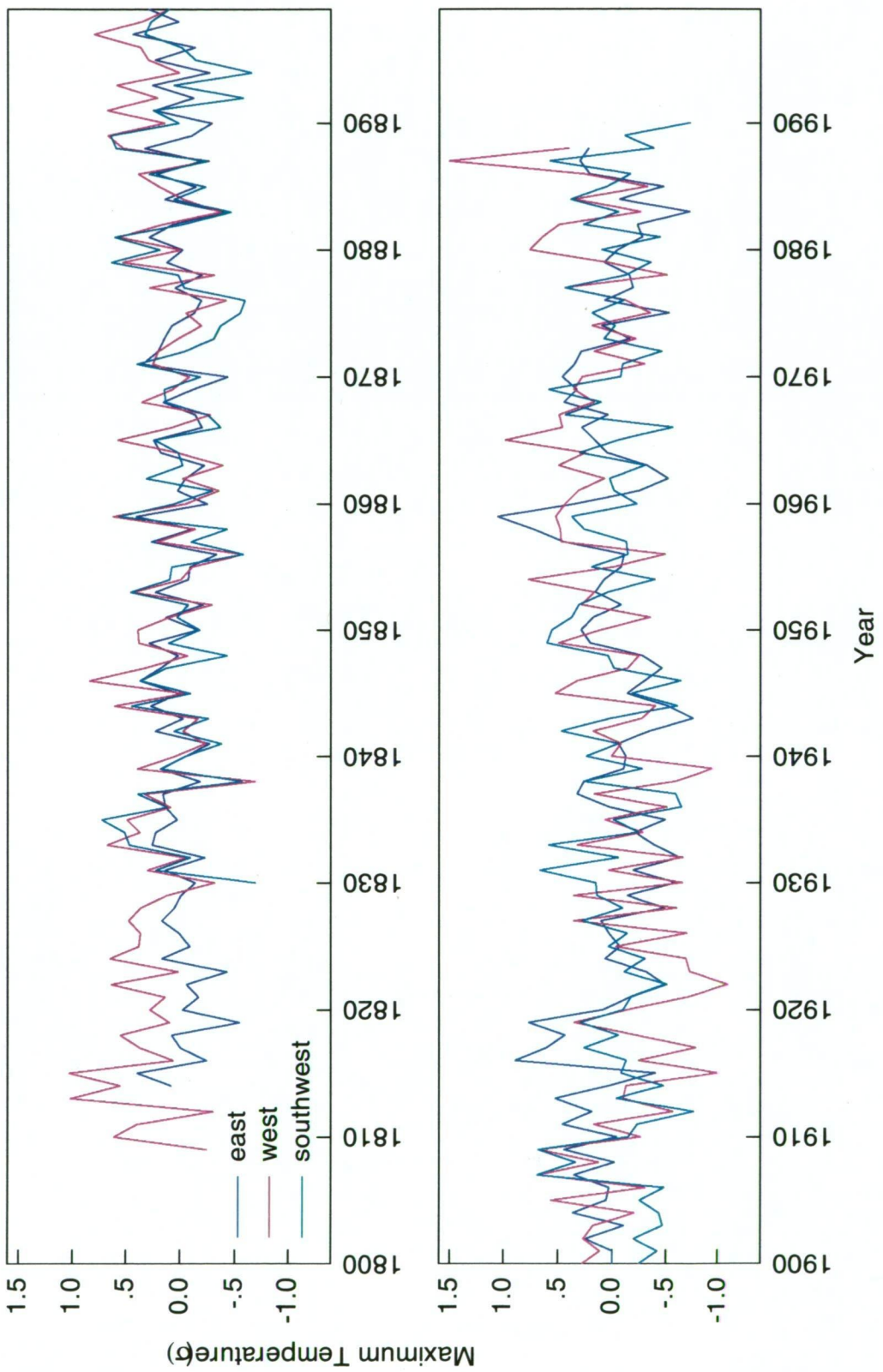
east
west
southwest
1.5
1.0
.5
0.0
-.5
-1.0
1800
1810
1820
1830
1840
1850
1860
1870
1880
1890
1900
1910
1920
1930
1940
1950
1960
1970
1980
1990
Year
Maximum Temperature(C)

P. aspleniifolius reconstruction indicates warmer than average temperatures (Figure 7.5). Opposite anomalies occur about 1915–1920 and in the early 1860s. Some general agreement between the two series can be seen, for example, the period from the 1880s to the mid 1890s is depicted as warmer than average and 1808–1832 also indicated to be warmer than average. Between 1940 and 1980, both reconstructions indicate increasing temperatures, although this trend is much more prominent in the *Lagarostrobos* reconstruction.

In general, however, there are large differences between the two reconstructions. It is possible that some of these differences may be attributed to elevational differences, as has been seen in the SRT (LOW) and MTREAD (HIGH) *Lagarostrobos franklinii* chronologies (Chapter 3). A further part of the difference is likely to be attributable to species differences.

7.4 Discussion

7.4.1 Validity of STS Reconstructions

Despite the fact that STS models have improved the quality of the reconstructions, explained variance in the models remains relatively low, suggesting that climatic reconstruction from this species may be neither viable nor reliable. The inferior performance of the STS model compared to the PC regression model for *Lagarostrobos franklinii* indicates that it may not be appropriate to model the relationship between *L. franklinii* and maximum temperature by STS. Indeed, Mavarall (1985) has commented that there are data sets for which an STS representation is inappropriate. In this study, the application of the simpler PC regression model has proven more suitable than the more complicated model.

With regard to the 'internal' validity of the *Phyllocladus aspleniifolius* reconstructions, some circumstantial evidence may be drawn from a comparison of the East and Southwest reconstructions over the past 180 years (Figure 7.4). The two series move closely together for the nineteenth century with an apparent change in their relationship immediately prior to the twentieth century. A change in the crossdating of the East and Southwest is also discernible at this time (Chapter 3). Prior to this, back to at least 1550, crossdating can readily be

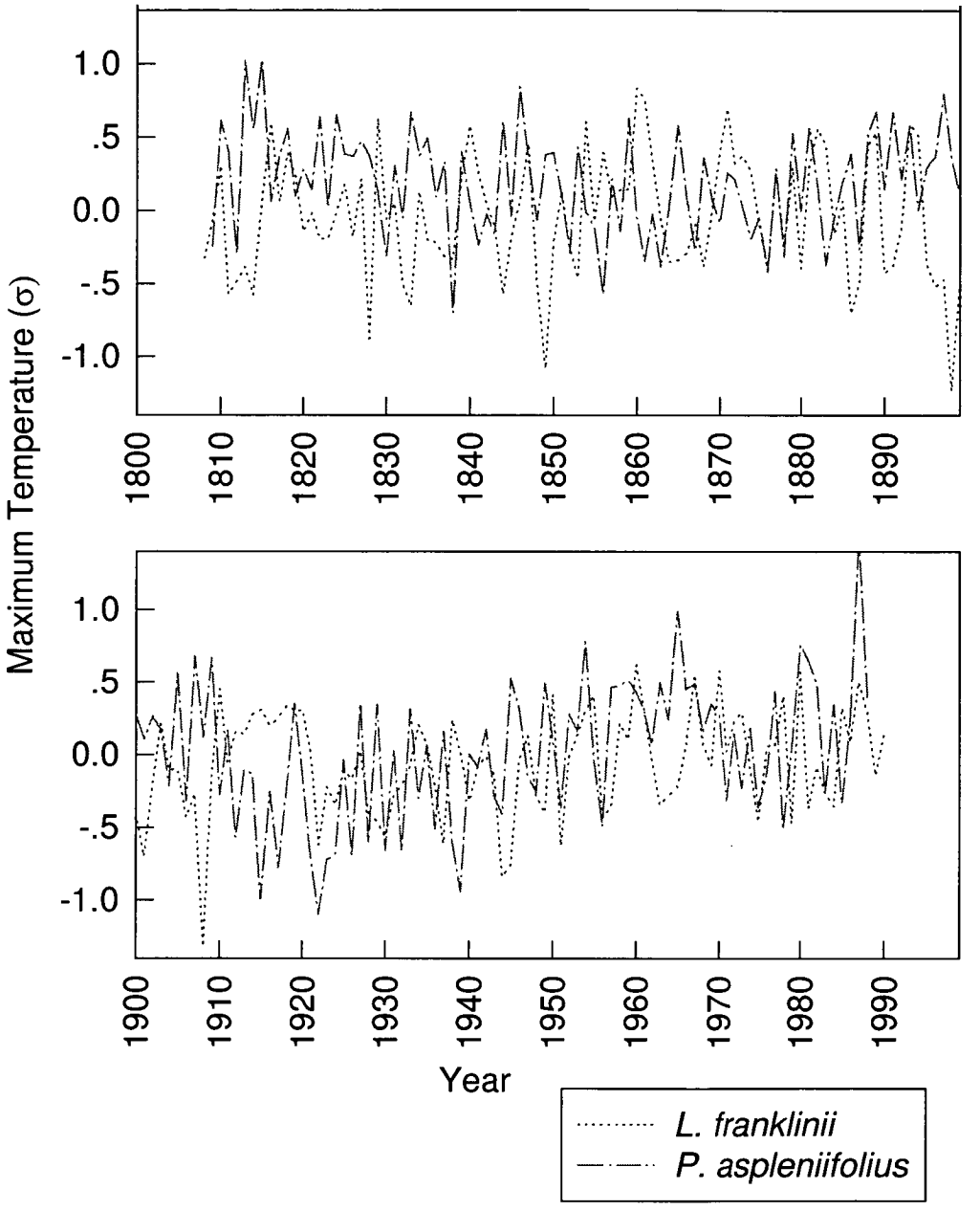

Figure 7.5: **Visual comparison of *Lagarostrobos franklinii* maximum temperature reconstruction with *Phyllocladus aspleniifolius* West maximum temperature reconstruction. Some commonality in trend is apparent but high frequency variation differs quite dramatically over the 180 years shown. This is not unexpected due to the lack of crossdating of the species. The greater higher frequency variability in the *P. aspleniifolius* reconstruction is a direct consequence of the high frequency variability inherent in the species**

established between these two regions, but becomes poor over the period 1890–1920. Two possible reasons for this are firstly, that disturbance over this time period has caused the change and, secondly, that climatic change is responsible.

During the nineteenth century, extensive tin mining existed around the township of Poimena on the top of Blue Tier, close to where many of the samples for the BLT_E site were collected. However, although gold was also found in the lower reaches of the northern slopes of Mt. Victoria and on the nearby Cottons Plains (Beaseley *et al.* 1993), the RFR_E site itself did not experience such extensive disturbance due to mining activities, but is also poorly correlated with the Southwest and West over this time period. This is not to entirely discount the impact of such extensive human disturbance on the BLT_E site. BEN_E, however, has been extensively disturbed in most recent times. It is also probable that the relative youth of this site is due to past Aboriginal burning in the area to the west of RFR_E (Beaseley *et al.* 1993).

Alternatively, Villalba *et al.* (1997) have commented on significant differences between nineteenth and twentieth century atmospheric circulation in the Southern Hemisphere, and Lamb and Johnson (1961) and Cook *et al.* (1996a) have described alternating periods of strong and weak westerly flow. The period from approximately 1800 to the late 1920s is characterised as one of enhanced zonal flow, while the period since the late 1920s is described as one of enhanced meridional flow, with a southward displacement of the subtropical high pressure belt, resulting in substantially drier and warmer conditions across the State. Regional temperature indices (Chapter 4) show an upward trend in the East and West only, implying that the effect of enhanced meridional flow is less evident in the Southwest of the State. However, as pointed out in Chapter 5, $CLAY_S$ has a response to temperature that is significantly different to those of SPR_S and LCR_S, and its inclusion in the transfer function may have had an important impact on the final Southwest reconstruction. Therefore, before much confidence can be placed in the Southwest reconstruction, it is advisable that a number of additional sites in the region, at greater elevation than $CLAY_S$, be sampled.

A further issue related to the validity of reconstructions is associated with the reliability of the initial instrumental data upon which the reconstructions

themselves are based. The work of LaMarche and Pittock (1982) discussed below is a prime example of this. The general agreement between a large number of records and studies based on these records does give some confidence in their reliability. The characteristics of data and the development of indices were described in Chapter 4, and it is believed that these indices are reliable representatives of regional climate. It must be recognised that the shortness and the relative sparseness of temperature records in the southwest of the State means that the Southwest reconstruction should be approached with additional caution.

7.4.2 The Tasmanian context

In order to establish whether or not the STS *Phyllocladus aspleniifolius* chronologies have any integrity, it is important to cross-check them with other reconstructions in the region. Two previously published temperature reconstructions for the Tasmanian region can be compared with the STS *P. aspleniifolius* reconstruction. The first is that of LaMarche and Pittock (1982), who have used a multispecies network to produce a single transfer function in order to reconstruct Statewide maximum temperatures (Figure 7.6). The second is the single species mean temperature reconstruction, based on higher elevation *Lagarostrobos franklinii*, by Cook *et al.* (1991, 1992, 1996a & b) and Buckley (1997) (Figure 7.7). Unfortunately, these two reconstructions conflict with one another. To some extent differences can be expected due to different climatic windows, as well as the reconstruction of different temperature variables and the use of different species. Perhaps the most important difference exists due to the inclusion of a number of different species with different responses to temperature in the one transfer function by LaMarche and Pittock. However, K. Peters (Lamont-Doherty Geological Earth Observatory, pers. comm.) has pointed out that the method of canonical regression analysis should, to some extent, have ameliorated these differences.

Two features which stand out as being very different in the reconstructions are the period at the turn of the century from approximately 1898–1910, and the more recent period, post 1950. The various *Lagarostrobos franklinii* reconstructions point to the turn of the century as being a particularly cool period and show a marked warming since these times. This is largely in accordance with

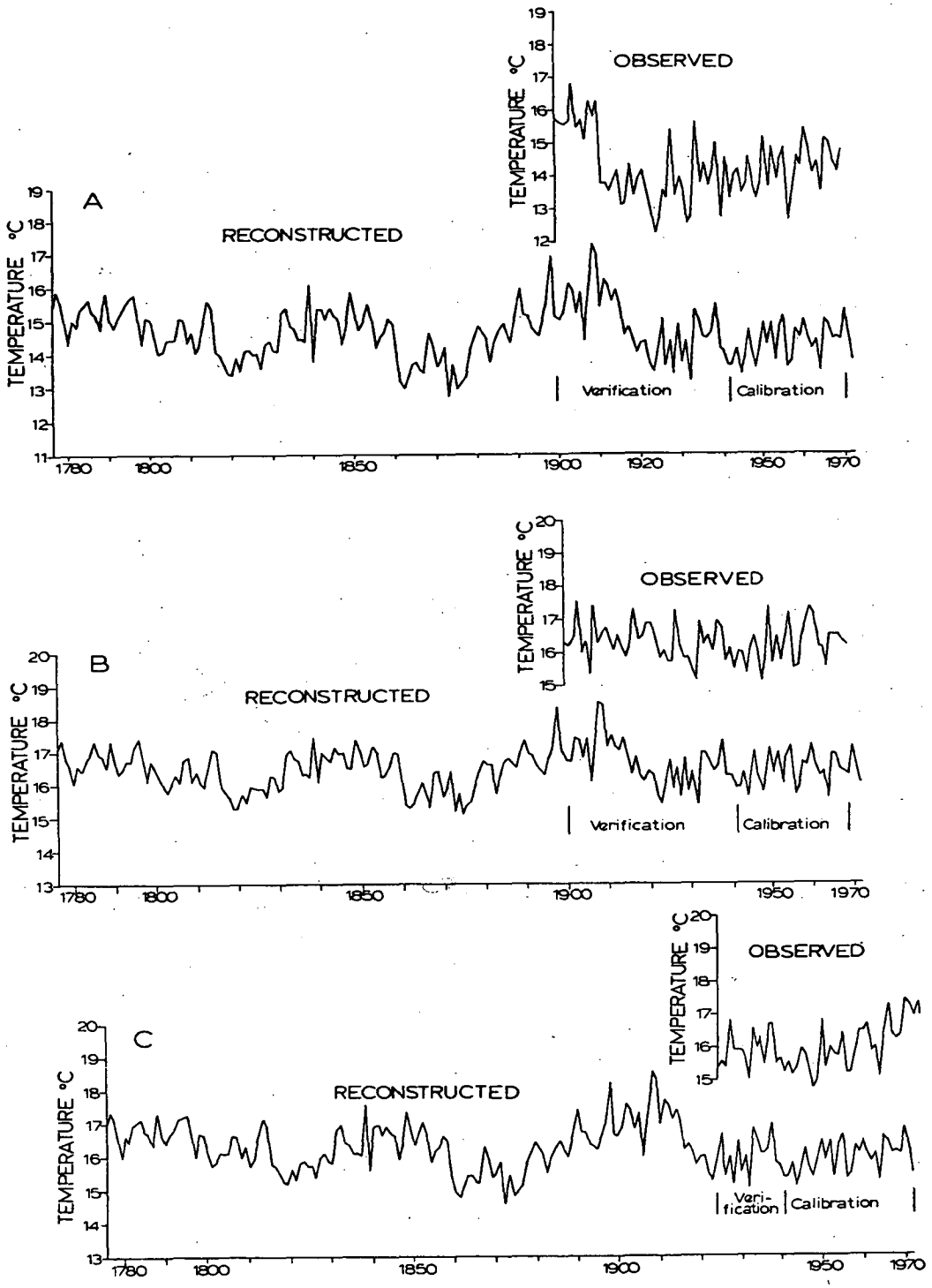

Figure 7.6: **LaMarche and Pittock warm season reconstructions (October–May) of mean maximum temperature for three Tasmanian stations: Waratah, Cape Sorell Lighthouse and Cape Bruny Lighthouse. Note the period around the turn of the twentieth century for all three reconstructions is given as warmer than average. Also note that neither the Waratah nor the Cape Bruny reconstructions successfully trace the observed temperature increase of most recent decades. Reconstructions were based on canonical components regression. Source: LaMarche and Pittock (1982)**

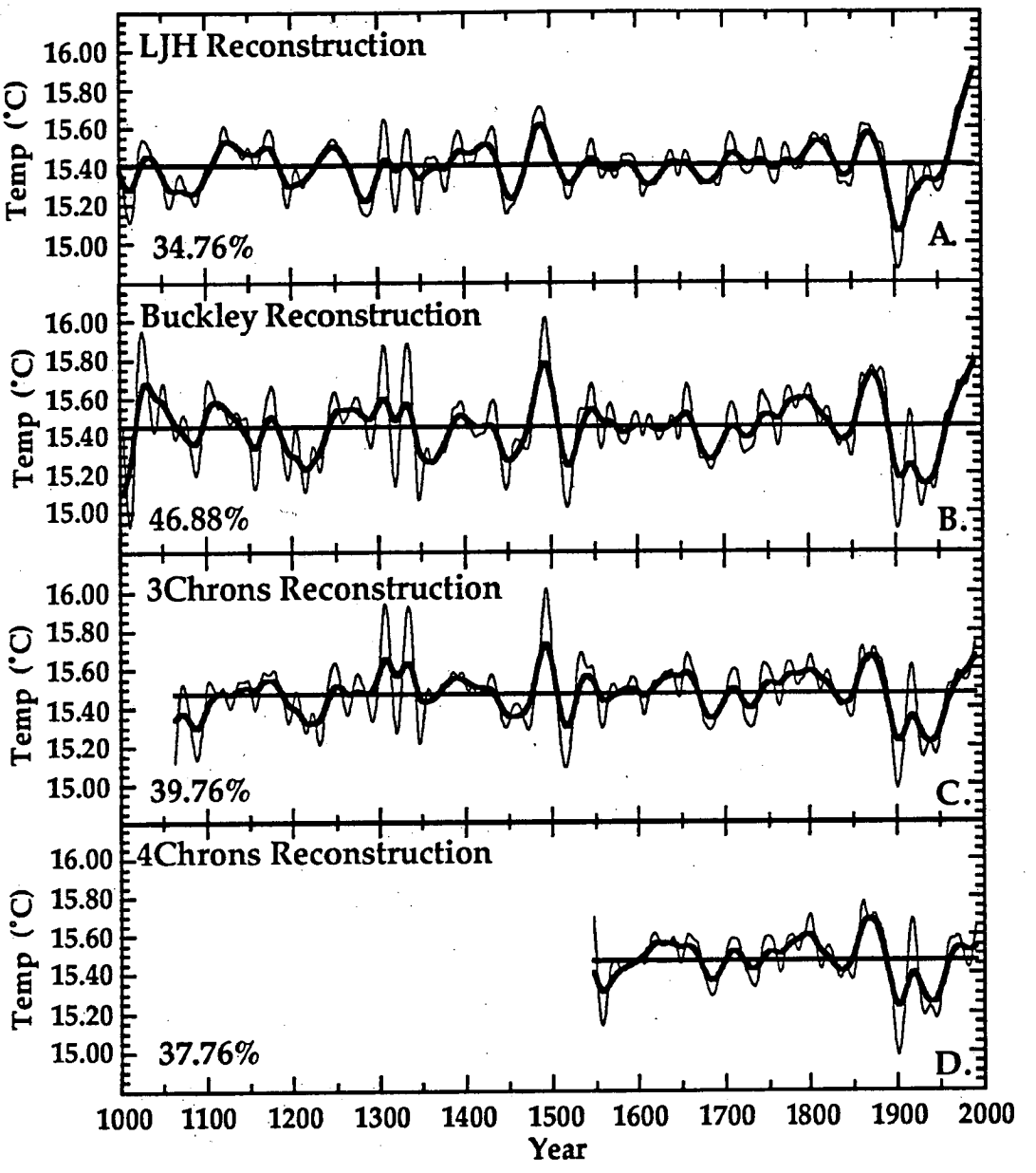

Figure 7.7: **The Buckley warm season (January–April) reconstructions of mean temperature. The four reconstructions are: A.: based on the Mt Read (LJH) site only, B. based on LJH and BCH (Frenchman's Cap area), C. LJH, BCH and LML (Frenchman's Cap area), D. all four chronologies above 700 m ASL: LJH, BCH, LML and LMH (Frenchman's Cap area). Source: Buckley (1997)**

available instrumental data at higher elevations, and much observational data in the Australia–New Zealand sector (D'Arrigo *et al.* 1995a). The LaMarche and Pittock reconstruction, on the other hand, shows the turn of the century as a markedly warm period and fails to reconstruct more recent temperature increases. While low elevation instrumental data does not imply the period around the turn of the century as markedly cool, it certainly does not suggest the period as the warmest period on record. One of the issues here is most likely related to the use of Waratah temperatures for verification. It is believed that the early portion of this temperature record is subject to serious error (Buckley 1997). The STS reconstruction does not reveal the late 1800s to early 1900s as either a particularly cold or warm period. This raises two issues: firstly, as Buckley suggested, that the use of the Waratah temperatures for verification influenced the LaMarche and Pittock reconstruction; and secondly, that species differences are likely to be important. In addition, differences in the two single species reconstructions may simply be the result of the lower elevation of the *Phyllocladus asplenifolius* sites in combination with the importance of physiological differences, as discussed in Chapter 5. It is important to note the poorer crossdating of higher and lower elevation *Lagarostrobos franklinii* sites at this point (Buckley 1997), and the closer association between different species at lower elevation sites for some time periods (Chapter 3).

The period of warming, depicted by Cook *et al.* (1991, 1992, 1996a & b) and Buckley (1997) as occurring since the 1920s, is also absent in the LaMarche and Pittock reconstruction, but present in their temperature data series. The STS reconstruction does reveal generally increasing temperatures between the late 1920s and approximately 1980, but for no region is this as pronounced as in the *Lagarostobos franklinii* reconstructions. The lower elevation of the *Phyllocladus* sites may be important in the de-emphasis of this trend, and it must also be noted that Buckley (1997) has failed to find evidence of increasing temperatures in the lowest elevation *L. franklinii* sites, at 225 and 450 m ASL.

7.4.3 Regional context

Tree-ring reconstructions from *Halocarpus biformis* (D'Arrigo *et al.* 1995) and *Nothofagus solandria* and *N. menziesii* (Norton 1983a & b) have traced the

temperature increase of recent decades (Figures 7.8 and 7.9). These chronologies also indicate the early 1800s as warm and the late 1840s and 1850s–1860s as being cool. The 1830s through to the 1860s has been noted as one of the coldest periods on record in New Zealand (Salinger *et al.* 1994), and the period around the turn of the century is noted as a cold period for the far south of New Zealand (D'Arrigo *et al.* 1995a & b). Buckley's (1997) reconstruction has also shown the late 1840s as a cold period, and the 1829–1854 as a generally cold period, corresponding with the New Zealand record. The West STS reconstruction (Figures 7.4, 7.5) indicates 1838 to be a cold year, but do not suggest the 1829–54 period as a whole to be particularly cold. Two members of the *Phyllocladus* genus, *P. trichomanoides* and *P. glaucus*, have been used by Palmer (1989) in an attempt to reconstruct summer temperatures (January–March) in New Zealand (Figure 7.9). This reconstruction does not reveal either of these features to the extent of the D'Arrigo *et al.* and Norton *et al* (1989) reconstructions and explains considerably less variance than either D'Arrigo *et al* or Norton *et al.* As has been commented upon in Chapter 5, Palmer (1989), and later Salinger *et al.* (1994) who have also used a number of *Phyllocladus* sites, note a definite difference between earlier and later calibration periods, with more variance being explained in the earlier period. This pattern is similar to the Tasmanian West and Southwest *Phyllocladus aspleniifolius* pattern (Chapter 5).

The fact that substantial differences between the New Zealand reconstructions themselves occur may again reflect species differences, although Palmer's sites are at considerably lower elevation than Norton's. This situation is not dissimilar to the *Lagarostrobos/Phyllocladus* situation in Tasmania. In turn, the clearer representation of increased temperatures in the Stewart Island chronologies of D'Arrigo *et al.* (1995a b) than in the Norton *et al.* (1989) chronologies may have been due either to species differences or to latitudinal differences.

Over the last 180 years in common among the various reconstructions, a general picture which emerges is one of increasing temperatures in the latter part of the record, and this is in agreement with almost all instrumental records for the region. The turn of the century as well as the approximate period 1830–1860, are

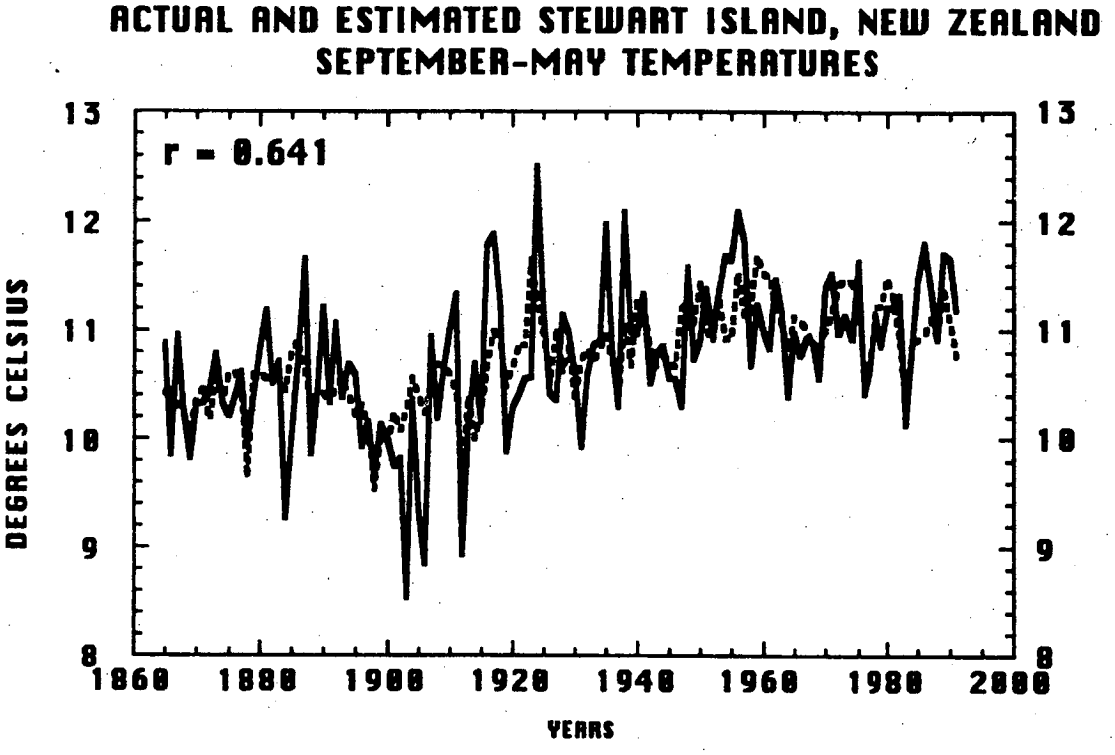

Figure 7.8: **D'Arrigo *et al.* (1995) reconstruction of Stewart Island temperatures. Actual (solid) September–May temperatures for 1865–1991 (based on 9:00 AM readings) and estimated (dashed) values based on ring-width chronology of *Halocarpus biformis*, Stewart Island. Tree estimates explain 41% of the variance in the instrumental temperature record. Adapted from D'Arrigo *et al.* (1995)**

depicted as being generally cool. From about 1880 to the late 1890s temperatures appear to have been above average. The fact that neither the Tasmanian species of the genus *Phyllocladus* nor the New Zealand species of the same genus convincingly reconstruct these features may be due to the standardisation techniques employed, elevational differences, sites not being at their limits with regard to temperature, and/or species differences.

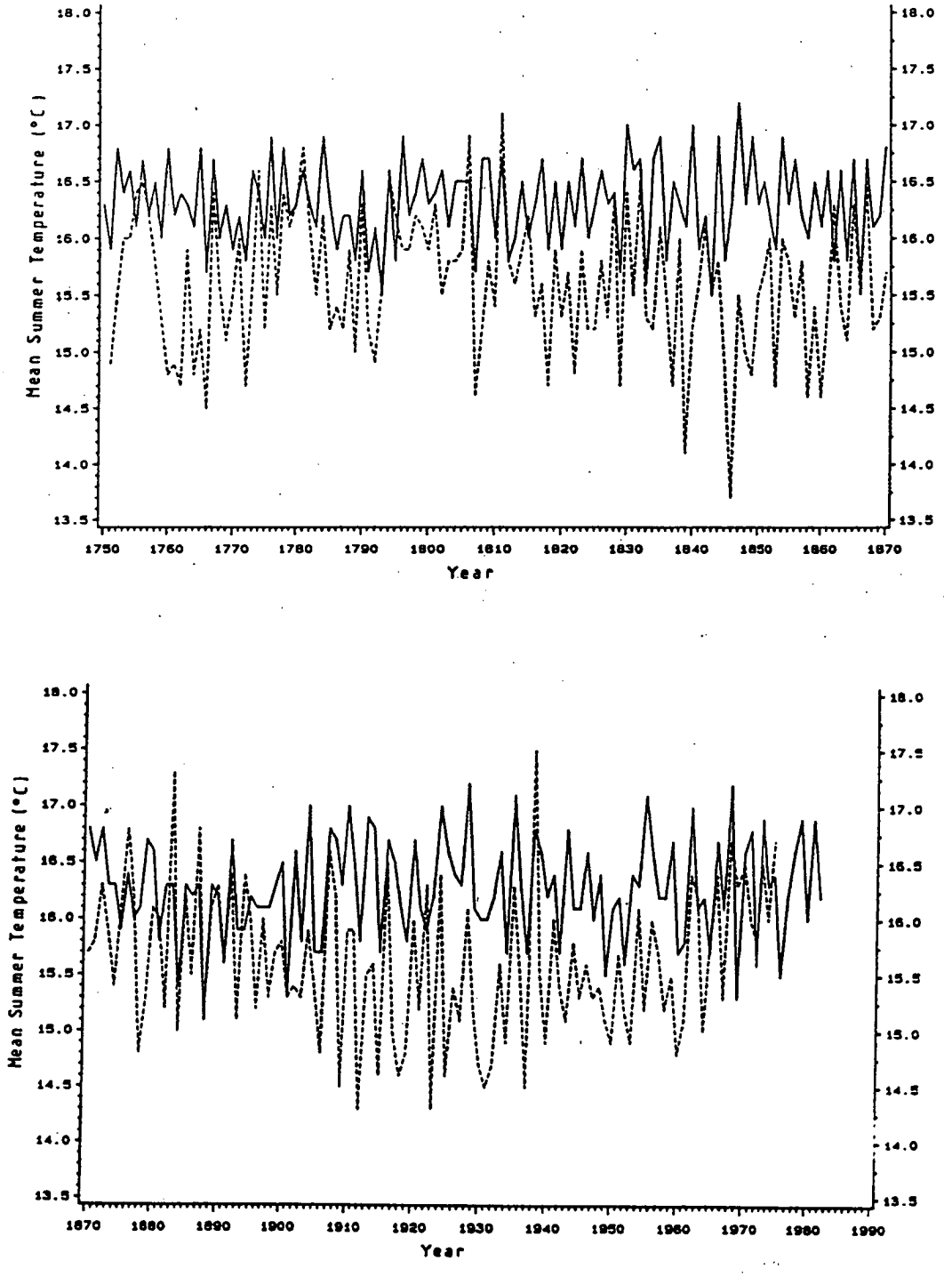

Figure 7.9: **Comparison of two reconstructions of New Zealand summer temperatures (1750–1982). Solid line is Palmer's (1989) reconstruction based on *P. glaucus and P. trichomanoides* and dashed line is Norton's (1983) reconstruction based on *Nothofagus sp.* Source: Palmer (1989)**

7.4.4 The STS Technique

The significant improvement in predictions, although insufficient to produce reconstructions from which one can draw confident inferences, suggests that STS modelling may represent a useful alternative to climate reconstruction techniques such as principal component regression if a number of limitations and theoretical issues can be resolved. One of the issues of concern in this study is the constancy or otherwise of the response to seasonalised data. Further work is required in order that this problem be more accurately gauged. The particular prospects and problems surrounding the use of STS in dendroclimatology fall into two broad classes: those issues concerning software applicability and workability and those concerning the methodology itself.

Diebold (1989) has pointed out several limitations of an earlier version of the package STAMP^{TM} used in this study. Although most of these have either been corrected in subsequent versions of the program or have had no bearing on the models utilised here, a number of problems remain. STAMP^{TM} has been designed with econometric applications in mind and an important limitation for dendroclimatology is the current inability of the program to generate 'forecasts' of more than 100 values. Because the use of STS models requires highly specialised software, few applications have been developed. Programs developed in the dendrochronological area which make use of the KF are currently being reviewed and updated in order that explanatory variables may be included (J. Gove, US Forest Service, pers. comm.).

In terms of the tenets of a good model, the STS technique provides a potentially more encompassing model, provides a better fit to the climatic data for *Phyllocladus aspleniifolius* and models are not unduly complicated although including a greater amount of information than the PC regression models. However, model verification is an important issue. Predictive testing does not provide the rigour of verification seen in PC regression models. This incompatiability with a split calibration–verification schemes, or to resampling techniques such as the bootstrap, is the most fundamental problem associated with the methodology. As Gordon and LeDuc (1981) have pointed out, the ability to successfully apply a calibrated model to an independent data set is imperative before any interpretation of a model can be made. So while internal statistics may

suggest a good model fit, it is not strictly possible to test the model on a temporally independent data set. Although this lack of verification on an independent data set is a weakness of the STS method, internal diagnostics provide a partial guide as to model performance and certainly provide valuable information on the *descriptive* value of the model. They cannot, however, be regarded as being equivalent to verification procedures.

Several authors have used relatively simple STS models in an analysis of the effect of climatic change or pollution on ring widths (e.g. Visser and Molenaar 1986, van Deusen 1989, 1990, 1991, Gove and Houston 1996), thereby concentrating on the trend component contained in the response functions. The emphasis in this chapter has been on the use of STS in the generation of a *transfer function* using a number of identified features of the climatic data as well as ring-width information.

Although it is apparent that the models produced are better in statistical terms than those produced by PC regression, it is not clear that the property of stochastic components is well suited to retrodiction of a climatic variable over a long time period. Due to the nature of the technique, each estimate is more heavily reliant on those immediately preceding it. In regression analysis, forecasting (or retrodiction) is based on the mean value of the process, while in STS it is based on the previous observations. In STS, as one becomes more distant from the 'end' of the climate data set, it is not implausible that the retrodicted vales produced by the model become increasingly tenuous as they are more dependent on those most recent retrodictions. The rate at which prior observations are discounted (and a high discount rate applies when disturbances are large) will be important in any determination of the point beyond which further retrodiction is inadvisable. In the PC regression model, the deterministic nature of the relationship means that this is not a problem. However, it is important to recognise that the use of the infinite memory filter by STS models ensures that the whole data set is used to calculate estimates and significant features, such as cycles or explanatory variables, and will be important in the regulation of the features of the series as retrodiction proceeds. Nevertheless, problems will arise if structural change occurs outside the period of the sampled dependent data (in this case, maximum temperature). This issue is not restricted

to the class of STS models, but also has important implications for the many regression models which can not, by their nature, consider structural change in their formulation.

The descriptive value of STS cannot be discounted, and the STS class of models provide the opportunity for far more encompassing and complete models than the PC regression method with which STS has been compared in this chapter. Such descriptive models allow some interpretation of the importance of particular climatic variables on ring-width growth in the presence of other components apparent in ring-width series. In this context then, STS models can provide an important starting point for some physiological investigations. For example, the use of statistically significant cycles as components distinct from the explanatory tree-ring variables adds a greater descriptive power to the climatic model. As discussed above, several investigators have already made use of KF-based models to examine changes in the trend component over time. In summary, the potential of STS models in climatic reconstruction requires further investigation into the nature of the technique, but as far as a descriptive model of tree growth is concerned, STS models of *Phyllocladus aspleniifolius* will often be superior to PC regression models.

7.5 Conclusions

The STS technique has resulted in improved estimates of temperature when using *Phyllocladus aspleniifolius*. However, the unsatisfactory results obtained when using *Lagarostrobos franklinii* demonstrate that this technique, like any other, is not universally applicable to the entire family of tree-ring indices. Although improvement of estimates occurs for *P. aspleniifolius*, the fundamental problem of a verification scheme remains a critical issue. The potential of STS models, especially with respect to their descriptive power, but also in terms of the role they might play in helping understand processes and improving the explanatory power of predictive models, requires further investigation, with attention being focussed on possible verification schemes and appropriate software.

Replicability and apparent strength of response function results across the State indicate that climatic information is contained in the rings of *Phyllocladus*

aspleniifolius. Consistency between the three regional reconstructions is highest for the nineteenth century, declining noticeably in the early 1900s. This may simply reflect changing atmospheric circulation patterns noted by numerous authors. Alternatively, it may reflect the importance of climatic changes on a regional basis (see Chapter 4), and associated changes in plant function due to the presence (for example) of temperature thresholds for these processes. Clear high frequency differences between the reconstruction of West *P. aspleniifolius* (STS) and *Lagarostrobos franklinii* (PC Regression) are most likely due to the QBORW in *P. aspleniifolius*. These two issues, the QBORW and a changing climate response over both time and space, require further investigation in order that differences in reconstructions between individual sites and different species can be better understood.

The relatively poor success in using *Phyllocladus* species in both Tasmania and New Zealand suggests that the genus itself responds in a different manner to climatic variables than a number of other species which have been used in dendroclimatology with greater success. Again, however, the role played by other factors, such as elevation and latitude, has not been sufficiently investigated. Although climatic information is contained within the ring widths of this species, a need still exists for a fuller understanding of its physiological characteristics before its full potential as a proxy climate indicator can be exploited. Once obtained, this information can be used to generate better statistical models which may in turn be used to produce more reliable climatic reconstructions. Due to characteristics identified as favourable for dendrochronology (see Ogden 1978a, Dunwiddie and LaMarche 1979, Campbell 1980, Bird *et al.* 1990), and also to the greater distribution of *Phyllocladus aspleniifolius*, compared to the long-lived *Lagarostrobos franklinii*, such information potentially enables a considerably richer understanding of climatic variability in the Tasmanian region.

Chapter 8: Conclusions

8.1 Summary

The richness of the Tasmanian dendroclimatological environment holds great promise, as discussed by previous authors (Ogden 1977, 1978a & b, LaMarche *et al.* 1979, Campbell 1980, Francey *et al.* 1984, Cook *et al.* 1991, Cook *et al.* 1992, Cook *et al.* 1996a & b, Buckley 1997). Little of this has yet been tapped despite over 20 years of research. Early efforts concentrated on the search for a number of species suitable for dendrochronology, while most recent efforts have been concentrated on the records provided by the long-lived and temperature sensitive *Lagarostrobos franklinii*. Crossdating of *Phyllocladus aspleniifolius* sites situated in a wide variety of environments is apparent across the State (Chapter 3), this confirming and expanding on the earlier work of Ogden (1978) and Dunwiddie and LaMarche (1980) who have previously demonstrated crossdating of the species in the west and southwest of the State. The existence of this Statewide crossdating confirms the importance of a macroscale influence on cambial growth. The weaker crossdating between the East and Southwest sites may reflect climatic differences, as intimated by Campbell (1980) and in Chapter 6, or be due to physiological plasticity of the species (Barker 1993).

The climate indices in Chapter 4 reveal a changing climate over the course of the twentieth century. The nature of the changing relationship between temperature and precipitation (significantly negative over the time scale studied) may well have some import for plant processes. These effects in turn can be expected to have an impact on the strength of the relationship between ring widths and climatic variables. In addition, the possibility that the south and north of the State have experienced different climatic changes over time (R. Allan, CSIRO, D. Shepherd, Bureau of Meteorology, pers. comm., Chapter 4 index series) creates further interest in the examination of proxy climate records extending back beyond the twentieth century.

The negative response to prior season temperature (minimum and maximum) shown in Chapter 5 has consistently been shown to be a feature of the species (Campbell 1980, LaMarche and Pittock 1982). A pattern of response to

precipitation across sites is less obvious, and more specific microsite information is necessary in order to gauge the true importance of moisture (as opposed to precipitation) to cambial growth of the species. Variability of site response is again obvious for ZI, MI and the SOI, although general patterns are apparent, especially for the ZI and SOI. Correlation with the ZI is essentially consistent between sites across the north of the State, regardless of region. Correlation between the SOI and cambial growth of Mersey, West and Southwest sites shows a remarkably consistent pattern while correlations with the East sites, while displaying a similar response, is less significant. The general pattern of response to temperature is similar to that for *Lagarostrobos franklinii*, although seasonality does differ somewhat, and a winter–spring correlation is more significant in *Phyllocladus aspleniifolius*.

The most consistent response, in space, is that of cambial growth to temperature. Regional differences do exist, however, and the Southwest is the most highly differentiated region. In this context, it can be seen that regionalisation has been a useful exercise in illuminating differences across the State. Whether or not these differences are directly related to climatic differences across such a small but topographically, vegetatively, geologically and geomorphologically diverse area, is unclear. The fact that no conclusions can be drawn regarding the influence of pH level, forest type, rock type and hence soil type, is consistent with Barker's (1993) finding that the species is insensitive to soil fertility and nutrient level. This provides some support for the supposition that sufficient differences in regional climates exist to produce different climate responses across sites.

At the same time, however, the responses described in Chapter 5 demonstrate that while *Phyllocladus aspleniifolius* does reflect climatic information of a 'broadscale nature', it is also sensitive to local conditions. This is highlighted in the changing responses to climate over the twentieth century, and Chapter 5 shows that few models, based on either the early or the late calibration periods, verify successfully. The response of sites within a region to temperature is considerably more coherent in the earlier time period than in the latter, suggesting temperature to be less limiting in the later period, and that individual site environments have become relatively more important. Figures 5.12–5.15 also

show that the responses to temperature and the ZI are also less defined for the later period, indicating less limiting conditions. Despite this, there are common patterns of change discernible across the sites, again inferring some macroscale control on cambial growth.

The existence of an elevational gradient in the response of *Lagarostrobos franklinii* to temperature is an important finding (Buckley *et al.* 1997). There is no strong evidence to support the existence of such a gradient in *Phyllocladus asplenifolius*. Nevertheless, weak evidence of it does exist, with a stronger current season response to temperature by the East sites, and $PILL_M$ (compared to other sites), all of which lie above 750 m ASL. On the other hand, $CLAY_S$, at sea level, displays a similar feature, and prior season response of the East sites and $PILL_M$ is not as clearly 'diminished' as Buckley found for *L. franklinii*. One possible reason for this latter feature is that the upper elevational limit in this study is not sufficient to see the same effect observed by Buckley.

The specific reason as to why such a gradient might occur is not clear, although the greater temperature limitation at higher elevations is likely to cause the current season response to be more pronounced at these sites. This is not, however, sufficient to explain why the prior season response is more emphasised at lower elevations and less significant at higher elevations. The photo-inhibition hypothesis briefly explored in Chapter 5 is one plausible mechanism for the differences, although it is by no means the only contender. Nor is it a completely satisfactory contender.

The clarity with which a climatic signal is present in the output of the QBORW has statistical implications when building and interpreting a chronology. If the QBORW is, by-and-large, a direct climatic signal, then the removal of the AR(2) process from models based on PC regression is inadvisable. At the present time, given the paucity of knowledge concerning the species and its physiological functions, the cause of the QBORW remains unelucidated. It is clear, however, that its cause cannot be resolved by simply subjecting it to statistical analyses, complex or otherwise.

Coupled with an inadequate understanding of plant physiological functions is an inability to apply appropriate statistical modelling procedures. Despite an attempt to apply an alternative set of more flexible models than the PC regression

models often used, satisfactory transfer functions have still not been successfully calculated. To date, dendroclimatological work has, understandably, concentrated on those species producing good statistical results. Other species, likely to contain important and supplementary information have been discarded due to what is perceived as greater complexity in their climatic response. It appears that at present, *Phyllocladus aspleniifolius* falls into this category. In essence, further efforts to extract information from these species by empirical means only are of little use until a fuller understanding of species physiology is attained. In Tasmania, *Lagarostrobos franklinii* has been the prized species for dendroclimatological investigation, both for its longevity, a number of excellent sites in limiting conditions, as well as its good temperature signal. It is not unlikely that further research on *Athrotaxis* spp. would show a similar potential for this species for related reasons. However, the broader ecological and geographical amplitude of *P. aspleniifolius*, while shorter lived, potentially provides information across the whole State, suggesting that further research into the species is warranted.

Although STS methodology has resulted in some improvements in reconstructions, this has not been sufficient to enable a high degree of confidence in the results. Regardless, any claim that a strong relationship between climate and the cambial growth of *Phyllocladus aspleniifolius* does not exist has not been shown to be true. Rather, what has been shown is that neither PC regression nor STS models provide a good statistical explanation of cambial growth, as dependent on temperature. It is certainly possible that the complexity of processes occurring within the tree prohibits finding a relatively simple mathematical relationship of any form between ring width and a climatic variable. Once again, the central and underlying issue is the lack of understanding of plant physiology.

Linked to this are the implications of the suggested nonconstant temperature response for climatic reconstruction. The reasons for the nonconstant response are not known, although it has been inferred that temperature thresholds for physiological processes may be important. Techniques relying on constant coefficients for climatic reconstruction can not be used in the face of a nonconstant relationship between independent and dependent variables.

Despite the difficulties encountered and the reasons for caution mentioned above, tentative temperature reconstructions of seasonalised maximum temperature (which shows a constant relationship with ring widths) based on the STS technique do show some similarities with other reconstructions in the region. Both *Lagarostrobos franklinii* and *Phyllocladus aspleniifolius* reconstructions show increasing temperatures over the latter part of this century, although this is less pronounced for *P. aspleniifolius* reconstructions. This trend of increasing temperatures is also seen in New Zealand reconstructions. However, other differences between *Phyllocladus* reconstructions and those based on other species remain and, in general, *Phyllocladus* spp. reconstructions, both in Tasmania and New Zealand, appear less robust than reconstructions from other species based on similar methodologies. It is important to note here that sites used in this thesis, although showing a temperature response, have not been severely limited by temperature. Palmer's (1989) study has suggested a similar reason for differences between *Nothofagus* spp. reconstructions and those of *Phyllocladus* spp in New Zealand. Additionally, at least some of the differences between the Tasmanian *Lagarostrobos franklinii* and *Phyllocladus aspleniifolius* reconstructions are likely to be related to elevational differences (Chapter 3). The QBORW in *P. aspleniifolius*, and the poor understanding of it, also creates some problems with respect to both the reconstruction process, and also to interpretations of any reconstructions.

8.2 Further Research

The dendrochronological and dendroclimatological investigation of *Phyllocladus aspleniifolius* has highlighted a number of areas requiring further research if the species is to be used to its full potential in climatic reconstruction. Several of the issues which arising during the course of this study can be considered to be fundamental in dendrochronological, dendroclimatological and dendroecological research. In broad terms, the recommended areas for further research fall into three categories.

The first of these relates to the *Phyllocladus* genus itself. The fact that the species is relatively long-lived, broadly distributed within New Zealand and Tasmania, crossdates well and is temperature-sensitive, points to it as a valuable

species for use in dendrochronological studies. The use of a network based on such a broadly distributed species eliminates uncertainties which might arise from using a network consisting of a number of species, each with its own limited distribution and individual response to climate. Nevertheless, problems surround attempts to reconstruct climate from its ring widths. A number of these relate to the unknowns of genus or species physiology which require further investigation. It may also be possible, through investigation of variables other than ring width, to obtain further useful information. Some information on $^{13}C/^{12}C$ variations (Pearman *et al.* 1976, Francey 1981, Francey and Farquhar 1982, Francey *et al.* 1984, Pepper, University of Sydney, pers. comm.), and ^{14}C variations (McPhail *et al.* 1983, Francey *et al.* 1984, Barbetti *et al.* 1992) in Tasmanian trees has already been obtained, and further research in this area may prove fruitful. Because measurements of wood density have been found at times to be more strongly related to climate than ring width information (e.g. Polge 1970, Parker and Henoch 1971, Briffa *et al.* 1998), such measurements for *P. aspleniifolius* may also prove to be more useful than ring widths in climatic reconstruction.

Secondly, throughout this study, the importance of, and need for, further detailed research into the physiology and growth of species useful in dendroclimatic research has been reinforced. Several other authors have also emphasised the need for such research (e.g. Palmer 1982, Buckley 1997). Buckley (1997) and Briffa *et al.* (1998) have both commented on the importance of thresholds in the response of ring width to climate, and Briffa *et al.* (1998) have alluded to their importance in a regime where climate is changing. The nonconstant nature of the growth response to monthly temperature, as found by Briffa *et al.* (1998), and in this study, presents a potentially serious obstacle to climate reconstruction. Furthermore, in considering responses of a number species jointly, as has been tentatively done here, it is important to acknowledge the differing thresholds and limits for these different species.

An issue which has attracted much attention over the past 20 years or so, and which uses dendroclimatological investigations as an important investigative tool, is that of global warming. To take just one simple example of how increasing temperatures might affect dendroclimatological records based on ring widths: it is known that if moisture stress occurs at a crucial time, a plant will

direct energy into reproduction (Kozlowski 1979). Kellomäki *et al.* (1997) noted that one of the effects of global warming on the timberline in Finland would be to increase both the quantity and quality of seed produced by *Pinus sylvestris.* The first question, which becomes apparent is, at what level will temperature become sufficiently high to inhibit cambial growth at the expense of reproductive processes at an individual site? Once this temperature threshold is reached, a narrow ring no longer implies a cold year, causing problems for dendroclimatic interpretation. Secondly, if considering sites of one species along an elavational transect (e.g. LaMarche 1974a, Buckley 1997), how will crossdating, and high and low frequency agreement between series be affected, and to what degree? Finally, how will any relationships established between different species be affected? Specifically focusing on *Phyllocladus asplenifolius*, what would be the effect of continuing temperature increases on the QBORW, especially if it is a reasonably direct function of alternating seed production? If indeed alternate years of heavy seed crops *do* result in the QBORW, then do past periods when the oscillation is more apparent in ring widths indicate warmer periods? A deeper understanding of thresholds may not only reduce errors in climatic reconstructions, but also assist with the interpretation of differences between disparate sites of a single species and between different species.

One starting point from which to more accurately assess the manner in which cambial growth of a species responds to climate would be to monitor the cambial response to a number of environmental variables simultaneously, at a fine resolution, such as monthly, weekly or even daily. Some variables of obvious interest are soil moisture, site temperatures (minimum and maximum), solar radiation, site humidity, leaf water potential and gas exchange. Evidence of different responses along an elevational gradient would seem to suggest the need for at least two monitoring stations — one at high elevation, and one at low elevation — in order to assess what differences between higher and lower elevation sites are due to exposure to different climatic conditions and what can be attributed to different physiological responses to different climatic conditions which exist at high and low elevations.

The third area of interest for further research is the development and effective use of a multiple species network. Potentially, such a network could provide immensely valuable insights in addition to those that have already been gained. Over 20 years ago, Ogden (1977) intimated that the use of a number of species, sensitive to different climatic variables, could provide a detailed portrait of past climatic variation in the State. In addition, a great deal of valuable ecological information may be gained. The approaches of the broader but less detailed early efforts and the most recent detailed but less broad investigations need to be combined to produce a multiple species network of well studied species. This would allow the integration of information concerning individual species characteristics with that available from a network of a number of different species across the State. Due to its relatively small size and numerous species already found to be suitable for dendrochronological work (Ogden 1977, 1978a, 1978b, Dunwiddie and LaMarche 1980, Bird *et al.* 1990), Tasmania represents an ideal testing ground for the additional utility of a multiple species network in the State.

The construction of an optimal network would provide a fuller understanding of climatic change and its effects across the State and in the region generally. Currently, dendrochronological sites of *L. franklinii* are restricted to the west coast area despite the occurrence of the species in the southwest of the State; at present these additional sites can not be utilised. The distribution of most species in the State already asserted to have dendroclimatological potential is restricted to the west and southwest of the State. However, information provided by the more broadly, and eastern, distributed species such as *Phyllocladus aspleniifolius* and some *Eucalyptus* species would provide an invaluable complement to that which has been obtained from the longer-lived, but distributionally restricted, species. Results here have shown that, although species differences are readily apparent between *L. franklinii* and *P. aspleniifolius*, some commonality does exist, as reflected in cross-spectral analyses. In addition, it is likely that not all differences will be directly related to species differences, with changes in response to temperature over time apparent for both species, but considerably less so for *L. franklinii* (see Chapter 5). Furthermore, the possibility

of an changing response to temperature with elevation by a number of species requires further investigation.

In order to effectively explore the uncertainties raised in this study, future research efforts need to be focused on both physiological investigation as well as on the development of multiple species networks. Further analysis of physiological responses to climatic variables is likely to result suggest more appropriate statistical methodologies for the production of reconstructions from species additional to those already producing high quality climate reconstructions.

But the issues raised here go beyond those which concern a single species, or even a small group of species. Why do a number of studies imply a time-dependence in the response of cambial growth to climate, and how important is the consideration of this time-dependence for climatic reconstructions? How important are thresholds for the cambial growth of different species? What are the implications of global warming for the interpretation of dendroclimatological records? How is it possible, using dendrochronological techniques, to paint a comprehensive, yet broad, picture of past climatic variability with regard to species and community changes? How might more accurate and relevant statistical models be developed for climatic reconstruction? These are fundamental questions, and it is time that additional effort be directed towards a fuller understanding of plant physiology which would undoubtedly assist the dendroclimatologist or dendroecologist in his/her endeavour.

References

Adamson, D.A., Whetton, P., and Salkirk, P.M., 1988; An analysis of air temperature records for Macquarie Island: decadal warming, ENSO cooling, and Southern Hemisphere circulation patterns Journal of the Royal Society of Tasmania 122(1), 107–111

Ahmed, M. and Ogden, J., 1985; Modern New Zealand tree-ring chronologies III *Agathis australis* (Salisb.) – *Kauri* Tree-ring Bulletin 45, 11–23

Akaike, H., 1974; A new look at the statistical model identification IEEE Transactions on Automatic Control AC19, 716–723

Allan, R.J., 1993; Historical fluctuations in ENSO and teleconnection structure since 1879: near global patterns, Paper presented at Quaternary Palaeoclimatic Mapping: A Protocol for Australia Monash Dec 2–4 1992

Allan, R.J., Lindesay, J.A. and Reason, C.J.C., 1995; Multidecadal variability in the climate system over the Indian Ocean region during the Austral summer Journal of Climate 8(7), 1,853–1,873

Allen, K., 1991; An Empirical Orthogonal Function and Spectral Analysis of Tasmanian Rainfall Unpublished Honours thesis, University of Tasmania, 137pp

Allen, K., 1997; A structural time series approach to dendroclimatology: *Phyllocladus aspleniifolius*, Proceedings of the Institute of Australian Geographer's and New Zealand Geographical Society Second Joint Conference, Hobart, Australia 1997, Dept. Geography, University of Waikato, 392–396

Anderson, R.Y., 1992, Long-term changes in the frequency of occurrence of El Niño events, in Diaz, H.F. and Markgraf, V. (Eds.) El Niño: Historical and Palaeoclimatic Aspects of the Southern Oscillation Cambridge University Press, Cambridge, 193–200

Angell, J.K, 1994; Global, hemispheric, and zonal temperature anomalies derived from radiosonde records, in Boden, T.A., Kaiser, R.J., Sepanski, R.J. and Stoss, F.W. (Eds.) Trends 93: A Compendium of Data on Climate Change ORNL/CDIA-65. Carbon Dioxide Information Analysis Centre, Oak Ridge National Laboratory Oak Ridge, Tennessee, USA, 636–672

Ash, J., 1983; Tree rings in tropical *Callitris macleayana* Australian Journal of Botany 31, 277–281

Baes, C.F. and McLaughlin, S.B., 1984, Trace elements in tree rings: evidence of recent and historical air pollution Science 224, 494–496

Balmer, J., 1991; Buttongrass moorlands vegetation, in Kirkpatrick, J.B., Pharo, A.J., Wells, A., Mendel, L. and Lynch, A.J.J. (Eds.) Tasmanian Native Bush: A Management Handbook Tasmanian Environment Centre, Hobart, 76–91

Banks, M. R., 1962; Cambrian system Journal of the Geological Society 9(2),127–146

Barbetti, M., Bird, T., Dolezal, G., Taylor, G., Francey, R., Cook, E. and Peterson, M., 1992; Radiocarbon variations from Tasmanian conifers: first results from late Pleistocene and Holocene logs Radiocarbon 34(3), 806–817

Barker, P.C.J., 1993; *Phyllocladus aspleniifolius* and *Anodopetalum biglandulosum:* A Comparative Autecology of Coexisting Wet Forest Trees in Tasmania Unpublished PhD thesis, University of Tasmania, 256pp

Barker, P.C.J., 1995; *Phyllocladus aspleniifolius*: Phenology, germination, and seedling survival New Zealand Journal of Botany 33, 325–337

Barker, P.C.J. and Kirkpatrick, J.B., 1994; *Phyllocladus aspleniifolius*: variability in the population structure, the regeneration niche and dispersion patterns in Tasmanian forests Australian Journal of Botany 42, 163–190

Beasley, C., Green, C., Hughes, L. and Pocock, C., 1993; An Archaeological Management Plan for the Mt Victoria Rockshelter Complex, Northeast Tasmania Draft Report, for the National Estate, Forestry Commission, Tasmania

Bender, M., Sowers, T., Dickson, M.-L., Orchardo, J., Grootes, P., Mayewski, P.A. and Meese, D.A., 1994; Climate correlations between Greenland and Antarctica during the past 100,000 years Nature 372, 663–666

Bieleski, R.L., 1959; Factors affecting growth and distribution of Kauri (*Agathis australis* Salisb.): I. The effect of light on the establishment of Kauri and *Phyllocladus trichomanoides* D. Don. Australian Journal of Botany 7, 252–267

Bird, T.B., Dolezal, J., Barbetti, M. and Francey, R., 1990; Tree-rings as indicators of environmental change Tasforests 2(2), 99–105

Bisset, I.J.W, Dadswell, H.E. and Wardrop, A.B., 1951; Factors influencing tracheid length in conifer stems Australian Forestry 15(1), 17–30

Bjerknes, J., 1969; Atmospheric teleconnections from the equatorial Pacific Monthly Weather Review 97(3), 163–172

Blasing, T.J., Duvick, D.N. and West, D.C.,1981, Dendroclimatic calibration and verification using regionally averaged and single station precipitation data Tree-Ring Bulletin 41, 37–43

Blasing, T.J., Solomon, A.M. and Duvivk, D.N., 1984; Response functions revisited Tree-Ring Bulletin 44, 1–15

Bloomfield, P., 1976; Fourier Analysis of Time Series: An Introduction John Wiley and Sons, New York, 258pp

Box, G.E.P. and Jenkins, G.M., 1970; Time Series Analysis: Forecasting and Control Holden-Day, San Fransisco, 553pp

Bradford, K.J., and Hsiao, 1981; Physiological responses to moderate water stress in Lange, O.L., Nobel, P.S., Ziegler, H. (Eds.) Physiological Plant Ecology II. Water Relations and Carbon Assimilates Springer-Verlag Berlin, 263–324

Bradley, R. S., 1985; Quaternary Palaeoclimatology: Methods of Palaeoclimatic Reconstruction Allen and Unwin, London, 472pp

Brázdil, R. and Zolotokrylin, A.N., 1995; The QBO signal in monthly precipitation fields over Europe Theoretical and Applied Climatology 51, 3–12

Brier, G.W., 1978; The quasi-biennial oscillation and feedback processes in the atmosphere-ocean-earth system Monthly Weather Review 106, 938–946

Briffa, K. and Jones, P.D., 1990; Basic chronology statistics and assessment, in Chapter 3 of Cook and Kariukstis (Eds.) Methods of Dendrochronology: Applications in the Environmental Sciences Kluwer Academic Publishers, Dordrecht, 394pp

Briffa, K.R., Schweingruber, F.H., Jones, P.D., Osborn, T.J., Shiyatov, S.G. and Vaganov, E.A., 1998; Reduced sensitivity of recent tree-growth to temperatures at high northern latitudes Nature 391(12), 678–682

Brinkmann, W.A.R., 1987; Water supplies to the Great Lake - reconstructed from tree-rings Journal of Climate and Applied Meteorology 26, 530–538

Brodribb, T., 1997; Southern Hemisphere Conifers: Distribution and History Interpreted From a Physiological Perspective Unpublished PhD thesis, University of Tasmania, 177pp

Brown, C.L., 1970; Physiology of wood formation in conifers Wood Science 3(1), 8–22

Brown, M.J. and Podger, F.D., 1982; Floristics and fire regimes of a vegetation sequence from sedge-land to rainforest at Bathurst Harbour, Tasmania Australian Journal of Botany 30, 659–676

Brown, P.M. and Sieg, C.H., 1996; Fire history in interior Ponderosa Pine communities of the Black Hills, South Dakota, USA International Journal of Wildland Fire 6(3), 97–105

Bryson, R.A., 1985; On climatic analogs in paleoclimatic reconstructions Quaternary Research 23, 275–286

Buchanan, A.M. (Ed.) 1995; A Census of the Vascular Plants of Tasmania and Index to The Student's Flora of Tasmania Tasmanian Herbarium Occasional Publication No. 5, Tasmanian Museum and Art Gallery, Hobart, Tasmania

Buckley, B.M., 1997; Climate Variability in Tasmania Based on Dendroclimatic Studies of *Lagarostobos franklinii* Unpublished PhD thesis, University of Tasmania, 167pp

Buckley, B.M., Barbetti, M. and Watanasak, M., 1995; On the prospect of large–scale spatial reconstruction of climate from tropical south–east Asian tree–rings, in Ohta, S., Fujii, T., Okada, N., Hughes, M.K. and Eckstein, D. (Eds.) Tree Rings: From the Past to the Future : Proceedings of The International Workshop on Asian and Pacific Dendrochronology, March 4–9, Tsukuba and Okutama, Japan, 76–87

Buckley, B.M., Cook, E.R., Peterson, M.J. and Barbetti, M., 1997; A changing temperature response with elevation for *Lagarostrobos franklinii* in Tasmania, Australia Climatic Change 36(3–4), 477–498

Burrett, C.F. and Martin, E.L., 1989; Geology and Mineral Resources of Tasmania Geological Society of Australia Incorporated, Special Publication No. 15, 574pp

Buszard, D. and Schwabe, W.W., 1995; Effect of previous crop load on stigmatic morphology of apple flowers Journal of the American Society of Horticultural Science 120(4), 566–570

Bureau of Meteorology, 1975; Climatic Averages: Tasmania and Miscellaneous Australian Government Publishing Service, 48pp

Bureau of Meteorology, 1993; Climate of Tasmania Commonwealth of Australia, 30pp

Campbell, D.A., 1980; The Feasibility of Using Tree-ring Chronologies to Augment Hydrologic Records in Tasmania, Australia Unpublished Masters thesis, University of Arizona, 175pp

Cannell, M.G.R. and Dewar, R.C., 1994; Carbon allocation in trees: a review of concepts for modelling Advances in Ecological Research 25, 59–104

Chatfield, C. 1975; The Analysis of Time Series Chapman and Hall, London, 263pp.

Cleaveland, M.K., 1986; Climatic response of densitometric properties in semi-arid site tree rings Tree-Ring Bulletin 46, 13–29

Colhoun, E.A. and Van De Geer, G., 1986; Holocene to Middle Last Glaciation vegetation history at Tullarbardine Dam, western Tasmania Proceedings of the Royal Society of London B 229, 177–207

Colhoun, E.A. and Fitzsimons, S.J., 1990; Late Cainozoic glaciation in western Tasmania Quaternary Science Reviews 9, 199–216

Colhoun, E.A., Van De Geer, G., and Hannan, D., 1991; Late glacial and Holocene vegetation history at Dublin Bog north-central Tasmania Australian Geographic Studies 29, 337–354

Colhoun, E.A., Van De Geer, G. and Fitzsimons, S.J., 1992; Late Quaternary organic deposits at Smelter Creek and vegetation history of the middle King Valley, western Tasmania Journal of Biogeography 19, 217–227

Cook, E.R., 1985; A Time Series Analysis Approach to Tree-ring Standardisation Unpublished PhD thesis, University of Arizona, 171pp

Cook, E.R., 1990; A conceptual linear aggregate model for tree rings, in Chapter 3 of Cook and Kariukstis (Eds.) Methods of Dendrochronology: Applications in the Environmental Sciences Kluwer Academic Publishers, Dordrecht, 98-104

Cook, E.R. and Peters, K., 1981; The smoothing spline: a new approach to standardizing forest interior tree-ring width series for dendroclimatic studies Tree-Ring Bulletin 41, 45–58

Cook, E.R. and Jacoby, G.C. Jr., 1979; Evidence for quasi-periodic July drought in the Hudson Valley, New York Nature 282, 390–392

Cook, E.R., Johnson, A.H. and Blasing, T.J., 1987; Forest decline: modeling the efect of climate in tree rings Tree Physiology 3, 27–40

Cook, E.R., Briffa, K., Shiyatov, S. and Mazepa, V., 1990a; Tree-ring standardisation and growth-trend estimation, in Chapter 3 of Cook and Kariukstis (Eds.) Methods of Dendrochronology: Applications in the Environmental Sciences Kluwer Academic Publishers, Dordrecht, 394pp

Cook, E.R., Shiyatov, S. and Mazepa, V., 1990b; Estimation of the mean ring width chronology, in Chapter 3 of Cook and Kariukstis (Eds.) Methods of Dendrochronology: Applications in the Environmental Sciences Kluwer Academic Publishers, Dordrecht, 394pp

Cook, E.R., Bird, T., Peterson, M., Barbetti, M., Buckley, B., Francey, R., Martins, D. and Tans, P., 1991; A 1089-year temperature record for Tasmania inferred from tree rings of subalpine Huon Pine Science 253, 1266–1268

Cook, E.R., Bird, T., Peterson, M., Barbetti, M., Buckley, B., D'Arrigo, R. and Francey, R., 1992; Climatic change over the last millenium in Tasmania reconstructed from tree-rings The Holocene 2(3), 205–217

Cook, E.R., Briffa, K.R. and Jones, P.D., 1994; Spatial regression methods in dendroclimatology: a review and comparison of two techniques International Journal of Climatology 14, 379–402

Cook, E.R., Briffa, K.R., Meko, D.M., Graybill, D.A. and Funkhouser, G., 1995; The 'segment length curse' in long tree-ring chronology development for palaeoclimatic studies The Holocene 5(2), 229–237

Cook, E.R., Buckley, B.M. and D'Arrigo, R.D., 1996a; Inter-decadal climate oscillations in the Tasmanian sector of the southern hemisphere: evidence from tree rings over the past three millenia, in Jones, P.D., Bradley, R.S., Jouzel, J (Eds.) Climate Variations and Forcing Mechanisms of the Last 2000 Years Springer-Verlag Berlin, 141–160

Cook, E.R., Francey, R.J., Buckley, B.M. and D'Arrigo, R.D., 1996b; Recent increases in Tasmanian Huon Pine ring widths from a subalpine stand: natural climate variability, or greenhouse warming? Papers and Proceedings of the Royal Society of Tasmania 130 (2), 65–71

Craddock, J.M., 1973; Problems and prospects for eigenvector analysis in meteorology The Statistician 22, 133–145

Crafts, N.F.R., Leybourne S.J. and Mills, T.C., 1990; Measurement of trend growth in European industrial output before 1914: Methodological issues and new estimates Explorations in Economic History 27, 442–467

Cullen, P.J., 1987; Regeneration patterns in population patterns of *Athrotaxis selaginoides* D. Don. from Tasmania Journal of Biogeography 14, 39–51

Cullen, P.J., 1991; Rainforest, in Kirkpatrick, J.B., Pharo, A.J., Wells, A., Mendel, L., Lynch, A.J.J. (Eds.) Tasmanian Native Bush: A Management Handbook Tasmanian Environment Centre, Hobart, 24–34

D'Arrigo, R.D. and Jacoby, G.C., 1991; A 1000-year record of winter precipitation from northwestern New Mexico, USA: a reconstruction from tree-rings and its relation to El Niño and the Southern Oscillation The Holocene 1(2), 95–101

D'Arrigo, R.D., Jacoby, G.C. and Free, R., 1992; Tree-ring width and maximum latewood density at the North American tree line: parameters of climatic change Canadian Journal of Forest Research 22, 1,291–1,296

D'Arrigo, R.D., Jacoby, G.J., Jr., 1993; Secular trends in high northern latitude temperature reconstructions based on tree rings Climatic Change 25, 163–177

D'Arrigo, R.D., Cook, E.R., Jacoby, G.C. and Briffa, K.R., 1993; NOA and sea surface temperature signatures in tree-ring records from the North Atlantic sector Quaternary Science Review 12, 431–440

D'Arrigo, R.D., Buckley, B.M., Cook, E.R. and Wagner, W., 1995a; Temperature-sensitive tree-ring width chronologies of pink pine (*Halocarpus biformis*) from Stewart Island, New Zealand Palaeogeography, Palaeoclimatology, Palaeoecology 119, 293–300

D'Arrigo, R.D., Cook, E.R., Buckley, B.M. and Krusic, P.J.,1995b; Tree-ring records from subantarctic forests in New Zealand, in Mikami, T., Matsumoto, E., Ohta, S., Sweda, T. (Eds.) Paleoclimate and Environmental Variability in Austral-Asian Transect During the Past 2000 Years: Proceedings of the 1995 Nagoya IGPB-PAGES/PEP-II Symposium, 126–137

Deacon, E.L., 1953; Climate in Australia since 1880 Australian Journal of Physics 6, 209–218

Dean, J., 1978; Tree-ring dating in archeology, in Miscellaneous Collected Papers 19–24, University of Utah Press, Salt Lake City, 129–163

de Jong, P. and Chu-Chun-Lin, S., 1994; Fast likelihood evaluation and prediction for nonstationary state space models Biometrika 81, 133–142

Demmig-Adams, B. and Adams, W.W., 1992; Photoprotection and other responses of plants to high light stress Annual Review of Plant Physiology and Molecular Biology 43, 599–626

Diebold, F.X., 1989; Structural time series analysis and modelling package: a Review Journal of Applied Econometrics 4, 195–204

Douglass, A.E., 1920; Evidence of climatic effects in the annual rings of trees Ecology 1, 24–32

Douglass, A.E., 1928; Climatic Cycles and Tree Growth. Vol II: A Study of the Annual Rings of Trees in Relation to Climate and Solar Activity Carnegie Institute of Washington Publication No. 289, 166 pp.

Drosdowsky, W., 1993; An analysis of Australian seasonal rainfall anomalies: 1950 –1987. II: Temporal variability and teleconnection patterns International Journal of Climatology 13, 111–149

Duncan, F., Introduction, in Kirkpatrick, J.B., Pharo, A.J., Wells, A., Mendel, L., Lynch, A.J.J. (Eds.), 1991; Tasmanian Native Bush: A Management Handbook Tasmanian Environment Centre, Hobart, 1–16

Duncan, F., Hocking, G.J. and Read, J., 1990; Rainforest, in Tasmanian Wilderness Royal Society of Tasmania and the Tasmanian Parks and Wildlife Service, Hobart, Tasmania

Dunwiddie, P.W., 1979; Dendrochronological studies of indigenous New Zealand trees New Zealand Journal of Botany 17, 251–266

Dunwiddie, P.W., 1982; Comment, in Hughes, M.K., Kelly, A.M., Pilcher, J.R., LaMarche, V.C. Jr. (Eds.) Climate from Tree Rings 103–104

Dunwiddie, P.W. and LaMarche V.C., Jr., 1980; Dendrochronological characteristics of some native Australian trees Australian Forestry 43 (2), 124–135

Dutilleul, P. and Till, C., 1989; Detection of atypical years in tree-ring series by construction of a temporal walk in the principal components planes Tree-Ring Bulletin 49, 11–21

Eckstein, D., Ogden, J., Jacoby, G.C. and Ash, J., 1981; Age and growth rate discrimination in tropical trees: the application of dendrochronological methods, in Borman, H.F. and Berlyn, G. (Eds.) Age and Growth of tropical Trees: New Directions for Research School of Forestry and Environmental Studies Bulletin No. 94, Yale University, New Haven, 83–106

Efron, B., 1979; Bootstrap methods: another look at the jackknife The Annals of Statistics 7(1), 1–26

Eis, S., Garman, E.H. and Ebell, L.F., 1965, Relation between cone production and diameter increment of Douglas Fir (*Pseudostuga menziesii* (Mirb.) Franco), Grand Fir (*Abies grandis* (Dougl.) Lindl.), and Western White Pine (*Pinus monticola* Dougl.) Canadian Journal of Botany 43, 1553–1559

Enfield, D.B. and Cid, L.S., 1991; Low-frequency changes in El Niño-Southern Oscillation Journal of Climate 4, 1137–1147

Epstein, S. and Yapp, C.J., 1976; Climatic implications of the D/H ratio of hydrogen in C–H groups in tree cellulose Earth and Planetary Science Letters 30, 252–261

Elliot, H.J., Kile, G.A., Candy, S.G. and Ratkowsky, D.A., 1987; The incidence and spatial pattern of *Nothofagus cunninghamii* (Hook.) Oerst. attacked by *platypus subgranuosus* Schedl in Tasmania's cool temperate rainforest Australian Journal of Ecology 12(2), 125–138

Ferguson, C.W., 1970; Concepts and techniques of dendrochronology, Chapter 4 in Berger, R. (Ed.), Scientific Methods in Medieval Archaeology University of California Press, Los Angeles, 183–200

Fitchner, K., Koch, G.W. and Mooney, H.A., 1994; Photosynthesis, storage and allocation, in Schulze, E. and Caldwell, M.M. (Eds.) Ecophysiology of Photosynthesis Springer-Verlag New York, 133–146

Francey, R.J., 1981; Tasmanian tree rings belie suggested anthropogenic $^{13}C/^{12}C$ trends Nature 290, 232–235

Francey, R.J. and Farquhar, G.D., 1982; An explanation of $^{13}C\backslash^{12}C$ variations in tree rings Nature 297, 28–31

Francey, R.J., Barbetti, M., Bird, T., Beardsmore, D., Coupland, W., Dolezal, J.E., Farquhar, G.D., Flynn, R.G., Fraser, P.J., Gifford, R.M., Goodman, H.S., Kunda, B., McPhail, S., Nanson, G., Pearman, G.I., Richards, N.G., Sharkey, T.D., Temple, R.B. and Weir, B., 1984; Isotopes in Tree Rings Division of Atmospheric Research Technical Paper No. 4, Commonwealth Scientific and Industrial Research Organisation, Melbourne, Australia, 86pp

Fritts, H.C., 1958; An analysis of radial growth of Beech in a central Ohio forest reserve during 1954-55 Ecology 39(4), 705–720

Fritts, H.C., 1963; Computer programs for tree-ring research Tree-Ring Bulletin 25(3–4), 2–7

Fritts, H.C., 1971; Dendroclimatology and dendroecology Quaternary Research 1, 419–449

Fritts, H.C., 1974; Relationships of ring widths in arid-site conifers to variations in monthly temperature and precipitation Ecological Monographs 44, 411–440

Fritts, H.C., 1976; Tree Rings and Climate Academic Press New York, 567pp

Fritts, H.C., 1979; Bristlecone Pine in the White Mountains of California: growth and ring-width characteristics Papers of the Laboratory of Tree Ring Research 4, University of Arizona Press, Tucson

Fritts, H.C., Smith, D.G., Cardis, J.W. and Budelsky, C.A., 1965; Tree-ring characteristics along a vegetation gradient in northern Arizona Ecology 46(4), 393–400

Fritts, H.C., Blasing, T.J., Hayden, B.P. and Kutzbach, J.E., 1971; Multivariate techniques for specifying tree-growth and climate relationships and for reconstructing anomalies in paleoclimate Journal of Applied Meteorology 10(5), 845–863

Fritts, H.C., Lofgren G.R. and Gordon, G.A., 1979; Variations in climate since 1602 as reconstructed from tree rings Quaternary Research 12, 18–46

Fritts, H.C. and Wu, X., 1986; A comparison between response function analysis and other regression techniques Tree-Ring Bulletin 46, 31–45

Fritts, H. C., Guiot, J. and Gordon, G.A., 1990; Verification, in Chapter 4 of Cook and Kariukstis (Eds.) Methods of Dendrochronology: Applications in the Environmental Sciences Kluwer Academic Publishers, Dordrecht, 394pp

Garfinkel, H.L. and Brubaker, L.B., 1980; Modern climate-tree growth relationships and climatic reconstruction in sub-Arctic Alaska Nature 286, 872–874

Gentilli, J., 1972; Australian Climate Patterns Griffin Press, Adelaide, 285pp

Gilbert, J.M., 1959; Forest succession in the Florentine Valley, Tasmania Papers and Proceedings of the Royal Society of Tasmania 93, 129–151

Gill, A.E., and Ramusson, E.M., 1983; The 1982–83 climate anomaly in the equatorial Pacific Nature 306, 229–234

Gordon, G.A. and LeDuc, S.K., 1981; Verification Statistics for Regression Models, in Reprints of 7th Conference on Probability and Statistics in Atmospheric Science, Monterey, Canada, 129–131

Gordon, G.A., Lough, J.M., Fritts, H.C. and Kelly, P.M., 1985; Comparison of sea level pressure reconstructions from western North American tree rings with a proxy record of winter severity in Japan Journal of Climatology and Applied Meteorology 24, 1219–1224

Goswami, B.N., 1995; A multiscale interaction model for the origin of the tropospheric QBO Journal of Climate 8, 525–534

Gove, J.H. and Houston, D.R.; 1996; Monitoring the growth of American Beech affected by Beech bark disease in Maine using the Kalman Filter Environmental and Ecological Statistics 3, 167–87

Graham, N.E. and White, W. B., 1988; The El Niño cycle: a natural oscillator of the Pacific Ocean- atmosphere system Science 240, 1293–1302

Graumlich, L.J. and Brubaker, L.B., 1986; Reconstruction of annual temperature (1590-1979) for Longmire, Washington, derived from tree rings Quaternary Research 25, 223–234

Gray, B.M., Wigley, T.M. and Pilcher, J.R., 1981; Statistical significance and reproducability of tree-ring response functions Tree-Ring Bulletin 41, 21–35

Graybill, D.A., 1979; Revised computer programs for tree-ring research Tree-Ring Bulletin 39, 77–82

Graybill, D. A., 1982; Chronology development and analysis, in Hughes, M.K., Kelly, A.M., Pilcher, J.R. and LaMarche, V.C. Jr. (Eds) Climate from Tree Rings, 21–28

Grier, C.C. and Waring, R.H., 1974; Conifer foliage mass related to sapwood area Forest Science 20(3), 206–206

Grosiman and Easterling, 1994; Century–scale series of annual precipitation over the contiguous United States and southern Canada, in Boden, T.A., Kaiser, R.J., Sepanski, R.J. and Stoss, F.W. (Eds.) Trends 93: A Compendium of Data on Climate Change ORNL/CDIA-65. Carbon Dioxide Information Analysis Centre, Oak Ridge National Laboratory Oak Ridge, Tennessee, USA, 770–782

Groves, D.I., Cocker, J.D. and Jennings, D.J., 1977; The Blue Tier Batholith Geological Survey Bulletin, Tasmania Department of Mines, 55, 171pp

Guiot, J., Berger, A.L. and Munaut, A.V., 1982; Response functions, in Hughes, M.K., Kelly, A.M., Pilcher, J.R., LaMarche, V.C. Jr. (Eds) Climate from Tree Rings 38–45

Guiot, J. 1985; The extrapolation of recent climatological series with spectral canonical regression Journal of Climatology 5, 325–335

Guiot, J., 1990; Methods of calibration, in Chapter 4 of Cook and Kariukstis (Eds.) Methods of Dendrochronology: Applications in the Environmental Sciences Kluwer Academic Publishers, Dordrecht, 394pp

Guiot, J., 1991; The bootstrapped response function Tree-Ring Bulletin 51, 39–41

Guiot, J., Keller,T. and Tessier,L., 1995; Relational databases in dendroclimatology and new nonlinear methods to analyse the tree response to climate and pollution, in Ohta, S., Fujii, T., Okada, N., Hughes, M.K. and Eckstein, D. (Eds.) Tree Rings: From the Past to the Future: Proceedings of the International Workshop on Asian and Pacific Dendrochronology, 17–23

Hajdas, I., Zolitschka, B., Ivy–Ochs, S.D., Beer, J., Bonami, G., Leroy, S.A.G., Negendank, J.W., Ramroth, M. and Suter, M., 1995; AMS radiocarbon dating of annually laminated sediments from Lake Holzmaar, Germany Quaternary Science Reviews 14, 137–143

Haggar, J.P., 1988; The structure, composition and status of the cloud forests of Pico Island in the Azores Biological Conservation 46, 7–22

Harris, G.P., Davies, P., Nunez, M. and Meyers, G., 1988; Interannual variability in climate and fisheries in Tasmania Nature 333, 754–757

Harris, S., 1991; Coastal vegetation, in Kirkpatrick, J.B., Pharo, A.J., Wells, A., Mendel, L., Lynch, A.J.J. (Eds.) Tasmanian Native Bush: A Management Handbook Tasmanian Environment Centre, Hobart, 128–147

Harvey, A.C. 1989; Forecasting, Structural Time Series and The Kalman Filter Cambridge University Press, Cambridge, 554pp

Harvey, A.C. and Todd, P.H.J., 1983; Forecasting economic time series with structural and Box-Jenkins models: a case study Journal of Business and Economic Statistics 1(4), 299–307

Harvey, A.C. and Durbin, J., 1986; The effects of seat belt legislation on British road casualties: a case study in structural time series modelling Journal of the Royal Statistical Society, Series A 149, 187–227

Harwood,C., 1991, Wetland vegetation, in Kirkpatrick, J.B., Pharo, A.J., Wells, A., Mendel, L., Lynch, A.J.J. (Eds.) Tasmanian Native Bush: A Management Handbook Tasmanian Environment Centre, Hobart, 110–116

Hawley, F.M., 1937; Relationship of southern Cedar growth to precipitation and runoff Ecology 18, 398–405

Henckel, P.A., 1964; Physiology of plants under drought Annual Review of Plant Physiology 15, 363–386

Hill, R.S., 1990a; The fossil history of Tasmania's rainforest tree types Tasforests 2(1), 5–12

Hill, R.S., 1990b; Sixty million years of change in Tasmania's climate and vegetation Tasforests 2(2), 89–98

Holmes, R.L., 1994; Dendrochronology Program Manual Laboratory of Tree-ring Research, Tucson, Arizona, 51 pp.

Holton, J.R. and Lindzen, R.S.; 1972; An updated theory for the quasi-beinnial cycle of the tropical stratosphere Journal of the Atmospheric Sciences 29, 1076–1080

Huesser, L.E. and Shackleton, N.J., 1994; Tropical climatic variation on the Pacific Slopes of the Ecuadorian Andes based on a 25 000-year pollen record from deep-sea sediment core tri 163-31b Quaternary Research 42, 222–225

Hughes, M., 1995; Role of dendrochronology in PAGES, in Mikami, T., Matsumoto, E., Ohta, S. and Sweda, T. (Eds.) Paleoclimate and Environmental

Variability in Austral-Asian Transect During the Past 2000 Years: Proceedings of the 1995 Nagoya IGPB-PAGES/PEP-II Symposium, 39-44

Hughes, M.K., Legget, P. and Milsom, S.J., Hibbert, F.A., 1978; Dendrochronology of oak in north Wales Tree-Ring Bulletin 38, 15–23

Hulme, M. and Zhao, Z., 1994; Century-scale series of annual and seasonal precipitation anomalies for East Asia (15^0–60^0 N; 70^0–140^0 E), in Boden, T.A., Kaiser, R.J., Sepanski, R.J. and Stoss, F.W. (Eds.) Trends 93: A Compendium of Data on Climate Change ORNL/CDIA-65. Carbon Dioxide Information Analysis Centre, Oak Ridge National Laboratory Oak Ridge, Tennesse, USA, 911–917

Hurvich, C.M. and Tsai, C.-L., 1989; Regression and time series model selection in small samples Biometrika 76, 297–307

Jackson, W.B., 1965; Vegetation, in Atlas of Tasmania Lands and Surveys Department, Hobart, 128pp

Jackson, J.E. and Hamer, P.J.C., 1980; The causes of year-to-year variation in the average yield of Cox's Orange Pippin Apple in England Journal of Horticultural Science 55(2), 149–156

Jacoby, G.C., Jr., 1983; A dendroclimatic study in the forest-tundra ecotone on the east shore of Hudson Bay, in Moiset, P., Payette, P. (Eds.) Tree-Line Ecology : Proceedings of the North Quebec Tree-Line Conference No. 47, Centre of Northern Studies University, Laval, Quebec, 95–99

Jacoby, G.C., 1988; Overview of tree-ring analysis in tropical regions IAWA Bulletin 10(2), 99–108

Jacoby, G.C., Jr., Sheppard, P.R. and Sieh, K.E., 1988; Irregular recurrence of large earthquakes along the San Andreas Fault: evidence from trees Science 241, 196–199

Jacoby, G.C., Williams, P.L. and Buckley, B.M., 1992; Tree ring correlation between prehistoric landslides and abrupt tectonic events in Seattle, Washington Science 258, 1621–1623

Jarman, S.J.and Brown, M.J., 1983; A definition of cool temperate rainforest in Tasmania Search 14(3–4), 81–87

Jarman, S.J., Brown, M.J. and Kantvilas, G., 1984; Rainforest in Tasmania National Parks and Wildlife Service, Tasmania, 201pp

Jolliffe, I.T., 1986; Principal Component Analysis Springer-Verlag, New York, 271pp

Jones, R.H., 1964; Prediction of multivariate time series Journal of Applied Meteorology 3(3), 285–289

Jones, P.D., 1994; Hemispheric surface air variations: a reanalysis and an update to 1993 Journal of Climate 7(11), 1794–1802

Jones, P.D. and Briffa, K.R., 1992; Global surface air temperature variations during the twentieth century: part I, spatial, temporal and seasonal details The Holocene 2(2), 165–179

Jones, S., 1977; A Review of Geological, Geomorpholical Landform and Landsystems Information for South-west Tasmania Occasional Paper 1 Tasmanian National Parks, Southwest Tasmania Resources Survey, 27pp

Judge, G.G., Carter Hill, R., Griffiths, W.E., Lütkepohl, H. and Tsoung-Chao, L., 1988; Introduction to the Theory and Practice of Econometrics John Wiley and Sons, New York, 1024pp

Jumppanen, P. 1993; The Free and Forced Response of a Propane/ Air Diffusion Flame Unpublished Masters Thesis, University of Tasmania, 276pp

Jury, M. R., McQueen, C. and Levey, K., 1994; SOI and QBO signals in the African region Theoretical and Applied Climatology 50, 103–115

Kaufman, M.R. and Troendle, C.A., 1981; The relationship of leaf area and foliage biomass to sapwood conducting area in four subalpine forest tree species Forest Science 27(3), 477–482

Kaufman, R.K. and Stern, D.I., 1997; Evidence for human influence on climate from hemispheric temperature relations Nature 388, 39–44

Kellomäki, S., 1979; The effect of solar radiation and air temperature on basic density of Scots Pine wood Silva Fennica 13(4), 304–315

Kellomäki, S., Väisänen, H. and Kolström, T., 1997; Model computations on the effects of elevating temperature and atmospheric CO_2 on the regeneration of Scots Pine at the timber line in Finland Climatic Change 37(4), 683–708

Kelly, P.E., Cook, E.R. and Larson, D.W., 1994; A 1397-year tree ring chronology of *Thuja occidentalis* from cliff faces of the Niagra Escarpment, southern Ontario, Canada Canadian Journal of Forest Research 24(5), 1049–1057

Kirkpatrick, J.B., 1977; The impact of man on the vegetation of the west coast region, in Proceedings of Symposium on Landscape and Man, by the Royal Society of Tasmania, November 1976

Kirkpatrick, J.B., Peacock, R.J., Cullen, P.J. and Neyland, M.J., 1988; The Wet Eucalypt Forests of Tasmania: A Report to the Australian Heritage Commission Department of Geography and Environmental Studies, 156pp

Kirkpatrick, J.B., 1991; Grassy vegetation, in Kirkpatrick, J.B., Pharo, A.J., Wells, A., Mendel, L. and Lynch, A.J.J. (Eds.) Tasmanian Native Bush: A Management Handbook Tasmanian Environment Centre, Hobart, 92–109

Kirkpatrick, J.B., Nunez, M., Bridle, K. and Chladil, M.A., 1996; Explaining a sharp transition from sedgeland to alpine vegetation on Mount Sprent, south-west Tasmania Journal of Vegetation Science 7(5), 763–768

Kodera, K., 1995; On the origin and nature of the interannual variability of the winter stratospheric circulation in the Northern Hemisphere Journal of Geophysical Research 100, 14,077–14,087

Koopman, S.J., Harvey, A.C., Doornik, J.A. and Sheppard, N., 1995; STAMP 5.0: Structrual Time Series Analyser, Modeller and Predictor Chapman and Hall, London, 382pp

Kozlowski, T.T., 1973; Extent and significance of shedding of plant parts, in Kozlowski, T.T. (Ed.) Shedding of Plant Parts Academic Press, New York, 1–37

Kozlowski, T.T., 1979; Tree Growth and Environmental Stress University of Washington Press, Washington, 192pp

Kozlowski, T.T., 1992; Carbohydrate sources and sinks in woody plants The Botanical Review 58, 107–223

Kozlowski, T.T. and Peterson, T.A., 1962; Seasonal growth of dominant, intermediate and supressed red pine trees Botanical Gazette 124(3), 146–154

Kramer, P.J., 1964; The role of water in wood formation, in Zimmerman (Ed.), The Formation of Wood in Forest Trees Academic Press, New York, 519–532

Kramer, P.J. and Kozlowski, T.T., 1979; Physiology of Woody Plants Academic Press, Orlando, Florida, 811pp

Kraus, E.B., 1954; Secular changes in the rainfall regime of SE Australia Quarterly Journal of the Royal Meteorological Society 80, 591–601

LaMarche, V.C., Jr., 1974a; Frequency-dependent relationships between tree-ring series along an ecological gradient and some dendroclimatic implications Tree-Ring Bulletin 34, 1–19

LaMarche, V.C., Jr., 1974b; Paleoclimatic inferences from long tree-ring records Science 183, 1043–1048

LaMarche, V.C., Jr., Holmes, R.L., Dunwiddie, P.W. and Drew, L.G., 1979; Tree-ring Chronologies of the Southern Hemisphere vol. 4: Australia Laboratory of Tree-ring Research, University of Arizona, Tucson

LaMarche, V.C., Jr., 1978; Tree ring evidence for chronic insect supression of productivity in subalpine *Eucalyptus* Science 201, 1244–1246

LaMarche, V.C., Jr., 1982; Sampling strategies, in Hughes, M.K., Kelly, A.M., Pilcher, J.R., LaMarche, V.C. Jr. (Eds) Climate from Tree Rings, 2–7

LaMarche, V.C. Jr., and Pittock, A.B., 1982; Preliminary temperature reconstructions for Tasmania, in Hughes, M.K., Kelly, A.M., Pilcher, J.R., LaMarche, V.C. Jr. (Eds) Climate from Tree Rings, 177–185

Lamb, H.H. and Johnson, A.I., 1961; Climatic variation and observed changes in the general circulation Geografiska Annaler 43, 363–400

Langford, 1965; Weather and climate, in Atlas of Tasmania Lands and Surveys Department, 2–10

Lara, A. and Villalba, R., 1993; A 3620-year temperature record from *Fitzroya cupressoides* tree rings in southern South America Science 260, 1104–1106

Larcher, W., 1994; Photosynthesis as a tool for indicating temperature stress events, in Schulze, E. D. and Caldwell, M.M. (Eds.) Ecophysiology of Photosynthesis Springer-Verlag, Berlin, 261–277

Lau, K.-M. and Sheu, P.J., 1988; Annual cycle, quasi-biennial oscillation and Southern Oscillation in global precipitation Journal of Geophysical Research 93, 10,975–10,988

Lavery, B., Kariko, A., Nicholls, N., 1992; A historical rainfall data set for Australia Australian Meteorological Magazine 40, 33–38

Leavitt, S.W. and Long, A., 1982; Stable isotopes as a potential supplemental tool in dendrochronology Tree-ring Bulletin 42, 49–55

Lindesay, A.A. and Vogel, C.H., 1990; Historical evidence for Southern-Oscillation African rainfall relationships International Journal of Climatology 10, 679–689

Ljung, G.M. and Box, G.E.P., 1978; On a measure of lack of fit in time series models Biometrika 65, 297–303

Lorenz, E.N., 1956; Empirical Orthogonal Functions and Statistical Weather Prediction Massachesetts Institute of Technology, Department of Meteorology, Cambridge, Massachesetts, 49pp

Lösch, R. and Schulze, 1994; Internal co-ordination of plant responses to drought and evaporation demand, in Schulze, E. D. and Caldwell, M.M. (Eds.) Ecophysiology of Photosynthesis Springer-Verlag, Berlin, 186–203

Lough, J.M., and Fritts, H.C., 1985; The Southern Oscillation and tree rings: 1600-1961 Journal of Climatology and Applied Meteorology 24, 952–966

Low, A.J., 1964; Compression wood in conifers: a review of the literature Forestry Abstracts 25(3), 35–51

Luckman, B.H., 1993; Glacier fluctuations and tree-ring records for the last millenium in the Canadian Rockies Quaternary Science Reviews 12, 441–450

McBride, J.L. and Nicholls, N., 1983; Seasonal relationships between Australian rainfall and the Southern Oscillation Monthly Weather Review 111, 1998–2004

McClenaghan, M.P. and Williams, P.R., 1982; Distribution and Characteristics of Granitoid Intrusions in the Blue Tier Area Geological Survey Paper 4, Tasmania Department of Mines, 32pp

McCulloch, M.T., Gagan, M.K. and Mortimer, G.E., Chivas, A.R., Isdale, P.J., 1994; A high-resolution Sr/Ca and $\delta^{18}O$ coral record from the Great Barrier Reef, Australia, and the 1982-1983 El Nino Geochimicia et Cosmochimicia Acta 58(12), 2747–2754

McDonald, A.D. and Hurn, A.S., 1995; Unobservable cyclical components in term premia of fixed-term financial instruments Mathematics and Computers in Simulation 39, 403–409, 1995

McKinnell, F.H. and Shepherd, K.R., 1971; The effect of moisture availability on density variation within the annual ring of Radiata Pine Journal of the Institute of Wood Science 5, 25–29

McPhail, S., Barbetti, M., Francey, R., Bird, T. and Dolezal, J., 1983; ^{14}C variations from Tasmanian trees — preliminary results Radiocarbon 25(3), 797–802

Macleod, W.N., Jack, R.H. and Threader, V.M., 1961; Explanatory Report: One Mile Geological Map Series K'55-11-52-Du Cane Tasmanian Department of Mines, Hobart, 42pp

MacPhail, M., 1980; Renergation processes in Tasmanian forests: a long term perspective based on pollen analysis Search 11(6), 184–190

MacPhail, M., 1981; Holocene pollen sequences, paper presented at Directions in Australian Quaternary Palynology symposium Kioloa, NSW, April 1981, 11pp.

Makrogiannis, T.J., Bloutsos, A.A. and Giles, B.D., 1982; Zonal Index and circulation change in the North Atlantic area, 1873-1972 Journal of Climatology 2, 159–169

Mark, A.F., 1970; Floral initiation and development in New Zealand alpine plants New Zealand Journal of Botany 8, 67–75

Mattheck, C., 1991; Trees: The Mechanical Design Springer-Verlag, Berlin, 121pp

Mavarall, A., 1985; On structural time series models and the characterization of components Journal of Businesss and Economic Statistics 3(4), 350–355

Meko, D.M., 1981; Applications of Box-Jenkins Methods of Time Series Analysis to the Reconstruction of Drought From Tree Rings Unpublished PhD Thesis, University of Arizona, 149pp

Meko, D.M., Stockton, C.W. and Boggess, R., 1980; A tree-ring reconstruction of drought in southern California Water Resources Bulletin 16(4), 594–600

Meko, D.M., Cook, E.R., Stahle, D.W., Stockton, C.W. and Hughes, M.K.,1993; Spatial patterns of tree-growth anomalies in the United States and southeastern Canada Journal of Climate 6(9), 1773–1786

Mendenhall, W., Reinmouth, J.E. and Beaver, R., 1989; Statistics for Management and Economics PWS-KENT Boston Publishing Company, Boston, 1108pp

Mocan, H.N. and Topyan, K., 1993; Real wages over the business cycle, evidence from a structural time series model Oxford Bulletin of Economics and Statistics 55(4), 363–387

Monselise, S.P. and Goldschmidt, E.E., 1982; Alternate bearing in fruit trees Horticultural Reviews 4, 128–173

Nanson, G.C., Barbetti, M. and Taylor, G., 1995; River stabilisation due to changing climate and vegetation during the late Quaternary in western Tasmania, Australia Geomorphology 13, 145–158

Nelson, C.D., 1964; The production and translocation of photosynthate-C^{14} in conifers, in Zimmerman (Ed.), The Formation of Wood in Forest Trees Academic Press, New York, 243–257

Neyland, M., 1990: Rainforest floristics and boundaries in eastern Tasmania, in Tasmanian Rainforest Research: Proceedings of a Seminar on Rainforest Research Tasmanian NRCP Report No. 1, Tasmanian component of the National rainforest Conservation program, Hobart

Neyland, M.G. and Brown, M.J., 1993; Rainforest in eastern Tasmania — floristics and conservation Papers and Proceedings of the Royal Society of Tasmania 127, 23–32

Nicholls, K.D., and Dimmock, G.M., 1965, Soils, in Atlas of Tasmania Lands and Surveys Department, Hobart, 128pp.

Nicholls, N., 1985; Towards the prediction of major Australian droughts Australian Meteorological Magazine 33, 161–166

Nicholls, N., 1989; Sea surface temperatures and Australian winter rainfall Journal of Climate 2, 965–973

Nicholls, 1992; Historical El Niño/Southern Oscillation variability in the Australasian region, in Diaz, H.F. and Markgraf, V. (Eds.), El Niño: Historical and Palaeoclimatic Aspects of the Southern Oscillation, 151–173

Nicholls, N. and Lavery, B., 1992; Australian rainfall trends during the twentieth century International Journal of Climatology 12, 153–163

Nicholls, N. and Kariko, A., 1993; East Australian rainfall events: interannual variations, trends, and relationships with the Southern Oscillation Journal of Climate 6, 1141–1152

Nicholson, S.E., 1994; Century-scale series of standardised annual departures of African rainfall, in Boden, T.A., Kaiser, R.J., Sepanski, R.J., Stoss, F.W. (Eds.) Trends 93: A Compendium of Data on Climate Change ORNL/CDIA-65. Carbon Dioxide Information Analysis Centre, Oak Ridge National Laboratory Oak Ridge, Tennessee, USA, 952–962

Nobori, Y., Ogata, T. and Takahashi, N., 1995; The relationship between El Niño, mast years and tree ring fluctuations of *Fagus crenata*, in Mikami, T., Matsumoto, E., Ohta, S. and Sweda, T. (Eds.) Paleoclimate and Environmental Variability in Austral-Asian Transect During the Past 2000 Years: Proceedings of the 1995 Nagoya IGPB-PAGES/PEP-II Symposium 205–210

North, G.R., Bell, T.L. and Cahalan, R.F., 1982; Sampling errors in the estimation of empirical orthogonal functions Monthly Weather Review 110, 699–706

Norton, D.A., 1983a; Modern New Zealand tree-ring chronologies I. *Nothofagus solandri* Tree-ring Bulletin 43, 1–17

Norton, D.A., 1983b; Modern New Zealand tree-ring chronologies II. *Nothofagus menziesii* Tree-ring Bulletin 43, 39–49

Norton, D.A., Palmer, J.G. and Ogden, J., 1987; Dendroecological studies in New Zealand: 1. An evaluation of tree age estimates based on increment cores New Zealand Journal of Botany 25, 373–383

Norton, D.A., Briffa, K.R. and Salinger, M.J., 1989; Reconstruction of New Zealand summer temperatures to 1730 AD using dendroclimatic techniques International Journal of Climatology 9, 633–644

Nunez, M., 1988; A regional lapse rate for Tasmania Papers and Proceedings of the Royal Society of Tasmania 122(2), 53–57

Ogden, J., 1977; Progress in dendrochronology in Australia, 1974–1977 Australian Quaternary Newsletter 9, 5–13

Ogden, J., 1978a; On the dendrochronological potential of Australian trees Australian Journal of Ecology 3, 339–356

Ogden , J., 1978b; Investigations on the dendrochronology of the genus *Athrotaxis* D. Don (Taxodiaceae) in Tasmania Tree-Ring Bulletin 38, 1–13

Ogden, J., 1981; Dendrochronological studies and determination of tree ages in the Australian tropics Journal of Biogeography 8, 405–420

Ogden, J., 1982; Australasia, in Hughes, M.K., Kelly, A.M., Pilcher, J.R., LaMarche, V.C. Jr. (Eds) Climate from Tree Rings, Cambridge University Press, Cambridge, 90–103

Ogden, J. and West, C.J., 1981; Annual rings in *Bielschmieda tawa* New Zealand Journal of Botany 19, 397–400

Olesen, A., Harris, S., and Allen, K., (in prep.); The significance of a forest boundary on Maria Island

Ong, C.K. and Baker, C.K. 1985; Temperature and leaf growth, in Baker N.R., Davies, W.J. and Ong, C.K. (Eds.), Control of Leaf Growth Cambridge University Press, Cambridge, 175–200

Packham, J., 1991; Myrtle Wilt Tasmanian NRCP Technical Report No. 2, Forestry Commission, 127pp

Palmer, J.G., 1989; A Dendroclimatic Study of *Phyllocladus trichomanoides* D. Don. (Tanekaha) Unpublished PhD thesis, University of Auckland, 241pp

Pankratz, A., 1983; Forecasting With Univariate Box-Jenkins Models: Concepts and Cases John Wiley and Sons, New York, 562pp

Parker, M.L., 1976; Improving tree-ring dating in northern Canada by X-ray densitometry Syesis 9, 163–172

Parker, M.L. and Hennoch, W.E.S., 1971; The use of Engleman Spruce latewood density for dendrochronological purposes Canadian Journal of Forest Research 1(2), 90–98

Payette, S., Filion, L. and Gauthier, L., 1985; Secular decline in old-growth tree-line vegetation of norther Quebec Nature 315, 135–138

Pearman, G.I., Francey, R.J. and Fraser, P.J.B., 1976; Climatic implications of stable carbon isotopes in tree rings Nature 260, 771–772

Percival, D.B. and Walden, A.T., 1993; Spectral Analysis for Physical Applications: Multitaper and Conventional Univariate Techniques Cambridge University Press, 583pp

Periera, J.S., 1994; Gas exchange and growth, in Schulze, E. and Caldwell, M.M. (Eds.) Ecophysiology of Photosynthesis Springer-Verlag New York, 147–181

Peters, K., Jacoby, G.C., Cook, E.R., 1981; Principal components analysis of tree-ring sites Tree-ring Bulletin 41, 1–19

Pittock, A.B., 1973; Global meridional interactions in stratosphere and troposphere Quarterly Journal of the Royal Meteorological Society 99, 424–437

Plummer, N. 1996; Temperature variability and extremes over Australia: part I - recent observed changes Australian Meteorological Magazine 45, 233–250

Pook, M.J., 1992; A note on the variability of the mid-tropospheric flow over the Southern Ocean in the Australian region Australian Meteorological Magazine 40(3), 169–177

Press, W.H., Teukolsky, S.A., Vetterling, W.T. and Flannery, B.P., 1992; Numerical recipes in FORTRAN: The Art of Scientific Computing 2nd edition, Cambridge University Press, Cambridge, 961pp

Pumijumnong, N., Eckstein, D. and Sass, U., 1995; A network of *Tectona grandis* tree–ring chronologies in Northern Thailand, in Tree Rings: From the Past to the Future: Proceedings of the International Workshop on Asian and Pacific Dendrochronology, March 4–9, Tsukuba and Okutama, Japan, 35–41

Quinn, W.H. and Neal, V.T., 1992; The historical record of El Niño events, in Bradley, R.S. and Jones, P.D., (Eds.) Climate Since AD 1500 Routledge, London, 623–648

Raven, P.H., Evert, R.F., Eichhorn, S.E., 1992; Biology of Plants Worth Publishers, New York, 791pp

Read, J., 1985; Photosynthetic and growth responses to different light regimes of the major canopy species of Tasmanian cool temperate rainforest Australian Journal of Ecology 10, 327–334

Read, J., 1989: Phenology and germination in some rainforest canopy species at Mt Field National Park, Tasmania Papers and Proceedings of the Royal Society of Tasmania 123, 211–221

Read, J. and Hill, R.S., 1988; Comparative responses to temperature of the major canopy species of Tasmanian cool temperate rainforest and their ecological significance. I. Foliar frost resistance Australian Journal of Botany 36, 131–143

Read, J. and Busby, J.R., 1990; Comparative responses to temperature of the major canopy species of Tasmanian cool temperate rainforest and their ecological significance. II. Net photosynthesis and climate analysis Australian Journal of Botany 38, 185–205

Read, J., 1995; The importance of comparative growth rates in determining the canopy composition of Tasmanian rainforest Australian Journal of Botany 43, 243–271

Richman, M.B., 1986; Rotation of principal components Journal of Climatology 6, 293–335

Roberts, M.S., Smart, P.L. and Baker, A., 1998; Annual trace element variations in a Holocene speleotherm Earth and Planetary Science Letters 154, 237–246

Ropelewski, C.F. and Jones, P.D., 1987; An extension of the Taihiti-Darwin Southern Oscillation index Monthly Weather Review 115, 2161–2165

Ropelewski, C.F., Halpert, M.S., Wang, X., 1992; Observed tropospheric biennial variability and its relationship to the Southern Oscillation Journal of Climate 5, 594–614

Sakai, A., Paton, D.M. and Wardle, P., 1981; Freezing resistance of trees of the south temperate zone, especially subalpine species of Australasia Ecology 62(3), 563–70

Salinger, M.J., Palmer, J.G., Jones, P.D. and Briffa, K.R., 1994; Reconstruction of New Zealand climate indices back to AD 1731 using dendroclimatic techniques: some preliminary results International Journal of Climatology 14, 1135–1149

Salinger, M.J., Fitzharris, B.B., Hay, J.E., Jones, P.D., Macveigh, J.P. and Schmidely-Leleu, I. 1995; Climate trends in the southwest Pacific International Journal of Climatology 15, 285–302

Salinger, M.J. and Jones, P.D., 1996; Southern Hemisphere climate: the modern record Papers and proceedings of the Royal Society of Tasmania 130(2), 101–107

Salisbury, F.B. and Ross, C.W., 1992; Plant Physiology Wadsworth Publishing Company, Belmont, California, 682pp

Scanlon, A., 1984; The Geology of Tasmania Education Department, Tasmania, 43pp

Scott, D., 1972; Correlation between tree-ring width and climate in two areas in New Zealand Journal of the Royal Society of New Zealand 2(4), 545–560

Schulman, E., 1945; Runoff histories in tree rings of the Pacific slope The Geographical Review 35, 59–73

Schulman, E., 1951; Tree-ring indices of rainfall, temperature, and river flow, in T.A. Malone (Ed.) Compendium of Meteorology American Meteorological Society, 1024–1029

Schulze, E.D. and Caldwell, M.C., (Eds.) 1994; Ecophysiology of Photosynthesis Springer Verlag, New York, 576pp

Schweingruber, F.H., Eckstein, D., Serre-Bachet, F. and Braker, O.U., 1990; Identification, presentation and interpretation of event years and pointer years in dendrochronology Dendrochronologia 8, 9–38

Scuderi, L.A., 1993; A 200-year tree ring record of annual temperatures in the Sierra Nevada mountains Science 259, 1433–1436

Shackley, S., Young, P. and Parkinson, S., 1998; Uncertainty, complexity and concepts of good science in climate modelling: are GCMs the best tools? Climatic Change 38, 159–205

Shapcott, A. 1991; Studies in the Population Biology and Genetic Variation of Huon Pine (*Lagarostobos franklinii*) Tasmanian NRCP Report No. 4, 84pp

Shashkin, A.V. and Fritts, H.C., 1995; TREERING 2.0: A model that simulates cambial activity and ring structure in conifers, in Mikami, T., Matsumoto, E., Ohta, S. and Sweda, T. (Eds.) Paleoclimate and Environmental Variability in Austral-Asian Transect During the Past 2000 Years: Proceedings of the 1995 Nagoya IGPB-PAGES/PEP-II Symposium 126–137

Shepherd, D., 1995; Some characteristics of Tasmanian rainfall Australian Meteorological Magazine 44(4), 261–274

Shigo, A., 1985; How branches are attached to trunks Canadian Journal of Botany 63, 1,391–1,401

Shiotani, M. and Hasebe, F., 1994; Stratospheric ozone variations in the equatorial region as seen in stratospheric aerosol and gas experiment data Journal of Geophysical Research 99, 14,575–14,584

Spry, A., 1962; Igneous activity Journal of the Geological Society 9(2), 255–284

Srikanthan, R. and Stewart, B.J., 1991; Analysis of Australian rainfall data with respect to climate variability and change Australian Meteorological Magazine 39, 11–20

Stahle, D.W. and Cleaveland, M.K., Hehr, J.G., 1985; A 450-year drought reconstruction for Arkansas, United States Nature 316, 530–532

Stahle, D.W., Cleaveland, M.K. and Hehr, J.G., 1988; North Carolina climate changes reconstructed from tree rings: AD 372-1985 Science 1517–1519

Stern, D.I. and Kaufman, R.K., 1997; Is there a global warming signal in hemispheric temperature series? Climatic Change Submitted and under review

Stidd, C.K., 1953; Cube-root-normal precipitation distributions Transactions of the American Geophysical Union 34, 31–35

Stockton, C.W., 1971; The Feasibility of Augmenting Hydrologic Records Using Tree-Ring Data Unpublished PhD thesis, University of Arizona, 172pp

Stockton, C.W. and Fritts, H.C., 1973; Long-term reconstructions of water level changes for Lake Athabasca by analysis of tree rings Water Resources Bulletin 9(5) 1,006–1,025

Stokes, M.A. and Smiley, T.L., 1968; An Introduction to Tree-ring Dating University of Chicago press,Chicago, 73pp

Strackee, J. and Jansma, E., 1992; The statistical properties of mean sensitivity - a reappraisal Dendrochronologia 10, 121–135.

Sustainable Development Advisory Council, 1996; State of the Environment:Tasmania: Volume 1 State of the Environment Unit, Department of Environment and Land Managament Hobart, Tasmania

Swetnam, T.W., Thompson, M.A. and Kennedy Sutherland, E., 1985; Spruce Budworms Handbook: Using Dendrochronology to Measure Radial Growth of Defoliated Trees United States Department of Agriculture, Forest Service, Cooperative State Research Service, United States, No. 639, 39pp

Swetnam, T.W. and Betancourt, J.L., 1990; Fire-Southern Oscillation relations in the southwestern United States Science 249, 1,016–1,021

Thomson, D.J., 1982; Spectrum estimation and harmonic analysis Proceedings of The IEEE 70(9), 1055–1096

Thompson, L.G., Mosley-Thompson, E., Davis, M.E., Lin, P.-N., Hendersen, K.A., Cole-Dai, J., Bolzan, J.F. and Liu, B.-B., 1995; Late glacial stage and Holocene tropical ice core records from Huascarán, Peru Science 269, 46–48

Till, C., 1984; A synthesis of response functions from eight Cedar forests located in northern Africa Dendrochronologia 2, 73–82

Tol, R.S.J., 1994; Greenhouse statistics - time series analysis: Part II Theoretical and Applied Climatology 49, 91–102

Tol, R.S.J. and A.F. de Vos, 1993; Greenhouse statistics - time series analysis Theoretical and Applied Climatology 48, 63–74

Tomlinson, P.B., Takaso, T., and Rattenbury, J.A., 1989; Cone and ovule ontogeny in *Phyllocladus* (Podcarpaceae) Botanical Journal of the Linnean Society 90, 209–221

Torok, S.J. and Nicholls, N., 1996; A historical annual temperature dataset for Australia Australian Meteorological Magazine 45, 251–260

Tranquillini, W., 1964; The physiology of plants at high altitudes Annual Review of Plant Physiology 15, 345–362

Trenberth, K.E., 1975; A quasi-biennial standing wave in the Southern Hemisphere and interrelations with sea surface temperature Quarterly Journal of the Royal Meteorological Society 101, 55–74

Trenberth, K.E., 1976; Fluctuations and trends in indices of the Southern Hemisphere circulation Quarterly Journal of the Royal Meteorological Society 102, 65–75

Trenberth, K.E., 1980; Atmospheric quasi-biennial oscillations Monthly Weather Review 108, 1,370–1,377

Trenberth, K.E., 1981; Internnual variability of the Southern Hemisphere 500 mb flow: regional characteristics Monthly Weather Review 109, 127–136

Troup, A.J. and Clarke, R.H., 1965; A closer examination of Hobart rainfall fluctuations Australian Meteorological Magazine 13(50), 35–43

Tsou, P.–S., Liu, T.–K., 1995; Dendrochronological and dendroclimatological studies of *Chamaecyparis fomosensis* in central Taiwan, in Tree Rings: From the Past to the Future Proceedings of the international workshop on Asian and Pacific Dendrochronology, March 4–9, Tsukuba and Okutama, Japan, 64–69

Van Deusen, P.C., 1989; A model-based approach to tree-ring analysis Biometrics 45, 763–779

Van Deusen, P.C., 1990; Evaluating time-dependent tree ring and climate relationships Journal of Environmental Quality 19, 481–19,488

Van Deusen, P.C., 1991; Trend monitoring with varying coefficient models Forest Science 37(5),1365–1375

van Loon, H. and Labitzke, K., 1988; Association between the 11-year solar cycle, the QBO, and the atmosphere. Part II: Surface and 700 mb in the Northern Hemisphere in winter Journal of Climate 1, 905–920

Villalba, R., Cook, E.R., D'Arrigo, R.D., Jacoby, G., Jones, P.D., Salinger, M.J. and Palmer, J., 1997; Sea-level pressure variability around Antarctica since AD 1750 inferred from subantarctic tree-ring records Climate Dynamics 13(6), 375–390

Vinnikov, K.Ya., Grosiman, P.Ya. and Lugina, K.M., 1994; Global and hemispheric temperature anomalies from instrumental surface air temperature records, in Boden, T.A., Kaiser, R.J., Sepanski, R.J. and Stoss, F.W. (Eds.) Trends 93: A Compendium of Data on Climate Change ORNL/CDIA-65. Carbon Dioxide Information Analysis Centre, Oak Ridge National Laboratory, Oak Ridge, Tennessee, USA, 615–627

Visser, H. and Molenaar, J. 1986; Time dependent responses of trees to weather variations: an application of the Kalman Filter Research and Development Division Report No. 50385-MOA 86-3041, 60pp.

Watson, M.W. and Engle, R.F., 1983; Alternative algorithms for the estimation of dynamic factor, mimic varying coefficient regression models Journal of Econometrics 23, 385–400

Wells, P., 1991; Wet forests, in Kirkpatrick, J.B., Pharo, A.J., Wells, A., Mendel, L. and Lynch, A.J.J. (Eds.) Tasmanian Native Bush: A Management Handbook Tasmanian Environment Centre, Hobart, 35–53

Westing, A.H., 1965; Formation and function of compression wood in gymnosperms The Botanical Review 31, 381–480

Whetton, P.H., 1986; A Synoptic Climatological Analysis of Victorian Rainfall Unpublished PhD thesis, Univeristy of Melbourne, 368pp.

White, J.W.C., Cook, E.R., Lawrence, J.R. and Broecker, W.S., 1985; The D/H ratios of sap in trees: implications for water sources and tree ring D/H ratios Geochimica et Cosmochimica Acta 49, 237–246

Whitmore, T.C., 1981; Wallace's Line and some other plants, Chapter 8 in Whitmore, T.C. (Ed.) Wallace's Line and Plate Tectonics Clarendon Press, Oxford, 91pp.

Wigley, T.M.L., Briffa, K.R. and Jones, P.D., 1984; On the average value of correlated time series, with applications in dendroclimatology and hydrometeorology Journal of Climate and Applied Meteorology 23, 201–213

Williams, K., 1991; Dry schlerophyll vegetation, in Kirkpatrick, J.B., Pharo, A.J., Wells, A., Mendel, L. and Lynch, A.J.J. (Eds.) Tasmanian Native Bush: A Management Handbook Tasmanian Environment Centre, Hobart, 54–75

Wilson, B.F., 1964; A model for cell production by the cambium of conifers, in Zimmerman (Ed.), The Formation of Wood in Forest Trees Academic Press, New York, 519–532

Wilson, H. and Hansen, J., 1994; Global and hemispheric temperature anomalies from instrumental surface air temperature records, in Boden, T.A., Kaiser, R.J., Sepanski, R.J. and Stoss, F.W. (Eds.) Trends 93: A Compendium of Data on Climate Change ORNL/CDIA-65. Carbon Dioxide Information Analysis Centre, Oak Ridge National Laboratory Oak Ridge, Tennessee, USA, 609–614

Wold, S., 1974; Spline functions in data analysis Technometrics 16(1), 1-11

Woodward, A., Silsbee, D.G., Schreiner, E.G. and Means, J.E. , 1994; Influence of climate and radial growth and cone production in Subalpine Fir (*Abies lasiocarpa*) and Mountain Hemlock (*Tsuga mertensiana*) Canadian Journal of Forest Research 24, 1,133–1,143

Young, P., 1997; Data-based mechanistic modelling of environmental, ecological, economic and engineering systems, Proceedings of MODSIM97: International Congress on Modelling and Simulation Hobart Dec. 8–11, 1997, 1,867–1,874

Zahner, R., 1963; Internal moisture stress and wood formation in conifers Forest Products Journal 13(6), 240–247

Zelawski, W., Szaniawski, R., Dybczynski, W. and Piechurowski, A., 1973; Photosynthetic capacity of conifers in diffuse light of high illuminance Photosynthetica 7(4), 351–357

Appendix 1

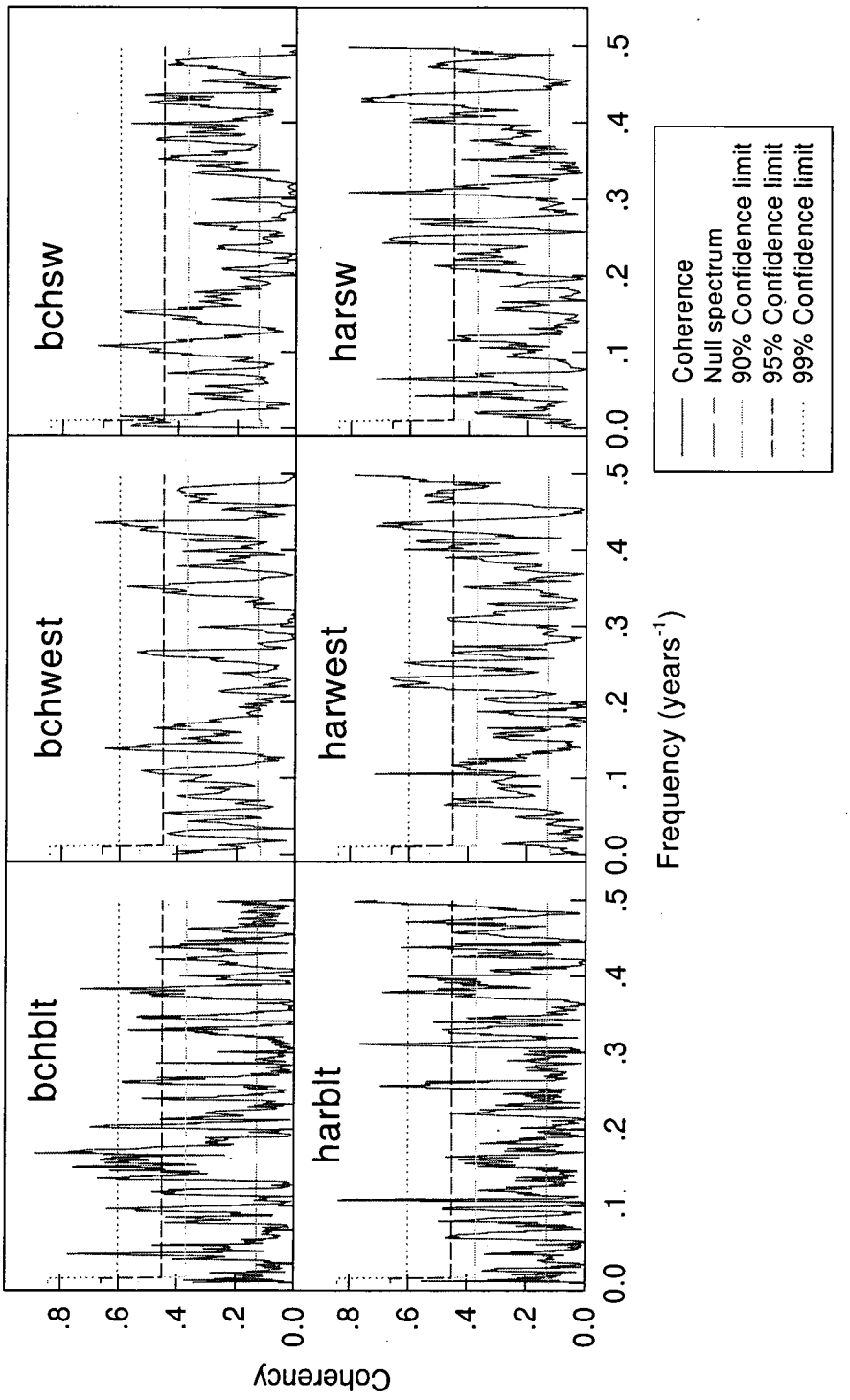
bchblt
bchwest
bchsw
harblt
harwest
harsw
Coherency
0.0
.2
.4
.6
.8
0.0
.1
.2
.3
.4
.5
Frequency (years^{-1})
Coherence
Null spectrum
90% Confidence limit
95% Confidence limit
99% Confidence limit

Appendix 2

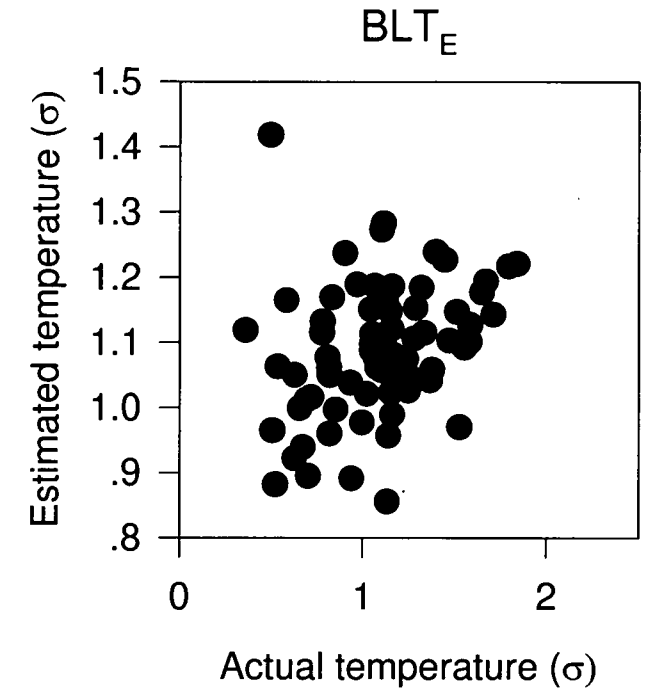
BLT$_E$
Estimated temperature (σ)
1.5
1.4
1.3
1.2
1.1
1.0
.9
.8
0
1
2
Actual temperature (σ)

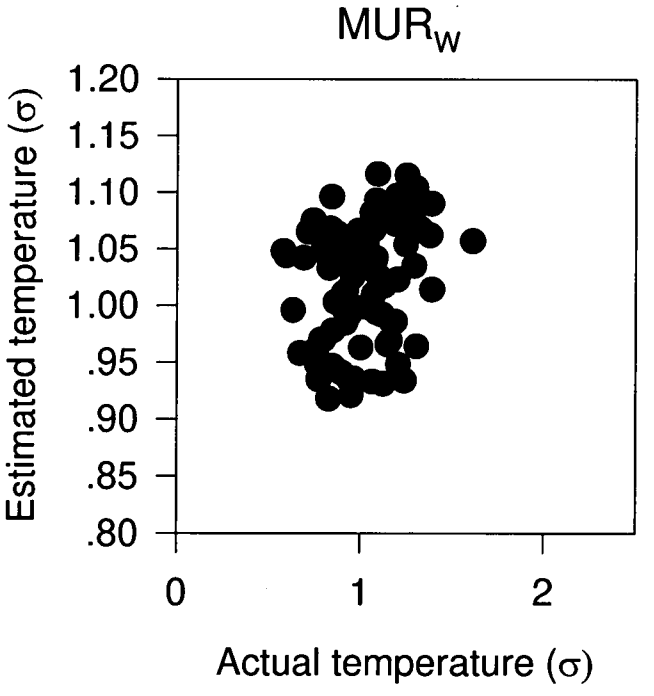
MUR$_W$
Estimated temperature (σ)
1.20
1.15
1.10
1.05
1.00
.95
.90
.85
.80
0
1
2
Actual temperature (σ)

Appendix 3

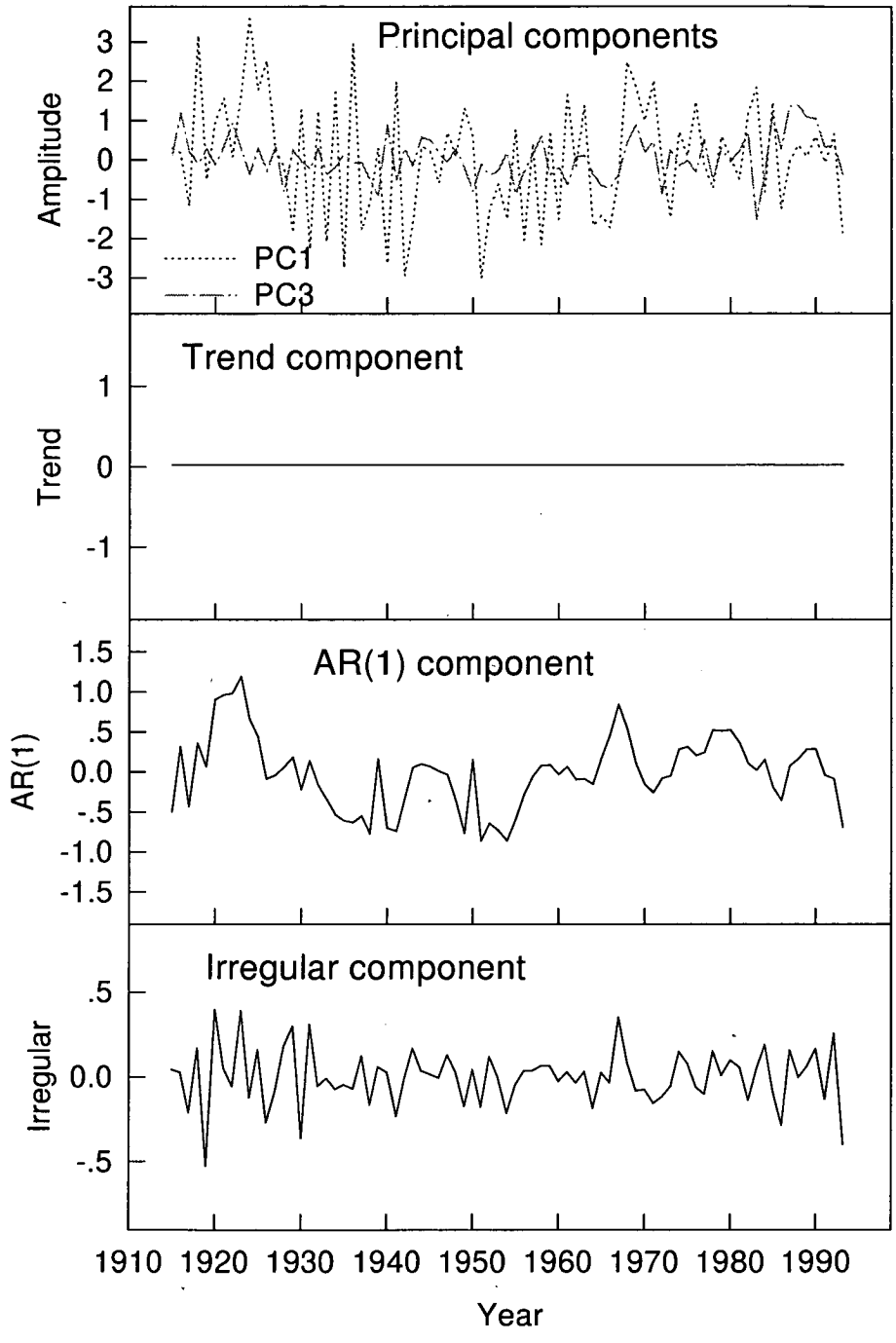

Figure A3a: **Time evolution of components of East STS model. Time period over which the estimates are made is 1915–1994. Both the AR(1) and PC1 components show general decreases up to 1950, and then increase. The flat trend component indicates that the trend is equivalent to the long-term mean**

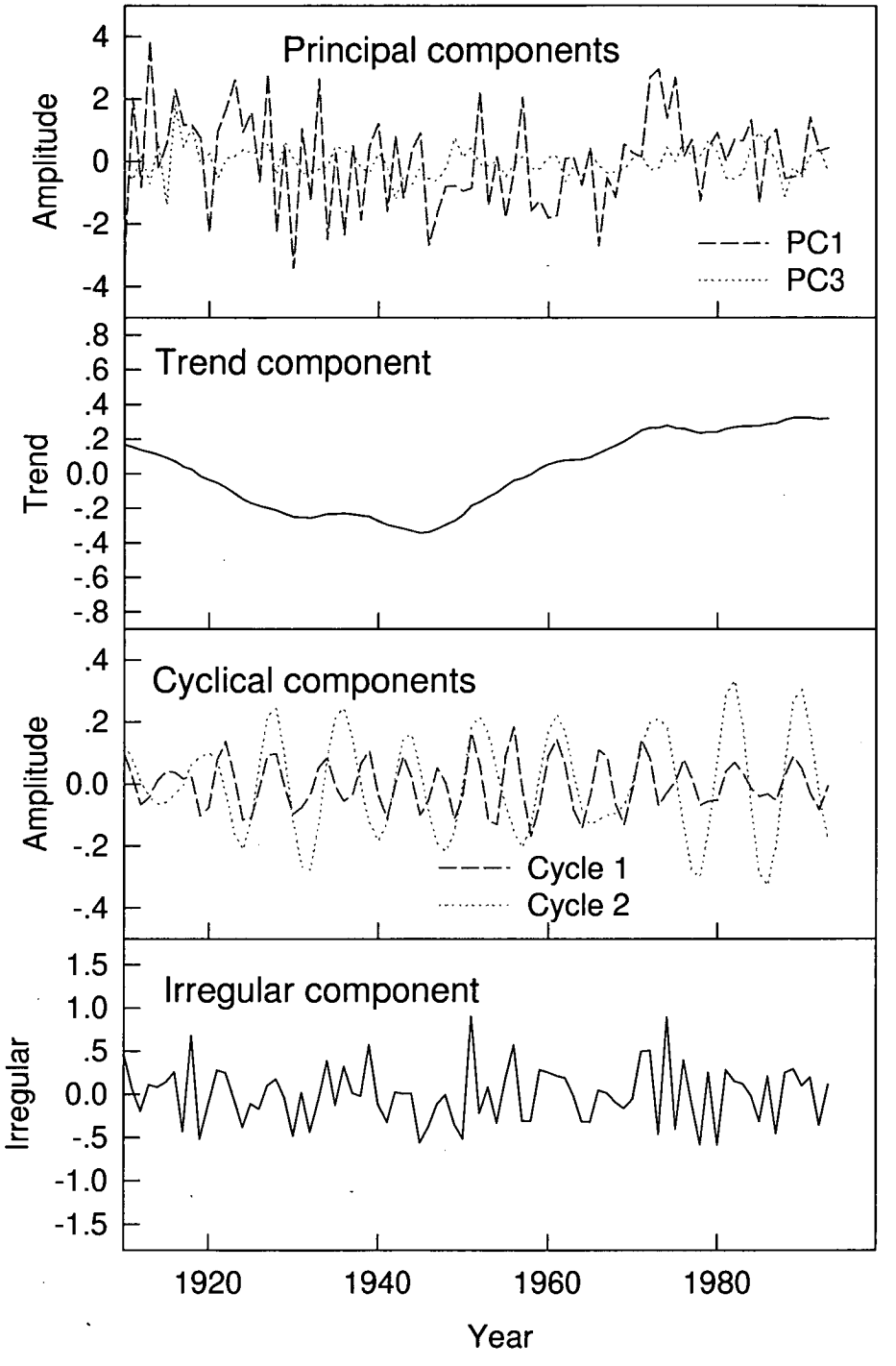

Figure A3b: **Time evolution of components of West STS model. Time period over which the estimates are made is 1915–1994. The trend component shows a decrease up to mid 1940s, and then increases to the present. This feature is also present in the PC1 component, although not as obviously so. The first cyclical component in particular shows amplitude variation over the period analysed.**

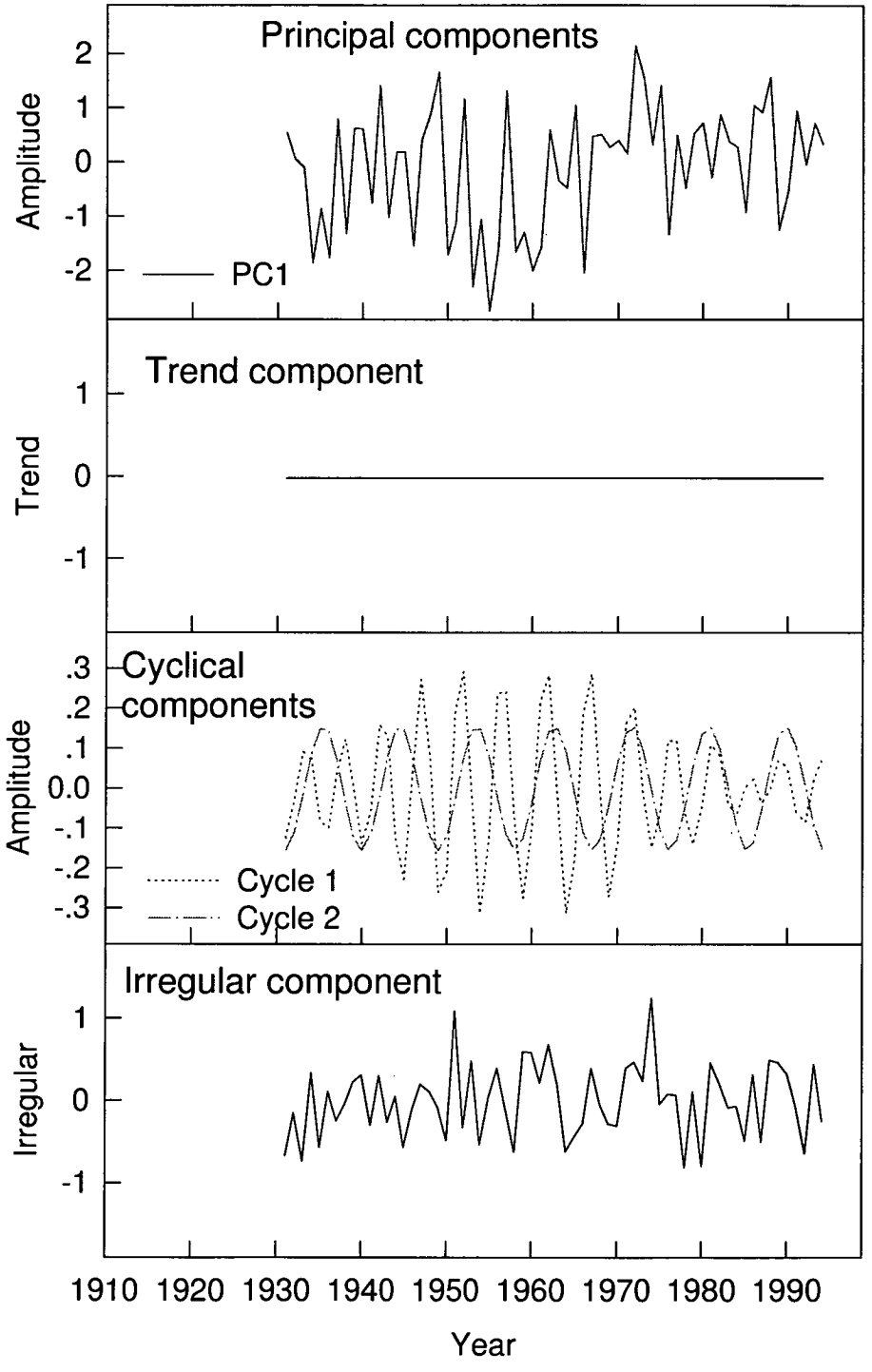

Figure A3c: **Time evolution of components of Southwest STS model. Time period over which the estimates are made is 1915–1994. As for the East model, the trend component is flat. The most obvious amplitude fluctuation in the the cyclical components occurs for cycle 1 which shows higher amplitude between 1940 and 1970. An increase in the amplitude of PC1 is evident**

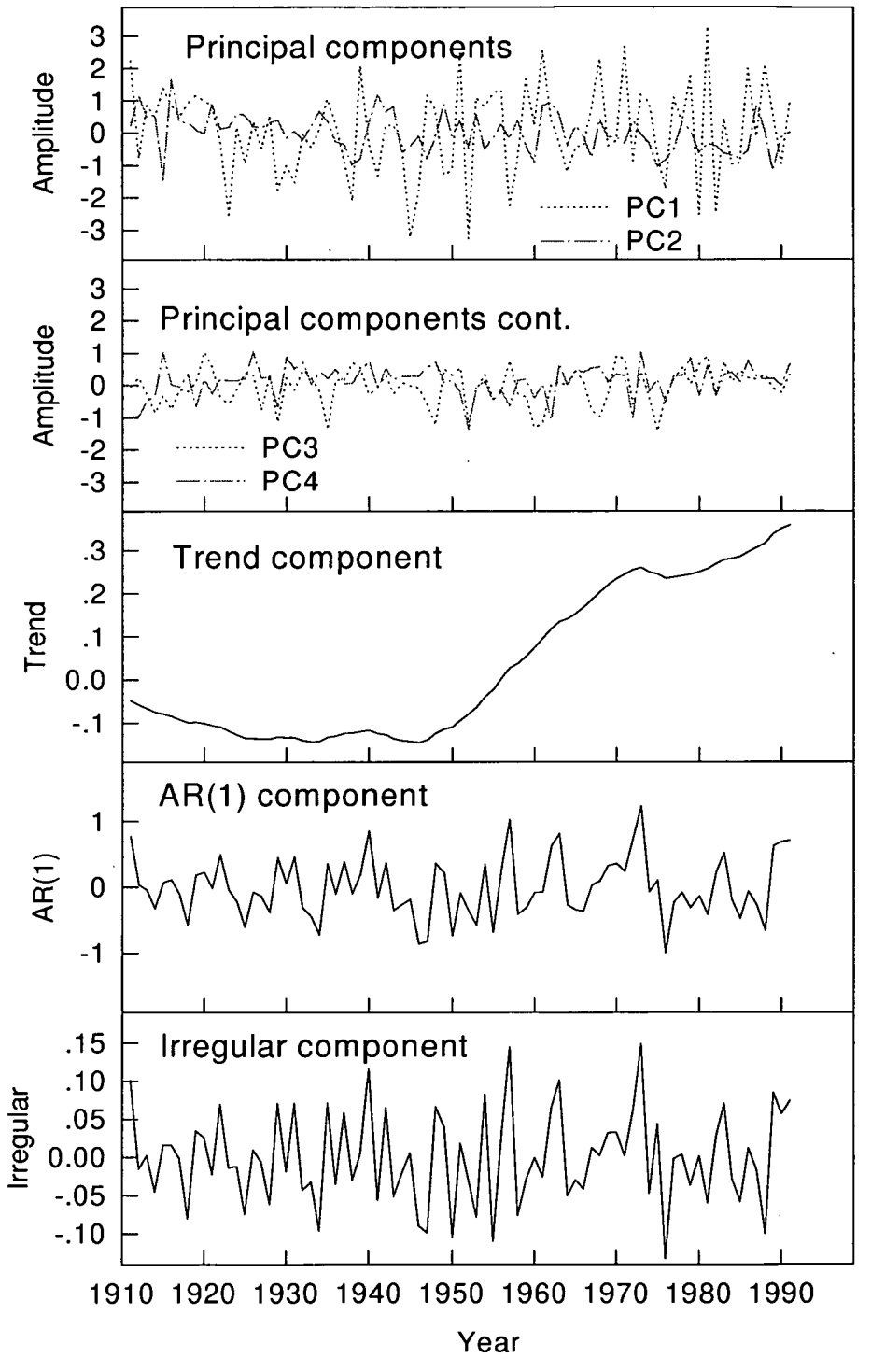

Figure A3d: **Time evolution of components of Huon STS model. Time period over which the estimates are made is 1915–1994. The first PC again shows an increasing amplitude over the current century, but the trend component shows this much more clearly**

Tales of the Trees: centuries of tittle-tattle

Now I've been and cored these 'orrible damn trees
And have amassed hundreds of time series
Over hundreds of years
Listened and ached to all the dried tears
Etched into every bloody ring
Put an ear to what will one day be dust
And its certainly killed my palaeo-lust

In those rings ride the widows of hysterical grey seas
drinking bottles of red as they shiver black
in borrowed and frayed wicker chairs.
There are tossed summers of murderous haste,
remembered in the letters they wrote to God
in the uncertain candlelight
of a drowning wick at New Year's dawn.
Then came the summers in which red farmers did plead
for darkening skies to precede the fires and wrath
they believed issued from the womb of Gehenna
like the excess gametes they deserted in their years of plenty

Along the twisted and battered roads
of many a statistical misadventure
The trees did appear to censure
the rules and regulations belonging to
modern mathematical machinery
and sophisticated statistical finery.
In the taciturn triumph of nature my trees quietly hiss
and silently rattle,
Telling all history as though it were nothing but tittle-tattle.

But in that other misty realm,
With the dignified reserve one may taste in that world
they softly await the interpreter
who will speak with the simplicity of firm earth
in the mother-tongue of the tree
Then what has seemed like tittle-tattle will become the tales
of centuries no longer hid in a widow-ship's ghostly sails.

A Structural Time Series Approach to The Reconstruction of Tasmanian Maximum Temperatures

Allen, K.*, R. Francey+, K. Michael* and M.Nunez*

*University of Tasmania, Hobart, Tasmania

+ CSIRO Division of Atmospheric Research, Aspendale, Victoria

In Press for special issue of Journal of Environmental Modeling and Software

ABSTRACT

Structural time series modelling was applied to the problem of reconstructing maximum temperatures from three regional *Phyllocladus aspleniifolius* tree-ring data sets from Tasmania, Australia. The resulting maximum temperature reconstructions span the past 190 years, and show considerable improvement over reconstructions produced by the more traditional technique of principal component regression. Reconstructions covering the period 1810–1990 reveal increased amplitude in all three time series in the twentieth as compared to the nineteenth century. Consistency between reconstructions also decreases in the twentieth century. Such changes are suggestive of differences in atmospheric circulation patterns of the two centuries. At a general level similarities between the *Phyllocladus aspleniifolius* and the much publicised *Lagarostrobos franklinii* reconstructions are apparent. However, some significant differences exist between the two, and are most likely attributable to biological differences between species and to the higher elevation of *Lagarostrobos franklinii* tree-ring sites.

SOFTWARE

STAMP® was first available in 1995 and has been developed by S.J. Koopman and A.C. Harvey in association with J.A. Doornik, D. Hendry and N. Shephard. It is written in C++. STAMP® is PC DOS or Windows based and requires DOS 3.12 or Windows 3.11 as a minimum. The size of the program is 2MB. The package consists of two 3.5" diskettes containing the software, and a 382 page manual. There are two versions of the program: the main one, stamp.exe, uses a DOS extender to access memory above the 640K boundary on 386 + computers, and a small memory version, stamps.exe, can be run on older machines. The program is available from International Thompson Business Press, 168–173 High Holborn, London WC1V 7AA, or directly form either S. Koopman or A. Harvey. Cost is 500 pounds sterling. Telephone contact is +44 (0)171 497 1422 or +31 13 466 3246, and fax. number is +31 13 466 3280. An email contact for the program is s.j.koopman@kub.nl. A web page for STAMP® can be found at: http://www.sosig.ac.uk/ctiecon/cheer/ch9_3/ch9_3p28.htm

PCREG is a FORTRAN program developed by E. Cook and K. Peters at the Lamont–Doherty Geological Earth Observatory, Palisades, NY 10964, USA. It is not commercially available, and has no support documentation. Enquiries may be directed to the authors at the above address, or to drdendro@ldeo.columbia.edu.

INTRODUCTION

The island state of Tasmania is home to a number of long–lived endemic conifers, including *Lagarostrobos franklinii* (Huon Pine) and *Phyllocladus aspleniifolius* (Celery Top Pine). The distribution of the former is limited to areas of the west and southwest of the State which are protected from fire. It has yielded one of the longest proxy climate records in the Southern Hemisphere (Cook *et al.* 1996). However, significant climatic differences may arise between the east and west of the State in years of strengthened meridional flow and weakened zonal flow, and vice versa. The shorter-lived *P. aspleniifolius* possesses a State–wide distribution, and has previously been assessed as having good dendroclimatic potential (Ogden 1978, Campbell 1980, LaMarche and Pittock 1982). Therefore this species has the potential to offer a spatial complement to the already impressive temporal record of *L. franklinii*. Figure 1 shows sites of *P. aspleniifolius* used in this study. The State has been divided into three regions: East (three sites), West (four sites) and Southwest (three sites).

The most popularly used technique to generate what is known as a *transfer function* in dendroclimatology is Principal Component regression (PC regression). Essentially, a Principal Component Analysis is performed on ring-width series from a number of sites, and the resultant statistically significant Principal Components (PCs) are used as regressors in a multiple regression framework. In dendroclimatology a *transfer function* is a relationship in which one or more independent variables (in PC regression the PCs of ring-widths) are used as an independent variables to map past climatic variation, in this case maximum temperature. Using the PC regression technique, Cook *et al.* (1992), and Buckley (1997) have shown *Lagarostrobos franklinii* ring-widths explain up to 46% of the variation in mean temperatures over the warm season. Similar success was not achieved with *Phyllocladus aspleniifolius* in this study; only 11–15% of climatic variance has been explained by ring-widths through the use of this technique.

The primary purpose of this paper is the application of a Structural Time Series (STS) technique to the reconstruction of past temperatures from tree-rings.

Specifically, this involves the calculation of the *transfer function* by the STS technique. In order to assess the potential of the methodology, results are compared to the PC regression results for the same species, and also to results for *L. franklinii.*

Recently, interest in the use of econometric methods in the physical sciences has increased. These techniques are not necessarily deterministic, nor as complex as models which rely on the current state of knowledge of the physical characteristics of a system. They represent an attempt to identify the major important behavioural modes contained within a data set. Structural time series (STS) techniques have been widely used in such econometric studies (e.g. Crafts *et al.* 1990, Mocan and Topyan 1993, McDonald and Hurn 1995). The ability to include frequency domain features, seasonality, autoregressive components as well as a local rather than global trend, represents an increased use of available information by a model. Although widely used in econometric studies, the use of STS approaches in the physical sciences has been extremely limited. However, a number of workers have applied such techniques to an examination of climatic data series (e.g. Tol and de Vos 199), Tol 1994, Kaufman and Stern 1997, Stern and Kaufman 1997, Young 1997). Young (1997) has emphasised the usefulness of first identifying model structure from information contained in the data itself. Stern and Kaufman (1997) have explicitly used a structural time series approach in investigation of the dynamics of hemispheric temperature series.

STS models are set up in terms of their components, which have a direct interpretation. For example, the decomposition of a given time series may show it to be modelled as a sum of a trend (μ), cyclical component (ψ), seasonal component (γ) explanatory component (δx) and an irregular component(ε). Each of these has a direct interpretation. The following provides a useful generalised mathematical expression of the decomposition of a time series:

$$y_t = \mu_t + \gamma_t + \delta x_t + \psi_t + \varepsilon_t \quad (1)$$

where the subscript t denotes time. A summarised description of each of these symbols, and those in the following equations, is given in Table 1.

Trend (μ) can be defined as that part of a time series which, when extrapolated, gives the clearest picture of future long term movements in the series (Harvey 1989). It need not be constrained to be global, nor must it take a linear form. There are two parts to a trend: *level* which refers to the value of the trend, and *slope* which may or may not be present. The simplest estimation of the level of a series is through the sample mean. A locally linear trend can be defined as:

$$\begin{aligned} \mu_t &= \mu_{t-1} + \beta_{t-1} + \xi_t \\ \beta_t &= \beta_{t-1} + \zeta_t \end{aligned} \qquad (2)$$

where μ_t is a linear trend (level), ξ_t denotes a white noise process associated with the trend, β_t the slope of the trend, and ζ_t a white noise process associated with the slope of the trend. The white noise processes, ξ_t and ζ_t, are mutually uncorrelated. If $\beta_t = 0$, then the process becomes a random walk.

Seasonal effects (γ) repeat themselves over a one-year time interval and are constrained to sum to zero over this period. They are generally included in a model as either trigonometric terms or as dummy variables. The following description treats the seasonal components as dummy variables. One way of allowing seasonal components to vary over time is to allow them to evolve as a random walk. This can be represented as:

$$\begin{aligned} \gamma_{jt} &= \gamma_{j,t-1} + \vartheta_{jt} \qquad j = 1,...,s \text{ and } t = 1,...,T \\ E(\vartheta_j) &= 0, VAR(\vartheta_t) = \sigma^2_{j\omega} \end{aligned} \qquad (3)$$

where j denotes the j^{th} seasonal component and ϑ_j is white noise.

A *cyclical* (ψ) phenomenon can be identified by an examination of the frequency domain. It repeats itself over time and can be defined in terms of its amplitude,

frequency and phase. In STAMP®, the program used for STS analysis in this paper, the spectra are estimated as:

$$\hat{f}(\lambda_i) = 1/2\pi \sum_{j=-m}^{m} \omega_j p\left(\lambda_{i+j}\right) \qquad (4)$$

where m is window length, ω_j are the normalised weights constrained by $\omega_{-j} = \omega_j$ for $j = 0,.....m$. The method used by STAMP® is based on a weighting procedure based on Pascal's triangle (Koopman *et al.* 1995).

In the present case, *explanatory variables* (δx) are the PCs of ring-widths, as will be explained below. x_t is the $k \times 1$ vector of explanatory variables, and δ contains the unknown parameters associated with them. The explanatory variables enter the model in a manner similar to which independent variables enter a regression model. Only those explanatory variables which are relevant should be included in a model.

The *irregular component* of the model, ε_t, captures nonsystematic movements, and is assumed to be normally and independently distributed with a mean of zero, and standard deviation σ, $\left(\text{NID}(0,\sigma)\right)$.

In addition to these components, STAMP® allows for the inclusion of an AR(1) term in model formulation if it is warranted. An interrogation of the correlogram is relatively straight forward.

It should be noted that there is not necessarily a unique solution to a problem when using the structural time series approach. Models are formulated on the basis of *a priori* information, goodness of fit and predictive power, should be parsimonous and not include extraneous components.

State Space Form (SSF) is a powerful tool opening the way for the handling of a wide range of time series models. Once in SSF, the Kalman Filter (discussed below) can be applied. The two basic equations comprising SSF are known as the *measurement* and *transition* equations. The measurement equation is a statement of relations between the state variables (which may be unobservable) and the observations, while the transition equation serves as a description of the evolution of

the characteristics of a physical process (Watson and Engle 1983). Following Harvey (1989), these are respectively:

$$y_t = Z_t\alpha_t + e_t \qquad (5)$$

$$\alpha_t = T_t\alpha_{t-1} + R_t\eta_t \qquad (6)$$

$$\text{for } t = 1...N$$

Here, y_t, the dependent variable (temperature indices in this study) can be expressed as a linear combination of the state and past errors (e_t and η_t). α_t, the *state vector*, is an $m \times 1$ vector linking the observations with the measurement equation. In SSF, the state of the system contains all the information from the past and present history of the system which is necessary to describe present and future behaviour of the system. It will contain the generally stochastic components, for example, cycles, trend, and seasonals. Ideally, its length (m) should be minimised in order that the model remain as simple as possible. The aim is to set up the state vector such that it contains all relevant information for a model while at the same time being the minimum possible length.

Elements in the state and error matrices are called *hyperparameters* and may be unknown. They govern the over-all movement of the series. Z_t', T_t and R_t, are known as system matrices. Z_t is an $N \times m$ matrix, essentially containing the coefficients of the state vector for each time, t. These coefficients are generally nonstochastic, meaning that although they may change over time, they do so in a deterministic manner (Harvey 1989). This implies that the model is linear and, that for any time period, y_t can be expressed as a linear combination of past and present e_ts and η_ts and the initial state, α_0. T_t, an $m \times m$ matrix, contains information such as the sine and cosine terms of a trigonometrically defined cycle and the ARMA effects of stationary components; R_t is an $m \times g$ matrix, where g refers to the number of errors associated with the components of the system. In many cases there will be one error process for each component, meaning that $g = m$. In some cases, however, the error process for one component may be the same as that for another, meaning that

$g < m$ in such cases. ε_t is an $N \times 1$ vector of serially uncorrelated disturbances: $\mathrm{E}(e_t) = 0$, and $\mathrm{Var}(e_t) = H_t$. η_t is also a $g \times 1$ vector of serially uncorrelated disturbances, i.e. $\mathrm{E}(\eta_t) = 0$, and $\mathrm{Var}(\eta_t) = Q_t$. Q_t and H_t are also system matrices.

Two further assumptions are required for the SSF formulation, and these are firstly, that:

$$E(\alpha_0) = a_0$$
$$VAR(\alpha_0) = P_0 \qquad (7)$$

and that the error terms, ε_t and η_t are uncorrelated with each other and the initial state, implying independence of transition and measurement equations, i.e.:

$$E(e_t \eta_s') = 0 \qquad \text{for all } s, t = 1,...,\mathrm{T}$$
$$E(e_t \alpha_0') = 0$$
$$E(\eta_t \alpha_0') = 0 \qquad \text{for } t = 1,...,\mathrm{T} \qquad (8)$$

The estimation of structural time series parameters proceeds through the Kalman Filter (KF), a recursive procedure which computes the optimal estimator at a given time with all available information which is contained in previous observations (Harvey 1989). The recursive KF is composed of two equation sets known as the predicting and updating equations. Through the application of these equations, an updated estimate of y_t (equation 1) is calculated. Their derivation is given in Harvey (1989). In the state space model, let a_{t-1} denote the optimal estimator of α_{t-1}. The covariance matrix of the estimation errors is:

$$P_{t-1} = E\left\{(\alpha_{t-1} - a_{t-1})(\alpha_{t-1} - a_{t-1})'\right\} \qquad (9)$$

The optimal estimator of the state at time t, given a_{t-1} and P_{t-1} is defined as:

$$a_{t|t-1} = T_t a_{t-1} \qquad (10)$$

The covariance matrix of the estimation error is:

$$P_{t|t-1} = T_t P_{t-1} T_t' + R_t Q_{t-1} R_t' \quad t = 1,\ldots,T \qquad (11)$$

These are the prediction equations of the Kalman Filter. The updating equations calculate a new estimator of the state as new information (observations) arrive. They are:

$$a_t = a_{t|t-1} + P_{t|t-1} Z_t' F_t^{-1} \left(y_t - Z_t a_{t|t-1} \right) \qquad (12)$$

$$P_t = P_{t|t-1} - P_{t|t-1} Z_t' F_t^{-1} Z_t P_{t|t-1} \qquad (13)$$

where

$$F_t = Z_t P_{t|t-1} Z_t' + H_t \quad t = 1,\ldots,T \quad (14)$$

Equation (12) is the mean of the multivariate normal distribution of α_t, conditional on the previous estimate, and (13) is a statement of its covariance matrix.

An underlying assumption is that both the disturbances and the state vector are normally distributed. The conditional distributions are also normal and therefore specified by their means and covariances as given above. If the disturbances and state vector are not normally distributed, it is not assured that the KF will produce the conditional mean, although it will remain an optimal estimator in the class of all linear estimators. As illustrated above, the KF makes use of all previous information when updating and predicting a new value. Because the more recent past is most likely to be relevant to the next data point, an exponential weighting function is used to place

more weight on the most recent observations. Both the predictions and estimator are continually updated as more observations become available and the amount of discounting is dependent on the relative values of the disturbances. The larger the disturbances, the greater the level of discounting of past observations.

The above serves as a brief descriptive of the 'mechanics' of STS. The estimation of the STS hyperparameters (cycles, trends, AR(p), seasonal terms) is based on the maximisation of a diffuse log likelihood function which is found by using the one step ahead predictions and their mean square errors. Because the KF is unable to handle situations where the initial state is unknown, a variation of the KF, known as the *diffuse KF*, has been used by STAMP® for an initial stretch of data (de Jong and Chu-Chun-Lin 1994). The reader is referred to de Jong and Chu-Chun-Lin 1994 and Koopman *et al.* (1995) for a thorough discussion of this issue.

STAMP® uses an iterative quasi-Newton method for the optimisation of the diffuse likelihood function (Koopman *et al.* 1995). Newton methods search for a maximum or a minimum of a function, i.e. they search for the point at which the function has a zero gradient. STAMP® uses the Broyden–Fletcher–Golfarb–Shanno method of finding this point in which a search direction is determined for the next step. A description of this method can be found in Press *et al.* (1992). A discussion of the iterative process can be found in Koopman *et al.* (1995) and comprehensive attention is given to the development of STS models in Harvey (1989), de Jonge and Chu-Chun-Lin (1994) and Koopman *et al.* (1995).

METHODOLOGY

Samples collected in the field included both increment cores and discs. Due to frequent ring wedging observed in *Phyllocladus*, three core samples were obtained from each tree cored. For each disc, three radii (where practical) were dated and measured. At each individual tree-ring site depicted in Figure 1, at least 20 trees were sampled. At the site in the far northeast of the state, over 40 trees were sampled.

Crossdating is the procedure whereby dendrochronologists match the sequences of narrow and wide rings from one sample with the ring-width sequences from other samples. In this way, rings which are missing in a particular sample can be identified. To be in error by a single year destroys the integrity of a chronology, and any further investigation based on an incorrect chronology will be fundamentally flawed. Crossdating between samples from one individual was first achieved, followed by cross-dating with other individuals at the same site. Crossdating procedures basically followed Stokes and Smiley (1968), with computerised assistance.

Standardisation aims to remove non-macroclimatic variance from samples, thereby maximising the macroclimatic signal present in ring widths. Early workers in dendrochronology have pointed out the existence of an ageing trend in many samples (e.g. Douglass 1928). To ignore the presence of such a trend would result in a chronology which was a function of average growth, which itself will partially be a function of sample depth. Therefore, detrending of individual samples is required prior to estimation of the mean site chronology. In this case, because *Phyllocladus* samples taken in Tasmanian mesic environments did not reveal a deterministic growth trend (Allen 1998), a stochastic 128-year 50% cut-off smoothing spline (Cook and Peters 1981) has been used to remove the growth trend. After detrending, data has been averaged to generate the mean ring width chronology, a stationary index series produced by the division of the raw ring width by its expected value — the expected value determined by detrending method used. Division rather than subtraction is used as local mean ring width is proportional to the local variance. When outliers exist, the simple arithmetic mean may be biased, as well as no longer being a minimum variance estimator of the mean. Here, a robust biweight mean has been used (Cook *et al.* 1990). Subsequently, the model of pooled autoregression has been estimated and then re-incorporated into the chronology. The rationale, again, is to maximise the climatic signal contained by the ring-width series prior to further analysis. A Principal Component Analysis has been performed on the tree-ring sites within each individual region for the years 1650–1994.

Each region noted in Figure 1 (East, West and Southwest) was modelled separately for both the PC regression and the STS techniques. The correlations

between a number of monthly climatic variables (maximum and minimum temperatures, precipitation, a Zonal Index, a Meridional Index, and the Southern Oscillation Index) and ring-widths of each region were initially tested. However, the strongest and most consistent response across sites was that to maximum temperature (Allen 1998), which is the subject of this paper. Temperature stations were initially chosen on the basis of their record length, homogeneity, and completeness. The monthly data of each station was converted to a dimensionless time series of standard normal deviates. For each region (Figure 1), the relevant individual station series were then averaged in order to create a single monthly index series for that region (after Meko 1981) which were then used in subsequent analyses.

The optimal climatic window upon which to base reconstructions can be defined as the period in which climate is indicated to be most important to tree growth. This window contained several consecutive months of significant, or near significant, correlations between ring-width and the temperature index. In order to determine the appropriate window for *Phyllocladus aspleniifolius*, correlations between annual ring-widths and monthly climatic data were calculated. It is known that biological processes occurring in the previous year will affect the width of the next year's ring (Fritts 1976). Therefore, each annual ring-width was correlated with 20 months of climatic data, extending from the September of the year prior to that in which growth occurred to April at the end of the current growing season over the entire 1915–1994 time period (1910–1994 for West).

Based on the monthly correlations with maximum temperature, the following windows were selected as optimal for each region: East coast, December–April of the previous growing season; West coast, November–March of the previous growing season; and Southwest, November–March of the previous growing season. For the high elevation *Lagarostrobos franklinii*, Buckley found that the optimal window is January–April of the current growing season. The monthly temperature data for each of these windows were then averaged to form a single seasonalised temperature series for each region. The variables to be reconstructed were, therefore, seasonal indices of maximum temperatures.

In PC regression, it is usual to calibrate a model against one data set, and then to verify it against an independent data set. This is commonly achieved by splitting the period of instrumental data in half, or through the use of resampling methods such as the bootstrap. However, because the KF is unsuited to these verification techniques, the whole period has been used to construct models for both techniques. This enabled comparison of methods over the longest possible time frame.

Program STAMP® was used for STS estimation, and the program PCREG was used for PC regression estimation. In both cases, maximum temperature was the dependent variable, and the principal components of the regional tree-ring chronologies were the independent/explanatory variables.

PC Regression Models

Both climatic and tree-ring data were prewhitened prior to modelling in order that subsequent statistical tests were valid. This resulted in the loss of two years of data (tree-ring series being modelled as AR(2) processes, climate as AR(1), as selected by the AIC_C). Only those PCs with an eigenvalue of one or greater were included as independent variables in the regression, with seasonalised maximum temperature as the dependent variable. The periods covered by models were: East 1916–1993, West 1913–1993, Southwest 1933–1994.

A model based on Buckley's (1997) high elevation *Lagarostrobos franklinii* sites was also estimated for the purposes of comparison with an STS model for the same species. The time span covered by the model was 1913–1993, with one year being lost due to prewhitening of data.

STS Models

Because STS models are designed to incorporate autoregression and include cyclical elements, chronologies which have not had autoregressive effects removed have been used. This contrasts with the use of chronologies which have had autoregressive effects removed for the estimation of PC regression models. Some differences between the results of the two techniques can therefore be expected due to this difference. Periods covered by the STS models were: East 1915–1993, West

1910–1993, and Southwest 1933–1994. As an example of model development, data and data interrogation for the West model is shown in Figure 2. Figure 3 shows the actual trace of the temperature data over the period 1910–1993.

Explanatory variables included in each model were the PCs of ring-width for an individual region. PCs not significant ($p = 0.10$) in the STS models were eliminated. For all STS models, trend was modelled as a random walk. Spectra of seasonalised temperature series were estimated by the Multiple Taper Method (Thompson 1982, Percival and Walden 1993) as an independent check of the frequency domain properties of the temperature data. Three tapers with bandwidth-frequency products of two were applied in all cases.

The spectra of seasonalised maximum temperature for the East did not show significant spectral peaks greater than 2.3 years. The correlogram, while not showing a classical AR(1) pattern, was suggestive of an AR(1) process. On the basis of this, an AR(1) term was included in the model. No cycles were incorporated, and explanatory variables, significant at the 0.10 level, were the first and third eigenvectors.

For West seasonalised maximum temperature data, the first and the third eigenvectors (Figure 2a), were indicated to be significant (0.10 level). The correlogram of West seasonalised maximum temperature did not show strong evidence of being an AR(1) process (Figure 2b). Additionally, four cyclical elements were indicated as being significant (Figure 2c). The lowest frequency cycle, however, was of a frequency too low to be resolvable given the length of the data set. Other periodicities occurred at 7.6 years and 2.42 years, with lesser peaks at 8.7 and 3.3 years. The peak at 3.3 years was significant at the 0.10 level, but not at 0.05. Initially three cycles were included in the model, but one of these had an amplitude which approached zero, and goodness of fit statistics suggested that the model was not the best available model. Therefore only two cycles were included in the model. The first and the third eigenvectors, significant at the 0.10 level, were included in the model along with these cycles.

For the Southwest, spectral peaks of greater than two years were evident at 7.8 and 2.44 years. Initially two cycles were included in the model, but one of these was insignificant with an amplitude which approached zero. It was therefore excluded from the model. Only the first eigenvector was significant at the 0.10 level.

An STS model for *Lagarostrobos franklinii* was also estimated, and covered the time period 1912–1993. The correlogram suggested the presence of an AR(1) process in the temperature data. No significant (0.05) spectral peaks were identified in the seasonalised January–April temperature data, other than one at zero frequency. Therefore, no cyclical component was included. This model used the four PCs of ring-width which were all significant at the 0.10 level and an AR(1) term.

RESULTS

Principal component regression models for *Phyllocladus aspleniifolius* were:

East

$$mxt\_1 = 0.372\,PC1 + \varepsilon \qquad (15)$$
$$(0.000)$$

West

$$mxt\_1 = 0.353\,PC1 + \varepsilon \qquad (16)$$
$$(0.000)$$

Southwest

$$mxt\_1 = -0.548\,PC1 + \varepsilon \qquad (17)$$
$$(0.000))$$

L. franklinii

$$mxt = -0.522\,PC1 + \varepsilon \qquad (18)$$
$$(0.000)$$

where *mxt_1* is maximum temperature of the prior season and *mxt* maximum temperature of the current season. Estimated and actual temperatures for these models are shown in Figure 3. None of the three *Phyllocladus aspleniifolius* models

provide a good visual fit, although they do appear to generally trace the series trend successfully. The *Lagarostrobos franklinii* PC regression model, although it does not explain a large proportion of the variance in maximum temperatures, is a better fit to the data than the *P. aspleniifolius* models (Figure 3), and this is confirmed by the results of Table 4.

STS Models

Table 2 reports descriptive statistics for each of the models below. The DW test indicates that very little first order autocorrelation remains in the residuals, although the Q statistic implies that significant autocorrelation (lags greater than one year) remains in the East (0.05 significance level). The distribution of the residuals for each of the models,(19)–(22), are indicated to be homogenous for East, West and *Lagarostrobos franklinii* models with the critical value of the F statistic being 1.44 (0.05 significance level). The critical value for the Southwest is F = 1.61, also indicating that heterogeneity of residuals is not significant in the Southwest either (0.05 significance level).

For each of the regional models, the form of the model is reported and Table 3 contains information on model parameters. The fitted STS models are:

East

$$mxt\_1 = level + AR(1) - PC1 - PC3 + \varepsilon \qquad (19)$$

West

$$mxt\_1 = level + \psi_1 + \psi_2 + PC1 + PC3 + \varepsilon \qquad (20)$$

Southwest

$$mxt\_1 = level + \psi_1 + \psi_2 + PC1 + \varepsilon \qquad (21)$$

L. franklinii

$$mxt = level + AR(1) + PC1 + PC2 + PC3 + PC4 + \varepsilon \qquad (22)$$

where *level* is a trend line without stochastic slope, *AR(1)* is the autoregressive order one component, *PC1–PC4* are the principal components of ring-width for each region, and ε the irregular component. For illustrative purposes, the time trace of each component on the left hand side of equation (20) is shown in Figure 4.

In the STS models, the explanatory variables, which enter the model in the same manner as independent variables in a regression, are deterministic. That is they do not vary over time. Despite the fact that the *level* is not statistically significant (Table 2) it has been included in the models as its non-inclusion leads to erratic and highly misleading temperature retrodictions being produced by resultant models. This has been ascertained by an examination of longer period temperature series such as the Cook and Buckley temperature series (Allen 1998).

Plots of STS estimated and actual temperatures are shown in the right panel of Figure 3. There is a visually apparent improvement over the PC regression models shown in the left panel. Goodness of fit statistics suggest definite improvements for all three *Phyllocladus aspleniifolius* models through the use of STS, both in terms of explained variance and model AIC_Cs (Table 4). The AIC_C for the Southwest is the least satisfactory of the three STS models. This may be due to the same reason that a PC regression model cannot be formulated in the later calibration period. As far as *Lagarostrobos franklinii* models are concerned, results suggest that the performance of the STS model is inferior to that of PC regression which has a lower AIC_C than the STS model (Table 4). A larger amount of explained variance in the STS model is likely to be caused by the inclusion of extra variables, inflating the statistic. Although the relationships between ring-width and maximum temperature remain relatively weak, better fits to the temperature data have been achieved through the use of STS.

Cycle periodicities for the West are reported by the model as 5.1 and 8.5 years. For the Southwest the periodicities are 4.86 and 9.06 years. It is probable that the differences between these estimates and the independent MTM estimates of periodicities in the temperature data (8.83 and 2.43 years West; 2.5 years for Southwest), most particularly for the Southwest, partially relate to the different technique used in STAMP® for estimating the spectra and also to the shortness of the maximum temperature data sets (see Percival and Walden 1993).

The improvement in explained variance for *Phyllocladus aspleniifolius* models does validate some tentative discussion of the STS temperature reconstructions. All three STS reconstructions show a great deal of similarity to one another over the period 1830 – late 1880s, indicating a similarity of conditions across the State (Figure 5). The periods 1815–1830 and 1915–1923, and the early 1980s, are instances of clear differences in the reconstructions. Temperatures for the West positively deviate from the long-term mean to a greater extent than for the East over 1815–1830, and for the East and Southwest in the early 1980s. Over the period 1915–1923, the East coast shows positive deviation from the mean, while the West, negative (on the whole). The year 1947 is indicated as being greater than 1σ below average for the Southwest while approaching the long-term mean temperature for East and West. There is a further anomaly between the Southwest and the more northern regions in the late 1960s/1970s. Again, these years are indicated to be cooler than average for the Southwest, but warmer than average for the West and East. In summary, warmer than average periods indicated by reconstructions are 1810–1830, mid 1840s, mid 1880s – late 1890s (West), 1915–1923 (East), late 1950s, mid 1960s – early 1970s, early 1980s (West). The northern reconstructions both indicate increasing temperatures, especially over the 1930–1960 period, most obviously so in the West. Cooler than average periods occur for 1818–1824, mid 1880s – mid 1890s (East), 1915–1945 (West), 1929–1945 and early 1980s (East). Temperature index series for the twentieth century indicate warmer than average conditions for the East from 1915–1921, in the late 1950s, the late 1960s – early 1970s; for the West temperatures are approximately average between 1910–1920, and since the 1950s have generally been above the long-term mean (Figure 3). This lends some credence to the reconstructions. However, the differences of the reconstructions in the late 1960s through to the late 1970s do not appear to be faithfully reproduced records of temperature, especially in the Southwest. The reason for this is unclear, but Norton *et al.* (1989), Salinger *et al.* (1994) and Briffa *et al.* (1998) have found that relationships between ring-widths (or ring density) and temperature has become less defined in the latter part of the twentieth century.

Because the *Lagarostrobos franklinii* and *Phyllocladus aspleniifolius* reconstructions are based on different climatic windows, it is not valid to compare

them statistically. A basic visual comparison, however, of the PC regression *L. franklinii* reconstruction and the STS *P. aspleniifolius* West reconstruction reveals some quite striking differences in the periods 1810–1815, 1849, the late 1890s and 1908, when *L. franklinii* indicates colder than average temperatures and the *P. aspleniifolius* reconstruction indicates warmer than average temperatures (Figure 6). Opposite anomalies also occur about 1915–1920 and in the early 1860s when the *L. franklinii* reconstruction indicates warmer than average temperatures, and the *P. aspleniifolius* reconstruction cooler than average temperatures. Some general agreement between the two series can be seen, for example, the 1808–1832 and from the 1880s to the mid 1890s are depicted as warmer than average. Between 1940 and 1980, both reconstructions indicate increasing temperatures, although this trend is much more prominent in the *Lagarostrobos* reconstruction. In general, however, there are large differences between the two reconstructions. It is possible that some of these differences may be attributed to elevational differences, and a further part to species differences (Allen 1998).

DISCUSSION

In terms of the tenets of a good model, the STS technique provides a potentially more encompassing method of estimating the transfer function, and has produced models which better fit the data in three of four cases here. Models remain relatively simple. The significant improvement in predictions of maximum temperature, although insufficient to produce reconstructions from which one can draw confident inferences, suggest that STS modelling may represent a useful alternative methodology for climate reconstruction if a number of limitations and theoretical issues can be resolved. The particular prospects and problems surrounding the use of STS in dendroclimatology fall into two broad classes: those issues concerning software applicability and workability and those concerning the methodology itself.

With respect to the software used in this study, Diebold (1989) has pointed out several limitations of an earlier version of the package STAMP®. Although most of these have either been corrected in subsequent versions of the program or have had no bearing on the models utilised here, a number of problems remain. Essentially, STAMP® has been designed for econometric applications, and some limitations apparent in dendroclimatic applications stem from this. An important limitation for dendroclimatology is the inability of the program to generate 'forecasts' of more than 100 values. Because the use of STS models requires highly specialised software, few applications have been developed. Of those that have been developed in the field of dendrochronology, very few currently handle explanatory variables, critical for dendroclimatology. These programs are currently being reviewed and updated in order that explanatory variables may be included (J. Gove, US Forest Service, pers. comm.). It is for reasons such as this that STAMP® has been used here.

The most fundamental methodological problem with STS methodology itself is its incompatibility with calibration/verification schemes currently used in dendroclimatology. As Gordon and LeDuc (1981) have pointed out, successful application of a calibrated model to an independent data set is imperative before any interpretation of a model can be made. Because the Kalman filter uses all prior information in updating the estimator, the use of a temporally independent verification period, as applied, for example, by Cook *et al.* (1992), is inappropriate because information is lost, potentially resulting in large differences in estimates. So while internal statistics may suggest a good STS model fit, it is not strictly possible to test the STS model on a temporally independent data set. Although this is a weakness of the STS method when compared to PC regression, internal diagnostics of STS models give a partial guide to model performance and certainly provide valuable information on the *descriptive* value of the model. They cannot, however, be regarded as being equivalent to verification procedures.

Despite the fact that STS models have improved the estimates available from chronologies, explained variance in the models remains relatively low, suggesting that maximum temperature reconstruction from *Phyllocladus asplenifolius* may be neither viable nor reliable. However, bearing both this and the calibration/verification issue

in mind, some tentative evidence for the integrity of the reconstruction may be drawn from a comparison of the East and Southwest reconstructions over the past 180 years. The two series move closely together (Figure 4) for the nineteenth century with an apparent change in their relationship immediately prior to the turn of the century. A change in the strength of crossdating of tree-ring series of the Southwest and East regions is also discernible at this time (Allen 1998). Prior to the turn of the century, back to at least 1550 AD, good crossdating can be readily established between these regions, but becomes poor over the period 1890–1920.

Villalba *et al.* (1997) have commented on significant differences between nineteeth and twentieth century atmospheric circulation in the Southern hemisphere. In addition, Lamb and Johnson (1961) and Cook *et al.* (1996), have described alternating periods of strong and weak westerly circulation. The period from approximately 1800 to the late 1920s is suggested as one of enhanced zonal flow with the period since the late 1920s described as one of enhanced meridional flow, with a southward displacement of the sub-tropical high pressure belt, resulting in substantially drier and warmer conditions across the state. Temperature data (Figure 3) show a clearly evident upward trend for West and East regions only, implying that the effect of enhanced meridional flow is less evident for the Southwest than for the rest of the state. This is one mechanism through which the Southwest and East reconstructions might be expected to differ over this time interval. The fact that crossdating only breaks down in the late 1800s – early 1900s over the past 450 years suggests that current differences between the north and south of the state have not otherwise existed over this time period.

With regard to the years of pronounced low temperatures in the *Lagarostrobos franklinii* reconstruction which are not evident in the lower elevation *Phyllocladus asplenifolius* reconstructions, historical records reveal that the summers of both 1898 and 1908 were particularly cold at higher elevations (Buckley 1997). At the same time, meteorological records for lower elevations do not concur with the suggested severity at these higher stations. Further, a lower optimal temperature for photosynthesis of *P. asplenifolius* than *L. franklinii* (Read and Busby 1990) suggests that years with colder than average maximum temperatures over the growing season may be detrimental to photosynthesis in higher elevation *L. franklinii* while at the

same time, being more favourable for woody growth in low elevation *P. aspleniifolius* with its lower optimal temperature for photosynthesis. The general trends of the reconstructions produced by the two species are similar, and a reasonable, although not optimal, degree of conformity between actual and STS estimates of temperature, implies that the use of the technique has produced useful information from the ring-widths of *P.aspleniifolius* which could not have been produced with the PC regression technique for this species.

CONCLUSIONS

The STS technique has resulted in improved estimates of temperature when using *Phyllocladus aspleniifolius*. However, the less satisfactory results obtained when using *Lagarostrobos franklinii* demonstrate that this technique, like any other, is not universally applicable to the entire family of tree ring indices. Although improvement of estimates occurs for *P. aspleniifolius*, the fundamental problem of a verification scheme remains a critical issue.

Consistency between the three regional reconstructions is highest for the nineteeth century, noticeably declining in the early 1900s. This may reflect changing atmospheric circulation patterns previously noted. Comparison with *Lagarostrobos franklinii* indicates broad agreement between reconstructions with regard to the upward trend, but high frequency differences prohibiting crossdating of the two species are likely to be due to biological factors.

STS reconstructions show dendroclimatological potential, and the technique deserves further investigation in the context of palaeoclimatic reconstruction with attention being focussed on possible verification schemes and appropriate software. The major benefit of the technique is its ability to model data based on the features contained within it, rather than imposing a rigid and deterministic model on a data set which does not explicitly recognise individual features of a time series. The identification of these major features within a time series, and their time-evolutions

provides an excellent descriptive basis of the time series. In addition, an understanding of the salient features in time series from tree-rings, and other proxy climate indicators, offer considerable potential for the improved reliability of palaeoclimatic reconstructions.

Acknowledgements Access to material held at the Laboratory of Tree-ring Research, Tucson, Arizona, and the assistance of Drs. E. Cook, D. McDonald and B. Buckley is gratefully acknowledged. Dr D. McDonald provided access to a copy of the program STAMP®, and Dr E. Cook provided the program PCREG.

REFERENCES

Allen, K., J.; *A Dendroclimatological Investigation of Phyllocladus aspleniifolius (Labill.) Hook. f.*, Unpub. PhD thesis, University of Tasmania, 1998

Buckley, B.M., *Climate Variability in Tasmania Based on Dendroclimatic Studies of Lagarostobos franklinii*, Unpub. PhD thesis, University of Tasmania, 1997

Briffa, K.R., Schweingruber, F.H., Jones, P.D., Osborn, T.J., Shiyatov, S.G. and Vaganov, E.A., Reduced sensitivity of recent tree-growth to temperatures at high northern latitudes, *Nature* 391(12), 678–682, 1998

Campbell, D.A., *The Feasibility of Using Tree-Ring Chronologies to Augment Hydrologic Records in Tasmania, Australia,* Unpub. Masters thesis, University of Arizona, 1980

Cook, E.R. and K. Peters, The smoothing spline: a new approach to standardizing forest interior tree-ring width series for dendroclimatic studies, *Tree-Ring Bulletin,* 41, 45–53, 1981

Cook, E.R., S. Shiyatov and V. Mazepa, Estimation of the mean chronology, in Chapter 3 of *Methods of Dendrochronology*, Cook and Kariukstis (Eds.), Kluwer Academic Publishers, Dordrecht, 394pp 1990

Cook, E.R., T. Bird, M. Peterson, M. Barbetti, R. D'Arrigo and R. Francey, Climatic change over the last millennium in Tasmania reconstructed from tree-rings, *The Holocene,* 2(3), 205–217, 1992

Cook, E.R., R.J. Francey., B.M. Buckley and R.D. D'Arrigo, Recent increases in Tasmanian Huon Pine ring widths from a subalpine stand: natural climate variability or greenhouse warming?, *Papers and Proceedings of the Royal Society of Tasmania,* 130(2), 65–72, 1996

Crafts, N.F.R., S.J. Leybourne and T.C. Mills, Measurement of trend growth in European industrial output before 1914: Methodological issues and new estimates, *Explorations in Economic History*, 27, 442–467, 1990

de Jong, P. and S. Chu-Chun-Lin, Fast likelihood evaluation and prediction for nonstationary state space models, *Biometrika* 81, 133–142, 1994

Diebold, F.X., Structural Time Series Analysis and Modelling Package: A Review, *Journal of Applied Econometrics* 4, 195–204, 1989

Douglass, A.E., *Climatic Cycles and Tree Growth. Vol II: A Study of the Annual Rings of Trees in Relation to Climate and Solar Activity* Carnegie Institute of Washington Publication No. 289, 166 pp, 1928

Fritts, H.C., *Tree Rings and Climate*, Academic Press New York, 567pp, 1976,

Gordon, G.A. and S.K. LeDuc, Verification statistics for regression models, in *Reprints of 7th Conference on probability and Statistics in Atmospheric Science*, Monterey Canada, 129–131, 1981

Harvey, A.C., *Forecasting, Structural Time Series and The Kalman Filter,* Cambridge University Press, Cambridge, 554pp, 1989

Kaufman, R.K. and D.I. Stern, Evidence for human influence on climate from hemispheric temperature relations, *Nature*, 388, 39–44, 1997

Koopman, S.J., A.C. Harvey, J.A. Doornik and N. Shephard, *STAMP 5.0: Structural Time Series Analyser, Modeller and Predictor*, Chapman and Hall, London, 382pp, 1995

Lamb, H.H. and A.I. Johnson, Climatic variation and observed changes in the general circulation, *Geografiska Annaler*, 43, 94–134, 1961

LaMarche, V.C. Jr., and A.B. Pittock, Preliminary temperature reconstructions for Tasmania, in *Climate from Tree Rings*, M.K. Hughes, A.M. Kelly, J.R. Pilcher. and V.C. LaMarche. Jr. (Eds.), 177–185, 1982

McDonald, A.D. and A.S. Hurn, Unobservable cyclical components in term premia of fixed-term financial instruments, *Mathematics and Computers in Simulation*, 39, 403–409, 1995

Meko, D.M, *Applications of Box-Jenkins Methods of Time Series Analysis to the Reconstruction of Drought from Tree Rings,* Unpub. PhD Thesis, University of Arizona, 1981

Mocan, H.N. and K. Topyan, Real wages over the business cycle, evidence from a structural time series model, *Oxford Bulletin of Economics and Statistics*, 55(4), 363–387, 1993

Norton, D.A., Briffa, K.R., and M.J. Salinger, Reconstruction of New Zealand summer temperatures to 1730 AD using dendroclimatic techniques, *International Journal of Climatology* 9, 633–644, 1989

Ogden, J., On the dendrochronological potential of Australian trees, *Australian Journal of Ecology*, 3, 339–356, 1978

Percival, D.B. and A.T. Walden, *Spectral Analysis for Physical Applications: Multitaper and Conventional Univariate Techniques*, Cambridge University Press, 583pp, 1993

Press, W.H., S.A. Teukolsky, W.T. Vetterling, and B.P. Flannery, *Numerical Recipes in FORTRAN: The Art of Scientific Computing*, 2nd edition, Cambridge University Press, Cambridge, 961pp, 1992

Read, J. and J.R. Busby, Comparative responses to temperature of the major canopy species of Tasmanian cool temperate rainforest and their ecological significance. II.

Net photosynthesis and climate analysis, *Australian Journal of Botany,* 38, 185–205, 1988

Salinger, M.J., Palmer, J.G., Jones, P.D., and K.R. Briffa, Reconstruction of New Zealand climate indices back to AD 1731 using dendroclimatic techniques: some preliminary results, *International Journal of Climatology* 14, 1135–1149, 1994

Stern, D.I. and R.K. Kaufman, Is there a global warming signal in hemispheric temperature series? Submitted and under review, *Climatic Change,* 1997

Stokes, M.A. and T.L. Smiley, *An Introduction to Tree-ring Dating,* University of Chicago press, Chicago, 1968

Thompson, D.J., Spectrum estimation and harmonic analysis, *Proceedings of The IEEE* 70(9), 1055–1096, 1982

Tol, R.S.J., Greenhouse statistics — time series analysis: Part II, *Theoretical and Applied Climatology,* 49, 91–102, 1994

Tol, R.S.J. and A.F. de Vos, Greenhouse statistics–time series analysis, *Theoretical and Applied Climatology,* 48, 63–74, 1993

Villalba, R., E.R. Cook, R.D. D'Arrigo, G. Jacoby, P.D. Jones, M.J. Salinger, and J. Palmer, Sea-level pressure variability around Antarctica since AD 1750 inferred from subantarctic tree-ring records, *Climate Dynamics* 13(6), 375–390, 1997

Watson, M.W. and R.F. Engle, Alternative algorithms for the estimation of dynamic factor, mimic varying coefficient regression models, *Journal of Econometrics,* 23, 385–400, 1983

Young, P., Data-based mechanistic modelling of environmental, ecological, economic and engineering systems, *Proceedings of MODSIM 97, International Congress on Modelling and Simulation, Hobart, 1997,*4, 1867–1874, 1997

FIGURE CAPTIONS

Figure 1: Location of Tasmanian tree-ring sampling sites and meteorological stations. Three regions have been delineated as East (3 sites), West (4 sites) and Southwest (3 sites)

Figure 2: Properties of West coast data.

a. The 4 West tree-ring chronologies over their entire periods. These chronologies have been detrended and autoregressively modelled and the pooled model of autoregression re-incorporated into them with the aim of maximising the macro-climatic signal present. KOA is the easternmost of the West sites, MUR is to the west of KOA, RCS to the north, and WEY is the most northerly of the West sites.

b. Correlogram of West temperature index. An AR(1) pattern in the seasonalised data is not evident.

c. Multiple Taper Method estimation of spectrum of West temperature index. Three data tapers with bandwidth frequency products of 2 have been applied, and significant spectral peaks occur at 0.0049 (204.08 years, obviously a spurious value), 0.1133 (8.83 years), 0.4121 (2.43 years). Period analysed is 1910–1994

Figure 3: Actual and estimated regional temperatures. Left hand column shows the PCREG estimates, and right hand column the STS estimates. Estimates are in standard deviations from the mean. 'Huon' refers to *L. franklinii*

Figure 4: Time traces of components for STS West model (equation 20). The PCA was performed on data of the four sites whose time series are shown in Figure 2 for the period 1650–1994. Only the two significant PCs included in (20) are shown, and for the period 1910–1994 only. The second frame shows the trend component which has been modelled as a random walk and shows a minimum in the 1940s, noted as a cold period in meteorological records generally. The third frame shows the two cyclical components, cycle 1 has a period of 5.149 years, and cycle 2, a period of 8.506 years. The final frame traces the irregular component over time.

Figure 5: Regional *P. aspleniifolius* reconstructions of maximum temperature. Relatively large differences between East and West occur between 1815–1825, and 1915–1925; differences between Southwest and the northern reconstructions occur in the mid 1970s. The West shows large positive deviations from mean maximum temperatures in the early 1980s while at the same time East and Southwest reconstructions indicate maximum temperatures to be below average.

Figure 6: West Coast *P. aspleniifolius* STS maximum temperature reconstructions and PC regression reconstruction of maximum temperature from *L. franklinii.* Top panel: AD 1800–1899, bottom panel AD 1900–1999. Years when large differences exist between the two reconstructions are 1849, 1898, 1908 and 1913–1915. The 1849, 1898 and 1908 cases all show maximum temperatures to be well below average according to *L. franklinii*, but close to or above average according to *P. aspleniifolius.*

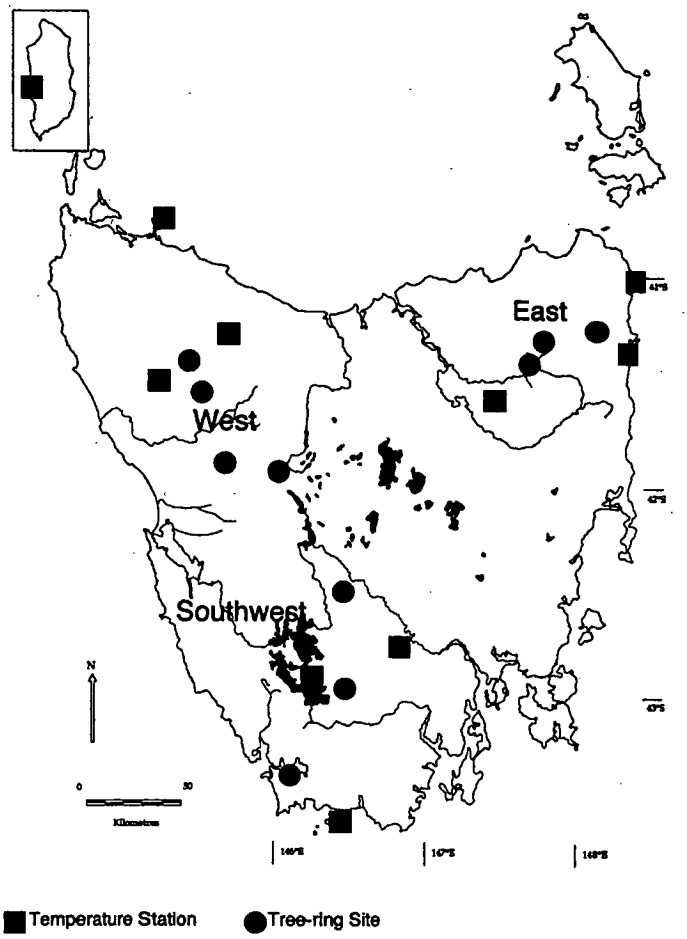

Figure 1

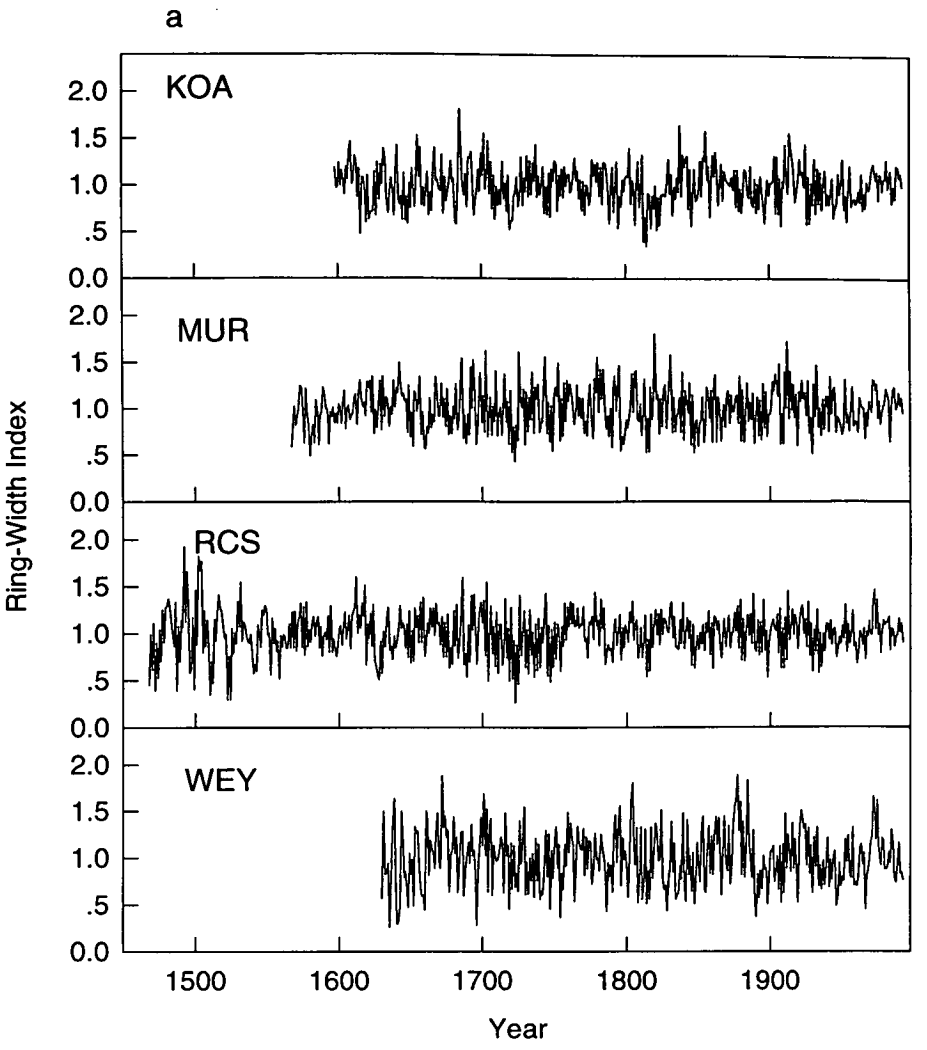
a
KOA
MUR
RCS
WEY
Ring-Width Index
2.0
1.5
1.0
.5
0.0
1500
1600
1700
1800
1900
Year

Figure 2a

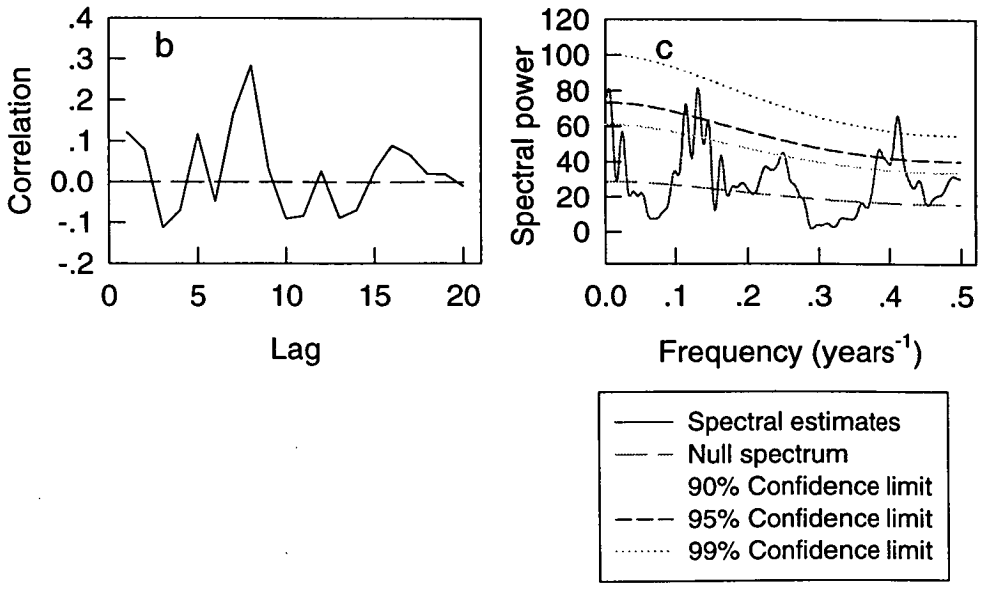

Figures 2b & 2c

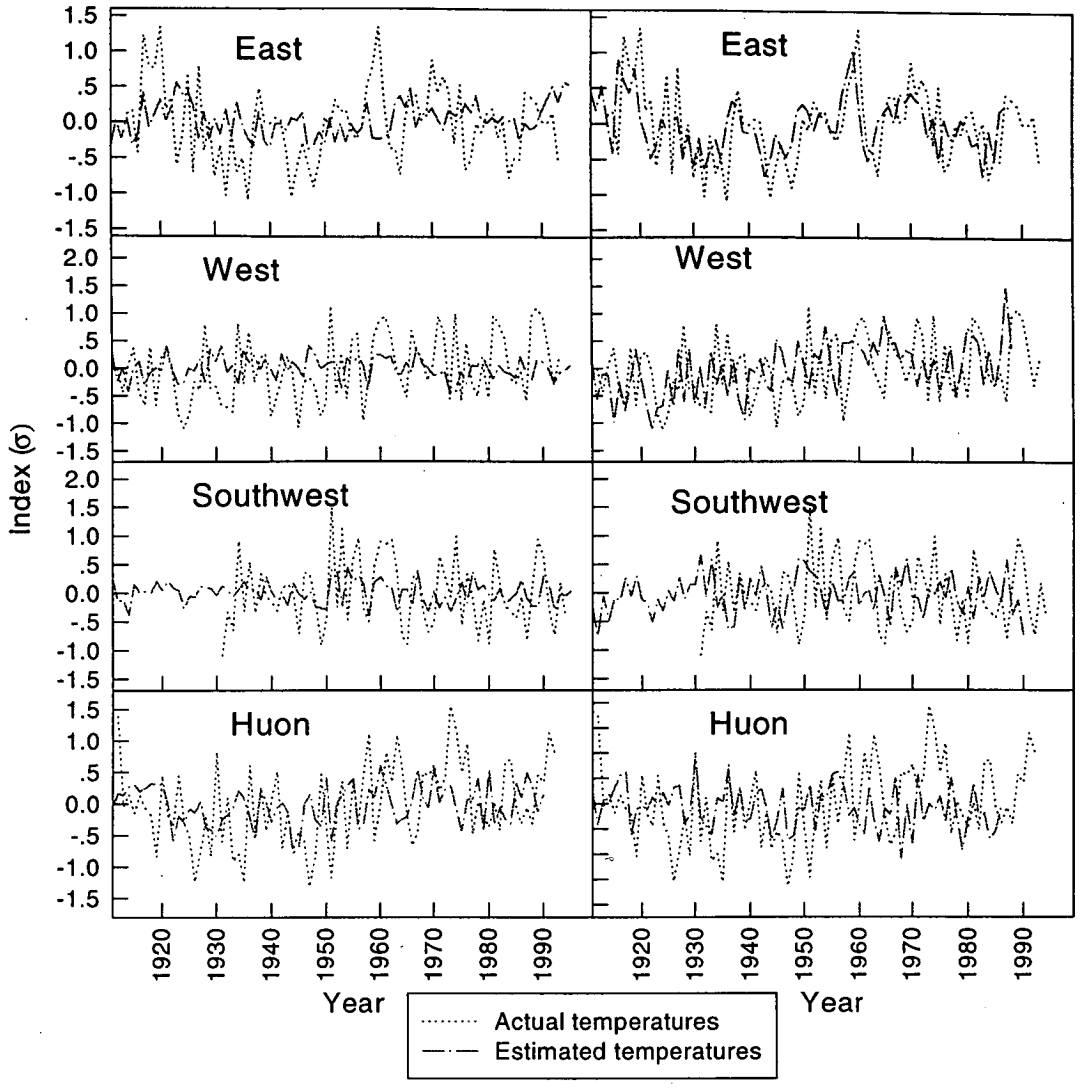
East
East
West
West
Southwest
Southwest
Huon
Huon
Index (σ)
Year
Year
1920
1930
1940
1950
1960
1970
1980
1990
Actual temperatures
Estimated temperatures

Figure 3

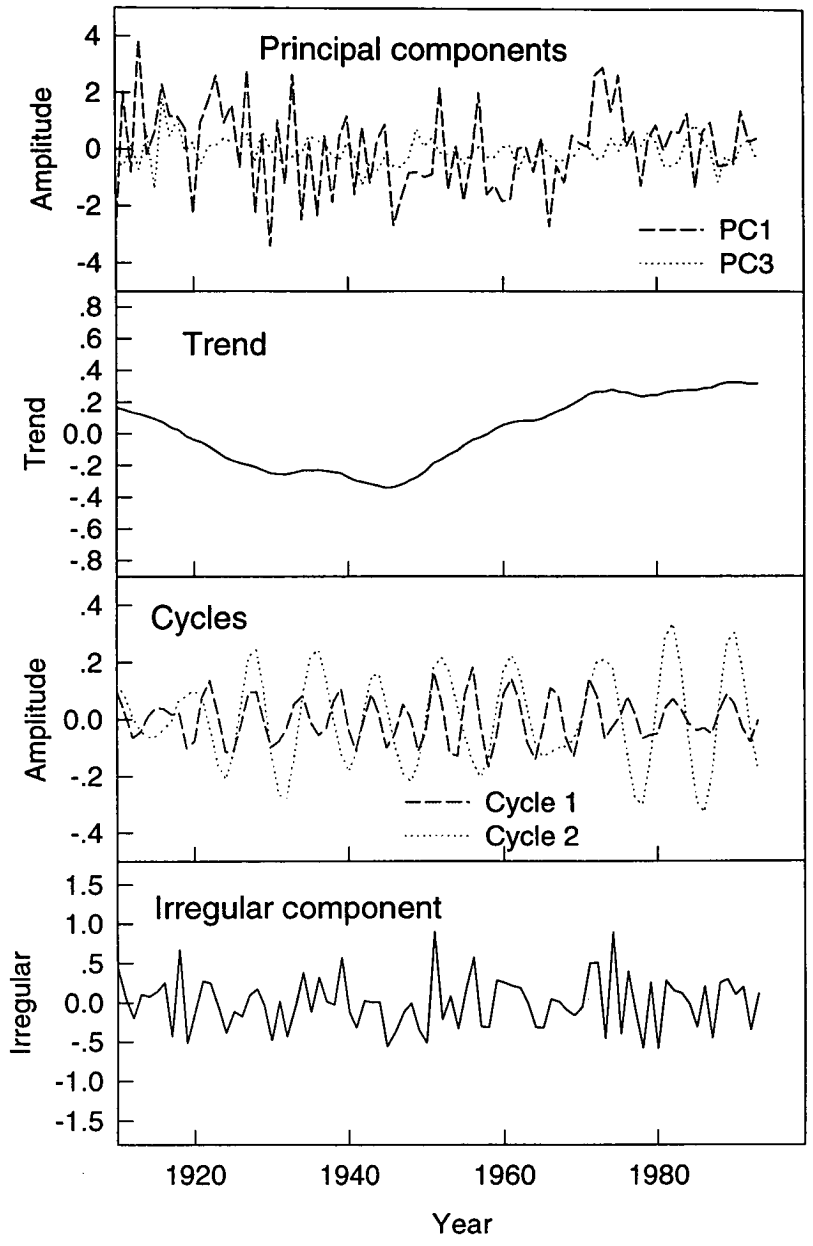
Principal components
Amplitude
4
2
0
-2
-4
PC1
PC3
Trend
Trend
.8
.6
.4
.2
0.0
-.2
-.4
-.6
-.8
Cycles
Amplitude
.4
.2
0.0
-.2
-.4
Cycle 1
Cycle 2
Irregular component
Irregular
1.5
1.0
.5
0.0
-.5
-1.0
-1.5
1920
1940
1960
1980
Year

Figure 4

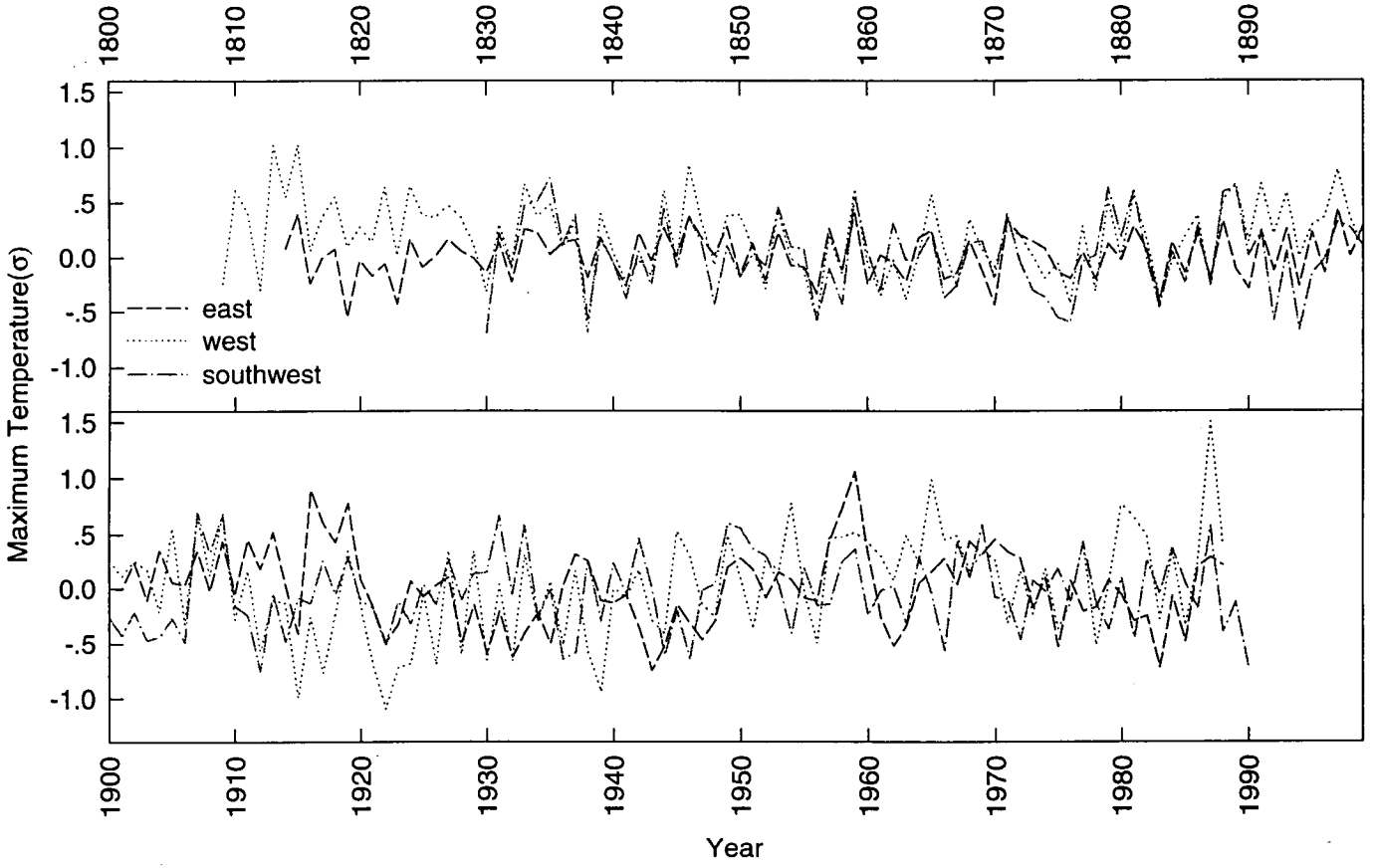
1800
1810
1820
1830
1840
1850
1860
1870
1880
1890
1.5
1.0
.5
0.0
-.5
-1.0
east
west
southwest
Maximum Temperature(σ)
1900
1910
1920
1930
1940
1950
1960
1970
1980
1990
Year

Figure 5

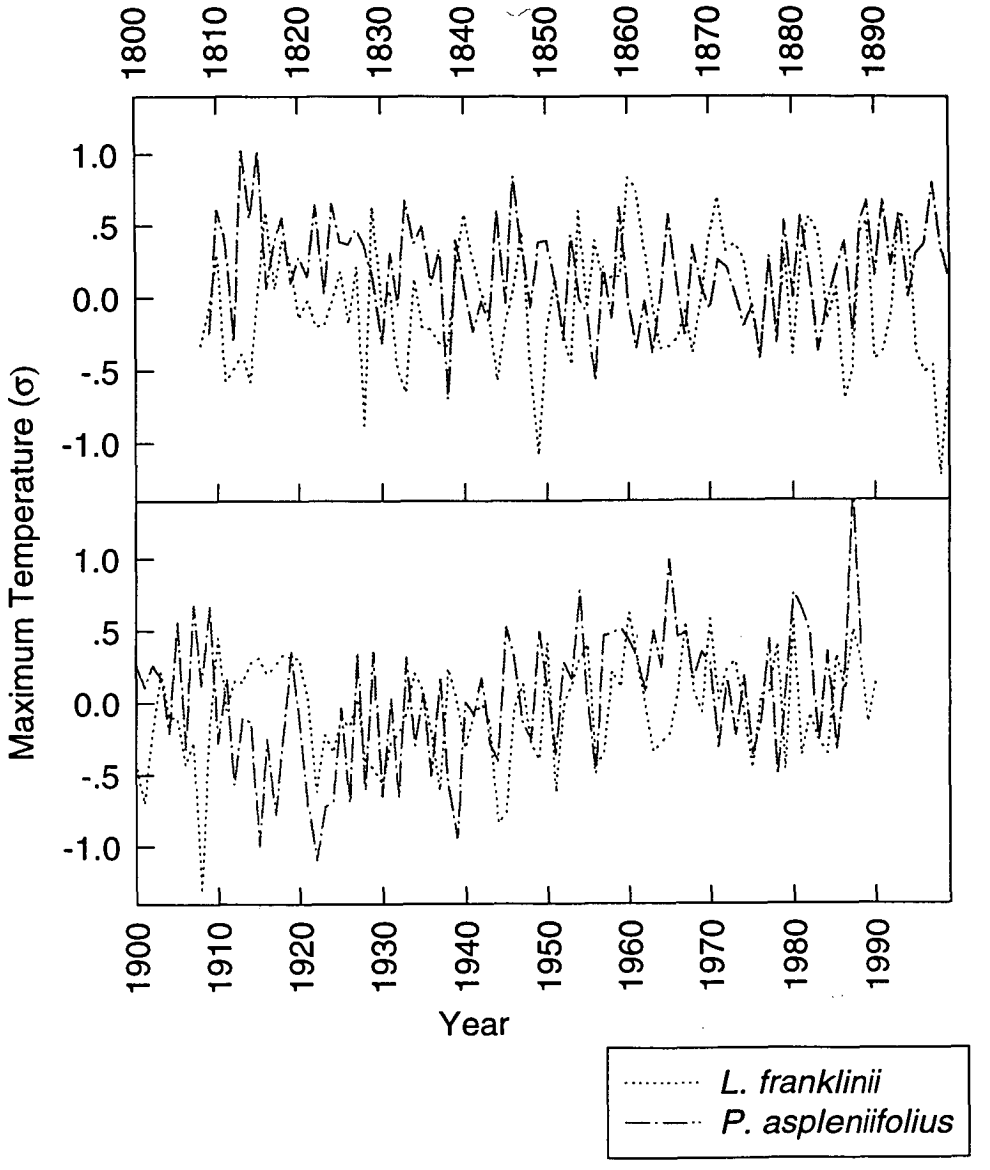
1800
1810
1820
1830
1840
1850
1860
1870
1880
1890
1.0
.5
0.0
-.5
-1.0
Maximum Temperature (σ)
1900
1910
1920
1930
1940
1950
1960
1970
1980
1990
Year
L. franklinii
P. aspleniifolius

Figure 6

TABLE CAPTIONS

Table 1: Summary of symbols used in text. Each symbol appears in the order it appeared in the text. More detail on the development of STS models can be found in Harvey (1989)

Table 2: STS Model diagnostics. The Bowman–Shenton (BS) test is a test of data normality. No value for any site is significant (0.05). DW is the Durbin–Watson statistic, centred around 2 for a series with no autocorrelation, and Q is the Box–Ljung Portmanteau statistic (Ljung and Box 1978) which tests for autocorrelation out to lag *p*. Significant autocorrelation remains (0.05 significance level) in the East

Table 3: Estimated parameters of STS models. Estimate of *level* is given for the final state, i.e. at $t = t$. Estimate for AR(1) parameter refers to the value of the ρ coefficient. A t statistic greater than 1.64 indicates significance at the 0.1 level and one greater than 1.96 is significant at the 0.05 level. For ψ_1 and ψ_2, the first value (A) refers to the amplitude of the cycle and the second value (λ) to the period of the cycle

Table 4: Goodness of fit statistics for PC regression (PCR) and Structural Time Series (STS) models. AIC has been calculated as the AIC corrected for inconsistency: $AIC_c = N*\log(MSE) + 2p + 2\{(p+1)(p+2)/(N-p-2)\}$, where N is the number of observations, MSE is mean square error and p the number of model parameters

Symbol	*Description*	*Equation*
y	Dependent variable	(1)
μ	Trend	(1), (2)
γ	Seasonal component	(1), 3)
δ	Parameters associated with explanatory variables	(1)
x	vector of explanatory variables	(1)
ψ	Cyclical component	(1)
ε	Irregular component	(1)
β	Slope of trend	(2)
ξ	A white noise process associated with trend slope	(2)
ϑ	White noise process associated with seasonal component	(3)
$\hat{f}(\lambda)$	Estimated spectrum	(4)
ω	Normalised weights used in spectral estimation	(4)
Z	System matrix, containing coefficients of state vector	(5)
α	State vector containing components of model	(5)
e	Error process associated with measurement equation	(5)
H	Variance of error process associated with measurement equation	
T	System matrix containing information on components	(6)
R	System matrix	(6)
η	Error process associated with transition equation	(6)
Q	Variance of error process associated with transition equation	
a	Expected value of the state	(7),(9), (10),(12)
P	Variance of the state	(7),(9), (11),(12),(13),(14)

Table 1

	Std Error	*BS*	*DW*	*Q*
East	0.444	0.615	2.051	12.590
West	0.4501	1.399	2.025	12.58
Southwest	0.506	1.510	2.087	10.400
L. franklinii	0.544	0.963	1.941	7.403

Table 2

Parameter	*Estimate*	*Standard Error*	*t statistic*
East			
level	0.023	0.152	0.147
AR(1)	0.759		
PC1	-0.123	0.030	-4.120
PC3	-0.189	0.102	-1.852
West			
level	0.167	0.176	0.948
ψ_1	0.097(A),5.149(λ)	0.168	
ψ_2	0.122(A), 8.506(λ)	0.229	
PC1	-0.185	0.034	-5.393
PC3	-0.179	0.106	-1.682
Southwest			
level	-0.023	0.061	-0.384
ψ_1	0.124(A), 0.4865(λ)	0.212	
ψ_2	0.155(A), 9.07(λ)	0.132	
PC1	-0.235	0.056	-4.218
Huon Pine			
level	-0.048	0.192	-0.252
AR(1)	0.212		
PC1	0.080	0.046	1.752
PC2	-0.244	0.110	-2.216
PC3	-0.31	0.111	-2.778
PC4	-0.441	0.141	-3.140

Table 3

	East	*West*	*Southwest*	*Lagarostobos*
R^2(PCREG)	0.138	0.117	0.149	0.252
AIC_C(PCREG)	-7.130	-13.600	-5.810	-19.330
R_D^2 (STS)	0.307	0.349	0.286	0.307
AIC_C (STS)	-35.586	-30.550	-22.503	-6.027

Table 4